Universitat de Girona

TRANSITION METAL-CATALYSED [2+2+2] CYCLOADDITION REACTIONS. METHODOLOGY AND MECHANISM

Magda PARERA BRIANSÓ

Dipòsit legal: Gi. 1088-2014
http://hdl.handle.net/10803/xxxxx

Doctoral thesis:

Transition metal-catalysed [2+2+2] cycloaddition reactions. Methodology and mechanism.

Magda Parera Briansó

2014

Doctorate Programme of Experimental Sciences and Sustainability

Supervised by:

Prof. Anna Roglans Ribas

Dr. Anna Pla Quintana

Presented in partial fulfillment of the requirements for a doctoral degree from the University of Girona

Les sotasignants **Anna Roglans Ribas** i **Anna Pla Quintana**, Professora Catedràtica i Professora Agregada del Departament de Química de la Universitat de Girona, respectivament,

CERTIFIQUEN, que la memòria que porta per títol "Transition metal-catalysed [2+2+2] cycloaddition reactions. Methodology and mechanism" que presenta la **Magda Parera Briansó** per a l'obtenció del títol de Doctor en Química, ha estat realitzat sota la seva direcció i que compleix els requisits per a poder optar a la Menció Internacional del títol.

I perquè així consti, signen el present certificat.

Prof. Anna Roglans Ribas

Dra. Anna Pla Quintana

Girona, 11 de febrer de 2014.

A la petita Afra

Acknowledgments

Ja fa sis anys que vaig arribar a la UdG i en aquest temps he cursat el màster de química mèdica i disseny de molècules MECHMOD i he realitzat el doctorat en el grup de Metalls de Transició en Síntesi Orgànica (METSO). Estic molt satisfeta de la feina feta i molt feliç d'haver conegut les persones amb qui he coincidit durant aquest temps. Valoro l'etapa del doctorat com un procés de consolidació dels coneixements de la carrera molt eficaç així com de creixement personal important. Tot aquest valor que he afegit a la meva formació no hagués estat possible sense el suport de les persones que han estat al meu costat, a les quals vull dedicar aquestes pàgines.

En primer lloc vull agrair a les meves directores de tesi, la Prof. Anna Roglans i la Dra. Anna Pla, l'oportunitat de realitzar la tesi al grup, així com d'engrescar-me i contagiar-me el seu interès per la recerca. En tot moment he rebut la vostra atenció i ajuda quan ho he necessitat. Gràcies a la vostra manera de guiar-me, he pogut afrontar-me a nous reptes, plantejar solucions als problemes, aprendre dels errors...garantint el meu autoaprenentatge.

El finançament d'aquesta tesi ha estat possible gràcies a una beca FI de la Generalitat de Catalunya i als projectes de recerca del MINECO de referència CTQ2008-05409 i CTQ2011-23121 i de l'AGAUR, de referència 2009SGR637.

Durant aquesta tesi he realitzat dues estades pre-doctorals, la primera als laboratoris del Prof. Jacques Muzart i Dr. Jean le Bras de la Universitat de Reims gràcies a una beca BE de la Generalitat de Catalunya i la segona en el grup del Prof. K.-R. Pörschke del Max-Planck Institut de Mülheim gràcies a un projecte AIB2010DE-00262. A tots ells, agrair-los la formació que m'han donat, la seva ajuda i atenció i també la bona rebuda i acollida que em van fer en els seus grups de recerca.

La determinació estructural dels diferents compostos sintetitzats durant la realització d'aquesta tesi no hagués estat possible sense els Serveis Tècnics de Recerca de la Universitat de Girona. Vull fer una menció especial a dues persones que sempre han estat disposades a donar un cop de mà: l'Anna Costa, per la realització de les anàlisis elementals, l'enregistrament dels espectres d'ESI-MS i, especialment, per fer-me tan agradables el munt d'hores que hem passat juntes davant de l'aparell d'ESI així com fent el curs de trampa iònica a Zaragoza, que recordo molt positivament. Amb ella he après molt sobre la tècnica i l'aparell d'ESI-MS, el qual hem netejat juntes algunes vegades i sempre ens ha quedat impecable! És clar que hem format un bon equip!; i a la Dra. Lluïsa Matas pels espectres de RMN realitzats i la seva predisposició en tot moment.

I a partir d'aquí, donar les gràcies a tota la gent amb qui he passat tantes bones estones al laboratori, despatx, classe o als congressos. Agraeixo a les meves companyes de grup Sandra, Lídia i Anna tota la paciència que han tingut i la seva ajuda sempre que l'he necessitada, així com el bon exemple que m'han donat, dins i fora del laboratori. A la Mònica, en Quim, la Mar i en Bernat els dedico un gran somriure per tots els que ells m'han regalat durant el seu pas pel laboratori. I a la Cristina, per ser la meva única i gran companya de màster! No puc deixar

d’anomenar la nova incorporació al grup, l’Ewelina, l’alegria del laboratori. Aquest últim any amb ella ha sigut genial. Hem tingut temps de coincidir a Polònia, a Viena i també al Montseny, a Banyoles i a Vic. Hem passat molt bones estones entre calçots, barraques, massatges, concerts i espectacles de circ! Gràcies per acollir-me, també, a Girona quan jo ja no hi tenia pis! dziękuję! A l’Òscar, al Martí i a l’Ouissam també vull agrair-los la seva col·laboració en tot moment en el laboratori, hem fet un bon equip! Que tingueu un futur ple d’èxits, que us el mereixeu!

Moltes gràcies, també, a la resta de companys químics d’altres àrees que m’han fet passar els dies més agradablement, sense notar tant la rutina. En especial els que em van socórrer quan em vaig accidentar al laboratori: Íngrid, Pep Duran, merci per les “gestions” que vàreu haver de fer!

D’altra banda, vull agrair als diferents companys de pis que he tingut durant aquesta època viscuda a Girona tots els moments fantàstics que no oblidaré mai i que han marcat un abans i un després a la meva vida: gràcies Berta, Jesús, Sònia, Sílvia, Laura, Xavi i Judit. Tot el que he rigut amb vosaltres farà que visqui uns quants anys més! Encara que ara estiguem separats, hem sigut una família i això m’ha fet sentir molt bé!

No voldria deixar d’anomenar les amigues de tota la vida de Mataró: la Marta, la Titi, l’Aleida, la Helen, la Laura, l’Andrea, la Meri i la Rebeca; i les de Gualba: Núria i Míriam. Són molts anys juntes i molts més que passarem encara que les coses al nostre voltant canviïn! A la colla de Girona, agrair el vostre acolliment, sempre tan càlid i atent. Gràcies, atzar, per fer que la Mireia i jo ens coneguéssim! Va ser l’inici d’un llarg camí! Carla, a tu t’agraeixo cada una de les abraçades que m’has fet plenes d’energia! Un plaer conèixer-te!

A la Dolors, vull agrair-li tota la seva atenció, companyia i generositat en aquests últims mesos, que han sigut durs. Gràcies per ajudar-me a trobar-me millor i també per posar-me un plat a taula cada dia.

Finalment vull que la meva família sàpiga com n’estic d’orgullosa i que sempre els agrairé tot el que han fet i fan, encara, per a mi. A ma mare, pels seus consells, per escoltar-me, pel seu suport, ànims i comprensió. Al meu pare, per la seva manera positiva de veure el món, per creure en mi i per fer-me riure sempre, fent-me el dia a dia més agradable. Sense vosaltres, no hauria arribat fins aquí, moltes gràcies. A la tieta, la millor del món: has estat sempre al meu costat des que vaig néixer i els moments que he passat amb tu han sigut dels més feliços de la meva vida. M’encanta dir-me igual que tu! Aquest any serà molt especial per les dues...

Ja només quedes tu, Rossend. Gràcies per la teva companyia, per la teva força i per la teva llum. Només tu ets el meu company de viatge i amic de debò. Només tu pots fer-me sentir aquesta alegria constant. Ara que estem més units que mai, desitjo que tot el que vingui a partir d’ara sigui una font d’inspiració per a ser millors i encara més feliços!

Moltes gràcies a tots!

Publications

This doctoral thesis has resulted in the following publications:

- *Chiral N-phosphino sulfinamide ligands in rhodium(I)-catalyzed [2+2+2] cycloaddition reactions.* Brun, S.; Parera, M.; Pla-Quintana, A.; Roglans, A.; León, T.; Achard, T.; Solà, J.; Verdaguer, X.; Riera, A. *Tetrahedron* **2010**, *66*, 9032.

- *P-Stereogenic Secondary Iminophosphorane Ligands and Their Rhodium(I) Complexes: Taking Advantage of NH/PH Tautomerism.* León, T.; Parera, M.; Roglans, A.; Riera, A. Verdaguer, X. *Angew. Chem. Int. Ed*. **2012**, *51*, 6951.

- *Direct Detection of Key Intermediates in Rhodium(I)-Catalyzed [2+2+2] Cycloadditions of Alkynes by ESI-MS.* Parera, M.; Dachs, A.; Solà, M.; Pla-Quintana, A.; Roglans, A. *Chem. Eur. J.* **2012**, *18*, 13097.

Abbreviations

v (in IR)	Frequency (units: cm^{-1})
APCI	Atmospheric Pressure Chemical Ionization
APPI	Atmospheric Pressure Photoionization
API	Atmospheric Pressure Interface
Ar	Aryl
ATR (in IR)	Attenuated Total Refractance
BIPHEP	Biphenylphosphine
Bn	Benzyl
Boc	*tert*-butyloxycarbonyl
Bu	Butyl
CID	Collision Induced Dissociation
COD	1,5-cyclooctadiene
Cp	Cyclopentadiene
Da	Dalton
DFT	Density Functional Theory
DMF	Dimethylformamide
EA	Elemental Analysis
ee	Enantiomeric excess
equiv.	Equivalent
ESI-MS	Electrospray Ionization-Mass Spectrometry
ESI-HRMS	Electrospray Ionization - High Resolution Mass Spectrometry
Et	Ethyl
et al.	Collaborators
EtOH	Ethanol
GC	Gas Chromatography

h	Hours
HPLC	High Performance Liquid Chromatography
^{i}Pr	*iso*-propyl
IMes	1,3-bis(2,4,6-trimethylphenyl)imidazol-2-ylidene
IR	Infrared Spectroscopy
LC	Liquid Chromatography
m-	*Meta-*
min.	Minutes
m/z	Mass to charge ratio
m.p.	Melting point
Me	Methyl
MeOH	Methanol
Mes	Mesityl (2,4,6-trimethylphenyl)
M.W.	Molecular Weight
o-	*Ortho-*
p-	*Para-*
Ph	Phenyl
r.t.	Room temperature
t	Time
T	Temperature
^{t}Bu	*tert*-butyl
Tf	Triflate
TFA	Trifluoroacetic acid
THF	Tetrahydrofuran
TLC	Thin Layer Chromatography
Ts	Tosyl (*p*-methylphenylsulfonyl)
V	Volts

Abbreviations used in Nuclear Magnetic Resonance (NMR)

δ	Chemical shift (units: ppm)
^{13}C-NMR	Nuclear magnetic resonance of carbon (13)
^{1}H-NMR	Nuclear magnetic resonance of proton
^{31}P-NMR	Nuclear magnetic resonance of phosphorous (31)
abs.	Absorption
d	Doublet
dd	Double doublet
dt	Double triplet
J	Coupling constant
m	Multiplet
q	Quadruplet
s	Singlet
t	Triplet

Graphical summary

Chapter 1. General introduction (p 11)

Chapter 2. General objectives (p 35)

Chapter 3. Hemilabile S-stereogenic and P-stereogenic ligands for the Rh(I)-catalysed [2+2+2] cycloaddition reactions (p 39)

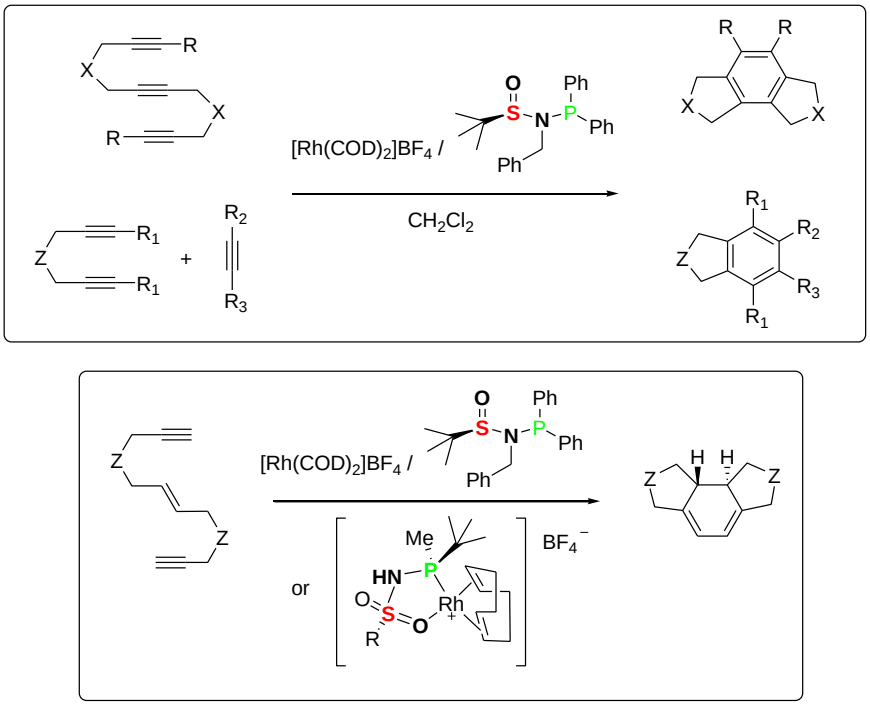

Chapter 4. Baylis-Hillman adducts as substrates of the [2+2+2] cycloaddition reaction (p 71)

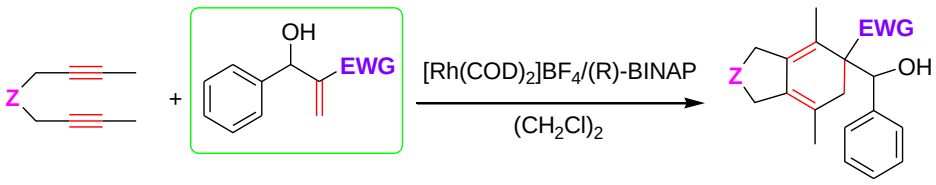

Z = NTs, O, $C(CO_2Et)_2$

EWG = COOMe, COOEt, COO^tBu

Chapter 5. Mechanistic study of [2+2+2] cycloaddition reactions by ESI-MS (p 95)

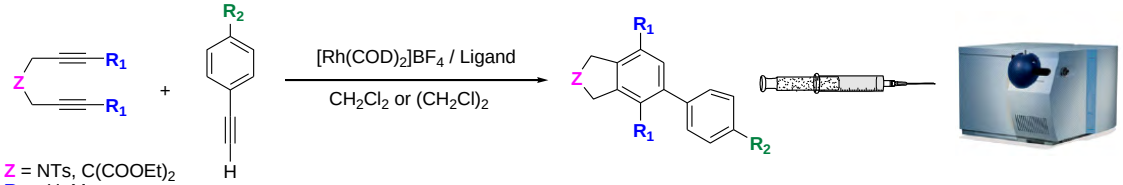

Z = NTs, $C(COOEt)_2$
R_1 = H, Me

R_2 = Me, OMe, H, *t*Bu, F, Br, NO_2, NMe_2, CN

Chapter 6. General conclusions (p 149)

Chapter 7. Methods (p 153)

Supplementary data

The material listed below is attached as supplementary data on the CD included in the thesis:

- **Thesis:** Memory of the thesis in .pdf format.

- **Chapter 3**:

  C3_Spectra: selection of the ^{1}H NMR, ^{13}C NMR, IR and MS spectra of the products synthesized in .pdf format.

- **Chapter 4**:

  C4_Spectra: selection of the ^{1}H NMR, ^{13}C NMR, IR and MS spectra of the products synthesized in .pdf format.

  C4_HPLC: HPLC chromatograms HPLC of the products obtained with enantiomeric excess in .pdf format.

- **Chapter 5**:

  C5_Spectra: selection of the ^{1}H NMR, ^{13}C NMR, IR and MS spectra of the products synthesized in .pdf format.

  C5_SI_2012CEJ13097: ESI-MS and ESI-MS/MS spectra of the reagents, products and intermediates detected in .pdf format.

- **Publications:** publications resulting from this thesis in .pdf format.

Table of contents

Summary

The development of new chemical processes and efficient catalysts for the formation of carbon-carbon bonds is an important topic in organic chemistry. In particular, the transition-metal catalysed [2+2+2] cycloaddition reaction is a highly efficient synthetic tool that allows six-membered polysubstituted carbo- and heterocyclic derivatives to be obtained in an atom economy process.

This doctoral thesis, divided into seven different chapters, is based on methodological and mechanistic studies of the rhodium(I)-catalysed [2+2+2] cycloaddition reaction. Chapter 1 contains a general introduction to this kind of process and makes reference to the main examples in the literature. Chapter 2 sets out the general objectives of the thesis. In Chapter 3, the use of hemilabile S-stereogenic and P-stereogenic ligands for the rhodium-catalysed [2+2+2] cycloaddition is described. The activity of these new catalytic systems is evaluated in the cycloaddition of three alkynes. Since these complexes are chiral they are also evaluated in the enantioselective cycloaddition of enediynes to obtain chiral cyclohexa-1,3-dienes. In Chapter 4, the participation of Baylis-Hillman adducts as alkene moieties for the partially intramolecular [2+2+2] cycloaddition is evaluated. This process allows the synthesis of a set of enantioenriched bicyclic cyclohexadienes featuring a quaternary stereogenic centre. In Chapter 5, the mechanistic study of [2+2+2] cycloaddition of alkynes by electrospray ionization mass spectrometry and DFT calculations is performed. These mechanistic studies result in all the reactive intermediates of the catalytic cycle being detected for the first time. Chapter 6 draws general conclusions from the results of these studies. Finally, Chapter 7 contains the experimental procedure for the compounds synthesised in this thesis.

Resumen

El desarrollo de nuevos procesos químicos y catalizadores eficientes para la formación de enlaces carbono-carbono es un campo importante en química orgánica. Concretamente, la reacción de cicloadición [2+2+2] catalizada por metales de transición es una herramienta muy eficiente que permite la formación de derivados carbo- y heterocíclicos polisustituidos de seis miembros en un proceso de economía atómica.

Esta tesis doctoral, dividida en siete capítulos, se ha basado en estudios metodológicos y mecanísticos de las reacciones de cicloadición [2+2+2] catalizadas por rodio(I). El Capítulo 1 contiene una introducción general de este tipo de procesos y los principales ejemplos descritos en la bibliografía. El Capítulo 2 incluye los objetivos generales de la tesis. En el Capítulo 3 se describe el uso de ligandos hemilábiles S-estereogénicos y P-estereogénicos para la reacción de cicloadición [2+2+2] catalizada por rodio. La actividad de estos nuevos sistemas catalíticos ha sido evaluada en la cicloadición de tres alquinos. Dado que estos complejos son quirales, también se han estudiado en la cicloadición enantioselectiva de endiinos para la obtención de ciclohexadienos quirales. En el Capítulo 4 se evalúa la participación de aductos de Baylis-Hillman como sustratos insaturados para la cicloadición [2+2+2] parcialmente intramolecular. Este proceso ha permitido la síntesis de un conjunto de ciclohexadienos bicíclicos quirales con un estereocentro cuaternario. El Capítulo 5 corresponde al estudio mecanístico de la cicloadición [2+2+2] de alquinos a través de la espectrometría de masas con ionización por electroespray y cálculos DFT. Estos estudios han permitido detectar experimentalmente por primera vez todos los intermedios reactivos del ciclo catalítico. El Capítulo 6 incluye las conclusiones generales que se pueden extraer de la tesis. Por último, el Capítulo 7 contiene el procedimiento experimental de los compuestos sintetizados en esta tesis.

Resum

El desenvolupament de nous processos químics i de catalitzadors eficients per la formació d'enllaços carboni-carboni és un tema rellevant en química orgànica. Concretament, la reacció de cicloaddició [2+2+2] catalitzada per metalls de transició és una eina molt eficient que permet la formació de derivats carbo- i heterocíclics polisubstituïts de sis membres en un procés d'economia atòmica.

Aquesta tesi doctoral, dividida en set capítols, es basa en l'estudi metodològic i mecanístic de les reaccions de cicloaddició [2+2+2] catalitzades per rodi(I). El Capítol 1 conté una introducció general d'aquest tipus de reaccions i els principals exemples descrits a la bibliografia. En el Capítol 2 es defineixen els objectius generals de la tesi. En el Capítol 3 es descriu l'ús de lligands hemilàbils S-estereogènics i P-estereògenics per a la reacció de cicloaddició [2+2+2] catalitzada per rodi. L'activitat d'aquests nous sistemes catalítics ha estat evaluada en la cicloaddició d'alquins. A més, com que aquests complexos són quirals, també s'han estudiat en la cicloaddició enantioselectiva d'endiïns per a l'obtenció de ciclohexadiens quirals. En el Capítol 4 s'estudia la participació d'adductes de Baylis-Hillman com a substrats olefínics en la cicloaddició [2+2+2] parcialment intramolecular. Aquest procés ha permès la síntesi d'un conjunt de ciclohexadiens quirals bicíclics amb un centre estereogènic quaternari. El Capítol 5 correspon a l'estudi mecanístic de les reaccions de cicloaddició [2+2+2] d'alquins a través de l'espectrometria de masses amb ionització per electroesprai i càlculs DFT. El Capítol 6 conté les conclusions generals que s'han extret de la tesi. Per últim, el Capítol 7 inclou el procediment experimental dels compostos sintetitzats en aquesta tesi.

Chapter 1. General introduction

1.1. Transition metal-catalysed [2+2+2] cycloaddition reactions

The development of new chemical processes and efficient catalysts to enable the formation of carbon-carbon bonds is an important topic in organic chemistry. One of these processes is the metal-catalysed [2+2+2] cycloaddition reaction where a wide range of six-membered carbo- and heterocyclic compounds with different functionalities can be obtained.

The first substrates involved in this reaction were the alkynes and their transition metal-catalysed [2+2+2] cycloaddition represents one of the most elegant methods for the construction of polycyclic aromatic compounds due to the fact that three carbon-carbon bonds are formed in an atom economy process (

Scheme **1**). In 1948, Reppe et al.[1] described the first transition metal-catalysed version of this transformation under nickel catalysis to obtain substituted benzene derivatives.

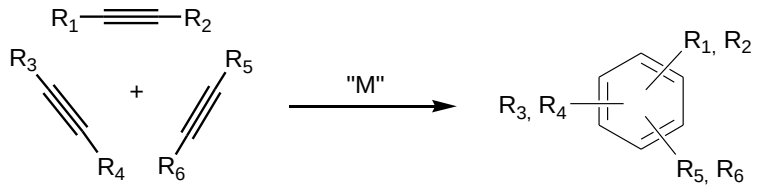

Scheme 1. Transition metal-catalysed [2+2+2] cycloaddition reaction of alkynes (M = transition metal catalyst).

Since this first study, many examples of alkyne cycloaddition catalysed by different transition metals have been described. The metals which have been used most have been Ni, Co, Pd, Rh, Ru, Zr, and Ir.[2] Over the last few years, this reaction, which originally required stoichiometric amounts of the transition metal and extreme reaction conditions, has become a highly efficient catalytic process which can be performed in mild conditions and with low catalyst loads.

[1] Reppe, W; Schweckendiek, W.J. *Justus Liebigs Ann. Chem*. **1948**, *560,*104.

[2] For monographs of [2+2+2] cycloadditions, see: Tanaka, K. *Transition-Metal-Mediated Aromatic Ring Construction*, Wiley, John & Sons, Inc., **2013**. For selected reviews, see: a) Shibata, Y; Tanaka, K. *Synthesis* **2012**, 323; b) Marinetti, A.; Jullien, H.; Voituriez, A. *Chem. Soc. Rev.,* **2012**, *41,* 4884; c) Broere, D. L. J.; Ruijter, E. *Synthesis* **2012**, 2639; d) Tanaka, K. *Heterocycles* **2012**, *85*, 1017; e) Okamoto, S. *Heterocycles* **2012**, *85*, 1579; f) Hua, R.; Abrenica, M. V. A.; Wang, P. *Curr. Org. Chem.* **2011**, *15*, 712; g) Wedling, N.; Hapke, M. *Chem. Soc. Rev.* **2011**, *40*, 4525; h) Domínguez, G.; Pérez-Castells, J. *Chem. Soc. Rev.* **2011**, *40*, 3430; i) Inglesby, P. A.; Evans, P. A. *Chem. Soc. Rev.* **2010**, *39*, 2791; j) Tanaka, K. *Chem. Asian J.* **2009**, *4*, 508; k) Galan, B. R.; Rovis, T. *Angew. Chem. Int. Ed.* **2009**, *48*, 2830; l) Tanaka, K. *Synlett* **2007**, 1977; m) Chopade, P. R.; Louie, J. *Adv. Synth. Catal.* **2006**, *348*, 2307; n) Gandon, V.; Aubert, C.; Malacria, M. *Chem. Commun.* **2006**, 2209; o) Yamamoto, Y. *Curr. Org. Chem.* **2005**, *9*, 503; p) Kotha, S.; Brahmachary, E.; Lahiri, K. *Eur. J. Org. Chem.* **2005**, 4741; q) Saito, S.; Yamamoto, Y. *Chem. Rev.* **2000**, *100*, 2901.

There are many aspects of this kind of reactions which are worthy of study. These include the study of catalysts with high levels of activity, the mechanistic aspects that govern these processes, the type of unsaturated substrates that can participate in the cycloaddition, the chemo- and regioselectivity, at times the enantioselectivity, and the application of these reactions especially in the synthesis of natural products. All of these aspects will be discussed here.

Given that this thesis is based on Rh-catalysed [2+2+2] cycloaddition reactions, the examples described will be mainly focused on this kind of catalytic systems.

1.1.1. The mechanism

Progress in computational chemistry has allowed a breakthrough in the knowledge of the mechanistic rationale of the transition metal-catalysed [2+2+2] cycloaddition reaction.[3] The specific reaction mechanism depends on the nature of the metal, ligands and substrate partners, but the most generally accepted pathway is shown in Scheme 2 .

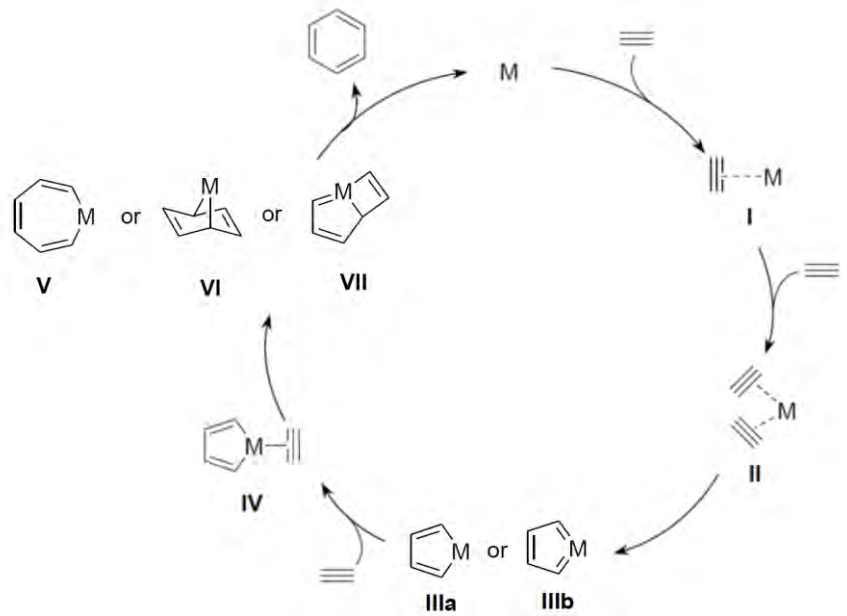

Scheme 2. Postulated general mechanism of alkyne [2+2+2] cycloaddition reaction, where M = transition metal catalyst.

[3] For selected recent references, see: a) Orian, L.; Swart, M.; Bickelhaupt, F. M. *ChemPhysChem*, DOI: 10.1002/cphc.201300934; b) Orian, L.; Wolters, L. P.; Bickelhaupt, F. M. *Chem. Eur. J.* **2013***, 19,* 13337*;* c) Calhorda, M. J.; Costa, P. J.; Kirchner, K. *Inorg. Chim. Acta* **2011**, *374*, 24; d) Li, X.; Xu, J. *Org. Biomol. Chem.* **2011**, *9*, 5997; e) Varela, J. A.; Saá, C. *J. Organomet. Chem.* **2009**, *694*, 143; f) Orian, L.; van Stralen, J. N. P.; Bickelhaupt, F. M. *Organometallics* **2007**, *26*, 3816; g) Agenet, N.; Gandon, V.; Vollhardt, K. P. C.; Malacria, M.; Aubert, C. *J. Am. Chem. Soc.* **2007**, *129*, 8860; h) Yamamoto, Y.; Kinpara, K.; Ogawa, R.; Itoh, K. *Chem. Eur. J.* **2006**, *12*, 5618. For contributions of our group on mechanistic DFT calculations on Rh-catalysed [2+2+2] cycloadditions, see: i) Dachs, A.; Pla-Quintana, A.; Parella, T.; Solà, M.; Roglans, A. *Chem. Eur. J.* **2011**, *17*, 14493; j) Dachs, A.; Roglans, A.; Solà, M. *Organometallics* **2011**, *30*, 3151; k) Dachs, A.; Osuna, S.; Roglans, A.; Solà, M. *Organometallics* **2010**, *29*, 562; l) Dachs, A.; Torrent, A.; Roglans, A.; Parella, T.; Osuna, S.; Solà, M. *Chem. Eur. J.* **2009**, *15*, 5289.

In a first step, the coordination of one alkyne partner to the metal takes place leading to species **I**, followed by a second alkyne coordination to form species **II**. There is then an oxidative addition of the metal to afford the metallacyclopentadiene **IIIa** or the metallacyclopentatriene **IIIb** with a biscarbene type structure (when M = Ru) in which the metal adopts an oxidation state two units greater than in its precursor **II**. This has been found to be the rate-determining step.[3e-g,l] It should be noted that a myriad of rodacyclopentadiene complexes of type **IIIa** have been isolated and characterized to date, experimentally supporting the structure of this intermediate.[4] The subsequent coordination of the third alkyne to intermediates **IIIa** or **IIIb** results in the formation of species **IV** and proceeds to either an alkyne insertion to form the metallacycloheptatriene **V** (the so-called Schore mechanism[5]), or by a metal-mediated [4+2] cycloaddition to afford the bicyclic complex **VI**, or by a formal [2+2] cycloaddition giving rise to metallabicyclo[3.2.0] heptatriene **VII**. Finally, reductive elimination of the metal results in the benzene ring formation and catalyst (M) being recovered.

The whole process is highly exothermic as the thermodynamic driving force is provided by the new σ-bonds formed and the aromaticity that is gained. Unlike the uncatalysed [2+2+2] cycloaddition of acetylenes, which presents a prohibitive energy barrier,[6] the barriers for the transition-metal-catalysed [2+2+2] cycloaddition are relatively low. This agrees with the fact that this reaction typically occurs under quite mild conditions.

1.1.2. Participating unsaturated substrates

In recent years, [2+2+2] cycloadditions have been modified to incorporate not only alkynes but also other unsaturated substrates such as olefins, nitriles, aldehydes, ketones, allenes, carbon dioxide, carbon disulfide, isocyanates, and isothiocyanates, which can react with two alkynes to afford the corresponding cyclohexadienic or heterocyclic compound (Scheme 3).[2f-j,l-q]

[4] Selected references: a) Dachs, A.; Torrent, A.; Pla-Quintana, A.; Roglans, A.; Jutand, A. *Organometallics* **2009**, *28*, 6063; b) Uchimura, H.; Ito, J. I.; Iwasa, S.; Nishiyama, H. *J. Organomet. Chem.* **2007**, *692*, 481; c) Xue, P.; Sung, H. S. Y.; Williams, I. D.; Jia, G. *J. Organomet. Chem.* **2006**, *691*, 1945; d) Nishiyama, H.; Niwa, E.; Inoue, T.; Ishima, Y.; Aoki, K. *Organometallics* **2002**, *21*, 2572; e) Rourke, J. P.; Batsanov, A. S.; Howard, J. A. K.; Marder, T. B. *Chem. Commun.* **2001**, 2626; f) Bianchini, C.; Meli, A.; Peruzzini, M.; Vacca, A.; Vizza, F. *Organometallics* **1991**, *10*, 645; g) Bianchini, C.; Caulton, K. G.; Chardon, C.; Eisenstein, O.; Folting, K.; Johnson, T. J.; Meli, A.; Peruzzini, M.; Tauscher, D. J.; Streib, W. E.; Vizza, F. *J. Am. Chem. Soc.* **1991**, *113*, 5127; h) Iglesias, M.; del Pino, C.; Ros, J.; García Blanco, S.; Carrera, S. M. *J. Organomet. Chem.* **1988**, *338*, 38; i) Gastinger, R. G.; Rausch, M. D.; Sullivan, D. A.; Palenik, G. J. *J. Organomet. Chem.* **1976**, *117*, 355; j) Müller, E. *Synthesis* **1974**, 761; k) Mague, J. T. *Inorg. Chem.* **1973**, *12*, 2649; l) Mague, J. T. *Inorg. Chem.* **1970**, *9*, 1610.

[5] Schore, N. E. *Chem. Rev.* **1988**, *88*, 1081.

[6] a) Santos, J. C.; Polo, V.; Andrés, J. *Chem. Phys. Lett.* **2005**, *406*, 393; b) Ioffe, A.; Shaik, S. *J. Chem. Soc., Perkin Trans. 2,* **1992**, 2101.

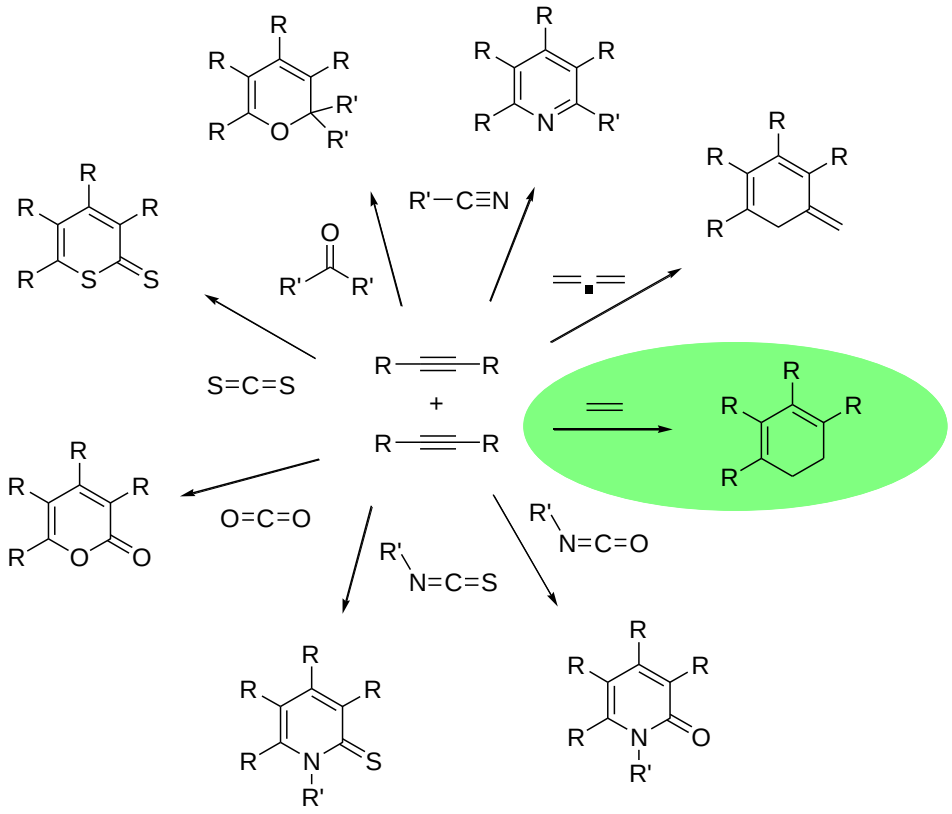

Scheme 3. Transition metal-catalysed [2+2+2] cycloadditions between two alkynes and different unsaturations.

Among the unsaturations depicted in Scheme 3, the most widely studied cases are the [2+2+2] cycloaddition between two alkynes and one nitrile and two alkynes and one alkene. In the first case pyridine derivatives are obtained, which represents one of the most efficient method for the synthesis of this kind of heterocycles.[7] In the case of two alkynes and one alkene, the reaction allows the formation of 1,3-cyclohexadienes in a highly efficient and selective way in mild reaction conditions. The synthesis of 1,3-cyclohexadienes by other means is not so easy [8] as their preparation is usually based on the dehydrobromination of 1,2-dibromocyclohexane[9] at high temperatures or by thermal electrocyclisation of hexatrienes.[10]

[7] a) Ref. 2d; b) Ref. 2e; c) Varela, J. A.; Saá, C. *Synlett* **2008**, 2571; d) Heller, B.; Hapke, M. *Chem. Soc. Rev*. **2007**, *36*, 1085; e) Varela, J. A.; Saá, C. *Chem. Rev*. **2003**, *103*, 3787.
[8] *Org. Synth.* **1973***, 5,* 285.
[9] *Org. Synth.* **1932**, *12*, 26.
[10] Roberts, S. *Comprehensive Organic Functional Group Transformations: Synthesis: Carbon with No Attached Heteroatoms* (**1995**) Cambridge; UK: Elsevier Science, p.419.

For this reason, the participation of alkenes in metal-catalysed [2+2+2] cycloadditions to obtain polysubstituted 1,3-cyclohexadienes has grown enormously in recent years.[11] In Chapter 2, intramolecular [2+2+2] cycloaddition of enediynes will be discussed and in Chapter 3 partially intramolecular [2+2+2] cycloaddition between diynes and alkenes will be commented on.

1.1.3. Chemoselective and regioselective features

Due to the atom economy and convergent nature of the [2+2+2] cycloaddition reaction, this process represents a useful tool for the preparation of polysubstituted hetero- and carbocyclic compounds and is considered as an example of de novo synthesis of this kind of products. As an advantage over conventional strategies for the construction of such derivatives, this approach enables the introduction of high functionality in a single reaction step. Despite its synthetic potential, controlling the chemo- and regioselectivity of this process still remains an important goal.

Alkyne [2+2+2] cycloadditions can be classified into the approaches shown in Scheme 4.

[11] For selected references of metal-catalysed [2+2+2] cycloaddition of diynes and one alkene, see: a) Kobayashi, M.; Suda, T.; Noguchi, K.; Tanaka, K. *Angew. Chem. Int. Ed*. **2011**, *50*, 1664; b) Jones, A. L.; Snyder, J. K. *J. Org. Chem*. **2009**, *74*, 2907; c) Tanaka, K.; Takahashi, M.; Imase, H.; Osaka, T.; Noguchi, K.; Hirano, M. *Tetrahedron* **2008**, *64*, 6289; d) Shibata, T.; Kawachi, A.; Ogawa, M.; Kuwata, Y.; Tsuchikama, K.; Endo, K. *Tetrahedron* **2007**, *63*, 12853; e) Tsuchikama, K.; Kuwata, Y.; Shibata, T. *J. Am. Chem. Soc.* **2006**, *128*, 13686; f) Ikeda, S.; Kondo, H.; Arii, T.; Odashima, K. *Chem. Commun*. **2002**, 2422.

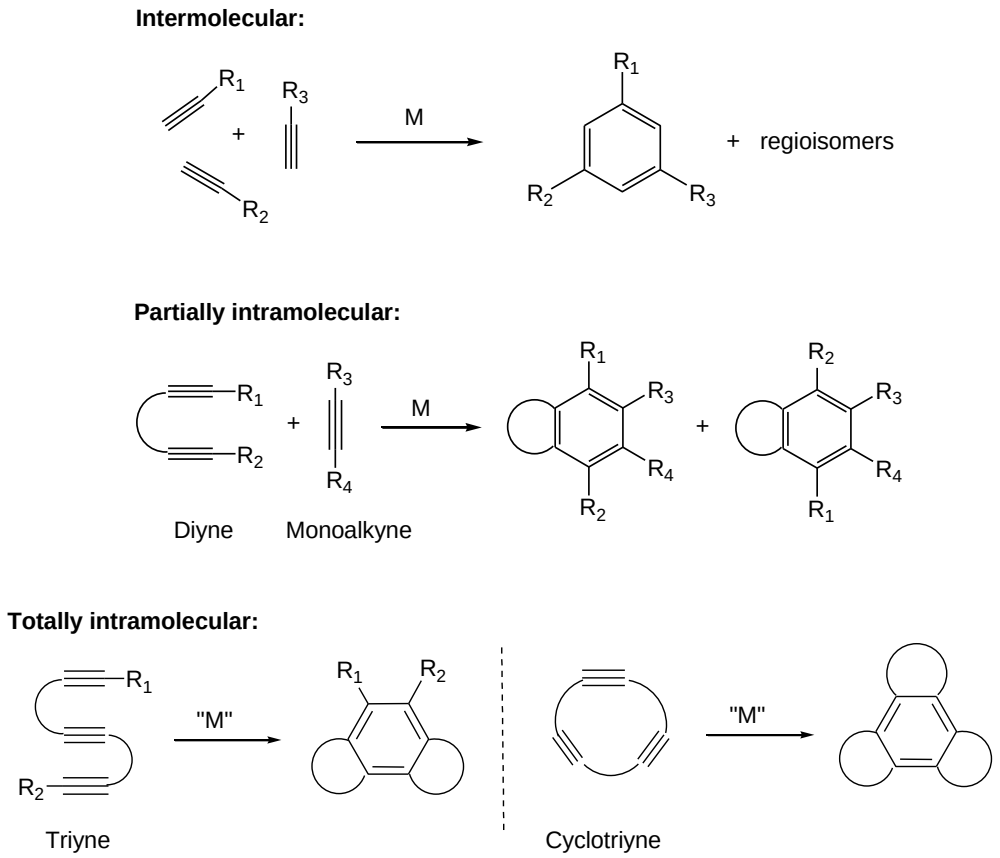

Scheme 4. [2+2+2] cycloaddition versions (M = transition metal catalyst).

The intermolecular approach is the most problematic in terms of regioselectivity due to the difficulty in the chemoselective and regioselective control during both the formation of the metallacycle and the subsequent insertion of the third component.[2c,k] Attempts to heterotrimerize two or more different alkynes has generally led to complex mixtures of regioisomers. However, promising advances have been made in this field and even a few cycloadditions of three different acetylenic derivatives have been performed in a catalytic and highly regioselective fashion.[12] Two main strategies have been used to overcome the regioselective problem in this approach. The first involves the employment of extreme electronically different alkyne components which can control the initial metallacycle formation. Acetylene dicarboxylates are good partners for heterotrimerization with terminal alkynes as they do not usually form the initial metallacyclopentadiene and thus are the last C2 unit to be incorporated. One of the first examples applying this principle in the intermolecular cyclotrimerization of alkynes is shown in Scheme 5,[12d] where the aromatic compounds were obtained in good yields and with highly regioisomeric ratios using a cationic Rh(I) complex and modified BINAP ligands.

[12] Selected references: a) Hara, H.; Hirano, M.; Tanaka, K. *Org. Lett.* **2008**, *10*, 2537; b) Yoshida, K.; Morimoto, I.; Mitsudo, K.; Tanaka, H. *Tetrahedron* **2008**, *64*, 5800; c) Tanaka, K.; Toyoda, K.; Wada, A.; Shirasaka, K.; Hirano, M. *Chem. Eur. J.* **2005**, *11*, 1145; d) Tanaka, K.; Shirasaka, K. *Org. Lett.* **2003**, *5*, 4697.

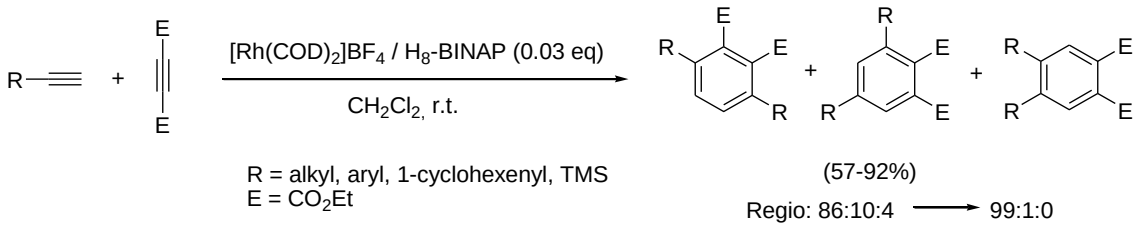

Scheme 5. Intermolecular [2+2+2]cycloaddition catalysed by Rh(I).

The second strategy to control the selectivity is the use of an alkyne surrogate. Examples to date have included the use of enol ethers, enol esters and easily enolizable ketones as alkyne equivalents that suffer dehydration after the cyclotrimerization, giving the aromatic final product. An example combining both enol esters and acetylene carboxylates consists in the Rh-catalysed chemo- and regioselective formal cross-alkyne cyclotrimerization described by Tanaka (Scheme 6)[12a] where the selective formation of a single regioisomer was achieved using this kind of alkyne surrogates. The two key steps controling the final chemo- and regioselectivity are the first metallacyclopentadiene intermediate formation, postulated to be selectively formed by the oxidative addition between the terminal alkyne and the electron-deficient internal monoyne, and the regioselective insertion of enol ester controlled by the coordination of the enol carbonyl moiety to the cationic Rh centre in the metallacyclopentadiene intermediate.

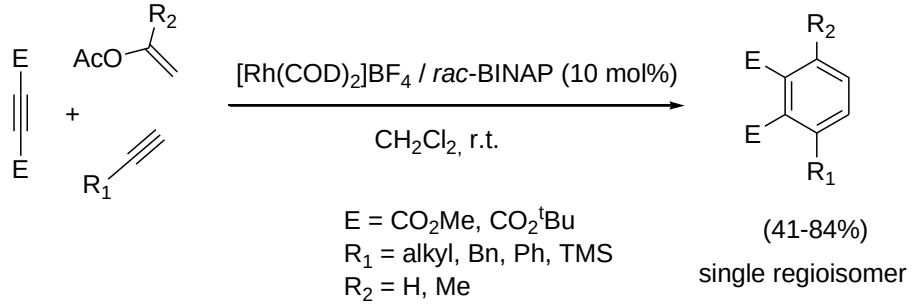

Scheme 6. Rh-catalysed intermolecular cycloaddition using alkyne surrogates.

Other strategies such as the use of a regiodirecting group[13] or a temporary tether[14] are also used. An example where electronics determine the chemoselectivity was reported by Takeuchi and Nakaya, who studied a ligand-controlled chemoselective iridium-catalysed [2+2+2] cyclotrimerization of an electron-deficient and electron-rich alkyne.[15] Another interesting example was reported by Hess[16] where the regioselectivity was affected by using different solvents.

[13] Sripada, L.; Teske, J. A.; Deiters, A. *Org. Biomol. Chem*. **2008***, 6*, 263.
[14] a) Yamamoto, Y.; Ishii, J.; Nishiyama, H.; Itoh, K. *J. Am. Chem. Soc*. **2005**, *127*, 9625; b) Yamamoto, Y.; Ishii, J.; Nishiyama, H.; Itoh, K. *J. Am. Chem. Soc.* **2004**, *126*, 3712.
[15] Takeuchi, R.; Nakaya, Y. *Org. Lett*. **2003**, *5,* 3659.
[16] Hilt, G.; Hengst, C.; Hess, W. *Eur. J. Org. Chem*. **2008**, 2293.

On the other hand, a commonly used strategy to minimize problems of regioselectivity in [2+2+2] cycloadditions is based on the union of at least two alkyne components, which allows the control of the formation of the first metallacyclic intermediate by geometrical and entropic restrictions. These cases correspond to intramolecular approaches (Scheme 4), which have been employed extensively in the synthesis of fused polycyclic compounds. The basic structure of these compounds can be found in many biologically interesting products.[2h]

While partially intramolecular methods have the advantadge of using readily accessible diynes and monoalkynes, the dimerization of the diyne component is a serious drawback. Thus, a considerable excess of monoalkyne or the slow addition of diyne is generally required to prevent such a side reaction. On the other hand, although the totally intramolecular cyclization of triynes or cyclotriynes allows the formation of the desired products with complete selectivity, the preparation of starting materials that possess the necessary substituents or functional groups at the desired positions is typically much more complex.

Partially intramolecular [2+2+2] cycloadditions between diynes and monoynes have been thoroughly studied using different transition metal complexes as the catalyst, where rhodium complexes are one of the most widely used.[17] The first example, published by Grigg et al.,[18] described the reaction between 1,6 diynes and monoalkynes under catalysis by rhodium. These authors demonstrated that various terminal diynes could be directly cyclized with acetylene and an array of monosubstituted alkynes in the presence of the Wilkinson's catalyst in good yields and with high chemoselectivities (Scheme 7).

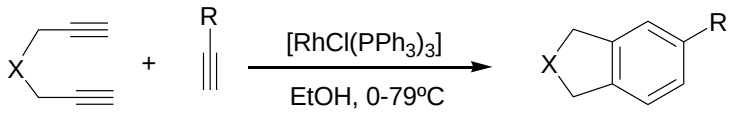

(58-76%)

X = CH_2, O, SO_2, NHAc, $C(COMe)_2$, $C(CO_2Et)_2$
R = H, C_3H_7, CH_2OH, Ph, TMS

Scheme 7. Partially intramolecular [2+2+2] cycloaddition catalysed by the Wilkinson's complex.

[17] For selected references of Rh-catalysed [2+2+2] cycloadditions between diynes and monoynes, see: a) Araki, T.; Noguchi, K.; Tanaka, K. *Angew. Chem. Int. Ed.* **2013**, *52*, 5617; b) Murayama, K.; Sawada, Y.; Noguchi, K.; Tanaka, K. *J. Org. Chem.* **2013**, *78*, 6202; c) Li, Y.; Zhu, J.; Zhang, L.; Wu, Y.; Gong, Y. *Chem. Eur. J.* **2013**, *19*, 8294; d) Garcia, L.; Roglans, A.; Laurent, R.; Majoral, J-P.; Pla-Quintana, A.; Caminade, A-M. *Chem. Commun*. **2012**, 9248; e) Cízková, M.; Kolivoska, V.; Cisarová, I.; Saman, D.; Pospisil, L.; Teplý, F. *Org. Biomol. Chem*. **2011**, *9*, 450; f) Suryawanshi, S. B.; Dushing, M. P.; Gonnade, R. G.; Ramana, C. V. *Tetrahedron* **2010**, *66*, 6085; g) Sedlák, D.; Novák, P.; Kotora, M.; Bartunek, P. *J. Med. Chem*. **2010**, *53*, 4290; h) Wu, W.; Zhang, X. Y.; Kang, S. X. Chin. *Chem. Lett*. **2010**, *21*, 18; i) Tanaka, K.; Sawada, Y.; Aida, Y.; Thammathevo, M.; Tanaka, R.; Sagae, H.; Otake, Y. *Tetrahedron* **2010**, *66*, 1563; j) Young, D. D.; Teske, J. A.; Deiters, A. *Synthesis* **2009**, 3785; k) Garcia, L.; Pla-Quintana, A.; Roglans, A. *Org. Biomol. Chem.* **2009**, *7*, 5020; l) Kotha, S.; Priti, K. *Eur. J. Org. Chem*. **2009**, 730; m) Komine, Y.; Kamisawa, A.; Tanaka K. *Org. Lett.* **2009**, *11*, 2361; n) Suda, T.; Noguchi, K.; Hirano, M.; Tanaka, K. *Chem. Eur. J.* **2008**, *14*, 6593; o) Novák, P.; Cíhalová, S.; Otmar, M.; Hocek, M.; Kotora, M. *Tetrahedron* **2008**, *64*, 5200; p) Nishida, G.; Noguchi, K.; Hirano, M.; Tanaka, K. *Angew. Chem. Int. Ed*. **2007**, *46*, 3951.

[18] Grigg, R.; Scott, R.; Stevenson, P. *J. Chem. Soc. Perkin Trans I*, **1988**, 1357.

This methodology has also been proven to be highly effective for the synthesis of several biologically interesting compounds, such as arylestradiols,[17g] which are polycyclic aromatic compounds that are difficult to prepare by conventional synthetic routes (Scheme 8).

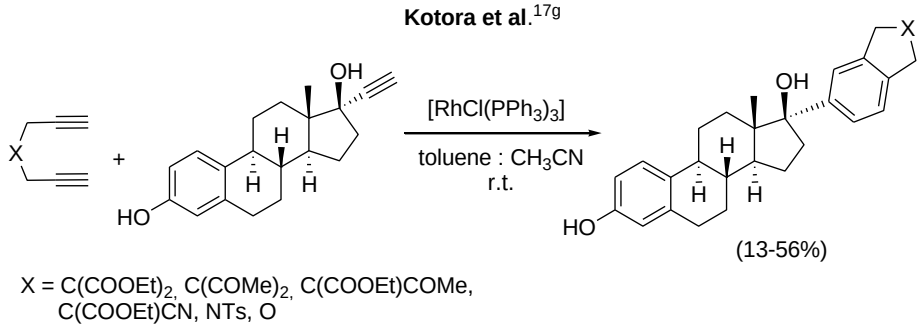

Scheme 8. Synthesis of fused polycyclic derivatives by Rh-catalysed [2+2+2] cycloaddition reaction.

Furthermore, in our research group,[17k] different phenylalanine non-natural amino acid derivatives were satisfactorily prepared through the Rh(I)-catalysed [2+2+2] cycloaddition reaction between propargyl glycine protected derivatives, both racemic and enantiopures, and different 1,6-diynes (Scheme 9). It is noteworthy that the stereogenic centre was configurationally stable under the reaction conditions used. The strategy also allowed the introduction of fluorescent labels in the corresponding amino acids when the X tether in the diyne is a dansyl or dabsyl sulfonamide group.

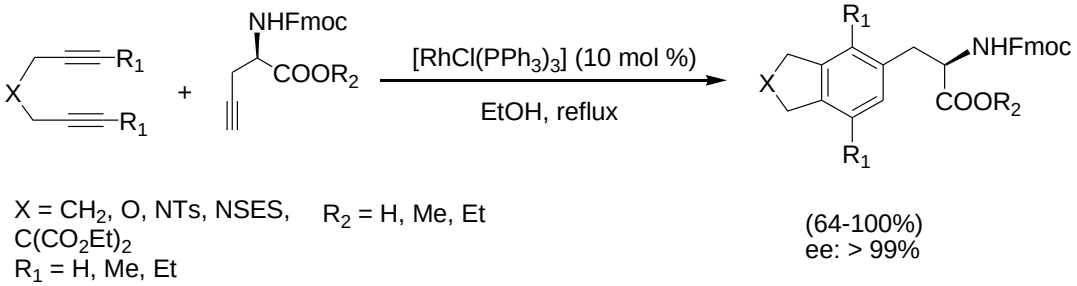

Scheme 9. Synthesis of phenylalanine derivatives by Rh(I)-catalysed [2+2+2] cycloaddition reaction.

The partially intramolecular [2+2+2] cycloaddition reaction has been used for the synthesis of natural products catalysed by different transition metals[19] (Scheme 10 and Scheme 11).

[19] For selected and recent examples, see: a) Changxia, Y.; Chih-Tsung, C.; Siegel, D. *J. Org. Chem*. **2013**, *78*, 5647; b) Ramana, C. V.; Dushing, M. P.; Mohapatra, S.; Mallik, R.; Gonnade, R. *Tetrahedron. Lett*. **2011**, *52*, 38; c) Yuan, C.; Chang, C-T.; Axelrod, A.; Siegel, D. *J. Am. Chem. Soc*. **2010**, *132*, 5924; d) Nicolau, K.C.; Tang, Y.; Wang. J. *Angew. Chem. Int. Ed.* **2009**, *48*, 3449.

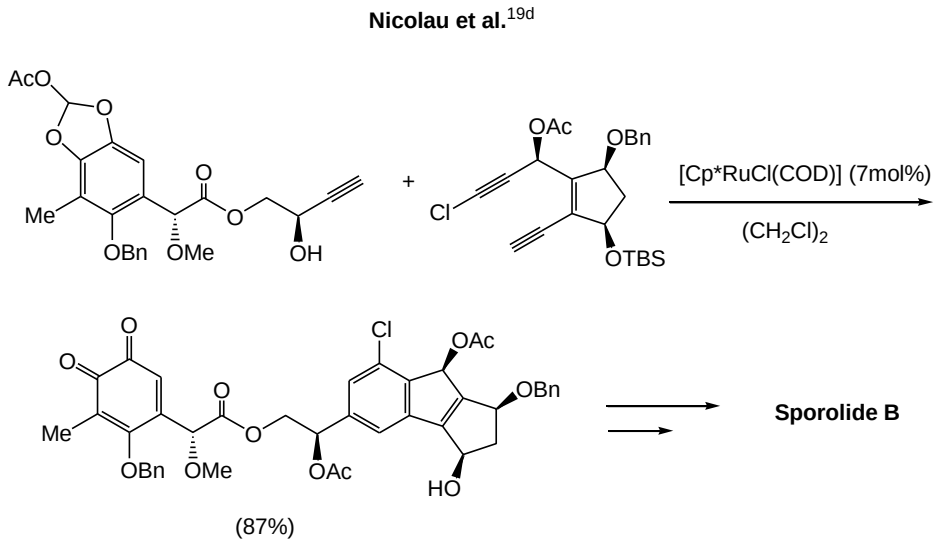

Scheme 10. Ruthenium-catalysed [2+2+2] cycloaddition reaction of a monoalkyne and a diyne for the synthesis of Sporolide B precursor.

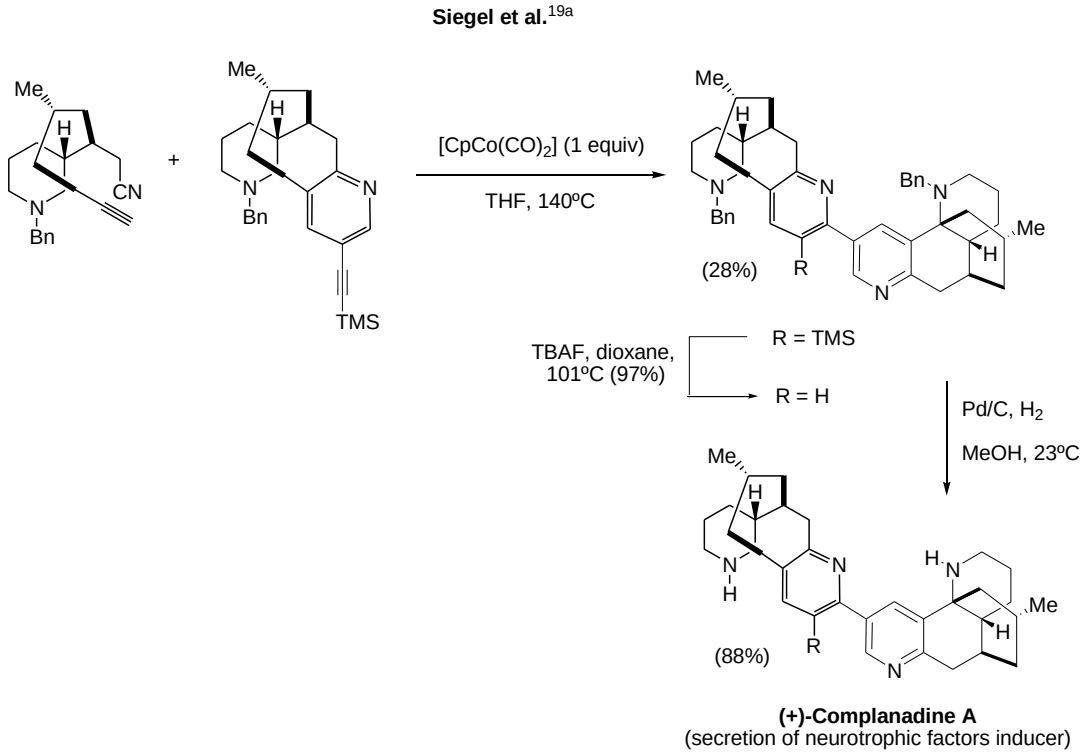

Scheme 11. Regioselective cobalt-mediated [2+2+2] cycloaddition of an alkyne-nitrile and a pyridylalkyne providing, after deprotection, Complanadine A.

As has been referred to earlier, the totally intramolecular approach also provides polycyclic compounds (structurally much more complex than the other cases) in a single synthetic operation. The first totally intramolecular [2+2+2] cycloaddition of triynes catalysed by the

Wilkinson's catalyst was described by Grigg et al.[18] Intramolecular cycloaddition reactions of triynes have also been used as a key step in the preparation of natural products containing polycyclic fused systems (Scheme 12 and

Scheme **13**).[20]

Witulski et al.[20h]

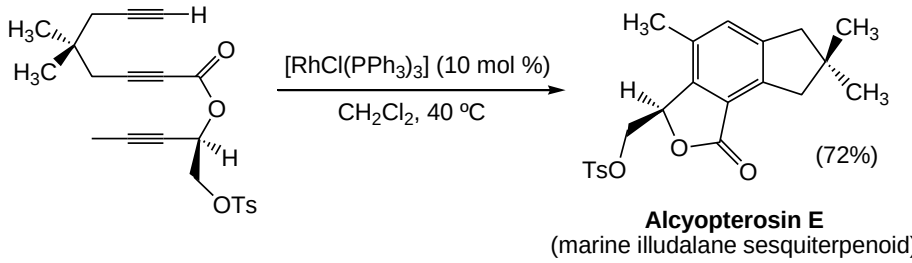

Alcyopterosin E
(marine illudalane sesquiterpenoid)

Scheme 12. Synthesis of Alcyopterosin E by totally intramolecular [2+2+2] cycloaddition reaction.

Sato et al.[20a]

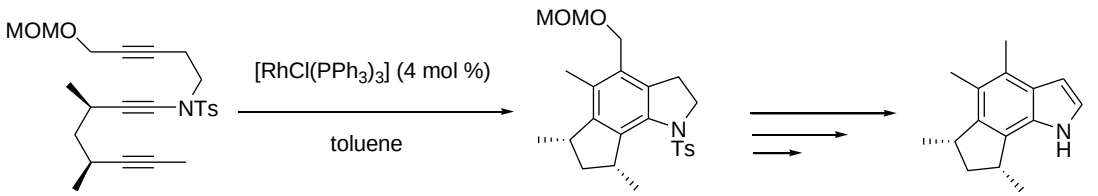

(97%)

(-)-Herbindole A
(KB cells cytotoxicity)

Scheme 13. Synthesis of (-)-Herbindole A by totally intramolecular [2+2+2] cycloaddition reaction (MOM = methoxy methyl).

In addition, if the three alkynes form part of a closed system (a macrocycle), fused tetracycles may easily be obtained (Scheme 4). Our research group has made some of the first contributions to this field. In recent years new types of poyalkyne azamacrocyclic systems have been prepared (Figure 1) and their [2+2+2] cycloaddition reactions have been studied.[21,22]

[20] a) Saito, N.; Ichimaru, T.; Sato, Y. *Org. Lett*. **2012**, *14*, 1914; b) Welsch, T.; Tran, H.-A.; Witulski, B. *Org. Lett.* **2010**, *12*, 5644; c) Zou, Y.; Deiters, A. *J. Org. Chem.* **2010**, *75*, 5355; d) Kesenheimer, C.; Kalogerakis, A.; Meiβner, A.; Groth, U. *Chem. Eur. J.* **2010**, *16*, 8805; e) Nicolaus, N.; Strauss, S.; Neudörfl, J-M.; Prokop, A.; Schmalz, H-G. *Org. Lett.* **2009**, *11*, 341; f) Anderson, E. A.; Alexanian, E. J.; Sorensen, E. J. *Angew. Chem. Int. Ed***. 2004**, *43*, 1998; g) Witulski, B.; Zimmermann, A. *Synlett* **2002**, 1855; h) Witulski, B.; Zimmermann, A.; Gowans, N. D. *Chem. Commun*. **2002**, 2984.

[21] a) Brun, S.; Garcia, L.; González, I.; Torrent, A.; Dachs, A.; Pla-Quintana, A.; Parella, T.; Roglans, A. *Chem. Commun*. **2008**, 4339; b) González, I.; Bouquillon, S.; Roglans, A.; Muzart, J. *Tetrahedron Lett.* **2007**, *48,* 6425; c) Torrent, A.; González, I.; Pla-Quintana, A.; Roglans, A. *J. Org. Chem*. **2005**, *70*, 2033; d)

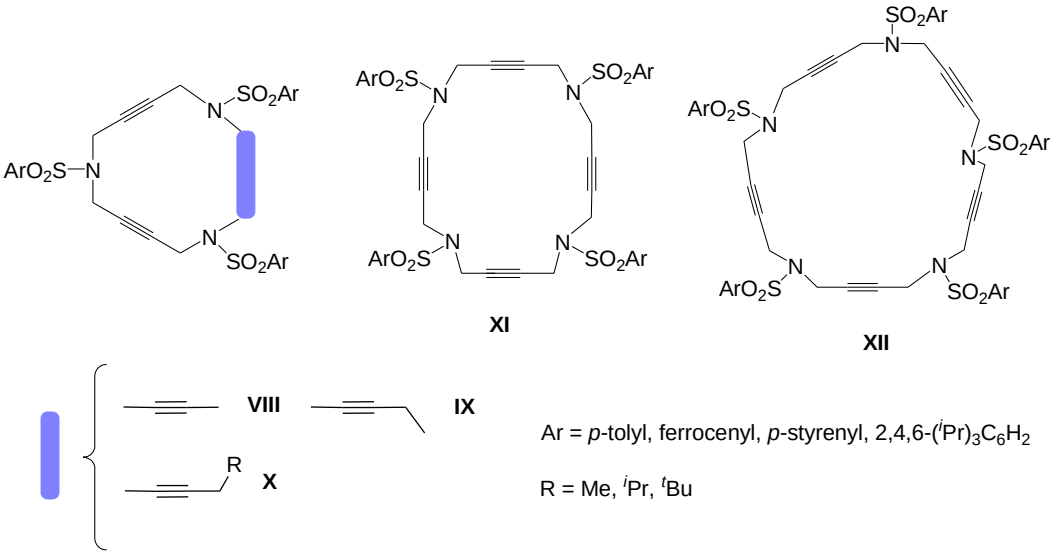

Figure 1. Polyacetylenic azamacrocycles prepared in our group.

All these macrocyclic compounds can be prepared stepwise from easily available arenesulfonamides and the corresponding simple alkyne compounds. Optimization of the synthesis of key intermediates has made it possible to prepare a wide range of polyunsaturated cyclic derivatives efficiently.[22]

Initially, the [2+2+2] cycloaddition reaction of macrocycles of type **VIII** was studied by using different transition metal catalysts based on Pd, Co, Ru, and Rh. The best results were obtained with the use of the Wilkinson's catalyst $[RhCl(PPh_3)_3]$.[21c] The Rh-catalysed cycloaddition of the other 15- and 16-membered macrocycles were studied next and the reaction temperature was optimized in each case (Scheme 14).[21c]

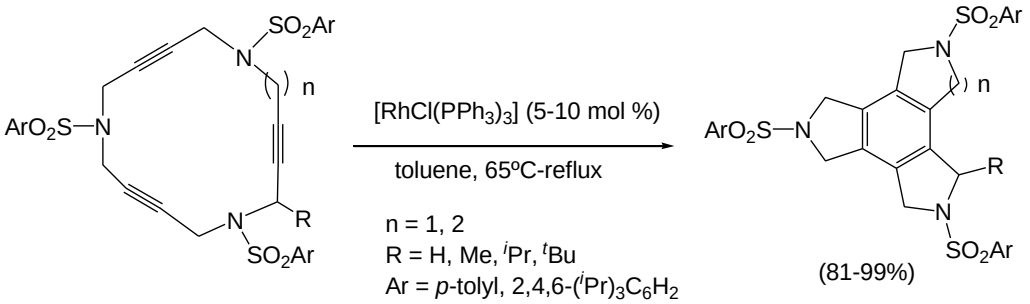

Scheme 14. Cycloisomerization of 15- and 16-membered triyne macrocycles.

Pla-Quintana, A.; Roglans, A.; Torrent, A.; Moreno-Mañas, M.; Benet-Buchholz, J. *Organometallics*, **2004**, *23*, 2762.

[22] For a review of [2+2+2] cycloadditions of macrocycles, see: Pla-Quintana, A.; Roglans, A. *Molecules* **2010**, *15*, 9230.

The Wilkinson's catalyst was also employed in the cycloaddition of higher order azamacrocycles (Scheme 15 and Scheme 16). When 20-membered macrocyclic derivatives of type **XI** were treated with $[RhCl(PPh_3)_3]$ in refluxing toluene, no reaction took place. Starting materials together with decomposition products were obtained.

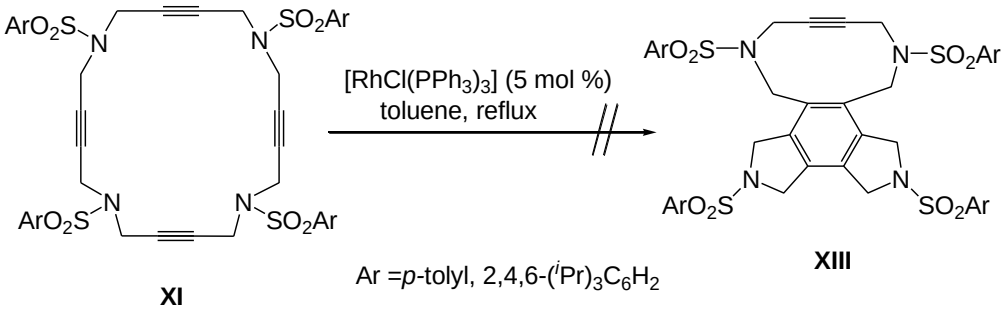

XI **XIII**

Scheme 15. Attempted cyclotrimerization of 10-membered macrocycle of type **XI**.

In contrast, when 25-membered macrocycle **XII** was tested with a catalytical amount of rhodium complex, cycloadduct **XIV**, resulting from the reaction of three contiguous alkynes, was obtained as the only product of the process (Scheme 16).

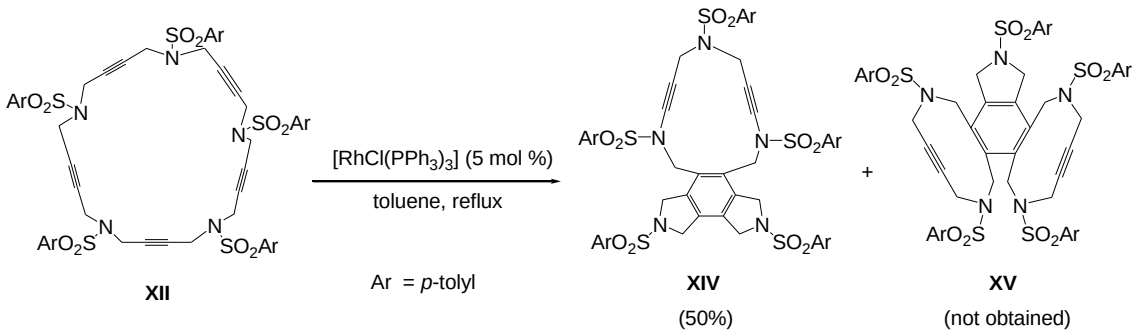

XII **XIV** (50%) **XV** (not obtained)

Scheme 16. [2+2+2] cycloaddition reaction of macrocycle **XII**.

The difference in reactivity of macrocycles type **XI** and **XII** as well as the formation of **XIV** has been justified by theoretical calculations.[3l]

1.1.4. Enantioselective features

The search for strategies that allow enantiomerically pure compounds to be obtained, constitute a milestone in organic synthesis. Asymmetric synthesis, defined by the IUPAC as "a chemical reaction (or reaction sequence) in which one or more new elements of chirality are formed in a substrate molecule and which produces the stereoisomeric (enantiomeric or diastereoisomeric) products in unequal amounts" is now the preferred strategy over racemate resolution and the use of the chiral pool. Among the different strategies for asymmetric synthesis, asymmetric catalysis, which makes use of a substoichiometric amount of a chiral catalyst to promote the reaction and, at the same time, the transferal of the asymmetry to the product, is especially relevant. The use of metallic catalysts, which generally uses metals complexed to chiral organic ligands, has grown significantly over the last two decades as their future potential has begun to be recognized.[23]

The enantioselective features have great interest in transition metal-catalysed [2+2+2] cycloaddition. In particular, among the catalysts used in this kind of processes, rhodium is one of the most efficient transition metals due to its ability to produce in situ complexes with different chiral ligands. Tanaka,[24,25] whose group has made the greatest contribution in this field, developed a methodology involving the use of a catalytic system formed by the cationic rhodium complex $[Rh(COD)_2]BF_4$ and BINAP-type chiral diphosphines (Figure 2). This has enabled the preparation of compounds with axial,[24] helical,[25b,c,h] planar,[25a,d,f] and central[25e,g,i,j] chirality with excellent enantiomeric excesses.

---

[23] For monographs and general reviews of asymmetric organometallic catalysis, see: a) Noyori, R. *Asymmetric Catalysis in Organic Synthesis*, **1994**, Wiley, New York; b) Jacobsen, E. N.; Pfaltz, A.; Yamamoto, H. *Comprehensive Asymmetric Catalysis*, **1999**, Springer, (vol. I-III), Berlin; c) Ojima, I. *Catalytic Asymmetric Synthesis*, **2000**, 2nd edition, Wiley-VCH, New York; d) Special number "*Catalytic Asymmetric Synthesis*", *Acc. Chem. Res*. **2000**, *33*, 323; e) Ma, J.-A.; Cahard, D. *Angew. Chem. Int. Ed.,* **2004**, *43*, 4566; f) Beller, M.; Bolm, C. *Transition Metals for Organic Synthesis*, **2004**, 2nd edition, Wiley-VCH, Weinheim; g) Christmann, M.; Bräse, S. *Asymmetric Synthesis*: *The Essentials*, Shibasaki, M.; Matsunaga, S. "*Part II, Metal Catalysed Asymmetric Synthesis*", **2007**, Wiley-VCH, Weinheim.

[24] For examples on axial chirality, see: a) Mori, A.; Araki, T.; Miyauchi, Y.; Noguchi, K.; Tanaka, K. *Eur. J. Org. Chem.* **2013**, 6774; b) Sakiyama, N.; Hojo, D.; Noguchi, K.; Tanaka, K. *Chem. Eur. J*. **2011**, *17*, 1428; c) Ogaki, S.; Shibata, Y.; Noguchi, K.; Tanaka, K. *J. Org. Chem*. **2011**, *76*, 1926; d) Mori, F.; Fukawa, N.; Noguchi, K.; Tanaka, K. *Org. Lett.* **2011**, *13*, 362; e) Nishida, G.; Ogaki, S.; Yusa, Y.; Yokozawa, T.; Noguchi, K.; Tanaka, K. *Org. Lett.* **2008**, *10*, 2849; f) Suda, T.; Noguchi, K.; Hirano, M.; Tanaka, K. *Chem Eur. J.* **2008**, *14,* 6593; g) Sagae, H.; Noguchi, K.; Hirano, M.; Tanaka, K. *Chem. Commun*. **2008**, 3804; h) Nishida, G.; Noguchi, K.; Hirano, M.; Tanaka, K. *Angew. Chem. Int. Ed*. **2007**, *46*, 3951; i) Tanaka, K.; Nishida, G.; Sagae, H.; Hirano, M. *Synlett* **2007**, 1426; j) Tanaka, K.; Suda, T.; Noguchi, K.; Hirano, M. *J. Org. Chem.* **2007**, *72*, 2243.

[25] For examples on other types of chirality, see: a) Ref. 17a; b) Sawada, Y.; Furumi, S.; Takai, A.; Takeuchi, M.; Noguchi, K.; Tanaka, K. *J. Am. Chem. Soc.* **2012**, *134*, 4080; c) Fukawa, N.; Suda, T.; Noguchi, K.; Tanaka, K. *Angew. Chem. Int. Ed*. **2009**, *48*, 5470; d) Tanaka, K.; Sagae, H.; Toyoda, K.; Hirano, M. *Tetrahedron* **2008**, *64*, 831; e) Nishida, G.; Noguchi, K.; Hirano, M.; Tanaka, K. *Angew. Chem. Int. Ed*. **2008,** *47,* 3410; f) Tanaka, K.; Sagae, H.; Toyoda, K.; Noguchi, K.; Hirano, M. *J. Am. Chem. Soc*. **2007**, *129*, 1522; g) Tanaka, K.; Osaka, T.; Noguchi, K.; Hirano, M. *Org. Lett.* **2007**, *9*, 1307; h) Tanaka, K.; Suda, T., Noguchi, K.; Hirano, M. *J. Am. Chem. Soc*. **2007**, *129*, 12078; i) Tanaka, K.; Wada, A.; Noguchi, K. *Org. Lett.* **2006**, *8*, 907; j) Tanaka, K.; Suzuki, N.; Nishida, G. *Eur. J. Org. Chem.* **2006**, 3917.

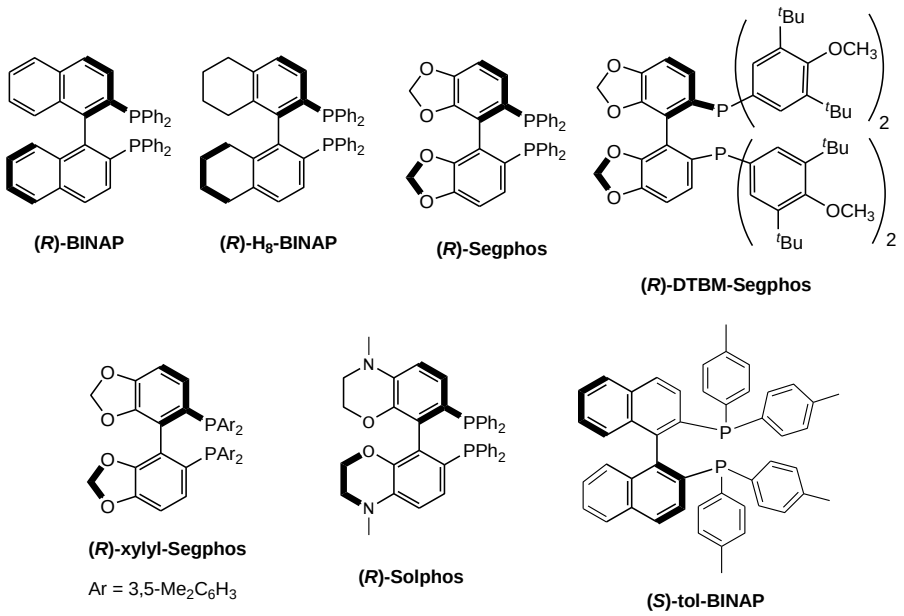

Figure 2. Selected examples of chiral BINAP-type diphosphines used in enantioselective Rh-catalysed [2+2+2] cycloaddition reactions.

An early example of the application of these kinds of ligands consisted in the asymmetric synthesis of 3,3-disubstituted phtalides with central chirality (Scheme 17),[25g] which represent a versatile route to the enantioselective synthesis of these compounds as it provides easy access to both coupling partners.

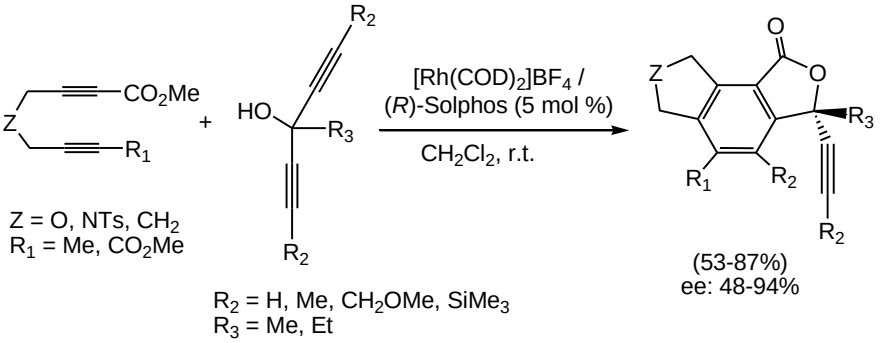

Scheme 17. Synthesis of enantiomerically enriched fused tricyclic phtalides with central chirality.

More recently, an asymmetric synthesis of axially chiral biaryl diphosphine compounds by the Rh-catalysed enantioselective intramolecular double [2+2+2] cycloadditions of hexayne diphosphine oxides has been reported (Scheme 18).[24d] The new chiral compounds were obtained in low to moderate yields but with good enantiomeric excesses. Furthermore, the diphenylphosphine oxide derivative was reduced to the corresponding phosphine and was tested as a ligand in catalytic asymmetric hydrogenations of disubstituted alkenes and in enantioselective partially intramolecular [2+2+2] cycloadditions providing good ee values in both cases.

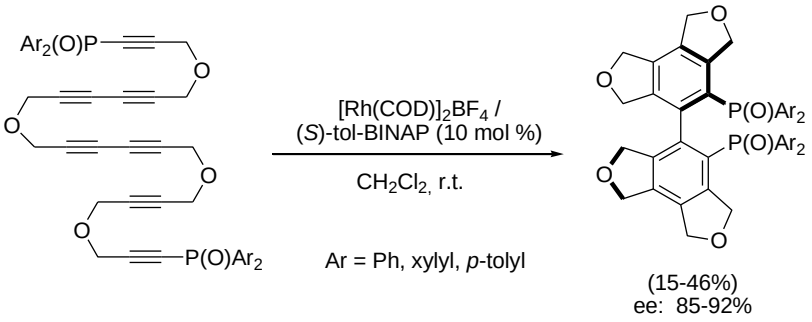

Scheme 18. Synthesis of axially chiral biaryl diphosphine oxides.

Our group, in collaboration with Dr. Caminade's group, has also contributed to the synthesis of axially chiral biaryl compounds by describing a highly efficient and recyclable catalytic system based on phosphorus dendrimers containing chiral phosphoramidite ligands as terminal groups (Figure 3).[17d] The Rh(I) catalysed [2+2+2] cycloaddition reaction of a diyne and 2-methoxynaphthalene alkynyl derivatives (Scheme 19) showed a strong positive dendritic effect both in the activity and enantiodiscrimination, constituting the strongest dendritic effect on the stereoselectivity reported to date. Furthermore, it was possible to recover the catalytic system by simple filtration and reuse it three times without observable reduction in the yield and enantioselectivity.

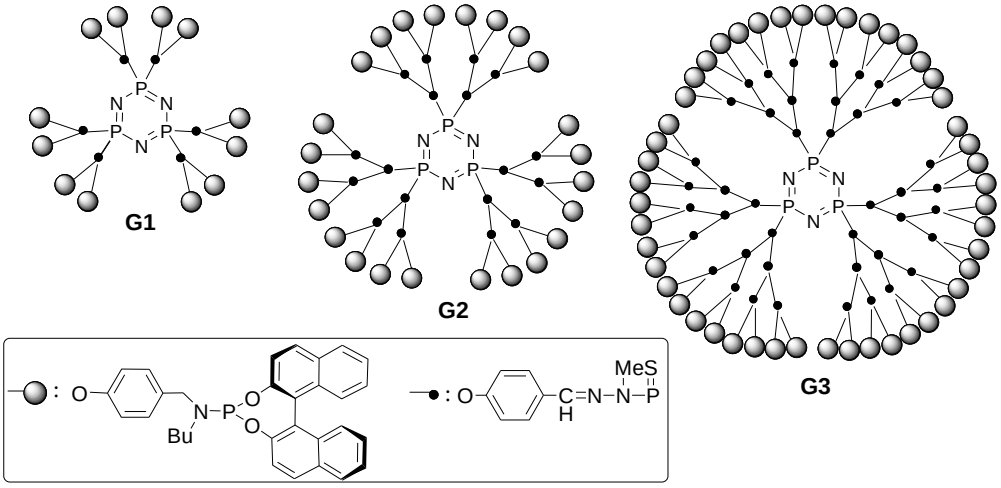

Figure 3. Structures of dendrimers **G1, G2** and **G3**.

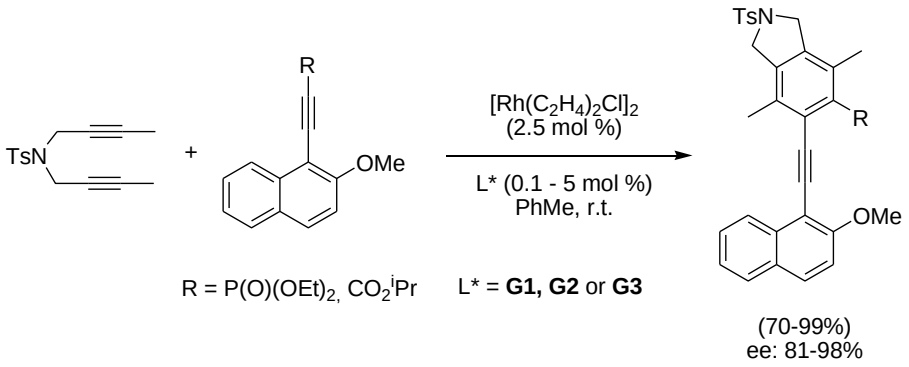

Scheme 19. [2+2+2] cycloaddition reaction between *N*-tosyl 1,6-diyne and 2-methoxynaphthalene alkynyl derivatives.

Furthermore, this kind of reaction has made it possible to form architectures with high structural complexity, such as [9]helicene-like derivatives or 1,1′-bitriphenylenes (Scheme 20[25c] and Scheme 21[25b]).

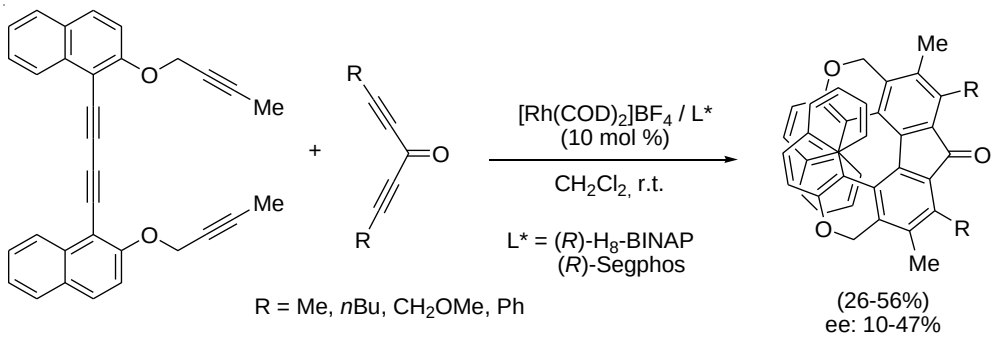

Scheme 20. Rh(I)-catalysed partially intramolecular double [2+2+2] cycloaddition leading to enantioenriched [9]helicene-like derivatives.

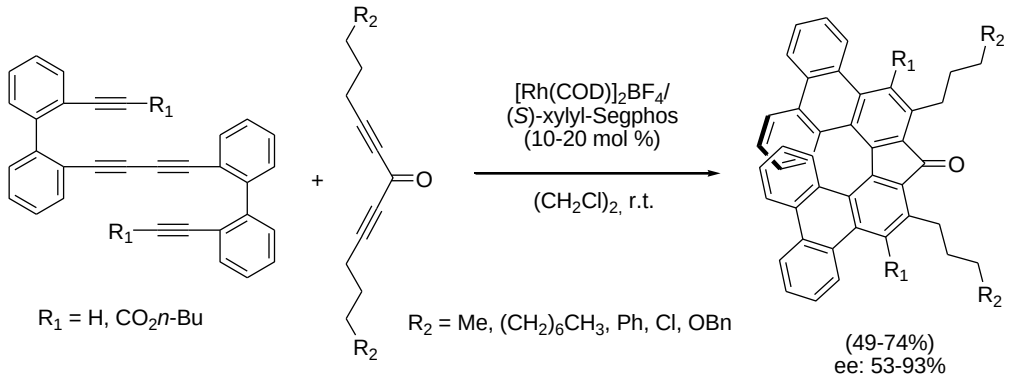

Scheme 21. Enantioselective synthesis of helically chiral 1,1′-bitriphenylenes via Rh(I)-catalysed partially intramolecular double [2+2+2] cycloaddition.

Planar-chiral derivatives have also been prepared recently by enantioselective Rh-catalysed partially intramolecular cycloadditions of cyclic diynes and terminal monoynes with good yields and enantiomeric excesses ranging from 64 to 93% (Scheme 22).[25a]

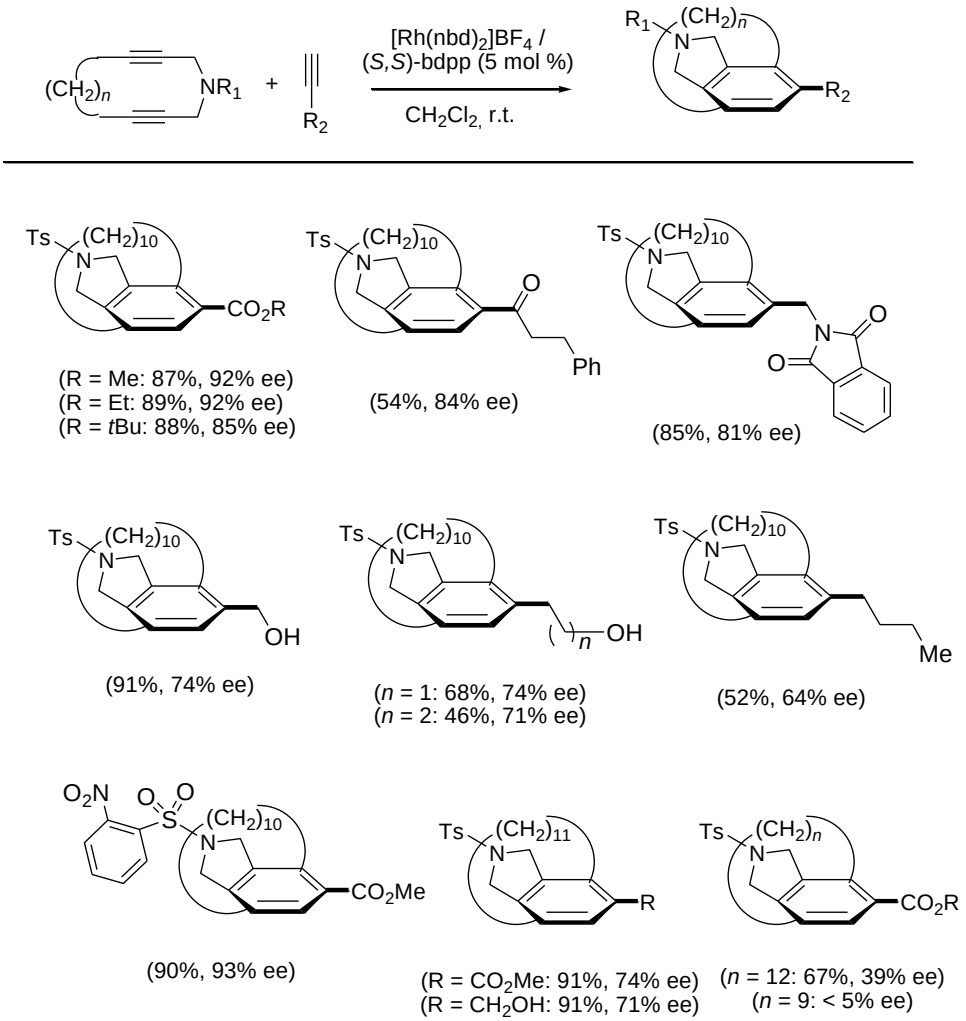

Scheme 22. Enantioselective synthesis of planar *para*-cyclophanes from cyclic diynes and terminal monoynes (nbd = norbornadiene, bdpp = 2,4-bis-(diphenylphosphino)pentane).

1.1.4.1. Rhodium-catalysed [2+2+2] cycloaddition reaction of two alkynes and one alkene

The participation of olefins in this kind of reaction is of great interest given that, depending on the nature of the double bond, chiral products can be obtained. Hence, the development of new catalytic systems allowing compounds to be obtained enantioselectively through [2+2+2] cycloaddition reactions is a field of great interest.[26]

a) Partially intramolecular reaction of enynes with monoalkynes

Oxidative addition of chiral Rh(I) complex to an enyne is a common scheme for the generation of an asymmetric stereocentre at the ring fusion carbon of a bicyclic metallacycle (Scheme 23). The [2+2+2] cycloaddition of enynes with a substituent at their olefinic moiety and alkynes provides an efficient protocol for the construction of a quaternary carbon at the ring-fused

[26] For a review of enantioselective [2+2+2] cycloadditions, see: Shibata, T.; Tsuchikama, K. *Org. Biomol. Chem.* **2008**, *6*, 1317.

position. Cationic chiral Rh-BINAP derivative complexes as a catalyst for the [2+2+2] cycloaddition of enynes with monoalkynes are known to work well as catalysts in the enantioselective formation of a bicyclic metallacycle (Scheme 23).

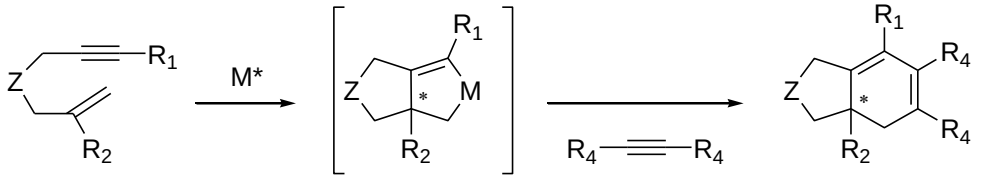

Scheme 23. Enantioselective formation of a bicyclic metallacycle in the [2+2+2] cycloaddition of enynes and monoalkynes.

As an example, Rh-tolBINAP complex efficiently catalysed the reaction of various enynes with substituents at their alkyne termini and olefinic moiety with a symmetric monoalkyne, and the corresponding bicyclic cyclohexa-1,3-dienes were obtained with good to excellent enantiomeric excesses (Scheme 24).[27]

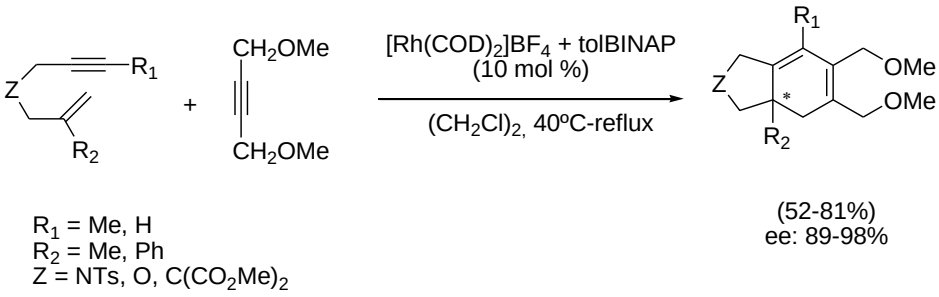

Scheme 24. Rh(I)-catalysed intermolecular [2+2+2] cycloaddition between enynes and monoalkynes.

At the same time, Evans et al.[28] published the enantioselective Rh-catalysed [2+2+2] cycloaddition of 1,6-enynes and asymmetric alkynes. Using (*S*)-Xylyl-P-PHOS as a chiral phosphine and $AgBF_4$ as the activating agent of rhodium catalyst $[RhCl(COD)]_2$, a highly enantioselective and regioselective process was achieved (Scheme 25).

[27] Shibata, T.; Arai, Y.; Tahara, Y. *Org. Lett.* **2005**, *7*, 4955.
[28] Lai, K. W.; Sawyer, J. R.; Evans, P. A. *J. Am. Chem. Soc.* **2005**, *127*, 12466.

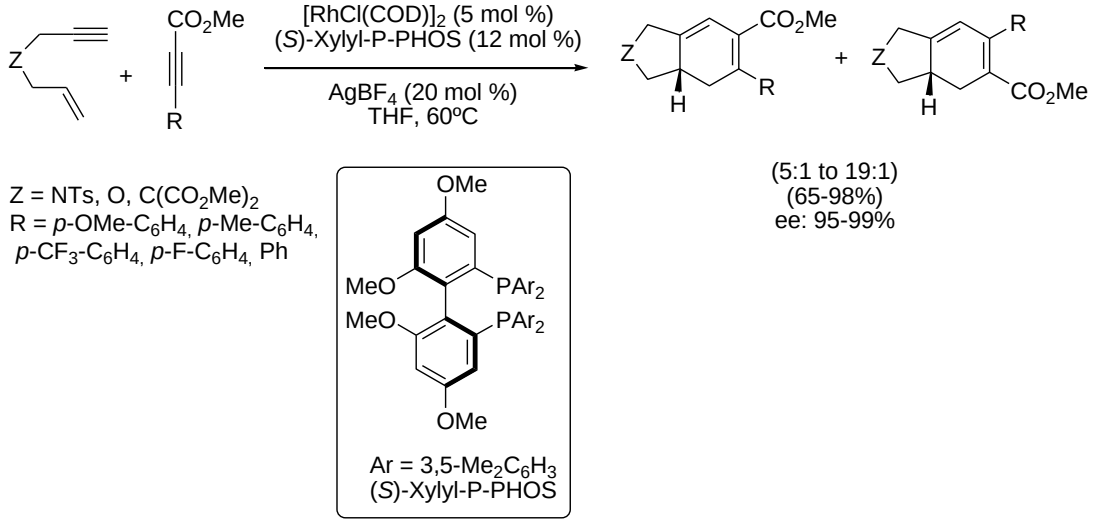

Scheme 25. [2+2+2] cycloaddition between 1,6-enynes and asymmetric alkynes for the synthesis of 1,3-cyclohexadienes.

b) Totally intramolecular reaction of enediynes

The formation of 1,3-cyclohexadienes through the totally intramolecular version of the [2+2+2] cycloaddition requires the preparation of enediyne substrates. In 2007, Shibata et al.[29] reported the enantioselective intramolecular [2+2+2] cycloaddition of different symmetric and asymmetric (*E*)-enediynes catalysed by $[Rh(COD)_2]BF_4$ complex and the chiral phosphine (*S*)-H_8-BINAP for the synthesis of chiral 1,3-cyclohexadienes (Scheme 26). This study involved internal and terminal alkynes as well as carbo- and heteatom-linked unsaturations. Although different cyclohexadienes were obtained in moderate to good yields and enantioselectivities, the study showed that the process was highly sensitive to the nature of the substrate as well as the phosphine used.

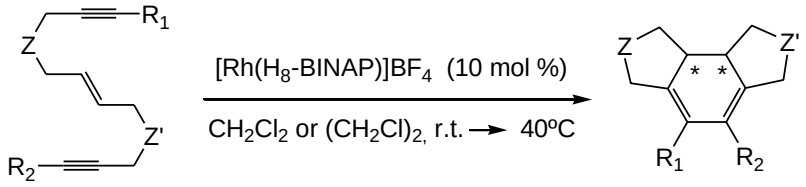

Z = $C(CO_2Me)_2$, NTs, $C(SO_2Ph)_2$
Z' = $C(CO_2Me)_2$, NTs, O, $C(SO_2Ph)_2$
R_1, R_2 = H, Me, Bu, Br, Ph, CO_2Me, CH_2OBn

(41-99%)
ee: 15-98%

Scheme 26. Rh(I)-catalysed enantioselective synthesis of 1,3-cyclohexadienes.

[29] Shibata, T.; Kurokawa, H.; Kanda; K. *J. Org. Chem*. **2007**, *72*, 6521.

In this study, the different enantioselectivities obtained were rationalized by different reaction pathways followed depending on the substrate structure (Scheme 27).

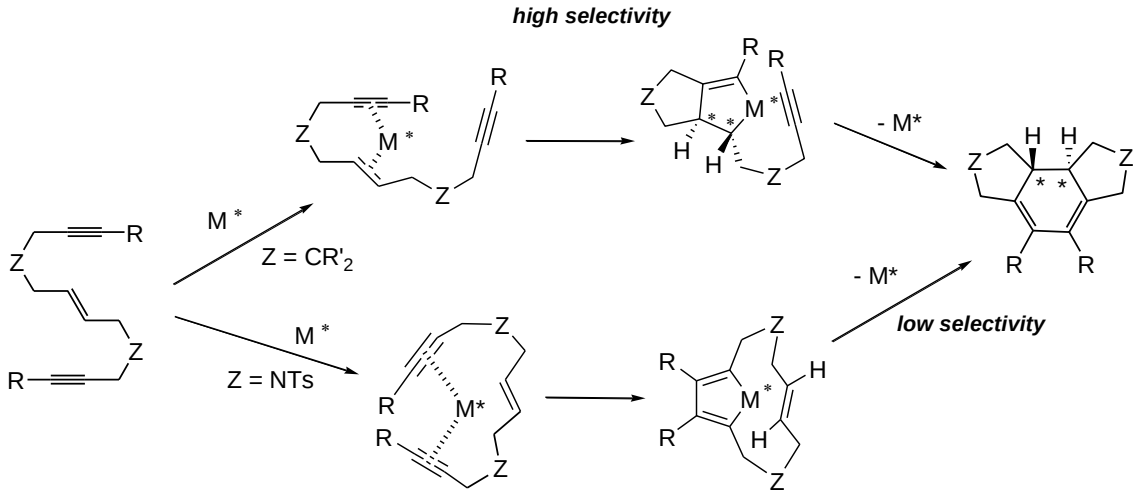

Scheme 27. Possible explanation proposed by Shibata[29] for the different enantioselectivities obtained in the [2+2+2] cycloadditions of (*E*)-enediynes.

The introduction of appropriate substituents on the alkyne termini of the enediyne to suppress the oxidative coupling of two alkyne moieties, which would decrease their reactivity, was crucial. In the case of enediynes with unsubstituted alkyne termini, the enantioselectivity was low, probably as a result of the high reactivity of the terminal alkynes that favour the oxidative coupling of two alkyne moieties over that of an enyne moiety. In the case of nitrogen-tethered enediynes, the choice of substituents on the alkyne termini was important to achieve high enantioselectivity and prevent alkyne-alkyne oxidative coupling of enediynes prior to alkyne-alkene coupling. The correct choice of chiral ligands was also essential as only H_8-BINAP achieved both a good yield and enantiomeric excess. Other BINAP derivatives, such as tolBINAP and BINAP, gave a poor yield and enantiomeric excess.

Tanaka et al.[30] also described the [2+2+2] cycloaddition of oxygen-linked terminal and internal (*E*)-enediyne systems using the same cationic rhodium complex as Shibata although with various chiral phosphines. The best results were again obtained with (*R*)-H_8-BINAP. Products were obtained with moderate to good yields but enantiomeric excesses reached 59% (Scheme 28). It should be noted that in the case of enediyne with methyl-substituted triple bonds, the corresponding 1,3-cyclohexadiene was not obtained. Therefore, once more, the sensitivity of the process proved to be strongly dependent on the nature of the substrates.

[30] Tanaka, K.; Nishida, G.; Sagae, H.; Hirano, M. *Synlett* **2007**, 1426.

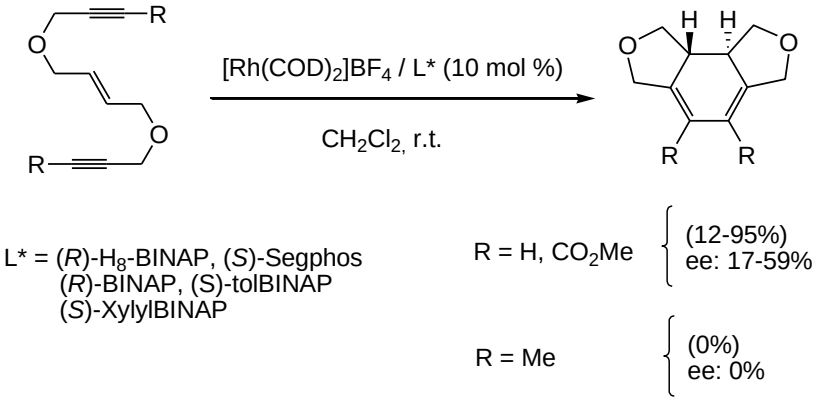

Scheme 28. Enantioselective [2+2+2] cycloaddition reactions of enediynes.

c) Partially intramolecular reaction of diynes with alkenes

The most challenging approach in terms of chemoselectivity and enantioselectivity is the partially intramolecular [2+2+2] cycloaddition between diynes and alkenes, due to the low reactivity of the alkene. In these cases, a considerable excess of the alkene or slow addition of the diyne are usually required to avoid the homocoupling of the diyne. Moreover, an asymmetric stereocentre is generated at the ring carbon atom when a 1,1-disubstituted unsymmetrical alkene is inserted into the metallacyclopentadiene intermediate (Scheme 29), which makes the steroselective control more difficult than in the two commented earlier cases.

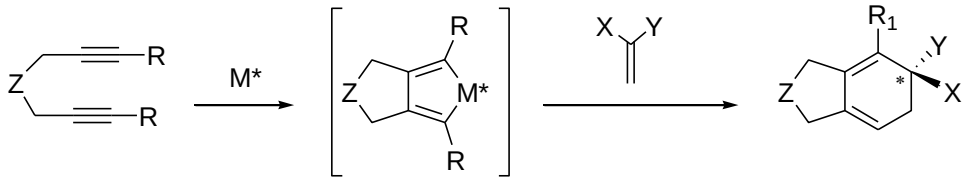

Scheme 29. Metallacyclopentadiene formed in the [2+2+2] cycloadditions of diynes and alkenes.

Examples of this kind of [2+2+2] cycloadditions will be discussed in detail in Chapter 3.

Chapter 2. General objectives

Despite the progress in the development of [2+2+2] cycloaddition reactions over the last few years, there is still a long way to go. Aspects still requiring particular attention are the search for more efficient catalytic systems, the search for new unsaturated substrates which can participate in the cycloaddition reactions, and the study of the mechanistic pathway, which is an issue that has been little studied experimentally. This thesis aims to make a contribution to these research fields by filling some of these gaps.

New catalytic systems. Rhodium-catalyzed stereoselective [2+2+2] cycloaddition reactions have mainly been achieved by using combinations of cationic rhodium complexes and BINAP type ligands. In these systems the chirality resides in the carbon backbone. The main goal of this thesis related to new catalytic systems deals with the search for catalysts in which the chirality is located in the coordinating heteroatom of the ligand. Therefore, in Chapter 3 of this thesis, we will study the efficiency of two sets of cationic rhodium complexes with S- and P-stereogenic ligands in the asymmetric [2+2+2] cycloaddition of enediyne substrates.

New unsaturated substrates. Alkenes have been used as substrates in the [2+2+2] cycloaddition reactions showing high versatility for the synthesis of cyclohexadiene derivatives. Among these challenging substrates, the involvement of 1,1-disubstituted alkenes provides access to chiral cyclohexadienic compounds featuring a quaternary stereogenic centre. In Chapter 4, Baylis-Hillman adducts, which are known as highly functionalized synthons, will be involved as new unsaturated substrates in partially intramolecular [2+2+2] cycloaddition reactions, giving particular importance to the stereoselective features of the process.

Mechanistic studies. Detailed study of mechanistic aspects of a chemical reaction helps to improve it. The mechanism of the [2+2+2] cycloaddition reaction has mainly been proposed based on theoretical calculations but experimental data is scarce. In Chapter 5, a complete mechanistic study of the Rh(I)-catalysed [2+2+2] cycloaddition of three alkynes will be undertaken experimentally through electrospray ionization mass spectrometry (ESI-MS). Given that, to date, the oxidative addition intermediate (rhodacyclopentadiene) is the only catalytic species that has been detected or isolated experimentally, this work will focus on the observation of all the intermediates in the catalytic cycle, especially the most advanced alkyne insertion intermediate.

Chapter 3.

Hemilabile S-stereogenic and P-stereogenic ligands for the Rh(I)-catalysed [2+2+2] cycloaddition reactions

---

Part of this chapter has been published on:

a) Brun, S.; Parera, M.; Pla-Quintana, A.; Roglans, A.; León, T.; Achard, T.; Solà, J.; Verdaguer, X.; Riera, A. *Tetrahedron* **2010**, *66*, 9032; b) León, T.; Parera, M.; Roglans, A.; Riera, A. Verdaguer, X. *Angew. Chem. Int. Ed*. **2012**, *51*, 6951.

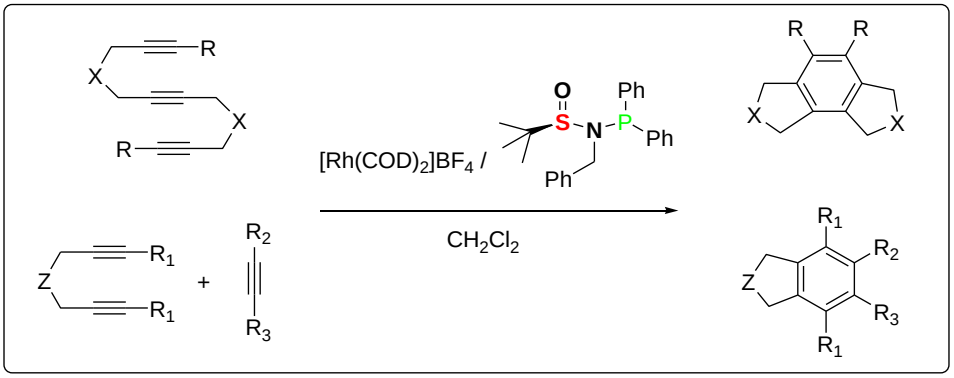

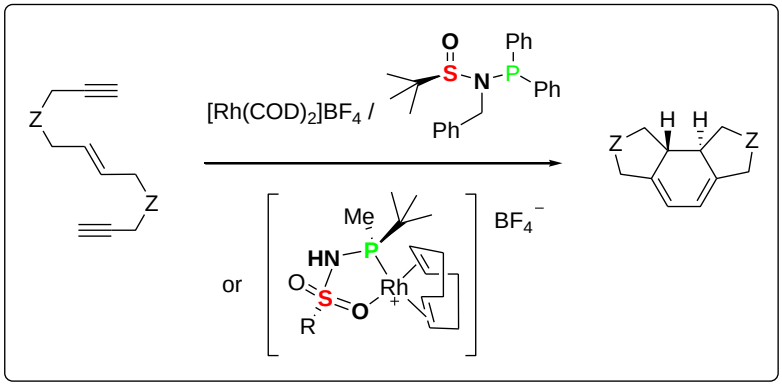

3.1. Precedents

Hybrid hemilabile ligands are polydentate ligands which contain at least two different types of chemical functionality capable of binding to metal centres in contrast to homofunctional polydentate ligands which contain only one type of functionality (Scheme 30).

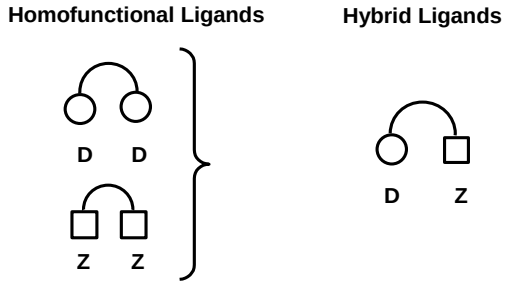

Scheme 30. General structure of homofunctional and hybrid bidentate ligands.

The functionalities in hybrid ligands are often chosen to be very different from each other to increase the differentiation between their resulting interactions with the metal centre and thereby their chemoselectivity (Scheme 31).

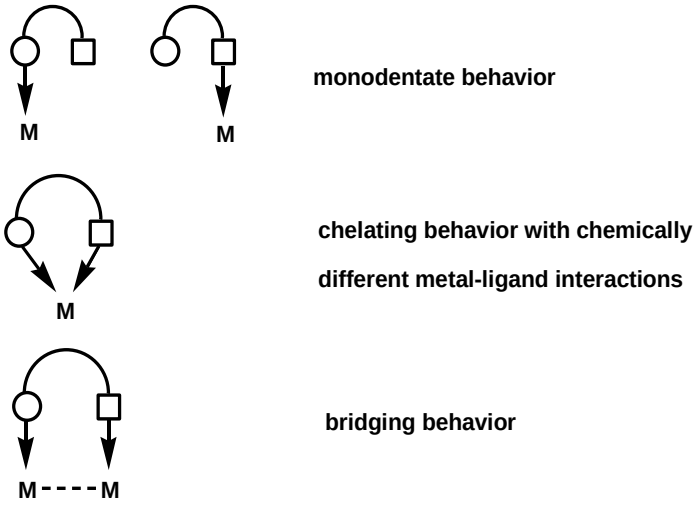

Scheme 31. Bonding modes of hybrid ligands.

The combination of soft and hard donors in the same ligand is an extremely important area of investigation that has led to novel and unprecedented properties been found for the resulting metal complexes.

An essential feature of hemilabile ligands is to have at least one substitutionally labile donor function Z while the other donor group(s) D remain firmly bound to the metal centre(s). The lability leads to selective breaking of the Z→metal interaction (Scheme 32) providing open

coordination sites at the metal centre during reactions that are "masked" in the ground-state structure and stabilize reactive intermediates.[31]

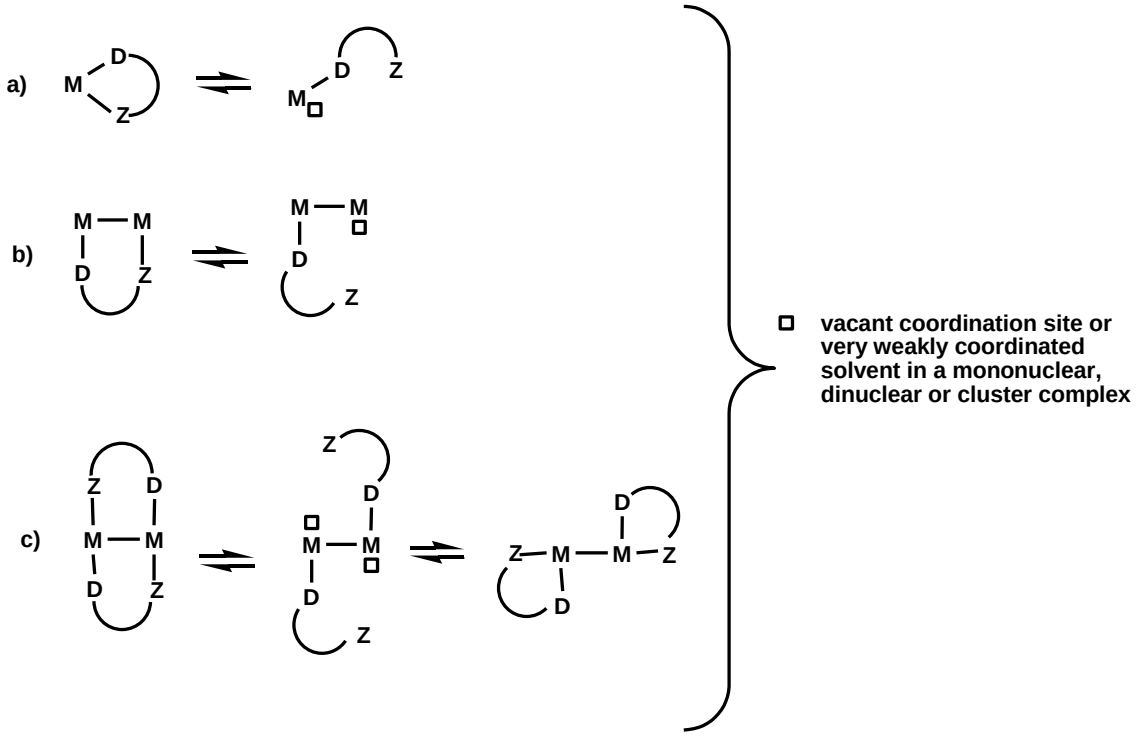

Scheme 32. Hemilabile situation of spontaneous "opening" of the D-Z chelate or bridge.

Another criterion to consider before assigning a hemilabile character to a ligand is the reversibility of the formation of the Z→metal interaction. Once the "opening" of a chelating ligand D-Z has occurred to give a Z-D →M monodentate system, "half" (hemi) of the ligand was indeed labile. After the opening of Z→metal bond, recoordination of the Z functionality may restore the original situation, usually after a chemical transformation has occurred within the metal coordination sphere.

The presence of a hemilabile ligand in a complex may significantly influence the reactivity of incoming substrates and promote transformations that would not otherwise occur. This further emphasizes the significance of hemilabile ligands in homogeneous or supported catalysis where the "opening" step allows coordination, activation, and transformation of a substrate molecule at the metal site while the "closing" step leads to stabilization of the metal coordination sphere and favours the elimination of the product.

[31] a) Braunstein, P.; Naud, F. *Angew. Chem. Int. Ed.* **2001**, *40*, 680; b) Bader, A.; Lindner, E. *Coord. Chem. Rev.* **1991**, *108*, 27.

3.1.1. *N*-phosphino-*tert*-butylsulfinamide (PNSO) ligands

The group of Prof. Riera and Dr. Verdaguer from the University of Barcelona has described a new class of chiral bidentate ligands which contain sulphur and phosphorous atoms in which the phosphorous atom provides metal affinity while the sulfur moiety is the source of chirality.

Only a few P,S=O ligands have been described in the literature. This lack of information is probably due to the low stability of phosphine-sulfoxide ligands as a result of sulfur-to-phosphorus oxygen migration.[32] Therefore, these authors have focused in the synthesis of *N*-phosphino-*tert*-butylsulfinamide ligands, called PNSO ligands.[33]

These ligands are modular since they are prepared from the commercially available enantiopure *tert*-butylsulfinamide, an aldehyde with a variable substituent R_1 and a chlorophosphine with identical substituents R_2 in only three steps of reaction (Scheme 33).

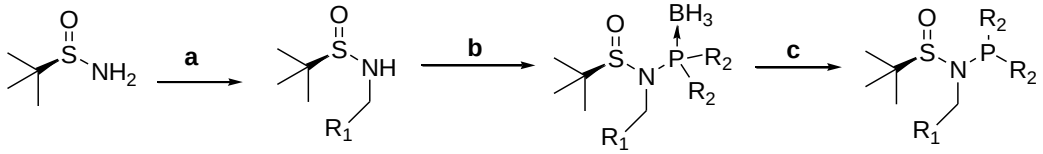

a i) R_1CHO, $Ti(OEt)_4$, ii) $NaBH_4$, **b** i) BuLi, R_2PCl, -78 ºC, ii) $BH_3 \cdot SMe_2$, -10 ºC, **c**) DABCO, r.t., toluene

Scheme 33. Synthesis of PNSO ligands developed in Riera and Verdaguer's group (DABCO = 1,4-diazabicyclo[2.2.2]octane).

Reductive amination with $Ti(OEt)_4$ in the presence of the corresponding aldehyde produced the intermediate sulfinimines, which were reduced in situ to the corresponding sulfinamides**.** Anion formation with *n*-BuLi at low temperature followed by the addition of chlorophosphine and the protection of the phosphine moiety with borane resulted in the corresponding borane-protected ligands. The borane-free ligand was obtained by deprotection with DABCO to afford PNSO ligands in good yields.

PNSO ligands are hemilabile ligands in which the sulfoxide moiety binds the metal through either sulfur or oxygen to provide either P,S or P,O chelation, depending on the electronic environment around the metal centre (Figure 4).

[32] a) Hiroi, K.; Suzuki, Y.; Kawagishi, R. *Tetrahedron Lett.* **1999**, *40*, 715; b) Alcock, N. W.; Brown, J. M.; Evans, P. L. *J. Organomet. Chem.* **1988**, *356*, 233; c) Wenschuh, E.; Fritzsche, B. *J.Prakt. Chem* **1970**, *312*, 29.

[33] a) Revés, M.; Riera, A.; Verdaguer, X. *Eur. J. Inorg. Chem*. **2009**, 4446; b) Revés, M.; Achard, T.; Solà, J.; Riera, A.; Verdaguer, X. *J. Org. Chem*. **2008**, *73*, 7080.

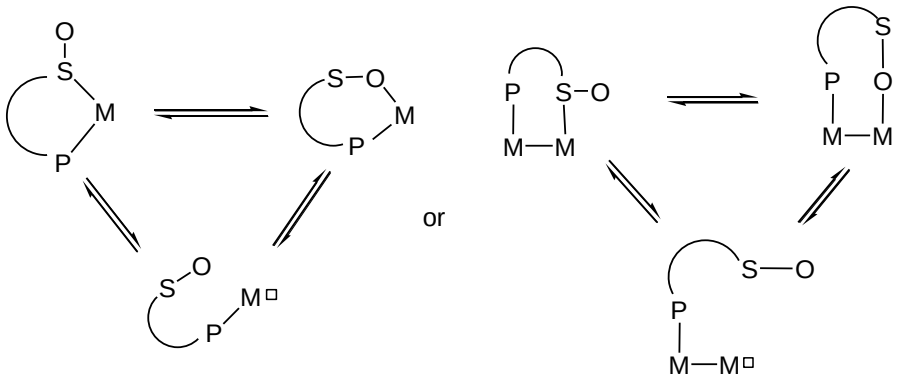

Figure 4. Possible coordination modes of the *N*-phosphino sulfinamide ligands with mono- and bimetallic complexes.

These PNSO ligands represent an efficient way of combining the easily accessible chirality of sulfur with the capacity for coordination of the phosphorous atom.[34] The Riera group has proved that some of these ligands, such as **1a** in Figure 5, are useful in the intermolecular asymmetric Pauson-Khand reaction acting as bidentate P,S ligands.[34]

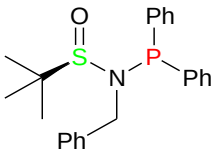

1a

Figure 5. Structure of PNSO ligand **1a**.

This study was the first example of a chiral sulfur atom coordinated to a cobalt centre. The intermolecular Pauson–Khand reaction of the corresponding PNSO-Co complexes with norbornadiene occurred with unprecedented stereoselectivity (Scheme 34).

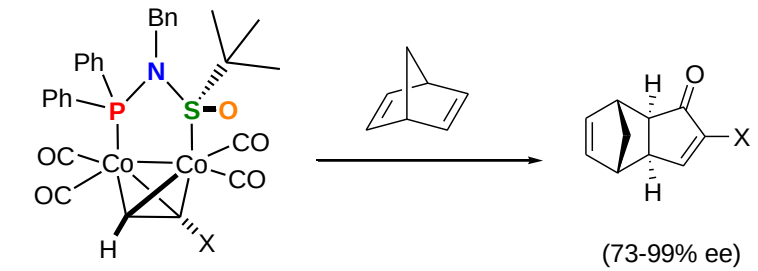

X = $C(CH_3)_2OH$, $CH_2OTBDPS$, TMS, Ph, CH_2OH

Scheme 34. Pauson-Khand reaction of the PNSO-dicobalt complexes with norbornadiene.

[34] Solà, J.; Revés, M.; Riera, A.; Verdaguer, X. *Angew. Chem. Int. Ed.* **2007**, *46*, 5020.

The same authors later published the synthesis and characterization of the first rhodium(I) complexes with ligand **1a.**[35] The reaction of $[RhCl(COD)]_2$ with one equivalent of **1a** in the presence of AgOTf afforded an 85% yield of complex [Rh(**1a**)(COD)]OTf, **2**, as an air-stable orange solid**.** The complex [Rh(**1a**)$_2$]OTf was obtained with a 90% yield using two equivalents of ligand **1a** (Scheme 35). Complex **3** was also an air-stable yellow compound.

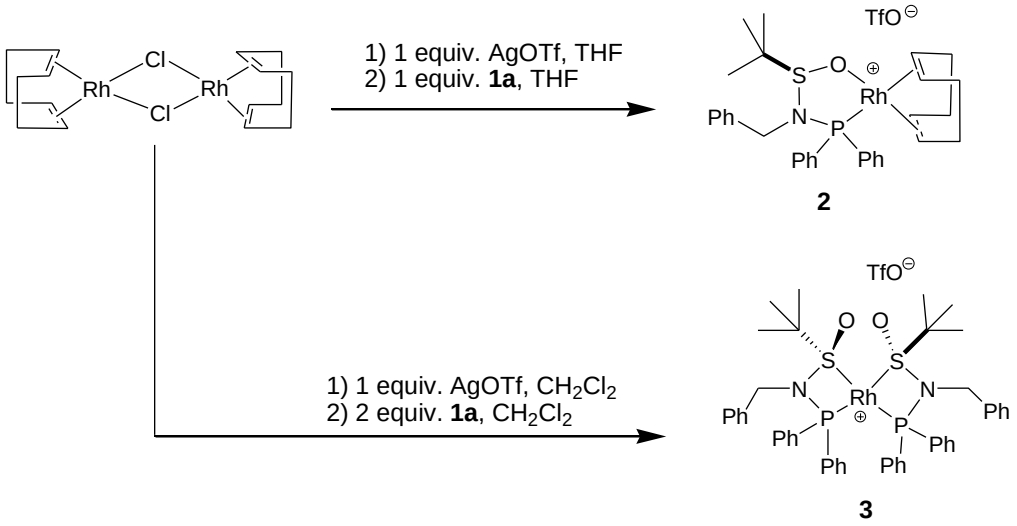

Scheme 35. Preparation of cationic rhodium complexes [Rh(**1a**)(COD)]OTf and [Rh(**1a**)$_2$]OTf.

It should be noted that when olefinic ligands such as COD are attached to the metal centre, ligand **1a** presents a P,O coordination (complex **2**, Scheme 35). On the other hand, rhodium complex with two PNSO ligands provide P,S coordination (complex **3**, Scheme 35). The coordination mode of the sulfinamide moiety in both complexes was determined by X-ray analysis.

3.1.2. P-stereogenic P,O hemilabile ligands

The synthesis of the *P*-stereogenic P,O hemilabile ligands was performed by Riera's group after their previous study of the synthesis of *P*-stereogenic aminophosphine **4** as a building block for the synthesis of chiral asymmetric iminodiphosphines **6** (Scheme 36).[36] The free primary aminophosphine was required for the reaction with the bulky *t*-Bu_2PCl. Compound **5** was found to exist exclusively as its P-H tautomer, which prevented the oxidation of phosphorous. Removal of the borane moiety with HBF_4 provided the air-stable phosphonium salt **6**, which exhibited rich coordination chemistry enabling the reaction with $[Rh(COD)_2]BF_4$, affording the corresponding cationic complex **7**, whose structure was confirmed by X-ray analysis.

[35] Achard, T.; Benet-Buchholz, J.; Riera, A.; Verdaguer, X. *Organometallics* **2009**, *28,* 480.
[36] a) Revés, M.; Ferrer, C.; León, T.; Doran, S.; Etayo, P.; Vidal- Ferran, A.; Riera, A.; Verdaguer, X. *Angew. Chem. Int. Ed.* **2010**, *49*, 9452.

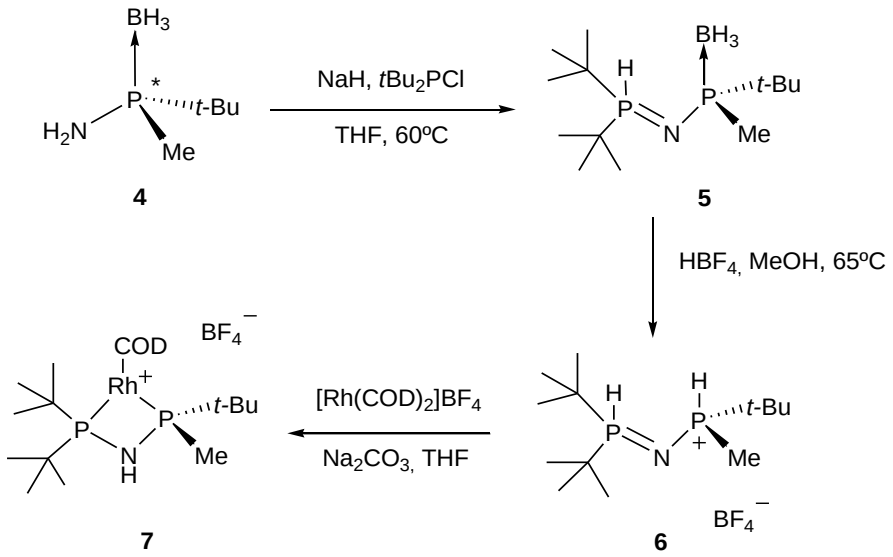

Scheme 36. Synthesis of the aminodiphosphine rhodium complex **7**.

Compound **4** is also a suitable building block for the synthesis of electron-rich *P**-sulfonyl iminophosphorane derivatives as shown in Scheme 37. Compound **4** was deprotonated with NaH and further reaction with commercially available sulfonylchlorides afforded the corresponding borane-protected phosphinosulfonamides **8** and **9** in good yields. Borane deprotection of compounds **8** and **9** was conducted under basic conditions in the presence of DABCO.

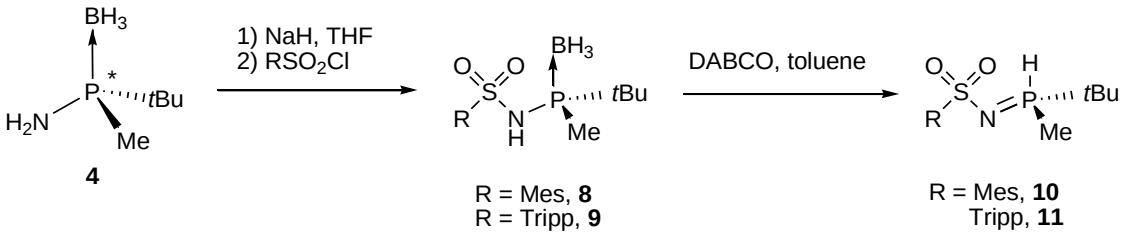

Scheme 37. Synthesis of iminophosphoranes **10** and **11** (Mes = 2,4,6-trimethylphenyl, Tripp = 2,4,6-tris(isopropyl)phenyl).

Moreover, the potential of these ligands arises from the NH/PH tautomeric equilibrium of the species that render them stable to oxidation (Scheme 38).

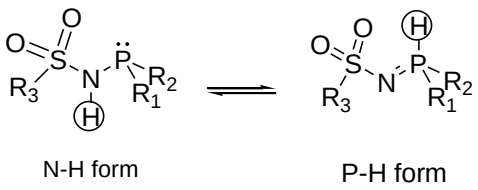

Scheme 38. NH/PH tautomeric equilibrium.

The equilibrium usually shifts towards the P^V form although it can shift to the aminophosphine form by the coordination of phosphorus to a metal. PH tautomer formation prevents the oxidation of phosphorous. Furthermore, P-stereogenic secondary iminophosphoranes are configurationally stable and thus chiral information is preserved through the PH/NH equilibrium. This equilibrium is presumably governed by the electronic properties of the phosphine atom rather than the nature of the substiutents of the sulfone.

These same authors then studied the capacity of this P, O ligands **10** and **11** to coordinate rhodium for their use in asymmetric catalysis. The reaction of bulky iminophosphoranes with $[Rh(COD)_2]BF_4$ resulted in the exchange of a single COD unit, as determined by ^1H NMR spectroscopy. The addition of an excess of secondary iminophosphoranes did not lead to a dimeric species; the steric bulk of the ligand may be responsible for this behavior. Complexes **12** and **13** were isolated as air-stable yellow solids (Scheme 39).

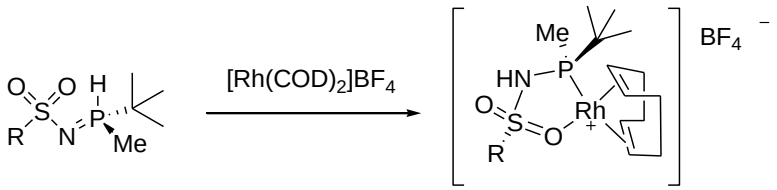

Scheme 39. Preparation of cationic Rh(I) complexes **12** and **13** with P,O ligands **10** and **11**.

Upon coordination to rhodium, the tautomeric equilibrium is effectively displaced towards the phosphinosulfonamide form. This leaves a relatively acidic NH group in place that shows a resonance around 8 ppm in the ^1H NMR spectrum ($CDCl_3$).

It is important to note that in the rhodium complexes **12** and **13**, the chirality remains in the *tert*-butylmethylphosphino moiety, which is strongly attached to the rhodium centre. In comparison, PNSO ligands have the chirality in the hemilabile sulphur atom (Figure 6).

Figure 6. Hemilabile S-stereogenic and P-stereogenic ligands.

3.1.3. Chiral catalysts for the Rh-catalysed [2+2+2] cycloaddition reactions

BINAP-type ligands are one of the most commonly used ligands in asymmetric Rh-catalysed [2+2+2] cycloaddition reactions since chelation provides the rigidity required to allocate the chiral information firmly around the metal centre.[37] However, hemilabile ligands have also been used satisfactorily in chiral induction.

Comparison of hemilabile S-stereogenic and P-stereogenic ligands with diphosphine ligands reveals that the chirality of the phosphine ligands resides in the carbon backbone whereas, in the other two cases, the chirality resides on one of the coordinating heteroatom (Figure 7).

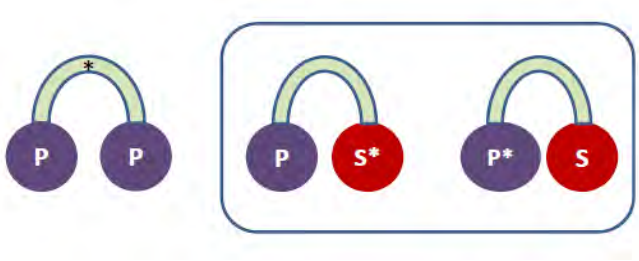

Figure 7. Different kind of chirality in phosphine-based ligands.

To investigate the hypothesis that rhodium complexes with S- and P-stereogenic ligands are active as catalysts in [2+2+2] cycloaddition reactions and especially as chiral ligands in asymmetric cycloaddition reactions, we embarked on a collaborative study with Prof. Riera and Dr. Verdaguer. As our main goal we decided to study the efficiency of the two sets of ligands in the asymmetric [2+2+2] cycloaddition of substrates such as enediynes. So, the specific objectives of this part of the thesis can be summarized as follows:

- To study the catalytic activity of S-stereogenic (PNSO) ligands in partially intramolecular and totally intramolecular Rh(I)-catalysed [2+2+2] cycloaddition reactions of alkynes.
- To study the efficiency of PNSO ligands in asymmetric intramolecular Rh(I)-catalysed [2+2+2] cycloaddition of enediynes.
- To study the catalytic activity of Rh(I) complexes with P-stereogenic ligands in the asymmetric intramolecular [2+2+2] cycloaddition reactions of enediynes.

[37] Shibata, Y.; Tanaka, K. *Synthesis* **2012**, *44*, 323.

3.2. Results and discussion

3.2.1. PNSO ligands in totally intramolecular [2+2+2] cycloaddition reactions of triynes

Given that the new Rh(I)-PNSO complexes had not been previously evaluated in [2+2+2] cycloaddition reactions, we first decided to test their catalytic efficiency in the most simple version, i.e., intramolecular [2+2+2] cycloadditions of triynes. *N*-Tosyl tethered triynes with terminal and non-terminal alkynes **14a-c** and *O*-linked tryine **14d** were the substrates of choice.

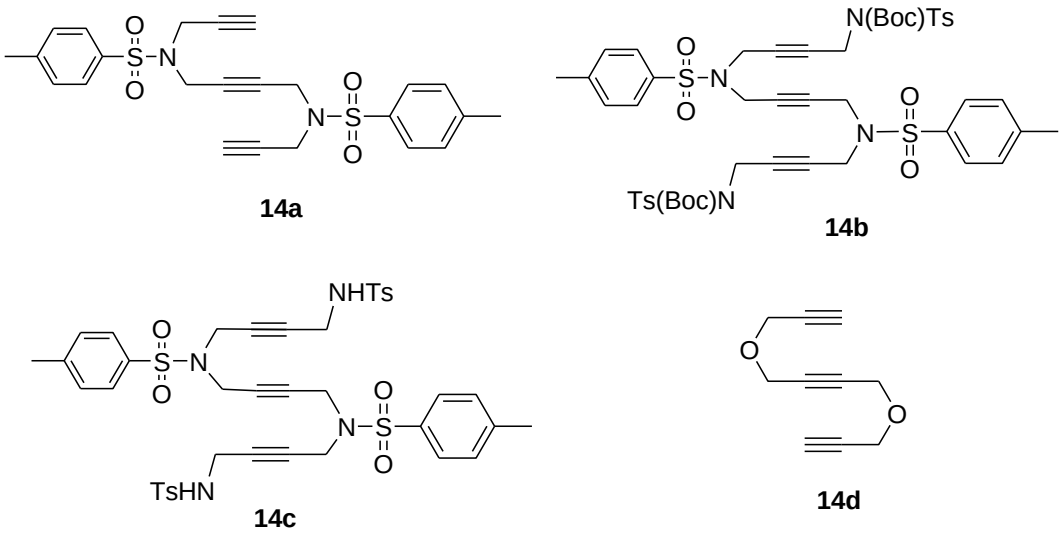

Figure 8. Triyne substrates tested in this study.

3.2.1.1. Synthesis of substrates

The triyne substrates used in this study were not commercially available and so were synthesized in our laboratories. Compounds **14b** and **14c** were prepared previously by Sandra Brun as part of her doctoral work. Compounds **14a**[38] and **14d**[39] were prepared following the method described previously in the literature.

Compound **14a** was prepared through the nucleophilic substitution of commercially available 1,4-dichloro-2-butyne with two equivalents of *N*-*p*-toluenesulfonyl-prop-2-yn-1-amine, synthesised previously from *p*-toluenesulfonyl chloride and propargylamine. Using sodium hydride as a base in anhydrous DMF, the reaction took place with a moderate yield (37%). This low yield was probably due to the low reactivity of 1,4-dichloro-2-butyne. This reagent was

[38] Ojima, I.; Vu, A. T.; McCullagh, J. V.; Kinoshita, A. *J. Am. Chem. Soc.* **1999**, *121*, 3230.
[39] Grigg, R.; Scott, R.; Stevenson, P. *J. Chem. Soc. Perkin Trans. I*, **1988**, 1357.

chosen rather than the more reactive 1,4-dibromo-2-butyne as the latter reagent is not commercially available and is difficult to use as it is a highly irritant compound.

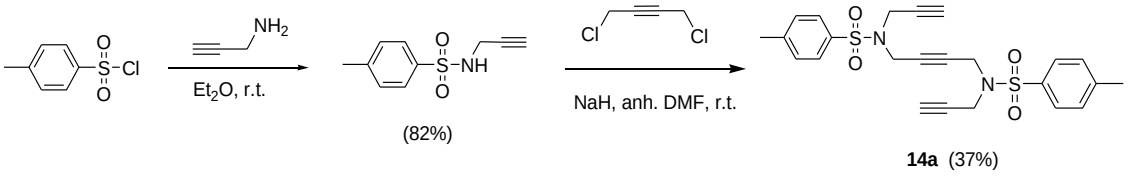

Scheme 40. Preparation of triyne **14a**.

For the preparation of triyne **14d**, two equivalents of propargyl bromide and one equivalent of 2-butyne-1,4-diol were used, both of which were commercially available. Potassium hydroxide was used as a base in DMSO at 70ºC to afford a 70% yield of compound **14d** together with a 16% yield of monosubstituted product 4-(prop-2-inyloxy)but-2-yn-1-ol **14dm**, which could be separated by column chromatography.

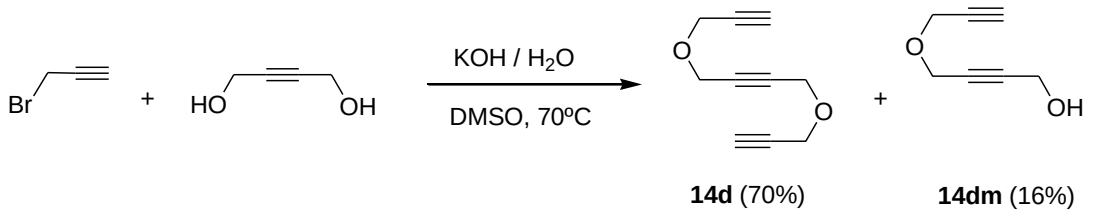

Scheme 41. Preparation of triyne **14d**.

3.2.1.2. [2+2+2] cycloaddition of triynes 14

After the synthesis of the triyne substrates we proceeded to evaluate their [2+2+2] cycloaddition reaction.[40, 41]

[40] For selected and recent examples of [2+2+2] cycloadditions of triynes using rhodium catalysts, see: a) Crittall, M. R.; Fairhurst, N. W. G; Carbery, D. R. *Chem. Commun*., **2012**, 11181; b) Shibata, T.; Uchiyama, T.; Hirashima, H.; Endo, K. *Pure Appl. Chem.,* **2011**, *83*, 597; c) Shibata, T.; Uchiyama, T.; Endo, K. *Org. Lett.* **2009**, *11*, 3906; d) Nicolaus, N.; Strauss, S.; Neudörfl, J.-M.; Prokop, A.; Schmalz, H.-G. *Org. Lett*. **2009**, *11*, 341; e) Tanaka, K.; Sagae, H.; Toyoda, K.; Hirano, M. *Tetrahedron* **2008**, *64*, 831.

[41] For selected examples of [2+2+2] cycloadditions of triynes using other metals, see: Cobalt: a) Geny, A.; Agenet, N.; Iannazzo, L.; Malacria, M.; Aubert, C.; Gandon, V. *Angew. Chem. Int. Ed.* **2009**, *48*, 1810; b) Chouraqui, G.; Petit, M.; Phansavath, P.; Aubert, C.; Malacria, M. *Eur. J. Org. Chem*. **2006**, 1413. Palladium: c) Yamamoto, Y.; Nagata, A.; Nagata, H.; Ando, Y.; Arikawa, Y.; Tatsumi, K.; Itoh, K. *Chem. Eur. J.* **2003***, 9*, 2469. Ruthenium: d) Yamamoto, Y.; Arakawa, T.; Ogawa, R.; Itoh, K. *J. Am. Chem. Soc*. **2003**, *125*, 12143; e) Hoven, G.; Efskind, J.; Rømming, C.; Undheim, K. *J. Org. Chem*. **2002**, *67*, 2459. Iridium: f) Shibata, T.; Tsuchikama, K.; Otsuka, M. *Tetrahedron: Asymmetry* **2006**, *17*, 614.

In a preliminary optimization of the reaction, monomeric Rh complex **2** and dimeric rhodium complex **3** (Figure 9) were evaluated and **2** was found to be the more active catalyst. Given that the catalyst was generated in situ and the reaction between $[Rh(COD)_2]BF_4$ and **1a** can give dimeric complex $[Rh(\mathbf{1a})_2]BF_4$, ^{31}P NMR studies were performed to find the best conditions to give monomeric $[Rh(\mathbf{1a})(COD)]BF_4$.

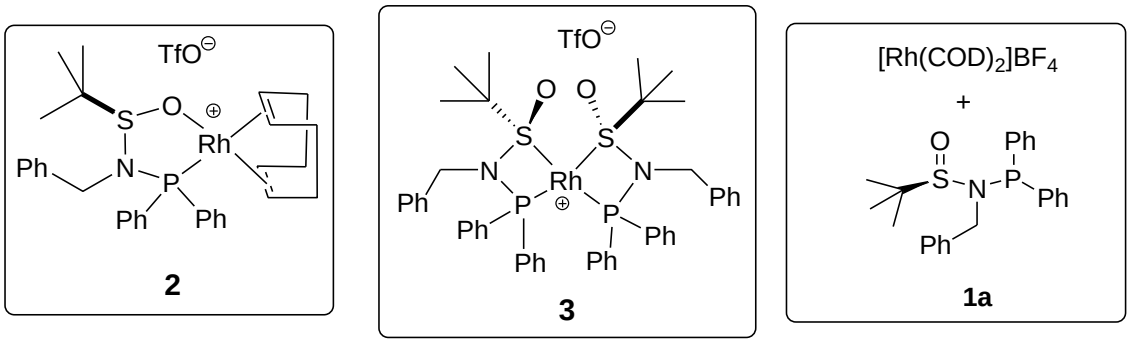

Figure 9. Structure of monomeric Rh complex **2**, dimeric rhodium complex **3** and in situ generation of catalytic system.

Mixtures containing $[Rh(COD)_2]BF_4$ and **1a** were prepared with a molar ratio ranging from 1:1 to 2:1. After hydrogenation, ^{31}P NMR analysis showed that when the ratio was 2:1 $[Rh(\mathbf{1a})(COD)]BF_4$ complex was the main compound (93% yield), and that a 7% yield of dimeric species $[Rh(\mathbf{1a})_2]BF_4$ was obtained. ESI-MS studies also confirmed the formation of the two rhodium complexes in solution.

Therefore, mixing 0.2 equivalents of cationic rhodium complex $[Rh(COD)_2]BF_4$ and 0.1 equivalents of PNSO ligand **1a** in dichloroethane afforded benzene derivatives **15a**-**15d** in excellent yields (Table 1).

N-Tosyl linked triynes **14a** and **14c** gave the corresponding benzene derivatives **15a** and **15c** at room temperature with short reaction times (Entries 1 and 3, Table 1). In order to cycloisomerize triyne **14b** to obtain a good yield of **15b,** it was necessary to heat the reaction at 50ºC for 24h. This might be due to the steric hindrance of the Boc groups in the two terminal nitrogen sulfonamides. *O*-tethered terminal triyne **14d** also gave excellent results (Entry 4, Table 1).

Table 1. Rh(I)-PNSO catalysed [2+2+2] cycloaddition reactions of triynes **14.**

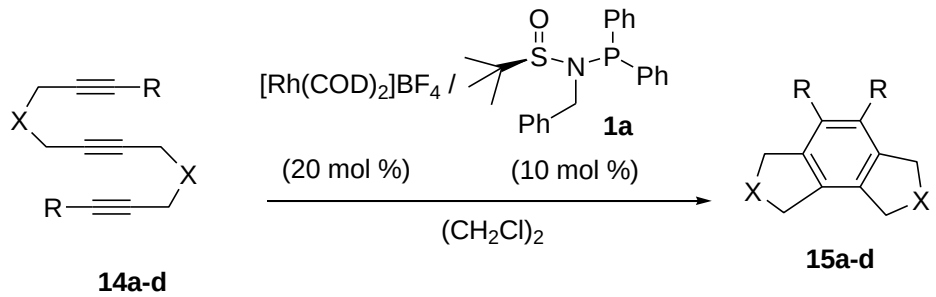

14a-d **15a-d**

Entry	Starting compound	Reaction conditions[a]	Product, yield (%)
1	**14a** (X = NTs, R = H)	r.t., 1 h.	**15a**, 100
2	**14b** (X = NTs, R = $CH_2N(Boc)Ts$)	50ºC, 24h.	**15b**, 81
3	**14c** (X = NTs, R = CH_2NHTs)	r.t., 1.5 h.	**15c**, 83
4	**14d** (X = O, R = H)	r.t., 45 min.	**15d**, 100

[a] Hydrogen gas was bubbled into the catalyst solution for 30 min., the hydrogen and solvent were then removed, the solvent was added again, and finally the substrate **14** was introduced.

3.2.2. PNSO ligands in partially intramolecular [2+2+2] cycloaddition reactions of diynes and monoynes

Since the totally intramolecular version was achieved with excellent results, the next step was to evaluate the chemoselectivity of the new catalytic system. Therefore, we tested it in the partially intramolecular version between diynes and monoynes (Scheme 42).[42,43]

[42] For selected and recent examples of [2+2+2] cycloadditions of diynes with monoynes using rhodium catalysts, see: a) Araki, T.; Noguchi, K.; Tanaka, K. *Angew. Chem. Int. Ed.* **2013**, *52*, 1 ; b) Shibata, Y.; Tanaka, K. *Synthesis*, **2012**, *3*, 323; c) Sakiyama, N.; Hojo, D.; Noguchi, K.; Tanaka, K. *Chem. Eur. J.* **2011**, *17*, 1428; d) Sedlák, D.; Novák, P.; Kotora, M.; Bartunek, P. *J. Med. Chem*. **2010**, *53*, 4290; e) Wu, W.; Zhang, X. Y.; Kang, S. X. *Chin*. *Chem. Lett.* **2010**, *21*, 18; f) Tanaka, K.; Sawada, Y.; Aida, Y.; Thammathevo, M.; Tanaka, R.; Sagae, H.; Otake, Y. *Tetrahedron* **2010**, *66*, 1563; g) Garcia, L.; Pla-Quintana, A.; Roglans, A. *Org. Biomol. Chem*. **2009**, *7*, 5020; h) Kotha, S.; Khedkhar, P. *Eur. J. Org. Chem.* **2009**, 730; i) Komine, Y.; Kamisawa, A.; Tanaka, K. *Org. Lett.* **2009**, *11*, 2361.

[43] For selected and recent examples of [2+2+2] cycloadditions of diynes with monoynes using other metals, see: Cooper: a) Yoshimatsu, M.; Sasaki, H.; Sugimoto, Y.; Nagase, Y.; Tanabe, G.; Muraoka, O. *Org. Lett*. **2012**, *14*, 3190. Cobalt: b) Iannazzo, L.; Kotera, N.; Malacria, M.; Aubert, C.; Gandon, V. *J. Organomet. Chem***. 2011***, 696,* 3906; c) Saino, N.; Kawaji, T.; Ito, T.; Matsushita, Y.; Okamoto, S. *Tetrahedron Lett*. **2010**, *51*, 1313. Palladium; d) Sato, Y.; Tamura, T.; Kinbara, A.; Mori, M. *Adv. Synth. Catal.* **2007**, *349*, 647. Ruthenium: e) Perekalin, D. S.; Trifonova, E. A.; Petrovskii,P. V.; Kudinov, A. R. *Russ. Chem. Bull., Int. Ed.,* **2011***, 60,* 2110*;* f) Shchetnikov, G. T.; Osipov, S. N.; Bruneau, C.; Dixneuf, P. H. *Synlett* **2008**, 578; g) Yamamoto, Y.; Hattori, K. *Tetrahedron* **2008**, *64*, 847. Iridium: h) Shibata, T.; Yoshida, S.; Arai, Y.; Otsuka, M.; Endo, K. *Tetrahedron* **2008**, *64*, 821; i) Matsuda, T.; Kadowaki, S.; Goya, T.; Murakami, M. *Org. Lett.* **2007**, *9*, 133. Nickel: j) Zou, Y.; Young, D. D.; Cruz-Montanez, A.; Deiters, A. *Org. Lett.* **2008**, *10*, 4661; k) Teske, J. A.; Deiters, A. *J. Org. Chem*. **2008**, *73*, 342.

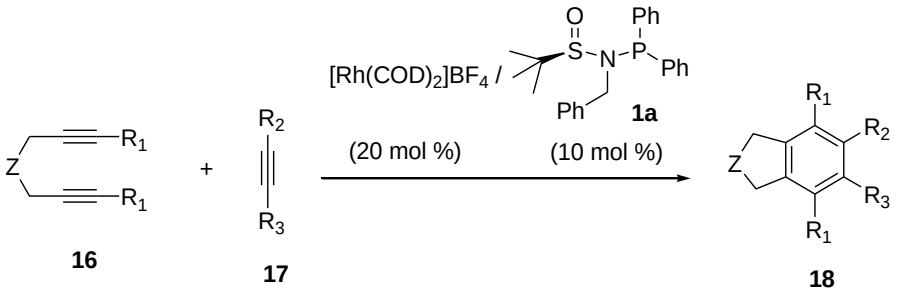

Scheme 42. Cycloaddition reactions between symmetrical diynes **16** and monoynes **17**.

Diynes and monoynes used in this section are represented in Figure 10. We chose *N*-tosyl- and malonate-tethered non-terminal diynes **16a** and **16b** since they are less prone to homocoupling reactions. We also wished to test terminal diynes with a wide range of tethers such as CH_2 **16c**, *N*-tosyl **16d**, malonate **16e** and *O*-tether **16f**. In order to study the scope of the reaction we chose monosubstituted monoynes **17a** and **17b** and disubstituted alkynes with different electronic demanding substituents **17c**-**17e**.

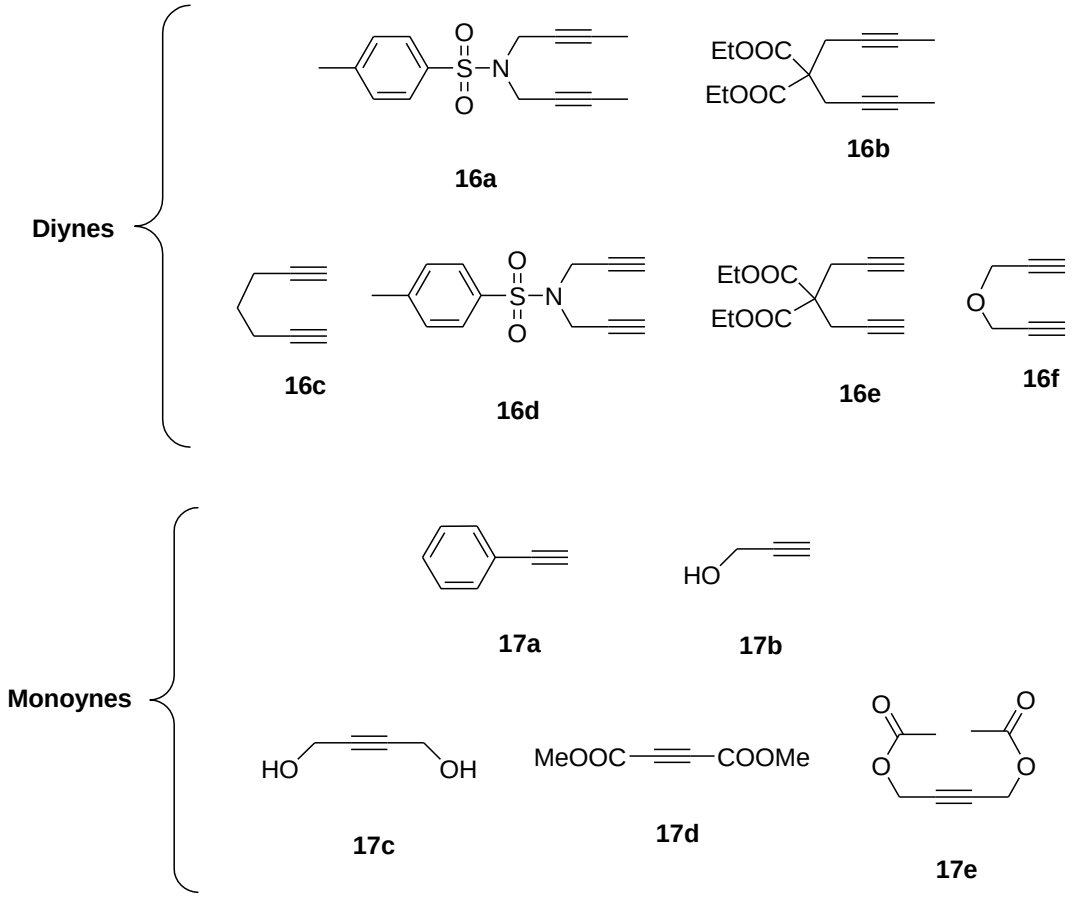

Figure 10. Diynes and monoynes used in this study.

3.2.2.1. Synthesis of substrates

Whereas most of the substrates are commercially available or were stored in the laboratory from other studies, diynes **16a**[44] and **16d**[45] were prepared in accordance with the methods described in the literature: *p*-toluenesulfonamide was reacted with 2 equivalents of 1-bromo-2-butyne and 1-bromo-2-propyne, respectively, in acetonitrile at reflux with a high excess of potassium carbonate as a base to afford a 94% yield of **16a** and a 90% of **16d**.

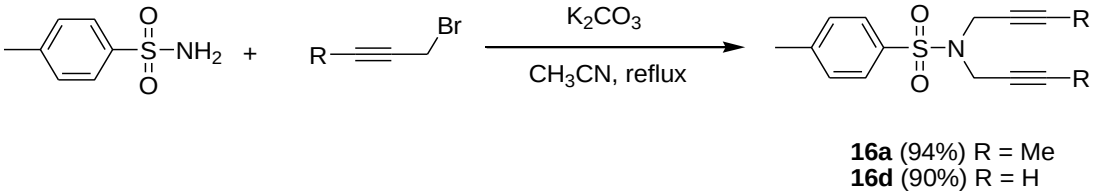

Scheme 43. Synthesis of diynes **16a** and **16d**.

Monoyne **17e**[46] was prepared by the reaction of 2-butyne-1,4-diol **17c** with three equivalents of acetyl chloride in dichloromethane at room temperature with a light excess of pyridine as a base, yielding 92% of 1,4-diacetyl-2-butyne **17e**.

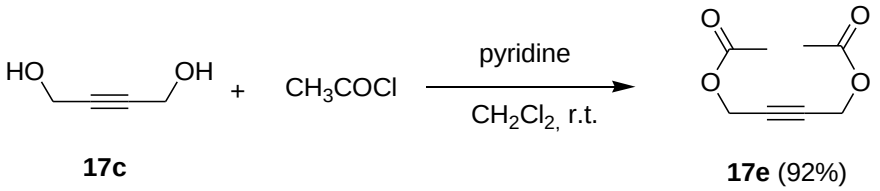

Scheme 44. Synthesis of monoyne **17e**.

3.2.2.2. [2+2+2] cycloaddition of diynes and monoynes

The first reaction conditions tested were the same as those we used in the cycloaddition of triynes. $[Rh(COD)_2]BF_4$/**1a** mixture was used as the catalyst and either dichloromethane or 1,2-dichloroethane was used depending on the temperature required. In all cases, an excess of monoyne of between 3 and 5 equivalents was used.

We first investigated the reaction of non-terminal diynes, which are generally less reactive than their terminal counterparts toward this reaction. *N*-tosyl-tethered diyne **16a** was reacted

[44] Nishida, M.; Shiga, H.; Mori, M. *J. Org. Chem*. **1998**, *63*, 8606.
[45] Brumwell, J. E.; Simplins, N. S.; Terrett, N. K. *Tetrahedron Lett.* **1993**, *34*, 1219.
[46] *Organic Synthesis*, **1998**, *9*, 507.

with phenylacetylene **17a** in the presence of cationic rhodium(I)/phosphinosulfinamide complex as a catalyst generated in situ. An 84% yield of **18aa** was obtained in short reaction times in dichloroethane at reflux (Entry 1, Table 2). We then studied the scope of the reaction by varying the monoyne counterpart. Monosubstituted alkyne **17b** (Entry 2, Table 2) as well as disubstituted alkynes **17c** (Entry 3, Table 2) and **17d** (Entry 4, Table 2) effectively participated in the [2+2+2] cycloaddition reaction.

Table 2. Rh(I)-PNSO catalysed [2+2+2] cycloaddition reactions of diyne **16a** and monoynes **17a-d.**

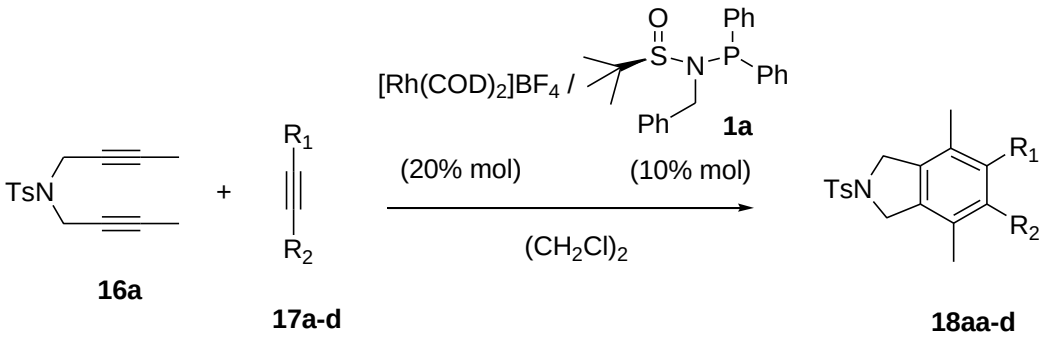

16a **17a-d** **18aa-d**

Entry	17 (R_1, R_2)	Reaction conditions	Product, yield (%)
1	**17a** (R_1 = Ph, R_2 = H)	reflux, 2 h	**18aa**, 84
2	**17b** (R_1 = CH_2OH, R_2 = H)	reflux, 24 h	**18ab**, 52
3	**17c**[a] (R_1 = R_2 = CH_2OH)	reflux, 24 h	**18ac**, 63
4	**17d** (R_1 = R_2 = COOMe)	reflux, 5 h	**18ad**, 44
5[b]	**17a** (R_1 = Ph, R_2 = H)	reflux, 2 h	**18aa**, 5

[a] Butyne-1,4-diol **17c** was added to the reaction mixture dissolved in THF (1 mL). [b] This reaction was performed in the absence of ligand **1a**.

The catalytic activity of the excess of $[Rh(COD)_2]BF_4$ present in the reaction media was evaluated by running a blank experiment excluding ligand **1a**. Only a 5% yield of benzene derivative **18aa** was achieved in the same reaction conditions leading us to conclude that the process is PNSO-ligand accelerated and that most of the catalytic activity is due to our new complex (Entry 5, Table 2).

It is worth mentioning that monoyne **17d** gave high quantities of the trimerization product, hexamethyl mellitate **19**, which was responsible for the decreased yield of the partially intramolecular reaction. Therefore, a completely intermolecular cycloaddition was run with alkyne **17d** alone. A 67% yield of hexamethyl mellitate **19** was obtained after 1.5 h of reaction (Scheme 45).

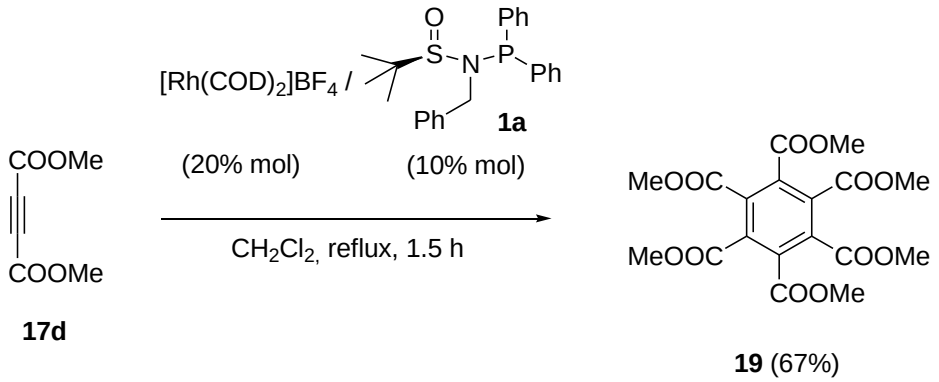

Scheme 45. Cyclotrimerization of **17d**.

The effect of the tether between the alkynes was also studied by reacting malonate-linked diyne **16b** with phenylacetylene **17a**. The reaction worked effectively in dichloroethane at reflux with a 78% yield of the cycloisomerized product **18ba** being achieved after 2 hours of reaction (Scheme 46).

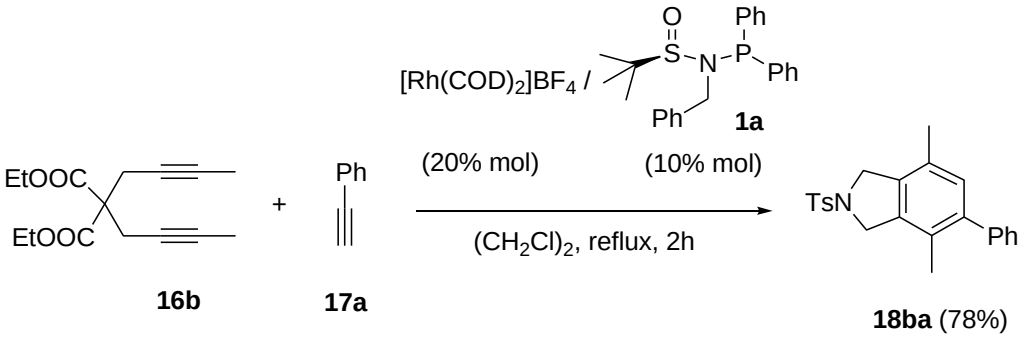

Scheme 46. Cycloaddition between non-terminal malonate-linked diyne **16b** and phenylacetylene **17a**.

In a second step, diynes featuring two terminal alkynes were submitted to the [2+2+2] cycloaddition reaction (Table 3).

1,6-heptadiyne **16c** was reacted with phenylacetylene **17a** in the presence of cationic rhodium(I)/phosphinosulfinamide complex as a catalyst generated in situ. A 60% yield of the biphenyl derivative **18ca** was achieved in just 15 minutes at room temperature (Entry 1, Table 3). The monoyne counterpart was varied and slightly better yields were achieved with propargyl alcohol **17b** (Entry 2, Table 3) and 2-butyne-1,4-diol **17c** (Entry 3, Table 3) except when 2-butyne-1,4-diol diacetate **17e** (Entry 4, Table 3) was used when only a 14% yield was obtained. This result might indicate that the electronic nature of the alkyne affects this reaction as those alkynes which are more reactive have electron withdrawing groups.

Table 3. Rh(I)-PNSO catalysed [2+2+2] cycloaddition reactions of diyne **16c** and monoynes **17a-c, 17e.**

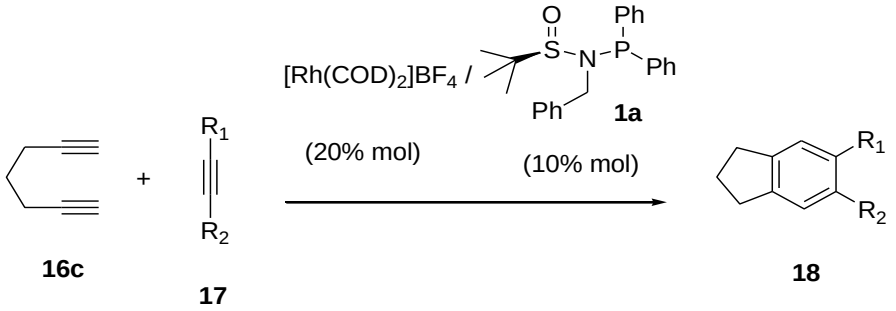

Entry	17 (R_1, R_2)	Reaction conditions	Product, yield (%)
1	**17a** (R_1 = Ph, R_2 = H)	CH_2Cl_2, r.t., 15 min	**18ca**, 60
2	**17b** (R_1 = CH_2OH, R_2 = H)	$(CH_2Cl)_2$, 84ºC, 1h	**18cb**, 73
3	**17c**[a] (R_1 = R_2 = CH_2OH)	$(CH_2Cl)_2$, 84ºC, 2h	**18cc**, 70
4	**17e** (R_1 = R_2 = CH_2OAc)	$(CH_2Cl)_2$, 84ºC, 5h	**18ce**, 14[b]
5[c]	**17a** (R_1 = Ph, R_2 = H)	CH_2Cl_2, r.t., 45 min	**18ca**, 11

[a] Butyne-1,4-diol **17c** was added to the reaction mixture dissolved in THF (1 mL). [b] 22% yield of homocoupling product **18ch** was also obtained. [c] This reaction was performed in the absence of ligand **1a**.

The low yield of product **18ce** can be explained by the competitive formation of the diyne dimerization product **18ch**. This reaction is more favoured when the alkyne is less reactive as is the case of diacetate **17e** (Figure 11).

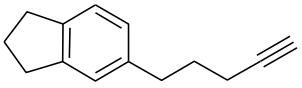

18ch

Figure 11. Homocoupling product of diyne **16c**.

The reaction was again shown to be PNSO-ligand accelerated by running a blank experiment that excluded ligand **1a**. In this case, only an 11% yield was obtained in the reaction between **16c** and **17a** with the same conditions and this was not improved when the reaction was left to run for 45 min (Entry 5, Table 3).

With respect to the tethers, *N*-tosyl-, malonate-, and oxygen-linked diynes could also be used for this reaction (Table 4, Table 5 and Table 6).

N-tosyl-tethered diyne **16d** gave a moderate 44% yield of **18da** when reacted with phenylacetylene **17a** for two hours at room temperature (Entry 1, Table 4), but the yield could be increased up to 78% in just 45 minutes when switching the reaction media to dichloroethane at reflux (Entry 2, Table 4). When monoyne **17e** was used, the yield decreased significantly (Entry 3, Table 4).

Table 4. Rh(I)-PNSO catalysed [2+2+2] cycloaddition reactions of diyne **16d** with monoynes **17a** and **17e.**

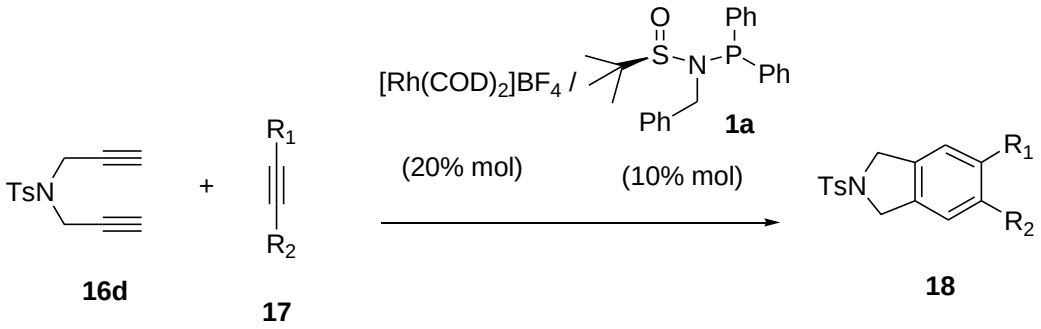

16d **17** **18**

Entry	17 (R_1, R_2)	Reaction conditions	Product, yield (%)
1	**17a** (R_1 = Ph, R_2 = H)	CH_2Cl_2, r.t., 2 h	**18da**, 44
2	**17a** (R_1 = Ph, R_2 = H)	$(CH_2Cl)_2$, 84ºC, 45 min	**18da**, 78
3	**17e** (R_1 = R_2 = CH_2OAc)	CH_2Cl_2, r.t., 28 h	**18de**, 26[a]

[a] 12% yield of homocoupling product **18dh** was also obtained.

The low yield of product **18de** can be explained by the competitive formation of the diyne dimerization product **18dh** (Figure 12).

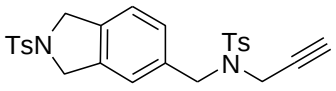

18dh

Figure 12. Homocoupling product of diyne **16d**.

Malonate-tethered diyne **16e** reacted with the three monoynes **17a-c** with yields above 70% (Table 5).

Table 5. Rh(I)-PNSO catalysed [2+2+2] cycloaddition reactions of diyne **16e** with monoynes **17a-c.**

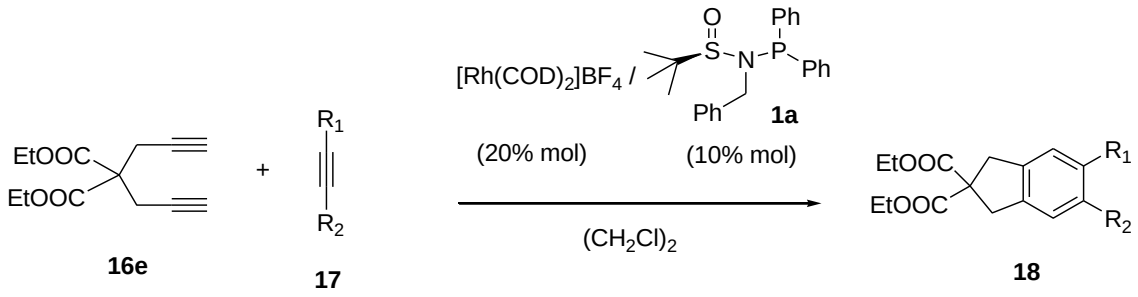

Entry	**17** **(R_1, R_2)**	Reaction conditions	Product, yield (%)
1	**17a** (R_1 = Ph, R_2 = H)	r.t., 6 h	**18ea**, 71
2	**17b** (R_1 = CH_2OH, R_2 = H)	84ºC, 2 h	**18eb**, 77
3	**17c**[a] (R_1 = R_2 = CH_2OH)	84ºC, 7 h	**18ec,** 72

[a] Butyne-1,4-diol **17c** was added to the reaction mixture dissolved in THF (1 mL).

Finally, oxygen-linked diyne **16f** was also shown to participate effectively in the [2+2+2] cycloaddition with monoynes **17a-c** in dichloroethane at room temperature (Table 6).

Table 6. Rh(I)-PNSO catalysed [2+2+2] cycloaddition reactions of diyne **16f** with monoynes **17a-c.**

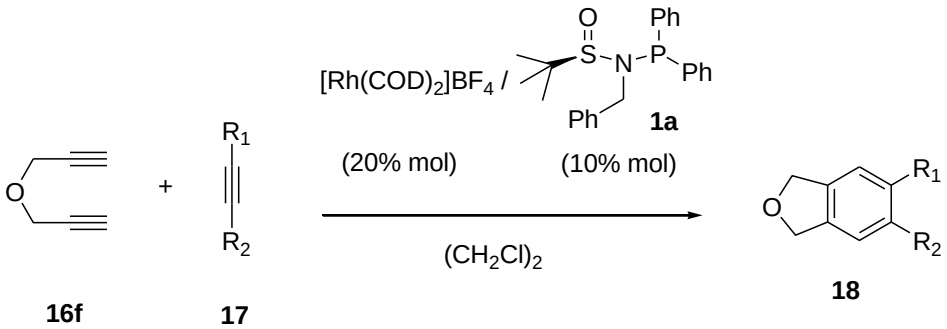

Entry	**17** **(R_1, R_2)**	Reaction conditions	Product, yield (%)
1	**17a** (R_1 = Ph, R_2 = H)	r.t., 3 h	**18fa**, 60
2	**17b** (R_1 = CH_2OH, R_2 = H)	r.t., 5 h	**18fb**, 99
3	**17c**[a] (R_1 = R_2 = CH_2OH)	r.t., 8 h	**18fc**, 48

[a] Butyne-1,4-diol **17c** was added to the reaction mixture dissolved in THF (1 mL).

Cyclotrimerized products **18ab**, **18ad**, **18ba**, **18ce** and **18de** have not been previously described and so have been completely characterized here.[47]

3.2.3. PNSO ligands in totally intramolecular [2+2+2] cycloaddition of open-chain and macrocyclic enediynes

Once the activity of PNSO ligands in the [2+2+2] cycloaddition of three alkynes had been established, we decided to test them in the more challenging cycloaddition of enediynes, which furthermore can generate enantioselectivity. For this reason, a complete study of intramolecular [2+2+2] cycloisomerizations of open-chained enediynes and macrocyclic enediynes catalysed by the combination of cationic Rh(I) catalysts with PNSO ligands was then undertaken. This work was performed by Sandra Brun in her doctoral thesis. As a summary, the best results obtained of yields and enantiomeric excesses are shown in the Scheme 47.

As we have previously commented in the Introduction, enediynes with terminal alkynes are challenging substrates to cyclize. To the best of our knowledge, only two significant cases of enantioselective intramolecular [2+2+2] cycloaddition of enediynes had been reported at that time. Tanaka et al.[48] found that the catalytic system formed by a cationic rhodium(I) complex with BINAP-type ligands catalysed enantioselective cycloadditions of enediyne **20** (Scheme 47) and its derivatives, which have different terminal substituents, resulting in good yields and moderate enantiomeric excesses. Shibata et al.,[49] using a similar catalytic system to that used by Tanaka, performed intramolecular cycloaddition of various carbon-, *N*-tosyl-, and oxygen-tethered enediynes, which gave the corresponding cyclohexa-1,3-dienes with high enantioselectivity.

Our study was initiated using *O*-tethered (*E*)-enediyne **20** as a substrate. A 92% yield of cyclohexadiene derivative **22** with a 32% of enantiomeric excess was obtained from the in situ-formed catalyst at reflux of dichloromethane after 3 hours of reaction. The enantioselectivity could not be improved at room temperature or using anhydrous dichloromethane. The results were similar when *N*-tosyl- tethered enediyne **21** was used with the same reaction conditions, yielding 86% of cyclohexadiene **23** with a 22% enantiomeric excess. Interestingly, in none of these cases was isomerization of the double bonds detected.

In this case, the catalytic activity of the excess of $[Rh(COD)_2]BF_4$ present in the reaction media was also evaluated by running a blank experiment excluding ligand **1a**. Only a 10% yield of cyclohexadiene derivative **22** was achieved after 3 hours in the same reaction conditions assuming that the process is PNSO-ligand accelerated and that most of the catalytic activity is due to the hemilabile complex.

[47] Compounds **18aa, 18cb, 18cc, 18ea, 18eb, 18ec, 18fa, 18fb** and **18fc** have been synthesized by Sandra Brun.
[48] Tanaka, K.; Nishida, G.; Sagae, H.; Hirano, M. *Synlett* **2007**, 1426.
[49] Shibata, T.; Kurokawa, H.; Kanda; K. *J. Org. Chem*. **2007**, *72*, 6521.

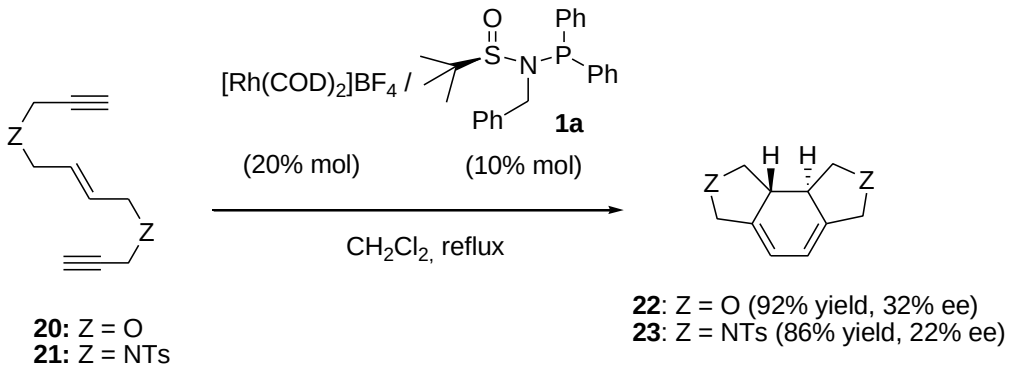

Scheme 47. Rh(I)-PNSO catalysed [2+2+2] cycloaddition reaction of enediynes **20** and **21.**

Sandra Brun also tested the new catalytic system in macrocyclic enediyne **24**[50] (Table 7). Using the catalyst generated in situ, an excellent yield of 91% but low enantioselectivity (11%) was obtained (Entry 1, Table 7). Therefore, the isolated complex [Rh(**1a**)(COD)]OTf was tested with the aim of improving the ee. The best result was achieved in toluene at room temperature since this solvent allowed the reaction time to be reduced considerably. A 79% yield of **25** with a 50% of ee was obtained after 5.5 hours (Entry 2, Table 7). This different behaviour of enantioselectivity can be explained with a blank experiment that demonstrates that the $[Rh(COD)_2]BF_4$ precursor is active, in this case, for the macrocyclic substrate **24** (Entry 3, Table 7).

Table 7. [2+2+2] cycloisomerizations of enediyne macrocycle **24** catalysed by Rh(I)-PNSO ligand generated in situ or as an isolated complex.

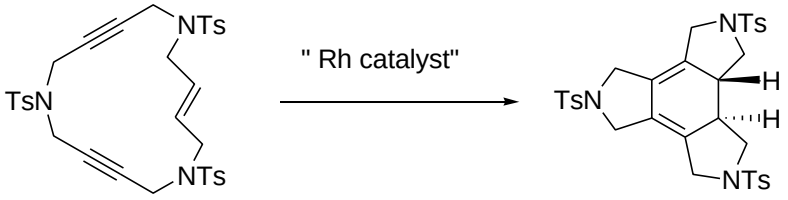

24 **25**

Entry	Catalyst	Reaction conditions	Yield (%)	ee (%)
1	$[Rh(COD)_2]BF_4$/**1a**	CH_2Cl_2, r.t., 2.5 h	91	11
2	[Rh(**1a**)(COD)]OTf	Toluene, r.t., 5.5 h	79	50
3	$[Rh(COD)_2]BF_4$	CH_2Cl_2, r.t., 2.5 h	84	n.d.

All the results presented here have been published in *Tetrahedron*[51].

[50] Torrent, A.; González, I.; Pla-Quintana, A.; Roglans, A.; Moreno-Mañas, M.; Parella, T.; Benet-Buchholz, J. *J. Org. Chem.* **2005**, *70*, 2033.
[51] Brun, S.; Parera, M.; Pla-Quintana, A.; Roglans, A.; León, T.; Achard, T.; Solà, J.; Verdaguer, X.; Riera, A. *Tetrahedron* **2010**, *66*, 9032.

3.2.4. Intramolecular [2+2+2] cycloaddition of enediynes catalysed by P-stereogenic Rh complexes

Once the efficiency of the Rh(I)-PNSO catalytic system was evaluated for the [2+2+2] cycloaddition of enediynes, we concluded that they render an acceptable reactivity profile but that the low selectivity (up to 32% ee) could be improved. This low ee was attributed to the fact that the chiral information in these ligands is located at the hemilabile sulfinyl group. Given that the chiral *tert*-butylmethylphosphino moiety of the rhodium–SIP complexes **12** and **13** synthesized in the group of Dr. Verdaguer and Prof. Riera were strongly attached to the rhodium centre, we tested them in the cyclization of this type of substrates in order to improve the ee. Therefore, we decided to test the enantioselective cycloaddition of enedyines **20**, **21**, **26**, **27** and **28** (see Figure 13). Firstly, we considered testing different tethered terminal diynes **20, 21** and **26**, which are more reactive than the internal ones. Then, as a more challenging objective, we wanted to involve internal enediynes **27** and **28** in this reaction.

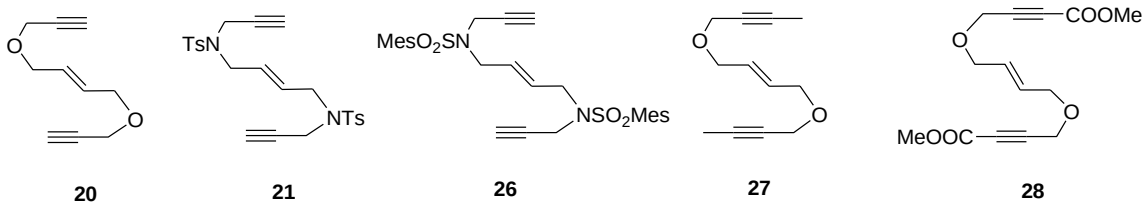

Figure 13. Terminal and internal enediynes used in this study.

3.2.4.1. Preparation of enediynes

First of all, it was necessary to synthesize enediyne substrates, which were not commercially available. Enediynes **21** and **26** were prepared by Thierry León (PhD student of the Riera's group). Synthesis of enediynes **20**[52], **27**[52] and **28**[53] was performed following the methodology previously described in the literature.

Compound **20** was prepared through the nucleophilic substitution of commercially available *trans*-1,4-dibromo-2-butene with an excess of 2-propyn-1-ol using sodium hydride as the base in anhydrous THF. After 6 hours, the reaction finished affording a 58% yield of the desired product (Scheme 48).

[52] Grigg, R.; Scott, R.; Stevenson, P. *J. Chem. Soc., Perkin Trans. 1,* **1988**, 1365.
[53] Yamamoto, Y.; Kuwabara, S.; Ando, Y.; Nagata, H.; Nishiyama, H.; Itoh, K. *J. Org. Chem.* **2004**, *69*, 6697.

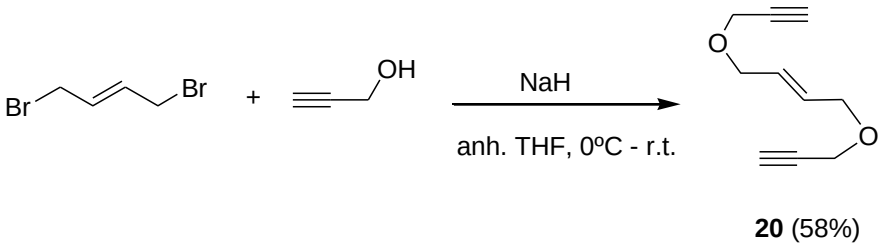

20 (58%)

Scheme 48. Synthesis of enediyne **20**.

Compound **27** was prepared using the same methodology as above starting with 2-butyn-1-ol. After 30 hours at room temperature, a mixture of the desired enediyne **27** was obtained in a 51% yield together with a 10% yield of monosubstituted derivative **27m**, which were then separated by column chromatography (Scheme 49).

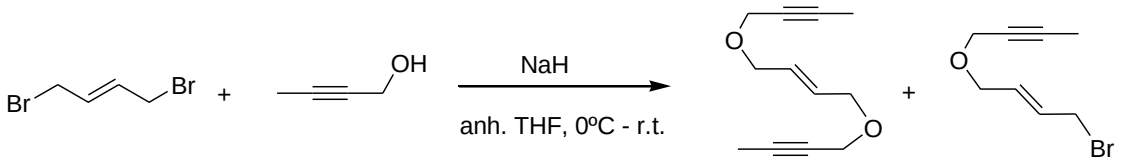

27(51%) **27m** (10%)

Scheme 49. Synthesis of enediyne **27.**

Compound **28** was prepared from the enediyne **20** with an excess of methyl chloroformate. *N*-butyllithium in anhydrous THF was used as a base at -78ºC. After 4 hours at room temperature the reaction was completed to afford 56% of enediyne **28** (Scheme 50).

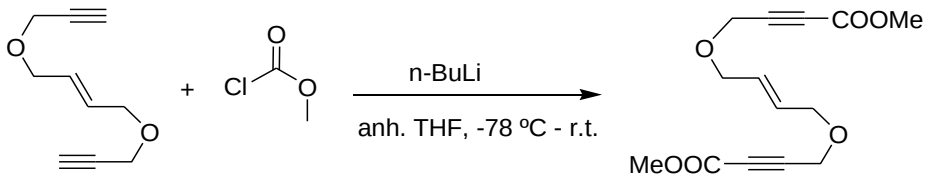

20 **28** (56%)

Scheme 50. Synthesis of enediyne **28.**

3.2.4.2. [2+2+2] Cycloaddition of enediynes 20, 21, 26, 27 and 28

Cationic complexes **12** and **13** (Figure 14) were used as catalysts in the cyclization of the oxygen-tethered enediyne **20** in refluxing CH_2Cl_2 (Table 8).

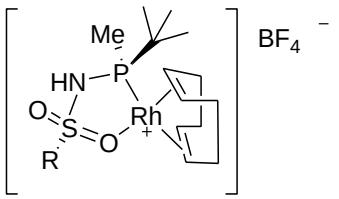

R = Mes, **12**
Tripp, **13**

Figure 14. Cationic rhodium complexes **12** and **13**.

Under these conditions, the reaction took place with complete conversion to afford cyclohexadiene **22** as the sole product with an enantiomeric excess of up to 63%. Catalyst **13**, which contains the bulky Tripp group, was more selective than mesityl complex **12** (Entries 1 and 2, Table 8). For this reason, the following experiments were performed using **13** as catalyst. Thus, using **13**, the selectivity was improved to 69% ee when the reaction was run at room temperature (Entry 3, Table 8). Non-terminal oxygen-tethered enediynes **27** and **28** were then tested using the cationic complex **13** in refluxing CH_2Cl_2 (Entries 4 and 5, Table 8). However, as only starting material was obtained after 22 and 28 hours, respectively, we decided to continue the study with the terminal substrates.

Afterwards, *N*-linked substrate **21** was cyclized with similar levels of selectivity than **20** (67% ee) at both room temperature and reflux (Entries 6 and 7, Table 8). At this point, we wanted to compare these results with those obtained from the reaction catalysed by the combination of $[Rh(COD)_2]BF_4$ with either (*R*)-(+)-BINAP or (*R*)-(+)-H_8-BINAP. These catalytic systems did not afford good yields when the reaction was conducted in dichloromethane at room temperature for 44 hours (Entries 8 and 9, Table 8).

After some experimentation, the addition of a catalytic amount of acid was found to enhance the selectivity with NTs linked substrate **21**. Thus, the addition of HBF_4 (10 mol%) allowed an increase of the ee to 90% (Entry 10, Table 8). This behaviour was also observed for substrate **26**, which, after 24h at reflux with a 10 mol % of HBF_4, yields the cycloadduct **29** with a 91% yield and an 83% ee (Entry 11, Table 8). Interestingly, upon addition of trifluoroacetic acid (TFA; 10 mol%) this result was improved to 99% yield and 94% ee (Entry 12, Table 8). This part of the study was performed by Thierry León in his doctoral thesis. One explanation for this improvement of selectivity in the presence of an acid could be that acid addition favours the formation of the cationic complexes **X** instead of the neutral complexes **Y** which proven to be inactive in cycloaddition reactions (Figure 15).

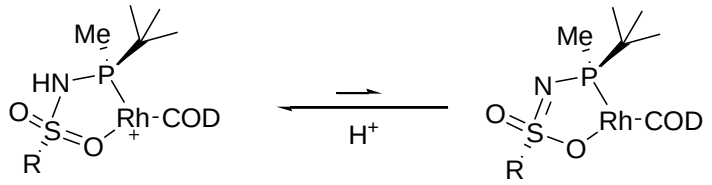

cationic complex, X **neutral complex, Y**

Figure 15. Possible explanation for the improvement of selectivities by adding acid to the reaction mixture.

Finally, for comparison, enediyne **26** was submitted to cyclization using the standard (*R*)-(+)-BINAP/$[Rh(COD)_2]BF_4$ (1:1) catalytic system to afford **29** in only 45% yield and 54% ee (Entry 13, Table 8). In these cases, when trifluoroacetic acid was added (10 mol %), the yield decreased whether or not the catalytic mixture was hydrogenated (Entries 14 and 15, Table 8).

Table 8. [2+2+2] intramolecular cycloaddition of enediynes catalysed by SIP-Rh complexes.

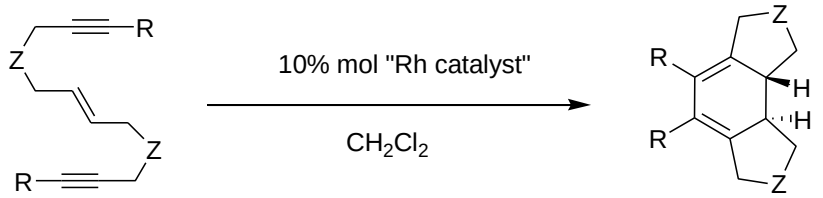

20: Z = O, R = H
27:Z = O, R = Me
28: Z = O, R = CO_2Me
21: Z = NTs, R = H
26: Z = NSO_2Mes, R = H

22: Z = O, R = H
30 : Z = O, R = Me
31: Z = O, R = CO_2Me
23: Z = NTs, R = H
29: Z = NSO_2Mes, R = H

Entry	Endiyne	Catalyst	Reaction Conditions	Conv (%)[a]	ee (%)[b]
1	**20**	**12**	reflux, 6h	99	59
2	**20**	**13**	reflux, 6h	99	63
3	**20**	**13**	r.t., 26h	98[c]	69
4	**27**	**13**	reflux, 22h	- [d]	-
5	**28**	**13**	reflux, 28h	- [d]	-
6	**21**	**13**	reflux, 8h	99	67
7	**21**	**13**	r.t., 15h	99	67
8	**21**	***(R)*-BINAP**[e,f]	r.t., 44h	26[g]	n.d.
9	**21**	***(R)*-H_8-BINAP**[e,f]	r.t., 44h	58[g]	n.d.
10	**21**	**13**	r.t., 24h, 10 mol%, HBF_4	99	90
11	**26**	**13**	reflux, 24h 10 mol% HBF_4	91[c]	83
12	**26**	**13**	reflux, 24h 10 mol% TFA	99	94
13	**26**	***(R)*-BINAP**[e]	reflux, 24h	45[c]	54
14	**26**	***(R)*-BINAP**[e,f]	reflux, 24h 10 mol% TFA	42[c]	n.d.
15	**26**	***(R)*-BINAP**[e]	reflux, 24h 10 mol% TFA	29[c]	52

[a] Conversion was determined by ^{1}H NMR spectroscopy. [b] In all cases the major product was the levorotatory one. [c] Yield of isolated product. [d] Enediyne was observed in the ^{1}H NMR of the crude. [e] A mixture of $[Rh(COD)_2]BF_4$/(*R*)-(+)-BINAP (1:1) was used as the catalyst. [f] Hydrogen gas was bubbled into the catalytic solution for 30 min., the hydrogen and solvent were then removed, the solvent was added again, and finally enediyne was introduced. [g] Yield determined by ^{1}H NMR.

As mentioned in the Introduction, cyclization of enediynes **20**, **21** and **26** can occur through pathways **I** or **II** (Scheme 51). It has been postulated that pathway **I**, which includes an early-stage stereodetermining step, provides a high level of stereocontrol, while pathway **II** leads to lower enantiomeric bias.[49]

DFT calculations of the intramolecular [2+2+2] cycloaddition of enediynes with different terminal substitution performed in our group[54] indicated that enediynes with terminal alkynes cyclize preferentially through initial alkyne-alkyne coupling (pathway **II**, Scheme 51), usually leading to low enantiomeric excess. Otherwise, the internal enediynes seems to cyclize through the more enantioselective pathway **I**.

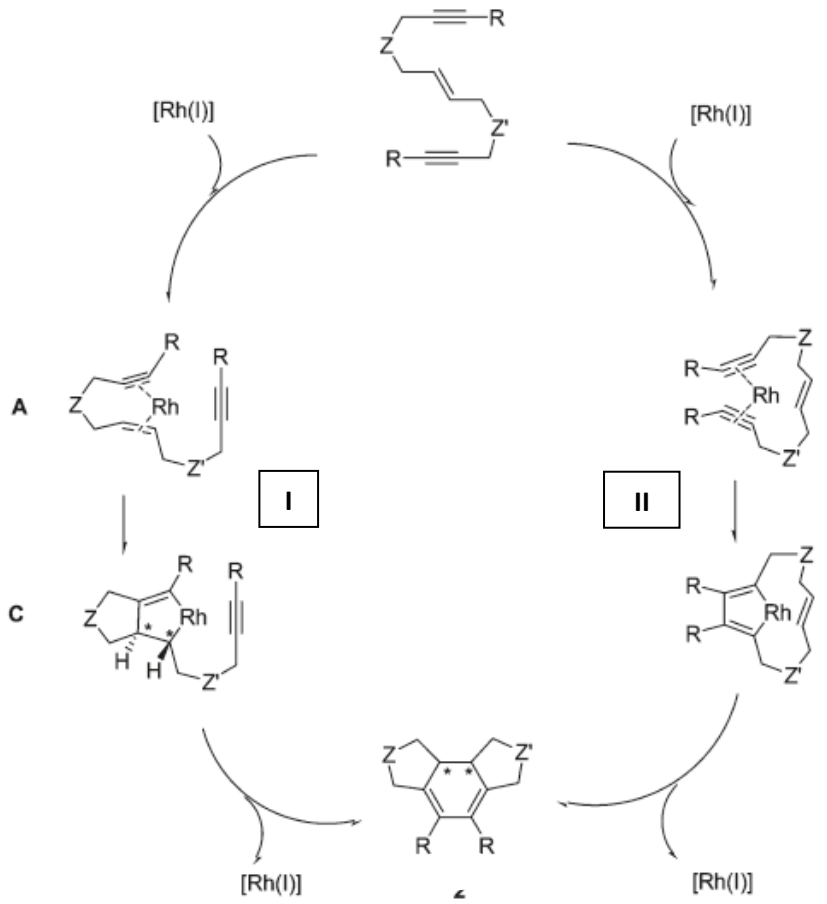

Scheme 51. Possible routes for the [2+2+2] cycloaddition process of enediynes.

According to the mechanistic hypothesis, the reaction pathway followed is pathway **II** (Scheme 51) as the iminophosphoranes showed to be active only for terminal enediynes. Most remarkably, the selectivities found in the study of new SIP preligands are the highest reported for terminal enediynes and thus highlight the utility of ligands with PH/NH tautomerism in catalysis.

All these results have been published in Angewandte Chemie.[55]

[54] Dachs, A.; Roglans, A.; Solà, M. *Organometallics* **2011**, *30*, 3151; b) Dachs, A.; Pla-Quintana, A.; Parella, T.; Solà, M.; Roglans, A. *Chem. Eur. J.* **2011**, *17*, 14493.
[55] León, T.; Parera, M.; Roglans, A.; Riera, A. Verdaguer, X. *Angew. Chem. Int. Ed*. **2012**, *51*, 6951.

3.2.4.3. Intramolecular [2+2+2] cycloaddition of macrocyclic enediyne catalysed by SIP-Rh complexes

Finally, we thought that it could be interesting to evaluate the activity and efficiency of cationic rhodium complex **13** in the cycloisomerization of the macrocyclic enediyne **24** (Scheme 52).

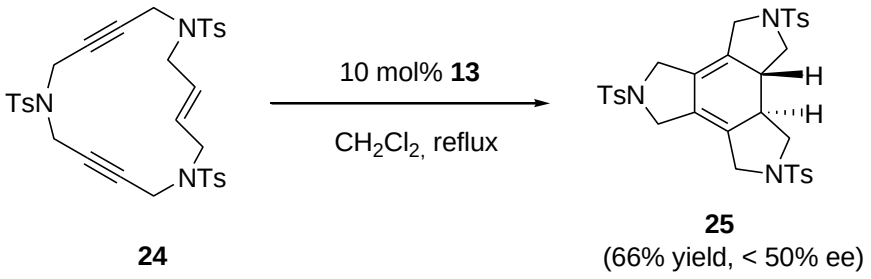

24 **25** (66% yield, < 50% ee)

Scheme 52. [2+2+2] cycloisomerization of macrocyclic enediyne **24** catalysed by Rh-complex **13**.

Thus, cyclohexadiene **25** was obtained with a 66% yield after 17 hours in refluxing dichloromethane showing that this new P-stereogenic-Rh complex was also active to the intramolecular [2+2+2] cycloisomerization of macrocyclic enediynes although the selectivity and yield did not improved the one obtained with S-stereogenic ligands (see, for instance, Table 7).

In conclusion, we have shown that *N*-phosphino *tert*-butylsulfinamide (PNSO) ligands are efficient in Rh(I)-catalysed [2+2+2] cycloaddition reactions. The scope of the cycloadditions has been firstly evaluated in the totally and partially intramolecular version of the [2+2+2] cycloaddition. The combination of $Rh(COD)_2]BF_4$ with PNSO ligand **1a** was found to be robust and applicable to a broad range of substrates independently of the nature of the linker between unsaturations and the substitution at the termini of the alkynes. We attribute the high activity of this complex to the hemilabile nature of the PNSO ligands since they provide vacant coordination sites to the substrate, so accelerating the cycloaddition process.

Moreover, the new catalytic system of $Rh(COD)_2]BF_4$ with PNSO ligand **1a** was also effective in the completely intramolecular cycloaddition of open-chained and macrocyclic enediynes. This process has been shown to be accelerated by PNSO ligands and in the case of (*E*)-enediynes, moderate enantiomeric excesses have been achieved. In PNSO ligands, the chiral information is located in the hemilabile moiety of the ligand, which can be far away from the metal center in the crucial C-C bond formation step. This fact may hinder the transfer of chiral information from the ligand to the cycloaddition product. For this reason, subsequent studies have been performed to improve the enantioselectivity in the [2+2+2] cycloaddition process by locating the chiral information closer to the metal center. To this aim, we disclosed *P*-stereogenic *N*-sulfonyl secondary iminophosphorane ligands as a novel class of preligands in metal catalysis.

These compounds are configurationally stable and thanks to the NH/PH tautomerism they do not undergo oxidation in air. We have shown that in the presence of a rhodium source, the tautomeric equilibrium is displaced towards the NH form allowing efficient P,O coordination with the metal centre. We have demonstrated that these rhodium complexes are efficient and selective catalysts for the [2+2+2] cycloaddition of enediynes with terminal alkynes. In this respect, our system provides good results where other existing methodologies fall short.

Chapter 4. Baylis-Hillman adducts as substrates of the [2+2+2] cycloaddition reaction

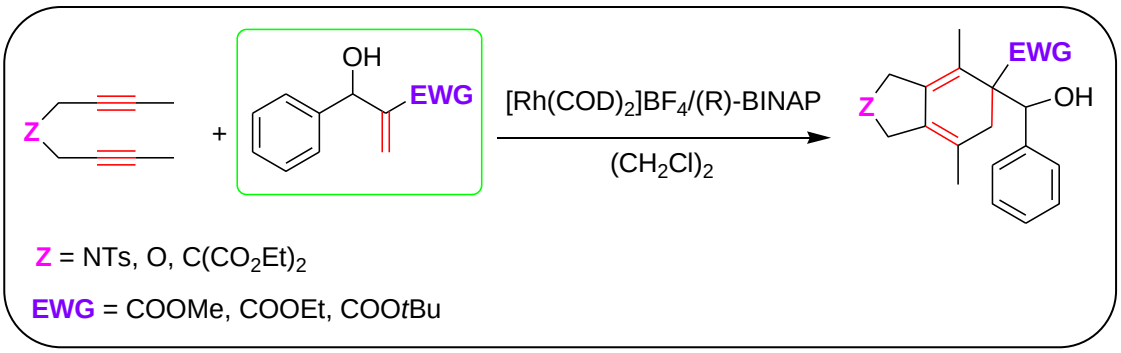

4.1. Precedents

4.1.1. Baylis-Hillman adducts

Baylis-Hillman adducts are densely functionalized molecules containing at least three functional groups in proximity which can participate in a wide range of organic transformations. Different perspectives of these compounds are pictorially presented in Figure 16.

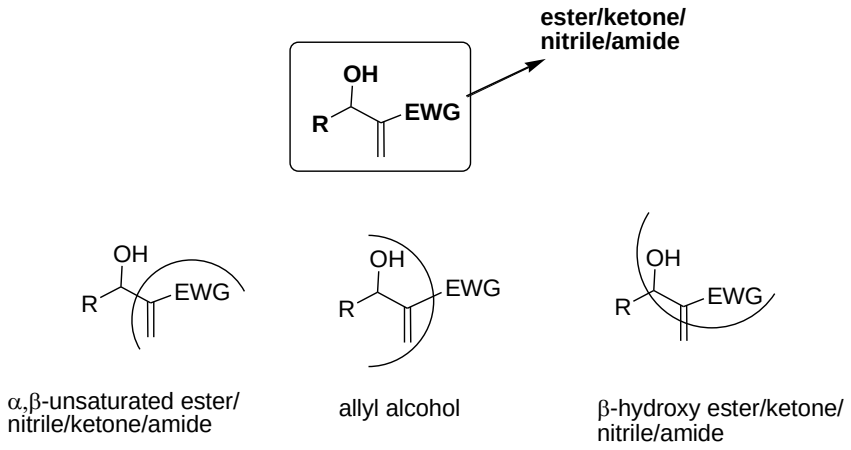

Figure 16. Baylis-Hillman adducts: different perspectives.

The synthesis of Baylis-Hillman (BH) adducts consists of a carbon-carbon bond-forming reaction, which involves an aldehyde and an activated alkene in the presence of a base. It is a three-step one-pot reaction involving successive Michael, aldol and elimination processes.[56] The reaction was discovered in 1968 when Morita reported that the reaction of an aldehyde with an activated alkene in the presence of tricyclohexylphosphine afforded a densely functionalized product (Scheme 53).[57] In 1972, Anthony Baylis and Melville Hillman were granted a German patent for performing the same reaction using a tertiary amine instead of a phosphine catalyst[58] (Scheme 53). Their greatest success was in the use of DABCO.

[56] For selected references related to the mechanistic aspects of this reaction, see: a) Amarante, G. W.; Benassi, M.; Milagre, H. M. S.; Braga, A. A. C.; Maseras, F.; Eberlin, M. N.; Coelho, F. *Chem. Eur. J.* **2009**, *15*, 12460; b) Amarante, G. W.; Milagre, H. M. S.; Vaz, B. G.; Ferreira, B. R. V.; Eberlin, M. N.; Coelho, F. *J. Org. Chem*. **2009**, *74*, 3031; c) Roy, D.; Sunoj, R. B. *Org. Lett*. **2007**, *9*, 4873; d) Robiette, R.; Aggarwal, V. K.; Harvey, J. N. *J. Am. Chem. Soc*. **2007**, *129*, 15513; e) Santos, L. S.; da Silveira Neto, B. A.; Consorti, C. S.; Pavam, C. H.; Almeida, W. P.; Coelho, F.; Dupont, J.; Eberlin, M. N. *J. Phys. Org. Chem.* **2006**, *19*, 731; f) Aggarwal, V. K.; Fulford, S. Y.; Lloyd-Jones, G. C. *Angew. Chem. Int. Ed*. **2005**, *44*, 1706; g) Price, K. E.; Broadwater, S. J.; Walker, B. J.; McQuade, D. T. *J. Org. Chem*. **2005**, *70*, 3980; h) Price, K. E.; Broadwater, S. J.; Jung, H. M.; McQuade, D. T. *Org. Lett*. **2005**, *7*, 147; i) Santos, L. S.; Pavam, C. H.; Almeida, W. P.; Coelho, F.; Eberlin, M. N. *Angew. Chem. Int. Ed*. **2004**, *43*, 4330.

[57] Morita, K.; Suzuki, Z.; Hirose, H. *Bull. Chem. Soc. Jpn*. **1968**, *41*, 2815.

[58] Baylis, A. B.; Hillman, M.E.D. *German Patent* 2155113, 1972; *Chem. Abstr*. **1972**, *77*, 34174.

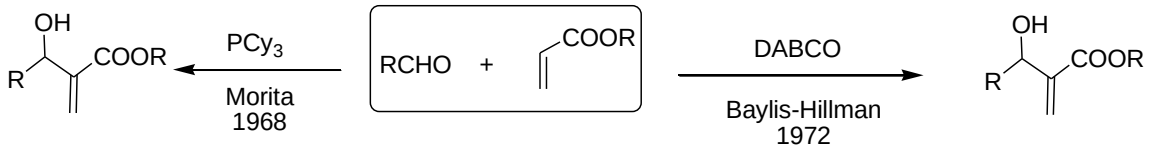

Scheme 53. Morita and Baylis-Hillman reactions.

In 1983, the reaction was taken up again and its scope was explored by Drewes and Basavaiah.[59] Since then, the scope of the reaction has broadened beyond the use of just aldehydes and acrylates to include alkyl vinyl ketones, acrylonitriles, vinyl sulfones among other groups.

The most generally accepted mechanism[60] of the amine-catalysed reaction is illustrated in Scheme 54, taking as a model the reaction between methyl vinyl ketone (as the activated alkene) and benzaldehyde (as the electrophile) under the catalytic influence of DABCO. The first step in this catalytic cycle involves the Michael-type nucleophilic addition of the tertiary amine to the activated alkene to produce a zwitterionic enolate, which makes a nucleophilic attack on the aldehyde in an aldol fashion to generate another zwitterion. Subsequent proton migration and release of the catalyst provide the desired multifunctional molecules. The main drawback of the Baylis-Hillman reaction is the extremely slow reaction rate. As the reaction can take from days to weeks to complete, considerable effort has been made to develop more efficient catalytic systems.

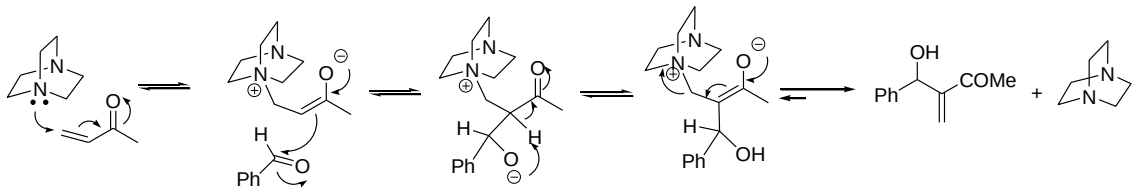

Scheme 54. Generally accepted mechanism of Baylis-Hillman reaction.

Of the multiple transformations in which BH adducts can be involved,[61] their use in the synthesis of cyclic compounds is particularly noteworthy (Scheme 55).

[59] Drewes, S.E.; Roos, G.H.P. *Tetrahedron* **1988**, *44*, 4653.

[60] a) Hill, J.S.; Isaacs, N.S. *J. Phys. Org. Chem*. **1990**, *3*, 285; b) Bode, M.L.; Kaye, P.T. *Tetrahedron Lett*. **1991**, *32*, 5611; c) Fort, Y.; Berthe, M.C.; Caubere, P. *Tetrahedron* **1992**, *48*, 6371; d) Basavaiah, D.; Dharma Rao, P.; Suguna Hyma, R. *Tetrahedron* **1996**, *52*, 8001; e) Ciganek, E. *Organic Reactions*: Paquette, L.A., Ed.; Wiley: New York, **1997**; Vol. 51, p 201; f) Langer, P. *Angew. Chem. Int. Ed*. **2000**, *39*, 3049.

[61] For reviews of BH adducts applications, see: Basavaiah, D.; Veeraraghavaiah, G. *Chem. Soc. Rev*. **2012**, *41*, 68; b) Basavaiah, D.; Reddy, B.S.; Badsara, S.S. *Chem. Rev*. **2010**, *110*, 5447; c) Declerck, V.; Martinez, J.; Lamaty, F. *Chem. Rev.* **2009**, *109*, 1; d) Singh, V.; Batra, S. *Tetrahedron* **2008**, *64*, 4511; e) Basavaiah, D.; Rao, K.V.; Reddy, R.J. *Chem. Soc. Rev*. **2007**, *36*, 1581; f) Basavaiah, D.; Rao, A. J.; Satyanarayana, T. *Chem. Rev*. **2003**, *103*, 811; g) Ref 60d.

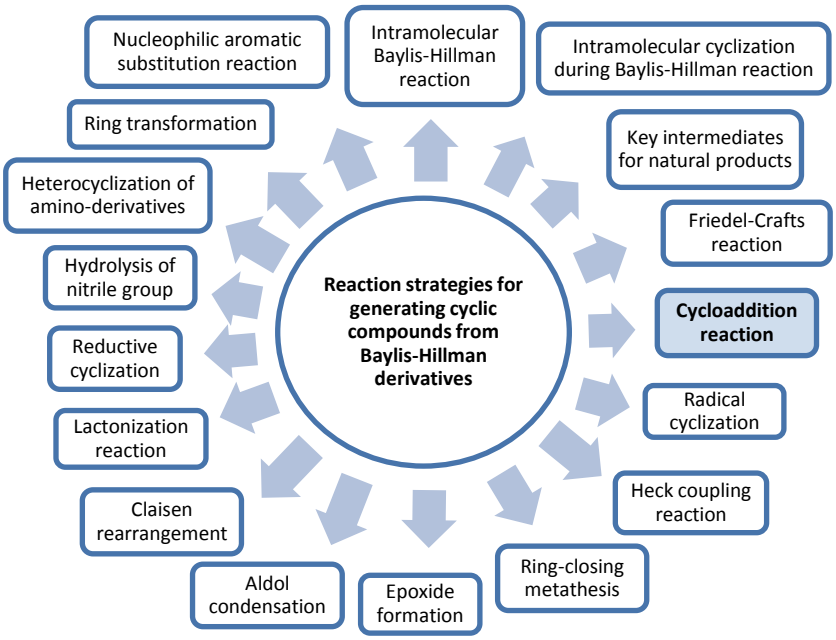

Scheme 55. Reaction strategies employed on the Baylis-Hillman derivatives for the generation of cyclic compounds.

BH adducts have been involved in Diels-Alder, [3+2] cycloaddition and 1,3-dipolar cycloaddition reactions. To the best of our knowledge, only Wang et al.[62] have reported the use of transition metals as catalysts for cycloaddition reactions in describing the use of BH adducts as effective dipolarophiles in copper(I)-catalysed 1,3-dipolar cycloaddition with azomethine ylides to construct pyrrolidine derivatives containing one quaternary and two tertiary stereogenic centres (Scheme 56).

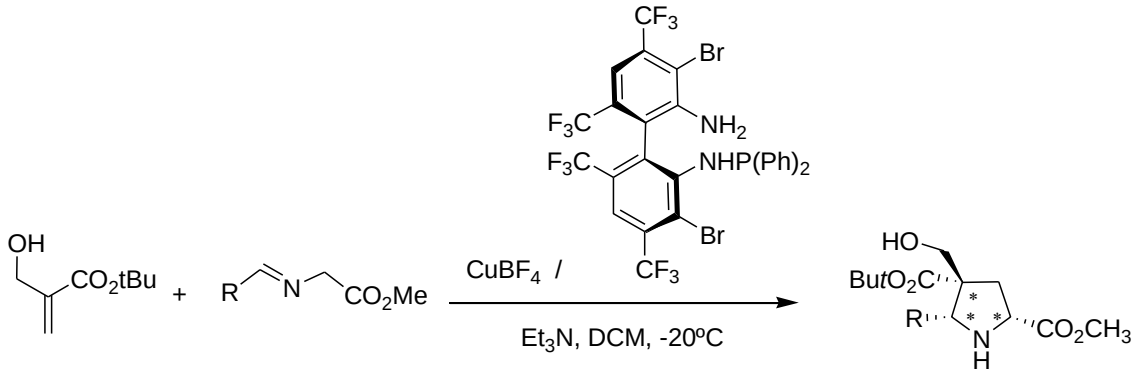

Scheme 56. Cu(I)-catalysed asymmetric 1,3-dipolar cycloaddition of various azomethine ylides with Baylis–Hillman adduct.

[62] Teng, H-L.; Huang, H.; Tao, H-Y.; Wang, C-J. *Chem. Commun*. **2011**, 5494.

4.1.2. [2+2+2] cycloaddition reactions between 1,1-disubstituted alkenes and diynes

There are few examples of [2+2+2] cycloaddition reactions between alkynes and 1,1-disubstituted alkenes. Shibata et al.[63] in 2006 reported the construction of chiral spirocyclic structures by [2+2+2] cycloaddition of diynes and *exo*-methylene cyclic compounds. In the same study, the authors describe three examples of [2+2+2] cycloaddition reactions of a diyne with acrylates as the alkenes (Scheme 57).

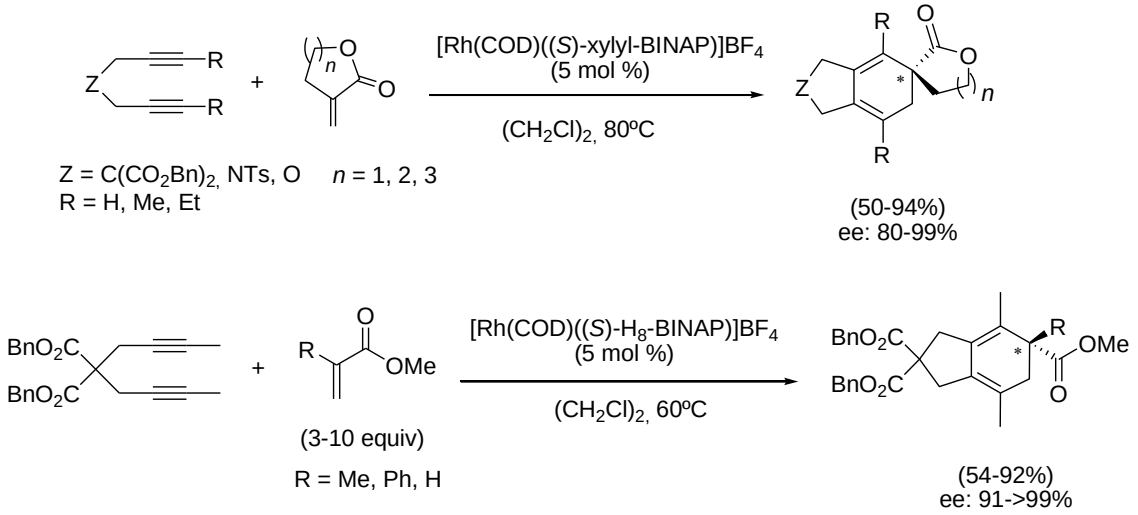

Scheme 57. [2+2+2] cycloaddition between 1,6-diynes and asymmetric alkenes.

Shibata et al.[64] also described four cases involving unfunctionalized 1,1-disubstituted alkenes in partially intramolecular Rh-catalysed [2+2+2] cycloaddition (Scheme 58). Good yields and enantioselectivities of bicyclic cyclohexa-1,3-dienes were obtained by using an excess of the corresponding alkenes.

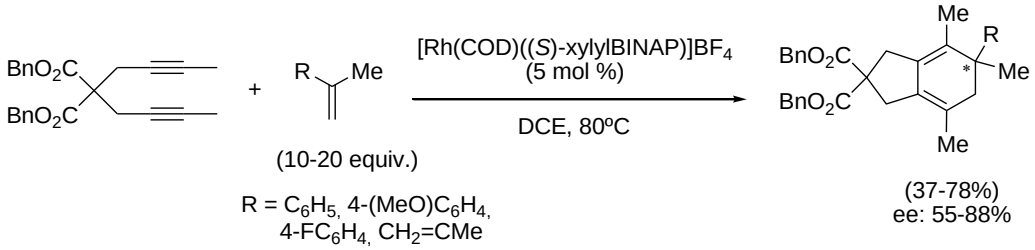

Scheme 58. Enantioselective [2+2+2] cycloaddition of diyne with styrene derivatives.

In 2008, Tanaka et al.[65] described the enantioselective synthesis of α,α–disubstituted α–amino acids by Rh-catalysed [2+2+2] cycloaddition of 1,6-diynes with protected dehydroamino acid

[63] Tsuchikama, K.; Kuwata, Y.; Shibata, T. *J. Am. Chem. Soc.* **2006**, *128*, 13686.
[64] Shibata, T.; Kawachi, A.; Ogawa, M.; Kuwata, Y.; Tsuchikama, K.; Endo, K. *Tetrahedron* **2007**, *63*, 12853.
[65] Tanaka, K.; Takahashi, M.; Imase, H.; Osaka, T.; Noguchi, K.; Hirano, M. *Tetrahedron* **2008**, *64*, 6289.

(Scheme 59). It is noteworthy that in this case only a slight excess of protected dehydroamino acid was necessary without the slow addition of diyne. They found that the use of sterically demanding phosphines (Segphos or xyl-BINAP) significantly decreased the yield.

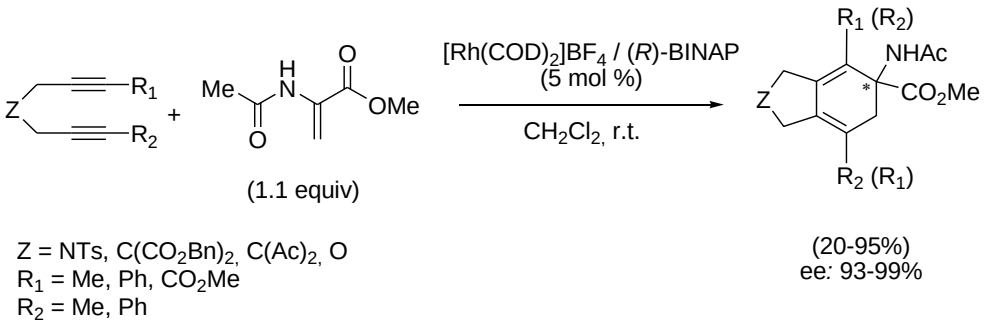

Scheme 59. Rh(I)-catalysed enantioselective [2+2+2] cycloaddition of diynes with dehydroaminoacid.

More recently, the same group[66] published the enantioselective construction of bridged multicyclic skeletons through a partially intramolecular [2+2+2] cycloaddition/intramolecular Diels-Alder reaction cascade. Amide-linked 1,5-dienes were used as the alkene partners (Scheme 60).

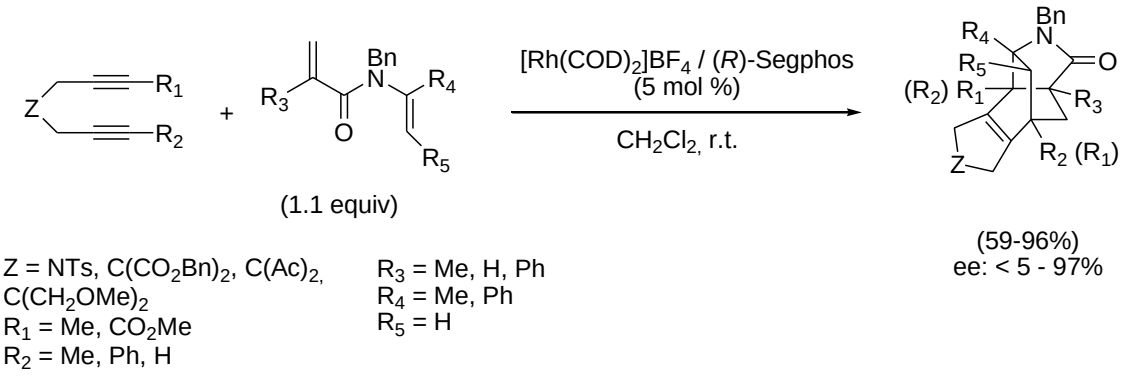

Scheme 60. Enantioselective cycloaddition cascade of 1,6-diynes with 1,5-dienes.

To the best of our knowledge, the participation of Baylis-Hillman adducts as alkene substrates in transition metal-catalysed [2+2+2] cycloaddition reactions has not been reported previously. For this reason, we decided to study the partially intramolecular [2+2+2] cycloaddition of symmetrical diynes with Baylis-Hillman adducts as 1,1-disubstituted alkenes in order to obtain bicyclic cyclohexa-1,3-dienes with a quaternary stereocentre (Scheme 61). We proposed the catalyst based on $[Rh(COD)_2]BF_4$ in combination with chiral diphosphines for these reactions since this system has, as has previously been commented, proven to be very useful in other examples of asymmetric [2+2+2] cycloadditions.

[66] Kobayashi, M.; Suda, T.; Noguchi, K.; Tanaka, K. *Angew. Chem. Int. Ed*. **2011**, *50*, 1664.

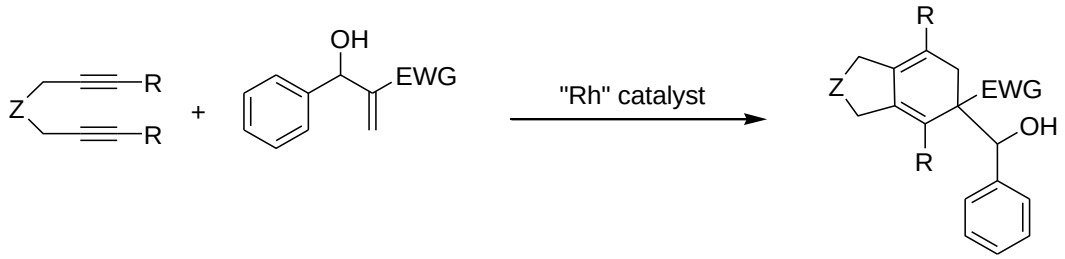

Scheme 61. [2+2+2] cycloaddition reactions between diynes and Baylis-Hillman adducts catalysed by $[Rh(COD)_2]BF_4$ with chiral diphosphines.

Therefore, the main goal of the study described in this section is to determine the reactivity of Baylis-Hillman adducts as new substrates involved in the partially intramolecular [2+2+2] cycloaddition reaction in combination with 1,6-diynes for the synthesis of chiral polysubstituted cyclohexa-1,3-dienes. The specific objectives of this study are:

- To determine the reactivity of different substituted BH adducts in the [2+2+2] cycloaddition reaction.

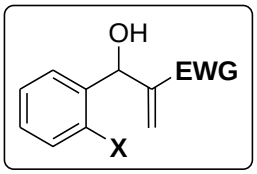

- To study the scope of the reaction (tethers and substituents on the diyne reagent).
- To study the chemoselectivity of the process.
- To study the diastereo- and enantioselectivity of the process.

4.2. Results and discussion

4.2.1. Synthesis of Baylis-Hillman substrates

The Baylis-Hillman adducts used as substrates were synthesized in the laboratories of the Université de Reims Champagne-Ardenne as a result of a four-month mobility grant to carry out a project entitled "intramolecular Heck cyclization of Baylis-Hillman adducts" under the supervision of Dr. Jean Le-Bras. A palladium-catalysed Heck 5-*endo-trig* cyclisation of Baylis-Hillman adducts with an *o*-bromosubstituted or an unsubstituted aryl and different electron withdrawing groups (COR, COOR and CN) was studied in this project (Scheme 62).

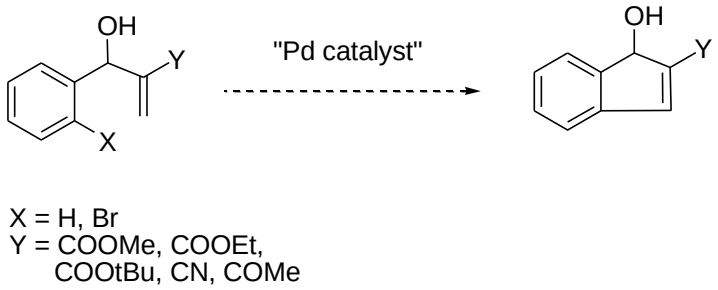

Scheme 62. Intramolecular Heck cyclisation of Baylis-Hillman adducts.

Hence, we decided to test some of the BH adducts prepared during the stay in the laboratories of Dr. Le-Bras as unsaturated substrates for the [2+2+2] cycloaddition reactions. In this case, β-hydroxy esters **32a-c** and **32e-g** as well as nitrile **32d** and ketone **32h** were the substrates of choice (Figure 17).

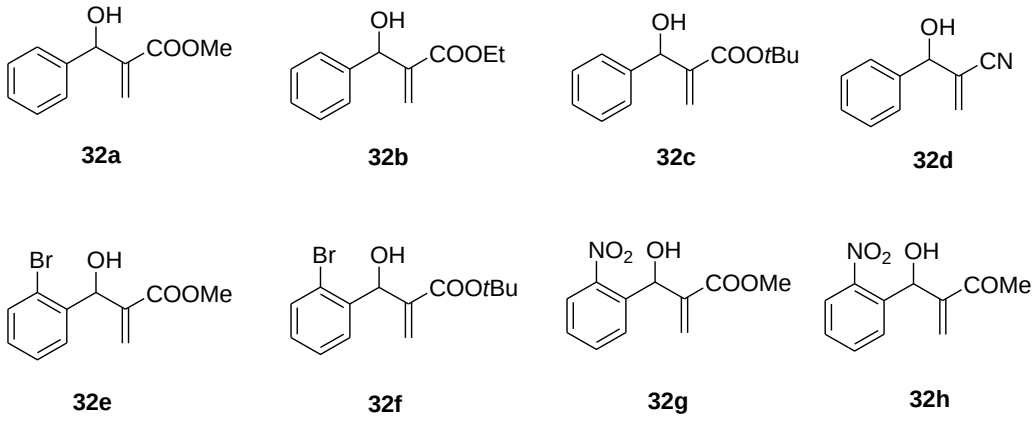

Figure 17. Baylis-Hillman substrates prepared and tested in this study.

The synthesis of the BH adducts was optimized starting from benzaldehyde **33** and different alkenes (Table 9). We first investigated some of the methods described in the literature based on the use of dioxane[67], acetonitrile[68] or a mixture of polyethylene glycol:water[69] as solvents

[67] Rafel, S.; Leahy, J.W. *J. Org. Chem*. **1997**, *62*, 1521.

(Entries 1-3, Table 9). None of these conditions allowed the formation of product **32a** so we then tested the use of polyethylene glycol with a molecular weight of 200 g/mol (PEG-200) as the solvent.[70] The use of PEG is described[70] as a recyclable solvent medium for the rapid Baylis–Hillman reaction between unreactive aldehydes and activated olefins. We started using a 20% mol of DABCO at room temperature. With these conditions, the reaction afforded only a 50% conversion of **33** after 1 day (Entry 4, Table 9). Changing the solvent for the heavier PEG-400 did not improve the results (Entry 5, Table 9). In order to improve the conversion and the reaction time, stochiometric amounts of DABCO were then used with the different acrylates and moderate yields of the Baylis Hillman adducts were obtained (Entries 6-8, Table 9). It should be noted that the reactivity of acrylates decreases with the size of substituent R since the reaction time is longer and the yields are decreased.[71] Acrylonitrile was then tested as the alkene partner. BH adduct **32d** was obtained in a high yield using only a 50 mol % of DABCO (Entry 9, Table 9). In an attempt to reducing the amount of catalyst required, the reaction was tested using a 20 mol% of DABCO but only a moderate yield of **32d** was obtained after 3 days at room temperature (Entry 10, Table 9).

Table 9. Synthesis of Baylis-Hillman substrates starting from benzaldehyde **33**.

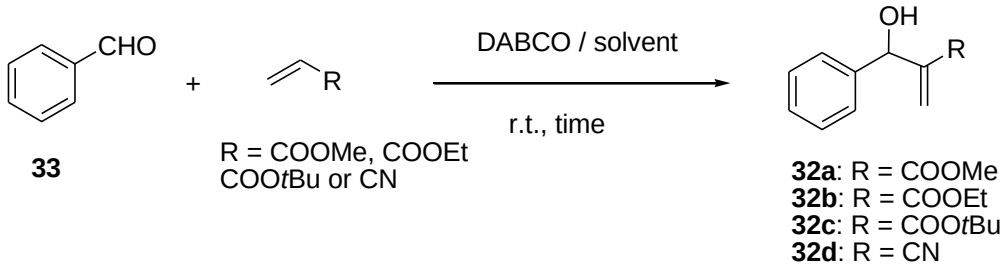

Entry	R	SOLVENT	% molar DABCO	t (h)	Product, Yield (%)
1	COOMe	dioxane	9	16	-
2	COOMe	CH_3CN	50	2	-
3	COOMe	PEG/H_2O (1:1)	20	72	-
4	COOMe	PEG-200	20	24	[a]
5	COOMe	PEG-400	20	24	[b]
6	COOMe	PEG-200	100	29	**32a**,73
7	COOEt	PEG-200	100	52	**32b**, 68
8	COO*t*Bu	PEG-200	100	72	**32c**, 48
9	CN	PEG-200	50	48	**32d,** 89
10	CN	PEG-200	20	72	**32d**, 53

[a] Ratio **33:32a** = 49:51, calculated by GC-MS. [b] **33:32a** =79:21.

[68] Lee, W-D.; Yang, K-S.; Chen, K. *Chem. Comm*. **2001**, 1612.

[69] The use of protic solvents to accelerate the reaction rate is described in: a) Aggarwal, V. K.; Dean, D. K.; Mereu, A.; Williams, R. *J. Org. Chem.* **2002**, *67*, 510; b) Augé, J.; Lubin, N.; Lubineau, A. *Tetrahedron Lett.* **1994**, *35*, 7947.

[70] a) Aravind, A.; George, S.; Kumar, S. *Chem. Cent. J.* **2012**, *6*, 30; b) Chandrasekhar, S; Narsihmulu, Ch; Saritha, B; Sultana, S. S. *Tetrahedron Lett.*, **2004**, *45*, 5865.

[71] a) Ref.69a; b) Aggarwal, V. K.; Mereu, A.; Tarver, G. J.; McCague, R. *J. Org. Chem.* **1998**, *63*, 7183; c) Ref. 60e; d) Aggarwal, V. K.; Tarver, G. J.; McCague, R. *Chem. Commun.* **1996**, 2713.

In addition, *ortho*-substituted BH adducts **32e-h** were prepared following the same procedure starting from the commercially available *ortho*-substituted benzaldehydes with good to excellent yields (Table 10).

Table 10. Synthesis of *ortho*-substituted BH adducts.

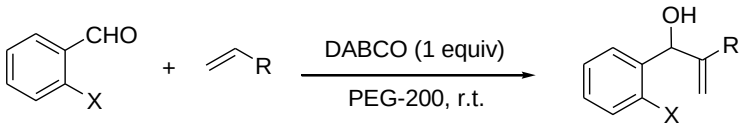

32e: X = Br, R = COOMe
32f: X = Br, R = COO^tBu
32g: X = NO_2, R = COOMe
32h: X = NO_2, R = COMe

Entry	X	R	t (h)	Product, Yield (%)
1	Br	COOMe	24	**32e**, 75
2	Br	COO^tBu	96	**32f**, 72
3	NO_2	COOMe	5.5	**32g,** 99
4	NO_2	COMe	24	**32h**, 55

4.2.2. Synthesis of diyne substrates

1,6-diynes used in this section are represented in Figure 18. We chose non-terminal diynes since they are less prone to [2+2+2] homocoupling reactions. We also wanted to evaluate the reactivity of heteroatom-linked diynes such as *N*-tosyl- and oxygen-linked diynes **16a, 34a, 34c** and **34d** and compare it with the reactivity of carbon-tethered diynes such as **16c**. 5-methyl-2-pyridinesulfonamide derivative **34b** had already been synthesised in our laboratories and we decided to test the effect of the coordination ability of pyridine in this reaction. Terminal substitution of diynes was also evaluated using different substituents such as esters (**34c**) or a phenyl group (**34d**). We also decided to test terminal diyne **16c**, which is commercially available, in order to compare its reactivity with that of the internal diynes.

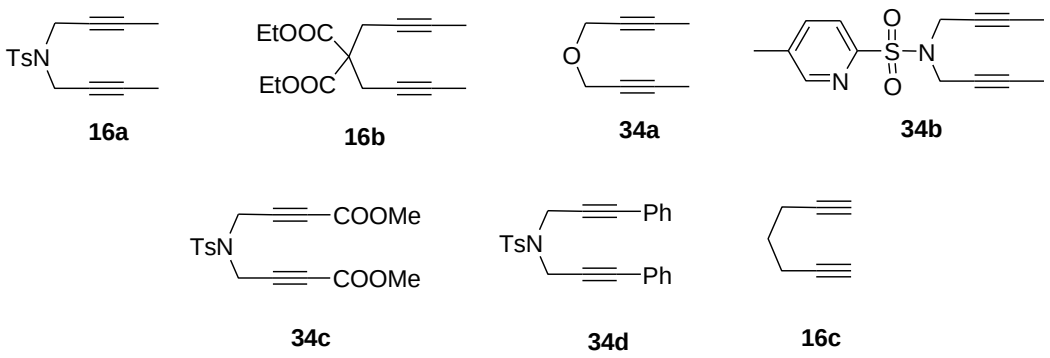

16a **16b** **34a** **34b**

34c **34d** **16c**

Figure 18. Diynes used in this study.

Whereas some of the substrates are commercially available or had already been prepared in our laboratories, diynes **34b**,[72] **34c**,[73] and **34d**[74] were prepared in accordance with the methods described in the literature.

For the synthesis of diyne **34b**, commercially available 5-methyl-2-pyridinesulfonamide **35** was reacted with 2 equivalents of alkylating agent 1-bromo-2-butyne in acetonitrile at reflux with an excess of potassium carbonate as a base to afford an 83% yield of dialkylated product (Scheme 63).

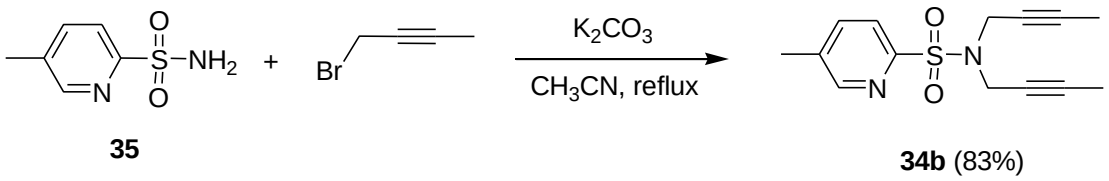

35 **34b** (83%)

Scheme 63. Synthesis of diyne **34b**.

The other two diynes **34c** and **34d** were prepared from diyne **16d**, the synthesis of which has already been described in Chapter 3. **16d** was treated with 2.2 equivalents of *n*-butyl lithium in anhydrous THF at -78ºC, followed by the addition of an excess of methyl chloroformate at this temperature in order to synthesize diyne **34c** (Scheme 64). After 22 hours at room temperature, the reaction was stopped to afford a mixture of diyne **34c** in a 12% yield together with a 41% yield of monosubstituted diyne **34cm**, which was then separated by column chromatography. The low yield obtained for diyne **34c** was possibly due to the low quantity of base used. The reaction was not optimised as the amounts of **34c** were sufficient for the catalytic tests.

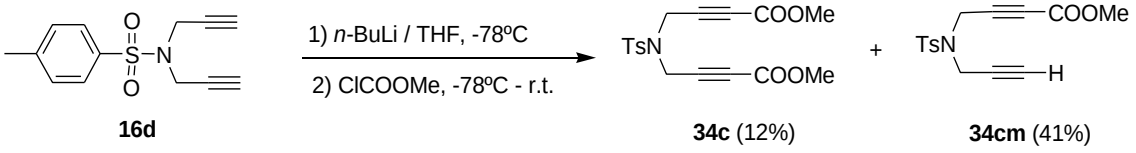

16d **34c** (12%) **34cm** (41%)

Scheme 64. Synthesis of diynes **34c** and **34cm**.

In order to introduce two phenyl groups in the terminal position of diyne **16d** we considered the Sonogashira cross-coupling reaction, which consists on the alkynylation of aryl halides by using a palladium catalyst with catalytic amounts of Cu(I) iodide as the cocatalyst. For the

[72] Nishida, M.; Shiga, H.; Mori, M. *J. Org. Chem*. **1998**, *63*, 8606.
[73] Kurokawa, H.; Kanda, K.; Shibata, T. *J. Org. Chem.* **2007**, *72*, 6521.
[74] Chen, Y.; Dubrovskiy, A.; Larock, R. C. *Org. Synth*. **2012**, *89*, 294.

synthesis of **34d**, a small excess of phenyl iodide, 10 mol % of copper iodide and 5 mol % of bis(triphenylphosphine)palladium dichloride catalyst was used. Triethylamine was used as a base and DMF as the solvent. After 19 hours at room temperature, the reaction was completed to afford a 23% yield of diyne **34d** (Scheme 65).

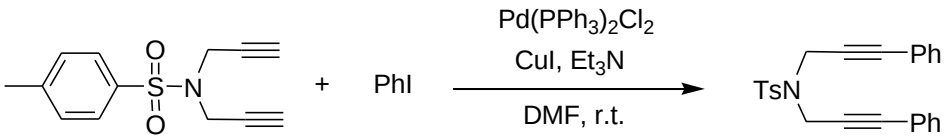

16d **34d** (23%)

Scheme 65. Synthesis of diyne **34d** by Sonogashira cross-coupling.

4.2.3. [2+2+2] cycloaddition of diynes and Baylis-Hillman adducts

Given that the partially intramolecular [2+2+2] cycloaddition between diynes and alkenes is a difficult reaction in terms of chemoselectivity and alkenes are less reactive than alkynes, 10 mol % of $[Rh(COD)_2]BF_4$/diphosphine mixture was used as the catalyst and 1,2-dichloroethane was the solvent of choice to make it possible to work at different temperatures.

We first investigated a Rh-BINAP catalysed reaction of *N*-tosyl-tethered symmetric diyne **16a** with 1.5 equivalents of BH adduct **32a** in dichloroethane at reflux. Only undesired products **36** and **37** (Figure 19) from the homocoupling reaction of **16a** and isomerization of BH adduct **32a** were obtained, respectively, when using *rac*-BINAP as the phosphine. One way to reduce homocoupling is to work with a high excess of monoalkene. However, this strategy was not explored due to the isomerization of the BH adduct observed in the reaction conditions. Thus, in all the cases that follow, 1.5 equivalents of BH adduct were used.

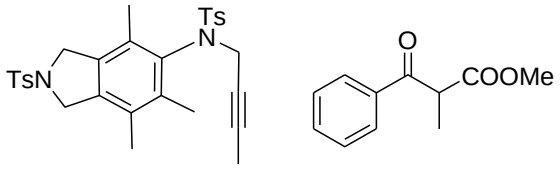

36 **37**

Figure 19. Homocoupling product **36** and isomerization product **37** obtained when the [2+2+2] cycloaddition reaction of **16a** and **32a** was performed with conventional heating.

Microwave-assisted organic synthesis (MAOS)[75] usually allows a dramatic diminution of the reaction time, an increase in yields and greater purity of the products. This fact can be

[75] For a monography about *MAOS*, see: a) *Microwave-Assisted Organic Synthesis*; Lidström, P.; Tierney, J. P. Eds.; Blackwell Scientific: Oxford, **2004**. For reviews, see: b) Kappe, C. O.; Dallinger, D. *Nature Rev.* **2006**, 5, 51; c) de la Hoz, A.; Díaz-Ortiz, A.; Moreno, A. *Chem. Soc. Rev.* **2005**, 34, 164; d) Kappe, C. O. *Angew. Chem. Int. Ed.* **2004**, 43, 6250.

explained through the temperature gradient inversion, which can be achieved by microwave irradiation instead of by conventional heating, due to the homogeneous heating which is achieved inside the reaction vessel by the direct coupling of the microwave energy with the molecules (solvent, reagents, catalyst) of the reaction mixture. Special conditions which can be achieved through the microwave heating cause, in some cases, modifications in the selectivity (chemo-, regio- and stereoselectivity) and, even, unusual reactivities.

The effect of microwave as the heating source (method **A**) was then evaluated by running the reaction in the microwave oven at a temperature of 80ºC for 10 minutes. A 55% yield of a cycloadduct was obtained and the formation of both homocoupled and isomerization products was supressed. A ^{1}H NMR analysis of the cycloadduct showed the formation of only one of the two possible diastereoisomers that can be formed (Scheme 66). The fact that one of the stereocentres generated is quaternary has made it difficult to identify the geometry of the diastereoisomer formed for the moment. Further work on this topic is needed.[76]

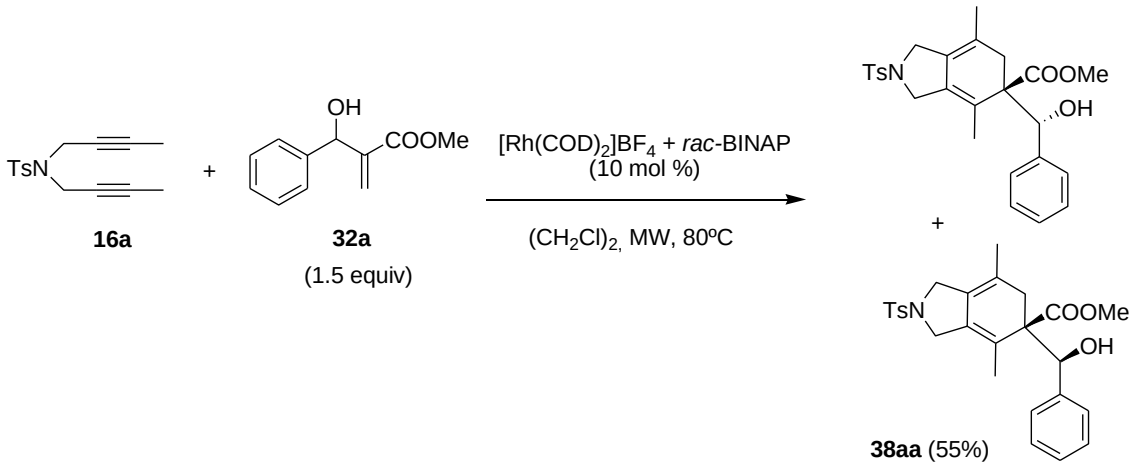

Scheme 66. [2+2+2] cycloaddition reaction between diyne **16a** and BH adduct **32a** leading to the formation of diastereoisomers.

As this was a diastereoselective process, we tackled the stereoselectivity study of this cycloaddition using different chiral phosphines (Table 11). The same reaction was repeated using the chiral (*R*)-BINAP ligand. A similar yield and excellent enantioselectivity of **38aa** was achieved after only 20 minutes at 60ºC (Entries 1 and 2, Table 11). Having started from a racemic mixture of the Baylis-Hillman adduct **32a**, an enantioenriched cycloadduct was obtained. This can only be explained if only one of the enantiomers of the Baylis-Hillman adduct has reacted in the [2+2+2] cycloaddition, suggesting that a kinetic resolution is operating.

[76] Since it has not been possible to identify which diastereoisomer has been formed, from here on the structure of the cycloadduct is represented without indicating the relative stereochemistry.

Another way in which a [2+2+2] homocoupling reaction may be avoided is through the slow addition of diyne[77] (method **B**) to the mixture of catalyst and **32a** using a syringe pump. In performing this experiment here, a similar yield was achieved but the enantioselectivity of **38aa** was less than the values obtained with microwave heating (compare Entry 3 with Entries 1-2, Table 11). It is noteworthy to comment here that when slow addition of the diyne was used homocoupling of **16a** was suppressed but isomerization of the BH adduct still occurred.

Given that microwave irradiation allowed shorter reaction times than conventional heating to obtain almost the same yield of **38aa** and better enantioselectivity, several BINAP derivatives were examined as chiral ligands under microwave irradiation in dichloroethane at 60ºC (Entries 4-6, Table 11). A good yield and excellent enantiomeric excess were obtained using (*R*)-H_8-BINAP as the ligand (Entry 4, Table 11). When (*R*)-Segphos was used, lower yield and enantiomeric excess were obtained (Entry 5, Table 11). With (*R*)-DTBM-Segphos, only starting material was observed after 40 minutes (Entry 6, Table 11) even when the reaction temperature was increased up to 80ºC. As a result, (*R*)-BINAP was chosen as the ligand of choice for the rest of the study.

We then tested (*S*)-BINAP to determine if it was possible to make the other enantiomer of the BH adduct to react. An 81% enantiomeric excess of the opposite enantiomer was obtained although with a lower yield than when using (*R*)-BINAP (Entry 7, Table 11).

[77] a) Sambaiah, T.; Li, L.P.; Huang, D. J.; Lin, C. H.; Rayabarapu, D. K.; Cheng, C. H. *J. Org. Chem*. **1999**, 3663; b) Ref. 65; c) Ref.63.

Table 11. Screening of phosphines for the [2+2+2] cycloaddition of diyne **16a** and BH adduct **32a**.

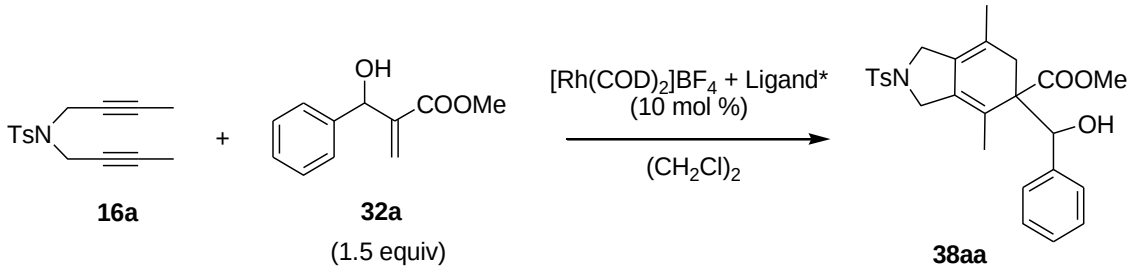

16a + **32a** (1.5 equiv) → **38aa**

Entry	Ligand	T (ºC)	t	Method[a]	Yield (%)[b]	ee (%)[c]
1	(*R*)-BINAP	60	20 min	**A**	50	93
2	(*R*)-BINAP	60	20 min	**A**	45	94[d]
3	(*R*)-BINAP	84	4.5 h	**B**	55[e]	73
4	(*R*)-H_8-BINAP	60	20 min	**A**	47	95
5	(*R*)-Segphos	60	20 min	**A**	35	72
6	(*R*)-DTBM-Segphos	80	40 min	**A**	-	-
7	(*S*)-BINAP	60	20 min	**A**	24	81[g]

[a] Method **A**: microwave heating. Method **B**: conventional heating and slow addition of diyne with syringe pump for 4 h. [b] Isolated product. [c] Calculated by chiral HPLC. [d] Calculated from the crude. [e] Isomerization product **37** was obtained together with the product. [g] The enantiomer obtained in this case was the opposite to that obtained using (*R*)-BINAP.

Using the conditions of methods **A** and **B** and BINAP as phosphine, different Baylis-Hillman adducts (**32b**-**d**) were subjected to the present enantioselective [2+2+2] cycloaddition (Table 12). The reaction with ethyl ester **32b** was first performed with (*R*)-BINAP under conventional heating with a slow addition of the diyne **16a** (Method **B**) and a moderate yield and lower enantioselectivity of **38ab** than that achieved with the methyl ester **32a** was obtained (compare Entry 3 of Table 11 and Entry 1 of Table 12). When (*S*)-BINAP was used for the same reaction, a good yield was also obtained but the enantioselectivity decreased significantly (Entry 2, Table 12). With ethyl ester **32b**, the use of microwave heating (Method **A**) did not improve the yield at 70ºC although the enantioselectivity was also good (Entry 3, Table 12). *Tert*-butyl ester **32c** proved to be less reactive than **32b** using the conditions of Method **B** since only a 32% yield of product **38ac** was obtained together with homocoupling product **36** (Entry 4, Table 12). However, high enantioselectivity was achieved. When acrylonitrile **32d** was tested under both conditions (Method **A** and **B**), the desired cycloadduct **38ad** was not obtained in none case. Therefore, the BH adduct with a nitrile as the electron withdrawing group was not a

good substrate for the [2+2+2] cycloaddition given that only starting material **16a** and the homocoupling product **36** were obtained in the two cases (Entries 5 and 6, Table 12).

Table 12. Effect of electron withdrawing group of BH adducts on yields and ee values of cyclohexa-1,3-dienes **38**.

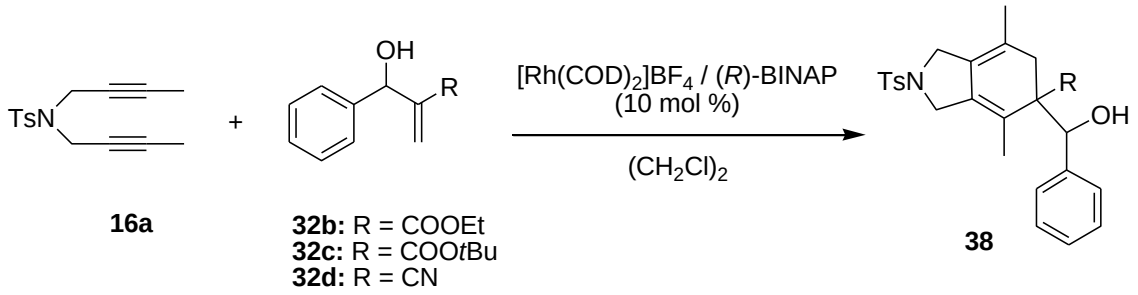

16a

32b: R = COOEt
32c: R = COO*t*Bu
32d: R = CN

38

Entry	BH adduct	BINAP	T (ºC)	t	Method[a]	Compound, Yield (%)	ee (%)[b]
1	**32b**	(*R*)-BINAP	84	4 h	**B**	**38ab**, 48	80
2	**32b**	(*S*)-BINAP	84	4 h	**B**	**38ab**, 53	58[c]
3	**32b**	(*R*)-BINAP	70	20 min	**A**	**38ab,** 21	84
4	**32c**	(*R*)-BINAP	84	4.5 h	**B**	**38ac,** 32[d]	95
5	**32d**	*rac*-BINAP	80	10 min	**A**	-[e]	-
6	**32d**	*rac*-BINAP	reflux	4h	**B**	-[e]	-

[a] Method **A**: microwave heating. Method **B**: conventional heating and slow addition of diyne with syringe pump for 4 h. [b] Calculated by chiral HPLC. [c] The enantiomer obtained in this case was the opposite to that obtained using (*R*)-BINAP. [d] Homocoupling product **36** (10% yield) was obtained together with the product. [e] Homocoupling product **36** was obtained.

When *ortho*-substituted BH adducts **32e-h** were used (Figure 20), the [2+2+2] cycloaddition did not proceed under microwave irradiation at 60ºC for 25 minutes and only starting material and homocoupling product **36** were obtained in all cases. As a result, these substrates were discarded for this study.

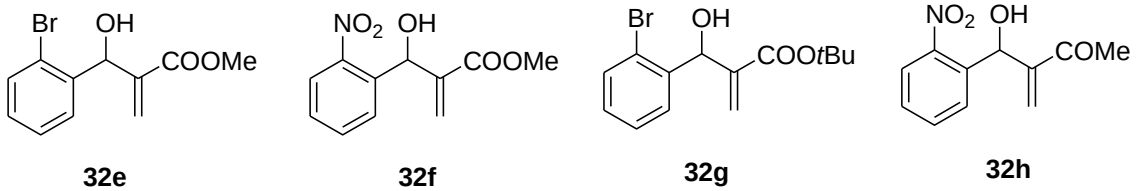

32e **32f** **32g** **32h**

Figure 20. *Ortho*-substituted Baylis-Hillman adducts which failed in the [2+2+2] cycloaddition reaction.

The scope of the reaction was then evaluated changing the diyne counterpart. The reaction of various symmetric diynes with some BH esters was examined (Table 13). Surprisingly, the

[2+2+2] cycloaddition reaction of ether- and malonate-linked diynes **34a** and **16b** was much more effective when the diyne was slowly added to the BH adduct (Method **B**) than when microwave heating was applied (Method **A**) (compare Entries 1 and 2, and 5 and 6, Table 13). The reactions run under microwave heating afforded homocoupling products **39** and **40** (Figure 21) when the ether-linked diyne **34a** was used. Only starting material was recovered when starting with the malonate-linked substrate **16b**. The reaction of oxygen-tethered diyne **34a** with ethyl ester BH adduct **32b** was not as effective as with methyl ester BH adduct **32a**, neither when (*R*)- nor (*S*)-BINAP were used since only 20% and 22% yields were obtained respectively (Entries 3 and 4, Table 13). Finally, 5-methyl-2piridinesulfonamide derivative **34b** was tested and the yield obtained was better than that obtained with other diynes although the enantiomeric excess was lower (Entry 7, Table 13).

Table 13. Diyne scope.

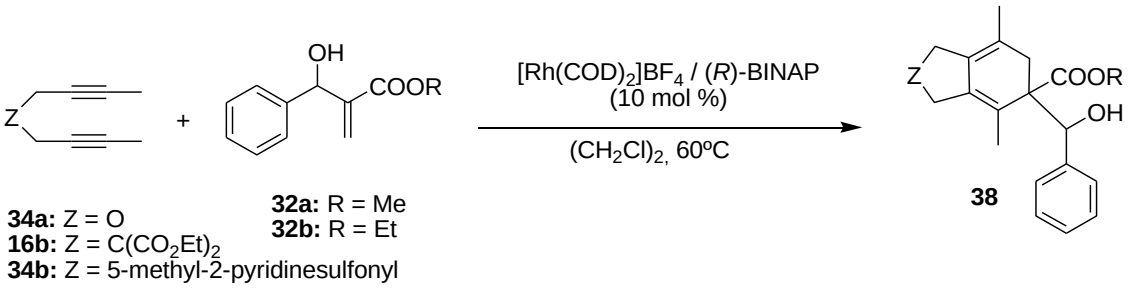

Entry	Diyne	BH adduct	t	Method[a]	Compound, Yield (%)	ee (%)[b]
1	**34a**	**32a**	4 h	**B**	**38ba**, 45[c]	90
2	**34a**	**32a**	10 min	**A**	**38ba**, 13[d],[e]	-
3	**34a**	**32b**	7.5 h	**B**	**38bb**, 20	80
4	**34a**	**32b**	4 h	**B**	**38bb**, 22	n.d.[f]
5	**16b**	**32a**	4 h	**B**	**38ca,** 41	n.d.
6	**16b**	**32a**	10 min	**A**	**38ca**, 13[d],[g]	-
7	**34b**	**32a**	4 h	**B**	**38da**, 56	73

[a] Method **A**: microwave heating. Method **B**: conventional heating and slow addition of diyne with syringe pump for 4 h. [b] Calculated by chiral HPLC. [c] Homocoupling product **40** (12% yield) was obtained together with the product. [d] *rac*-BINAP and microwave heating at 80ºC were used. [e] Isomerization product **37** and homocoupling products **39** and **40** were also obtained. [f] (*S*)-BINAP was used. [g] Isomerization product **37** was also obtained.

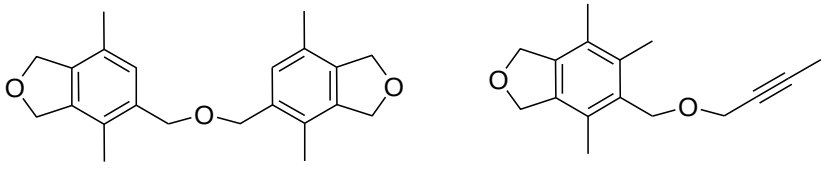

39 **40**

Figure 21. Homocoupling products of diyne **34a**.

Diynes and BH adducts were also reacted using *rac*-BINAP in order to be able to determine the enantiomeric excess (Table 14). All reactions gave moderate to good yields of the cycloadducts except when the BH **32c** was reacted with the diyne **34a** (Table 14). For this reason, the enantioselectivity of the reaction was not studied in this case (Entry 5, Table 14).

Table 14. Diyne scope (with racemic BINAP).

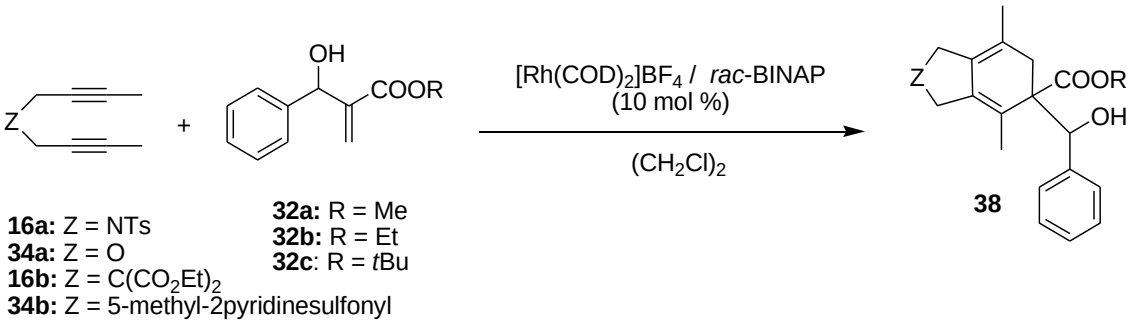

16a: Z = NTs
34a: Z = O
16b: Z = $C(CO_2Et)_2$
34b: Z = 5-methyl-2pyridinesulfonyl

32a: R = Me
32b: R = Et
32c: R = *t*Bu

Entry	Diyne	BH adduct	t	Method[a]	Compound, Yield (%)
1	**16a**	**32b**	10 min	**A**	**38ab**, 40
2	**16a**	**32c**	10 min	**A**	**38ac**, 33
3	**34a**	**32a**	3 h	**B**	**38ba**, 60
4	**34a**	**32b**	4 h	**B**	**38bb**, 55
5	**34a**	**32c**	4 h	**B**	**38bc**, 28
6	**16b**	**32a**	4 h	**B**	**38ca,** 35
7	**34b**	**32a**	4 h	**B**	**38da**, 63

[a] Method **A**: microwave heating at 80ºC. Method **B**: conventional heating and slow addition of diyne with syringe pump at 84ºC.

The effect of substitution on the alkyne terminus of the diyne was then evaluated. The reaction of methyl ester substituted diyne (**34c**), phenyl substituted diyne (**34d**), and unsubstituted diyne (**16c**) with BH adduct **32a** using racemic BINAP as the phosphine was studied (Scheme 67). When the reaction was run under the conditions of Method **B**, the cycloadducts were not formed.

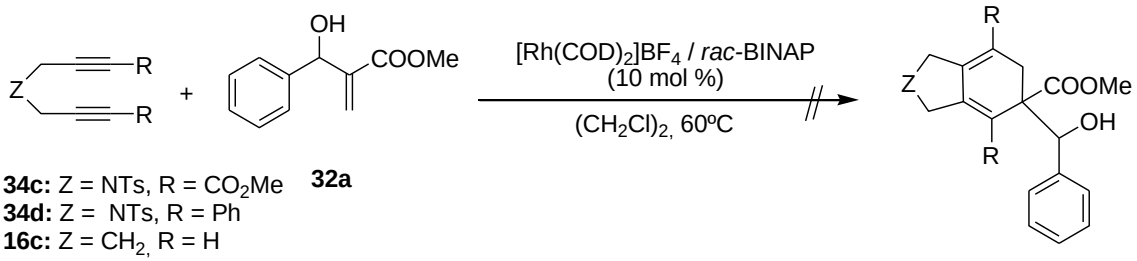

34c: Z = NTs, R = CO_2Me
34d: Z = NTs, R = Ph
16c: Z = CH_2, R = H

32a

Scheme 67. Diyne substrates that failed in the [2+2+2] cycloaddition with **32a**.

The reactions led to the formation of the isomerization product of the BH adduct **32a** and also homocoupling product **41** when diyne **16c** was used (Figure 22).

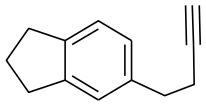

41

Figure 22. Homocoupling product of diyne **16c.**

As a summary, the yields obtained with heteroatom-tethered diynes were higher than those obtained with malonate-tethered diyne **16b** for the same BH adduct. Moreover, when the less reactive BH adducts with ethyl ester or *tert*-butyl ester group were used, the yield decreased significantly due to the formation of the diyne homocoupling products. Finally, carbon tethered terminal diyne **16c** as well as internal diynes **34c** and **34d** proved to be unsuitable substrates for this reaction.

In order to study the activity of another catalyst in this reaction, [RuCp*(COD)Cl] was tested in the reactions involving diyne **16a** and different BH adducts (Table 15). This ruthenium catalyst is known to be highly active in [2+2+2] cycloaddition reactions, particularly those that involve nitriles as substrates for the formation of pyridines.[78] For this reason, BH adduct **32d**, which has a nitrile as an electron withdrawing group, was tested under ruthenium catalysis.

[78] a) Varela, J. A.; Saá, C. *Synlett* **2008**, 2571; b) Heller, B.; Hapke, M. *Chem. Soc. Rev*. **2007**, *36*, 1085; c) Varela, J. A.; Saá, C. *Chem. Rev*. **2003**, *103*, 3787.

Table 15. [2+2+2] cycloaddition reaction catalysed by [RuCp*(COD)Cl] catalyst.

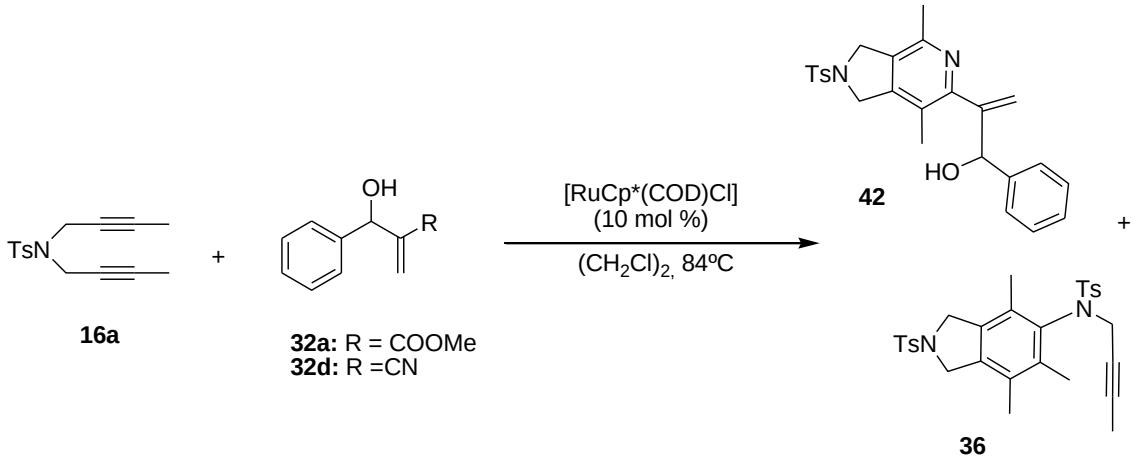

Entry	BH adduct	Catalyst	t	Yield of 42 (%)	Yield of 36 (%)
1	**32d**	[RuCp*(COD)Cl]	4 h	46	-
2	**32d**	[RuCp*(COD)Cl]	10 min[a]	60	-
3	**32d**	$Rh(COD)_2BF_4$/*rac*-BINAP	10 min[a]	-	13
4	**32d**	$Rh(COD)_2BF_4$/BIPHEP	3 h	-	26
5	**32a**	[RuCp*(COD)Cl]	3 h	-	24

[a] Microwave heating was used at 80ºC.

These experiments revealed that the ruthenium catalyst was active when the substrate involved has a nitrile (Entry 1, Table 15) since pyridine cycloadduct **42** was formed with a 46% yield after 4 hours at reflux (without slow addition with syringe pump). The same reaction was tested under microwave heating and the yield was improved to 60% (Entry 2, Table 15). To compare the behaviour of ruthenium and rhodium catalysts, the reactions of Entries 1 and 2 were repeated but using $[Rh(COD)_2]BF_4$ in combination with racemic BINAP or BIPHEP (Entries 3 and 4, Table 15). In both cases the only product obtained was the homocoupling of diyne **16a** with low yield. In contrast, when the BH adduct involved was the ester **32a** instead of the nitrile **32d** under ruthenium catalysis, the reaction between diyne **16a** and **32a** did not work and only the homocoupling product **36** was formed with a 24% yield (Entry 5, Table 15). Hence, the reactivity of these two catalysts was completely different: while the rhodium catalyst was not active for the BH adduct with a nitrile group (Entries 3 and 4, Table 15), the ruthenium catalyst was not active for the BH adduct with an ester group (Entry 5, Table 15).

Once the pyridine **42** was obtained, we planned to test the subsequent [2+2+2] cycloaddition reaction between the alkene **42** and diyne **16a** catalysed by $[Rh(COD)_2]BF_4$/racemic BINAP in dichloroethane at reflux (Scheme 68). Cycloadduct **42** was not reactive enough and the homocoupling product **36** (22% yield) was obtained together with ketone **43** (Figure 23) in a 47% yield resulting from the isomerization of **42**. We decided to repeat the reaction but using the conditions of Method **A** (microwave heating at 60ºC during 20 minutes) and homocoupling

of diyne **16a** was also obtained (7% yield) together with the starting materials (**42** and **16a**). In this case isomerization product **43** was not formed.

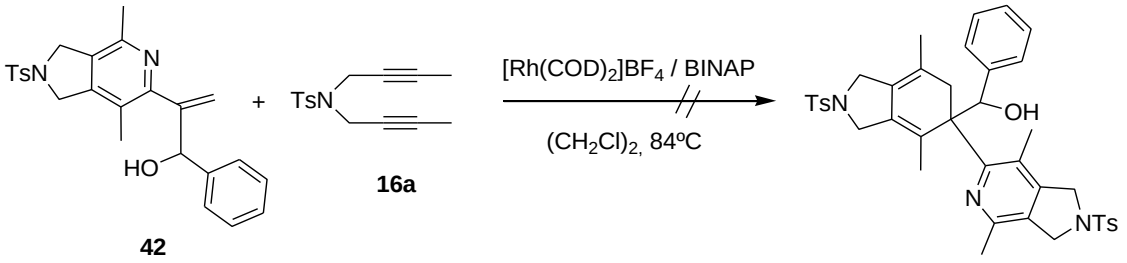

42

Scheme 68. Attempted reaction between pyridine **42** and diyne **16a** catalysed by Rh(I).

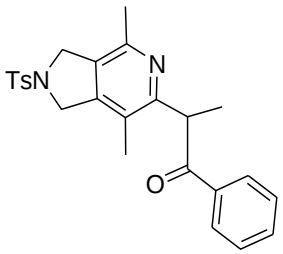

43

Figure 23. Isomerization product **43** of pyridine **42**.

As a summary, we can conclude that Baylis-Hillman adducts can be used as substrates for the rhodium-catalysed [2+2+2] cycloaddition reaction with diynes affording highly functionalized bicyclic compounds with a cyclohexadiene core. The reaction is diastereoselective and highly enantioselective when chiral BINAP-type diphosphines were used allowing for the preparation of a set of compounds with a quaternary carbon stereocentre. These preliminary results show that the process is governed by a kinetic resolution affording only one stereoisomer starting from a racemic mixture of the Baylis-Hillman adduct. In order to achieve the cycloaddition product, it has been necessary to suppress the homocoupling reaction of the diyne and the isomerization of the BH adduct. Two strategies have been shown to be effective towards this end: to decrease the reaction time by microwave heating (method **A**) and the slow addition of the diyne over the BH adduct and catalyst mixture (method **B**). Although slow addition was an effective strategy in all of the tethers explored, the use of microwave heating was only effective when N-tethered diynes were reacted.

The scope of the reaction has been evaluated in the case of the BH adduct and diyne reagents. Only BH adducts with an ester group resulted active in the rhodium-catalysed [2+2+2] cycloaddition reaction. The reactivity trend of the different esters tested conformed to the bulkiness of the substituent (COOMe > COOEt > COO*t*Bu). Nitrile-containing BH adducts were not active in the rhodium-catalysed [2+2+2] cycloaddition reaction but afforded pyridine bicyclic structures when ruthenium-based catalysts were used.

With regards to the scope of the diyne, nitrogen, carbon and oxygen tethered diynes have all been shown to be effective in the reaction. Alkyne terminus substitution has been found to have a dramatic effect on the reaction, as only methyl substituted alkynes can successfully be involved in the present cycloaddition reaction.

Further experimentation is needed to identify the diastereoisomer that has been formed and to study in detail whether or not the process is governed by kinetic resolution.

Chapter 5. Mechanistic study of the [2+2+2] cycloaddition reactions by ESI-MS

Part of this chapter has been published on:

Parera, M.; Dachs, A.; Solà, M.; Pla-Quintana, A.; Roglans, A. *Chem. Eur. J.* **2012**, *18*, 13097.

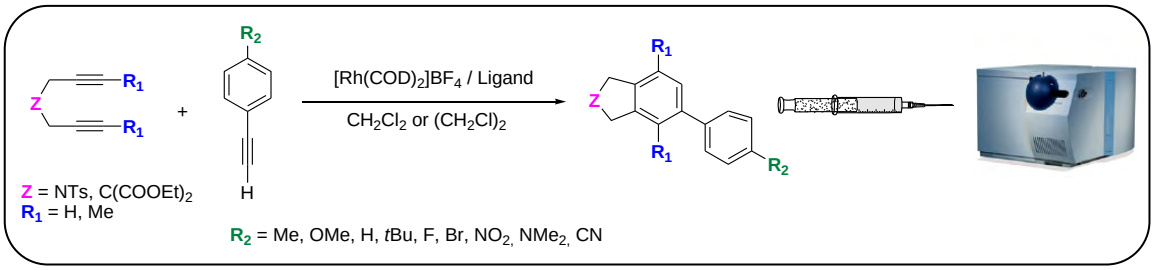

5.1. Precedents

5.1.1. Electrospray ionization mass spectrometry (ESI-MS): soft ionization technique

Mass spectrometry, which allows the determination of the mass to charge *(m/z)* ratio of compounds, is one of the oldest instrumental analytical techniques. Different ionization techniques can be identified based on the energy transferred during the ionization process. The first instruments developed used "hard" techniques, such as electron ionization, which produce ions with a large excess of energy, which generally leads to extensive fragmentation. Thus, the number of compounds that could be analyzed was limited by the extreme temperature conditions used for the ionization as well as the high volatility of compounds to be analyzed. Moreover, the molecules of the analyte were ionized in the mass spectrometer under vacuum. These approaches were only successful for a very limited number of compounds.

As a result of the need to develop softer techniques, atmospheric pressure ionization (API) mass spectrometry was implemented in which ions are generated in a reaction chamber that is external to the low pressure region of mass analyzers. Samples may be introduced in solvent-free fashion (by vaporization in a stream of preheated carrier gas, or in the effluent stream from a gas chromatograph) or with solvents (by injection of solutions, or in the effluent stream from a liquid chromatograph). The most commonly used API techniques are electrospray ionization (ESI), atmospheric pressure chemical ionization (APCI) and atmospheric pressure photoionization (APPI). In APCI, the ionization occurs in the gas phase, unlike ESI, where the ionization occurs in the liquid phase.

Electrospray ionization was applied to mass spectrometry at the end of the 1980's by Fenn et al[79]. ESI-MS has taken on such importance as it permits the introduction of samples in solution at atmospheric pressure, so allowing the ionization of high polar and non-volatile compounds. The significance of this advance in the study of biological macromolecules resulted in Fenn being awarded the Nobel Prize of Chemistry in 2002.[80] The electrospray technique has become extremely popular due to its ability to investigate species in solution even when concentrations are extremely low and in complex mixtures. Apart from the detection of biomolecules[81], the development of this technique has resulted in new applications, such as

[79] a) Fenn, J. B.; Mann, M.; Meng, C.K.; Wong, S.F.; Whitehouse, C.M. *Science*, **1989**, *246*, 64; b) Fenn, J. B.; Mann, M.; Meng, C.K.; Wong, S.F.; Whitehouse, C.M. *Mass Spectrom. Rev*. **1990**, *9*, 37.

[80] Fenn, J.B. *Electrospray Wings for Molecular Elephants*. Nobel Lecture available on web: http://nobelprize.org/nobel_prizes/chemistry/laureates/2002/fenn-lecture.pdf.

[81] For significant examples, see: a) Aramendía, M. A.; Borau, V.; Garcia, I.; Jimenez, C.; Lafont, F.; Marinas, J. M.; Porras, A.; Urbano, F. J. *J. Mass Spectrom.* **1995**, S153; b) Kerwin, J. L.; Wiens, A. M; Ericsson, L. H. *J. Mass Spectrom*. **1996**, *31*, 184; c) Kotiaho, T.; Eberlin, M. N.; Vainiotalo, P.; Kostiainen, R. *J. Am. Soc. Mass Spectrom*. **2000**, *11*, 526; d) Potterat, O.; Wagner, K.; Haag, H. *J. Chromatograph. A.* **2000**, *872*, 85; e) Cooks, R. G.; Zhang, D.; Koch, K. J.; Gozzo, F. C.; Eberlin, M. N. *Anal. Chem*. **2001**, *73*, 3646; f) Koch, K. J.; Gozzo, F. C.; Nanita, S. C.; Takats, Z.; Eberlin, M. N.; Cooks, R. G. *Angew. Chem. Int.*

the study of organometallic compounds in solution, being found.[82] ESI-MS is one of the softest methodologies given that it allows the analysis of high polar and thermally unstable molecules. Furthermore, the appearance of multiple-charged species enables ESI to characterize compounds whose molecular weight would otherwise be far in excess of what most mass analysers are capable of (molecules as large as 150000 mass units can be analyzed even though the mass-to-charge range for typical MS instruments is around 3000 *m/z*).

Electrospray is partially dependent on its own chemistry to generate analyte ions in solution before the analyte reaches the mass spectrometer. The sample is dissolved in a volatile mobile phase and the solution is then sprayed through a needle into a spray chamber with high electric potential (3-6 kV) at one end, which produces droplets of solvent and sample. The droplets are also subjected to a high-voltage electrostatic gradient at atmospheric pressure in the spray chamber, which produces oxidation-reduction reactions and forces the liquid to emerge as charged drops (spray). A heated drying gas, usually nitrogen, which flows perpendicularly to the capillary, is introduced into the spray chamber to help evaporate the solvent from the droplets (Scheme 69).

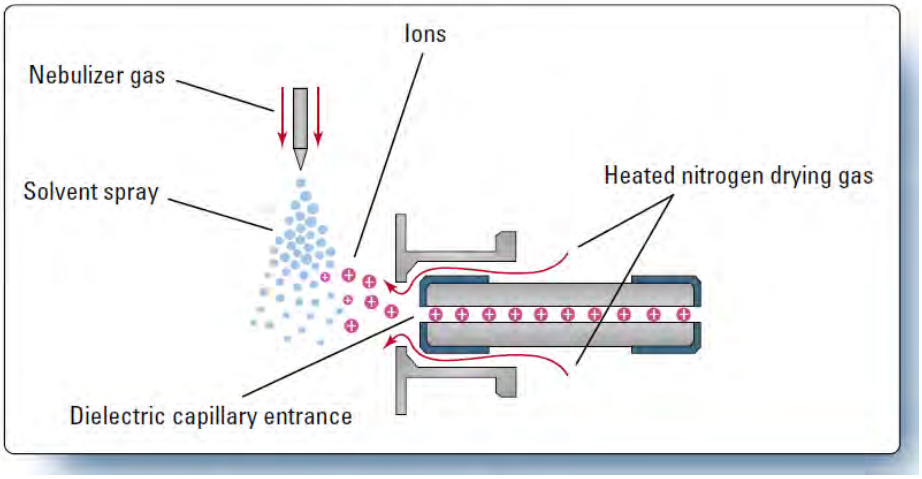

Scheme 69. Electrospray ion source (Source: "Basics of LC-MS". Agilent Technologies, Printed in the U.S.A. February 15, 2001, 5988-2045EN).

As the droplets shrink, the concentration of the charge increases. Eventually, the repulsive force between ions with identical charges exceeds the cohesive forces and ions are ejected (desorbed) into the gas phase (Scheme 70).

Ed. **2002**, *41*, 1721; g) Lenz, C.; Kühn-Hölsken, E.; Urlaub, H. *J. Am. Mass. Spectrom*. **2007**, *18*, 869; h) Lomeli, S. H.; Yin, S.; Loo, R. R. O.; Loo, J. A. *J. Am. Mass Spectrom.* **2009**, *20*, 593.

[82] For a monography, see: *Mass Spectrometry of Inorganic, Coordination and Organometallic Compounds. Tools-Techniques-Tips.* Henderson, W.; Mc Indoe, J. S. **2005**, John Wiley & Sons, Chichester, England.

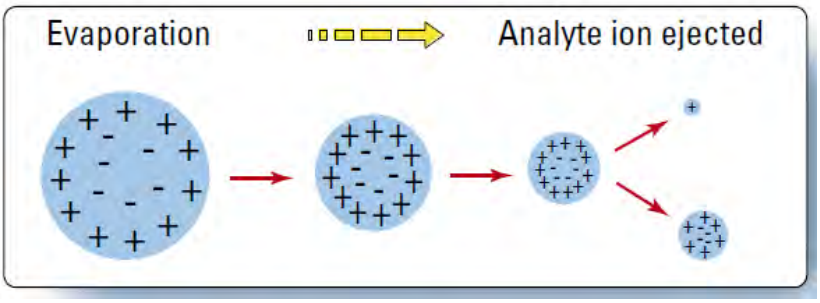

Scheme 70. Desorption of ions from solution (Source: "Basics of LC-MS". Agilent Technologies, Printed in the U.S.A. February 15, 2001, 5988-2045EN).

Given the operational mechanism of ESI-MS, neutral molecules must be converted into ionic species in solution to make them detectable. The most common mechanisms to generate these charged species is either by protonation of the analyte to generate the corresponding ion $[M+H]^+$ in ESI(+) mode or by deprotonation to generate the ion $[M-H]^-$ in ESI(-) mode. Therefore, polar solvents are the most widely used in ESI-MS to facilitate the ionization of the analytes. Another common mechanism to form ions is the association of the substrate with other ions with a trace presence in HPLC grade solvents in cases where analytes do not have protonation sites or are not sufficiently basic to be deprotonated. Hence, the observation of ions such as $[M+NH_4]^+$, $[M+Na]^+$ or $[M+Cl]^-$ is usual.

In some cases, the metallic capillary of electrospray can act as an electrode in a reduction reaction promoting ionization by oxidation of electron-rich substrates generating ions such as $[M]^+$.[83] These oxidation processes are difficult to predict and usually depend on the compound, the solvent used and the equipment.

Adducts with solvents such as $[M+solvent+H]^+$ and aggregates with high molecular weight such as $[2M+H]^+$ or $[2M+Na]^+$ are also commonly observed. This is due to the incomplete desorption of drops generated in the spray. In addition, multiple-charged species can be detected which have a particular isotopic distribution of only 1/n units of mass of difference (n is the number of charges) instead of 1 unit since the mass-to-charge ratio is less than mono-charged ones.

As an example of the observation of polycharged species, the spectrum in Figure 24 has been selected from a publication where native polysaccharide from pineapple gum (PANP) has been characterized.[84] The authors applied low energy in a first approach in order to prevent in-source fragmentation. The oligosaccharides appeared as multi-charged ions.

[83] Van Berkel, G. J.; Zhou, F. *Anal. Chem*. **1995**, *67*, 3958.
[84] Simas-Tosin, F. F.; de Souza, L. M.; Wagner, R.; Pereira, G. Z. P.; Barraza, R. R; Wendel, C. F.; Sassaki, G. L.; Iacomini, M.; Gorin, P. A. J. *Carbohydrate Polymers* **2013**, *94*, 704.

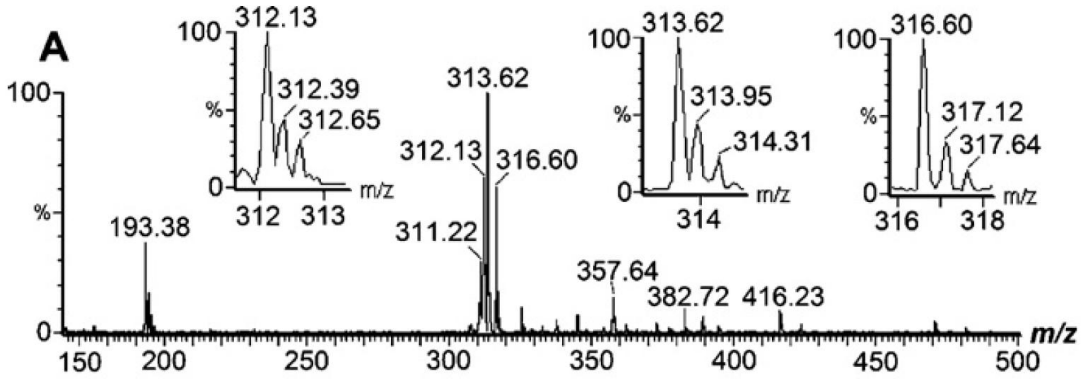

Figure 24. ESI-MS of multi-charged oligosaccharides from fraction PANP-PH. Insets: zoom of main ions showing isotopic distribution indicating the presence of 4, 3 and 2 charges at ions with *m/z* 312.13, 313.62 and 316.60, respectively.

Special care has to be taken when working with ESI-MS to avoid error or misinterpretation resulting from the formation of aggregates during the ionization process inside the apparatus or the dissociation of non-covalent complexes during ionization. Furthermore, it is important to note that the intensities of peaks in the mass spectrum are not necessarily related to the concentrations.[85]

Once the ions are formed, they are transferred through a capillary and an octopole ion guide to the mass analyzer under vacuum, which separates the ions from the ion flow by their *m/z* and focuses them by electric and magnetic field lenses towards the detector.

In this study we used a simple ion-trap mass analyzer which was robust and fast. An ion trap performs several important functions including mass accumulation and sequential mass ejection to produce the mass spectrum. For efficient trapping and cooling of the ions, helium gas is introduced into the ion trap. As the ions collide with helium and lose further energy, they are slowed down and focused at the centre of the trap. A resonant frequency is then applied to selectively expel ions of a given *m/z* ratio (Scheme 71).

[85] Leize, E.; Jaffrezic, A.; Van Dorsselaer, A. *J. Mass Spectrom*. **1996**, *31*, 537.

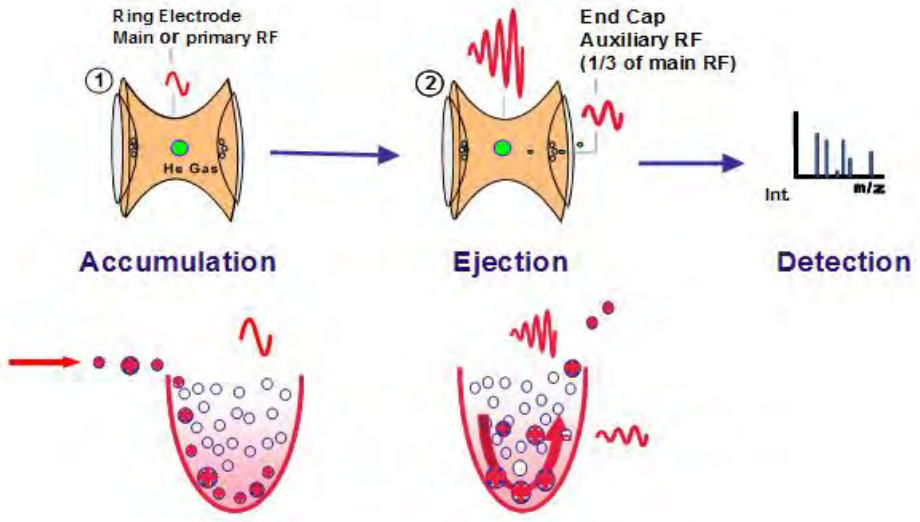

Scheme 71. Ion trap mass analyzer.

Furthermore, ion traps are able to selectively isolate and excite a mass: a feature that can be used to perform MS/MS experiments. The main advantage of the ion trap instrument is that MS/MS experiments take place at the same location (in the trap) and so are separated in time rather than space, without the need for additional mass analyzers.

Tandem mass spectrometry or collision induced dissociation (CID) consists in the isolation and excitation of an ion of interest by increasing the resonance frequency of the dipolar field in the trap followed by their fragmentation through collision with the surrounding buffer gas (He). The fragmented ions are then trapped again at the centre of the apparatous and no further fragmentation takes place as the excitation is specific just for the *m/z* of the precursor ion. The procedure can still be repeated several times (MS^n) as the dissociation products remain in the trap (Scheme 72). This is a powerful technique to determine important structural information of the analytes since almost no fragmentation occurs using softer techniques.

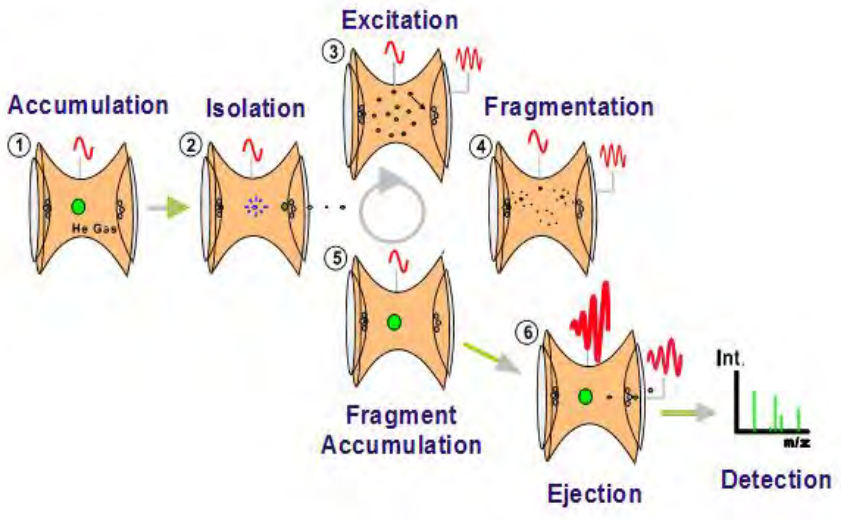

Scheme 72. MS/MS in an ion trap.

5.1.2. Electrospray ionization mass spectrometry: a powerful tool to study reaction mechanisms

A reaction mechanism is defined as the step-by-step description of a chemical reaction. In general, reactions take place through a complex sequence of steps *via* reactive intermediates. Except for a few concerted reactions in which all bond breaking and bond making occurs in a single elementary step, most chemical reactions occur in a stepwise manner with a complex sequence of steps via the formation and consumption of intermediates. Thus, knowledge of reactive intermediates plays a key role in the understanding of reaction mechanism.

A reaction intermediate is a molecular entity, such as an atom, ion or molecule, with an appreciably longer lifetime than the molecular vibration that directly or indirectly arises from the reactants, and which further reacts to give the final products of a chemical reaction. They are often metastable species, and many intermediates are usually short-lived and highly reactive. Therefore, these common characteristics of the reaction intermediates together with the low concentrations at which they are found, when compared with final stable reaction products, makes their capture extremely challenging.

In 1993, the validity of using ESI-MS to detect and examine transient ionic intermediates directly from solution was successfully tested in organic reactions (Wittig, Mitsunobu, and Staudinger) to provide a mechanistic probe for well-studied phosphine-mediated reactions. Wilson et al.[86] identified the cationic intermediates postulated for the three reactions by ESI-MS which correlated with those proposed on the basis of ^{31}P-NMR analysis.

Since then, the investigation of reaction mechanisms by ESI-MS has taken on increasing relevance.[87] The methodology is especially well-suited for reactions involving ionic intermediates. As an example, one of the first ESI-MS mechanistic studies involving organometallic catalityc cycles was undertaken by Canary et al. in 1994.[88] Canary published the first complete study of palladium-catalysed Suzuki-Miyaura cross-coupling reactions between several arylboronic acids and bromopyridines using the ESI-MS technique. The Suzuki-Miyaura reaction involves the cross-coupling between organoboron compounds and organic halides or triflates and is one of the most convenient synthetic methods for the formation of carbon-

[86] Wilson, S.R.; Perez, J.; Pasternak, A. *J. Am. Chem. Soc*. **1993**, *115*, 1994.

[87] For recent and selected references, see: a) Wang, H.-Y.; Yim, W.-L.; Klüner, T.; Metzger, J. O. *Chem. Eur. J.* **2009**, *15*, 10948; b) Müller, C. A.; Markert, C.; Teichert, A. M.; Pfaltz, A. *Chem. Commun*. **2009**, 1607; c) Schade, M. A.; Fleckenstein, J. E.; Knochel, P.; Koszinowski, K. *J. Org. Chem*. **2010**, *75*, 6848; d) Fernandes, T. A.; Vaz, B. G.; Eberlin, M. N.; da Silva, A. J. M.; Costa, P. R. R. *J. Org. Chem*. **2010**, *75*, 7085; e) Beierlein, C. H.; Breit, B.; Schmidt, R. A. P.; Plattner, D. A. *Organometallics* **2010**, *29*, 2521; f) Agrawal, D.; Schröder, D.; Frech, C. M. *Organometallics* **2011**, *30*, 3579; g) Agrawal, D.; Schröder, D. *Organometallics* **2011**, *30*, 32; h) Henderson, M. A.; Luo, J.; Oliver, A.; McIndoe, J. S. *Organometallics* **2011**, *30*, 5471; i) Vikse, K. L.; Ahmadi, Z.; Manning, C. C.; Harrington, D. A.; McIndoe, J. S. *Angew. Chem. Int. Ed*. **2011**, *50*, 8304; j) Wang, H. Y.; Yim, W. L.; Guo, Y. L.; Metzger, J. O. *Organometallics* **2012**, *31*, 1627; k) He, X.; Zhang, S.; Guo, Y.; Wang, H.; Lin, G. *Organometallics* **2012**, 31, 2945; l) Henderson, M. A.; Trefz, T. K.; Collins, S.; Wang, M. Y.; McIndoe, J. S. *Organometallics* **2013**, *32*, 2079; m) Hyvl, J.; Agrawal, D.; Pohl, R.; Suri, M.; Glorius, F.; Schröder, D. *Organometallics* **2013**, *32*, 807.

[88] Aliprantis, A. O.; Canary, J.W. *J. Am. Chem. Soc*. **1994**, *116*, 6985.

carbon bonds. Canary used pyridyl halides (**44** and **45**) instead of the typically used phenyl derivatives to introduce a protonable group into the complexes, which otherwise might not be detected by the ESI-MS (Scheme 73).

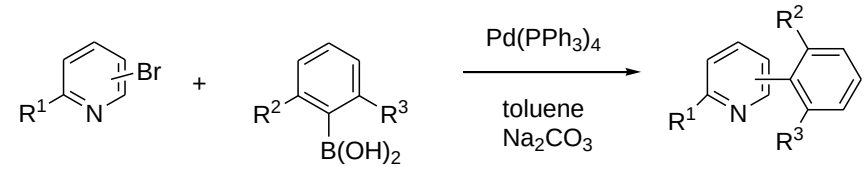

44 3-Br, R^1 = H
45 6-Br, R^1 = CHO

46
$R^2 = R^3 = H$
$R^2 = H$, $R^3 = Me$
$R^2 = R^3 = Me$

47
3-Ar, $R^1 = R^2 = R^3 = H$
3-Ar, $R^1 = R^2 = H$, $R^3 = Me$
3-Ar, $R^1 = H$, $R^2 = R^3 = Me$
6-Ar, $R^1 = CHO$, $R^2 = R^3 = H$
6-Ar, $R^1 = CHO$, $R^2 = H$, $R^3 = Me$
6-Ar, $R^1 = CHO$, $R^2 = R^3 = Me$

Scheme 73. Suzuki-Miyaura cross-coupling reactions of pyridyl halides **44** and **45** with arylboronic acids **46** studied by ESI-MS.

The reaction was studied by taking aliquots from the organic layer of the reaction mixture at regular time intervals until the reaction was completed. The aliquot was quenched in cold methanol and then warmed to room temperature before injection into the spectrometer.

Scheme 73 shows the reactions studied and Figure 25 shows the intermediates detected by ESI-MS. The two key intermediates of the Suzuki-Miyaura reaction, species **A** and **B** corresponding to oxidative addition intermediates, and species **C** corresponding to transmetallation intermediates, were detected by ESI-MS in all the reactions for the first time in authentic reaction mixtures. Species **D** and **E**, detected in most cases, were assigned to $[ArPd(PPh_3)_2]^+$ and $[Pd(PPh_3)_4]^{2+}$ respectively and were also observed in control experiments when the aryl halide was excluded from the reaction mixture. The authors postulate that intermediate **D** is a result of transmetallation with **E**. This first study showed for the first time that the ESI-MS technique has great potential as a complementary analytical tool for the determination of reaction mechanisms.

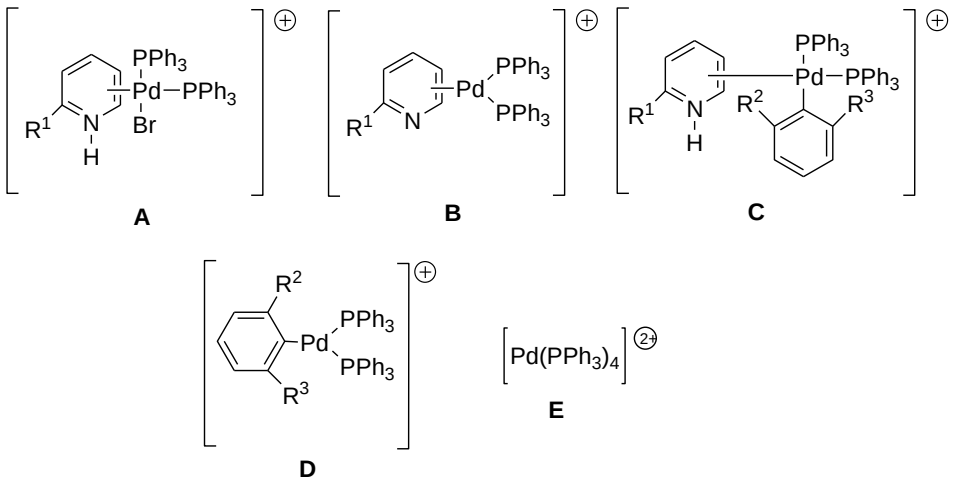

Figure 25. Intermediate species detected by ESI-MS in Suzuki-Miyaura reactions.

When reaction intermediates are not charged they are blind to the technique. Therefore, they can only be detected if ionized or if a chemical derivatization strategy that facilitates pulling out a desired species by way of selective labelling with charge substrates (charged tags) is used. The most common purposes of chemical derivatization in ESI-MS are to achieve optimal chemical properties (such as polarity, ionizability, stability and fragmentability), to enhance ionization efficiency and to increase detection specificity. Charge-tagged substrates[89] or charged ligands[90] (by replacement of a neutral ligand with a charged analogue) render intermediates amenable to manipulation and detection using a standard ESI-MS technique. This strategy has allowed the detection of intermediates in reactions where neutral intermediates are postulated. Commonly employed tags are quaternary ammonium cations and sulfonate anions. The charge tag can be directly incorporated into an organic moiety covalently bounded to the metal centre (Scheme 74). For instance, Koszinowski et al.[89b] reported a study of insertion reactions of different metals (Pd, Zn, Mg and In) into charge-tagged organic iodides analyzed by ESI-MS to compare the results with data available for the related untagged systems.

[89] For selected examples, see: a) Santa, T. *Biomed. Chromatogr.* **2011**, *25*, 1; b) Schade, M. A.; Fleckenstein, J. E.; Knochel, P.; Koszinowski, K. *J. Org. Chem.* **2010**, *75*, 6848.

[90] For selected examples, see: a) Farrer, N. J.; McDonald, R.; McIndoe, J. S. *Dalton Trans*. **2006**, 4570; b) Chisholm, D. M.; McIndoe, J. S. *Dalton Trans.* **2008**, 3933; c) Wang, H.-Y.; Metzger, J. O. *Organometallics* **2008**, *27*, 2761; d) Chisholm, D. M.; Oliver, A. G.; McIndoe, J. S. *Dalton Trans.* **2010**, *39*, 364; e) Beierlein, C. H.; Breit, B.; Schmidt, R. A. P.; Plattner, D. A. *Organometallics* **2010**, *29,* 2521; f) Jackson, S. M.; Chisholm, D. M.; McIndoe, J. S.; Rosenberg, L. *Eur. J. Inorg. Chem*. **2011**, 327.

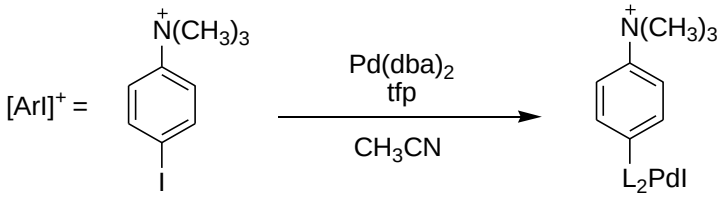

Scheme 74. Insertion of zerovalent metals into charge-tagged organic iodides (oxidative addition step). (Tfp = tri(2-furyl)phosphine).

Moreover, they demonstrated that ESI-MS was useful for monitoring cross-coupling reactions such as Pd-catalysed Negishi reaction of charge-tagged substrates (Scheme 75).

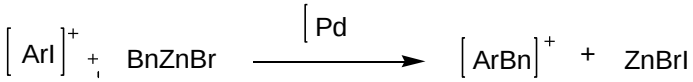

Scheme 75. Pd-catalysed cross-coupling of $[ArI]^+$ with benzylzinc bromide (Negishi reaction).

It is assumed that the reactions start by the oxidative addition of the organic halide to the zerovalent Pd catalyst. The resulting insertion product then undergoes transmetalation by the organozinc reagent and finally yields the coupling product by reductive elimination.[91] In this study, $Pd(dba)_2$/tfp in acetonitrile was employed as the catalytic system, which efficiently adds $[ArI]^+$. In the presence of BnZnBr, the expected coupling product $[ArBn]^+$ (*m/z* 226) could indeed be detected by ESI mass spectrometry (Figure 26).

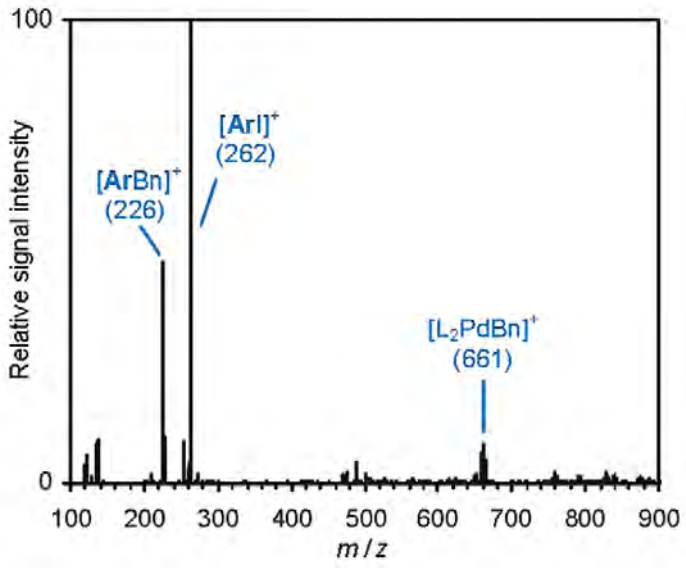

Figure 26. Positive ion mode ESI mass spectrum of a solution of (*p*-iodophenyl)-trimethylammonium iodide ($[ArI]^+$), BnZnBr, $Pd(dba)_2$, and tri(2-furyl)phosphine in CH_3CN.

[91] Frisch, A. C.; Beller, M. *Angew. Chem. Int. Ed.* **2005**, *44*, 674.

Another simple method for cationization of neutral species is the addition of traces of salts to the sample, which leads to the corresponding alkali cation adducts. Metal-ion adduct formation is known to be a favourable process to convert inorganic or organometallic neutral molecules into cationic derivatives.[92]

For instance, Metzger et al.[87a,j] studied olefin metathesis reactions catalysed by the first generation Grubb's catalyst through ESI-MS using the formation of adducts with alkaline metals to help to ionize the species (Scheme 76). The authors added potassium or lithium salts to the reaction and, after proving that these salts did not affect the catalytic activity, succeeded in detecting all the intermediates in the catalytic cycle.[87a] Through CID experiments of [**48**·M]$^+$ species, they observed a main fragment due to the loss of the PCy_3 group (Figure 27). The isotopic distribution of [**48a**·K]$^+$ is shown in Figure 28.

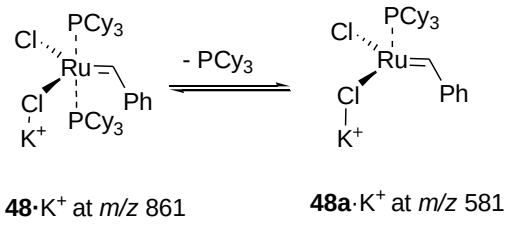

48·K$^+$ at *m/z* 861 **48a**·K$^+$ at *m/z* 581

Scheme 76. Potassium adducts of the first generation Grubb's catalyst.

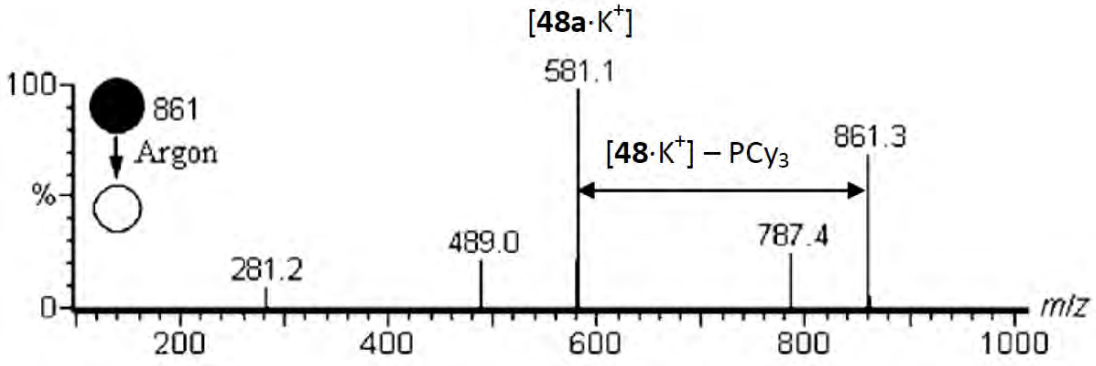

Figure 27. ESI-MS/MS spectrum for the CID of [**48**·K]$^+$ at *m/z* 861, collision energy of 9 eV.

[92] Colton, R.; D'Agostino, A.; Traeger, J. C. *Mass Spectrom. Rev*. **1995**, *14,* 79; b) Traeger, J. C. *Int. J. Mass Spectrom*. **2000**, *200*, 387.

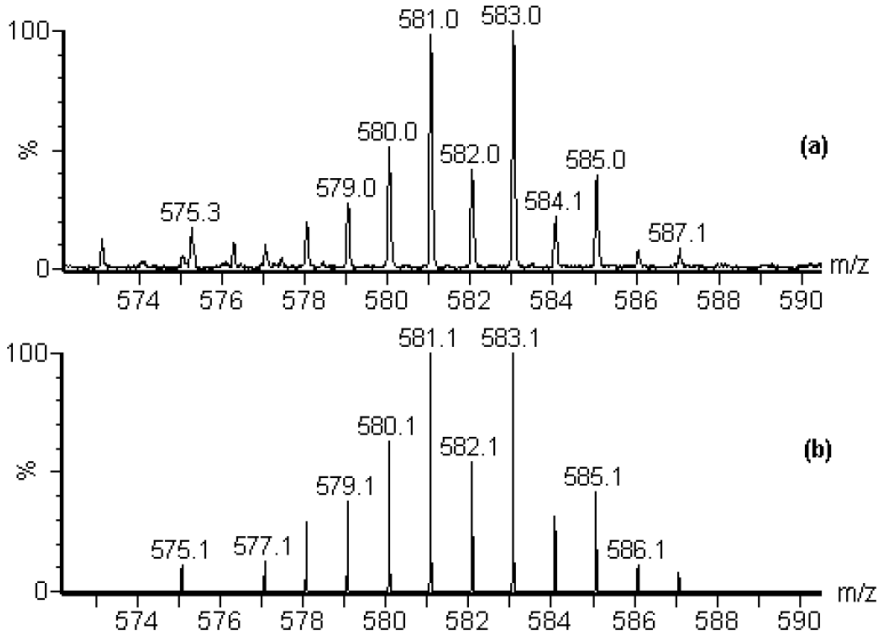

Figure 28. a) Isotopic pattern of [**48a**·K]$^+$; b) theoretical isotopic pattern of [**48a**·K]$^+$.

With the aim of determining whether the modification used changed the mechanism of the reaction, the authors extended the study with theoretical calculations to analyse the effect of the alkali cation on the Gibbs free energy of the catalytically active Ru species. They found that the energy profile of the reaction of **48**·K$^+$ and **48**·Li$^+$ was similar to the bare Ru complex **48**, which agreed well with the experimental results.

ESI-MS approaches to probing transient species in reaction mixtures as a function of time can be classified into two categories: *off*-line consecutive sampling and continuous *on*-line reaction screening. The operation of *off*-line monitoring can be accomplished by taking aliquots from the reaction mixture at pre-determined time intervals during a reaction period. The aliquots are analyzed either immediately or after quenching and storing. This strategy allows detailed structural identification of solution compositions or even putative transient species (*via* intermediate complex[88]) as long as they are present in reasonable concentrations and are not degraded within the first few minutes.

On-line strategies have been developed to overcome the inherent limitations of the *off*-line scenario. A continuous transfer of reaction mixtures directly to ESI-MS is achieved by connecting a reaction vessel, such as a syringe or microreactor, to the ESI source. This allows for real-time monitoring with millisecond time resolution of reactive intermediates occurring at very low concentrations even when they are short-lived.

One of these *on*-line strategies, which was introduced by Metzger et al. in 2003, consists in the connection of a microreactor (also called a mixing tee) to the ESI-MS (Figure 29).[93a] This clever system of sample introduction consists in injecting two solutions with reagents in two separate

syringes, which are pumped at the same velocity through two identical capillaries inside the microreactor. After mixing, the solution is sent to the ESI ion source. The reaction takes place during the time required to transport the mixture of solutions to the end of the capillary. The use of microreactors has allowed the mechanistic study of a high variety of organic reactions that have failed with *off*-line strategies.[93]

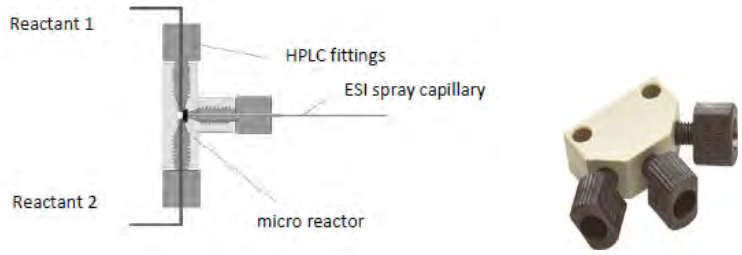

Figure 29. Microreactor joined to ESI-MS for the study of fast reactions.

5.1.3. Precedents from the METSO group

In our research group, mechanistic studies of different transition metal-catalysed reactions have been performed. The most remarkable contributions, some of which have been performed in collaboration with other research groups, relate to palladium chemistry.[94] Some of these studies will be commented as examples.

The first study was based on the characterization of the reactive intermediates of Heck-Matsuda reactions using a Pd(0) azamacrocyclic triolefinic complex as a recoverable and recyclable catalyst (Scheme 77).[94a,b] This study was performed using arenediazonium salts as electrophiles.

[93] For articles of mechanistic studies of reactions by ESI-MS using *Mixing Tee*, see: a) Meyer, S.; Koch, R.; Metzger, J. O. *Angew. Chem., Int. Ed.* **2003**, *42*, 4700; b) Meyer, S.; Metzger, J. O. *Anal. Bioanal. Chem.* **2003**, *377*, 1108; c) Wilson, D. J; Konermann, L. *Anal. Chem*. **2003,** *75*, 6408; d) Fürmeier, S.; Metzger, J.O. *J. Am. Chem. Soc*. **2004**, *126*, 14485; e) Santos, L. S.; Knaack, L.; Metzger, J. O. *Int. J. Mass Spectrom*. **2005**, *246*, 84; f) Eberlin, M. N. *Eur. J. Mass Spectrom*. **2007**, *13*, 19; g) Santos, L. S.; Metzger, J. O. *Angew. Chem*. **2006**, *118*, 991; h) Santos, L. S.; Metzger, J. O. *Angew. Chem. Int. Ed*. **2006,** *45*, 997; i) Marquez, C. A.; Fabbretti, F.; Metzger, J. O. *Angew. Chem. Int. Ed*. **2007**, *46*, 6915; j) Santos, L. S.; Metzger. J. O. *Rapid Commun. Mass Spectrom*. **2008**, *22*, 898; k) Santos, L. S. *Eur. J. Org. Chem*. **2008**, *23*, 5; l) Wang, H.-Y.; Metzger, J. O. *Organometallics* **2008**, *27*, 2761; m) Marquez, C. A.; Wang, H.-Y.; Fabbretti, F.; Metzger, J. O. *J. Am. Chem. Soc*. **2008**, *130*, 17208.

[94] a) Masllorens, J.; Moreno-Mañas, M.; Pla-Quintana, A.; Roglans, A. *Org. Lett*. **2003**, *5*, 1559; b) Pla-Quintana, A.; Roglans, A. *Arkivoc* **2005**, IX, 51; b) Masllorens, J.; González, I.; Roglans, A. *Eur. J. Org. Chem.* **2007**, 158; c) Moreno-Mañas, M.; Pleixats, R.; Spengler, J.; Chevrin, C.; Estrine, B.; Bouquillons, S.; Hénin, F.; Muzart, J.; Pla-Quintana, A.; Roglans, A. *Eur. J. Org. Chem*. **2003**, 274; d) Chevrin, C.; Le Bras, J.; Hénin, F.; Muzart, J.; Pla-Quintana, A.; Roglans, A.; Pleixats, R. *Organometallics* **2004**, *23,* 4796; e) Comelles, J.; Moreno-Mañas, M.; Pérez, E.; Roglans, A.; Sebastián, R. M.; Vallribera, A. *J. Org. Chem.* **2004**, *69*, 6834; f) Comelles, J.; Pericas, A.; Moreno-Mañas, M.; Vallribera, A.; Drudis-Solé, G.; Lledós, A.; Parella, T.; Roglans, A.; García-Granda, S.; Roces-Fernández, L. *J. Org. Chem*. **2007**, *72*, 2077.

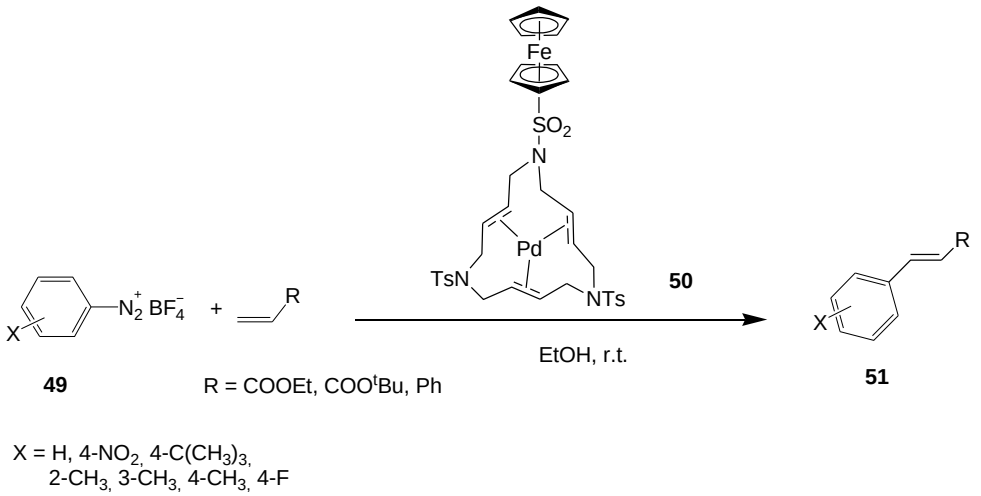

Scheme 77. Heck reaction of arenediazoium salts catalysed by macrocyclic Pd(0) complex **50**.

Apart from being highly reactive electrophiles, diazonium salts have the advantage of generating cationic reaction intermediates, so the mechanism was studied using ESI-MS. The mechanistic study was undertaken to determine the rate-determining step of the reaction and to detect the catalytic species. To this end, an equimolar quantity of arenediazonium tetrafluoroborate **49** and the alkene (Scheme 77) was mixed with palladium(0) complex in ethanol and the whole mixture was injected into the mass spectrometer. The oxidative addition intermediate was observed at *m/z* = 945.6 (**F** intermediate, Scheme 78) but the olefin insertion intermediate **G** could not be detected. Otherwise, the peak corresponding to the recovered catalyst **50** appeared at the end of the reaction.

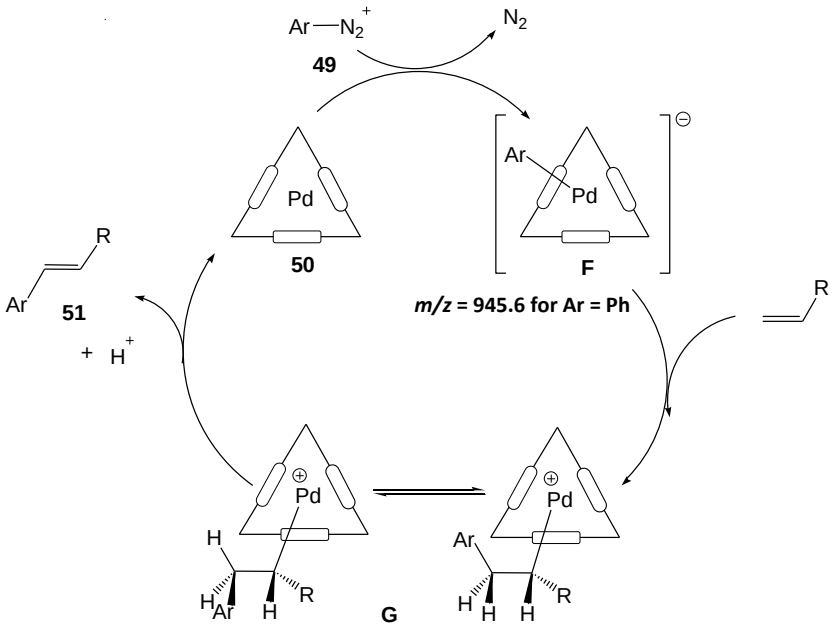

Scheme 78. Mechanistic role proposed for the Pd(0) complex **50** in Heck-Matsuda reaction with arenediazonium salts.

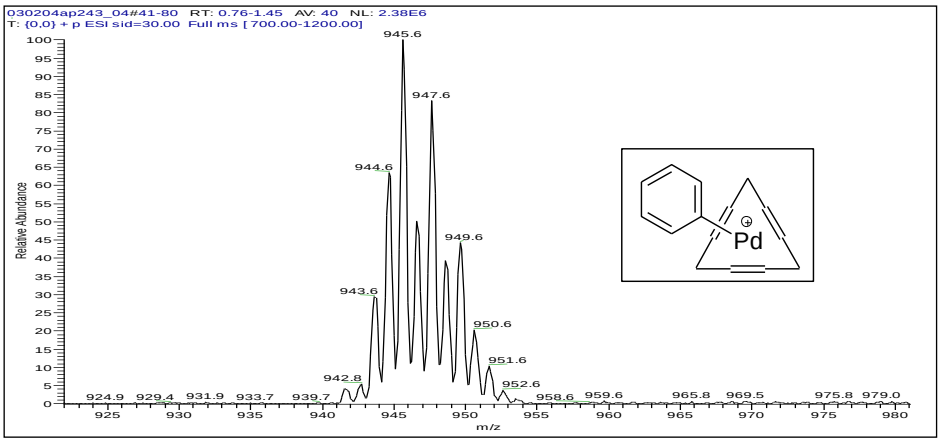

Figure 30. Isotopic pattern of intermediate **F** when Ar = phenyl (*m/z* = 945.6).

Based on these ESI-MS results (Figure 30), the reaction was postulated as occurring with the palladium stabilized inside the macrocyclic system. Since intermediate **F** was generated easily and remained until the end of the reaction, the olefin insertion was postulated as the rate-determining step of the reaction.

Mechanistic studies by ESI-MS of Michael addition reactions under catalysis by copper[94e] and lanthanides[94f] were performed in collaboration with Dr. Vallribera from the Universitat Autònoma de Barcelona. In a first study, UV-VIS, IR and ESI-MS were used together to suggest that the in situ formed copper enolates of the *β*-dicarbonyl compound were the active nucleophilic species in the Michael addition of *β*-ketoester **52** and butenone **53** (Scheme 79). ESI-MS studies of the ongoing reaction were not able to show more advanced intermediates and the copper enolate **H** was the only intermediate observed during the reaction (Figure 31).

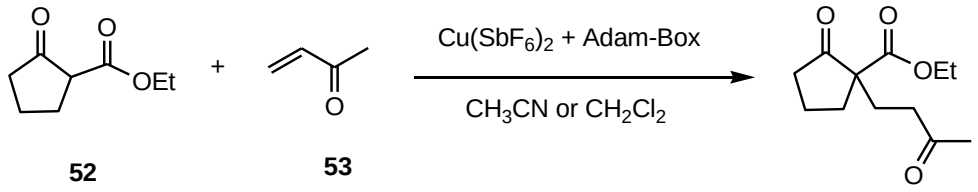

52 **53**

Scheme 79. Michael addition reaction between ethyl *β*-ketoester **52** and butenone **53** catalysed by copper salt with 2,2'-Isopropylidenebis[(4*R*)-(1-adamantyl)-2-oxazoline] (Adam-Box) ligand.

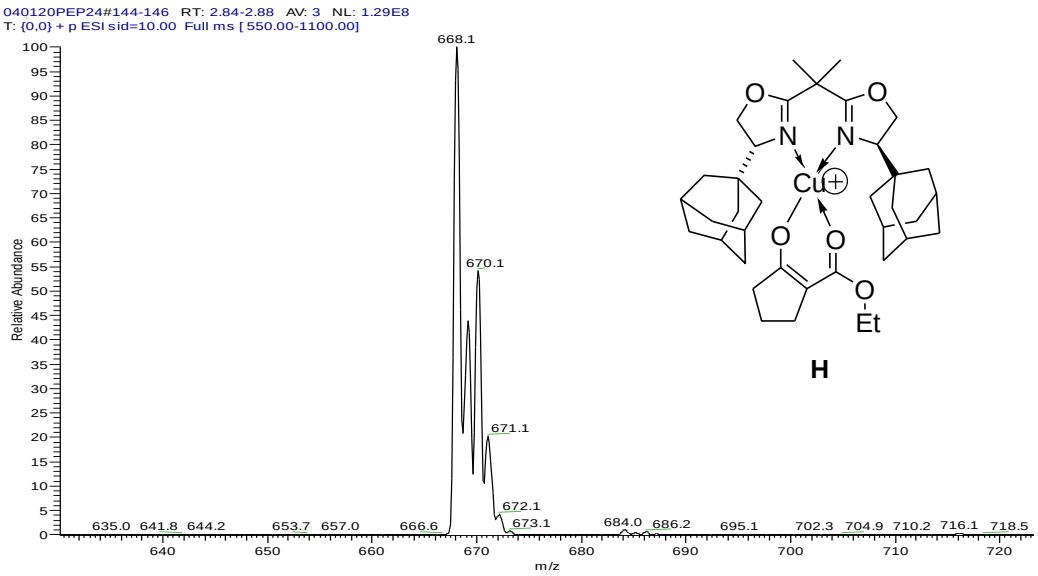

Figure 31. Copper enolate **H** was detected at *m/z* = 668.1 by ESI-MS and postulated as a reaction intermediate.

In the second case, the study was based on the reaction of 1-adamantyl ketoester **54** with two different electrophiles, butenone **53** and azodicarboxylate **55** and using La(OTf)$_3$/(S,S)-ip-pybox as the catalytic system in acetonitrile at room temperature (Scheme 80).

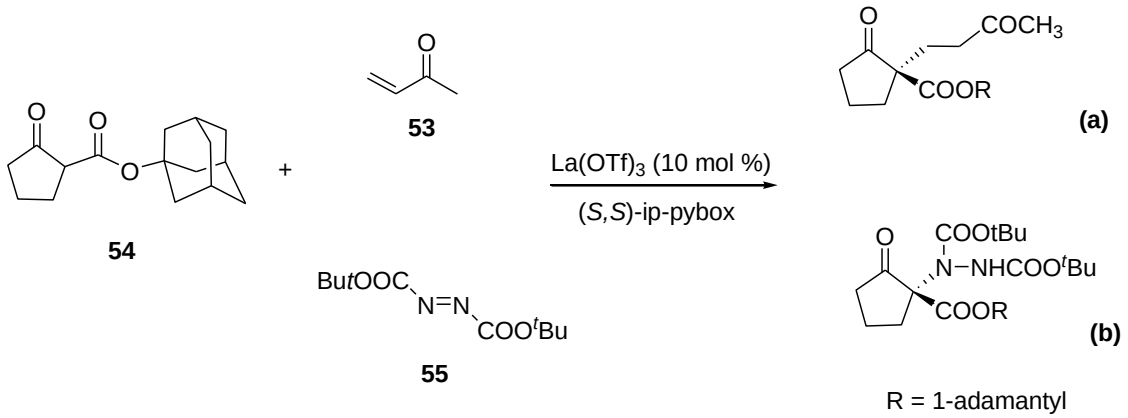

Scheme 80. Michael addition reaction between adamantyl β-ketoester **54** and methylvinylketone **53** (reaction a) or azodicarboxylate **55** (reaction b) catalysed by La(OTf)$_3$ and 2,6-Bis[(*S*)-4'-isoprpopyloxazolin-2'-yl]pyridine ((S,S)-ip-pybox) ligand.

ESI-MS experiments were used to detect reaction intermediates. A simultaneous coordination of the lanthanide with the chiral ligand and the enolate of the *β*–ketoester derivative **54** was proposed as the key intermediate and the mechanistic pathway was proposed based on that finding (Figure 32).

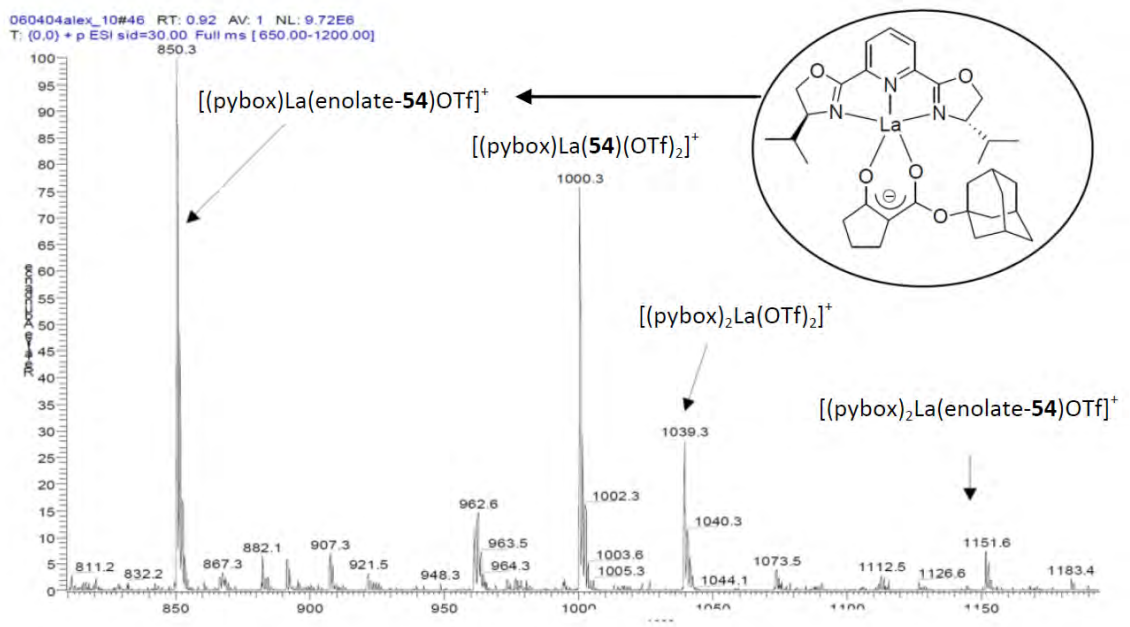

Figure 32. Enolate intermediate detected at *m/z* = 850.3, agreeing with the in situ formation of lanthanum enolate with one pybox ligand [(pybox)La(enolate-**54**)OTf]$^+$.

5.1.4. Previous mechanistic studies of cationic Rh(I)-catalysed reactions by ESI-MS

In 2009, Krische's group investigated the catalytic mechanism of hydrogen-mediated coupling of 1,6-diynes **56** and **57** to carbonyl compounds to afford (*Z*)-butadienyl allylic alcohols **58** and **59** using triphenylacetic acid (TPAA) as cocatalyst by ESI-MS and computational modelling (Scheme 81).[95]

In this study, they proposed a catalytic cycle based on the insertion of a carbonyl compound **60** to the rhodacyclopentadiene intermediate **I** obtained from the oxidative addition of the diyne, followed by hydrogenolysis assisted by a Brönsted acid of the oxarhodacyclopentadiene **J** formed, as is shown in Scheme 81. The first steps of this reaction are analogous to those of the [2+2+2] cycloaddition reaction (see the Scheme 2 of the mechanism in the General Introduction chapter).

[95] Williams, V.; Kong, J. R.; Ko, B J.; Mantri, Y.; Brodbelt, J. S.; Baik, M. H.; Krische, M. J. *J. Am. Chem. Soc.* **2009**, *131*, 16054.

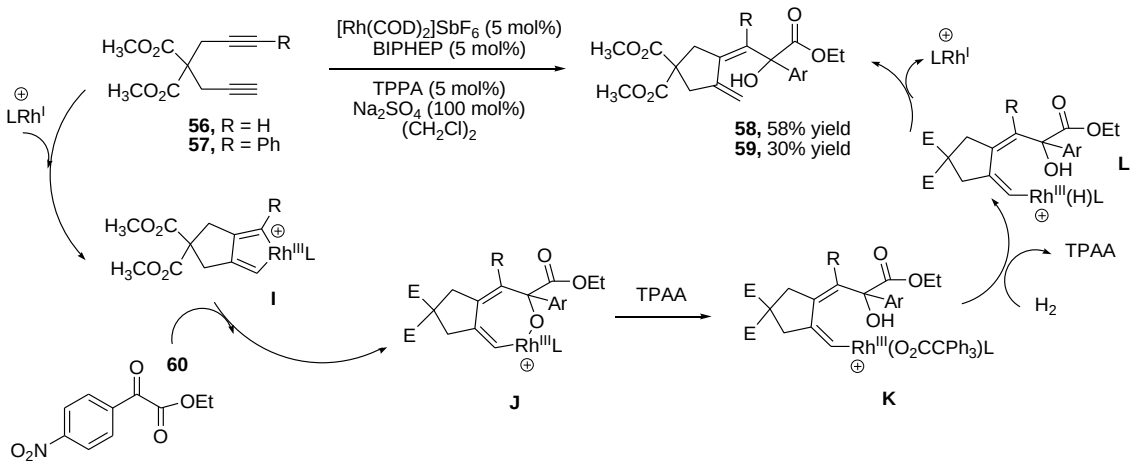

Scheme 81. Proposed catalytic mechanism for the hydrogen-mediated coupling of 1,6-diynes **56** and **57** to α-ketoester **60** using triphenylacetic acid as cocatalyst (L = BIPHEP, E = CO_2CH_3, Ar = *p*-NO_2phenyl, TPAA = triphenylacetic acid).

Different 1,6-diynes were hydrogenated in the presence of α-ketoester **60** using a cationic rhodium catalyst and the reaction mixture was studied by ESI-MS. To determine the formation of the proposed species in solution, an aliquot of the crude reaction mixture diluted 5000-fold in methanol was analyzed by ESI-MS.

The two most abundant ions observed included one that matched the mass of the cationic rhodacyclopentadiene **I** (*m*/*z* 909) and another that matched the mass of the cationic oxarhodacycloheptadiene **J** (*m*/*z* 1132) (Scheme 82a). Upon MS/MS studies, the ion of *m*/*z* 1132 dissociates by loss of 223 Da, consistent with the elimination of **60** to regenerate the rhodacyclopentadiene (*m*/*z* 909) (Scheme 82b). They also observed an ion of *m*/*z* 1195 corresponding to the mass of [Rh(BIPHEP)(**57**)(**60**)(OMe)(HOMe)], which may correspond to the methanol-methoxide adduct of the cationic oxarhodacycloheptadiene **J**.

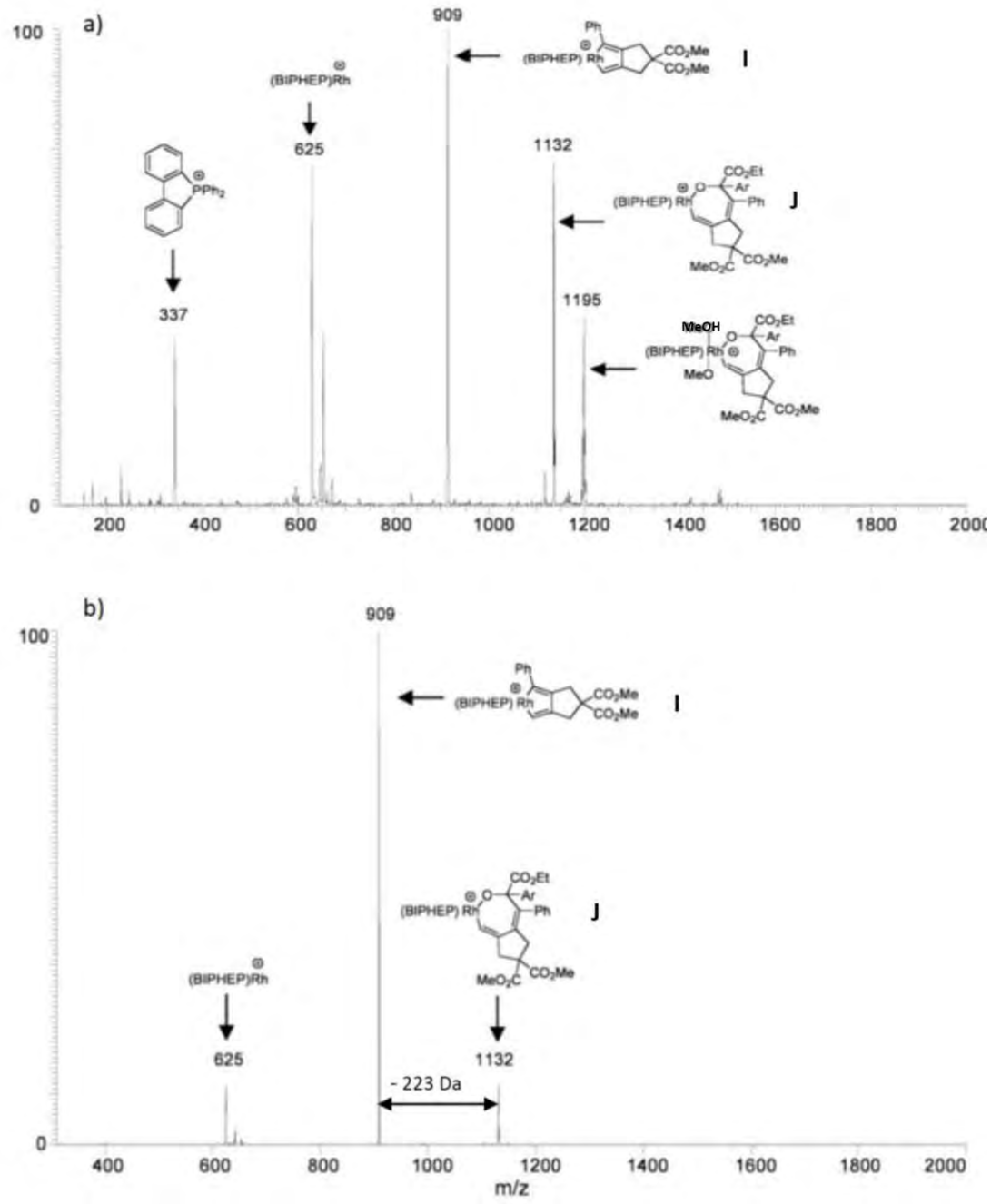

Scheme 82. a) ESI mass spectrum with proposed structural assignment of observed ions; b) MS/MS spectrum of the ion of *m/z* 1132 with proposed structural assignment of observed ions.

5.1.5. Previous mechanistic studies of Rh-catalysed [2+2+2] cycloaddition reactions by ESI-MS

Given the importance of transition-metal catalysed [2+2+2] cycloaddition reactions in organic synthesis, knowledge of its reactive intermediates, which play a key role in the understanding of the reaction mechanism, is of great interest. Although many transition-metal-catalysed

reactions have already been studied using ESI-MS, to the best of our knowledge the metal-catalysed [2+2+2] cycloaddition reaction has never been analyzed in this way as we have commented in the General Introduction of this thesis. The generally accepted reaction mechanism for this cycloaddition involving three alkynes is shown in Scheme 83.

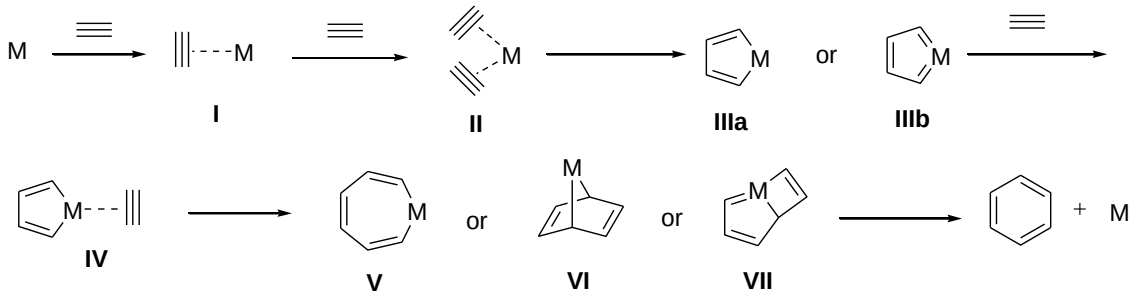

Scheme 83. Mechanistic proposal for the [2+2+2] cycloaddition reaction of three alkynes.

In 2009 our group described rhodium *N*-heterocyclic carbene complexes as being efficient catalysts for the cycloisomerization of both triyne and enediyne azamacrocicles as well as open-chain triyne substrates.[96] Futhermore, a partially intramolecular version between diynes and monoynes was also achieved. We also analyzed the intermolecular version, where there is a mass difference between substrates and products, by ESI-MS (Scheme 84).

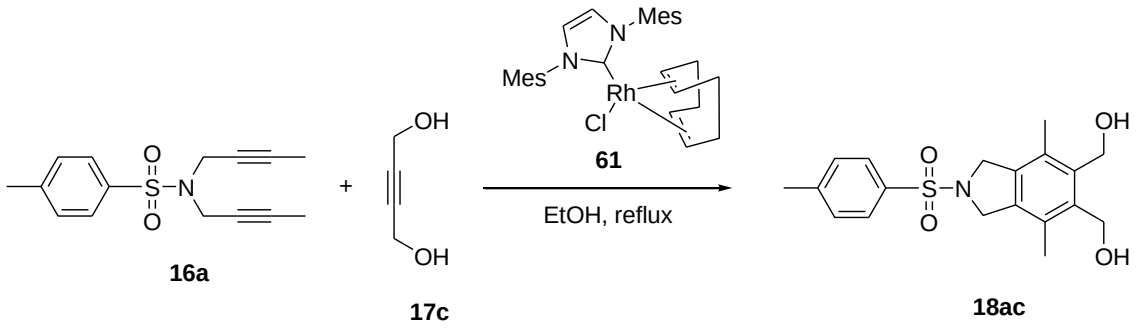

Scheme 84. Partially intramolecular reaction studied by ESI-MS(+).

The oxidative addition intermediate generated from diyne and Rh was detected by ESI-MS after 30 minutes of diyne **16a** addition to the solution of Rh-NHC complex **61** in ethanol. A cluster corresponding to the oxidative addition intermediate could be detected centred at *m/z* 790.2 ([Rh(IMes)(COD)(**16a**)]$^+$), which retains both the NHC and COD ligands in the rhodium metal (Figure 33).

[96] González, I.; Pla-Quintana, A.; Roglans, A. *Synlett*, **2009**, 2844.

However, no further intermediate could be observed involving the monoalkyne reacting partner.

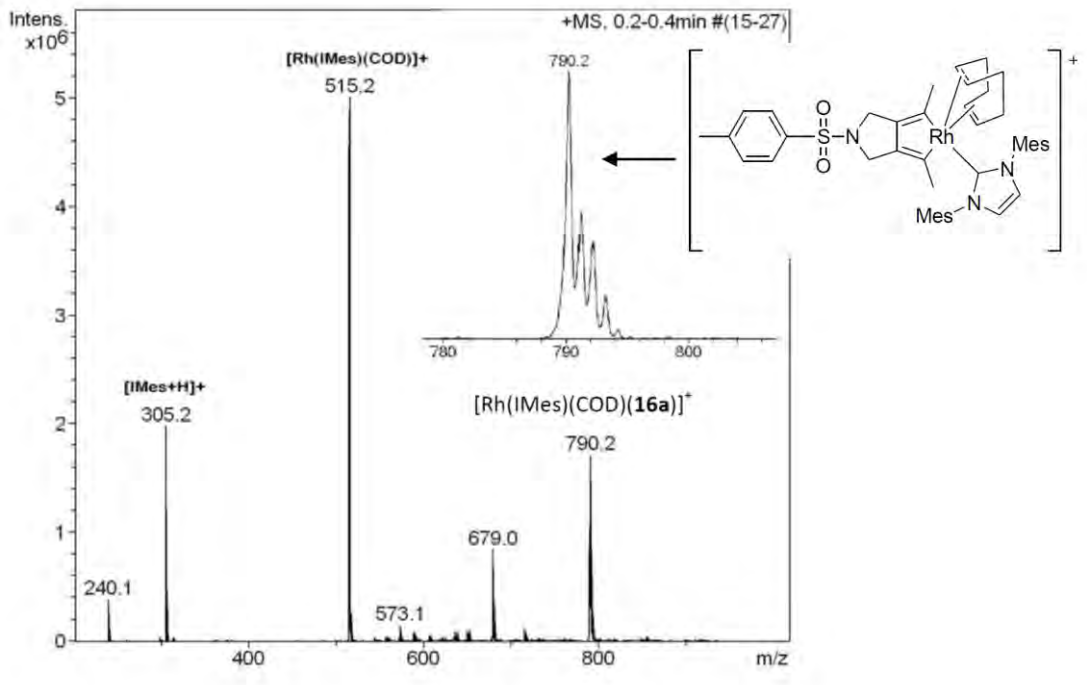

Figure 33. Oxidative coupling intermediate at *m/z* = 790.2 generated from diyne **16a** and Rh carbene complex.

In another study, performed in collaboration with Prof. Anny Jutand of CNRS, Paris, we for the first time found kinetic data for the catalytic cycle of the $RhCl(PPh_3)_3$-catalysed [2+2+2] cycloaddition of alkynes.[97] The partially intramolecular version between different diynes and 2-butyn-1,4-diol was analyzed by cyclic voltammetry, conductivity measurements, ^{31}P NMR, and ESI-MS (Scheme 85). The two main steps of the catalytic cycle, oxidative addition and insertion of the monoyne, were kinetically characterized by electrochemical monitoring of the formation and further reaction of the oxidative addition intermediate.

[97] Dachs, A.; Torrent, A.; Pla-Quintana, A.; Roglans, A.; Jutand, A. *Organometallics* **2009**, *28*, 6036.

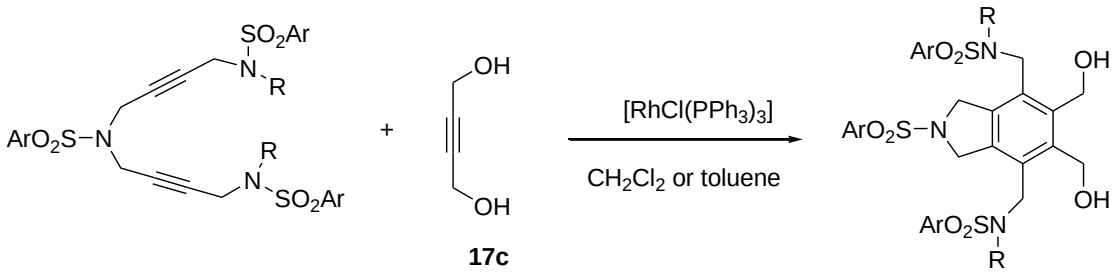

62a: R = Boc, Ar = 2,4,6-triisopropylphenyl
62b: R = H, Ar = 2,4,6-triisopropylphenyl
62c: R = H, Ar = 4-methylphenyl

Scheme 85. [2+2+2] Cycloaddition reaction between diynes **62** and 2-butyn-1,4-diol **17c** catalysed by Wilkinson's catalyst studied by ESI-MS.

Rhodacyclopentadiene intermediates were further characterized by ESI-MS. In all cases, cationic species were formed due to the loss of the chlorine atom of the catalyst. Two different species with one or two triphenylphosphines were detected for rhodacyclopentadiene **63c**, which contained the less sterically demanding arylsulfonamide. The other two rhodacylopentadienes, **63a** and **63b**, only showed ionic adducts containing one triphenylphosphine coordinated to the Rh(III) atom (Figure 34).

a)

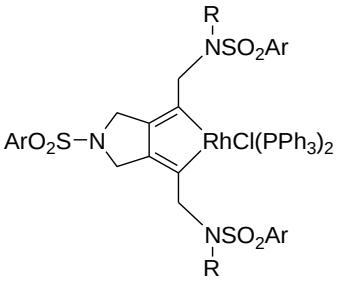

63a: R = Boc, Ar = 2,4,6-triisopropylphenyl
63b: R = H, Ar = 2,4,6-triisopropylphenyl
63c: R = H, Ar = 4-methylphenyl

b)

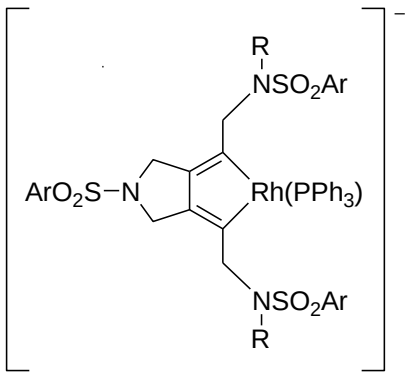

m/z = 1514.6 [**63a**-Cl-PPh_3]$^+$

m/z = 1314.3 [**63b**-Cl-PPh_3]$^+$

m/z = 978.0 [**63c**-Cl-PPh_3]$^+$

m/z = 1239.8 [**63c**-Cl]$^+$

Figure 34. a) Rhodacyclopentadiene intermediates **63a**, **63b** and **63c**; b) Rhodacyclopentadiene species detected by ESI-MS(+) due to the loss of chlorine atom and one triphenylphosphine group.

When 2-butyn-1,4-diol **17c** was added to the reaction mixture, no peak associated with a more advanced intermediate could be detected even when isolated rhodacyclopentadiene species were injected into the mass spectrometer and the monoalkyne was added. After the addition of the monoalkyne, the composition of the cationic species changed gradually over time: the intensity of the rhodacyclopentadiene species faded, the cycloaddition product was observed and increased in intensity over time, and triphenylphosphine oxide-related peaks appeared.

Furthermore, the formation of rhodacyclopentadiene **64** was confirmed again by injecting a 2:1 molar mixture of 2-butyn-1,4-diol and the Wilkinson's catalyst in dichloromethane into the mass spectrometer (Scheme 86). A new peak emerged which we identified as rhodacylcopentadiene **64** after having lost its chlorine atom and a triphenylphosphine ligand.

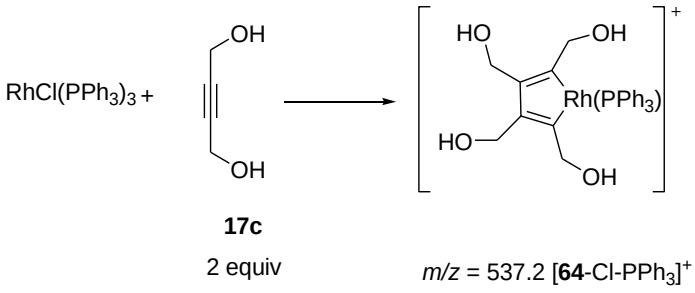

Scheme 86. Rhodacyclopentadiene intermediate between two alkynes and Wilkinson's catalyst detected at *m/z* = 537.2 by ESI-MS(+).

In summary, in these studies our group detected the oxidative coupling intermediate but in no case were we able to detect the alkyne insertion intermediate. The aim of the study will be to analyze the whole mechanism of the rhodium-catalysed [2+2+2] cycloaddition reaction of diynes and monoynes by means of ESI-MS in order to detect and characterize all of the intermediates in the catalytic cycle.

Given that, to date, the oxidative addition intermediate (rhodacyclopentadiene) is the only catalytic specie that has been detected or isolated experimentally, this work will focus on the observation of all the intermediates in the catalytic cycle, especially the most advanced alkyne insertion intermediate. The strategy proposed is to use the combination of a cationic rhodium(I) complex ($[Rh(COD)_2]BF_4$) with diphosphine ligands, which generates highly active complexes that can be detected by ESI(+) experiments. Moreover, the structural assignments of ions will be supported by tandem mass spectrometry analyses.

To complete the experimental results, computer model studies based on density functional theory (DFT) will be performed to support the structural proposal of the intermediates detected by ESI-MS.

5.2. Results and discussion

5.2.1. Experimental design

The first step of the study was to choose the reaction to be studied by ESI-MS. Among the different versions of the [2+2+2] cycloaddition reaction, the completely intramolecular version was discarded because the mass of the intermediates does not change during the whole reaction. The completely intermolecular [2+2+2] cycloaddition is rather difficult due to the regio- and chemoselectivity issues. Therefore, the partially intramolecular [2+2+2] cycloaddition between diynes and monoynes was chosen. This version of the reaction allows the consumption of the reagents and the formation of the intermediates and the final product to be followed due to the different mass/charge ratio of the compounds involved in the reaction (Scheme 87). The possibility of changing the diyne linkage (Z in Scheme 87) is also interesting to aid ionization and to compare the intermediates detected in each case as well as their CID behaviour.

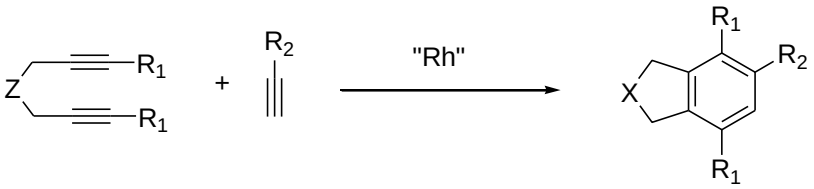

Scheme 87. General partially intramolecular [2+2+2] cycloaddition reactions studied by ESI-MS.

We then attempted to find a good catalytic system. Among the more usual rhodium catalysts, cationic Rh(I) complex $[Rh(COD)]_2BF_4$ in combination with BINAP-type ligands has been shown to be an efficient catalyst for [2+2+2] cycloaddition reactions. This was selected as the catalytic system for the present study for various reasons: a) it is cationic and is postulated to form cationic intermediates unlike the Wilkinson's catalyst, which is neutral; b) the catalytically active species are generated in situ by hydrogenation of a solution containing the cationic complex $[Rh(COD)]_2BF_4$ and diphosphines, so it constitutes a modular platform that allows the ligand to be changed with relative ease.

The final step in the experimental design consisted in optimizing the reaction in the laboratory (solvent, concentration, reagents ratio and temperature). Optimization led to the use of refluxing dichloroethane or dichloromethane at a concentration of 0.036 M of diyne and a diyne:monoyne ratio of 1:1.5, which, after two to three hours depending on the substrates afforded quantitative yields of the cycloadducts (see the experimental section for a detailed description of the procedure). We noted that the order of addition of reagents was important since diyne selfcoupling could be minimized by adding monoyne before diyne.

5.2.2. Scope of the reaction

A series of reactions was performed between different diynes and monoynes in order to obtain a full set of reactions for study by ESI-MS (Scheme 88). The reactions were first run in the laboratory in order to determine yields and reaction times. These results are also set out in Table 16-18 to facilitate the comparison of the reactivity of different substrates and catalytic systems.

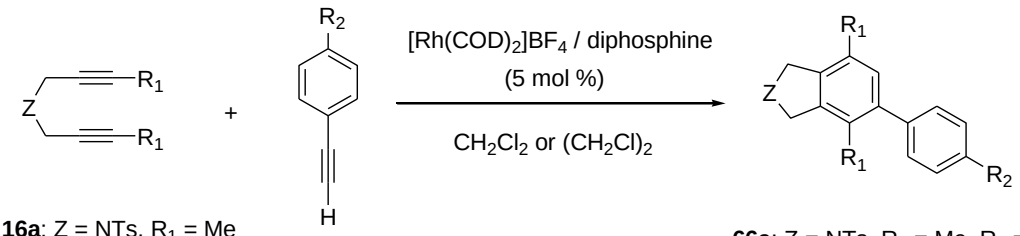

16a: Z = NTs, R_1 = Me
16d: Z = NTs, R_1 = H
16e: Z = C(COOEt)$_2$, R_1 = H
16b: Z = C(COOEt)$_2$, R_1 = Me

65a: R_2 = Me
65b: R_2 = OMe
17a: R_2 = H
65c: R_2 = ^{t}Bu
65d: R_2 = F
65e: R_2 = Br
65f: R_2 = NO_2
65g: R_2 = NMe_2
65h: R_2 = CN

66a: Z = NTs, R_1 = Me, R_2 = Me
66b: Z = NTs, R_1 = Me, R_2 = OMe
18aa: Z = NTs, R_1 = Me, R_2 = H
66c: Z = NTs, R_1 = Me, R_2 = ^{t}Bu
66d: Z = NTs, R_1 = Me, R_2 = F
66e: Z = NTs, R_1 = Me, R_2 = Br
66f: Z = NTs, R_1 = Me, R_2 = NO_2
66g: Z = NTs, R_1 = Me, R_2 = NMe_2
66h: Z = NTs, R_1 = Me, R_2 = CN
18da: Z = NTs, R_1 = H, R_2 = H
66i:Z = C(COOEt)$_2$, R_1 = H, R_2 = Me
18ea: Z = C(COOEt)$_2$, R_1 = H, R_2 = H
66j: Z = C(COOEt)$_2$, R_1 = Me, R_2 = Me

Scheme 88. [2+2+2] Cycloaddition reactions monitored by ESI-MS.

We started by evaluating the reaction between *N*Ts-linked diynes. Diyne **16a,** which has non-terminal alkynes, was first reacted with phenylacetylene **17a** and the diphosphine of the catalytic system was varied (Table 16). Comparison between racemic-BINAP and (*R*)-H_8-BINAP revealed that the first diphosphine was the most efficient since the reaction was finished after 1 hour with an excellent yield (compare Entries 1 and 2, Table 16). Although (*R*)-H_8-BINAP was found to be the most efficient phosphine, we chose to use *rac*-BINAP, which unlike (*R*)-H_8-BINAP is commercially available in racemic form, as it also gave good results and was considerably less expensive. When BIPHEP was used, it was necessary to heat under reflux in dichloroethane to reduce the reaction time (Entry 3, Table 16). The results of the cycloaddition between *N*Ts-linked terminal diyne **16d** and phenylacetylene **17a** using different diphosphines were then evaluated. When BINAP was used, a 53% yield of the cycloadduct was obtained in one hour at room temperature (Entry 4, Table 16). When BIPHEP was used at room temperature the yield increased to 74% but the reaction time increased significantly (Entry 5, Table 16). The same yield with a shorter reaction time (four hours) was obtained when BIPHEP was used at an increased temperature (Entry 6, Table 16). Terminal diyne **16d** is more prone to form homocoupling products, which explains the lower yields obtained with this diyne in comparison with non-terminal diyne **16a**.

Table 16. [2+2+2] Cycloaddition of different diynes with phenylacetylene **17a** using different phosphines.

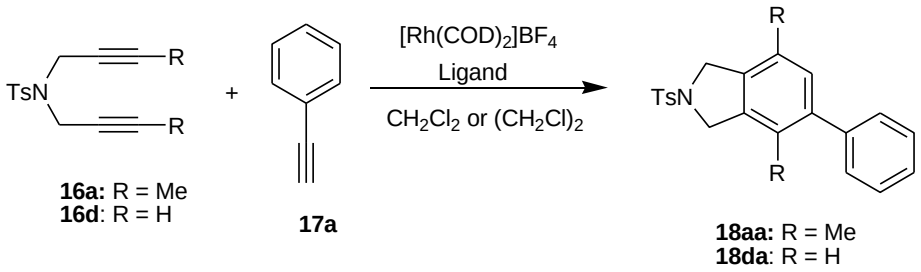

16a: R = Me
16d: R = H

17a

18aa: R = Me
18da: R = H

Entry	Diyne	Ligand	Reaction conditions	Product, Yield (%)
1	**16a**	*rac*-BINAP	CH_2Cl_2, r.t., 1h	**18aa**, 80
2	**16a**	(*R*)-H_8-BINAP	CH_2Cl_2, r.t., 1h	**18aa**, 99
3	**16a**	BIPHEP	$(CH_2Cl)_2$, 84ºC, 1h	**18aa**, 88
4	**16d**	*rac*-BINAP	CH_2Cl_2, r.t., 1h	**18da**, 53[a]
5	**16d**	BIPHEP	CH_2Cl_2, r.t., 21 h	**18da**, 74
6	**16d**	BIPHEP	$(CH_2Cl)_2$, 84ºC, 4h	**18da**, 73

[a]Homocoupling of diyne **16d** was also obtained.

Cycloaddition between internal *N*Ts-linked diyne **16a** and different *para*-substituted phenylacetylenes **65a-h** was then performed (Table 17). For these cases, *rac*-BINAP in reflux conditions was necessary since the reactions were slower than when phenylacetylene **17a** was used. Between four and five hours were required to complete the reaction. Excellent yields were obtained in all cases. With phenylacetylenes having a fluorine or cyano substituent (monoynes **65d** and **65h**) the yield decreased to 60% (Entries 5 and 9, Table 17).

Table 17. [2+2+2] Cycloaddition of internal diyne **16a** and different phenylacetylenes **65a-h**.

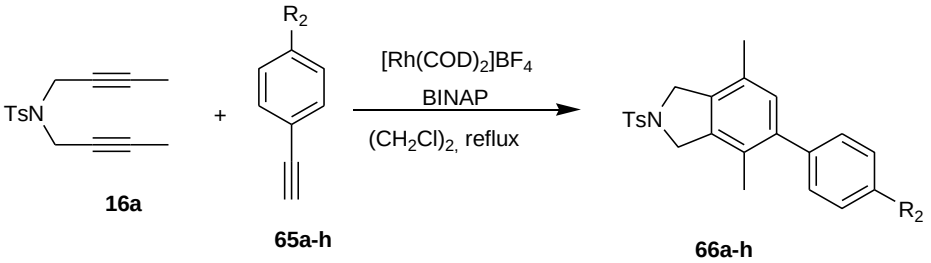

16a

65a-h

66a-h

Entry	Monoyne / R_2	Reaction conditions	Product, Yield (%)
1	**65a** / Me	$(CH_2Cl)_2$, 84ºC, 5h	**66a**, 100
2	**65b** / OMe	$(CH_2Cl)_2$, 84ºC, 4.5 h	**66b,** 96
3	**17a** / H	CH_2Cl_2, r.t., 1h	**18aa,** 80
4	**65c** / ^{t}Bu	$(CH_2Cl)_2$, 84ºC, 5h	**66c,** 100
5	**65d** / F	$(CH_2Cl)_2$, 84ºC, 4h	**66d,** 60
6	**65e** / Br	$(CH_2Cl)_2$, 84ºC, 5h	**66e,** 100
7	**65f** / NO_2	$(CH_2Cl)_2$, 84ºC, 4h	**66f,** 100
8	**65g** / NMe_2	$(CH_2Cl)_2$, 84ºC, 4.5 h	**66g,** 95
9	**65h** / CN	$(CH_2Cl)_2$, 84ºC, 5h	**66h**, 60

Finally, the tether of the diyne was varied. Terminal and internal malonate-tethered diynes **16e** and **16b** were evaluated with phenylacetylene **17a** and *p*-methylphenylacetylene **65a** (Table 18). For the terminal diyne **16e**, the reactions could be performed at room temperature due to the fast formation of the product, but for the internal diyne **16b** it was necessary to heat at reflux to accelerate the reaction. It is important to note that terminal diyne gave worse yields (Entries 1 and 2, Table 18) than the internal one (Entry 3, Table 18) due to the parallel formation of diyne homocoupling products.

Table 18. [2+2+2] cycloaddition reactions between malonate-tethered diynes **16e** and **16b** and phenylacetylenes **65a** and **17a**.

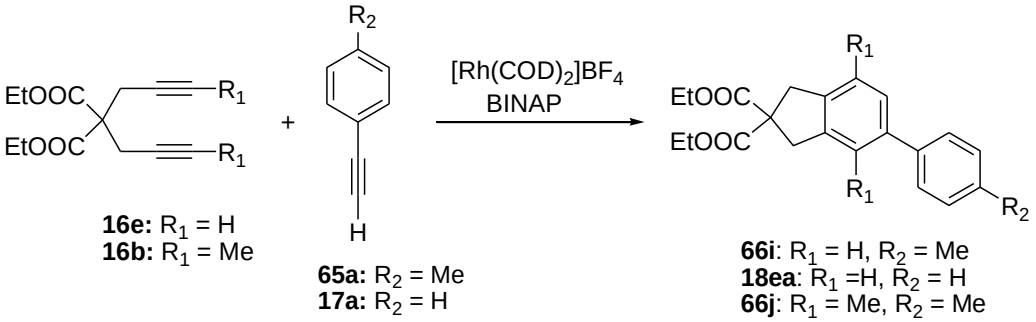

16e: R_1 = H
16b: R_1 = Me

65a: R_2 = Me
17a: R_2 = H

66i: R_1 = H, R_2 = Me
18ea: R_1 =H, R_2 = H
66j: R_1 = Me, R_2 = Me

Entry	Diyne	Monoyne	Reaction conditions	Product, Yield (%)
1	**16e**	**65a**	CH_2Cl_2, r.t., 2h	**66i**, 49
2	**16e**	**17a**	CH_2Cl_2, r.t., 2h	**18ea**, 82
3	**16b**	**65a**	$(CH_2Cl)_2$, 84ºC, 1.5 h	**66j**, 98

After the optimization of the reaction conditions, we concluded that terminal diynes were more reactive than the internal ones (they reacted at shorter reaction times and gave greater amounts of homocoupling products than the internal ones).

Once the best reaction conditions were achieved, all the reactions in Scheme 88 were followed by ESI-MS. However, only those reactions which gave us interesting new information are described in this chapter.

5.2.3. Characterization of the catalytic mixture

The components of the catalytic system were first analysed. $[Rh(COD)_2]BF_4$ was dissolved in methanol and injected into the mass spectrometer.[98] One peak was observed at *m/z* = 211.0, corresponding to the complex $[Rh(COD)]^+$ that had lost a COD ligand. Analysis of the BINAP ligand by ESI-MS gave the molecular peak $[BINAP + H]^+$ at *m/z* = 623.2, but the peak of an

[98] All of the species detected in the present study were assigned by comparison of the experimentally obtained isotopic pattern and the theoretically calculated one. Only the most relevant spectra are shown in this chapter. The whole set of experiments can be found in the supplementary information.

a)

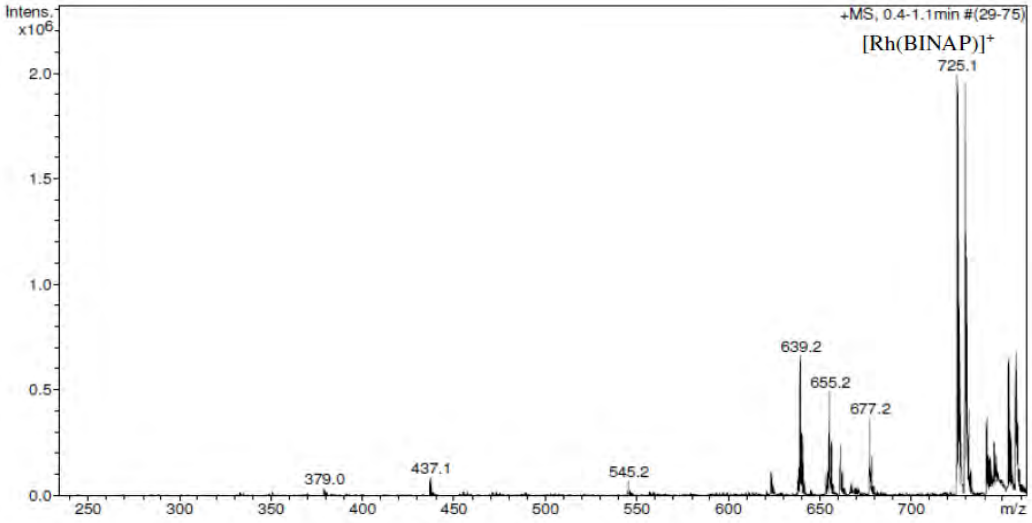

b)

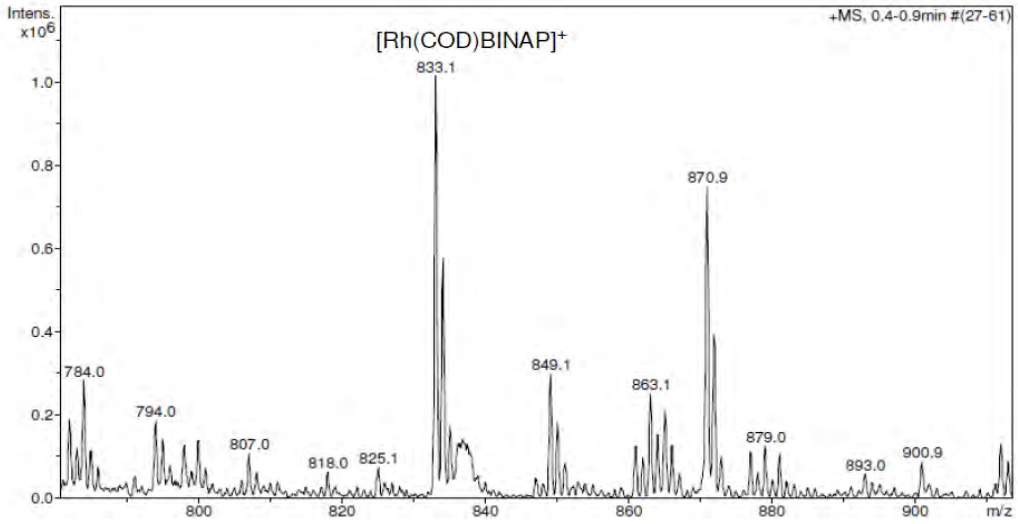

c)

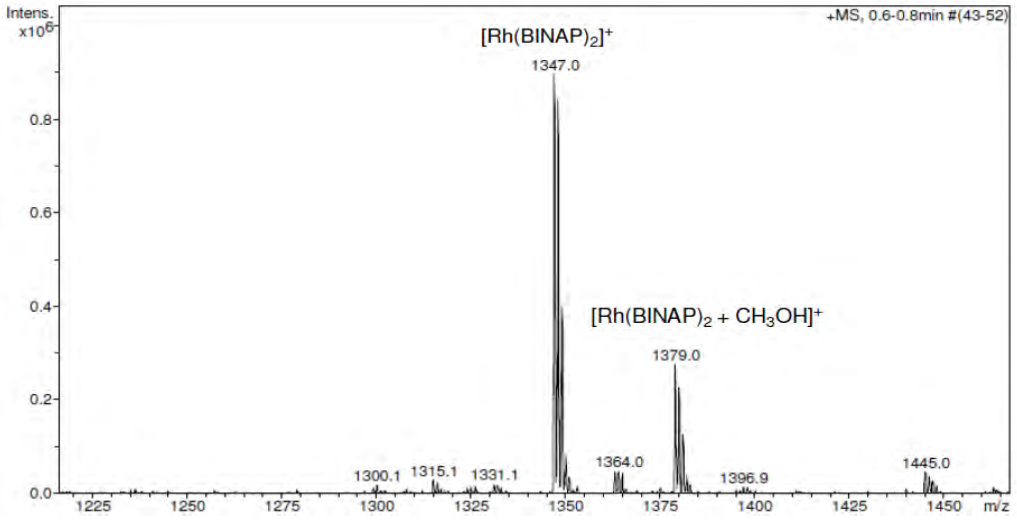

Figure 35. ESI(+) mass spectra of a solution of $[Rh(COD)_2]BF_4$/BINAP (1:1) diluted in methanol. a) *m/z* 240-770 range, b) *m/z* 780-920 range, c) *m/z* 1200-1500 range.

oxidized species $[BINAP=O + H]^+$ was also observed at *m/z* = 639.2. This oxidized species could be formed in the same mass spectrometer since an oxidative positive ESI mode was used and the presence of traces of oxygen was possible given the purity of the nebulizing nitrogen employed.

The active catalytic species was then generated by hydrogenating[99] a 1:1 mixture of $[Rh(COD)_2]BF_4$ and the BINAP ligand in dichloromethane. Upon dilution with methanol, this mixture was analysed by ESI-MS (Figure 35). The spectrum showed the species $[Rh(BINAP)]^+$ at *m/z* = 725.1, $[Rh(COD)BINAP]^+$ at *m/z* = 833.1, and $[Rh(BINAP)_2]^+$ at *m/z* = 1347.0. Then, the peak at *m/z* = 833.1 was fragmented by CID, resulting in the loss of the COD ligand and leading to the formation of $[Rh(BINAP)]^+$ at *m/z* = 725.0 (Figure 36).

We postulate that methanol is not only a better suited solvent for ESI-MS but that it also helps to stabilize the short-lived intermediates by forming solvent adducts or complexes which can then be split in the ESI source, thus facilitating their detection by mass spectrometry. Methanol has been shown not to have a deleterious effect on the reaction since the cycloaddition of diyne **16a** and *p*-methylphenylacetylene **65a** (Scheme 89) works satisfactorily (75% conversion in five hours at reflux) when run in a mixture of DCE/MeOH (1:10, v/v).

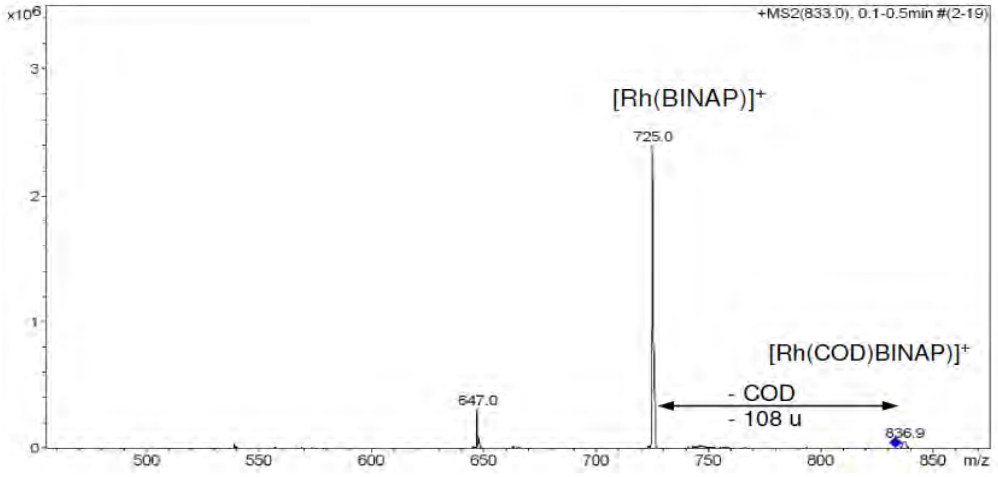

Figure 36. ESI(+)-MS/MS spectrum of the ion $[Rh(COD)(BINAP)]^+$ at *m/z* = 833 (collision energy of 1 V).

[99] Hydrogenation of the catalytic mixture is a usual procedure for the activation of the catalyst.

5.2.4. Study of the reaction mixture

As a first test reaction we chose the cycloaddition of diyne **16a** and *p*-methylphenylacetylene **65a** (Scheme 89).

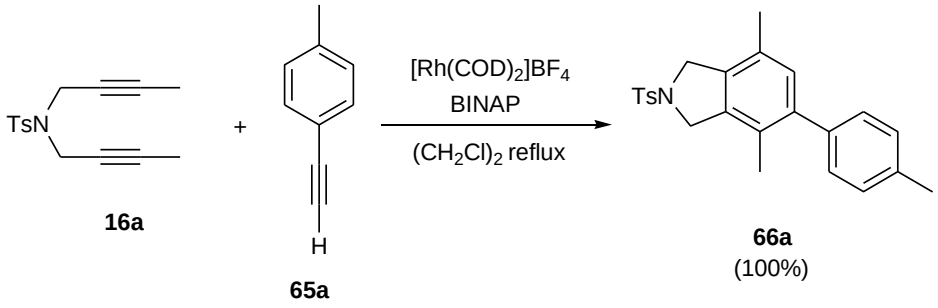

Scheme 89. [2+2+2] Cycloaddition reaction between diyne **16a** and *p*-methylphenylacetylene **65a** studied by ESI-MS.

In order to determine the sensitivity of the technique towards the species present in the reaction, the first step was to analyze each of the components separately by ESI-MS. The starting diyne **16a** and final product **66a** both gave peaks corresponding to the $[M + H]^+$ and $[M + Na]^+$ adducts. Phenylacetylene **65a** was not observed given its high apolar nature. Cycloadduct **66a** was submitted to CID and the loss of 156 mass units corresponding to the TsH group was observed (Figure 37).

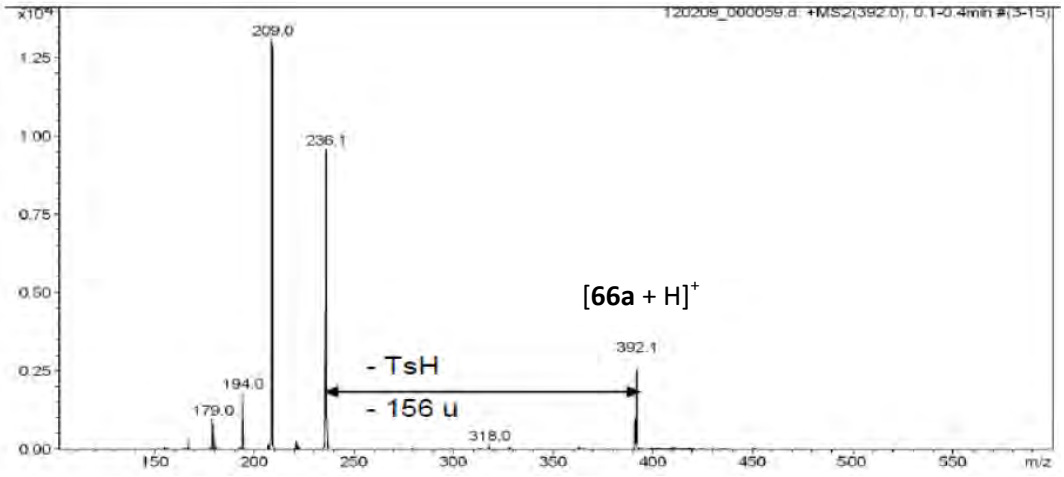

Figure 37. ESI(+)MS/MS spectrum of the ion at *m/z* = 392.

The complete reaction resulting from the addition of diyne **16a** to the mixture of hydrogenated $[Rh(COD)_2]BF_4$ and BINAP together with 1.5 equivalents of *p*-methylphenylacetylene **65a** in dichloroethane was the next mixture to be analysed by ESI-MS. After heating at reflux for 15 minutes in an inert atmosphere, a sample was diluted in methanol and injected into the mass spectrometer (Figure 38).

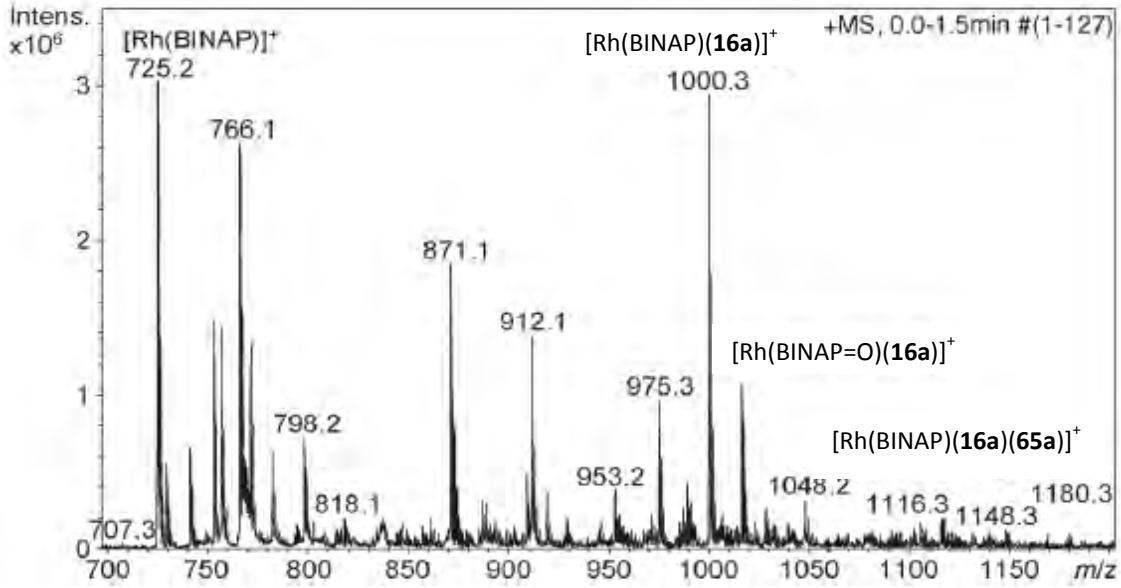

Figure 38. ESI mass spectrum of a mixture of ($[Rh(COD)_2]BF_4$ + BINAP) (5 mol%) + **65a** + **16a** after 15 min.

The postulated catalytically active species $[Rh(BINAP)]^+$ was detected at *m/z* = 725.2. The peak observed at *m/z* = 1000.3 corresponds to the mass of a cluster containing $[Rh(BINAP)(\mathbf{16a})]^+$. Since the peak may correspond to two possible intermediates, one resulting from the coordination of the diyne to rhodium and the other resulting from oxidative addition of the diyne to the metal, we further characterized it by conducting an MS/MS analysis (Figure 39).

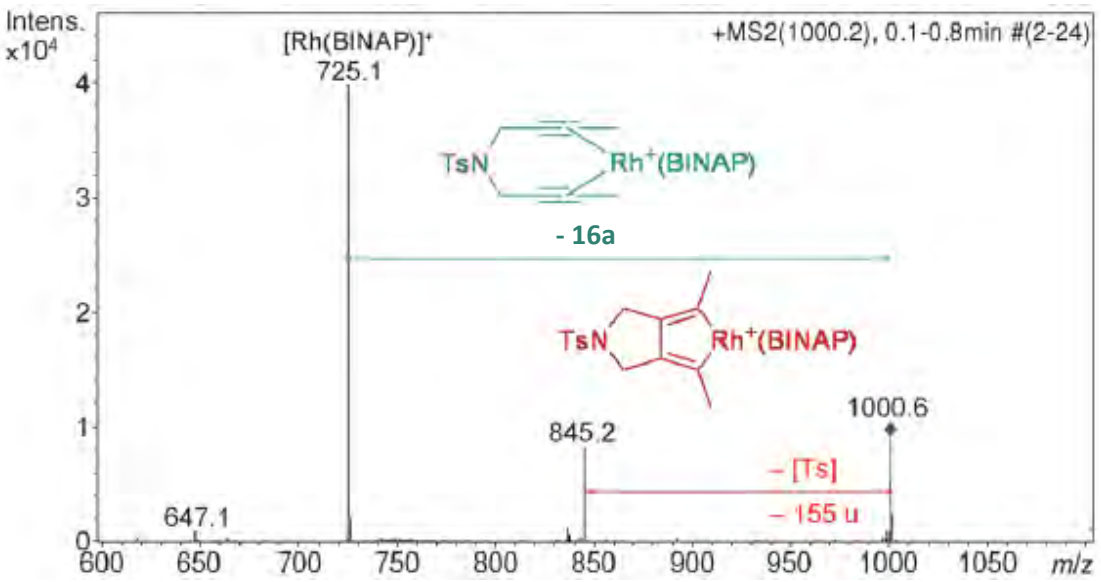

Figure 39. CID mass spectrum of the ion at *m/z* = 1000.3.

The peak at *m/z* = 1000.3 suffered fragmentation resulting in a peak at *m/z* = 725.0, corresponding to the fragment $[Rh(BINAP)]^+$, and another cleavage to release a fragment $[M-155]^+$ corresponding to loss of the tosyl group. Had the insertion step already occurred, $[Rh(BINAP)]^+$ would not have been observed as the insertion step is irreversible.[95] Therefore, we assign the cluster at *m/z* = 1000.3 to a mixture of the two intermediates: the coordination intermediate fragmenting to $[Rh(BINAP)]^+$ by dissociation of the diyne component from the metal, and the oxidative addition intermediate fragmenting by tosyl loss through S-N bond fragmentation, which is a common fragmentation suffered by aryl sulfonamides in mass spectrometry.[100] A peak was also observed in the reaction mixture at *m/z* = 1016.3 which is attributable to the $[Rh(BINAP=O)(\mathbf{16a})]^+$ species. MS/MS studies of this compound (Figure 40) indicated that it was cleaved to release a fragment $[M-155]^+$ corresponding to the loss of the tosyl group, from which we concluded that it corresponds to the oxidized form of the oxidative addition intermediate.

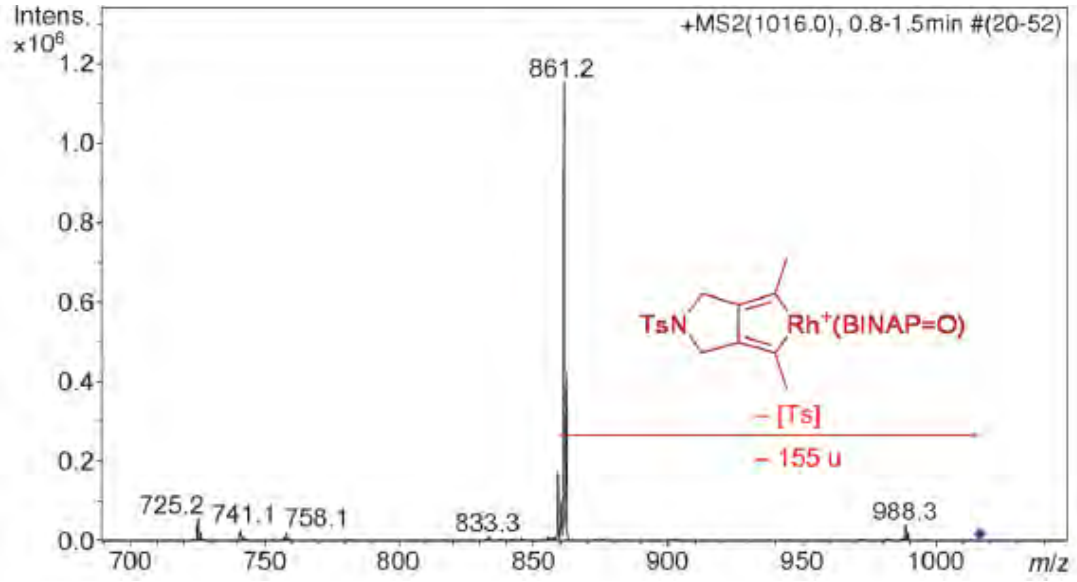

Figure 40. CID mass spectrum of the ion at *m/z* = 1016.3.

The oxidative addition is thought to be the rate-determining step of the [2+2+2] cycloaddition reaction. The ensuing intermediates might therefore be present at very low concentrations and so are likely to be detected, if at all, as minor ions. In the search for these minor ions, spectra were expanded paying special attention to the *m/z* 1110–1120 region. We were delighted to observe a small peak at *m/z* = 1116.3, corresponding to the formal addition of *p*-methylphenylacetylene to the intermediate $[Rh(BINAP)(\mathbf{16a})]^+$. This peak may also correspond to different intermediates: one involving π-coordination of acetylene **65a** to rhodacyclopentadiene, another resulting from alkyne insertion into the same intermediate,

[100] a) Hu, N.; Tu, Y.-P.; Jiang, K.; Pan, Y. *J. Org. Chem*. **2010**, *75*, 4244; b) Xu, G.; Huang, T.; Zhang, J.; Huang, J. K.; Carlson, T.; Miao, S. *Rapid Commun. Mass Spectrom*. **2010**, *24*, 321; c) Fitch, W. L.; He, L.; Tu, Y.-P.; Alexandrova, L. *Rapid Commun. Mass Spectrom*. **2007**, *21*, 1661; d) Thurman, E. M.; Ferrer, I.; Pozo, O. J.; Sancho, J. V.; Hernandez, J. *Rapid Commun. Mass Spectrom*. **2007**, *21*, 3855.

and a third which might correspond to a coordination species of the final product **66a** with the catalyst (Scheme 90).

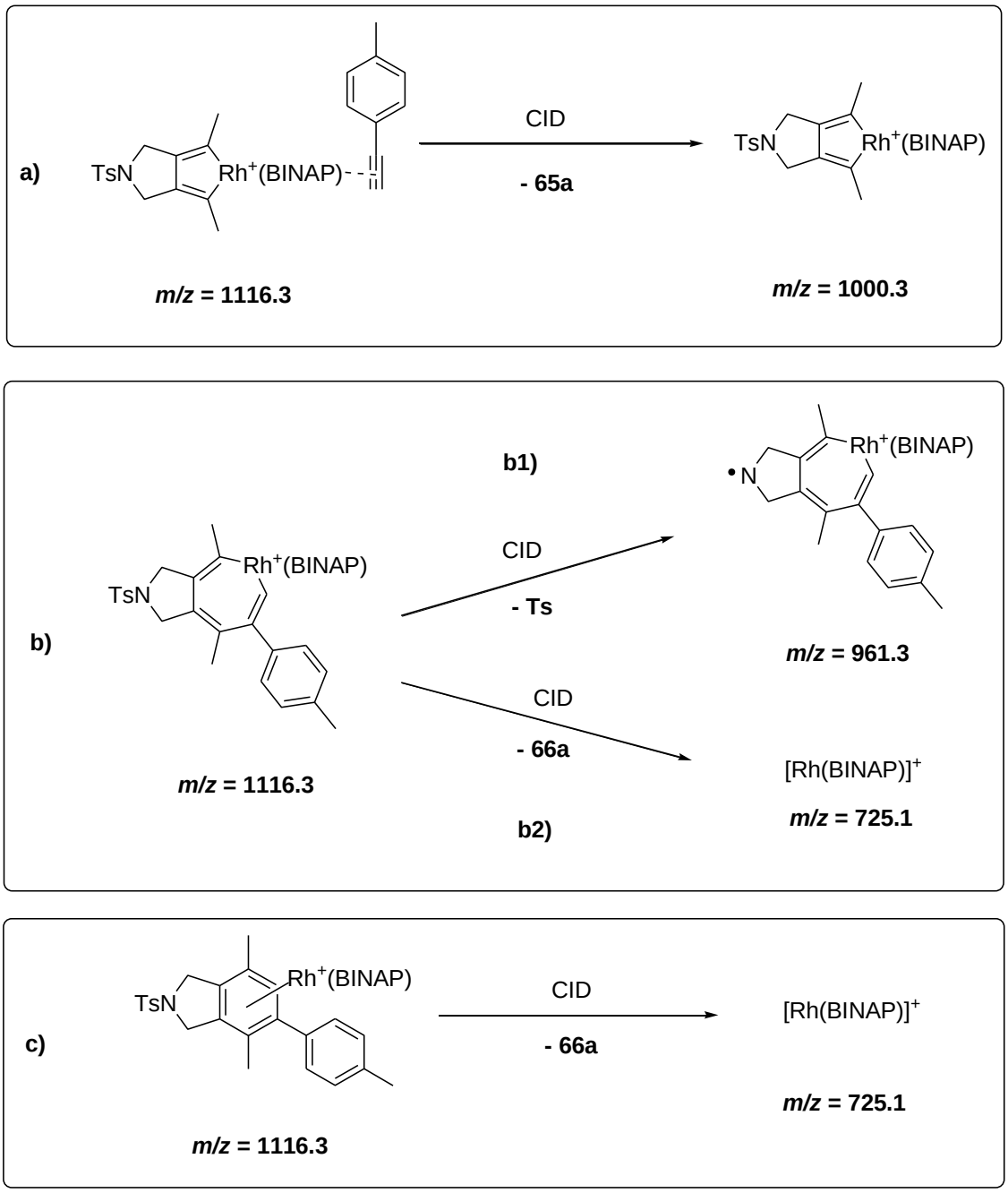

Scheme 90. Expected fragmentations of the peak with *m/z* = 1116.3; a) Dissociation of acetylene **65a** from the oxidative coupling intermediate; b1) Loss of the tosyl group from the alkyne insertion intermediate; b2) Reductive elimination; c) Final product dissociation from the catalyst.

Given the importance of the observation of the peak at *m/z* = 1116.3, we proceeded to further characterize the nature of this intermediate by MS/MS (Figure 41). If the insertion step had not occurred, fragmentation would have caused simple *p*-methylphenylacetylene dissociation and

the formation of a fragment at *m/z* = 1000.3 (Scheme 90a). Since this was not observed, a π-coordination intermediate can be ruled out. In fact, two main fragments arose after CID of the peak at *m/z* = 1116.3, one at *m/z* = 961.3 corresponding to the loss of the tosyl group (Scheme 90b1), and another at *m/z* = 725.1 corresponding to the mass of $[Rh(BINAP)]^+$ (Scheme 90c). This last fragment was derived from the loss of 391 mass units, exactly the weight of the final product **66a**. Whereas the formation of $[Rh(BINAP)]^+$ may be the result of either reductive elimination from the insertion intermediate (Scheme 90b2) or product dissociation from the complex formed by coordination of the catalyst to the final product (Scheme 90c), the tosyl group is presumably lost from the olefin insertion intermediate.

Further evidence of this hypothesis was gained by injecting into the mass spectrometer a mixture of **66a** in dichloroethane and 5 mol % of the catalytic mixture. The mixture was stirred for 5 minutes and then diluted with methanol prior to injection. The catalytic mixture gave the three peaks that have already been observed for the catalytic mixture ($[Rh(BINAP)]^+$ at *m/z* = 725.1, $[Rh(COD)BINAP]^+$ at *m/z* = 833.1, and $[Rh(BINAP)_2]^+$ at *m/z* = 1347.0) and an extra peak at *m/z* = 1115.9 corresponding to the coordination of **66a** with the catalytic species $[Rh(BINAP)]^+$ was observed (Figure 41). When this peak was submitted to CID at the same collision energy as in the previous experiment (fragmentation of the peak at *m/z* = 1116.3 detected for the ongoing reaction), it only gave the $[Rh(BINAP)]^+$ fragment at *m/z* = 725.1 without loss of the tosyl group (compare Figure 41 and Figure 42).[101]

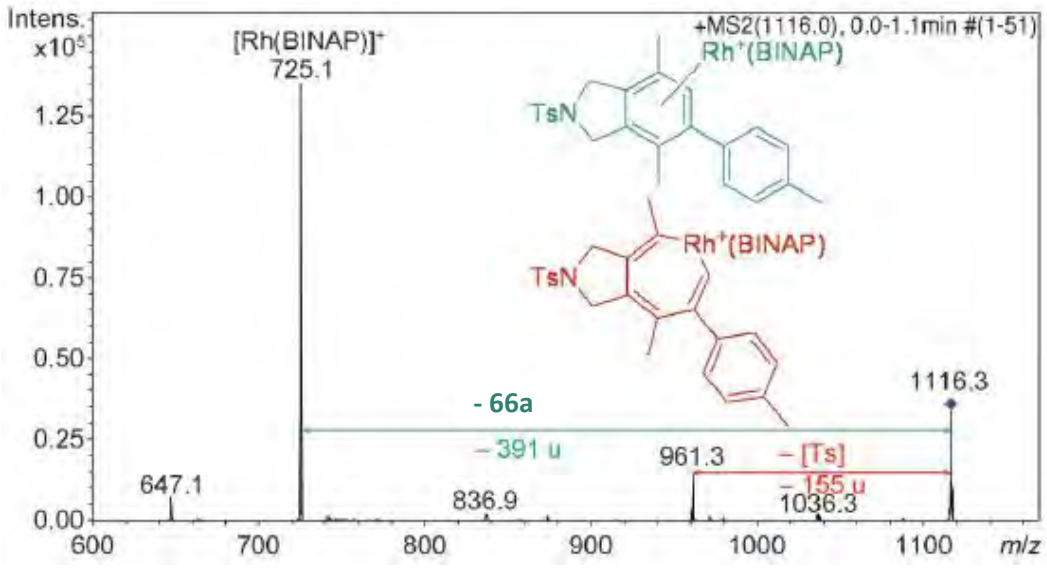

Figure 41. CID mass spectrum of the ion at *m/z* = 1116.3 at a collision energy of 0.95 V.

[101] The alkyne insertion intermediate has been drawn as the rhodacycloheptatriene in accordance with the results obtained by DFT calculations, which are commented on in section 5.2.8.

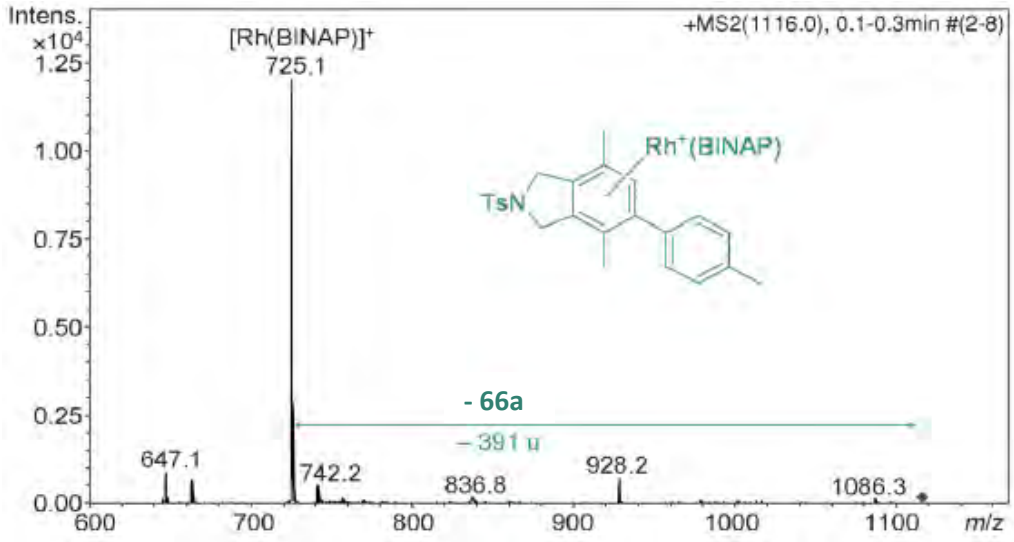

Figure 42. CID mass spectrum of the ion at *m/z* = 1115.9 at a collision energy of 0.95 V originating from a mixture of **66a** + rhodium catalyst.

We therefore conclude that we have detected for the first time the most advanced insertion intermediate. The reaction was monitored at fixed time intervals by ESI-MS and was complete after 2 hours (TLC monitoring), as shown by the disappearance of the ions corresponding to the intermediates at *m/z* = 1000 (oxidative addition) and *m/z* = 1116 (alkyne insertion) and the formation of the final product **66a**.

5.2.5. Study of different monoyne substrates

To confirm the species detected and to test the general applicability of the method, we studied the cycloaddition reaction by varying the nature of the monoalkyne. Cycloaddition reactions with a series of *para*-substituted phenylacetylenes **65b-f** and **17a** with the same tosyl-tethered diyne **16a** were analysed (Table 19).

Table 19. [2+2+2] Cycloaddition reactions between diyne **16a** and *p*-phenylacetylenes **65b-e** and **17a** studied by ESI-MS.

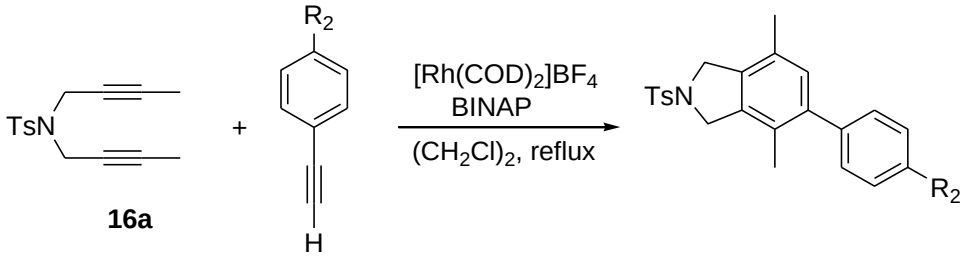

16a

65b: R_2 = OMe
17a: R_2 =H
65c: R_2 = ^{t}Bu
65d: R_2 = F
65e: R_2 = Br

66b (R_2 = OMe, 96% yield)
18aa (R_2 = H, 80% yield)
66c (R_2 = ^{t}Bu, 100% yield)
66d (R_2 = F, 60% yield)
66e (R_2 = Br, 100% yield)

Entry	Monoyne 65 / R_2	MS (*m/z*) / identified species	MS/MS (*m/z*) / identified species
1	**65b** / OMe	1131.8 / [Rh(BINAP)(**16a**)(**65b**)]$^+$	977.0 / [Rh(BINAP)(**16a**)(**65b**) – Ts]$^+$ 725.0 / [Rh(BINAP)]$^+$
2	**17a** / H	1101.9 / [Rh(BINAP)(**16a**)(**17a**)]$^+$	946.9 / [Rh(BINAP)(**16a**)(**17a**) – Ts]$^+$ 725.0 / [Rh(BINAP)]$^+$
3	**65c** / ^{t}Bu	1158.0 / [Rh(BINAP)(**16a**)(**65c**)]$^+$	1003.3 / [Rh(BINAP)(**16a**)(**65c**) – Ts]$^+$ 725.1 / [Rh(BINAP)]$^+$
4	**65d** / F	1119.8 / [Rh(BINAP)(**16a**)(**65d**)]$^+$	964.9 / [Rh(BINAP)(**16a**)(**65d**) – Ts]$^+$ 724.9 / [Rh(BINAP)]$^+$
5	**65e** / Br	1179.9-1181.7 / [Rh(BINAP)(**16a**)(**65e**)]$^+$	1026.8 / [Rh(BINAP)(**16a**)(**65e**) – Ts]$^+$ 724.9 / [Rh(BINAP)]$^+$

When the reactions were studied by ESI-MS following the same methodology as before, data analogous to the results with *p*-methylphenylacetylene were obtained, confirming our initial assignments. In Table 19, only the clusters corresponding to the second intermediate and their further characterization by MS/MS are shown in detail as the oxidative addition intermediate is the same in all the examples. In all cases, the MS/MS experiments showed both the loss of tosyl groups and, by dissociation of the final product from the catalyst or by the reductive elimination process from the alkyne insertion intermediate, formation of the [Rh(BINAP)]$^+$ fragment at *m/z* = 725.0. In order to confirm the detection of the alkyne insertion intermediate and to exclude the mere formation of a species corresponding to coordination of the catalyst to the final product, a mixture of cycloadduct **66** and 5 mol% of $[Rh(COD)_2]BF_4$ and BINAP was analysed in each case. The spectra showed that the fragmentation of the peak observed with the mass corresponding to [RhBINAP(**16a**)(**65**)]$^+$ was different from the alkyne insertion intermediate detected for the ongoing reaction. These experiments showed that coordinated species did not fragment by losing the tosyl group when they were submitted to MS/MS, confirming the observation of the alkyne insertion intermediate in the ensuing reactions.

Just as an example, the particular case of *p*-bromophenylacetylene, with its characteristic distribution due to the presence of the bromide atom is shown in Figure 43. The experimental and calculated isotopic patterns of this peak corresponding to the alkyne insertion intermediate at *m/z* = 1179.9-1181.7 match well.

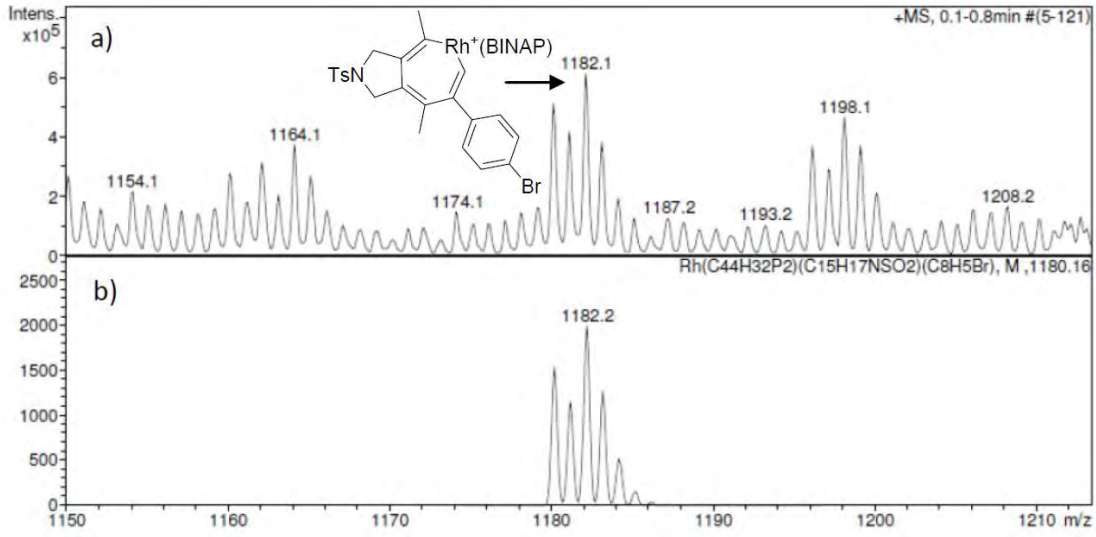

Figure 43. Isotopic pattern experimentally obtained compared to that calculated for the [Rh(BINAP)(**16a**)(**65e**)]$^+$ cluster.

5.2.6. Study of different diyne substrates

We then studied the effect of the variation of the diyne and performed the reaction with *N*Ts-tethered terminal diyne **16d** and phenylacetylene **17a** (Table 20).

Table 20. [2+2+2] Cycloaddition reaction between diyne **16d** and phenylacetylene **17a** studied by ESI-MS.

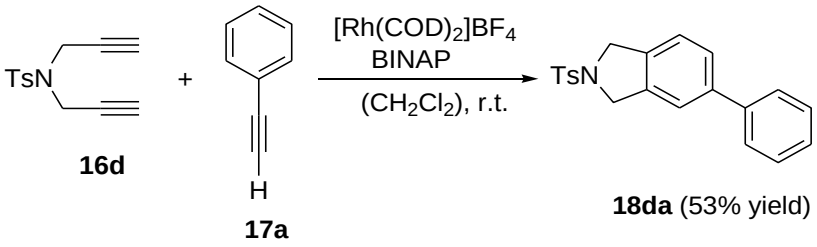

16d **17a** **18da** (53% yield)

Sample[a]	MS (*m/z*) / identified species	MS/MS (*m/z*) / identified species
$[Rh(COD)_2]BF_4$ + BINAP + **16d** + **17a**	972.1 / $[Rh(BINAP)(\mathbf{16d})]^+$	816.9 $[Rh(BINAP)(\mathbf{16d}) - Ts]^+$ 725.1 $[Rh(BINAP)]^+$
	988.1 / $[Rh(BINAP{=}O)(\mathbf{16d})]^+$	833.1 $[Rh(BINAP{=}O)(\mathbf{16d}) - Ts]^+$
	1074.1 / $[Rh(BINAP)(\mathbf{16d})(\mathbf{17a})]^+$	919.1 $[Rh(BINAP)(\mathbf{16d})(\mathbf{17a}) - Ts]^+$ 724.9 $[Rh(BINAP)]^+$
	1218.9 / $[Rh(BINAP)(\mathbf{16d})_2]^+$	1063.9 $[Rh(BINAP)(\mathbf{16d})_2 - Ts]^+$
$[Rh(COD)_2]BF_4$ + BINAP + **18da**	1074.3 / $[Rh(BINAP)(\mathbf{18da})]^+$	725.1 $[Rh(BINAP)]^+$

[a] 5 mol% of rhodium complex and diphosphine were used.

The starting diyne **16d** and the final product **18da** were individually injected into the mass spectrometer for analysis. Both were detected as protonated species or sodium adducts. When diyne **16d** and cycloadduct **18da** were submitted to MS/MS experiments, tosyl loss occurred by heterolytic cleavage as a result of the loss of a neutral molecule (Figure 44).

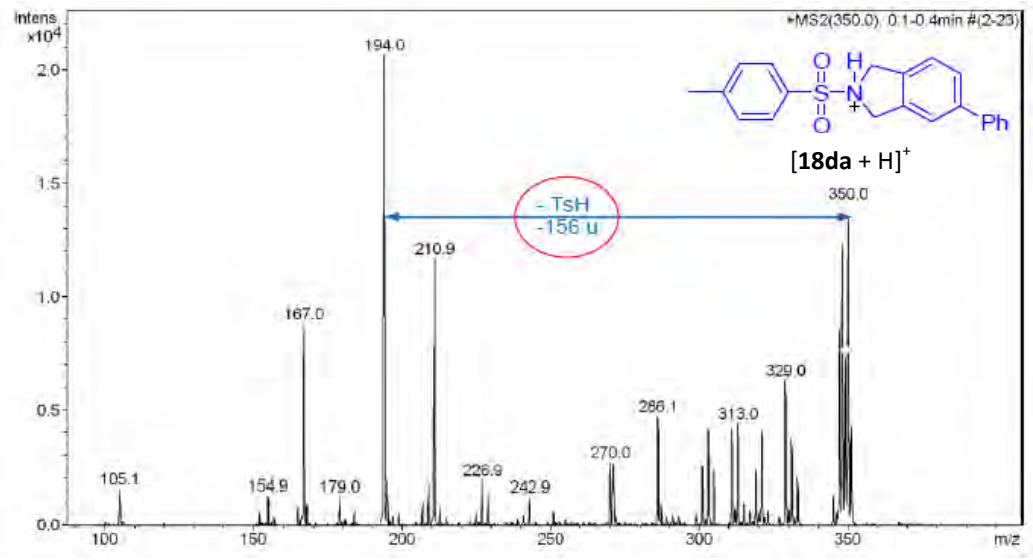

Figure 44. ESI(+)-MS/MS spectrum of the ion [**18da** + H]$^+$ at *m/z* = 350 (collision energy of 1 V).

This heterolytic cleavage differs from the behaviour of the previously observed intrinsically ionic rhodium intermediates in which homolytic cleavage led to the loss of radical Ts and the detection of a cationic radical fragment (Scheme 91).[102]

This difference in behaviour between the two species (reaction intermediate and final product) is due to their different electronic configurations: cationic Rh intermediates are odd-electron ions and favour the radical losses while the protonated species [M+H]$^+$ are even-electron ions and favour the less energetic neutral losses.

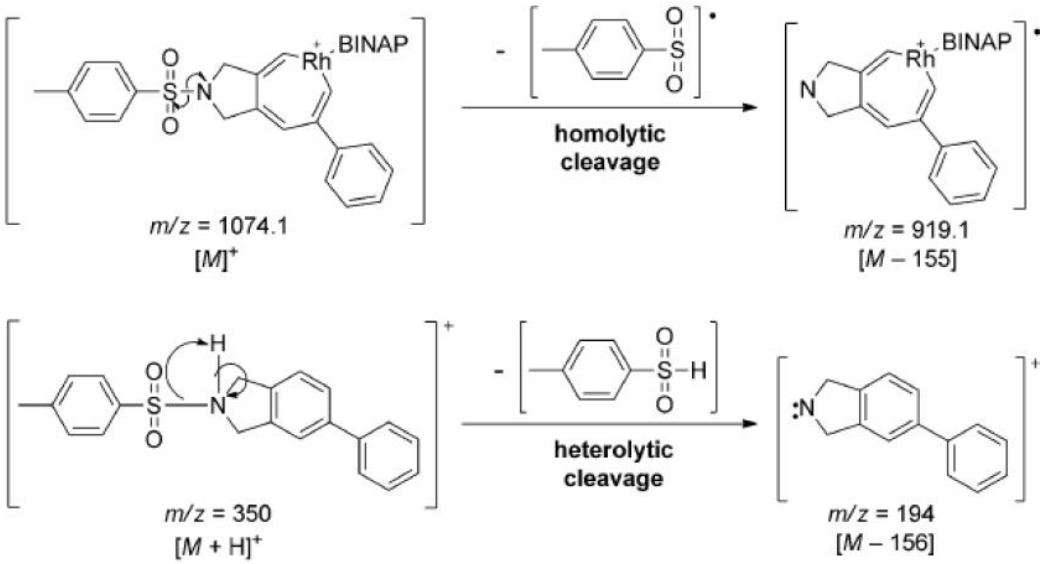

Scheme 91. Homolytic *vs.* heterolytic cleavage of tosyl-containing species.

[102] a) Cai, Y.; Mo, Z.; Rannulu, N. S.; Guan, B.; Kannupal, S.; Gibba, B. C.; Colea, R. B. *J. Mass. Spectrom.* **2010**, *45*, 235; b) Ref. 100d.

It is important to note that when electrospray ionization is used, the formation of the precursor ion results in a closed-shell ion that is stable (even electron ion). In contrast, electronic impact ionization led to the formation of an open-shell (odd electron) ion that is energetically unstable.

The even-electron rule[103] is a useful guideline for the analysis of fragmentation behaviour in ESI-MS. It is based on the fact that even-electron (EE) ions mostly fragment into other EE ions or suffer EE neutral losses. In addition, it has been observed for the ESI-MS that the base peak fragment ion is almost always an EE ion and that most fragment ions are also EE ions. Odd-electron (OE) ions are formed when the leaving group is strongly electronegative and this favours the open shell of the OE fragment. Neutral radical losses are less common in ESI but in some cases have been observed[102] leading OE ions in this approximate order of stability $\cdot SO_2CH_3 > \cdot NO_2 > \cdot CH_3 > \cdot Cl > \cdot SCH_3 > \cdot CH_2CH > \cdot OH$ (Scheme 92). It appears that loss of the more electronegative radical is favoured.

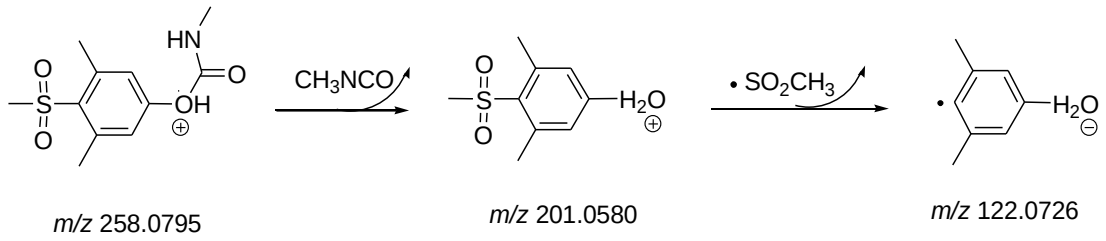

Scheme 92. Example of a neutral radical loss of SO_2CH_3 group from as a result of a CID fragmentation of an odd-electron ion.

The solution resulting from the reaction between *N*-tosyl diyne **16d** and phenylacetylene **17a** was injected into the mass spectrometer after 15 minutes of reaction at room temperature and dilution with methanol. Intermediates analogous to those detected for *N*-tosyl diyne **16d** were observed and found to display similar behaviour in the fragmentation experiments with CID with the exception of the observation of a new cluster at *m/z* = 1218.9 corresponding to the mass of [Rh(BINAP)(**16d**)$_2$]$^+$. This cluster can be assigned either to insertion of a second molecule of *N*-tosyl diyne **16d** into the oxidative addition intermediate (an intermediate that led to the homocoupling of *N*-tosyl diyne **16d**) or to complexation of the catalyst with the homocoupled product. ESI-MS/MS analysis showed the loss of the Ts group and the dissociation of the final homocoupled product, so this cluster was a mixture of both species (Figure 45).

[103] Karni, M.; Mandelbaum, A. *Org. Mass Spectrom*. **1980,** *15,* 53.

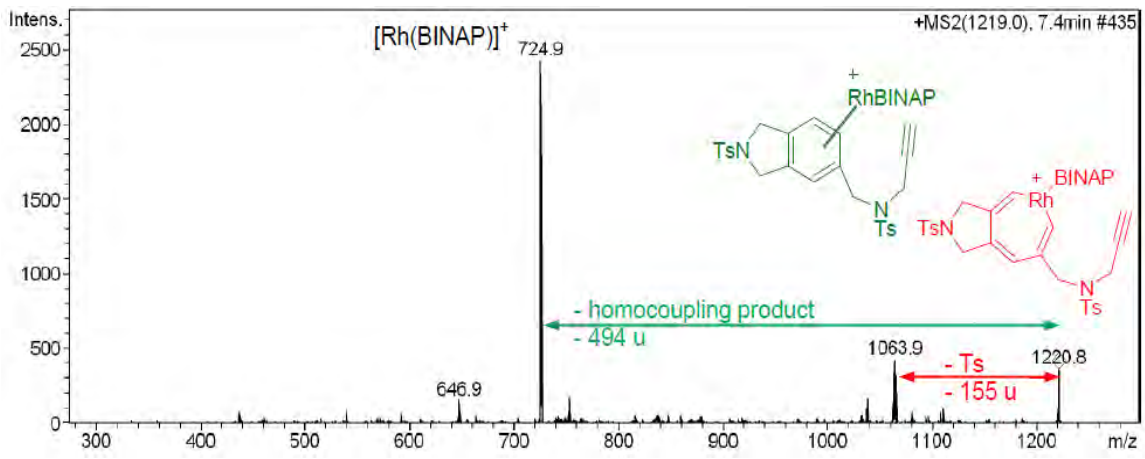

Figure 45. ESI(+)-MS/MS spectrum of the ion at *m/z* = 1219.0 (collision energy of 1 V, width = 4 *m/z*).

After one hour, the reaction mixture was analysed and the peaks corresponding to sodium adducts of the final product **18da** were observed as well as a peak corresponding to the mass of the sodium adduct of homocoupled product (Figure 46). Apart from this, the peaks corresponding to the catalytic species [Rh(COD)BINAP]$^+$ at *m/z* = 725 and intermediates at *m/z* = 972 and 1074 assigned to [RhBINAP(**16d**)]$^+$ and [RhBINAP(**16d**)(**17a**)]$^+$ respectively, were not observed, so we could demonstrate that these intermediates were, certainly, reactive intermediates as they have disappeared as expected for catalytic species at the end of the reaction. On the other hand, [Rh(BINAP)$_2$]$^+$ observed at *m/z* = 1347.1 is still observed so we can assume that it corresponds to a resting state.

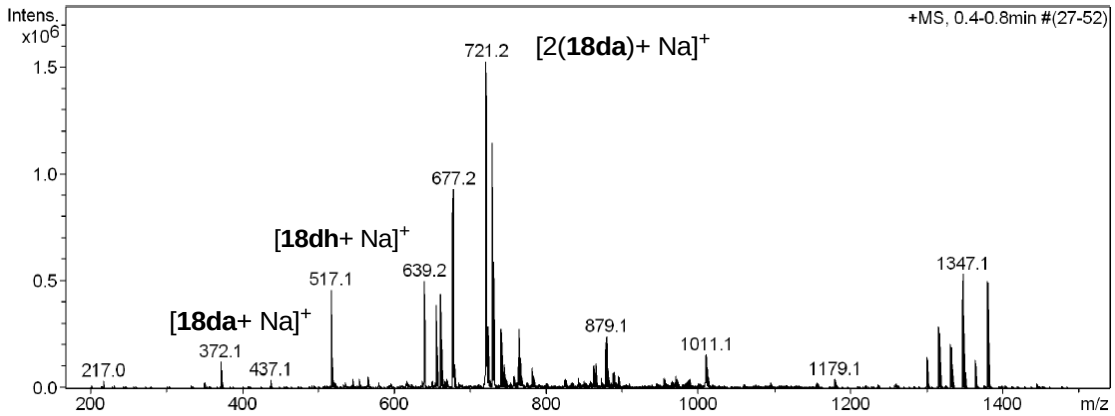

Figure 46. ESI(+) mass spectra of a solution of the mixture of [Rh(COD)$_2$]BF$_4$/BINAP (5% molar) + **16d** + **17a** at the reaction time of 1 hour diluted in methanol.

The fact that terminal alkynes are more prone to homocoupling than their non-terminal counterparts may explain why these intermediates were exclusively observed in this set of experiments.

To characterize in depth the nature of the species detected at *m/z* = 972 corresponding to [RhBINAP(**16d**)]$^+$, a series of experiments were run to study the dependence of fragment yields on the collision energy (Figure 47). We hypothesized that this species was a mixture of the diyne coordinated to the catalyst and the oxidative addition intermediate and that each fragmented through a characteristic pathway. This is corroborated in the present study, since the fragmentation of non-covalent bonds (i.e., diyne dissociation from the catalyst leading to the catalyst fragment at *m/z* = 725) starts to take place at lower amplitudes (A>0.15) than the fragmentation of covalent bonds (A>0.17) (tosyl cleavage from the oxidative coupling intermediate leading to the fragment at *m/z* = 817). The breaking of coordination bonds occurs to a much greater extent than the breaking of the *N*-Ts covalent bond throughout the collision energy range studied. Furthermore, on increasing the collision energy, the difference in the relative abundance of the two fragments (725 *vs* 817) is increased. We rule out the possibility that the fragment at *m/z* = 817 originates from the coordination intermediate since the dissociation of non-covalent bonds would be expected to be much more favourable than for the breaking of a covalent bond.

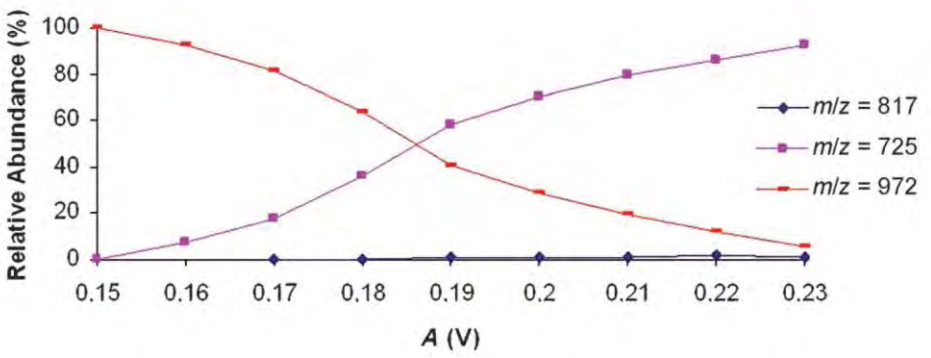

Figure 47. Study of the dependence of fragment yields on the collision energy at a reaction time of 45 minutes.

In line with the study of the variation of the diyne reagent, we performed a second set of experiments using a malonate tethered diyne **16e** in order to obtain a different fragmentation pattern of the reaction products and intermediates (Scheme 93).

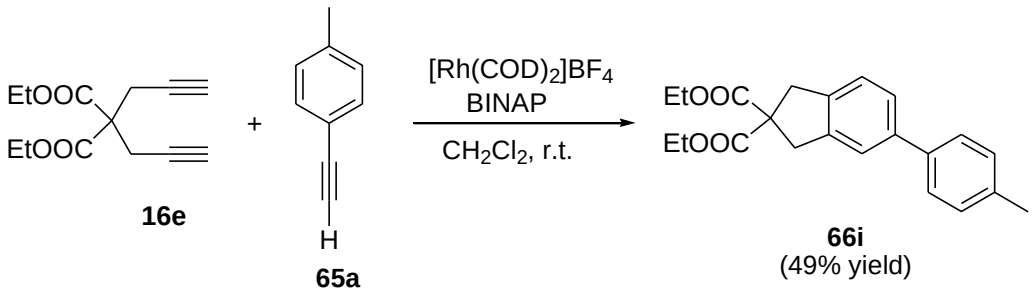

Scheme 93. [2+2+2] Cycloaddition reaction between malonate tethered diyne **16e** and *p*-methylphenylacetylene **65a** studied by ESI-MS.

To prove this hypothesis, cycloadduct **66i** was first injected into the ESI-MS apparatus giving an adduct at *m/z* = 353.0 corresponding to $[M+H]^+$, which underwent CID fragmentation to give a peak at *m/z* = 325.0 arising from a McLafferty rearrangement ($[\mathbf{66i}\text{-}C_2H_4]^+$), and another peak at *m/z* = 279.0 resulting from the neutral loss of COOEt + H (Figure 48). Therefore, we proceeded to analyse the whole reaction mixture. The ensuing reaction was then analysed under the standard conditions. Apart from the species $[Rh(BINAP)(COD)]^+$ at *m/z* = 833.3 and $[Rh(BINAP)_2]^+$ at *m/z* = 1347.3 that were assigned to the catalytic system, new signals appeared relating to intermediates in the reaction. In the *m/z* 960–980 region, in which peaks due to oxidative addition intermediates were expected, a peak at *m/z* = 977.3 was assigned to the $[Rh(BINAP{=}O)(\mathbf{16e})]^+$. CID fragmentation of this compound showed the formation of a peak at $[M\text{-}73]^+$ (Figure 49), corresponding to the loss of a COOEt group, which indicated that the cluster at *m/z* = 977.3 corresponded to the oxidized form of the oxidative addition intermediate and not to a coordination species. A possible explanation for the observation of this intermediate in this particular case is that it accumulates on ceasing to be catalytically active when it is oxidised.

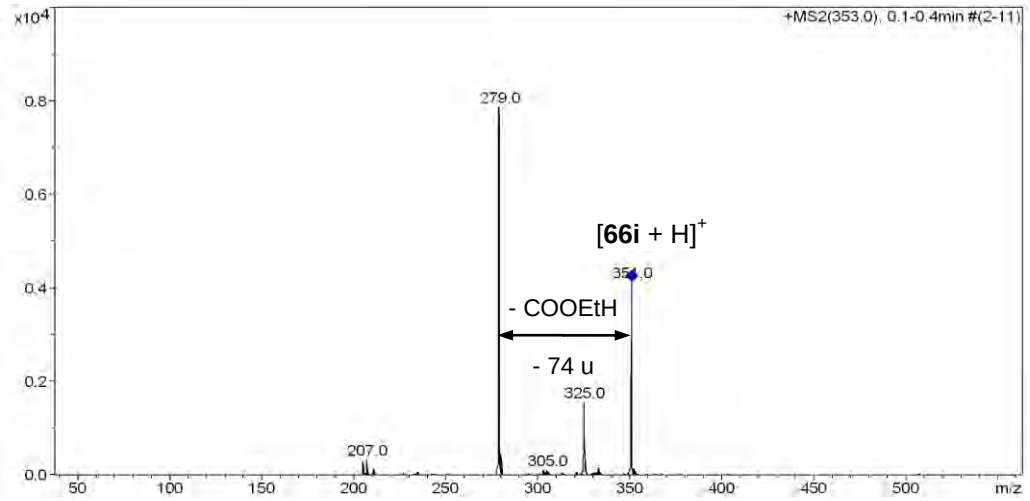

Figure 48. ESI(+)MS/MS spectrum of the ion $[\mathbf{66i} + H]^+$ at *m/z* = 353.0 (collision energy of 0.30 V).

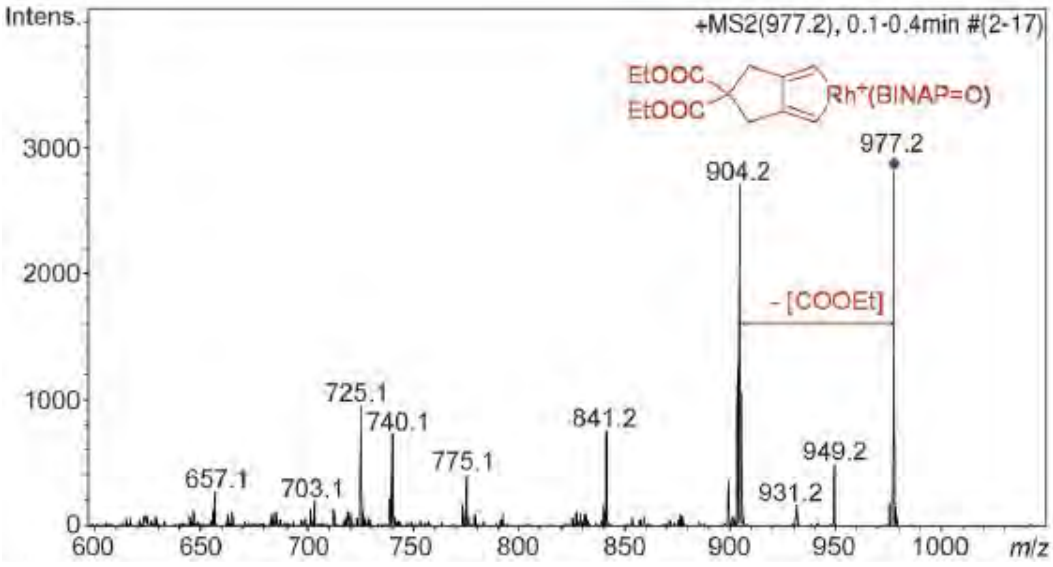

Figure 49. CID mass spectrum of the ion at *m/z* = 977.3

The low intensity of the small peak observed at *m/z* = 961.3 corresponding to [Rh(BINAP)(**16e**)]$^+$ prevented full isolation and fragmentation. The mass region corresponding to the alkyne insertion intermediate was then analysed. A peak at *m/z* = 1077.3 was observed, which could be assigned to a cluster incorporating both the diyne and monoyne, [Rh(BINAP)(**16e**)(**65a**)]$^+$. MS/MS analysis of this peak was performed to assign it to monoyne coordination to the oxidative addition intermediate, alkyne insertion intermediate, or coordination of the cycloadduct **66i** to the catalyst. The main fragment at *m/z* = 725.1 corresponded to [Rh(BINAP)]$^+$, which indicated the presence of a species involving coordination of cycloadduct **66i** to the catalyst, although we cannot rule out the possibility that it was formed through reductive elimination from the alkyne insertion intermediate (Figure 50). Unfortunately, as no fragmentation of the tether (loss of an ester group) was observed, we do not have unequivocal proof of the formation of the alkyne insertion intermediate.

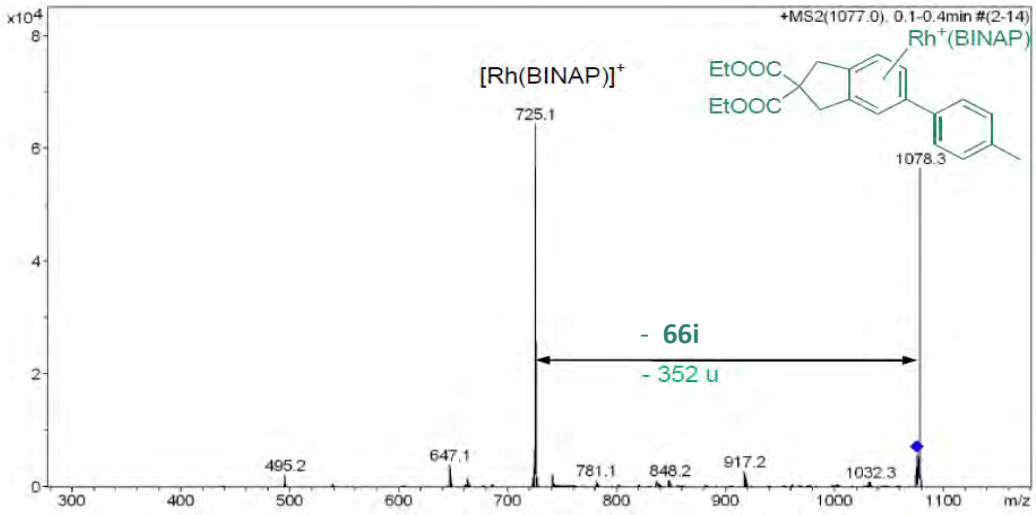

Figure 50. ESI(+)MS/MS spectrum of the ion [Rh(BINAP)(**66i**)]$^+$ at *m/z* = 1077.3 (collision energy of 0.30 V).

A peak attributable to [Rh(BINAP=O)(**16e**)(**65a**)]$^+$ was also observed at *m/z* = 1093.3. CID analysis revealed two main peaks. The first fragment at *m/z* = 741.1 corresponded to [Rh(BINAP=O)]$^+$ and, analogously to the peak of the non-oxidized species, indicated the presence of the later intermediate involving coordination of the cycloadduct **66i** to the catalyst, although it could possibly also have been formed from the alkyne insertion intermediate. However, unlike the peak of the non-oxidized species, a fragment attributable to [Rh(BINAP=O)(**16e**)]$^+$ was observed at *m/z* = 977.2 (Figure 51). The formation of this fragment indicated the presence of an intermediate in which monoyne **65a** was coordinated to the oxidative addition intermediate, which fragmented by dissociation of the metal from the monoyne (Scheme 94a).

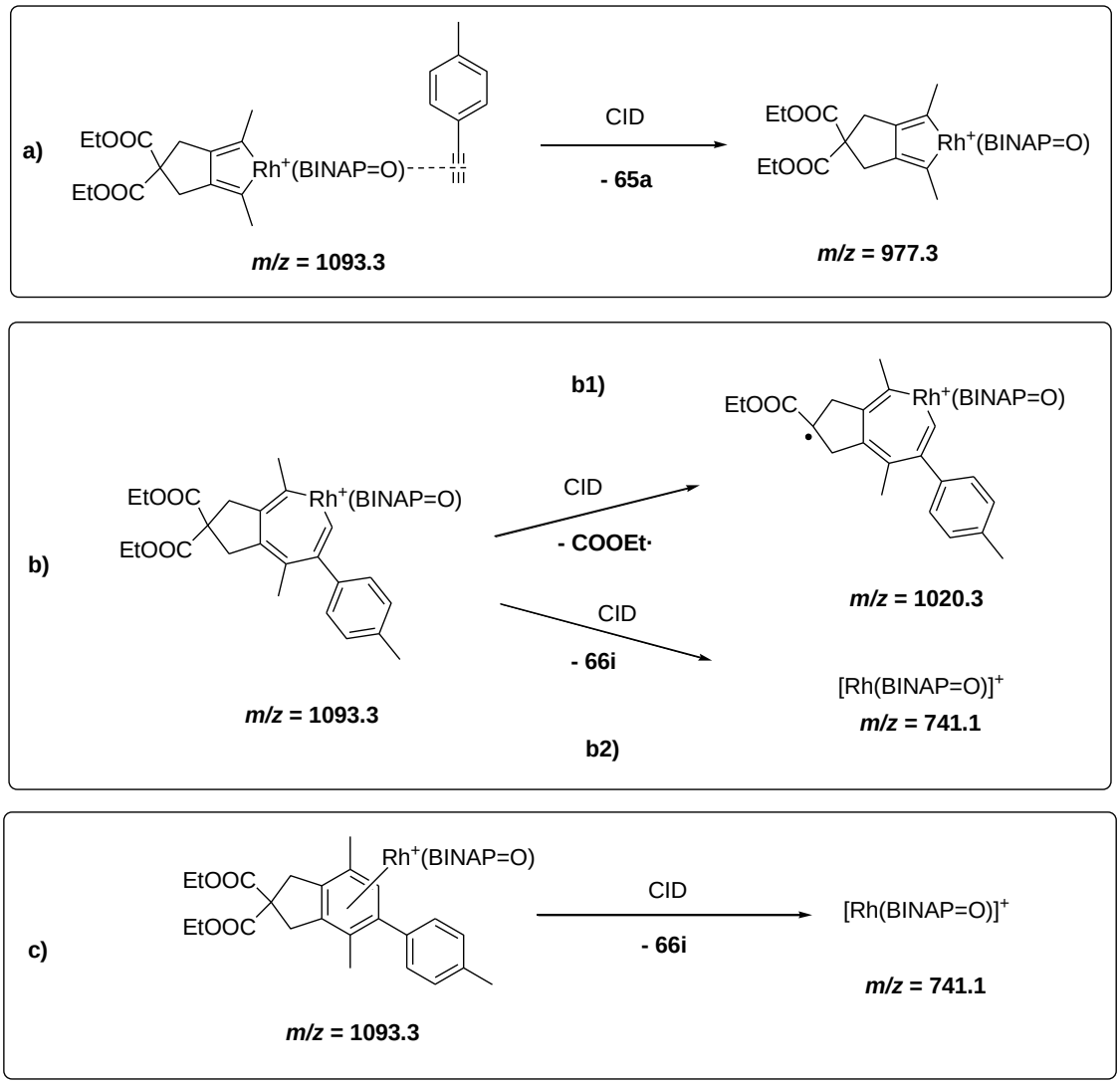

Scheme 94. Hypothesis of CID fragmentation of the three different possible structures with the *m/z* = 1093.3; a) Dissociation of the monoyne from the oxidative coupling intermediate; b1) Unobserved loss of an ester group from the alkyne insertion intermediate; b2) Reductive elimination; c) Dissociation of the cycloadduct **66i** from the catalyst.

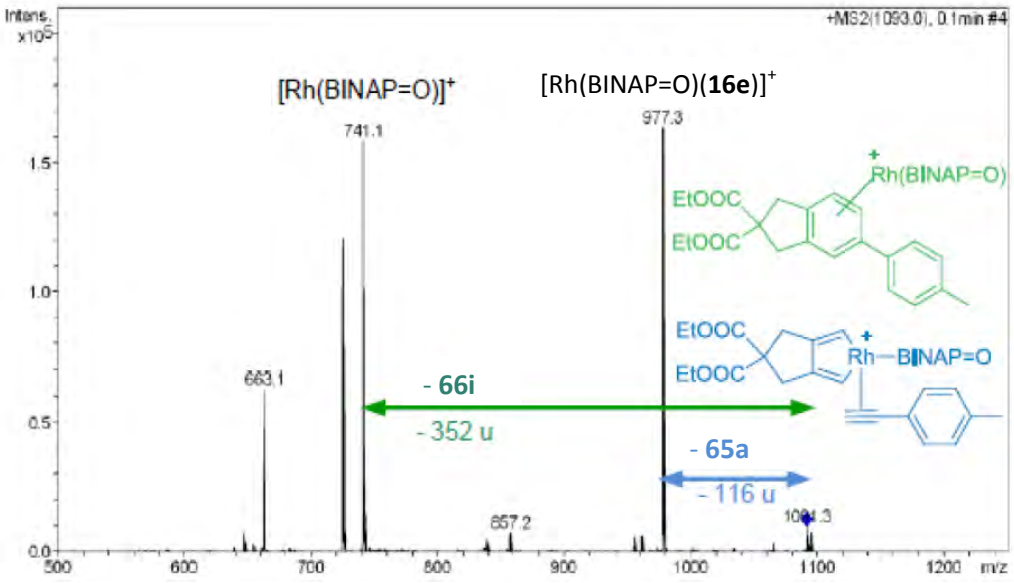

Figure 51. CID mass spectrum of the ion at *m/z* = 1093.3 showing the dissociation of the metal from the monoyne.

Moreover, MS^3 analysis of this peak showed that the fragment ion at 977.2 was not a coordination specie because when it was submitted to CID, the loss of another COOEt group was observed instead of the formation of $[RhBINAP=O]^+$ ion at 741 *m/z* (Figure 52). This evidence corroborates that the peak at 1093 is a mixture of two species with different fragmentation behaviour. We can therefore conclude that we also observed the hitherto elusive intermediate of coordination of the monoyne to the oxidative addition intermediate.

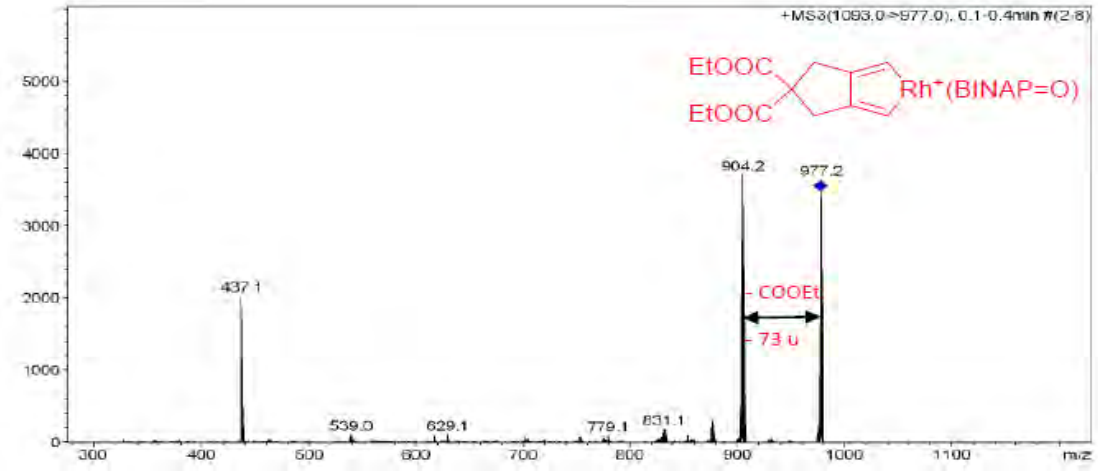

Figure 52. ESI(+)MS^3 spectrum of the ion $[Rh(BINAP=O)(\mathbf{16e})(\mathbf{65a})]^+$ at *m/z* = 1093.3 (collision energy of 0.30 V).

Given that diyne **16e** bears terminal alkyne moieties, intermediates leading to the homocoupled products were also observed at *m/z* = 1197.0, assigned to $[Rh(BINAP)(\mathbf{16e})_2]^+$, and at *m/z* = 1213.4, assigned to $[Rh(BINAP=O)(\mathbf{16e})_2]^+$. Both peaks fragmented by dissociation

of the homocoupled product from the ligand or by reductive elimination to give $[Rh(BINAP)]^+$ and $[Rh(BINAP=O)]^+$, respectively. It should be noted that the peaks of oxidised species were much more intense in the case of the malonate-tethered diyne than for the *N*Ts-tethered diynes.

5.2.7. Study of different catalysts

After varying the monoyne and diyne reactants, a third set of experiments was conducted on the cycloaddition of diyne **16d** and phenylacetylene **17a** (Table 21) with different diphosphines, (*R*)-H_8-BINAP and BIPHEP (BIPHEP = 2,2'-bis(diphenylphosphino)-1,1'-biphenyl) to compare the behaviour of three different catalytic systems.

The data extracted from these experiments were analogous to those obtained with BINAP (with the obvious changes in the expected mass shifts arising from the different masses of the various phosphines). Therefore, the presence of the proposed species in the cycloaddition reactions was confirmed. In Table 21 we show the most relevant spectra and data in order to demonstrate that their fragmentation behaviour was reproducible.

Table 21. Electrospray mass spectral data for mixtures of the reaction between diyne **16d** and phenylacetylene **17a** using (*R*)-H_8-BINAP and BIPHEP as ligands.

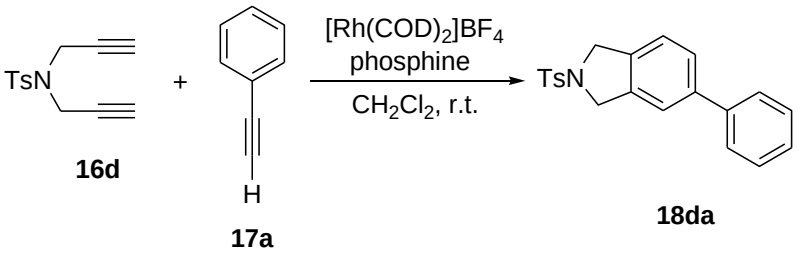

16d **17a** **18da**

Sample[a]	MS (*m/z*) / identified species	MS/MS (*m/z*) / identified species
$[Rh(COD)_2]BF_4$ + H_8-BINAP + **16d** + **17a**	980.3 / $[Rh(H_8\text{-BINAP})(\mathbf{16d})]^+$	825.2 $[Rh(H_8\text{-BINAP})(\mathbf{16d})$ - Ts$]^+$ 733.2 $[Rh(H_8\text{-BINAP})]^+$
	1082.3 / $[Rh(H_8\text{-BINAP})(\mathbf{16d})(\mathbf{17a})]^+$	733.2 $[Rh(H_8\text{-BINAP})]^+$
	1227.3 / $[Rh(H_8\text{-BINAP})(\mathbf{16d})_2]^+$	733.2 $[Rh(H_8\text{-BINAP})]^+$
$[Rh(COD)_2]BF_4$ + BIPHEP+ **16d** + **17a**	872.0 / $[Rh(BIPHEP)(\mathbf{16d})]^+$	717.1 / $[Rh(BIPHEP)(\mathbf{16d})$ - Ts$]^+$ 625.1 / $[Rh(BIPHEP)]^+$
	888.0 / $[Rh(BIPHEP{=}O)(\mathbf{16d})]^+$	733.1 / $[Rh(BIPHEP{=}O)(\mathbf{16d})$ - Ts$]^+$ 625.1 / $[Rh(BIPHEP)]^+$
	974.1 / $[Rh(BIPHEP)(\mathbf{16d})(\mathbf{17a})]^+$	819.1 / $[Rh(BIPHEP)(\mathbf{16d})(\mathbf{17a})$ - Ts$]^+$ 625.1 / $[Rh(BIPHEP)]^+$
	1119.2 / $[Rh(BIPHEP)(\mathbf{16d})_2]^+$	964.2 / $[Rh(BIPHEP)(\mathbf{16d})_2$ - Ts$]^+$ 625.1 / $[Rh(BIPHEP)]^+$
$[Rh(COD)_2]BF_4$ + BIPHEP + **18da**	974.1 / $[Rh(BIPHEP)(\mathbf{18da})]^+$	625.1 / $[Rh(BIPHEP)]^+$

[a] 5 mol % of rhodium complex and diphosphine were used.

ESI-MS experiments with (*R*)-H_8-BINAP showed that the reaction was faster than when the other phosphines were used. We were unable to observe the alkyne insertion intermediate with clarity. Only the coordination of the final product to the catalyst was observed since the ion corresponding to the mass of [Rh(H_8-BINAP)(**16d**)(**17a**)]$^+$ at *m/z* = 1082 was fragmented leading mainly to the formation of [Rh(H_8-BINAP)]$^+$. In this case, the fragment ion at *m/z* = 927.3 resulting from the loss of the tosyl group of the insertion intermediate was observed but with very low intensity (Figure 53). On the other hand, the diyne insertion intermediate at *m/z* = 1227.3 (resulting from the homocoupling reaction) was not detected since the loss of the tosyl group was not observed.

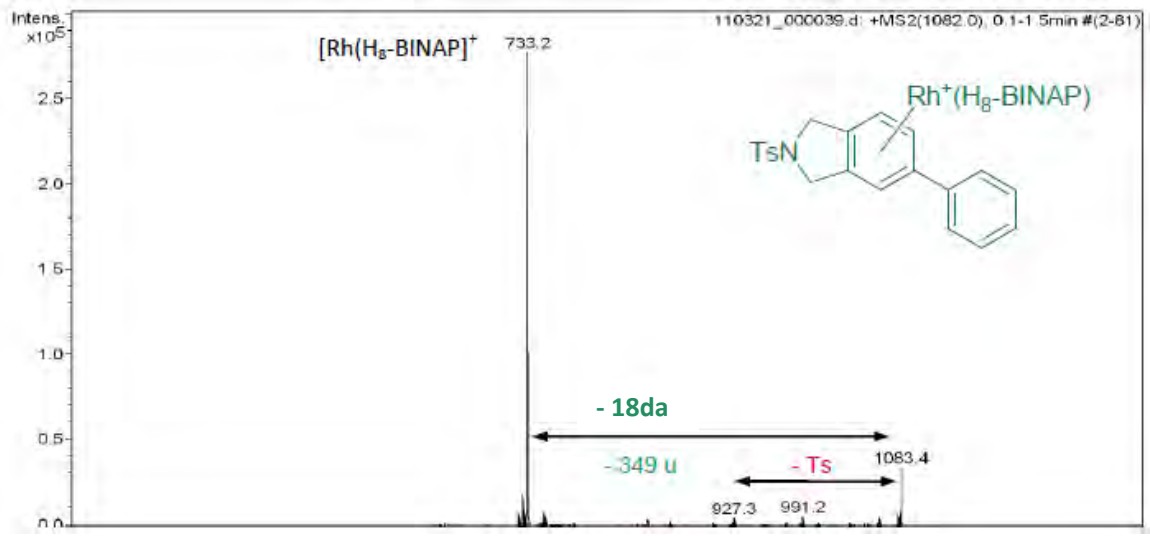

Figure 53. ESI(+)MS/MS spectrum of the ion [Rh(H_8-BINAP=O)(**16d**)(**17a**)]$^+$ at *m/z* = 1082.2 (collision energy of 1 V).

When BIPHEP was used, the reaction was slower and it was possible to detect all the intermediates and characterize them in more detail by CID experiments. The alkyne insertion intermediate was detected since the loss of the tosyl group was observed (Figure 54). When cycloadduct **18da** was injected with 5% of catalytic mixture, coordination took place and its fragmentation corresponded to the dissociation of **18da** from the catalyst with no loss of the tosyl group.

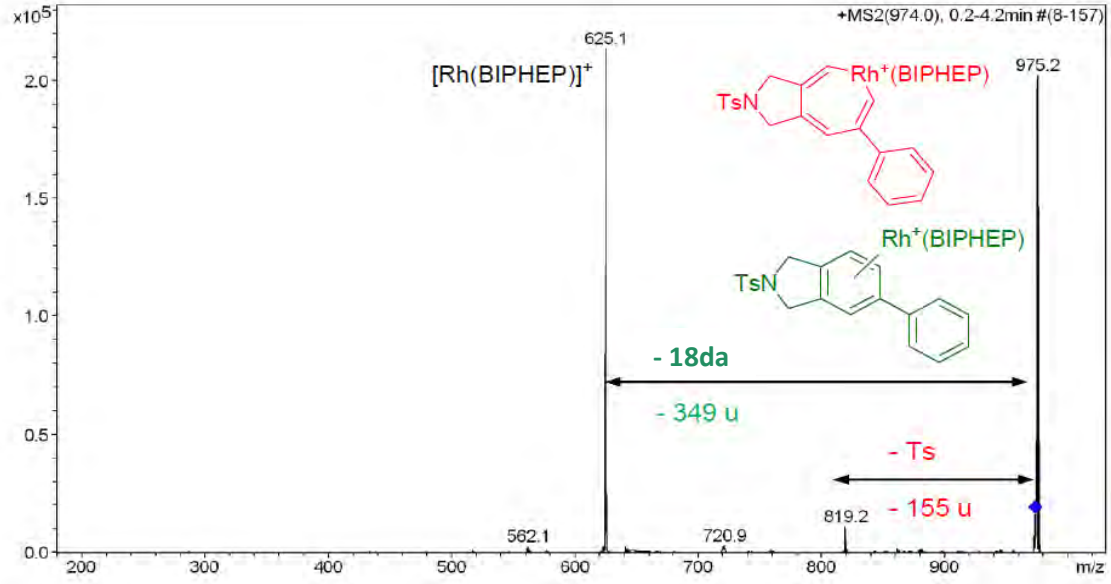

Figure 54. ESI(+)MS/MS of the ion [Rh(BIPHEP)(**16d**)(**17a**)]$^+$ at *m/z* = 974 (collision energy of 0.23 V).

In this case, the insertion of a second diyne molecule was also observed at *m/z* = 1119. When this peak was fragmented by MS/MS/MS, two consecutive losses of the two tosyl groups in the molecule were observed (Figure 55).

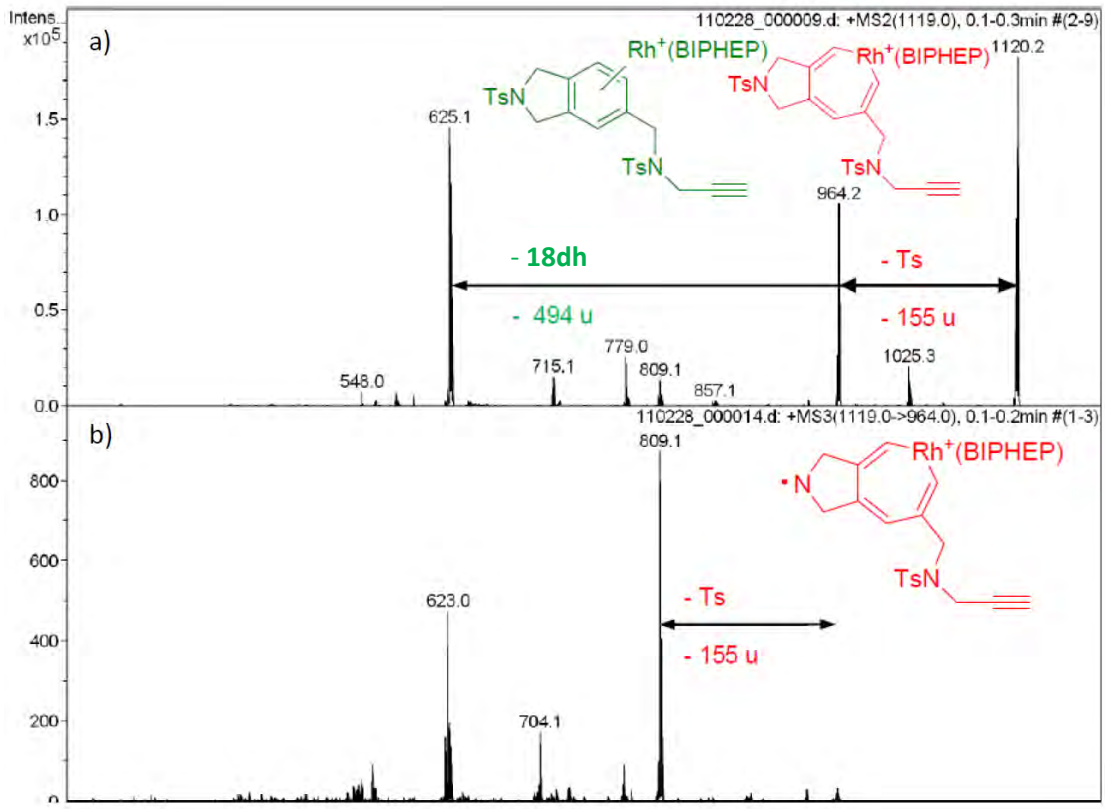

Figure 55. a) ESI(+)MS/MS; b) MS^3 spectra of the ion [Rh(BIPHEP)(**16d**)$_2$]$^+$ at *m/z* = 1119 (collision energy of 0.25 V).

At the end of the reaction, the homocoupled product was observed as a protonated species at *m/z* = 495. The MS^3 analysis of this peak showed two consecutive losses of the TsH group.

5.2.8. Theoretical Calculations

After the experimental detection of the intermediates, the challenge remained as to how to draw a structure for the monoyne insertion intermediate. To this end, we carried out DFT calculations to determine whether this intermediate was one of the three possible structures (**V**, **VI**, or **VII**) represented in the mechanistic proposal in Scheme 83 (page 115). This part of the study was performed by Dr. Anna Dachs as part of her thesis work under the supervision of Prof. Miquel Solà from the University of Girona.

The reaction mechanism involving diyne **16d** and alkyne **17a** with Rh/BIPHEP as the catalytic system was studied at the B3LYP/cc-pVDZ-PP level of theory. To reduce the computational cost, the Ts group was replaced by an SO_2CH_3 substituent. Our simulations started from complex **A** (the π-complex between phenylacetylene **17a** and our model of the [Rh(BIPHEP)(**16d**)]$^+$ species), since this is the first structure in the whole reaction mechanism with the required number and type of atoms to be the experimentally detected intermediate [Rh(BIPHEP)(**16d**)(**17a**)]$^+$. Scheme 95 shows the Gibbs energy profile for the transformation of complex **A** into final product **D**.

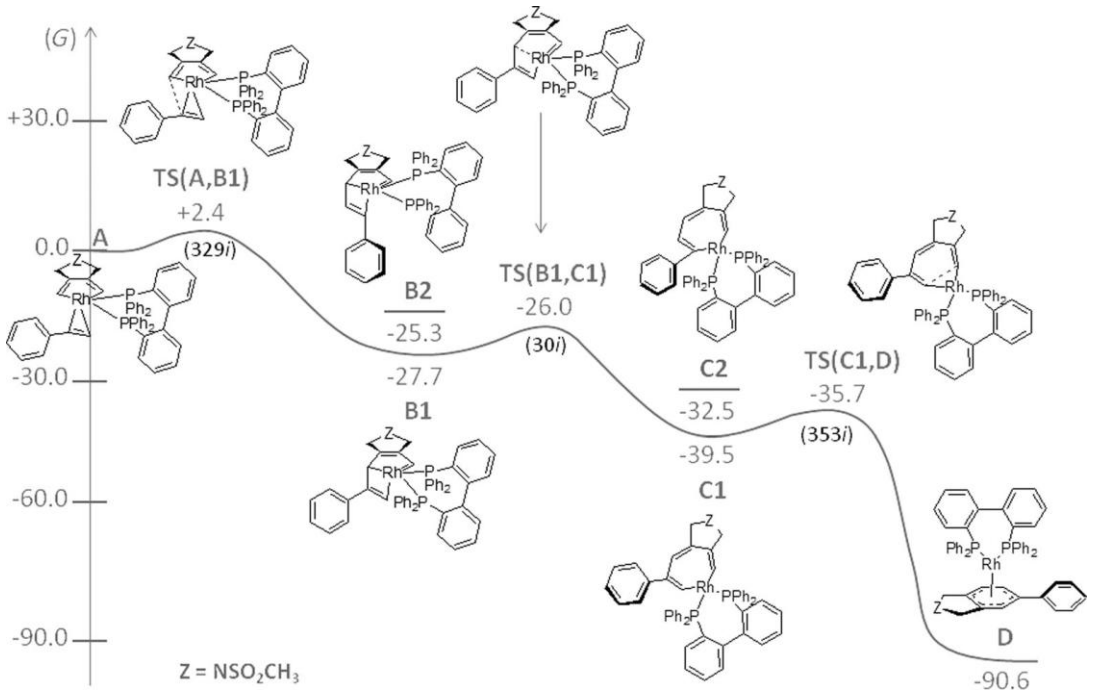

Scheme 95. Gibbs energy profile (in kcalmol^{-1}) for the formation of product **D** from **A** with Z = NSO_2CH_3.

The relative Gibbs energy of **A** with respect to $[Rh(BIPHEP)]^+$, phenylacetylene **17a**, and our model of diyne **16d** is -44.8 kcalmol^{-1}. This represents the stabilization gain in Gibbs energy during the initial oxidative coupling together with the π-complexation of phenylacetylene. Subsequent formal [5+2] alkyne addition of phenylacetylene **17a** in π-complex **A** leads to the rhodabicyclo[3.2.0]heptatriene complex **B1**. Another rhodabicyclo[3.2.0]heptatriene complex **B2** could have been formed from an initial π-complexation of phenylacetylene with the phenyl group of **17a** pointing in the direction of the BIPHEP group. However, complex **B1** with the phenyl group of the phenylacetylene species pointing away from the BIPHEP substituent is more favourable than **B2** by 2.4 kcalmol^{-1} due to the lower steric repulsion and, for this reason, the reaction through intermediate **B2** was discarded. The transition state (TS) for the conversion of **A** to **B1**, TS(**A**,**B1**) has a Gibbs energy barrier of 2.4 kcalmol^{-1} and the process is exergonic by 27.7 kcalmol^{-1}. The five- and four-membered bicyclic ring **B1** evolves to the cycloheptatriene complex **C1** through the transition state TS(**B1**,**C1**) with a Gibbs energy barrier of 1.7 kcalmol^{-1}. This process is exergonic by 11.8 kcalmol^{-1}. Intermediate **B2** could also have been transformed into **C2**. However, **C2** is 7.0 kcalmol^{-1} less stable than **C1** and it is therefore likely that the route through **C2** is not operative. In the final step, complex **D** is formed through a very exergonic reductive elimination step (51.1 kcalmol^{-1}) through TS(**C1**,**D**), which has a barrier of 2.2 kcalmol^{-1}. Finally, the dissociation of product **18da** and the recovery of the Rh^{I}/BIPHEP catalyst from complex **D** is a slightly endergonic process that only requires 5.8 kcal·mol^{-1}. Our B3LYP/cc-pVDZ-PP results indicate that the overall cycloaddition reaction of diyne **16d** and alkyne **17a** catalysed by Rh/BIPHEP is exergonic by -129.7 kcalmol^{-1}. Moreover, reaction **16d** + **17a** + Rh/BIPHEP to yield **D** is exergonic by -135.5 kcal·mol^{-1}. Most theoretical studies of [2+2+2] reaction mechanisms carried out to date have yielded either the rhodabicyclo[3.2.0]heptatriene or the cycloheptatriene complex. The coexistence of both in the same route is not common, although it is not unprecedented.[104] Our simulations exclude the 7-metallanorbornadiene complex **VI** as the monoyne insertion intermediate, since it has not been possible to locate such a complex on the potential energy surface. On the other hand, our results favour the assignment of the cycloheptatriene complex **V** as the insertion intermediate since the forward barrier on the way to the products is slightly higher for **C1** than for **B1**. The small energy difference between the two Gibbs energy barriers (just 0.5 kcal mol^{-1}) prevents a definitive conclusion being drawn and the assignment of this intermediate as the rhodabicyclo [3.2.0]heptatriene complex **VII** cannot be completely excluded.

To sum up, the picture of the catalytic cycle obtained after ESI-MS and DFT calculations of the studied reactions is shown in Scheme 96. As an example, the *m/z* ratios for the detected species together with their characteristic CID fragmentations are shown for the reaction between diyne **16d** and phenylacetylene **17a**, using Rh(I)/BIPHEP as the catalytic system.

All these results have been published in Chemistry, A European Journal.[105]

[104] a) Kirchner, K.; Calhorda, M. J.; Schmid, R.; Veiros, L. F. *J. Am. Chem. Soc.* **2003**, *125*, 1172; b) Yamamoto, Y.; Arakawa, T.; Ogawa, R.; Itoh, K. *J. Am. Chem. Soc.* **2003**, *125*, 12143; c) Dachs, A.; Osuna, S.; Roglans, A.; Solà, M. *Organometallics* **2010**, *29*, 562.
[105] Parera, M.; Dachs, A.; Solà, M.; Pla-Quintana, A.; Roglans, A. *Chem. Eur. J.* **2012**, *18*, 13097.

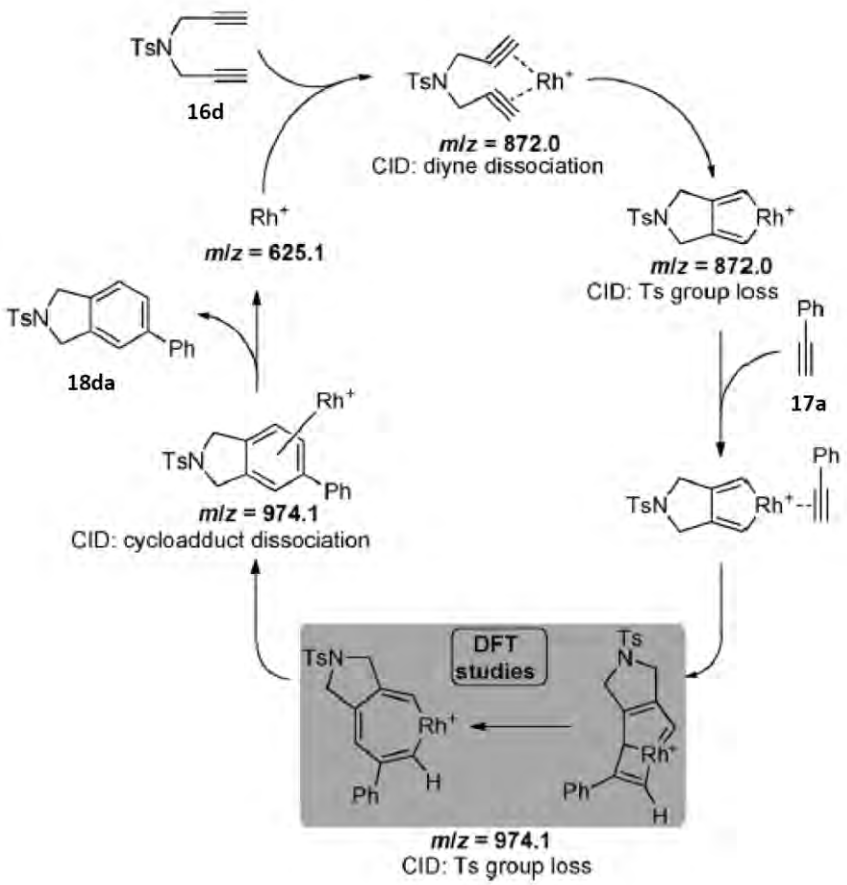

Scheme 96. Catalytic cycle proposed for the [2+2+2] cycloaddition of diynes and monoynes under Rh/diphosphine catalysis (the BIPHEP ligand has been omitted for clarity) with detected ESI-MS species and CID characterization.

In conclusion, ESI-MS offers a fruitful approach to the analysis of reaction intermediates in the Rh-catalysed [2+2+2] cycloaddition of diynes and monoynes. Complete monitoring of the reaction has been possible due to the cationic nature of the reaction intermediates provided by the inherently cationic catalytic system used (BINAP/$[Rh(COD)_2]BF_4$), as opposed to the neutrality of the reactants and the products of the reaction.

Observation of the intermediates present in particularly low concentrations has been possible with this technique, especially the direct detection of the elusive intermediates resulting from the insertion of the monoyne into the rhodacyclopentadiene for the first time. The fragmentation pattern of this intermediate consisted in breaking a covalent bond (loss of the tosyl group for the *N*-tethered diynes and loss of the ester group for the malonate-tethered diyne) that differs from the fragmentation of coordination species which dissociated from the catalyst. CID experiments have been fundamental in ensuring the existence of this intermediate since the coordinated species (coordination of the monoyne to the

rhodacyclopentadiene and coordination of the cycloadduct to the catalyst) have the same mass. In all the cases, the peaks observed corresponded with a mixture of these species.

This was the first time that the cationic rhodium catalyst had been investigated in a theoretical study of a [2+2+2] cycloaddition reaction. DFT results indicated that the cycloheptatriene intermediate was the most likely structure for the monoyne insertion intermediate, since it had the highest forward barrier for the different steps of the analysed reaction mechanism. However, the small differences in energy barriers did not allow us to rule out the possibility of this insertion intermediate being the rhodabicyclo[3.2.0]heptatriene complex.

Chapter 6. General conclusions

In this thesis, the following advances in methodological and mechanistic aspects of the Rh(I)-catalysed [2+2+2] cycloaddition reactions have been achieved:

- In Chapter 3 the synthesis of two sets of hemilabile S-stereogenic (PNSO) and P-stereogenic ligands capable of inducing chirality in the Rh(I)-catalysed intramolecular [2+2+2] cycloaddition of enediynes has been described. The efficiency and chemoselectivity of the Rh(I)/PNSO-catalysed [2+2+2] cycloaddition has been evaluated using triynes or diynes and monoynes as substrates. The enantioselective formation of chiral cyclohexa-1,3dienes from terminal (*E*)-enediynes has then been studied with both types of ligands. It is particularly noteworthy that the enantioselectivities found in the study of P-stereogenic hemilabile ligands have been the highest reported for terminal enediynes and thus highlight their utility in catalysis.

- In Chapter 4 a series of new bicyclic cyclohexa-1,3-dienes with a quaternary stereocentre have been successfully synthesized by Rh(I)-catalysed partially intramolecular [2+2+2] cycloadditions of diynes and Baylis-Hillman adducts. In this study it has been demonstrated that microwave irradiation is crucial to obtain the cycloadducts and avoid side-reactions. Slow addition of diynes is another methodology used to avoid the formation of diyne homocoupling products. The process is diastereoselective and high enantioselectivities have been achieved using commercially available chiral phosphine ligands starting from the racemic Baylis-Hillman adducts suggesting that a kinetic resolution process is taking place.

- Finally, in Chapter 5 all the intermediates of the [2+2+2] cycloaddition reaction of alkynes have been detected for the first time by ESI-MS. In the case of all of the ESI-MS experiments, the structural assignments of ions are supported by tandem mass spectrometry analyses. In addition, the structure of some of the intermediates has been determined by DFT calculations. These studies taken together provide new insight into the reactivity of cationic rhodacyclopentadienes, which should facilitate the design of related rhodium-catalysed carbon-carbon couplings.

Chapter 7. Methods

7.1. General materials and instrumentation

Materials

Unless otherwise noted, materials were obtained from commercial suppliers and used without further purification. All reactions requiring anhydrous conditions were conducted in oven-dried glassware under a dry nitrogen atmosphere. Dichloromethane and THF were degassed and anhydrized under nitrogen atmosphere through solvent purification columns (MBraun, SPS-800). Toluene was distilled under nitrogen over sodium as a drying reagent. DMF was distilled under reduced pressure using molecular sieves as a drying reagent. $[Rh(COD)_2]BF_4$ is air sensitive and was stored and weighted in a glove box. Solvents were removed under reduced pressure with a rotary evaporator. Residues were chromatographed on a silica gel column (230-400 mesh) using a gradient solvent system (hexane/ethyl acetate or hexane/dichloromethane) as the eluent.

Instrumentation

NMR spectroscopy: ^{1}H and ^{13}C NMR spectra were measured on a Bruker Avance III 400 (^{1}H (400 MHz) and ^{13}C (100 MHz)) or Bruker DPX300 (^{1}H (300 MHz) and ^{13}C (75 MHz)) NMR spectrometers of the Serveis Tècnics de Recerca (Research Technical Services department) of the Universitat de Girona, and Bruker Avance DRX (^{1}H (250 MHz) and ^{13}C (62.5 MHz)) from the Université de Reims Champagne-Ardenne. Chemical shifts (δ) for ^{1}H and ^{13}C were referenced to internal solvent resonances and reported relative to $SiMe_4$.

IR spectroscopy: IR spectra were measured on a FT-IR spectrophotometer Mattson-Galaxy Satellite, using an MKII Golden Gate Single Reflection ATR System of the Chemistry Department of the Universitat de Girona and Bruker Alpha FT-IR spectrometer of the Serveis Tècnics de Recerca of the Universitat de Girona.

Electrospray Ionization Mass Spectrometry spectra were registered in an Esquire 6000 ESI Ion Trap LC/MS (Bruker Daltonics) with an electrospray ionization source of the Serveis Tècnics de Recerca of the Universitat de Girona. Samples were studied in positive-ion mode using nitrogen as the nebulizer gas. Pure samples such as rhodium pre-catalyst, phosphines, diyne reagents, and isolated cycloadducts were introduced as $2.5 \cdot 10^{-3}$m solutions in methanol into the ESI source by means of a liquid chromatographic system (HPLC P1200, Agilent) at a flow rate of 100 $mLmin^{-1}$. The catalytic system and the aliquots sampled from the reaction mixture (100 mL in dichloromethane or dichloroethane) were analysed after dilution in methanol (1 mL at room temperature) by direct infusion into the ESI source by a syringe pump at a flow rate of 5 $mLmin^{-1}$. The time elapsed between sampling and injection was kept below 1 min. A spray voltage of 4.5 kV, a capillary voltage of about 40 V, a drying temperature of 350ºC, and a

sheath gas flow rate of 7 $Lmin^{-1}$ were adjusted to ensure reasonably soft ionization. Using two octopoles, the ions were guided from the source into the ion trap for storage and manipulation in the presence of about 10^{-5} mbar helium as a trapping gas. For detection, the ions were ejected from the trap to an electron multiplier. For collision-induced-dissociation (CID) spectra, the ions were mass-selected in the ion trap and then kinetically accelerated within the helium gas present in the ion trap as the collision and cooling gas. Collision energies and window widths were chosen to provide reasonable yields of the fragmented ions while maintaining the parent ion as the most abundant one. The maximum accumulation time was in the 50–100 ms range. Mass spectra were recorded from *m/z* 200 to 1400 and seven spectral averages were accumulated to improve the signal-to-noise ratio. The isotope pattern was calculated using a Bruker Daltonics programme.

High Resolution Mass Sepectrometry (ESI-HRMS) spectra were registered in a Bruker Micro TOF-Q spectrometer with a quadrupole-Time-Of-Flight hybrid analyzer of the Universidad de Zaragoza (Instituto de Ciencias de los Materiales de Aragón).

High Performance Liquid Chromatography (HPLC): HPLC analysis have been performed using a CHIRALPAK AD-H column (4.6 x 250 mm, 5 µm) on a Spectra System Thermo chromatograph (Shimadzu) equipped with a SN4000 connector, a SCM1000 degasser, a P2000 pump and a UV6000LP detector with a of 20 µm loop.

Elemental Analysis: were registered on a PerkinElmer type 2400 analyzer in the Serveis Tècnics of the Universitat de Girona**.**

Melting points: were measured in a SMP10 apparatus from Stuart without any correction.

Thin Layer Chromatography (TLC): were performed with pre-coated (0.20 mm width) chromatography plates Alugram Sil G/UV254.

Column chromatography: were performed using silica gel SDS with a size of 35-70 µm mesh particle size.

Microwaves heating: a CEM Discover S-Class microwave synthesizer was used (250 W/250 psi). Microwave heated reactions were performed in sealed vials in an Ethos SEL Lab station (Milestone Inc.), a multimode microwave with a dual magnetron (1600 W). During the experiments, the time, temperature, and the power were measured with an “EasyControl” software package. The temperature was monitored and controlled throughout the reaction by an ATC-400FO Automatic Fiber Optic Temperature Control system. The wattage was automatically adjusted to maintain the desired temperature for the desired period of time.

7.2. Experimental procedure for the products synthesised in Chapter 3

7.2.1. Synthesis of triynes 14a and 14d

7.2.1.1. Synthesis of N-tosyl-prop-2-yn-1-amine

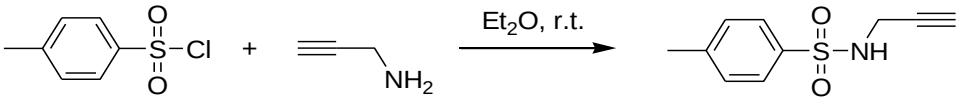

A stirred mixture of *p*-toluenesulfonyl chloride (4.09 g, 20.98 mmol) in diethyl ether (20 mL) was cooled at 0ºC in an ice bath. Propargylamine (2.94 mL, 41.96 mmol) was then added dropwise. The reaction mixture was stirred at room temperature for 2.5 h (TLC monitoring). The solvent was evaporated and the residue was purified by column chromatography on silica gel with hexanes/ethyl acetate (7:3) to afford *N*-tosyl-prop-2-yn-1-amine[106] (3.60 g, 82% yield) as a colourless solid. **Molecular formula**: $C_{10}H_{11}NSO_2$; **MW**: 209.20 g/mol; **^{1}H NMR (400 MHz, $CDCl_3$) δ (ppm):** 2.10 (t, $^4J_{H,H}$ = 2.6 Hz, 1H), 2.43 (s, 3H), 3.80-3.85 (m, 2H), 4.56 (s, 1H), 7.31 (AA' part of AA'BB' system, $^3J_{H,H}$ = 8.4 Hz, 2H), 7.77 (BB' part of AA'BB' system, $^3J_{H,H}$ = 8.4 Hz, 2H).

7.2.1.2. Synthesis of 4,9-bis(p-toluenesulfonyl)-4,9-diazadodeca-1,6,11-triyne, **14a**

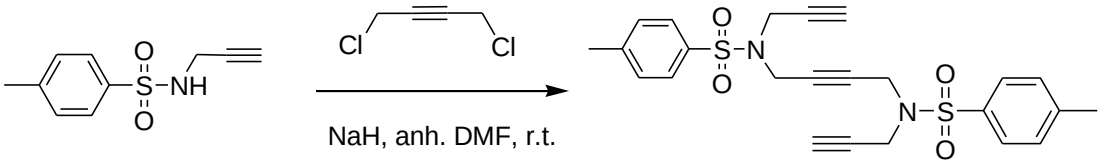

14a (37%)

A stirred mixture of sodium hydride in 60% oil dispersion (0.30 g, 5.93 mmol of pure NaH) in anhydrous DMF (8 mL) was cooled at 0ºC in an ice bath. Propargyl(*p*-toluenesulfonyl)amine (0.99 g, 4.75 mmol) in anhydrous DMF (8mL) was added slowly at 0ºC. The mixture was stirred for 1 hour while warming to room temperature under nitrogen atmosphere. 1,4-dichloro-2-butyne (0.29 g, 2.37 mmol) in DMF (2 mL) was then added dropwise via an addition funnel and the reaction was stirred for additional 2 hours at room temperature (TLC monitoring). NH_4Cl was added to quench the reaction and the mixture was extracted with ethyl acetate. The organic phase was washed with brine, dried over sodium sulfate, filtered and concentrated. The crude was purified by recrystallization in ethyl acetate to afford 4,9-bis(*p*-toluenesulfonyl)-4,9-diazadodeca-1,6,11-triyne **14a**[38] (0.41 g, 37%) as a colourless solid. **Molecular formula**: $C_{24}H_{24}N_2S_2O_4$; **MW**: 468.15 g/mol; **m.p.** 161-163 ºC; **IR (ATR) ν (cm^{-1}):** 3265, 2339, 1340, 1321,

[106] Deng, J. Tabei, J.; Shiotsuki, M.; Sanda, F.; Masuda, T. *Macromolecules* **2004**, *37*, 5538.

1157, 1090, 896, 747, 664, 570; **^{1}H NMR (400 MHz, $CDCl_3$) δ (ppm):** 2.13 (t, $^{4}J_{H,H}$ = 2.8 Hz, 2H), 2.44 (s, 6H), 3.99 (d, $^{4}J_{H,H}$ = 2.8 Hz, 4H), 4.02 (s, 4H), 7.31 (AA' part of AA'BB' system, $^{3}J_{H,H}$ = 8.4 Hz, 4H), 7.67 (BB' part of AA'BB' system, $^{3}J_{H,H}$ = 8.4 Hz, 4H); **^{13}C NMR (100 MHz, $CDCl_3$) δ (ppm):** 21.6, 36.2, 36.3, 74.1, 76.1, 78.3, 127.8, 129.6, 135.1, 144.1; **ESI-MS (*m/z*)**: 469 $[M+H]^+$, 486 $[M+NH_4]^+$, 491$[M+Na]^+$.

7.2.1.3. Synthesis of 4,9-dioxa-dodeca-1,6,11-triyne, **14d**

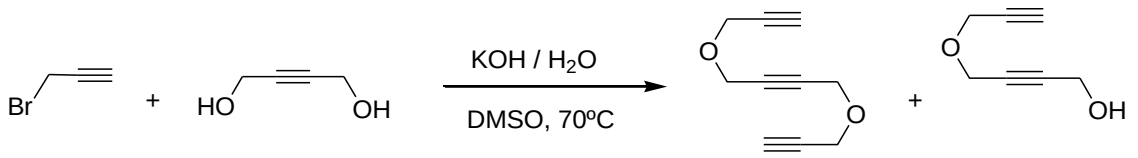

14d (70%) **14dm** (16%)

A stirred mixture of 1-bromo-2-propyne (2.01 g, 23.23 mmol) in DMSO (8 mL) and KOH (6.26 g, 58.08 mmol) in 3 mL of water (3 mL) was cooled at 0ºC in an ice bath. 2-Butyne-1,4-diol (5.18 mL, 58.08 mmol) in DMSO (3 mL) was then added dropwise. The reaction was stirred at 0ºC for 30 minutes and heating at 70ºC for 5.5 hours (TLC monitoring). The salts were filtered off, water (10 mL) was added to the filtrate and it was extracted with ethyl acetate (3 x 15 mL). The solvent was evaporated and the residue was purified by column chromatography on silica gel with hexanes/dichloromethane (7:3) to afford 4,9-dioxa-dodeca-1,6,11-triyne **14d**[39] (2.65 g, 70% yield) as a yellow oil. **Molecular formula**: $C_{10}H_{10}O_2$; **MW**: 162.07 g/mol; **IR (ATR) ν (cm^{-1}):** 3291, 2953, 2906, 2856, 1442, 1344, 1141, 1120, 1069, 933, 885, 735, 637; **^{1}H NMR (400 MHz, $CDCl_3$) δ (ppm):** 2.46 (t, $^{4}J_{H,H}$ = 2.4 Hz, 2H), 4.25 (d, $^{4}J_{H,H}$ = 2.4 Hz, 4H), 4.32 (s, 4H); **^{13}C NMR (100 MHz, $CDCl_3$) δ (ppm):** 56.4, 56.7, 75.1, 78.8, 82.1.

Further elution with hexanes/dichloromethane (7:3) afforded the monoalkylation product 4-(prop-2-inyloxy)but-2-yn-1-ol, **14dm** (0.46 g, 16% yield) as a yellow oil. **Molecular formula**: $C_7H_8O_2$; **MW**: 124.14 g/mol; **^{1}H NMR (400 MHz, $CDCl_3$) δ (ppm):** 2.35 (s, 1H), 2.48 (t, $^{4}J_{H,H}$ = 2.4 Hz, 1H), 4.25 (d, $^{4}J_{H,H}$ = 2.4 Hz, 2H), 4.30 (s, 4H).

7.2.2. Rh-catalysed [2+2+2] cycloaddition reactions of triynes 14a and 14d

7.2.2.1. Synthesis of 2,7-bis-(p-toluenesulfonyl)-1,2,3,6,7,8-hexahydro-2,7-diaza-as-indacene, **15a**

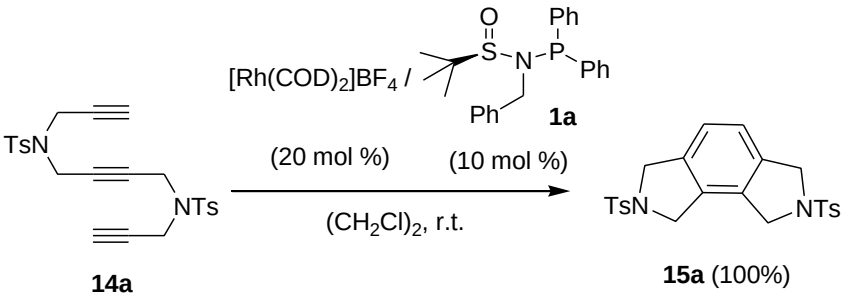

A stirred mixture of ligand PNSO **1a** (4.5 mg, 0.011 mmol) and rhodium complex $[Rh(COD)_2]BF_4$ (8.7 mg, 0.021 mmol) in 1,2-dichloroethane (3 mL) was degassed under nitrogen. Hydrogen gas was introduced to the catalyst solution and stirred for 30 minutes. The resulting mixture was then concentrated to dryness. 1,2-Dichloroethane (10 mL) was added and the solution was stirred under N_2 atmosphere. Triyne **14a** (0.05 g, 0,161 mmol) in 1,2-dichloroethane (3 mL) was then added and the reaction was stirred at room temperature for 1 h (TLC monitoring). The solvent was evaporated and the residue was purified by column chromatography on silica gel with dichloromethane/hexanes (8:2) to afford 2,7-bis-(toluene-4-sulfonyl)-1,2,3,6,7,8-hexahydro-2,7-diaza-*as*-indacene, **15a**[38] (0.05 g, 100% yield) as a colourless solid. **Molecular formula**: $C_{24}H_{24}N_2S_2O_4$; **MW**: 468.15 g/mol; **m.p.** 245-247 ºC; **IR (ATR) ν (cm^{-1}):** 2923, 1343, 1158; **^{1}H NMR (400 MHz, $CDCl_3$) *δ* (ppm):** 2.4 (s, 6H), 4.45 (s, 4H), 4.57 (s, 4H), 7.04 (s, 2H) 7.31 (AA' part of AA'BB' system, $^3J_{H,H}$ = 8.4 Hz, 4H), 7.74 (BB' part of AA'BB' system, $^3J_{H,H}$ = 8.4 Hz, 4H); **^{13}C NMR (100 MHz, $CDCl_3$) *δ* (ppm):** 21.5, 52.2, 53.5, 122.1, 127.6, 130.0, 130.9, 133.6, 136.1, 143.9; **ESI-MS (*m/z*):** 469 $[M+H]^+$, 486 $[M+NH_4]^+$, 491 $[M+Na]^+$.

7.2.2.2. Synthesis of 1,3,6,8-tetrahydro-2,7-dioxa-as-indacene, **15d**

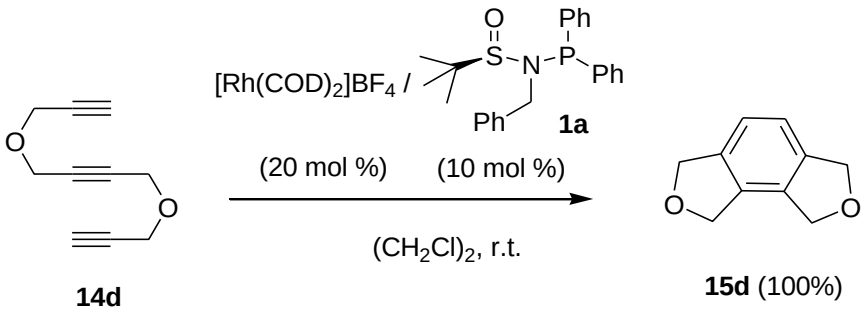

A stirred mixture of PNSO ligand **1a** (12.4 mg, 0.031 mmol) and rhodium complex $[Rh(COD)_2]BF_4$ (25.1 mg, 0,062 mmol) in 1,4-dichloromethane (4 mL) was degassed under nitrogen. Hydrogen gas was introduced to the catalyst solution and stirred for 30 minutes. The resulting mixture was then concentrated to dryness. 1,2-dichloroethane (9 mL) was added and the solution was stirred under N_2 atmosphere. Triyne **14d** (0.05g, 0.324 mmol) in 1,2-

dichloroethane (3 mL) was added and the reaction was stirred for 45 min. at room temperature (TLC monitoring). The solvent was evaporated and the residue was purified by column chromatography on silica gel with dichloromethane/hexanes (7:3) to afford 1,3,6,8-tetrahydro-2,7-dioxa-*as*-indacene **15d** (0.05 g, 100% yield) as a colourless solid. **Molecular formula**: $C_{10}H_{10}O_2$; **MW**: 162.07 g/mol; **m.p.** 78-80 ºC (Lit.[39] **m.p.** 83ºC); **IR (ATR) ν (cm^{-1}):** 2921, 2850, 1462, 1352, 1054, 1029; **^{1}H NMR (400 MHz, $CDCl_3$) δ (ppm):** 5.03 (t, $^4J_{H,H}$ = 1.6 Hz, 4H), 5.12 (t, $^4J_{H,H}$ = 1.6 Hz, 4H), 7.15 (s, 2H); **^{13}C NMR (100 MHz, $CDCl_3$) δ (ppm):** 72.2, 73.4, 119.9, 132.4, 138.7; **ESI-MS (*m/z*):** 163 $[M+H]^+$.

7.2.3. Synthesis of diynes 16d, 16a and monoyne 17e

7.2.3.1. Synthesis of N,N-bis(2-butinyl)-(p-methylphenyl)sulfonamide, 16a

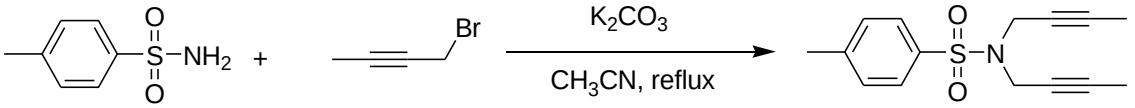

16a (94%)

A stirred mixture of *p*-toluenesulfonamide (1.20 g, 6.94 mmol) and K_2CO_3 (4.98 g, 35.95 mmol) in acetonitrile (60 mL) was heated at reflux. 1-bromo-2-butyne (1.22 mL, 13.93 mmol) was then added slowly and the reaction was stirred at reflux for 4 h (TLC montiring). The salts were filtered off and the solvent was evaporated. The residue was purified by column chromatography on silica gel with dichloromethane/hexanes (5:1) to afford *N,N*-bis(2-butinyl)-(4-methylphenyl)sulfonamide, **16a**[44] (1.79 g, 94% yield) as a colourless solid. **Molecular formula**: $C_{15}H_{17}NSO_2$; **MW**: 275.37 g/mol; **m.p.** 83-84 ºC; **^{1}H NMR (400 MHz, $CDCl_3$) δ (ppm):** 1.64 (t, $^5J_{H,H}$ = 2.4 Hz, 6H), 2.42 (s, 3H), 4.07 (q, $^5J_{H,H}$ = 2.4 Hz, 4H), 7.10 (AA' part of AA'BB' system, $^3J_{H,H}$ = 8.0 Hz, 2H), 7.28 (BB' part of AA'BB' system, $^3J_{H,H}$ = 8.0 Hz, 2H).

7.2.3.2. Synthesis of N,N-bis(2-propinyl)-(p-methylphenyl)sulfonamide, 16d

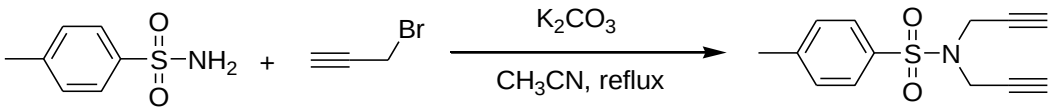

16d (90%)

A stirred mixture of *p*-methylsulfonamide (0.99 g, 5.84 mmol), 1-bromo-2-propyne (1.19 mL, 13.43 mmol) and K_2CO_3 (4.84 g, 35.04 mmol) in acetonitrile (60 mL) was heated at 80ºC for 4 hours (TLC monitoring). The salts were filtered off and the solvent was evaporated. The residue was purified by column chromatography on silica gel with dichloromethane/hexanes

(5:1) to afford *N,N*-bis(2-propinyl)-(4-methylphenyl)sulfonamide, **16d**[45] (1.30 g, 90% yield) as a colourless solid. **Molecular formula**: $C_{13}H_{13}NSO_2$; **MW**: 247.31 g/mol; **m.p.** 63-64 ºC; **^{1}H NMR (400 MHz, $CDCl_3$) δ (ppm):** 2.15 (t, $^4J_{H,H}$ = 2.4 Hz, 2H), 2.42 (s, 3H), 4.16 (d, $^4J_{H,H}$ = 2.4 Hz, 4H), 7.30 (AA' part of AA'BB' system, $^3J_{H,H}$ = 8.4 Hz, 2H), 7.71 (BB' part of AA'BB' system, $^3J_{H,H}$ = 8.4 Hz, 2H).

7.2.3.3. Synthesis of 1,4-diacetyl-2-butyne, **17e**

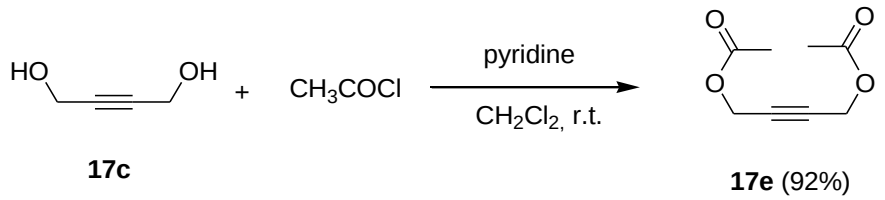

17c **17e** (92%)

A stirred mixture of 2-butyn-1,4-diol **17c** (0.99 g, 11.62 mmol) and pyridine (2.3 mL, 29.04 mmol) in dichloromethane (4.4 mL) was cooled at 0ºC in an ice bath. Acetyl chloride (2.5 mL, 34.48 mmol) was then added in dichloromethane (6.4 mL). The reaction mixture was stirred at room temperature for 4 hours (TLC monitoring). The organic phase was washed with water (3 x 15 mL) and dried over anhydrous sodium sulfate. The salts were filtered off and the solvent was evaporated. The residue was purified by column chromatography on silica gel with hexanes/ethyl acetate (6:4) to afford 1,4-diacetyl-2-butyne **17e**[46] (1.82 g, 92% yield) as a colourless oil. **Molecular formula**: $C_8H_{10}O_4$; **MW**: 170.16 g/mol; **^{1}H NMR (400 MHz, $CDCl_3$) δ (ppm):** 2.10 (s, 6H), 4.71 (s, 4H).

7.2.4. Rh-catalysed [2+2+2] cycloaddition reactions between diynes and monoalkynes

7.2.4.1. Synthesis of cycloadduct **18da**

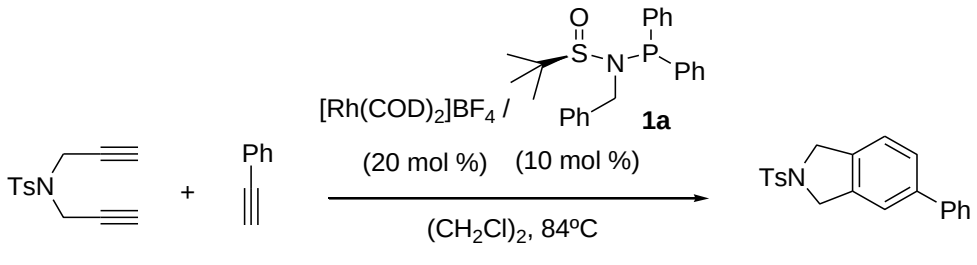

16d **17a** **18da** (78%)

A stirred mixture of $[Rh(COD)_2]BF_4$ (10 mg, 0.025 mmol, 0.2 equiv.) and PNSO ligand **1a** (5 mg, 0.013 mmol, 0.1 equiv.) in dichloromethane (4 mL) was degassed under nitrogen. Hydrogen gas was introduced to the catalyst solution and stirred for 30 minutes. The resulting mixture

was then concentrated to dryness. 1,2-dichloroethane (10 mL) was then added and the solution was stirred under nitrogen atmosphere. Monoalkyne **17a** (0.07 mL, 0.619 mmol, 5 equiv.) in dichloroethane (3 mL) was then added. Finally diyne **16d** (0.03 g, 0.129 mmol, 1 equiv.) in 3 mL of dichloroethane (3 mL) was added dropwise to the reaction mixture. The reaction mixture was heated at reflux for 45 minutes (TLC monitoring). The solvent was evaporated and the residue was purified by column chromatography on silica gel with dichloromethane/hexanes (1:1) to afford **18da**[107] (0.04 g, 78% yield) as a colourless solid. **Molecular formula**: $C_{21}H_{19}NSO_2$; **MW**: 349.45 g/mol; **m.p.** 170-173 ºC; **IR (ATR) (cm^{-1}):** 2919, 2850, 1465, 1343, 1160; **^{1}H NMR (400 MHz, $CDCl_3$) δ (ppm):** 2.38 (s, 3H), 4.64 (br. s, 4H), 7.20 (AA' part of AA'BB' system, $^3J_{H,H}$ = 8.0 Hz, 1H), 7.26-7.36 (m, 4H), 7.37-7.44 (m, 3H), 7.45-7.52 (m, 2H), 7.77 (BB' part of AA'BB' system, $^3J_{H,H}$ = 8.4 Hz, 2H); **^{13}C NMR (100 MHz, $CDCl_3$) δ (ppm):** 21.7, 53.8, 53.9, 121.5, 123.1, 127.1, 127.3, 127.7, 127.8, 129.0, 130.0, 133.9, 135.3, 137.0, 140.7, 141.5, 143.9; **ESI-MS (*m/z*):** 372 $[M+Na]^+$, 388 $[M+K]^+$.

7.2.4.2. Synthesis of cycloadduct 18ad

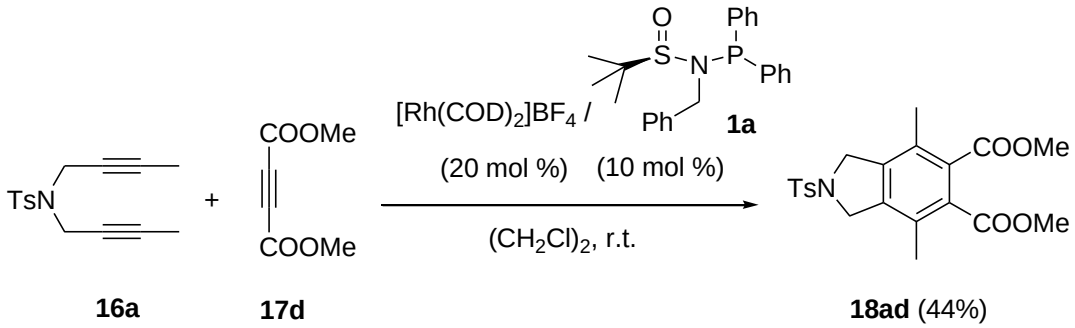

16a **17d** **18ad** (44%)

Using the same experimental procedure as for compound **18da, 18ad** was obtained as a colourless solid (0.02 g, 44% yield) after 5 hours.

Molecular formula: $C_{21}H_{23}NSO_6$; **MW**: 417.48 g/mol; **m.p.** 193-195 ºC. **IR (ATR) ν (cm^{-1})** 2920, 2850, 1722, 1344, 1319, 1216, 1158; **^{1}H NMR (400 MHz, $CDCl_3$) δ (ppm):** 2.20 (s, 6H), 2.42 (s, 3H), 3.84 (s, 6H), 4.61 (s, 4H), 7.33 (AA' part of AABB' system $^3J_{H,H}$ = 8.0 Hz, 2H), 7.77 (BB' part of AABB' system $^3J_{H,H}$ = 8.0 Hz, 2H); **^{13}C NMR (100 MHz, $CDCl_3$) δ (ppm):** 16.7, 21.9, 52.9, 54.3, 127.9, 129.5, 130.4, 132.6, 134.0, 138.5, 144.5, 168.6; **ESI-MS (*m/z*)**: 418 $[M+H]^+$; **ESI-HRMS (*m/z*) calcd. for** $[C_{21}H_{23}NSO_6 + H]^+$ 418.1319; **found**: 418.1316.

[107] Son, S.U.; Choi, D.S.; Chung, Y.K. *Org. Lett.* **2000**, *2*, 2097.

7.2.4.3. Synthesis of cycloadduct 19

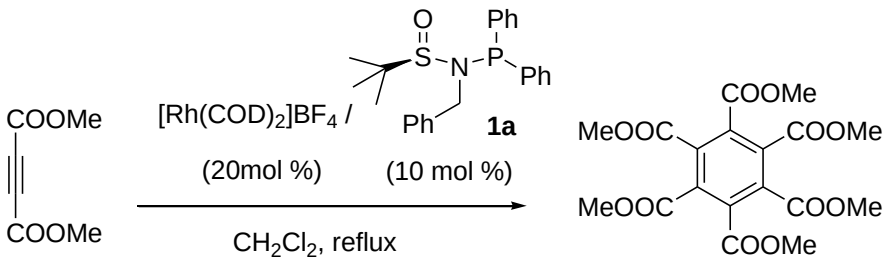

17d

19 (67%)

A stirred mixture of $[Rh(COD)_2]BF_4$ (0.017 g, 0.042 mmol) and ligand **1a** (8 mg, 0.021 mmol) in dichloromethane (4 mL) was degassed under nitrogen. Hydrogen gas was introduced to the catalyst solution and stirred for 30 minutes. The resulting mixture was then concentrated to dryness. Dichloromethane (10 mL) was added and the solution was stirred under nitrogen atmosphere. **17d** (0.03 mL, 0.211 mmol) in dichloromethane (3 mL) was then added. The reaction mixture was stirred for 5 hours at room temperature but it was necessary to heat at reflux for 1.5 hours more (TLC monitoring). The solvent was evaporated and the residue was purified by column chromatography on silica gel with hexanes/ethyl acetate (7:3) to afford hexamethyl benzene-1,2,3,4,5,6-hexacarboxylate **19** (0.01 g, 67% yield) as a colourless solid. **Molecular formula**: $C_{18}H_{18}O_{12}$; **MW**: 426,33 g/mol; **m.p.** 180-183ºC (Lit.[108] **m.p.** 186 ºC); **IR (ATR) ν (cm^{-1}):** 2921, 1726, 1442, 1225; **^{1}H NMR (400 MHz, $CDCl_3$) δ (ppm):** 3.88 (s, 18H); **^{13}C NMR (100 MHz, $CDCl_3$) δ (ppm):** 53.5, 133.9, 165.1; **ESI-MS (*m/z*)**: 427 $[M+H]^+$, 444 $[M+NH_4]^+$, 449 $[M+Na]^+$.

7.2.4.4. Synthesis of cycloadduct 18ce

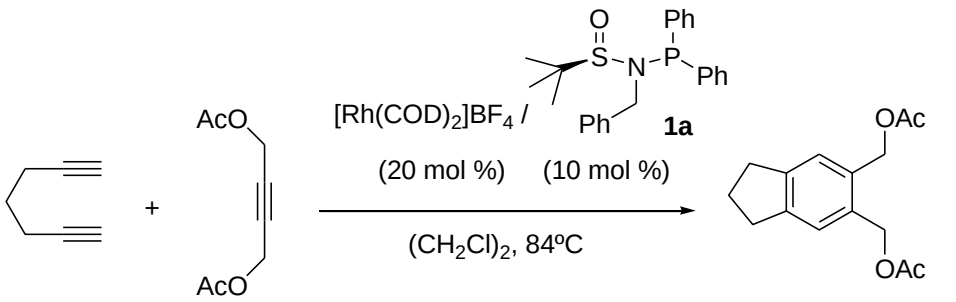

16c

17e

18ce (14%)

Using the same experimental procedure as for compound **18da, 18ce** was obtained as a colourless solid (0.01 g, 14% yield).

[108] Desroy, N.; Robert-Peillard, F.; Toueg, J.; Hénaut, C.; Duboc, R.; Rager, M.N.; Savignac, M.; Genêt, J.P. *Synthesis* **2004**, 2665.

Molecular formula: $C_{15}H_{18}O_4$; **MW**: 263.2 g/mol; **m.p.** 70-72 ºC; **IR (ATR) ν (cm^{-1}):** 2929, 1737, 1223, 1212; **^{1}H NMR (400 MHz, $CDCl_3$) δ (ppm):** 2.05-2.15 (m, 2H), 2.07 (s, 6H), 2.90 (t, $^3J_{H,H}$ = 7.4 Hz, 4H), 5.16 (s, 4H), 7.27 (s, 2H); **^{13}C NMR (100 MHz, $CDCl_3$) δ (ppm):** 21.0, 25.4, 32.6, 64.1, 126.2, 132.4, 145.2, 170.8; **ESI-MS (*m/z*):** 285 $[M+Na]^+$; **Anal. Calcd. for** $C_{15}H_{18}O_4$: C, 68.68; H, 6.92; **found**: C, 68.64; H, 7.02.

Diyne homocoupling product (7 mg, 22% yield) was also obtained as a 2,3-dihydro-5-(pent-4-ynyl)-1*H*-indene, **18ch** by eluting with hexanes/ethyl acetate (7:3)**. Molecular formula:** $C_{14}H_{16}$; **MW**: 184.28 g/mol; **^{1}H NMR (400 MHz, $CDCl_3$) δ (ppm):** 1.78-1.85 (m, 2H), 1.97 (s, 1H), 2.00-2.26 (m, 5H), 2.68 (m, 1H), 2.84-2.88 (m, 4H), 6.94 (m, 1H), 7.05 (s, 1H), 7.13 (m, 1H).

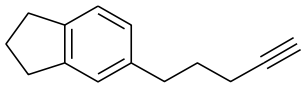

18ch

7.2.4.5. Synthesis of cycloadduct 18de

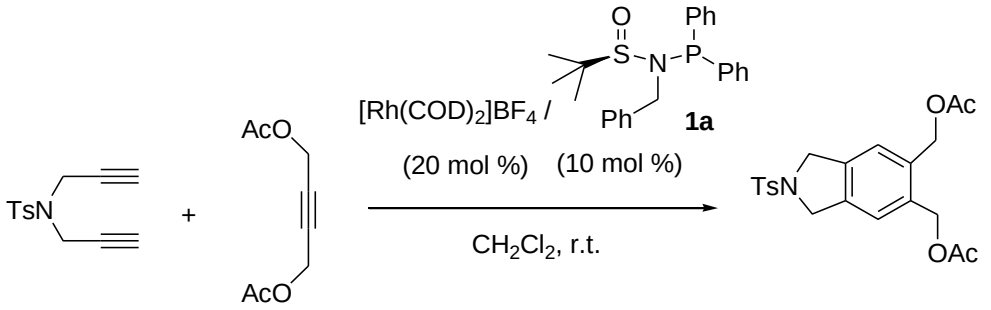

16d **17e** **18de** (26%)

Using the same experimental procedure as for compound **18da, 18de** was obtained as a colourless solid (0.02 g, 26% yield) after 28 hours.

Molecular formula: $C_{21}H_{23}NSO_6$; **MW**: 417.48 g/mol; **m.p.** 143-145 ºC; **IR (ATR) (cm^{-1}):** 2920, 1726, 1340, 1241, 1155; **^{1}H NMR (400 MHz, $CDCl_3$) δ (ppm):** 2.06 (s, 6H), 2.40 (s, 3H), 4.60 (s, 4H), 5.13 (s, 4H), 7.22 (s, 2H), 7.30 (AA' part of AABB' system $^3J_{H,H}$ = 8.0 Hz, 2H), 7.75 (BB' part of AABB' system $^3J_{H,H}$ = 8.0 Hz, 2H); **^{13}C NMR (100 MHz, $CDCl_3$) δ (ppm):** 21.0, 21.6, 53.7, 63.6, 124.2, 127.7, 130.0, 133.6, 134.6, 136.9, 144.0, 170.7; **ESI-MS (*m/z*)**: 418 $[M+H]^+$, 440 $[M+Na]^+$; **ESI-HRMS (*m/z*) calcd. for $[C_{21}H_{23}NSO_6 + H]^+$:** 418.1319; **found** 418.1313.

Further elution with hexanes/ethyl acetate (1:1) afforded *N*-tosyl-*N*-((2-tosylisoindolin-5-yl)methyl)prop-2-yn-1-amine **18dh** as a colourless solid (6 mg, 12% yield). **Molecular formula**: $C_{26}H_{26}N_2S_2O_4$; **MW**: 494.63 g/mol; **^{1}H NMR (400 MHz, $CDCl_3$) δ (ppm):** 2.00 (t, $^4J_{H,H}$ = 2.4 Hz, 1H), 2.40 (s, 3H), 2.44 (s, 3H), 3.9 (d, $^4J_{H,H}$ = 2.4 Hz, 2H), 4.30 (s, 2H), 4.59-4.72 (m, 4H), 7.12 (AA' part of AABB' system $^3J_{H,H}$ = 7.6 Hz, 1H), 7.18 (s, 1H), 7.20 (AA' part of AABB' system $^3J_{H,H}$ = 7.6 Hz, 1 H), 7.31 (BB' part of AABB' system $^3J_{H,H}$ = 8.0 Hz, 4H), 7.76 (BB' part of AABB' system $^3J_{H,H}$ =

8.0 Hz, 4H). **^{13}C NMR (100 MHz, $CDCl_3$) δ (ppm):** 21.55, 35.6, 49.5, 53.5, 122.8, 127.8, 128.3, 129.5, 129.8, 133.7, 135.0, 135.8, 136.2, 136.8, 143.7. **ESI-MS (*m/z*):** 495 $[M+H]^+$, 512 $[M+NH_4]^+$, 517 $[M+Na]^+$.

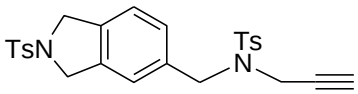

18dh

7.2.4.6. Synthesis of cyclohexadiene derivative 22*: blank test*

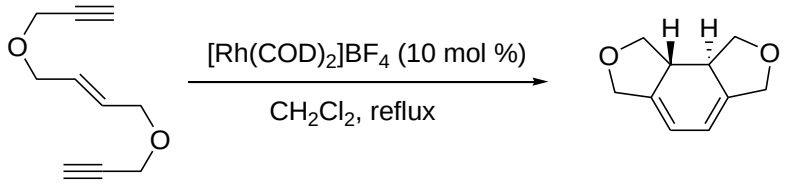

20 **22** (10 %)

A stirred mixture of $[Rh(COD)_2]BF_4$ (7 mg, 0.018 mmol) in dichloromethane (3 mL) was degassed under nitrogen. Hydrogen gas was introduced to the catalyst solution and stirred for 30 minutes. The resulting mixture was then concentrated to dryness. Dichloromethane (2.5 mL) was added and the solution was heated at reflux and stirred under N_2 atmosphere. Then, enediyne **20** (0.04 g, 0.183 mmol) was added in dichloromethane (2 mL) and the reaction mixture was stirred for 3 hours. The solvent was evaporated and the residue was purified by column chromatography on silica gel with hexanes/ethyl acetate (7:3) to afford (*E*)-2,7-dioxa-1,3,6,8,8a,8b-hexahidro-*as*-indacene, **22**[109] (3 mg, 10% yield) as a colourless solid. **Molecular formula**: $C_{10}H_{12}O_2$; **MW**: 164.20 g/mol; **^{1}H NMR (400 MHz, $CDCl_3$) δ (ppm):** 2.73(s, 2H), 3.43-3.48 (m, 2H), 4.24-4.28 (m, 2H), 4.35 (d, $^2J_{H,H}$ = 13.4 Hz, 2H), 4.55 (d, $^2J_{H,H}$ = 13.4 Hz, 2H), 5.85 (s, 2H).

7.2.5. Synthesis of enediynes 20, 27 and 28

7.2.5.1. Synthesis of enediyne 20

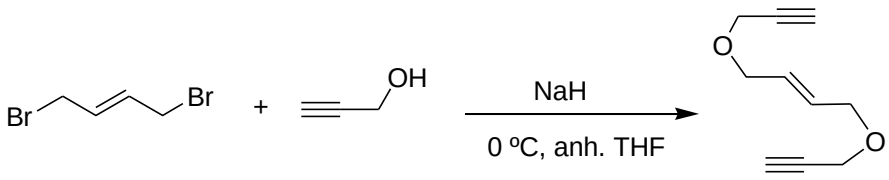

20 (58%)

[109] Tanaka, K.; Nishida, G.; Sagae, H.; Hirano, M. *Synlett* **2007**, 1426.

A stirred mixture of sodium hydride in 60% oil dispersion (1.12 g, 28.05 mmol of pure NaH) and prop-2-yn-1-ol (2.45 mL, 42.07 mmol) in anhydrous THF (20 mL) was cooled at 0ºC. The mixture was stirred for 1 hour at 0ºC under nitrogen atmosphere. (*E*)-1,4-dibromo-2-butene (3 g, 14.02 mmol) in THF (7 mL) was added dropwise at 0ºC and then, the mixture was warmed at room temperature for further 6 hours (TLC monitoring). The residue was quenched with saturated solution of ammonium chloride (30 mL) and extracted with ethyl acetate (3 x 30 mL). The organic phase was dried over anhydrous sodium sulfate and the solvent was evaporated. The residue was purified by column chromatography through silica gel with hexanes/ethyl acetate (9:1) to afford (*E*)-1,4-bis(prop-2-ynyloxy)but-2-ene, **20**[52] (1.32 g, 58% yield) as a yellow oil. **Molecular formula**: $C_{10}H_{12}O_2$; **MW**: 164.20 g/mol; **^{1}H NMR (400 MHz, $CDCl_3$) δ (ppm):** 2.43 (t, $^4J_{H,H}$ = 2.4 Hz, 2H), 4.08 (d, $^3J_{H,H}$ = 1.2 Hz, 4 H), 4.14 (d, $^4J_{H,H}$ = 2.4 Hz, 4H), 5.83 (t, $^3J_{H,H}$ = 1.2 Hz, 2H).

7.2.5.2. Synthesis of enediyne **27**

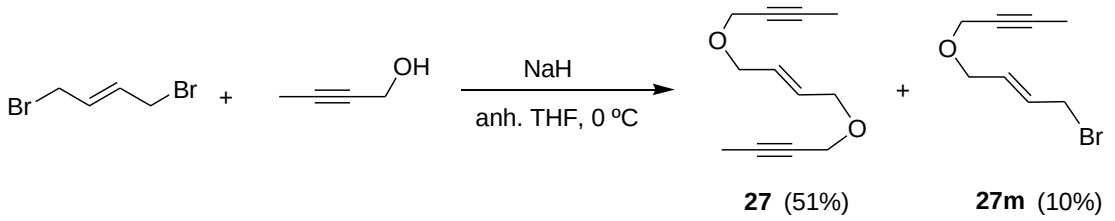

27 (51%) **27m** (10%)

A stirred mixture of sodium hydride in 60% oil dispersion (3.95 g, 98.80 mmol of pure NaH) in anhydrous THF (20 mL) was cooled at 0ºC under nitrogen atmosphere. But-2-yn-1-ol (3.88 mL, 52.00 mmol) was then added dropwise in THF (10 mL). After 30 minutes at 0ºC, (*E*)-1,4-dibromo-2-butene (8.29 g, 38.76 mmol) in THF (10 mL) was added dropwise to the solution. The reaction was warmed at room temperature for 30 hours (TLC monitoring). The residue was treated with saturated solution of ammonium chloride (30 mL) and extracted with ethyl acetate (3 x 30 mL). The organic phase was dried over anhydrous sodium sulfate and the solvent was evaporated. The residue was purified by column chromatography on silica gel with hexanes/ethyl acetate (15:1) to afford (*E*)-1,4-bis(but-2-ynyloxy)but-2-ene **27**[52] (2.57 g, 51% yield) as a yellow oil. **Molecular formula**: $C_{12}H_{16}O_2$; **MW**: 192.25 g/mol; **^{1}H NMR (400 MHz, $CDCl_3$) δ (ppm):** 1.79 (t, $^5J_{H,H}$ = 2.4 Hz, 6H), 3.98 (d, $^3J_{H,H}$ = 1.5 Hz, 4H), 4.03 (q, $^5J_{H,H}$ = 2.4 Hz, 4H), 5.76 (t, $^3J_{H,H}$ = 1.5 Hz, 2H); **^{13}C NMR (75 MHz, $CDCl_3$) δ (ppm):** 3.9, 58.0, 69.6, 75.3, 82.8, 129.8.

Monosusbtituted alkene (*E*)-1-bromo-4-(but-2-ynyloxy)but-2-ene **27m** was also obtained (0.275 g, 10% yield) as a yellow oil. **Molecular formula:** $C_8H_{11}OBr$; **MW**: 184.28 g/mol; **^{1}H NMR (400 MHz, $CDCl_3$) δ (ppm):** 1.80 (t, $^5J_{H,H}$ = 2.4 Hz, 3H), 3.90 (dd, $^3J_{H,H}$ = 7.2 Hz, $^4J_{H,H}$ = 0.6 Hz, 2H), 3.99 (dd, $^3J_{H,H}$ = 5.4 Hz, $^4J_{H,H}$ = 0.6 Hz, 2H), 4.04 (q, $^5J_{H,H}$ = 2.4 Hz, 2H), 5.79 (m, 1H), 5.91 (m, 1H).

7.2.5.3. Synthesis of enediyne 28

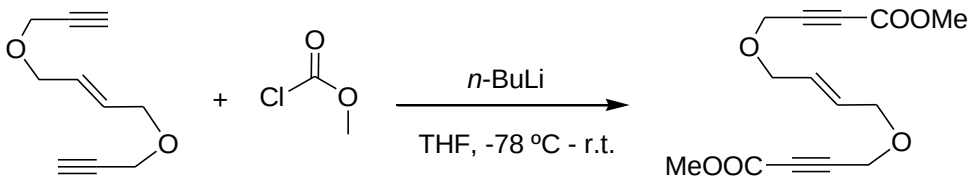

20 **28** (56%)

A stirred mixture of **20** (0.508 g, 3.1 mmol) in anhydrous THF (40 mL) was cooled at -78ºC in a CO_2/acetone bath. Then, *n*-butyllithium (5 mL of 1.35 M, 6.69 mmol) was added dropwise at -78ºC under nitrogen atmosphere. The mixture was stirred for 1 hour at this temperature and finally, methyl chloroformate (0.706 mL, 9.14 mmol) was added. After 1 hour at -78ºC the reaction was heated at room temperature for 4 hours (TLC monitoring). The residue was treated with a saturated solution of ammonium chloride (20 mL) and extracted with ethyl acetate (3 x 20 mL). Then, organic phase was dried over anhydrous sodium sulfate and the solvent was evaporated. The residue was purified by column chromatography through silica gel with hexanes/ethyl acetate (9:1) to afford **28**[53] (0.47 g, 56% yield) as a yellow oil**. Molecular formula**: $C_{14}H_{16}O_6$; **MW**: 280.27 g/mol; **^{1}H NMR (400 MHz, $CDCl_3$) δ (ppm):** 3.78 (s, 6H), 4.09 (d, $^3J_{H,H}$ = 1.6 Hz, 4H), 4.28 (s, 4H), 5.83 (t, $^3J_{H,H}$ = 1.6 Hz, 2H).

7.2.6. Rh-Catalysed [2+2+2]cycloaddition reactions of enediynes 21 and 26

7.2.6.1. Synthesis of cyclohexadiene 23 with (*R*)-BINAP as ligand

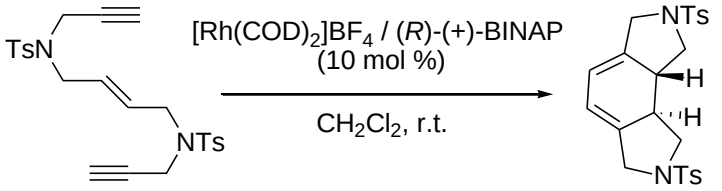

21 **23** (26%)

A stirred mixture of $[Rh(COD)_2]BF_4$ (3 mg, 0.006 mmol) and (*R*)-(+)-BINAP (4 mg, 0.006 mmol) in anhydrous dichloromethane (3 mL) was degassed under nitrogen. Hydrogen gas was introduced to the catalyst solution and stirred for 30 minutes. The resulting mixture was then concentrated to dryness. Dichloromethane (3 mL) was added and the solution was stirred under nitrogen atmosphere. (*E*)-4,9-bis[(4-methylphenyl)sulfonyl)]-4,9-diazadodeca-6-en-1,11-diyne **21** (0.031 g, 0.066 mmol) in dichloromethane (1 mL) was then added. The reaction mixture was stirred under nitrogen atmosphere at room temperature for 44 hours (TLC monitoring). The solvent was evaporated and the residue was purified by column chromatography through silica gel with hexanes/dichloromethane (3:7) to afford (*E*)-2,7-bis[(4-methylphenyl)sulfonyl]-1,3,6,8,8a,8b-hexahydro-2,7-diaza-*as*-indacene, **23**[55] (0.01 g, 26% yield)

as a colourless solid. **Molecular formula**: $C_{24}H_{26}N_2O_4S_2$; **MW**: 470.61 g/mol; **^{1}H NMR (400 MHz, $CDCl_3$) δ (ppm):** 2.44 (s, 6H), 2.62-2.64 (m, 2H + 2H), 3.67 (d, $^2J_{H,H}$ = 14.4 Hz, 2H), 3.79-3.81 (m, 2H), 4.09 (d, $^2J_{H,H}$ = 14.8 Hz, 2H), 5.73 (s, 2H), 7.33 (AA' part of AA'BB' system, $^3J_{H,H}$ = 8 Hz, 4H), 7.69 (BB' part of AA'BB' system, $^3J_{H,H}$ = 8 Hz, 4H).

7.2.6.2. Synthesis of cyclohexadiene 23 with (*R*)-H_8-BINAP as ligand

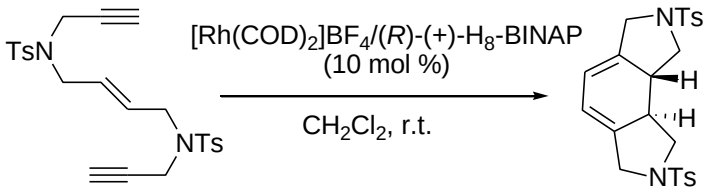

21 **23** (58%)

A stirred mixture of $[Rh(COD)_2]BF_4$ (3 mg, 0.006 mmol) and (*R*)-H_8-(+)-BINAP (4 mg, 0.006 mmol) in anhydrous dichloromethane (3 mL) was degassed under nitrogen. Hydrogen gas was introduced to the catalyst solution and stirred for 30 minutes. The resulting mixture was then concentrated to dryness. Dichloromethane (3 mL) was added and the solution was stirred under nitrogen atmosphere. Then, (*E*)-4,9-bis[(4-methylphenyl)sulfonyl)]-4,9-diazadodeca-6-en-1,11-diyne **21** (0.031 g, 0.065 mmol) in dichloromethane (1 mL) was added. The reaction mixture was stirred under nitrogen atmosphere at room temperature for 44 hours (TLC monitoring). The solvent was evaporated and the residue was purified by column chromatography through silica gel with hexanes/dichloromethane (1:4) to afford (*E*)-2,7-bis[(4-methylphenyl)sulfonyl]-1,3,6,8,8a,8b-hexahydro-2,7-diaza-*as*-indacene, **23**[55] (0.02 g, 58% yield) as a colourless solid.

7.2.6.3. Synthesis of cyclohexadiene 29

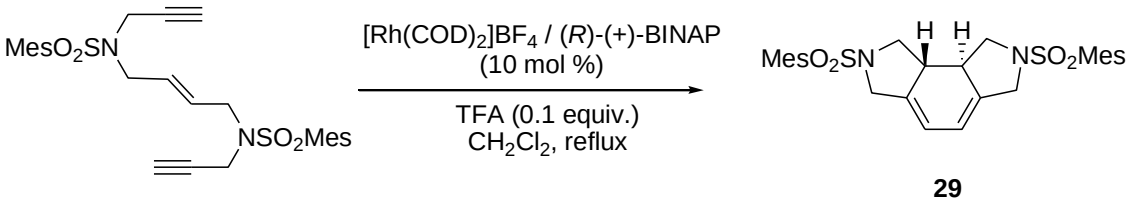

26 **29** (29%, 52 ee)

A stirred mixture of $[Rh(COD)_2]BF_4$ (5.4 mg, 0.013 mmol) and (*R*)-(+)-BINAP (8.28 mg, 0.133 mmol) in anhydrous dichloromethane (3 mL) was degassed under nitrogen. Then, trifluoroacetic acid (0.001 mL, 0.013 mmol) and **26** (0.070 g, 0.131 mmol) in dichloromethane (2 mL) were added. The reaction mixture was heated to reflux and stirred for 24 h (TLC monitoring). The solvent was evaporated and the residue was purified by column chromatography through silica gel with hexanes/ethyl acetate (8:2) to afford **29**[55] **(**0.02 g, 29%

yield) of a colourless solid. **Molecular formula**: $C_{28}H_{34}N_2O_4S_2$; **MW**: 526.71 g/mol; **^{1}H NMR (400 MHz, $CDCl_3$) δ (ppm):** 2.30 (s, 6 H), 2.60 (s, 12 H), 2.76 (broad s, 2H), 2.93-2.98 (m, 2H), 3.61-3.65 (m, 2H), 3.97 (s, 4 H), 5.82 (s, 2 H), 6.95 (s, 4 H).

7.2.7. Synthesis of cyclohexadienes from macrocyclic enediynes

7.2.7.1. Synthesis of cyclohexadiene 25

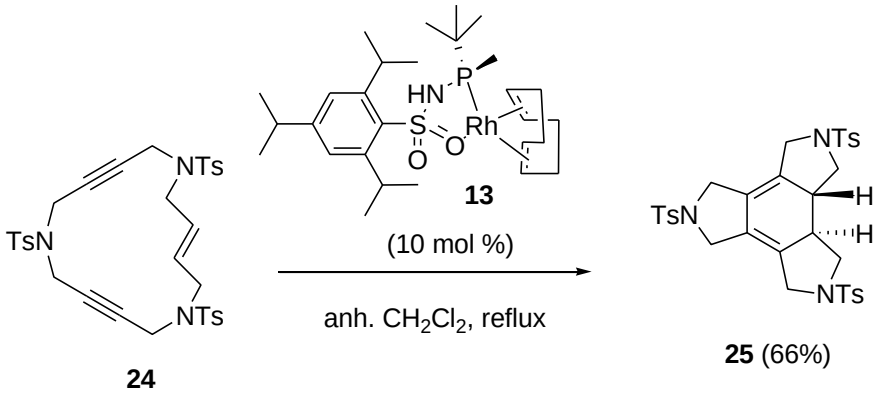

24 **25** (66%)

A stirred mixture of rhodium complex **13** (20 mg, 0.003 mmol) in anhydrous dichloromethane (4 mL) was degassed under nitrogen atmosphere. Then, macrocycle **24** (0.021 g of 0.03 mmol) in dichloromethane (4 mL) was added and the reaction was heated to reflux for 17 hours (TLC monitoring) to afford cyclohexadiene derivative **25**[50] (5 mg, 66% yield) as a colourless solid. **Molecular formula**: $C_{33}H_{35}N_3O_6S_3$; **MW**: 665.84 g/mol; **^{1}H NMR (400 MHz, CD_2Cl_2) δ (ppm)**: 2.30 (s, 3H), 2.35 (s, 6H), 2.46-2.49 (m, 4H), 3.44 (d, $^2J_{H,H}$ = 14.0 Hz, 2H), 3.69 (br abs, 6H), 3.89 (d, $^2J_{H,H}$ = 14.0 Hz, 2H), 7.18 (AA' part of a AA'BB' system, $^3J_{H,H}$ = 8.0 Hz, 2H), 7.28 (AA' part of AA'BB' system, $^3J_{H,H}$ = 8.0 Hz, 4H), 7.53 (BB' part of AA'BB' system, $^3J_{H,H}$ = 8.0 Hz, 2H), 7.58 (BB' of AA'BB' system, $^3J_{H,H}$ = 8.0 Hz, 4H).

7.3. Experimental procedure for the products synthesised in Chapter 4

7.3.1. Synthesis of Baylis-Hillman adducts

7.3.1.1. Synthesis of 32a

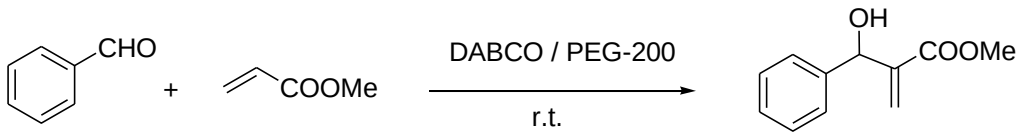

33 **32a** (73%)

In a 50 mL flask, a mixture of benzaldehyde **33** (1.01 mL, 10.0 mmol), methyl acrylate (1.35 mL, 15.0 mmol) and DABCO (1.12 g, 10.0 mmol) was dissolved in polyethylene glycol with a molecular weight of 200 g/mol (10 mL). The solution was stirred at room temperature until completion (TLC monitoring). Water was added (10 mL) and the product was then extracted with ethyl ether (4 x 10 mL). The organic phase was dried over magnesium sulfate, the solvent was evaporated and the residue was purified by column chromatography through silica gel with essence G/ethyl acetate (8:2) to afford methyl 2-(hydroxy(phenyl)methyl)acrylate, **32a**[110] (1.4 g, 73%) as colourless oil. **Molecular formula**: $C_{11}H_{12}O_3$; **MW**: 192.21 g/mol; **^{1}H NMR (250 MHz, $CDCl_3$) δ (ppm):** 3.10 (broad s, 1H), 3.72 (s, 3H), 5.57 (s, 1H), 5.84 (s, 1H), 6.34 (s, 1H), 7.28-7.39 (m, 5 H).

7.3.1.2. Synthesis of 32b

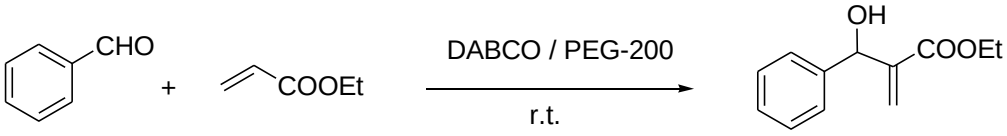

33 **32b** (68%)

This compound was obtained following the general procedure described for **32a** with the specific conditions:

Benzaldehyde: 2.02 mL (20 mmol)
Ethyl acrylate: 3.25 mL (30 mmol)
DABCO: 2.24 g (20 mmol)
PEG-200: 10 mL
Purification: essence G/ethyl acetate (85:15)

[110] Kinsella, M.; Duggan, P. G.; Muldoon, J.; Eccles, K. S.; Lawrence, S. E.; Lennon, C. M. *E. J. Org. Chem*. **2011**, 1125.

After purification, 2.77 g (68% yield) of a colourless oil was obtained which was identified by spectroscopic data as ethyl 2-(hydroxy(phenyl)methyl)acrylate, **32b**[56f]. **Molecular formula**: $C_{12}H_{14}O_3$; **MW**: 206.24 g/mol; **^{1}H NMR (250 MHz, $CDCl_3$) δ (ppm):** 1.19 (t, $^3J_{H,H}$ = 7.25, 3H), 3.60 (d, $^3J_{H,H}$ = 5.25, 1H), 4.10 (q, $^3J_{H,H}$ = 7.25, 2H), 5.51 (d, $^3J_{H,H}$ = 5.25, 1H), 5.85 (s, 1H), 6.31 (s, 1H), 7.24-7.36 (m, 5H).

7.3.1.3. Synthesis of **32c**

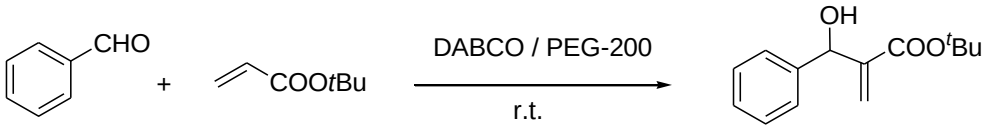

33 **32c** (48%)

This compound was obtained following the general procedure described for **32a** with the specific conditions:

Benzaldehyde: 1.01 mL (10 mmol)
tert-Butyl acrylate: 2.21 mL (15 mmol)
DABCO: 1.12 g (10 mmol)
PEG-200: 10 mL
Purification: essence G/ethyl acetate (90:10)

After purification, 1.13 g (48% yield) of a colourless oil was obtained which was identified by spectroscopic data as *tert*-butyl 2-(hydroxy(phenyl)methyl)acrylate, **32c**.[110] **Molecular formula**: $C_{14}H_{18}O_3$; **MW**: 234.29 g/mol; **^{1}H NMR (250 MHz, $CDCl_3$) δ (ppm):** 1.40 (s, 9H), 3.09 (d, $^3J_{H,H}$ = 7.5 Hz, 1H), 5.50 (d, $^3J_{H,H}$ = 7.5 Hz, 1H), 5.72 (s, 1H), 6.26 (s, 1H), 7.34-7.37 (m, 5H).

7.3.1.4. Synthesis of **32d**

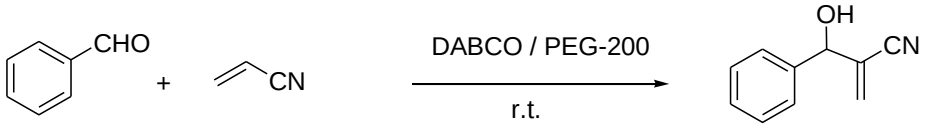

33 **32d** (89%)

This compound was obtained following the general procedure described for **32a** with the specific conditions:

Benzaldehyde: 3.04 mL (30 mmol)
Acrylonitrile: 2.98 mL (45 mmol)
DABCO: 1.68 g (15 mmol)
PEG-200: 10 mL
Purification: essence G/ethyl acetate (80:20→75:25)

After purification, 4.24 g (89% yield) of a colourless oil was obtained which was identified by spectroscopic data as 2-(hydroxy(phenyl)methyl)acrylonitrile, **32d.**[111] **Molecular formula**: $C_{10}H_9NO$; **MW**: 159.18 g/mol; **^{1}H NMR (250 MHz, $CDCl_3$) δ (ppm):** 2.39 (broad s, 1H), 5.31 (s, 1H), 6.02 (d, $^2J_{H,H}$ = 2.5 Hz, 1H), 6.12 (d, $^2J_{H,H}$ = 2.5 Hz, 1H), 7.40 (s, 5H).

7.3.1.5. Synthesis of **32e**

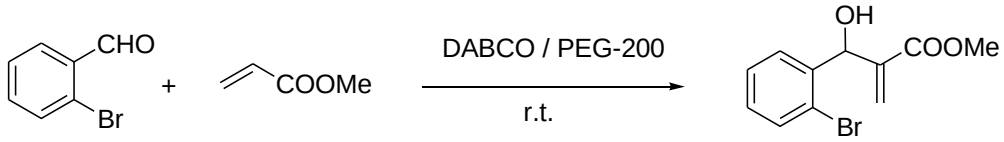

32e (75%)

This compound was obtained following the general procedure described for **32a** with the specific conditions:

2-Bromobenzaldehyde: 1.17 mL (10 mmol)
Methyl acrylate: 1.35 mL (15 mmol)
DABCO: 1.12 g (10 mmol)
PEG-200: 10 mL
Purification: essence G/ethyl acetate (80:20)

After purification, 2.04 g (75% yield) of a colourless oil was obtained which was identified by spectroscopic data as methyl 2-((2-bromophenyl)(hydroxy)methyl)acrylate, **32e.**[112] **Molecular formula**: $C_{11}H_{11}BrO_3$; **MW**: 271.11 g/mol; **^{1}H NMR (250 MHz, $CDCl_3$) δ (ppm):** 3.36 (broad s, 1H), 3.78 (s, 3H), 5.57 (s, 1H), 5.95 (s, 1H), 6.35 (s, 1H), 7.14-7.38 (m, 2H), 7.55 (d, $^3J_{H,H}$ = 7.5 Hz, 2H).

7.3.1.6. Synthesis of **32f**

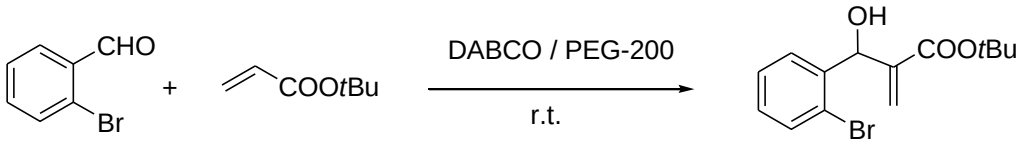

32f (72%)

[111] Cai, J.; Zhou, Z.; Zhao, G.; Tang, C. *Org. Lett*. **2002**, *4*, 4723.
[112] Coelho, F.; Almeida, W. P.; Veronese, D.; Mateus, C. R.; Silva Lopes, E. C.; Rossi, R. C.; Silveira, G. P. C.; Pavam. C. H. *Tetrahedron* **2002**, *58*, 7437.

This compound was obtained following the general procedure described for **32a** with the specific conditions:

2-Bromobenzaldehyde: 1.17 mL (10 mmol)
tert-Butyl acrylate: 2.20 mL (15 mmol)
DABCO: 1.12 g (10 mmol)
PEG-200: 10 mL
Purification: essence G/ethyl acetate (80:20)

After purification, 2.27 g (72% yield) of a colourless oil was obtained which was identified by spectroscopic data as *tert*-butyl 2-((2-bromophenyl)(hydroxy)methyl)acrylate **32f. Molecular formula**: $C_{14}H_{17}BrO_3$; **MW**: 313.19 g/mol; **^{1}H NMR (250 MHz, $CDCl_3$) δ (ppm):** ^{1}H-NMR ($CDCl_3$, 250 MHz): 1.67 (s, 9 H), 3.45 (d, $^3J_{H,H}$ = 5 Hz, 1H), 5.77 (s, 1H), 6.13 (d, $^3J_{H,H}$ = 5 Hz, 1H), 6.51 (s, 1H), 7.40 (t, $^3J_{H,H}$ = 7.5 Hz, 1H), 7.57 (t, $^3J_{H,H}$ = 7.5 Hz, 1H), 7.76 (m, 2H).

7.3.1.7. Synthesis of 32g

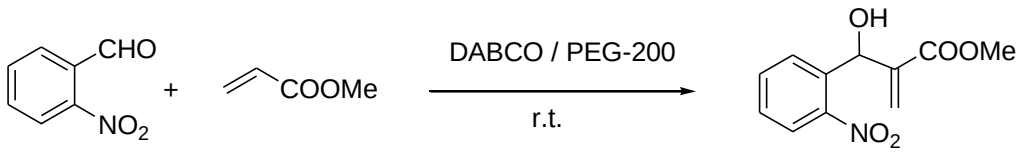

32g (99%)

This compound was obtained following the general procedure described for **32a** with the specific conditions:

2-Nitrobenzaldehyde: 3.02 g (20 mmol)
Methyl acrylate: 2.70 mL (30 mmol)
DABCO: 2.24 g (20 mmol)
PEG-200: 10 mL
Purification: essence G/ethyl acetate (80:20)

After purification, 3.41 g (99% yield) of a colourless oil was obtained which was identified by spectroscopic data as methyl 2-(hydroxy(2-nitrophenyl)methyl)acrylate, **32g**[110]. **Molecular formula**: $C_{11}H_{11}NO_5$; **MW**: 237.21 g/mol; **^{1}H NMR (250 MHz, $CDCl_3$) δ (ppm):** 3.43 (d, $^3J_{H,H}$ = 5 Hz, 1 H), 3.73 (s, 3H), 5.73 (s, 1H), 6.20 (d, $^3J_{H,H}$ = 5 Hz, 1 H), 6.37 (s, 1H), 7.47 (t, $^3J_{H,H}$ = 2.5 Hz, 1H), 7.65 (t, $^3J_{H,H}$ = 2.5 Hz, 1 H), 7.75 (d, $^3J_{H,H}$ = 2.5 Hz, 1 H), 7.95 (d, $^3J_{H,H}$ = 2.5 Hz, 1 H).

7.3.1.8. Synthesis of **32h**

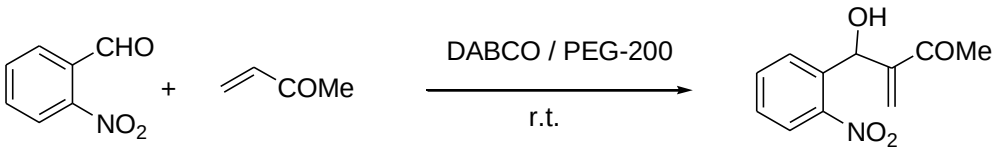

32h (55%)

This compound was obtained following the general procedure described for **32a** with the specific conditions:

2-Nitrobenzaldehyde: 3.02 g (20 mmol)
Methyl vinyl ketone: 2.43 mL (30 mmol)
DABCO: 0.45 g (4 mmol)
PEG-200: 10 mL
Purification: essence G/ethyl acetate (80:20)

After purification, 2.44 g (55% yield) of a colourless solid was obtained which was identified by spectroscopic data as methyl 3-[hydroxy(2-nitrophenyl)methyl]but-3-en-2-one **32h**[113]. **Molecular formula**: $C_{11}H_{11}NO_4$; **MW**: 221.21 g/mol; **^{1}H NMR (250 MHz, $CDCl_3$) δ (ppm):** 2.38 (s, 3H), 3.51 (d, $^3J_{H,H}$ = 5 Hz, 1H), 5.80 (s, 1H), 6.18 (s, 1H), 6.23 (d, $^3J_{H,H}$ = 5 Hz, 1H), 7.47 (t, $^3J_{H,H}$ = 7.5 Hz, 1H), 7.66 (t, $^3J_{H,H}$ = 7.5 Hz, 1 H), 7.78 (d, $^3J_{H,H}$ = 7.5 Hz, 1 H), 7.97 (d, $^3J_{H,H}$ = 7.5 Hz, 1 H).

7.3.2. Synthesis of diynes

7.3.2.1. Synthesis of diyne **34b**

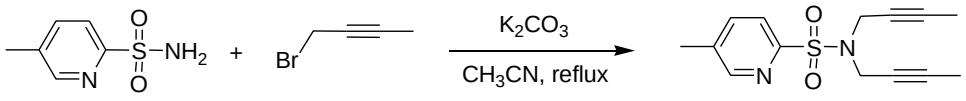

35 **34b** (83%)

A stirred mixture of 5-methyl-2-pyridinesulfonamide **35** (1.20 g, 6.97 mmol) and potassium carbonate (4.95 g, 34.85 mmol) in acetonitrile (60 mL) was heated at reflux. Then, 1-bromo-2-butyne (1.22 mL, 13.94 mmol) was added. The solution was stirred at reflux for 4 hours (TLC monitoring). The salts were filtered off and the residue was purified by column chromatography through silica gel with hexanes/dichloromethane (1:7) to afford diyne **34b** (1.59 g, 83%) as a colourless solid. **Molecular formula**: $C_{14}H_{16}N_2O_2S$; **MW:** 276.35 g/mol; **^{1}H NMR (400 MHz, $CDCl_3$) δ (ppm):** 1.60 (t, $^5J_{H,H}$ = 2.4 Hz, 6H) 2.42 (s, 3H), 4.23 (q, $^5J_{H,H}$ = 2.4 Hz, 4H), 7.75 (m, 1H), 7.86 (d, $^3J_{H,H}$ = 8 Hz, 1H), 8.51 (m, 1H).

[113] Oh, K.; Li, J. Y.; Ryu, J. *Org. Biomol. Chem.* **2010**, *8*, 3015.

7.3.2.2. Synthesis of diyne **34c**

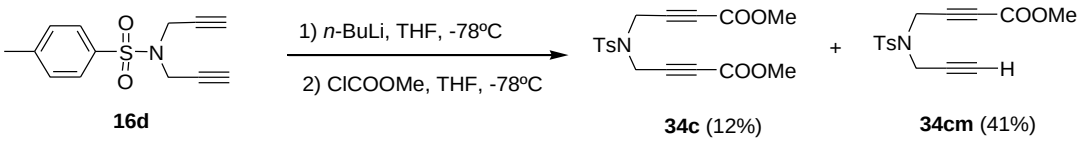

16d **34c** (12%) **34cm** (41%)

A stirred mixture of **16d** (0.58 g, 2.30 mmol) in anhydrous THF (35 mL) was cooled at -78ºC in an ethyl acetate/nitrogen bath. Then, *n*-butyllithium (3.20 mL of a 1.6 M solution in hexanes, 5.17 mmol) was added dropwise at -78ºC under nitrogen atmosphere. The mixture was stirred for 1 hour at this temperature and then methyl chloroformate (0.54 mL, 7.04 mmol) was added. After 1 hour at -78ºC the reaction was warmed to room temperature and stirred at this temperature for 22 hours (TLC monitoring). The residue was treated with a saturated solution of ammonium chloride (20 mL) and extracted with ethyl acetate (3 x 20 mL). Then, the organic phase was dried over anhydrous sodium sulfate and the solvent was evaporated. The residue was purified by column chromatography through silica gel with hexanes/ethyl acetate (8:2) to afford diyne **34c** (0.11 g, 12% yield) and diyne **34cm** (0.30 g, 41% yield) as colourless solids.

Diyne **34c**: **Molecular formula**: $C_{17}H_{17}NO_6S$; **MW**: 363.38 g/mol; **^{1}H NMR (300 MHz, $CDCl_3$) δ (ppm):** 2.42 (s, 3H), 3.72 (s, 6H), 4.27 (s, 4H), 7.32 (AA' part of AA'BB' system, $^3J_{H,H}$ = 8.4 Hz, 2H), 7.71 (BB' part of AA'BB' system, $^3J_{H,H}$ = 8.4 Hz, 2H).

Diyne **34cm**: **Molecular formula**: $C_{15}H_{15}NO_4S$; **MW**: 305.35 g/mol; **^{1}H NMR (300 MHz, $CDCl_3$) δ (ppm):** 2.19 (t, $^4J_{H,H}$ = 2.4 Hz, 1H), 2.43 (s, 3H), 3.73 (s, 3H), 4.14 (d, $^4J_{H,H}$ = 2.4 Hz, 2H), 4.31 (s, 2H), 7.29-7.35 (m, 2H), 7.69-7.73 (m, 2H).

7.3.2.3. Synthesis of diyne **34d**

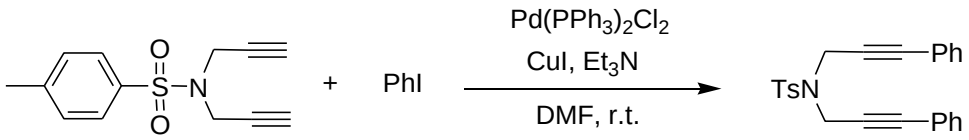

16d **34d** (23%)

A mixture of **16d** (0.195 g, 0.79 mmol), phenyl iodide (0.177 mL, 1.58 mmol), copper iodide (0.015 g, 0.079 mmol) and bis(triphenylphosphine)palladium dichloride (0.027 g, 0.040 mmol) in dry degassed triethylamine (2 mL) and anhydrous dimethylformamide (0.9 mL) was stirred at room temperature for 19 hours (TLC monitoring). The residue was treated with a saturated solution of ammonium chloride (1 mL) and extracted with ethyl acetate (3 x 2 mL). The organic phase was washed with a saturated solution of sodium chloride, dried over anhydrous sodium sulfate and the solvent was evaporated. The residue was purified by column chromatography through silica gel with hexanes/ethyl acetate (8:2) to afford diyne **34d** (0.071 g, 23%) as a

colourless solid. **Molecular formula**: $C_{25}H_{21}NO_2S$; **MW:** 399.5 g/mol; **^{1}H NMR (400 MHz, $CDCl_3$) δ (ppm):** 2.31 (s, 3H), 4.44 (s, 4H), 7.18-7.30 (m, 12H), 7.79 (d, $^3J_{H,H}$ = 8.3 Hz, 2H).

7.3.3. General procedure for [2+2+2] cycloaddition reactions of diynes with BH adducts using microwave heating (Method A)

7.3.3.1. Synthesis of 38aa

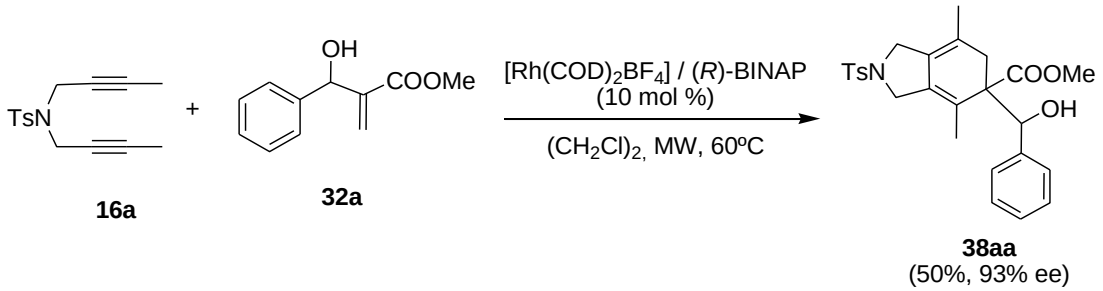

16a **32a** **38aa** (50%, 93% ee)

A stirred mixture of $[Rh(COD)_2]BF_4$ (5 mg, 0.012 mmol, 0.1 equiv.) and (*R*)-BINAP (8 mg, 0.013 mmol, 0.1 equiv.) in dichloromethane (2 mL) was degassed under nitrogen. Hydrogen gas was introduced to the catalyst solution and stirred for 30 minutes. The resulting mixture was then concentrated to dryness. 1,2-dichloroethane (1 mL) was then added and the solution was stirred under nitrogen atmosphere. The solution was introduced in a 10 mL microwave reaction vial together with a solution of Baylis-Hillman adduct **32a** (0.03 g, 0.164 mmol, 1.5 equiv.) and diyne **16a** (0.03g, 0.109 mmol, 1 equiv.) in dichloroethane (2 mL) under a nitrogen atmosphere. The vial was then placed inside the cavity of the microwave synthesizer. The reaction mixture was heated at 60ºC under microwave irradiation (TLC monitoring). Upon completion, the solvent was evaporated and the residue was purified by column chromatography on silica gel with hexanes/ethyl acetate (6:4) to afford cycloadduct **38aa** (0.023 g, 50% yield) as a colourless solid. **Molecular formula**: $C_{26}H_{29}NO_5S$; **MW**: 467.58 g/mol; **m.p.** 75-77ºC; **IR (ATR)** 2923, 1717, 1342, 1159, 1095, 1046 cm^{-1}; **^{1}H NMR ($CDCl_3$, 300 MHz): δ (ppm**): 1.41 (s, 3H), 1.72 (s, 3H), 2.35 (d, $^2J_{H,H}$ = 17.6 Hz, 1H), 2.47 (s, 3H), 2.52 (d, $^2J_{H,H}$ = 17.6 Hz, 1H), 3.28 (d, $^3J_{H,H}$ = 4.2 Hz, 1H), 3.26-3.32 (m, 1H), 3.72 (s, 3H), 3.71-3.77 (m, 1H), 3.82 (d, $^2J_{H,H}$ = 12.4 Hz, 1H), 4.00 (d, $^2J_{H,H}$ = 12.4 Hz, 1H), 4.96 (d, $^3J_{H,H}$ = 4.2 Hz, 1H), 6.95-7.00 (m, 2H), 7.04-7.09 (m, 3H), 7.38 (AA' part of AA'BB' system, $^3J_{H,H}$ = 8.1 Hz, 2H), 7.70 (BB' part of AA'BB' system, $^3J_{H,H}$ = 8.1 Hz, 2H); **^{13}C NMR ($CDCl_3$, 100 MHz): δ (ppm**): 17.9, 19.2, 21.9, 36.2, 50.3, 51.3, 52.7, 58.3, 77.9, 119.9, 122.5, 126.1, 127.2, 127.4, 127.4, 127.8, 128.1, 128.2, 130.0, 133.1, 133.3, 139.9, 144.1, 176.5; **ESI-MS (*m/z*):** 468.1 $[M+H]^+$, 490.1 $[M+Na]^+$; **Anal. Calc. for $C_{26}H_{29}NO_5S \cdot 2\ H_2O$:** C, 62.01, H, 6.60, N, 2.78; **found:** C, 62.25; H, 6.04; N, 3.17. Enantiomeric excess was determined with HPLC analysis (Daicel Chiralpak column (4.6 x 250 mm, 5 µm); 1 mL/min flow rate of a 50% 2-propanol : 50% heptane mobile phase during 30 min.; λ = 254 nm.; Rt = 8 min for major isomer and Rt = 15 min for minor isomer).

7.3.4. General procedure for [2+2+2] cycloaddition reactions of diynes with BH adducts using conventional heating and slow addition of diyne with syringe pump (Method B)

7.3.4.1. Synthesis of 38ab

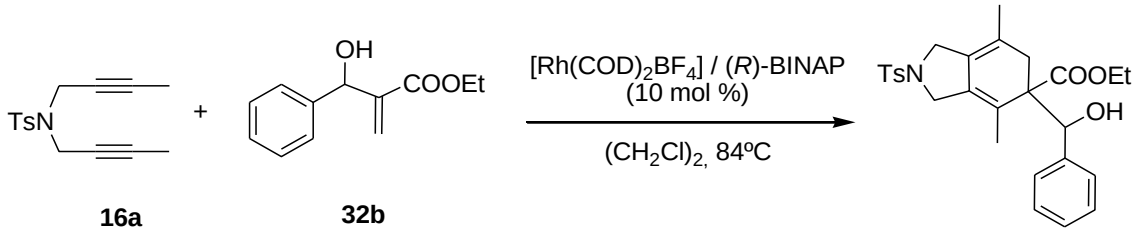

16a **32b** **38ab** (48%, 80% ee)

In a 10 mL flask, a mixture of $[Rh(COD)_2]BF_4$ (5 mg, 0.011 mmol) and (*R*)-BINAP (7 mg, 0.011 mmol) was dissolved in CH_2Cl_2 (2 mL). Hydrogen gas was introduced to the catalyst solution and stirred for 30 min. The resulting mixture was then concentrated to dryness. 1,2-dichloroethane (1 mL) was added and the solution was stirred under a nitrogen atmosphere. A solution of Baylis-Hillman adduct **32b** (0.034 g, 0.163 mmol) in dichloroethane (1 mL) was then added at room temperature and the resulting solution was heated at 84ºC. Diyne **16a** (0.03 g, 0.109 mmol) in dichloroethane (1 mL) was then slowly added with a syringe pump during 4 hours. The reaction was stirred until completion (TLC monitoring). The solvent was evaporated and the residue was purified by column chromatography through silica gel with hexanes/ethyl acetate (6:4) to afford cycloadduct **38ab** as a colourless solid (25 mg, 48% yield). **Molecular formula**: $C_{27}H_{31}NO_5S$; **MW**: 481.6 g/mol; **IR (ATR)** 2923, 1719, 1343, 1160, 1094, 1045 cm^{-1}; **^{1}H NMR ($CDCl_3$, 300 MHz): δ (ppm)**: 1.25 (t, $^3J_{H,H}$ = 7.2 Hz, 3H), 1.41 (s, 3H), 1.72 (s, 3H), 2.35 (d, $^2J_{H,H}$ = 17.7 Hz, 1H), 2.47 (s, 3H), 2.52 (d, $^2J_{H,H}$ = 17.7 Hz, 1H), 3.28 (d, $^2J_{H,H}$ = 12.8 Hz, 1H), 3.41 (d, $^3J_{H,H}$ = 4.4 Hz, 1H), 3.75 (d, $^2J_{H,H}$ = 12.8 Hz, 1H), 3.81 (d, $^2J_{H,H}$ = 13.0 Hz, 1H), 4.00 (d, $^2J_{H,H}$ = 13.0 Hz, 1H), 4.14-4.23 (m, 2H), 4.94 (d, $^3J_{H,H}$ = 4.4 Hz, 1H), 6.93-6.98 (m, 2H), 7.01-7.10 (m, 3H), 7.38 (AA' part of AA'BB' system, $^3J_{H,H}$ = 8.2 Hz, 2H), 7.70 (BB' part of AA'BB' system, $^3J_{H,H}$ = 8.2 Hz, 2H)**; ESI-MS (*m/z*):** 482.1 $[M+H]^+$; 504.1 $[M+Na]^+$. Enantiomeric excess was determined with HPLC analysis (Daicel Chiralpak column (4.6 x 250 mm, 5 µm); 1 mL/min flow rate of a 60% 2-propanol : 40% heptane mobile phase during 30 min.; λ = 254 nm.; Rt = 7 min for major isomer and Rt = 24 min for minor isomer).

7.3.4.2. Synthesis of **38ac**

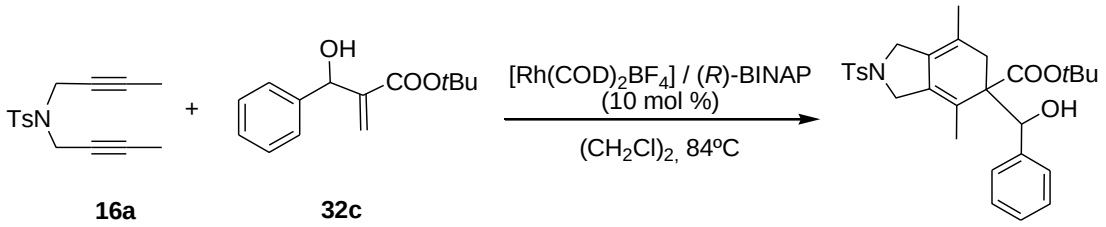

16a **32c**

38ac
(32%, 95% ee)

This compound was obtained following the general procedure described for cycloadduct **38ab**.

After purification by column chromatography through silica gel with hexanes/ethyl acetate (8:2), cycloadduct **38ac** was obtained as a colourless solid (11 mg, 32% yield). **Molecular formula**: $C_{29}H_{35}NO_5S$; **MW**: 509.66 g/mol; **m.p.** 68-70ºC**; ^{1}H NMR ($CDCl_3$, 400 MHz): δ (ppm**): 1.41 (s, 3H), 1.44 (s, 9H), 1.68 (s, 3H), 2.31 (d, $^2J_{H,H}$ = 17.6 Hz, 1H), 2.48 (s, 3H), 2,54 (d, $^2J_{H,H}$ = 17.6 Hz, 1H), 3.22 (d, $^2J_{H,H}$ = 12.8 Hz, 1H), 3.58 (d, $^3J_{H,H}$ = 4.4 Hz, 1H), 3.77-3.79 (m, 2H), 4.00 (d, $^2J_{H,H}$ = 12.8 Hz, 1H), 4.86 (d, $^3J_{H,H}$ = 4.4 Hz, 1H), 6.90-6.95 (m, 2H), 7.00-7.07 (m, 3H), 7.39 (AA' part of AA'BB' system, $^3J_{H,H}$ = 8.8 Hz, 2H), 7.71 (BB' part of AA'BB' system, $^3J_{H,H}$ = 8.8 Hz, 2 H); **^{13}C NMR ($CDCl_3$, 75 MHz): δ (ppm**): 18.1, 19.1, 21.9, 28.3, 37.0, 50.3, 51.2, 58.6, 78.2, 82.6, 120.4, 122.2, 126.1, 127.2, 127.4, 127.9, 128.2, 130.0, 132.7, 133.0, 140.3, 144.0, 175.7; **ESI-MS (*m/z*):** 510.1 $[M+H]^+$; **Anal. Calc. for $C_{29}H_{35}NO_5S \cdot H_2O$:** C, 66.01; H, 7.07; N, 2.65; **found:** C, 65.74; H, 6.54; N, 3.10. Enantiomeric excess was determined with HPLC analysis (Daicel Chiralpak column (4.6 x 250 mm, 5 μm); 1 mL/min flow rate of a 40% 2-propanol : 60% heptane mobile phase during 30 min.; λ = 254 nm.; Rt = 8 min for major isomer and Rt = 15 min for minor isomer).

Further elution with hexanes/ethyl acetate (8:2) afforded the homocoupling product *N*-((4,5,7-trimethyl-2-tosylisoindolin-6-yl)methyl)-N-tosylbut-2-yn-1-amine, **36** (3.1 mg, 10% yield) as a colourless solid. **Molecular formula**: $C_{30}H_{34}N_2O_4S_2$; **MW**: 550.73 g/mol; **^{1}H NMR (300 MHz, $CDCl_3$) *δ* (ppm):** 1.41 (t, $^5J_{H,H}$ = 2.4 Hz, 3H), 2.07 (s, 3H), 2.19 (s, 3H), 2.27 (s, 3H), 2.32 (s, 3H), 2.40 (s, 3H), 2.45 (s, 3H), 3.60 (q, $^5J_{H,H}$ = 2.4 Hz, 2H), 4.42 (s, 2H), 4.46 (d, $^2J_{H,H}$ = 6.9 Hz, 4H), 7.32 (AA' part of AA'BB' system, $^3J_{H,H}$ = 8.4 Hz, 4H), 7.78 (BB' part of AA'BB' system, $^3J_{H,H}$ = 8.4 Hz, 4H 4H).

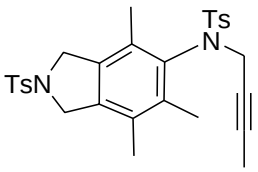

36

7.3.4.3. Synthesis of **38ba**

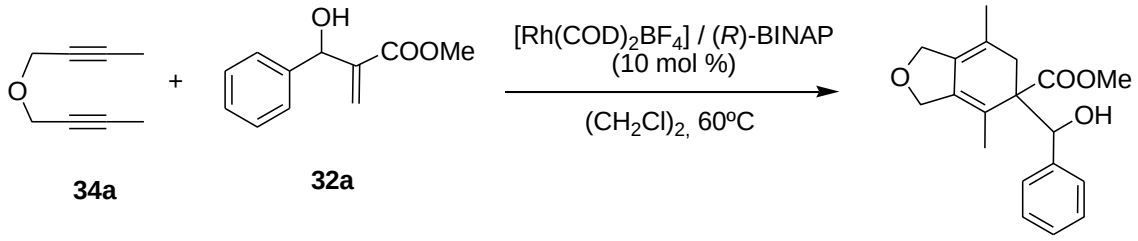

34a **32a**

38ba
(45%, 90% ee)

This compound was obtained following the general procedure described for cycloadduct **38ab** but with a slow addition of diyne **34a** over **32a** during 4 hours at 60ºC. Cycloadduct **38ba** was isolated after column chromatography through silica gel with hexanes/ethyl acetate (20:1) as a yellow oil (57 mg, 45% yield). **Molecular formula**: $C_{19}H_{22}O_4$; **MW:** 314.38 g/mol; **IR (ATR)** 2950, 1716, 1434, 1203; **^{1}H NMR ($CDCl_3$, 400 MHz): δ (ppm)**: 1.49 (s, 3H), 1.69 (s, 3H), 2.50 (d, $^2J_{H,H}$ = 17.6 Hz, 1H), 2.60 (d, $^2J_{H,H}$ = 17.6 Hz, 1H), 3.36 (d, $^3J_{H,H}$ = 4.8 Hz, 1H), 3.74 (s, 3H), 4.02 (d, $^2J_{H,H}$ = 12.4 Hz, 1H), 4.28 (d, $^2J_{H,H}$ = 12.4 Hz, 1H), 4.42 (d, $^2J_{H,H}$ = 12.0 Hz, 1H), 4.48 (d, $^2J_{H,H}$ = 12.0 Hz, 1H), 5.05 (d, $^3J_{H,H}$ = 4.8 Hz, 1H), 7.20-7.25 (m, 5H). **^{13}C NMR ($CDCl_3$, 75 MHz): δ (ppm)**: 17.8, 19.4, 36.5, 52.7, 58.6, 70.3, 70.9, 77.2, 117.3, 120.2, 127.5, 127.8, 128.2, 129.3, 136.8, 140.3, 176.7; **ESI-MS (*m/z*)**: 337.2 $[M+Na]^+$; **ESI-HRMS (*m/z*) calcd. for $[M+Na]^+$:** 337.1410; **found:** 337.1410. Enantiomeric excess was determined with HPLC analysis (Daicel Chiralpak column (4.6 x 250 mm, 5 µm); 1 mL/min flow rate of a 5% 2-propanol : 95% heptane mobile phase during 40 min.; λ = 254 nm.; Rt = 28 min for major isomer and Rt = 33 min for minor isomer).

Further elution with hexanes/ethyl acetate (20:1) afforded the homocoupling product 5-((but-2-ynyloxy)methyl)-1,3-dihydro-4,6,7-trimethylisobenzofuran, **40** (0.012 g, 12% yield) as a colourless solid. **Molecular formula**: $C_{16}H_{20}O_2$; **MW**: 244.33 g/mol; **^{1}H NMR (400 MHz, $CDCl_3$) *δ* (ppm):** 1.89 (t, $^5J_{H,H}$ = 2.0 Hz, 3H), 2.12 (s, 3H), 2.25 (s, 3H), 2.31 (s, 3H), 4.16 (t, $^5J_{H,H}$ = 2.0 Hz, 2H), 4.62 (s, 2H), 5.11 (s, 4H).

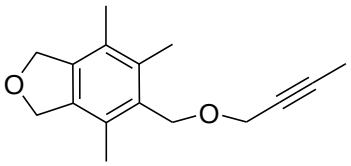

40

7.3.4.4. Synthesis of **38bb**

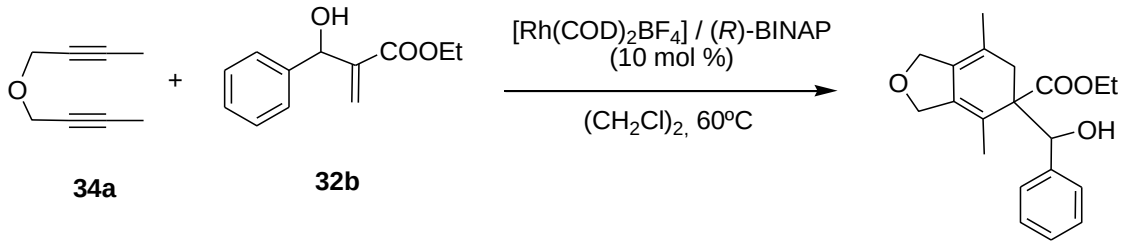

34a **32b** **38bb**
(20%, 80% ee)

This compound was obtained following the general procedure described for cycloadduct **38ab** but with a slow addition of diyne **34a** over **32b** during 7.5 hours. Cycloadduct **38bb** was isolated after column chromatography on silica gel with hexanes/ethyl acetate (20:1) together with homocoupling product **40** (27 mg, 20% yield as calculated by ^{1}H-NMR). **Molecular formula**: $C_{20}H_{24}O_4$; **MW:** 328.4 g/mol; **^{1}H NMR ($CDCl_3$, 300 MHz): δ (ppm)**: 1.29 (t, $^{3}J_{H,H}$ = 7.2 Hz, 3H), 1.51 (s, 3H), 1.70 (s, 3H), 2.51 (d, $^{2}J_{H,H}$ = 17.1 Hz, 1H), 2.62 (d, $^{2}J_{H,H}$ = 17.1 Hz, 1H), 3.56 (d, $^{3}J_{H,H}$ = 4.8 Hz, 1H), 4.03 (d, $^{2}J_{H,H}$ = 12.6 Hz, 1H), 4.23 (q, $^{3}J_{H,H}$ = 7.2 Hz, 2H), 4.30 (d, $^{2}J_{H,H}$ = 12.3 Hz, 1H), 4.42 (d, $^{2}J_{H,H}$ = 12.9 Hz, 1 H), 4.50 (d, $^{2}J_{H,H}$ = 12.9 Hz, 1 H), 5.04 (d, $^{3}J_{H,H}$ = 4.8 Hz, 1H); 7.24-7.26 (m, 5H). Enantiomeric excess was determined with HPLC analysis (Daicel Chiralpak column (4.6 x 250 mm, 5 μm); 1 mL/min flow rate of a 5% 2-propanol : 95% heptane mobile phase during 40 min.; λ = 254 nm.; Rt = 24 min for major isomer and Rt = 31 min for minor isomer).

7.3.4.5. Synthesis of **38ca**

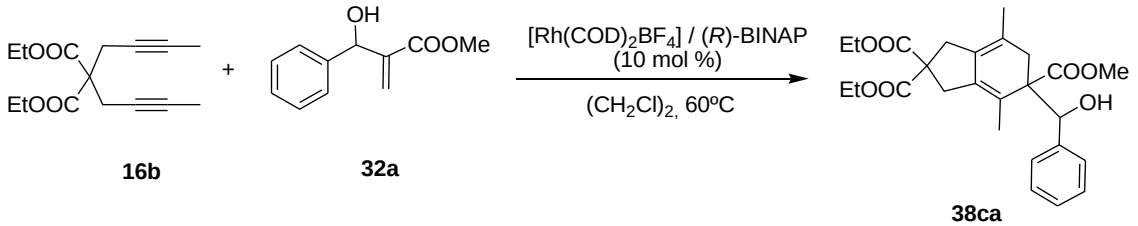

16b **32a** **38ca**
(41%, n.d. ee)

This compound was obtained following the general procedure described for cycloadduct **38ab**. After purification by column chromatography through silica gel with dichloromethane/ hexanes/methanol (7:3:0.2) cycloadduct **38ca** was obtained as a yellow oil (35 mg, 41%). **Molecular formula**: $C_{26}H_{32}O_7$; **MW:** 456.53 g/mol; **IR (ATR)** 2927, 1726, 1435, 1244, 1186; **^{1}H NMR ($CDCl_3$, 400 MHz): δ (ppm)**: 1.22 (t, $^{3}J_{H,H}$ = 7.2 Hz, 3H), 1.27 (t, $^{3}J_{H,H}$ = 7.2Hz, 3H), 1.52 (s, 3H), 1.60 (s, 3H), 2.55 (s, 2H), 2.65 (d, $^{2}J_{H,H}$ = 16.4 Hz, 1H), 2.83 (d, $^{2}J_{H,H}$ = 16.4 Hz, 1H), 2.94 (s, 2H), 3.59 (d, $^{3}J_{H,H}$ = 5.6 Hz, 1H), 3.70 (s, 3H), 4.17 (q, $^{3}J_{H,H}$ = 7.2 Hz, 2H), 4.22 (q, $^{3}J_{H,H}$ = 7.2 Hz, 2H), 4.93 (d, $^{3}J_{H,H}$ = 5.2 Hz, 1H), 7.20-7.24 (m, 5H); **^{13}C NMR ($CDCl_3$, 75 MHz): δ (ppm)**: 14.3, 14.4, 17.6, 19.4, 36.5, 36.9, 38.1, 52.4, 58.5, 58.8, 61.8, 61.9, 76.3, 119.9, 122.5, 127.8, 127.8, 127.8, 129.3, 136.5, 140.9, 171.9, 172.0, 177.0; **ESI-MS (*m/z*):** 474.1 $[M+NH_4]^+$; **Anal. Calc. for**

$C_{26}H_{32}O_7$: C, 68.40, H, 7.07; **found:** C, 67.95, H, 6.92. The enantiomeric excess could not be determined because the columns that are available in the lab could not separate the two enantiomers.

7.3.4.6. Synthesis of 38da

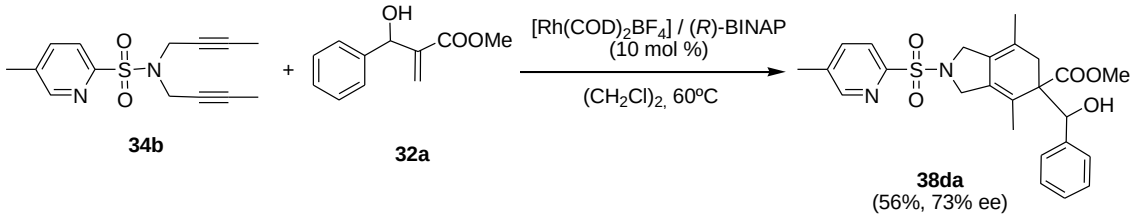

34b **32a** **38da** (56%, 73% ee)

This compound was obtained following the general procedure described for cycloadduct **38ab**. After purification by column chromatography through silica gel with hexanes/ethyl acetate (8:2) cycloadduct **38da** was obtained as a colourless solid (37 mg, 56%). **Molecular formula**: $C_{25}H_{28}N_2SO_5$; **MW:** 468.17 **g/mol**; **m.p.** 48-50ºC; **IR (ATR)** 2923, 1718, 1340, 1169 cm^{-1}; **^{1}H NMR ($CDCl_3$, 300 MHz): δ (ppm)**: 1.45 (s, 3H), 1.68 (s, 3H), 2.43-2.47 (m, 1H), 2.46 (s, 3H), 2.53 (d, $^2J_{H,H}$ = 17.7 Hz, 1H), 3.36 (d, $^3J_{H,H}$ = 4.8 Hz, 1H), 3.66 (d, $^2J_{H,H}$ = 13.8 Hz, 1H), 3.72 (s, 3H), 3.98 (d, $^2J_{H,H}$ = 13.8 Hz, 1H), 4.16-4.20 (m, 2H), 5.0 (d, $^3J_{H,H}$ = 4.8 Hz, 1H), 7.07-7.15 (m, 5H), 7.72 (m, 1H), 7.85 (d, $^3J_{H,H}$ = 8.4 Hz, 1H), 8.55 (m, 1H); **^{13}C NMR ($CDCl_3$, 75 MHz): δ (ppm)**: 17.6, 18.7, 19.1, 35.9, 50.8, 51.8, 52.5, 58.0, 77.1, 119.8, 122.5, 123.0, 126.1, 127.2, 127.4, 128.0, 133.3, 137.4, 138.0, 140.0, 150.8, 153.3, 176.1; **ESI-MS (*m/z*):** 469.0 $[M+H]^+$; **Anal. Calc. for $C_{25}H_{28}N_2SO_5 \cdot 2H_2O$:** C, 59.51, H, 6.39, N, 5.55; **found:** C, 59.96, H, 5.63, N, 5.64. Enantiomeric excess was determined with HPLC analysis (Daicel Chiralpak column (4.6 x 250 mm, 5 µm); 1 mL/min flow rate of a 40% 2-propanol:60% heptane mobile phase during 30 min.; λ = 254 nm.; Rt = 9 min for major isomer and Rt = 14 min for minor isomer).

7.3.4.7. Synthesis of 42

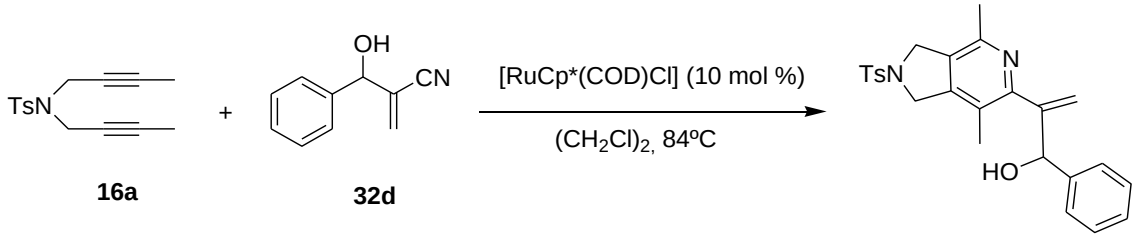

16a **32d** **42** (46%)

In a 10 mL flask, a mixture of [RuCp*(COD)Cl] (8.3 mg, 0.022 mmol), diyne **16a** (0.061 g, 0.22 mmol) and Baylis-Hillman adduct **32d** (0.055 g, 0.33 mmol) was dissolved in 1,2-dichloroethane (4 mL). The solution was heated at reflux and stirred under a nitrogen atmosphere for 4 hours (TLC monitoring). The solvent was evaporated and the residue was purified by column chromatography on silica gel with hexanes/ethyl acetate (2:1) to afford cycloadduct **42** as a colourless solid (43.6 mg, 46% yield). **Molecular formula**: $C_{25}H_{26}N_2O_3S$; **MW**: 434.55 g/mol; **^{1}H**

NMR ($CDCl_3$, 300 MHz): δ (ppm): 1.96 (s, 3H), 2.35 (s, 3H), 2.41 (s, 3H), 4.43-4.54 (m, 2H), 4.52-4.55 (m, 2H), 5.17 (s, 1H), 5.53 (s, 1H), 5.65 (s, 1H), 6.45 (br. s, 1H), 7.13-7.27 (m, 5H), 7.33 (AA' part of AA'BB' system, $^3J_{H,H}$ = 8.7 Hz, 2H), 7.75 (BB' part of AA'BB' system, $^3J_{H,H}$ = 8.7 Hz, 2H); **^{13}C NMR ($CDCl_3$, 100 MHz): δ (ppm)**: 15.8, 21.6, 21.7, 52.7, 53.6, 78.9, 119.7, 124.1, 126.0, 127.1, 127.7, 128.1, 129.2, 130.2, 133.8, 142.7, 144.2, 145.8, 146.6, 148.1, 156.7.

7.3.4.8. Characterization data for compound 43*:*

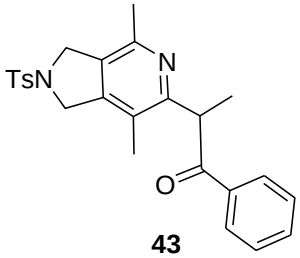

43

Molecular formula: $C_{25}H_{26}N_2O_3S$; **MW**: 434.55 g/mol; **^{1}H NMR ($CDCl_3$, 300 MHz): δ (ppm)**: 1.49 (d, $^3J_{H,H}$ = 6.9 Hz, 3H), 2.18 (s, 3H), 2.22 (s, 3H), 2.41 (s, 3H), 4.28-4.54 (m, 4H), 4.80 (q, $^3J_{H,H}$ = 6.9 Hz, 1H), 7.29-7.35 (m, 4H), 7.43 (m, 1H), 7.75-7.79 (m, 4H).

7.3.4.9. Characterization data for compound 37*:*

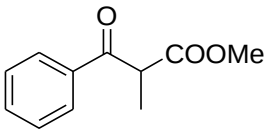

37

Molecular formula: $C_{11}H_{12}O_3$; **MW**: 192.21 g/mol; **^{1}H NMR ($CDCl_3$, 400 MHz): δ (ppm)**: 1.50 (d, $^3J_{H,H}$ = 7.2 Hz, 3H), 3.69 (s, 3H), 4.41 (q, $^3J_{H,H}$ = 7.2 Hz, 1H), 7.44-7.51 (m, 2H), 7.55-7.60 (m, 1H), 7.95-7.99 (m, 2H); **^{13}C NMR ($CDCl_3$, 75 MHz): δ (ppm)**: 14.2, 48.4, 52.8, 128.9, 129.1, 133.8, 136.0, 171.6, 196.1; **ESI-MS (*m/z*):** 215.0 $[M+Na]^+$.

7.4. Experimental procedure for the products synthesised in Chapter 5

7.4.1. Experimental procedure for the partially intramolecular [2+2+2] cycloaddition reactions catalysed by Rh(I)-BINAP-type ligands

7.4.1.1. Synthesis of 4,7-dimethyl-5-phenyl-2-tosylisoindoline, **18aa**

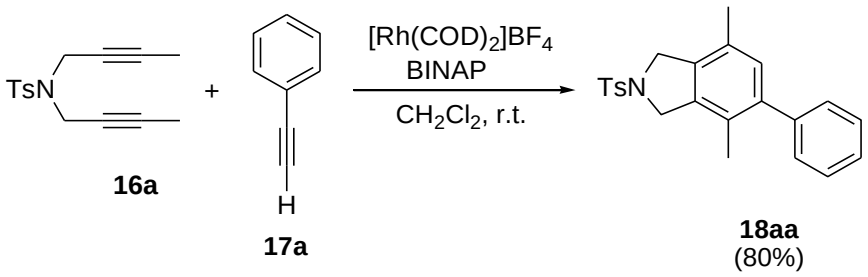

16a **17a** **18aa** (80%)

A mixture of $[Rh(COD)_2]BF_4$ (2.21 mg, 0.005 mmol, 0.05 equiv) and BINAP (3.39 mg, 0.005 mmol, 0.05 equiv) was dissolved in dichloromethane (3 mL) in a 25 mL flask. Hydrogen gas was introduced into the catalyst solution with stirring for 30 min. The resulting mixture was then concentrated to dryness, the residue was redissolved in dichloroethane (1 mL) and the solution was stirred under nitrogen atmosphere. A solution of *p*-methylphenylacetylene **17a** (0.018 mL, 0.163 mmol, 1.5 equiv) in dichloroethane (0.5 mL) was then added at room temperature followed by a solution of diyne **16a** (0.030 g, 0.109 mmol, 1 equiv) in dichloroethane (0.5 mL). The reaction mixture was heated under reflux until completion (TLC monitoring). The solvent was evaporated and the residue was purified by column chromatography on silica gel with hexanes/dichloromethane (1:2) to afford 0.033 g (80% yield) of a colourless solid, which was identified by spectroscopic data as 4,7-dimethyl-5-*p*-tolyl-2-tosylisoindoline, **18aa**. **Molecular formula**: $C_{23}H_{23}NO_2S$; **MW:** 377.5 g/mol; **M.p**. 201-203ºC (Lit.[96] **m.p**. 156-158ºC); **IR (ATR) (cm^{-1}):** 2922, 1333, 1155cm^{-1}; **^{1}H NMR (400 MHz, $CDCl_3$) δ (ppm):** 2.06 (s, 3H), 2.19 (s, 3H), 2.42 (s, 3H), 4.62 (s, 4H), 6.95 (s, 1H), 7.21-7.23 (m, 2H), 7.32-7.40 (m, 5H), 7.81 (d, $^3J_{H,H}$ = 8.4 Hz, 2H); **ESI-MS (*m/z*):** 400.1 $[M+Na]^+$, 777.1 $[2M+Na]^+$.

7.4.1.2. Synthesis of 4,7-dimethyl-5-phenyl-2-tosylisoindoline, **18aa** *using (R)-H_8-BINAP*

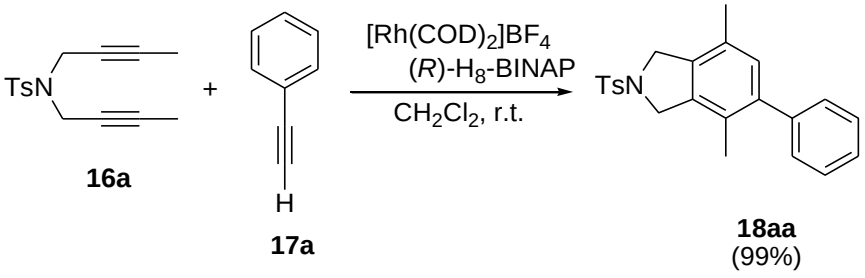

16a **17a** **18aa** (99%)

This compound was obtained using the general procedure described for **18aa** with the following specific conditions:

$[Rh(COD)_2]BF_4$: 2.21 mg (0.005 mmol)
H_8-BINAP: 3.44 mg (0.005 mmol)
Monoyne **17a**: 0.018 mL (0.163 mmol)
Diyne **16a**: 0.030 g (0.109 mmol)
Dichloromethane: 3 mL
Reaction time: 1 hour
Purification: hexanes/dichloromethane (2:3)

After purification, 0.041 g (99% yield) of a colourless solid was obtained which was identified by spectroscopic data as 4,7-dimethyl-5-*p*-tolyl-2-tosylisoindoline, **18aa**.

7.4.1.3. Synthesis of 5-phenyl-2-tosylisoindoline, **18da**

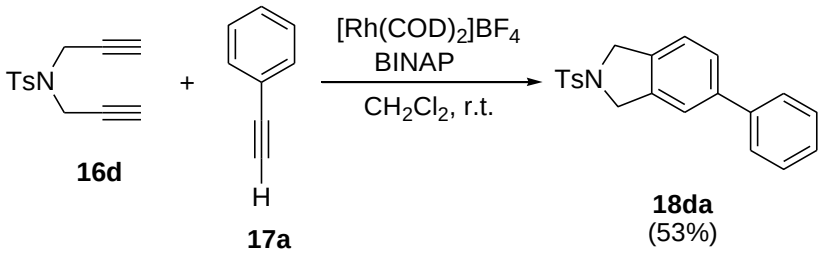

This compound was obtained using the general procedure described for **18aa** with the following specific conditions:

$[Rh(COD)_2]BF_4$: 2.46 mg (0.008 mmol)
BINAP: 5.04 mg (0.008 mmol)
Monoyne **17a**: 0.030 g (0.243 mmol)
Diyne **16d**: 0.041 g (0.162 mmol)
Dichloromethane: 5 mL
Reaction time: 1 hour
Purification: hexanes/dichloromethane (6:4)

After purification, 0.030 g (53% yield) of a colourless solid was obtained which was identified by spectroscopic data as 5-phenyl-2-tosylisoindoline*,* **18da**.[114] **Molecular formula**: $C_{21}H_{19}NO_2S$; **MW**: 349.45 g/mol; **M.p.** 170-173 ºC; **IR (ATR) ν (cm^{-1}):** 2919, 2850, 1465, 1343, 1160 cm^{-1}; **^{1}H NMR (400 MHz, $CDCl_3$) δ (ppm):** 2.38 (s, 3H), 4.64 (br. s , 4H), 7.20 (d, *J* = 8.0 Hz, 1H), 7.26-7.36 (m, 4H), 7.37-7.44 (m, 3H), 7.45-7.52 (m, 2H), 7.77 (d, *J* = 8.4 Hz, 2H) ppm; **^{13}C NMR (100 MHz, $CDCl_3$) δ (ppm):** 21.7, 53.8, 53.9, 121.5, 123.1, 127.1, 127.3, 127.7, 127.8, 129.0, 130.0, 133.9, 135.3, 137.0, 140.7, 141.5, 143.9; **ESI-MS (*m/z*):** 350.1 $[M+H]^+$, 372.1 $[M+Na]^+$, 388.1 $[M+K]^+$.

[114] Son, S. U.; Choi, D. S.; Chung, Y. K. *Org. Lett*. **2000**, *2,* 2097.

7.4.1.4. Synthesis of 4,7-dimethyl-5-p-tolyl-2-tosylisoindoline, 66a

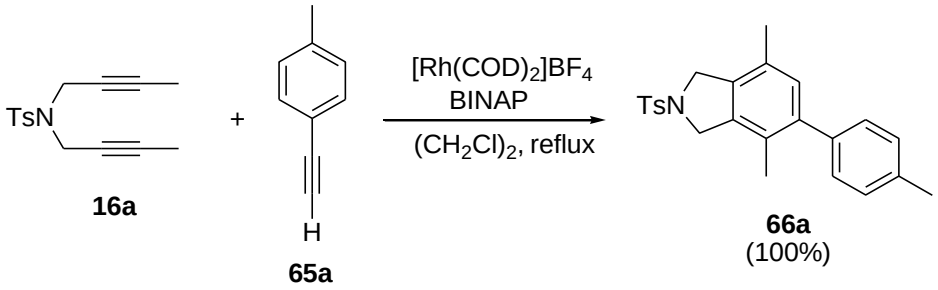

This compound was obtained using the general procedure described for **18aa** with the following specific conditions:

$[Rh(COD)_2]BF_4$]: 2.75 mg (0.007 mmol)
BINAP: 4.23 mg (0.007 mmol)
Monoyne **17a**: 0.019 g (0.163 mmol)
Diyne **16a**: 0.03 g (0.109 mmol)
Dichloromethane: 2 mL
Reaction time: 5 hours
Purification: hexanes/dichloromethane (1:1)

After purification, 0.047 g (quantitative yield) of a colourless solid was obtained which was identified by spectroscopic data as 4,7-dimethyl-5-*p*-tolyl-2-tosylisoindoline, **66a**. **Molecular formula**: $C_{24}H_{25}NSO_2$; **MW:** 391.53 g/mol; **M.p.** 150–152ºC; **IR (ATR) ν (cm^{-1}):** 2918, 1340, 1159, 1098; **^{1}H NMR (300 MHz, $CDCl_3$) δ (ppm):** 2.05 (s, 3H), 2.18 (s, 3H), 2.38 (s, 3H), 2.41 (s, 3H), 4.61 (s, 4H), 6.92 (s, 1H), 7.09 (AA' part of AA'BB' system, $^3J_{H,H}$ = 8.1 Hz, 2H), 7.18 (AA' part of AA'BB' system, $^3J_{H,H}$ = 8.1 Hz, 2H), 7.32 (BB' part of AA'BB' system, $^3J_{H,H}$ = 8.4 Hz, 2H), 7.80 ppm (BB' part of AA'BB' system, $^3J_{H,H}$ = 8.4 Hz, 2H); **^{13}C NMR (75 MHz, $CDCl_3$) δ (ppm):** 16.3, 18.2, 21.1, 21.5, 53.5, 53.9, 127.2, 127.6, 128.8, 129.0, 129.5, 129.8, 130.6, 133.7, 135.7, 136.6, 138.0, 141.9, 143.6; **ESI-MS (*m/z*)**: 392.1 $[M+H]^+$, 414.1 $[M+Na]^+$, 805.1 $[2M+Na]^+$; **Anal. Calc. for $C_{24}H_{25}NO_2S·0.5(C_6H_{14})$:** C 74.96, H 6.99, N 3.24; **found:** C 75.26, H 7.20, N 3.46.

7.4.1.5. Synthesis of 5-(4-methoxyphenyl)-4,7-dimethyl-2-tosylisoindoline, 66b

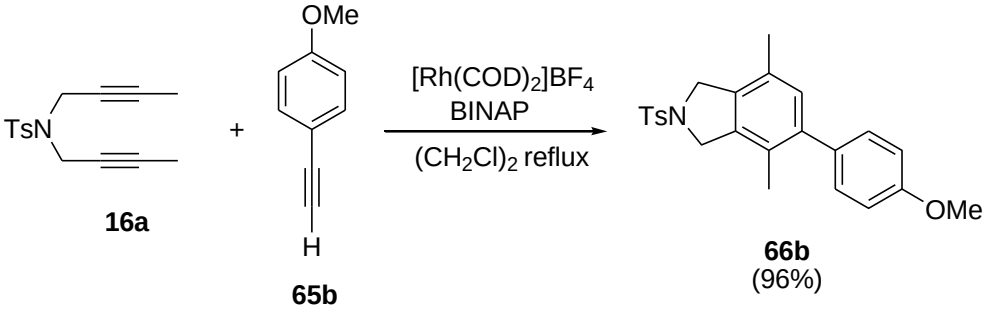

This compound was obtained using the general procedure described for **18aa** with the following specific conditions:

$[Rh(COD)_2]BF_4$: 2.21 mg (0.005 mmol)
BINAP: 3.39 mg (0.005 mmol)
Monoyne **65b**: 0.022 g (0.163 mmol)
Diyne **16a**: 0.030 g (0.109 mmol)
Dichloroethane: 3 mL
Reaction time: 4.5 hours
Purification: hexanes/dichloromethane (1:2)

After purification, 0.043 g (96% yield) of a colourless solid was obtained which was identified by spectroscopic data as 5-(4-methoxyphenyl)-4,7-dimethyl-2-tosylisoindoline, **66b**. **Molecular formula**: $C_{24}H_{25}NO_3S$; **MW:** 407.53 g/mol; **M.p**. 128–130ºC; **IR (ATR) ν (cm^{-1}):** 2921, 2851, 1347, 1161; **^{1}H NMR (400 MHz, $CDCl_3$) δ (ppm):** 2.06 (s, 3H), 2.19 (s, 3H), 2.42 (s, 3H), 3.84 (s, 3H), 4.62 (s, 4H), 6.91 (AA' part of AA'BB' system, $^3J_{H,H}$ = 8.8 Hz, 2H), 6.93 (s, 1H), 7.15 (AA' part of AA'BB' system, $^3J_{H,H}$ = 8.4 Hz, 2H), 7.33 (BB' part of AA'BB' system, $^3J_{H,H}$ = 8.8 Hz, 2H), 7.81 (BB' part of AA'BB' system, $^3J_{H,H}$ = 8.4 Hz, 2H); **^{13}C NMR (100 MHz, $CDCl_3$) δ (ppm):** 16.4, 18.2, 21.5, 53.5, 53.9, 55.3, 113.6, 127.3, 127.6, 129.5, 129.8, 130.3, 130.6, 133.3, 133.6, 133.8, 135.7, 141.5, 143.6, 158.6; **ESI-MS (*m/z*)**: 430.2 $[M+Na]^+$, 446.1 $[M+K]^+$, 837.2 $[2M+Na]^+$; **ESI-HRMS (*m/z*) calcd. for $[C_{24}H_{25}NO_3S+H]^+$:** 408.1628; **found:** 408.1643.

7.4.1.6. Synthesis of 5-(4-tert-butylphenyl)-4,7-dimethyl-2-tosylisoindoline, 66c

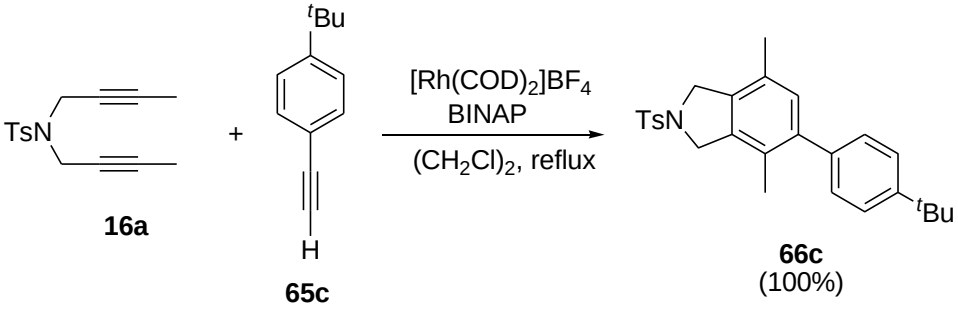

This compound was obtained using the general procedure described for **18aa** with the following specific conditions:

$[Rh(COD)_2]BF_4$: 2.75 mg (0.006 mmol)
BINAP: 4.23 mg (0.006 mmol)
Monoyne **65c**: 0.026 g (0.163 mmol)
Diyne **16a**: 0.030 g (0.109 mmol)
Dichloroethane: 2 mL
Reaction time: 5 hours
Purification: hexanes/dichloromethane (1:1)

After purification, 0.047 g (quantitative yield) of a colourless solid was obtained which was identified by spectroscopic data as 5-(4-tert-butylphenyl)-4,7-dimethyl-2-tosylisoindoline, **66c. Molecular formula**: $C_{27}H_{31}NO_2S$; **MW:** 433.61 g/mol; **M.p.** 203–205ºC; **IR (ATR) ν (cm^{-1}):** 2918, 1335, 1159; **^{1}H NMR (400 MHz, $CDCl_3$) δ (ppm):** 1.35 (s, 9H), 2.08 (s, 3H), 2.19 (s, 3H), 2.42 (s, 3H), 4.62 (s, 4H), 6.95 (s, 1H), 7.15 (AA' part of AA'BB' system, $^3J_{H,H}$ = 8.4 Hz, 2H), 7.33 (AA' part of AA'BB' system, $^3J_{H,H}$ = 8.4 Hz, 2H), 7.38 (BB' part of AA'BB' system, $^3J_{H,H}$ = 8.4 Hz, 2H), 7.81 (BB' part of AA'BB' system, $^3J_{H,H}$ = 8.4 Hz, 2H); **^{13}C NMR (100 MHz, $CDCl_3$) δ (ppm):** 16.4, 18.2, 21.5, 31.4, 34.5, 53.5, 53.9, 125.0, 127.3, 127.6, 128.8, 129.4, 129.8, 130.7, 133.7, 134.0, 135.7, 137.9, 141.8, 143.6, 149.8; **ESI-MS (*m/z*)**: 434.2 $[M+H]^+$, 456.1 $[M+Na]^+$, 472.1 $[M+K]^+$, 889.2 $[2M+Na]^+$; **Anal. Calc. for $C_{27}H_{31}NO_2S$·0.5(C_6H_{14}):** C 75.91, H 7.64, N 2.95; **found:** C 75.68, H 7.85, N 3.34.

7.4.1.7. Synthesis of 5-(4-fluorophenyl)-4,7-dimethyl-2-tosylisoindoline, 66d

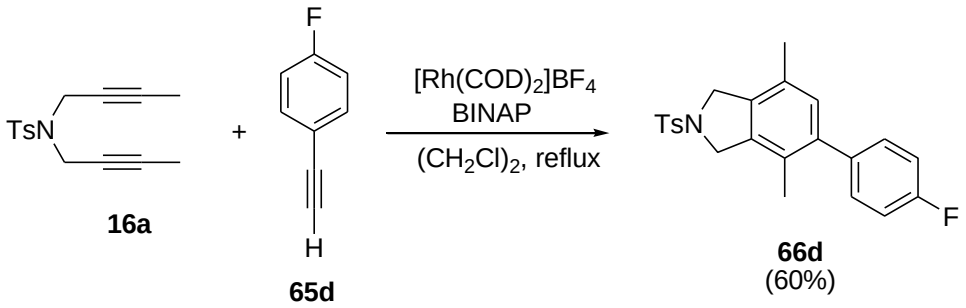

This compound was obtained using the general procedure described for **18aa** with the following specific conditions:

$[Rh(COD)_2]BF_4$]: 2.21 mg (0.005 mmol)
BINAP: 3.39 mg (0.005 mmol)
Monoyne **65d**: 0.018 g (0.163 mmol)
Diyne **16a**: 0.030 g (0.109 mmol)
Dichloroethane: 3 mL
Reaction time: 4 hours
Purification: hexanes/dichloromethane (6:4)

After purification, 0.026 g (60% yield) of a colourless solid was obtained which was identified by spectroscopic data as 5-(4-fluorophenyl)-4,7-dimethyl-2-tosylisoindoline, **66d**. **Molecular formula**: $C_{23}H_{22}FNO_2S$; **MW:** 395.49 g/mol; **M.p.** 138–140ºC; **IR (ATR) ν (cm^{-1}):** 2935, 1345, 1221, 1163; **^{1}H NMR (400 MHz, $CDCl_3$) δ (ppm):** 2.03 (s, 3H), 2.19 (s, 3H), 2.42 (s, 3H), 4.61 (s, 4H), 6.91 (s, 1H), 7.07 (dd, $^3J_{H,H}$ = 8.8 Hz, $^3J_{H,F}$ = 8.8 Hz, 2H), 7.18 (dd, $^3J_{H,H}$ = 8.8 Hz, $^4J_{H,F}$ =5.6 Hz, 2H), 7.33 (BB' part of AA'BB' system, $^3J_{H,H}$ = 8.0 Hz, 2H), 7.80 (BB' part of AA'BB' system, $^3J_{H,H}$ = 8.0 Hz, 2H); **^{13}C NMR (100 MHz, $CDCl_3$) δ (ppm):** 16.3, 18.2, 21.5, 53.4, 53.8, 115.0 (d, $^2J_{C,F}$ = 21.0 Hz), 127.2, 127.6, 129.6, 129.9, 130.5, 130.7 (d, $^3J_{C,F}$ = 6.7 Hz), 133.8, 134.1, 135.8, 136.8 (d, $^4J_{C,F}$ = 3.7 Hz), 140.8, 143.7, 161.9 (d, $^1J_{C,F}$ = 245 Hz); **ESI-MS (*m/z*)**: 418.2 $[M+Na]^+$, 434.1

$[M+K]^+$, 813.1 $[2M+Na]^+$; **ESI-HRMS (*m/z*) calcd. for $[C_{23}H_{22}FNO_2S + H]^+$:** 396.1428; **found:** 396.1429.

7.4.1.8. Synthesis of 5-(4-bromophenyl)-4,7-dimethyl-2-tosylisoindoline, 66e

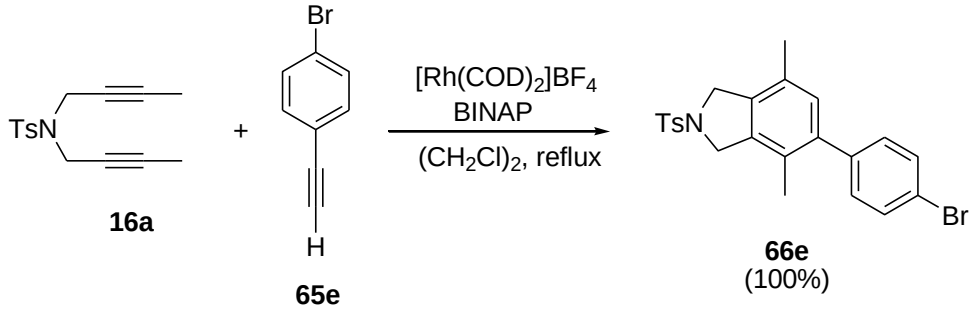

This compound was obtained using the general procedure described for **18aa** with the following specific conditions:

$[Rh(COD)_2]BF_4$]: 2.75 mg (0.006 mmol)
BINAP: 4.23 mg (0.006 mmol)
Monoyne **65e**: 0.030 g (0.163 mmol)
Diyne **16a**: 0.030 g (0.109 mmol)
Dichloroethane: 2 mL
Reaction time: 5 hours
Purification: hexanes/dichloromethane (1:1)

After purification, 0.050 g (quantitative yield) of a colourless solid was obtained which was identified by spectroscopic data as 5-(4-bromophenyl)-4,7-dimethyl-2-tosylisoindoline*,* **66e. Molecular formula**: $C_{23}H_{22}NO_2SBr$; **MW:** 456.40 g/mol; **M.p.** 61–63ºC; **IR (ATR) ν (cm^{-1}):** 2920, 1340, 1158 2.03 (s, 3 H), 2.19 (s, 3H), **^{1}H NMR (300 MHz, $CDCl_3$) δ (ppm):** 2.42 (s, 3H), 4.61 (s, 4H), 6.90 (s, 1H), 7.09 (AA' part of AA'BB' system, $^3J_{H,H}$ = 8.5 Hz, 2H), 7.33 (AA' part of AA'BB' system, $^3J_{H,H}$ = 8.5 Hz, 2H), 7.51 (BB' part of AA'BB' system, $^3J_{H,H}$ = 8.4 Hz, 2H), 7.81 (BB' part of AA'BB' system $^3J_{H,H}$ = 8.4 Hz, 2H); **^{13}C NMR (75 MHz, $CDCl_3$) δ (ppm):** 16.6, 18.5, 21.8, 53.8, 54.2, 121.5, 127.4, 127.9, 130.1, 130.2, 130.7, 131.2, 131.6, 134.3, 134.7, 136.3, 140.2, 140.9, 144.0; **ESI-MS (*m/z*)**: 456–458 $[M+H]^+$, 478–480 $[M+Na]^+$, 494–496 $[M+K]^+$, 935 $[2M+Na]^+$; **Anal. Calcd. for $[C_{23}H_{22}NO_2SBr]$:** C 64.68, H 5.99, N 2.60; **found**: C 63.92, H 6.26, N 2.68.

7.4.1.9. Synthesis of 4,7-dimethyl-5-(4-nitrophenyl)-2-tosylisoindoline, 66f

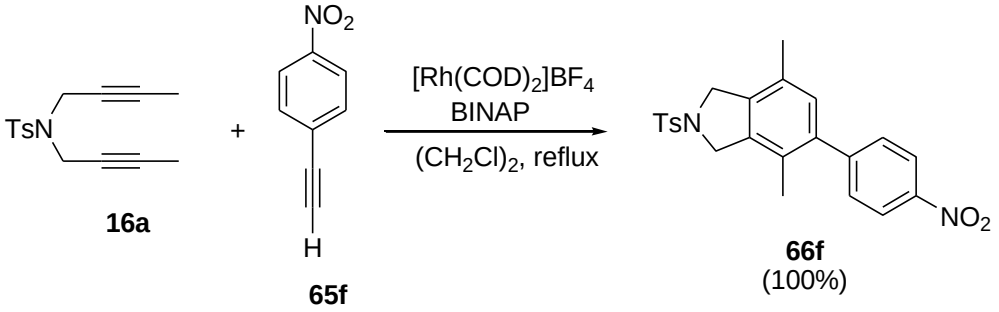

16a **65f** **66f** (100%)

This compound was obtained using the general procedure described for **18aa** with the following specific conditions:

$[Rh(COD)_2]BF_4$: 2.21 mg (0.005 mmol)
BINAP: 3.39 mg (0.005 mmol)
Monoyne **65f**: 0.024 g (0.163 mmol)
Diyne **16a**: 0.030 g (0.109 mmol)
Dichloroethane: 3 mL
Reaction time: 4 hours
Purification: hexanes/dichloromethane (6:4)

After purification, 0.048 g (quantitative yield) of a yellow solid was obtained which was identified by spectroscopic data as 4,7-dimethyl-5-(4-nitrophenyl)-2-tosylisoindoline*,* **66f. Molecular formula**: $C_{23}H_{22}N_2O_4S$; **MW**: 422.50 g/mol; **M.p.** 196-198ºC; **IR (ATR) ν (cm^{-1}):** 2920, 1510, 1343, 1160; **^{1}H NMR (300 MHz, $CDCl_3$) δ (ppm):** 2.06 (s, 3H), 2.22 (s, 3H), 2.43 (s, 3H), 4.63 (s, 4H), 6.93 (s, 1H), 7.36 (AA' part of AA'BB' system, $^3J_{H,H}$ = 8.4 Hz, 2H), 7.41 (AA' part of AA'BB' system,$^3J_{H,H}$ = 6.9 Hz, 2H), 7.81 (BB' part of AA'BB' system, $^3J_{H,H}$ = 8.1 Hz, 2H), 8.26 (BB' part of AA'BB' system, $^3J_{H,H}$ = 6.9 Hz, 2H); **^{13}C NMR (75 MHz, $CDCl_3$) δ (ppm):** 16.4, 18.3, 21.6, 53.5, 53.8, 123.5, 127.1, 127.6, 127.7, 127.7, 127.7, 127.7, 130.0, 130.2, 130.2, 130.2, 133.8, 135.3, 135.4, 136.3, 139.6, 143.9, 147.0, 148.0; **ESI-MS (*m/z*)**: 445.2 $[M+Na]^+$, 461.3 $[M+K]^+$.

7.4.1.10. Synthesis of N,N-dimethyl-4-(4,7-dimethyl-2-tosylisoindolin-5-yl)benzenamine, 66g

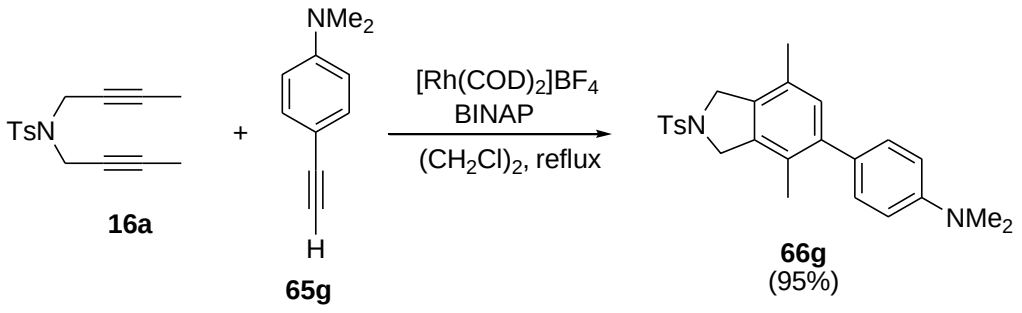

16a **65g** **66g** (95%)

This compound was obtained using the general procedure described for **18aa** with the following specific conditions:

$[Rh(COD)_2]BF_4$]: 2.21 mg (0.005 mmol)
BINAP: 3.39 mg (0.005 mmol)
Monoyne **65g**: 0.024 g (0.163 mmol)
Diyne **16a**: 0.030 g (0.109 mmol)
Dichloroethane: 3 mL
Reaction time: 4.5 hours
Purification: hexanes/dichloromethane (1:1)

After purification, 0.043 g (95% yield) of a colourless solid was obtained which was identified by spectroscopic data as N,N-dimethyl-4-(4,7-dimethyl-2-tosylisoindolin-5-yl)benzenamine, **66g. Molecular formula**: $C_{25}H_{28}N_2O_2S$; **MW**: 420.57 g/mol; **M.p.** 181-183ºC; **IR (ATR) ν (cm^{-1}):** 2843, 1346, 1165; **^{1}H NMR (400 MHz, $CDCl_3$) δ (ppm):** 2.09 (s, 3H), 2.18 (s, 3H), 2.42 (s, 3H), 2.98 (s, 6H), 4.61 (s, 4H), 6.75 (AA' part of AA'BB' system, $^3J_{H,H}$ = 8.0 Hz, 2H), 6.94 (s, 1H), 7.11 (BB' part of AA'BB' system, $^3J_{H,H}$ = 9.6 Hz, 2H), 7.33 (AA' part of AA'BB' system, $^3J_{H,H}$ = 8.0 Hz, 2H), 7.80 (BB' part of AA'BB' system, $^3J_{H,H}$ = 8.4 Hz, 2H); **^{13}C NMR (75 MHz, $CDCl_3$) δ (ppm):** 16.5, 18.3, 21.5, 53.5, 54.0, 127.3, 127.6, 129.4, 129.8, 130.0, 130.7, 133.1, 133.8, 135.7, 143.6; **ESI-MS (*m/z*)**: 421.4 $[M+H]^+$, 443.3 $[M+Na]^+$, 459.2 $[M+K]^+$, 863.2 $[2M+Na]^+$; **Anal. Calcd. for [$C_{25}H_{28}N_2O_2S$]:** C 71.40, H 6.71, N 6.66; **found**: C 71.06, H 6.98, N 6.76.

7.4.1.11. Synthesis of 4-(4,7-dimethyl-2-tosylisoindolin-5-yl)benzonitrile, **66h**

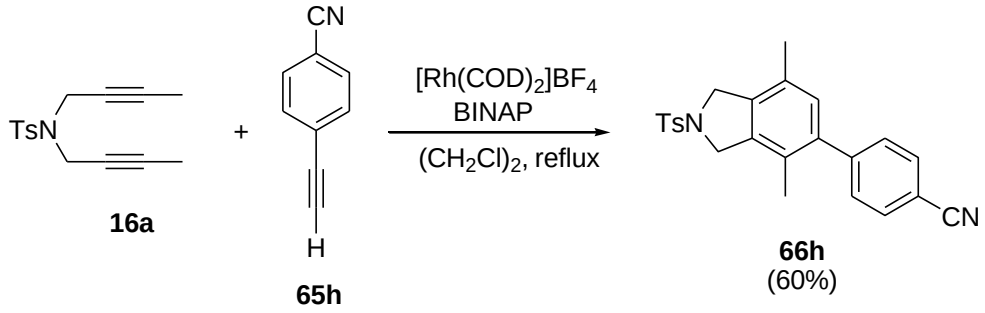

This compound was obtained using the general procedure described for **66a** with the following specific conditions:
$[Rh(COD)_2]BF_4$]: 2.75 mg (0.005 mmol)
BINAP: 4.23 mg (0.005 mmol)
Monoyne **65h**: 0.024 g (0.163 mmol)
Diyne **16a**: 0.030 g (0.109 mmol)
Dichloroethane: 2 mL
Reaction time: 5 hours
Purification: dichloromethane

After purification, 0.026 g (60% yield) of a colourless solid was obtained which was identified by spectroscopic data as 4-(4,7-dimethyl-2-tosylisoindolin-5-yl)benzonitrile, **66h. Molecular**

formula: $C_{24}H_{22}N_2O_2S$; **MW**: 402.51 g/mol; **IR (ATR) ν (cm^{-1}):** 2327, 2155, 1982, 1163; **^{1}H NMR (400 MHz, $CDCl_3$) δ (ppm):** 2.04 (s, 3H), 2.20 (s, 3H), 2.42 (s, 3H), 4.62 (s, 4H), 6.90 (s, 1H), 7.32-7.36 (m, 4H), 7.68 (BB' part of AA'BB' system, $^3J_{H,H}$ = 8.4 Hz, 2H), 7.81 (BB' part of AA'BB' system, $^3J_{H,H}$ = 8.4 Hz, 2H); **^{13}C NMR (100 MHz, $CDCl_3$) δ (ppm):** 16.3, 18.2, 21.5, 53.4, 53.8, 111.0, 118.8, 127.0, 127.6, 129.9, 130.0, 130.2, 132.0, 134.0, 135.1, 136.2, 140.0, 143.7, 145.9; **ESI-MS (*m/z*)**: 403.1 $[M+H]^+$, 425.1 $[M+Na]^+$, 441.0 $[M+K]^+$, 827.0 $[2M+Na]^+$.

7.4.1.12. Synthesis of diethyl 5-p-tolyl-1H-indene-2,2(3H)-dicarboxylate, **66i**

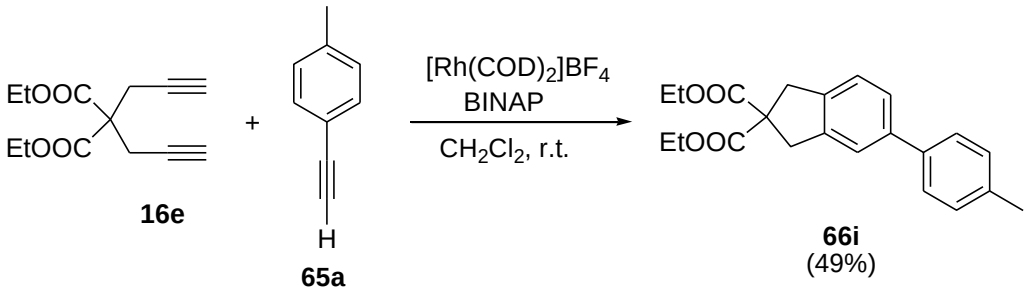

This compound was obtained using the general procedure described for **18aa** with the following specific conditions:

$[Rh(COD)_2]BF_4$]: 2.58 mg (0.006 mmol)
BINAP: 3.95 mg (0.006 mmol)
Monoyne **65a**: 0.024 mL (0.191 mmol)
Diyne **16e**: 0.030 g (0.127 mmol)
Dichloroethane: 3 mL
Reaction time: 2 hours
Purification: hexanes/dichloromethane (3:7)

After purification, 0.022 g (49% yield) of a colourless solid was obtained which was identified by spectroscopic data as diethyl 5-*p*-tolyl-1*H*-indene-2,2(3*H*)-dicarboxylate, **66i. Molecular formula**: $C_{22}H_{24}O_4$; **MW**: 352.42 g/mol; **M.p**. 72–74ºC; **IR (ATR) ν (cm^{-1}):** 2922, 1729, 1241, 1185, 1067; **^{1}H NMR (300 MHz, $CDCl_3$) δ (ppm):** 1.26 (t, $^3J_{H,H}$ = 7.2 Hz, 6H), 2.38 (s, 3H), 3.61-3.63 (m, 4H), 4.21 (q, $^3J_{H,H}$ = 7.2 Hz, 4H), 7.20–7.25 (m, 3H), 7.37 (AA' part of AA'BB' system, $^3J_{H,H}$ = 8.1 Hz, 2H), 7.44 (BB' part of AA'BB' system, $^3J_{H,H}$ = 8.1 Hz, 2H); **^{13}C NMR (100 MHz, $CDCl_3$) δ (ppm):** 14.4, 21.4, 60.8, 62.1, 123.1, 124.7, 126.3, 127.3, 129.7, 137.1, 138.7, 139.2, 140.6, 141.0, 172.0; **ESI-MS (*m/z*)**: 353.2 $[M+H]^+$, 375.2 $[M+Na]^+$, 727.3 $[2M+Na]^+$; **Anal. Calcd. for $C_{22}H_{24}O_4 \cdot 0.5(C_6H_{14})$:** C 75.73, H 8.13; **found**: C 75.66, H 7.89.

7.4.1.13. Synthesis of diethyl diethyl 5-phenyl-1H-indene-2,2(3H)-dicarboxylate, **18ea**

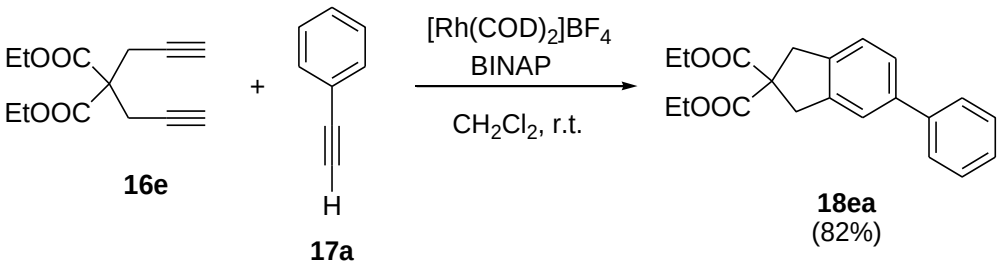

This compound was obtained using the general procedure described for **18aa** with the following specific conditions:

$[Rh(COD)_2]BF_4$: 2.58 mg (0.006 mmol)
BINAP: 3.95 mg (0.006 mmol)
Monoyne **17a**: 0.024 mL (0.191 mmol)
Diyne **16e**: 0.030 g (0.127 mmol)
Dichloromethane: 3 mL
Reaction time: 2 hours
Purification: hexanes/dichloromethane (7:3)

After purification, 0.038 g (82% yield) of a yellow oil was obtained which was identified by spectroscopic data as *diethyl* 5-phenyl-1*H*-indene-2,2(3*H*)-dicarboxylate, **18ea**.[115] **Molecular formula**: $C_{21}H_{22}O_4$; **MW**: 338.40 g/mol; **^{1}H NMR (400 MHz, $CDCl_3$) δ (ppm):** 1.26 (t, $^3J_{H,H}$ = 7.2 Hz, 6H), 3.61-3.64 (m, 4H), 4.21 (q, $^3J_{H,H}$ = 7.2 Hz, 4H), 7.27 (m, 1H), 7.35 (m, 1H), 7.40 (m, 4H), 7.53 (BB' part of AA'BB' system, $^3J_{H,H}$ = 8.4 Hz, 2H); **ESI-MS (*m/z*)**: 339.2 $[M+H]^+$, 361.1 $[M+Na]^+$, 699.0 $[2M+Na]^+$.

7.4.1.14. Synthesis of diethyl 4,7-dimethyl-5-p-tolyl-1H-indene-2,2(3H)-dicarboxylate, **66j**

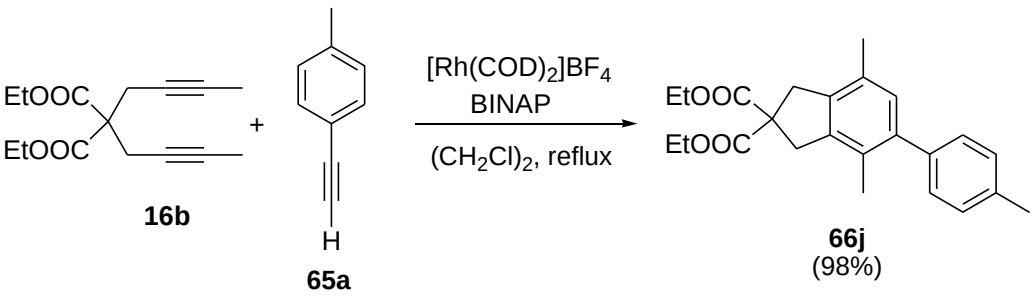

[115] Yoshida, K.; Morimoto, I.; Mitsudo, K.; Tanaka, H. *Tetrahedron* **2008**, *64*, 5800.

This compound was obtained using the general procedure described for **18aa** with the following specific conditions:

$[Rh(COD)_2]BF_4$]: 5 mg (0.012 mmol)
BINAP: 7 mg (0.013 mmol)
Monoyne **65a**: 0.027 mL (0.214 mmol)
Diyne **16b**: 0.038 g (0.143 mmol)
Dichloroethane: 2 mL
Reaction time: 1.5 hours
Purification: hexanes/ethyl acetate (9:1)

After purification, 0.053 g (98% yield) of a colourless solid was obtained which was identified by spectroscopic data as diethyl 4,7-dimethyl-5-p-tolyl-1H-indene-2,2(3H)-dicarboxylate, **66j**. **Molecular formula**: $C_{24}H_{28}O_4$; **MW**: 380.48 g/mol; **IR (ATR) ν (cm^{-1}):** 2921, 1729, 1248, 1080; **^{1}H NMR (300 MHz, $CDCl_3$) δ (ppm):** 1.28 (t, $^3J_{H,H}$ = 7.2 Hz, 6H), 2.13 (s, 3H), 2.24 (s, 3H), 2.38 (s, 3H), 3.57-3.59 (m, 4H), 4.23 (q, $^3J_{H,H}$ = 7.2 Hz, 4H), 6.89 (s, 1H), 7.18 (m, 4H); **^{13}C NMR (100 MHz, $CDCl_3$) δ (ppm):** 14.4, 17.0, 19.0, 21.5, 39.9, 40.5, 59.9, 62.1, 128.6, 129.0, 129.6, 130.3, 130.8, 136.5, 137.8, 139.3, 139.7, 141.2, 172.3; **ESI-MS (*m/z*)**: 381.2 $[M+H]^+$, 403.2 $[M+Na]^+$, 783.4 $[2M+Na]^+$.

This doctoral thesis has been undertaken in the Chemistry Department (Organic Chemistry area) of the Universitat de Girona and has been made possible thanks to a predoctoral fellowship (FI) from the Generalitat de Catalunya and the financial support of the Spanish Ministry of Economy and Competitiveness (Project No.: CTQ2011-23121/BQU) and the previous Ministry of Science and Innovation (Project No.: CTQ2008-05409) and the Department for Innovation, Universities and Enterprise (DIUE) of the Generalitat de Catalunya (Project No.: 2009SGR637).

Supplementary Data

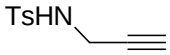

^{1}H RMN (400 MHz, $CDCl_3$)

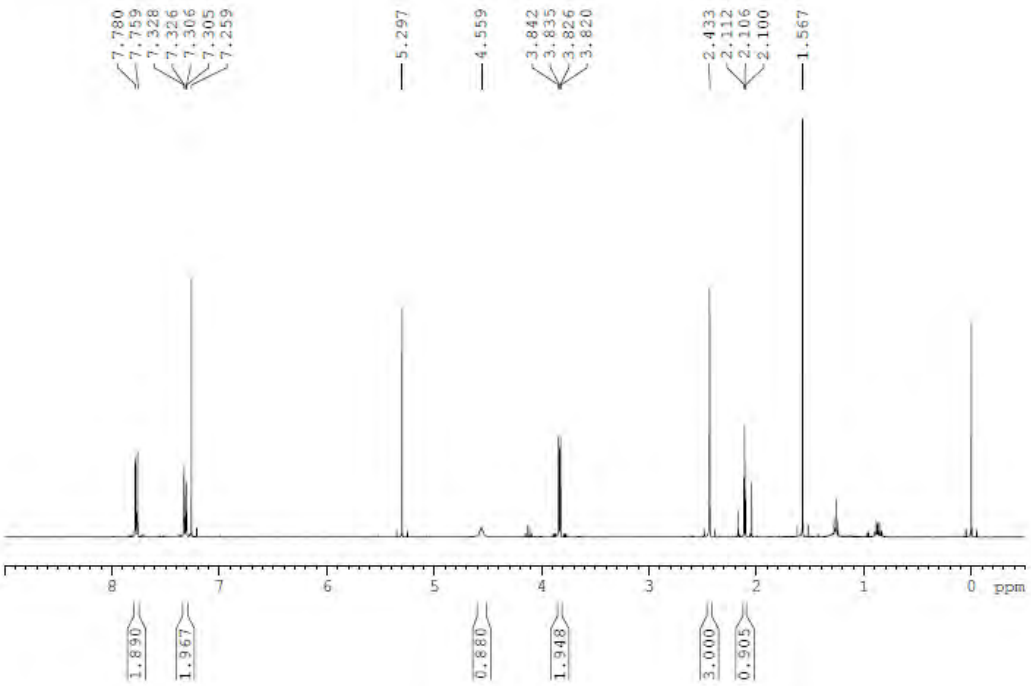

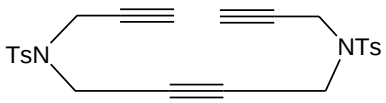

^{1}H RMN (400 MHz, $CDCl_3$)

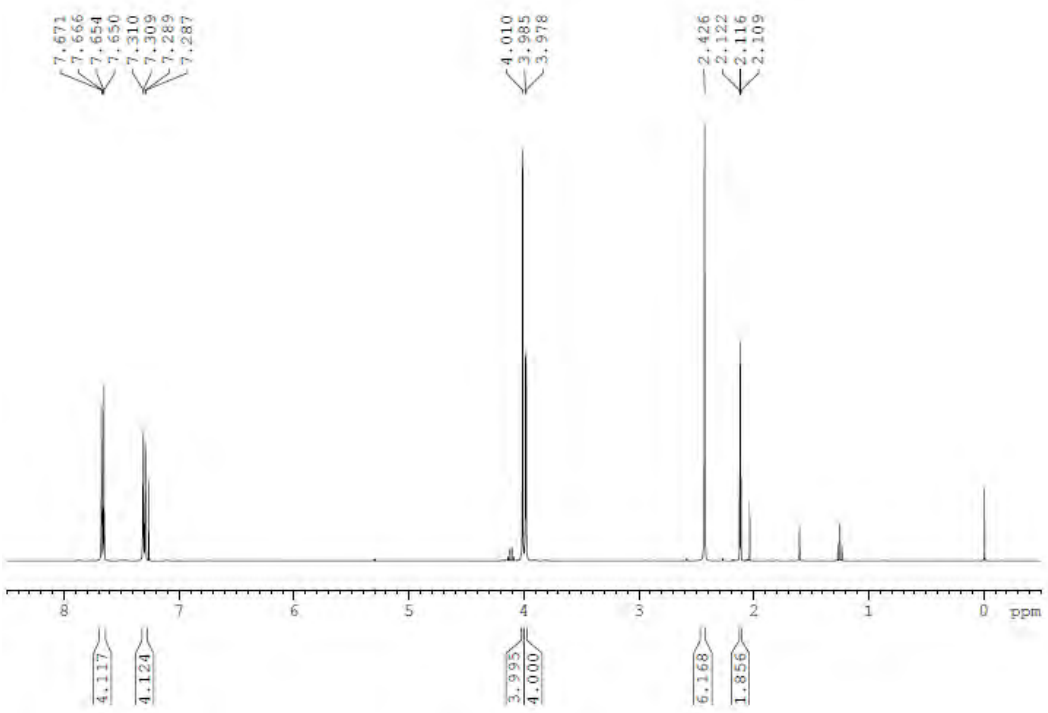

^{13}C RMN (100 MHz, $CDCl_3$)

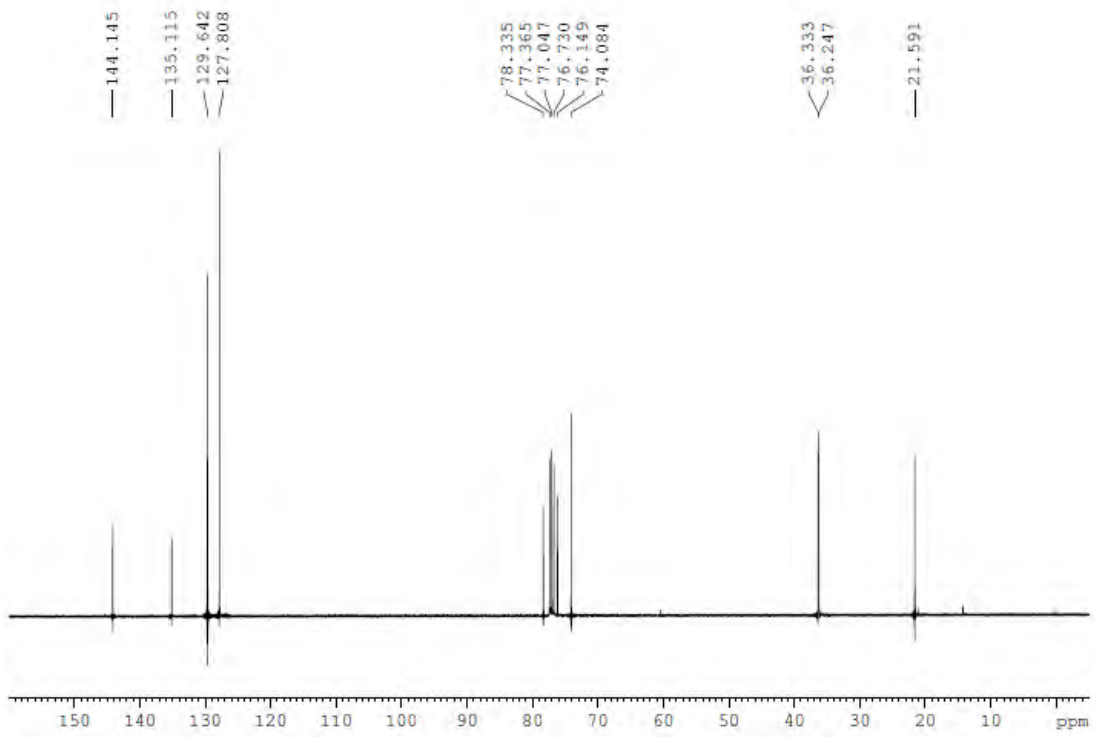

IR (ATR)

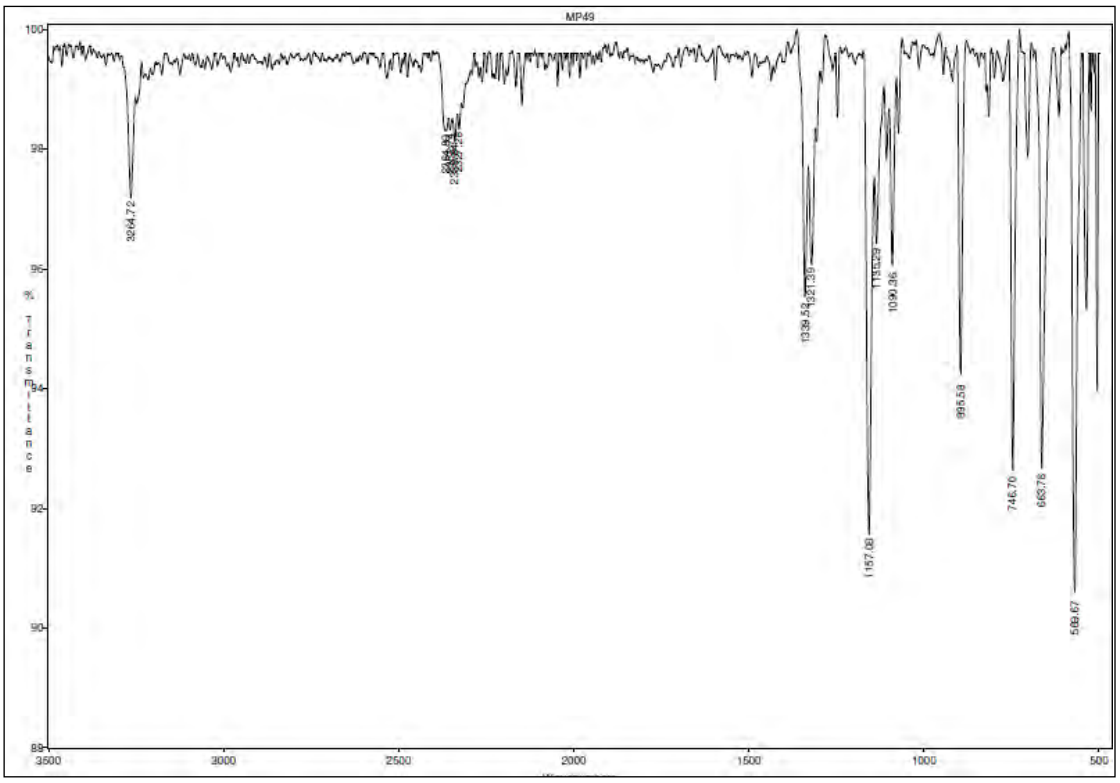

ESI-MS(+)

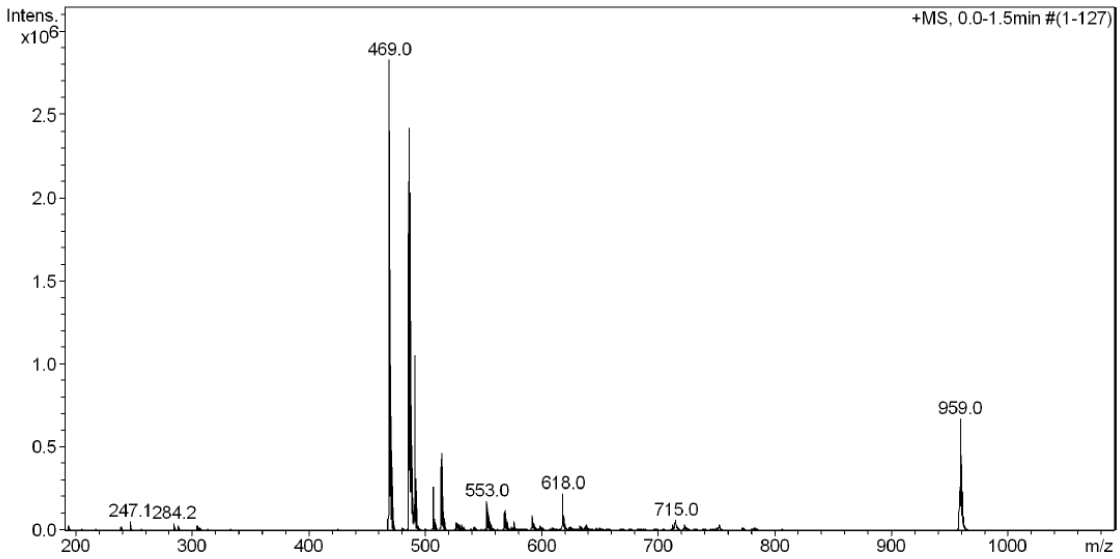

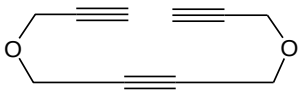

^{1}H RMN (400 MHz, $CDCl_3$)

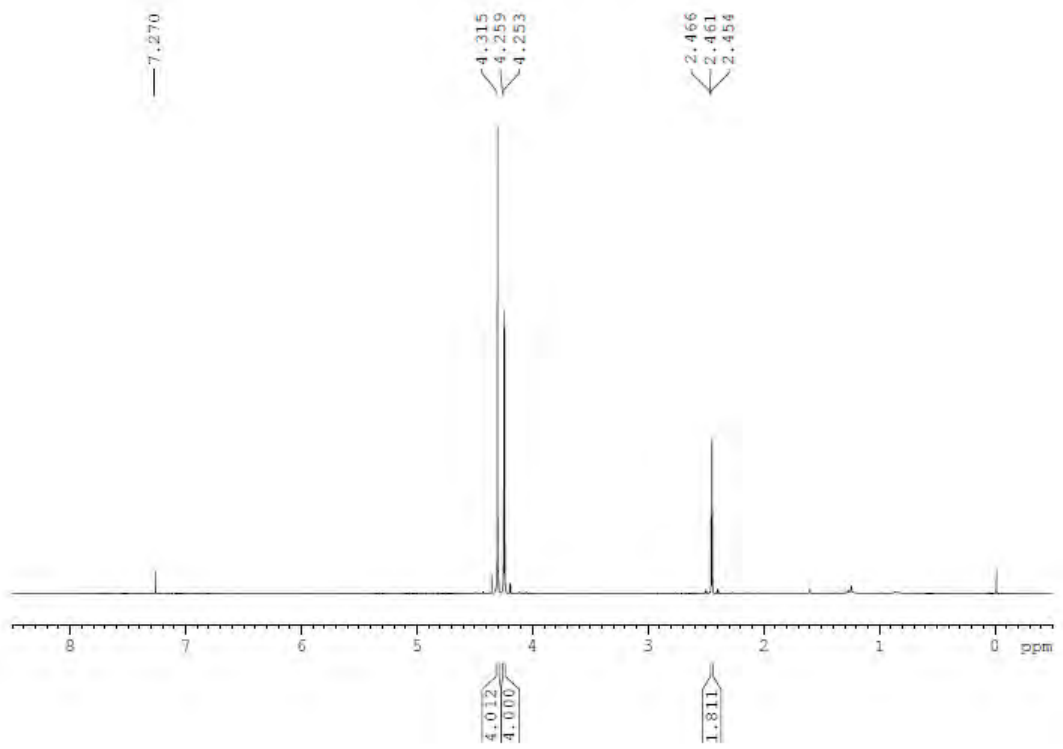

^{13}C RMN (100 MHz, $CDCl_3$)

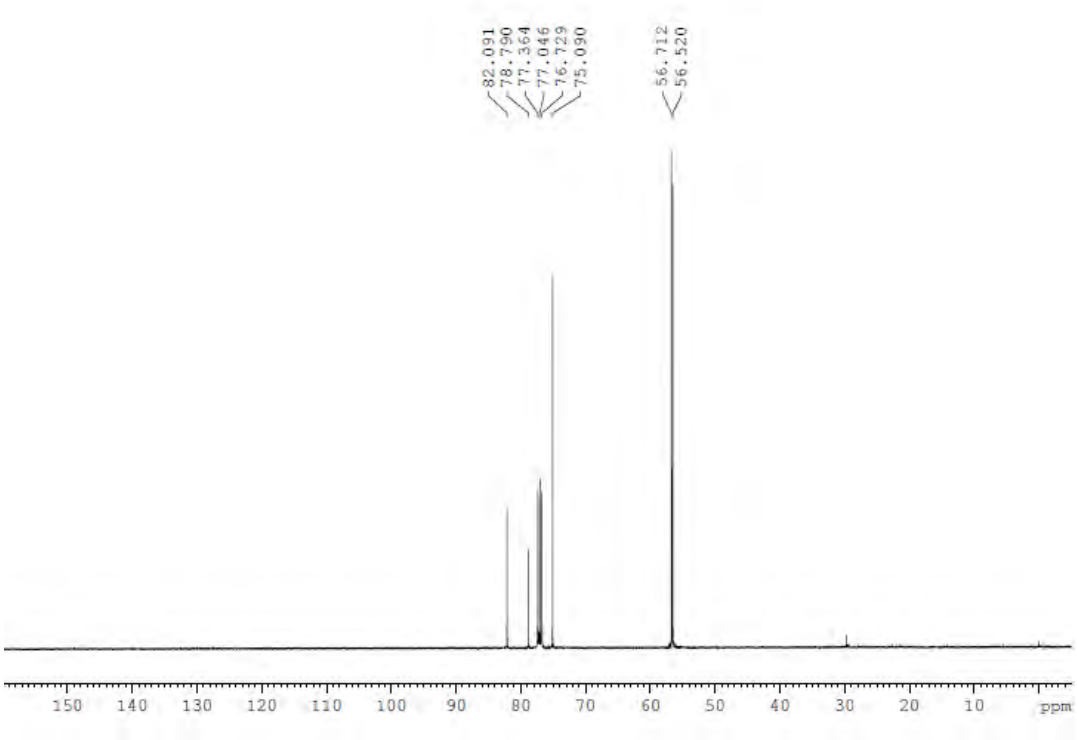

IR (ATR)

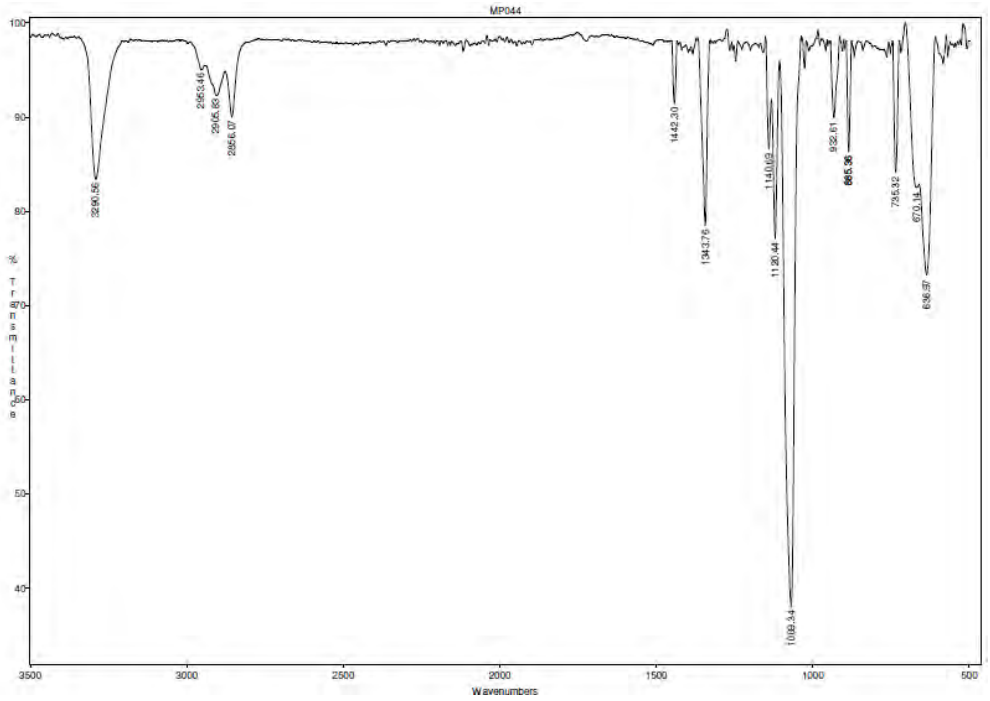

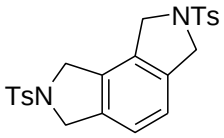

^{1}H RMN (400 MHz, $CDCl_3$)

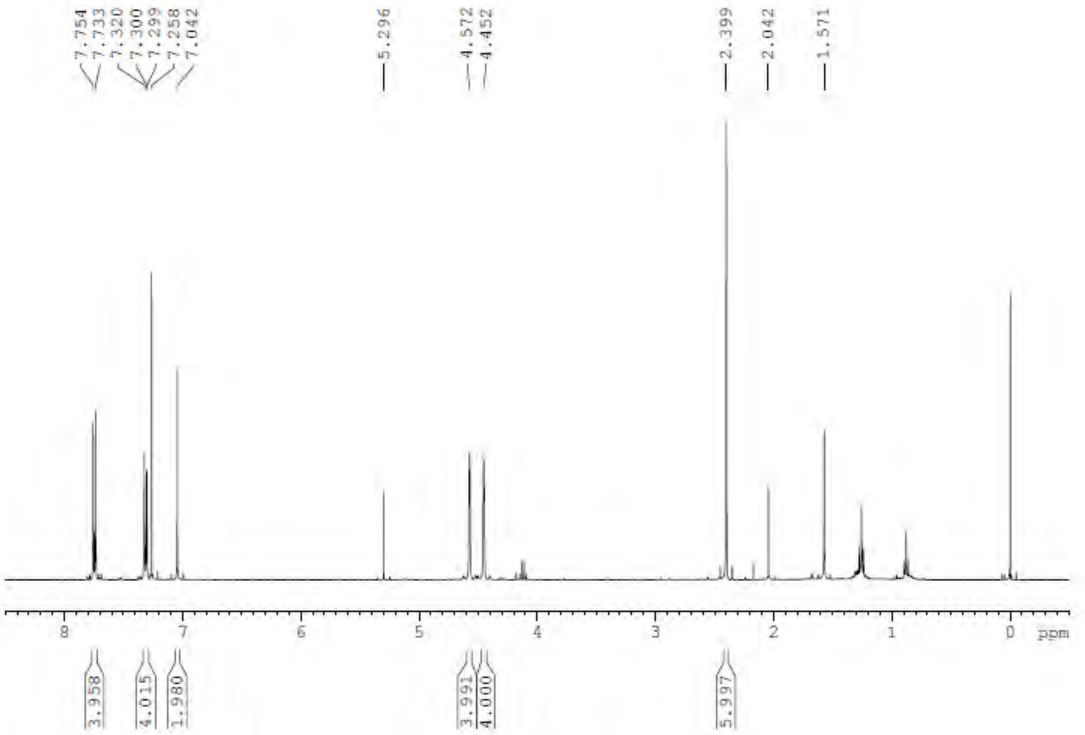

^{13}C RMN (100 MHz, $CDCl_3$)

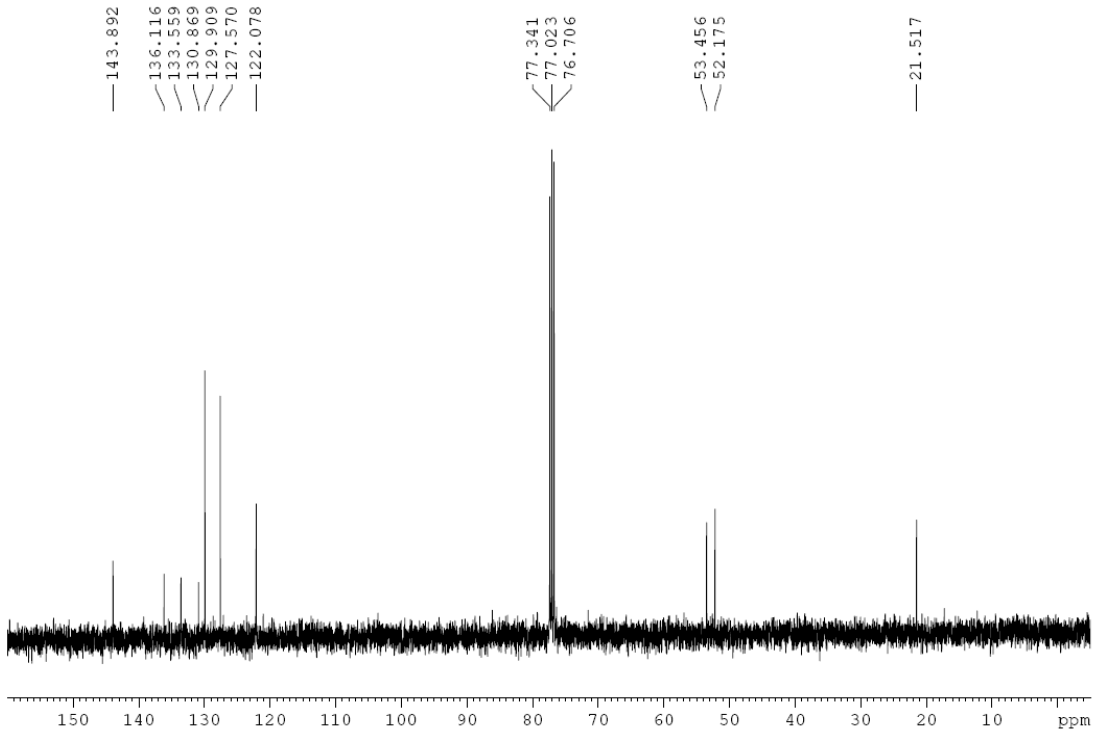

IR (ATR)

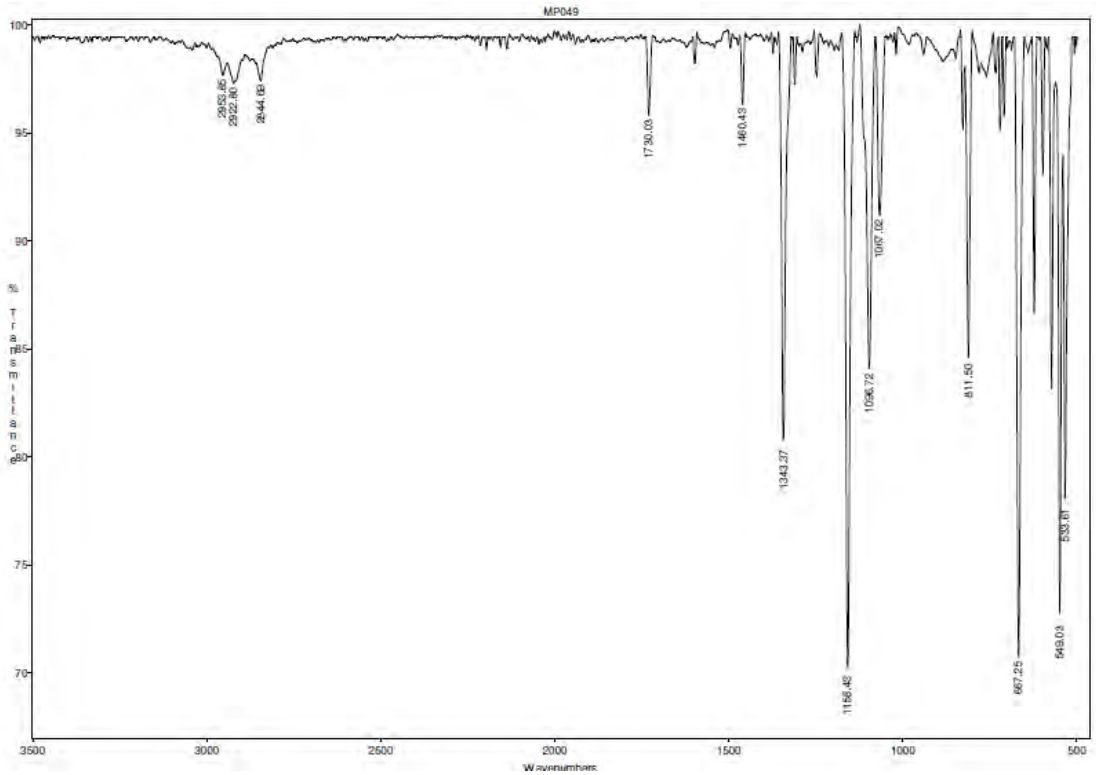
MP049
100
95
90
85
80
75
70
%
Transmittance
2955.85
2922.80
2844.09
1730.03
1460.43
1343.37
1158.48
1096.72
1067.02
811.50
667.25
649.03
533.81
3500
3000
2500
2000
1500
1000
500
Wavenumbers

ESI-MS(+)

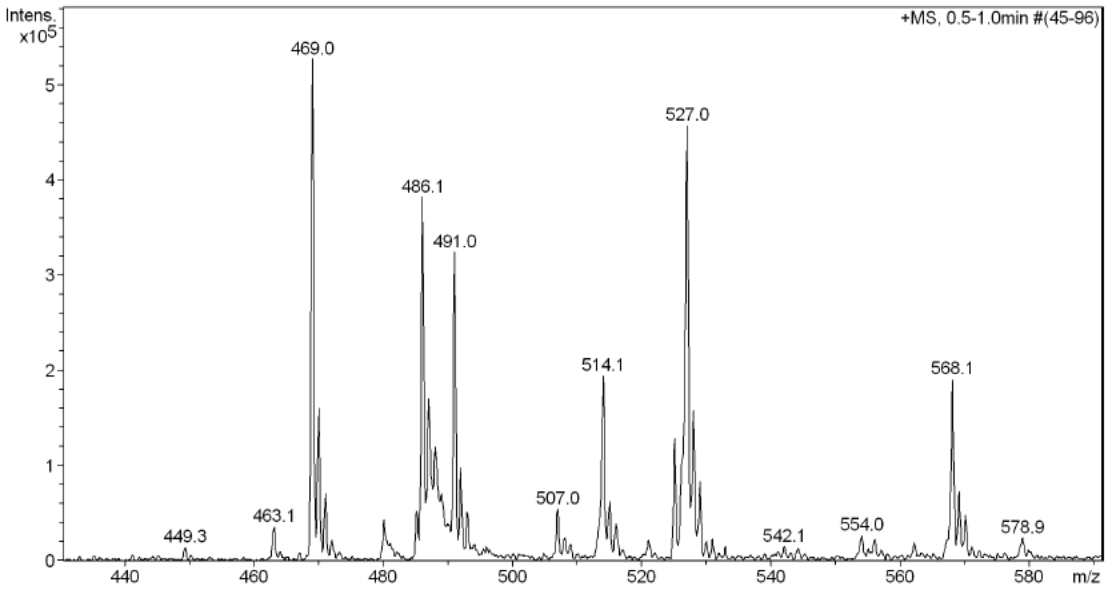
Intens.
x10^5
+MS, 0.5-1.0min #(45-96)
469.0
527.0
486.1
491.0
514.1
568.1
507.0
463.1
449.3
542.1
554.0
578.9
0
1
2
3
4
5
440
460
480
500
520
540
560
580
m/z

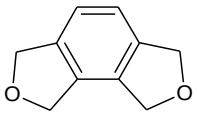

^{1}H RMN (400 MHz, $CDCl_3$)

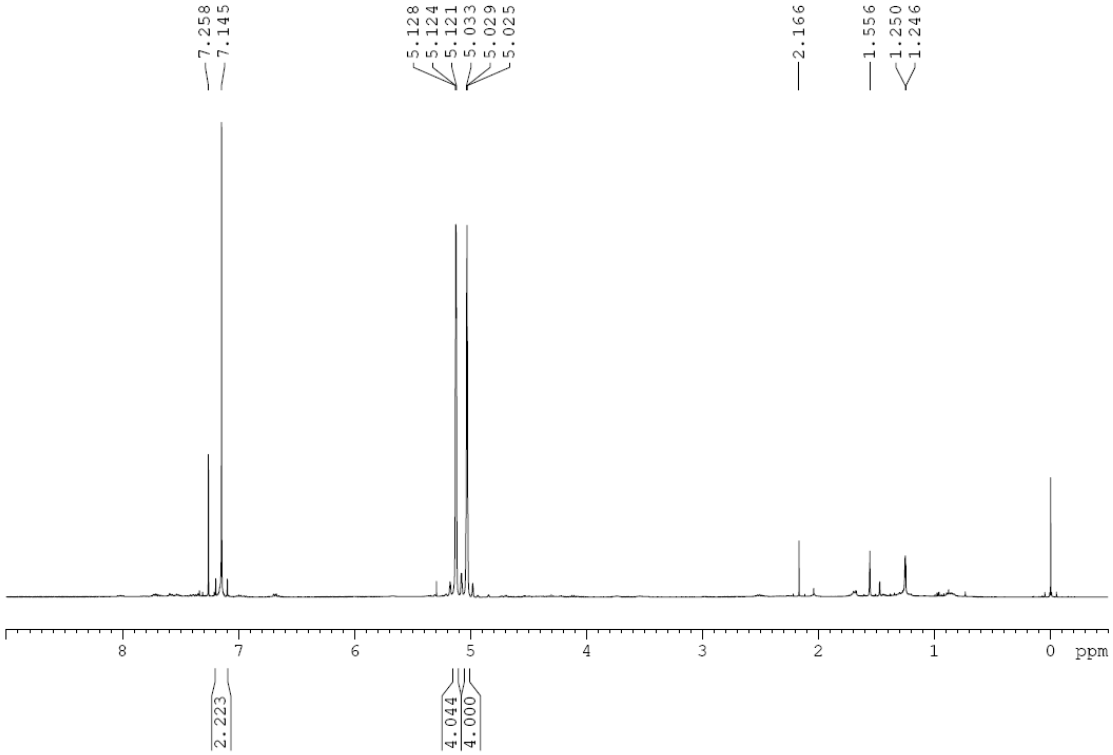

^{13}C RMN (100 MHz, $CDCl_3$)

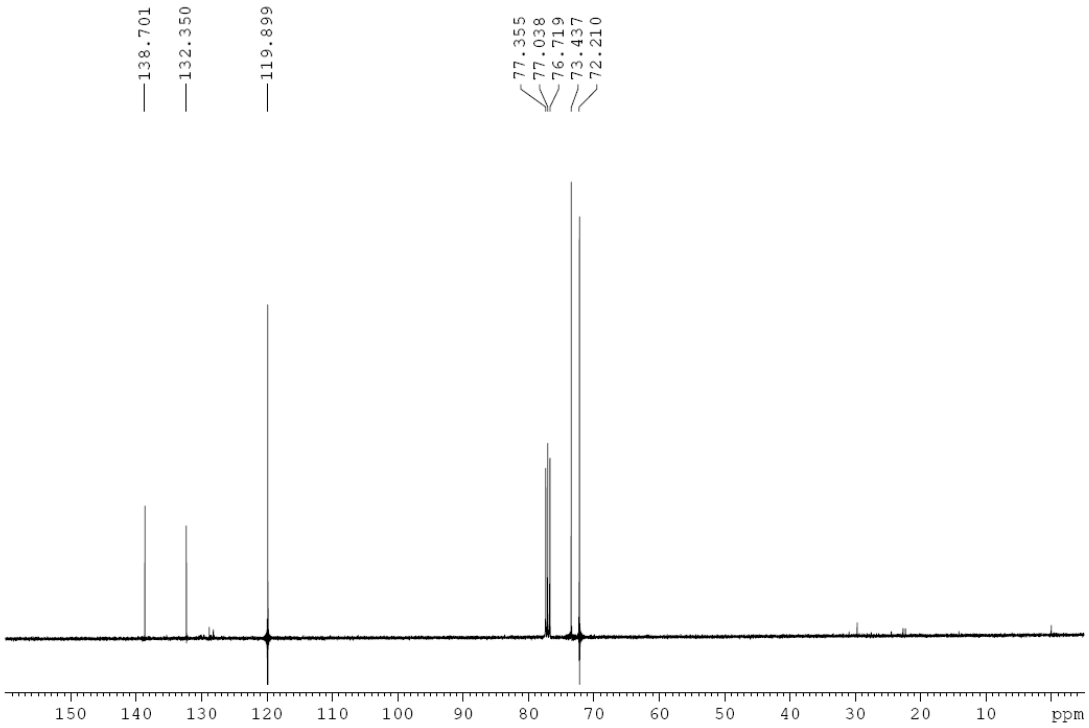

IR (ATR)

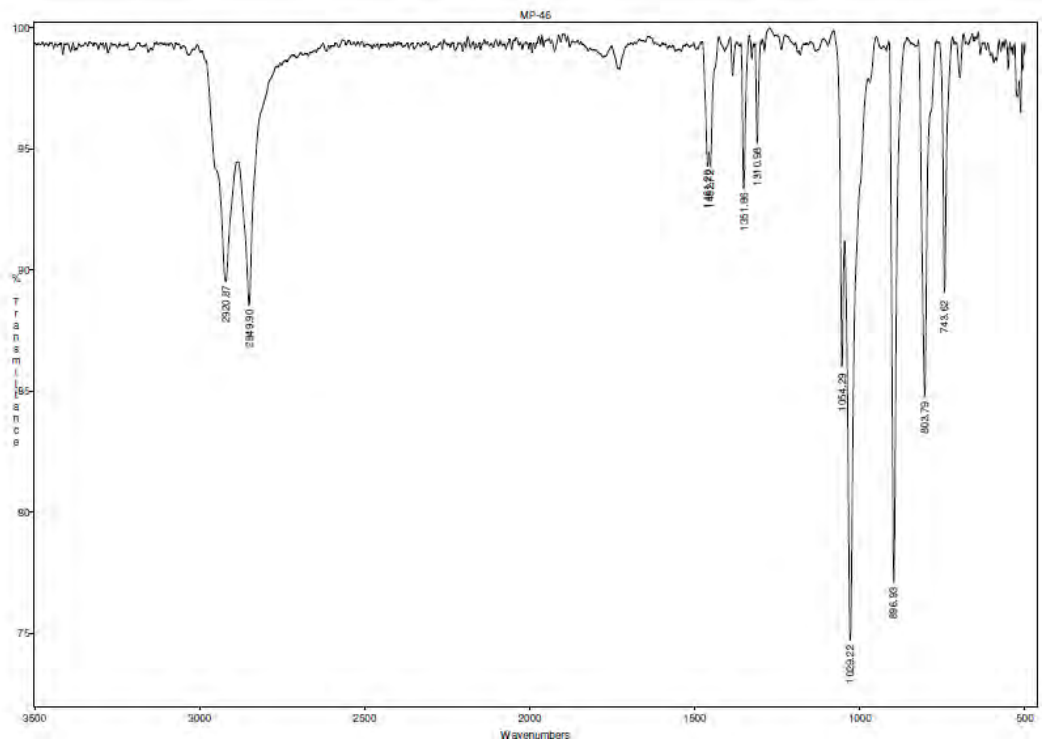
MP-46
100
95
90
85
80
75
% Transmittance
2920.87
2849.30
1464.79
1351.98
1310.98
1054.29
1003.22
896.99
803.79
743.62
3500
3000
2500
2000
1500
1000
500
Wavenumbers

ESI-MS(+)

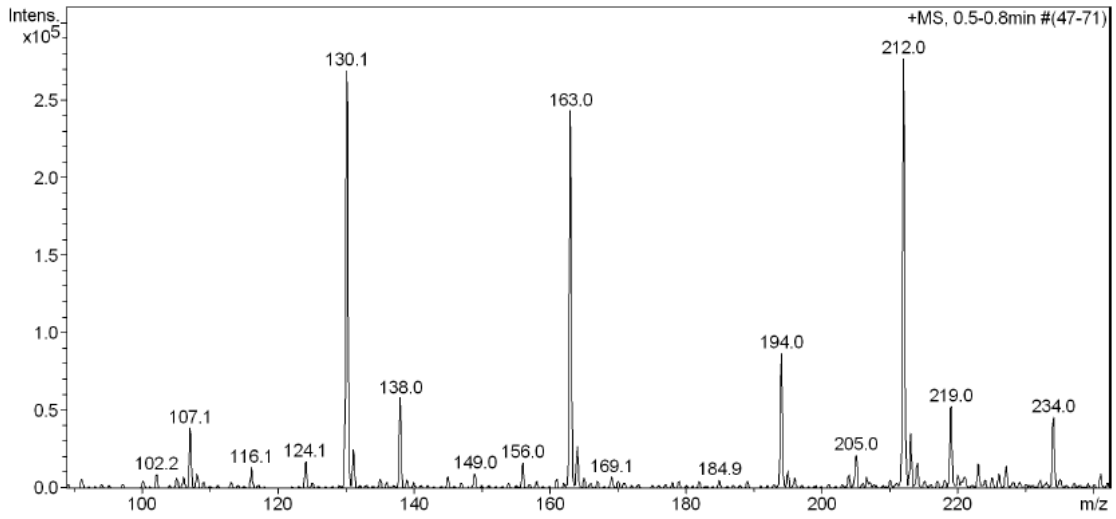
Intens.
x10^5
+MS, 0.5-0.8min #(47-71)
2.5
2.0
1.5
1.0
0.5
0.0
130.1
212.0
163.0
194.0
138.0
219.0
234.0
107.1
205.0
102.2
116.1
124.1
149.0
156.0
169.1
184.9
100
120
140
160
180
200
220
m/z

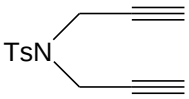

^{1}H RMN (400 MHz, $CDCl_3$)

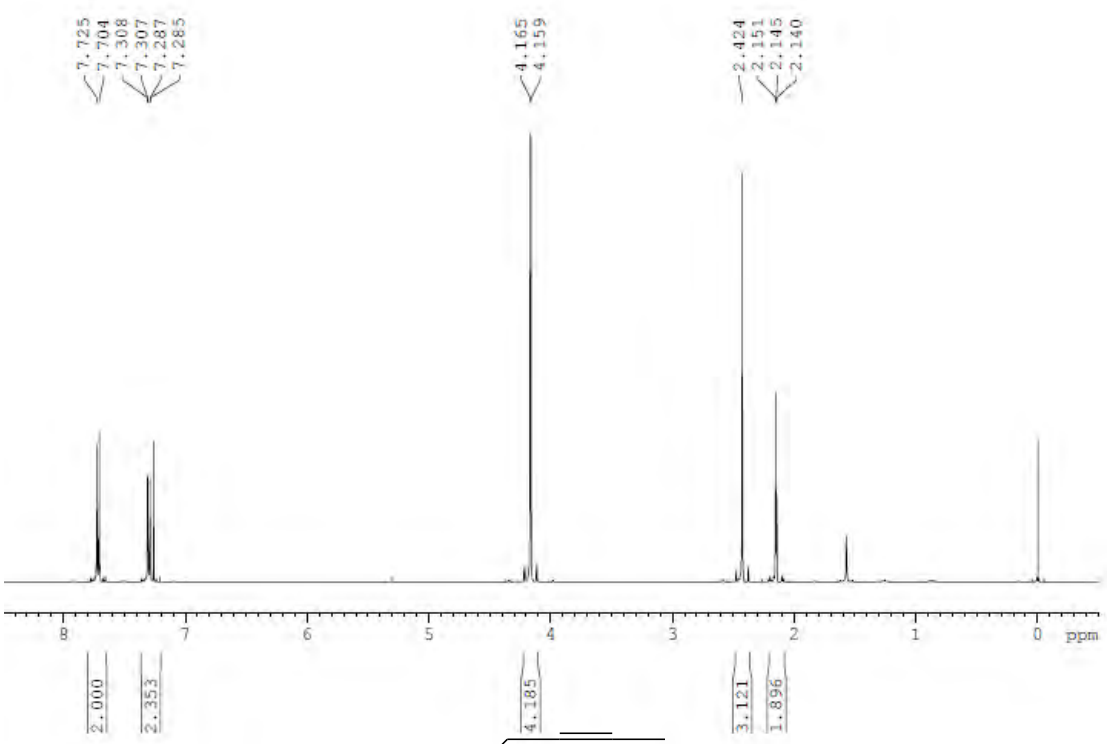

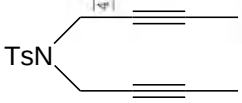

^{1}H RMN (400 MHz, $CDCl_3$)

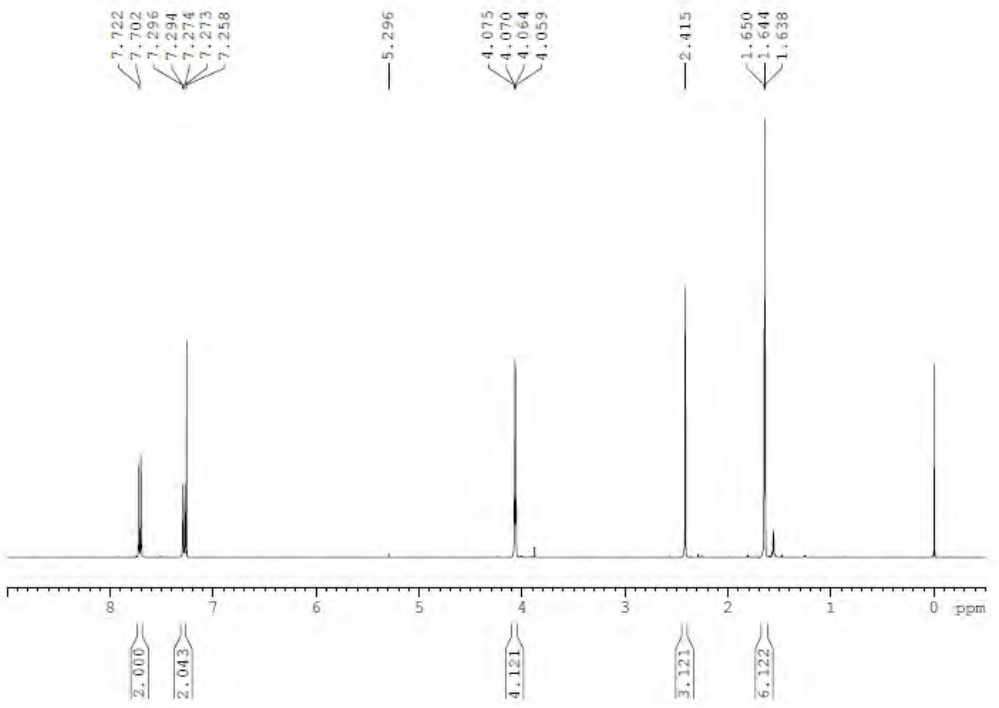

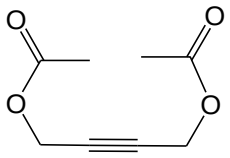

^{1}H RMN (400 MHz, $CDCl_3$)

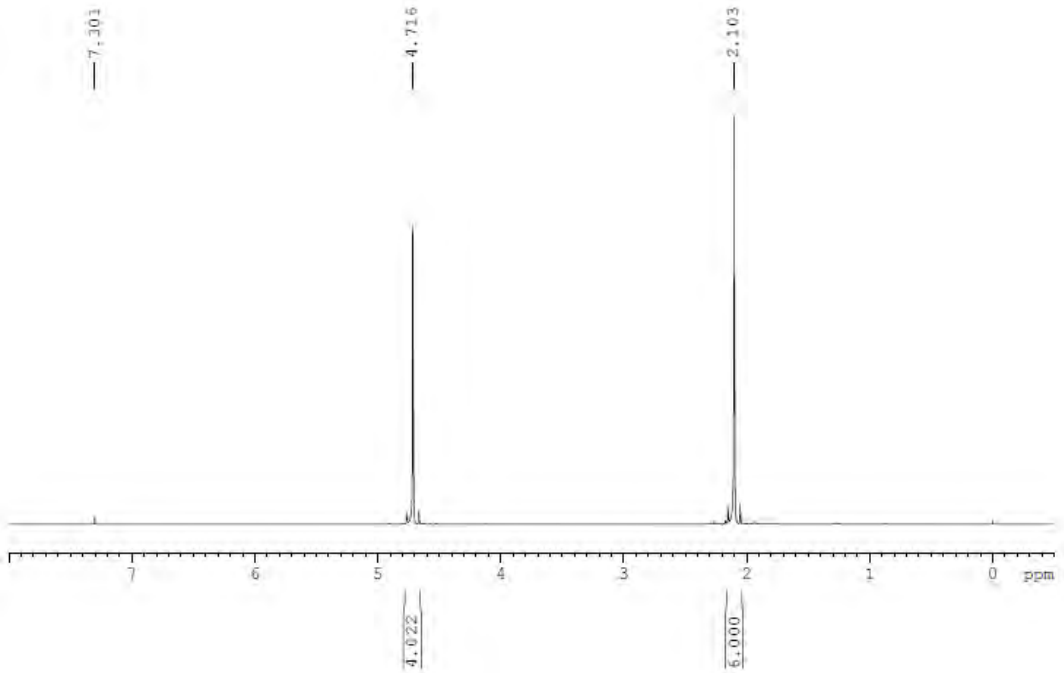

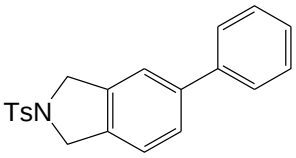

^{1}H RMN (400 MHz, $CDCl_3$)

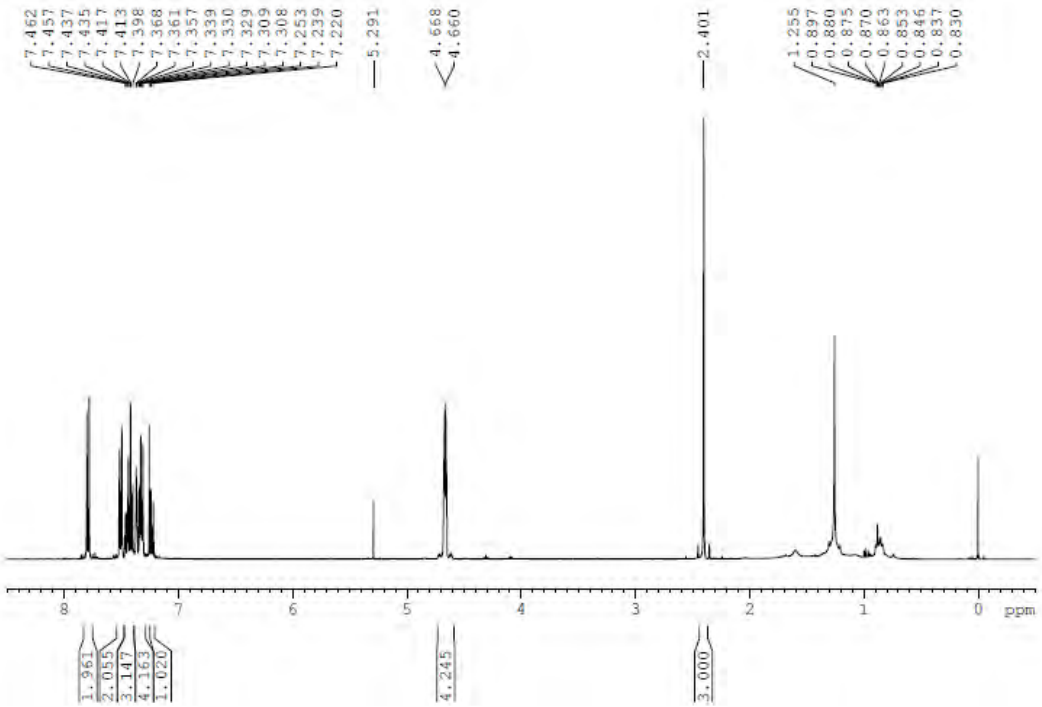

^{13}C RMN (100 MHz, $CDCl_3$)

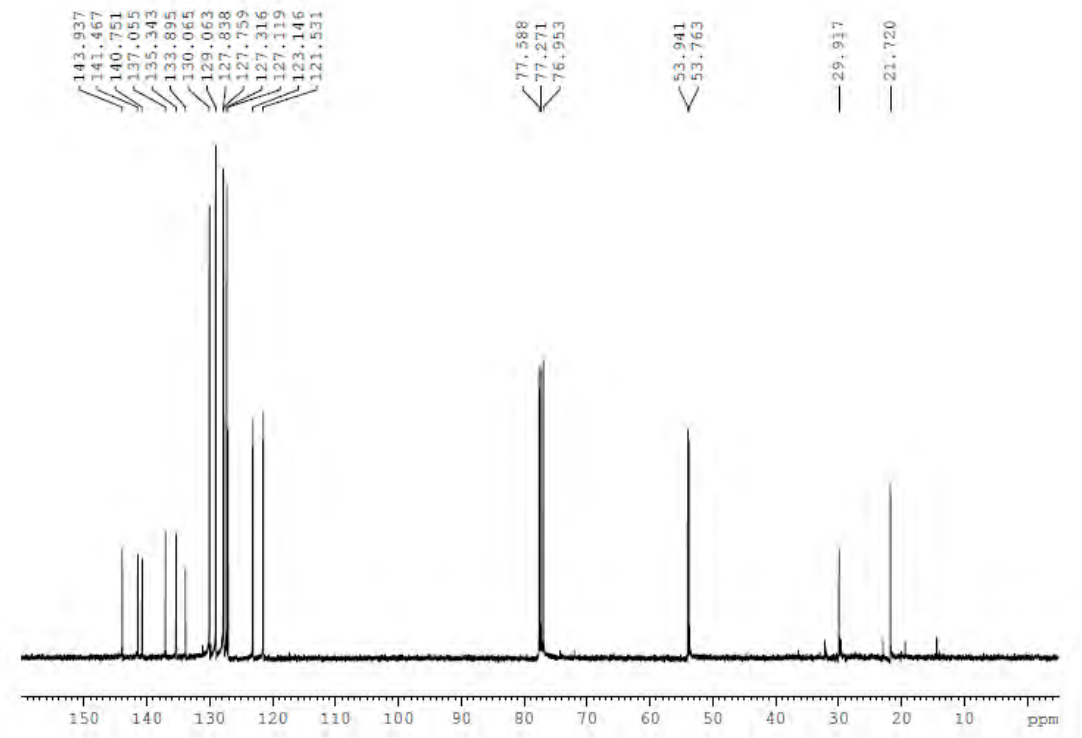

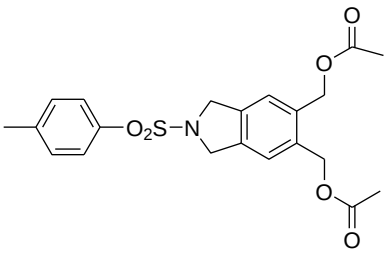

^{1}H RMN (400 MHz, $CDCl_3$)

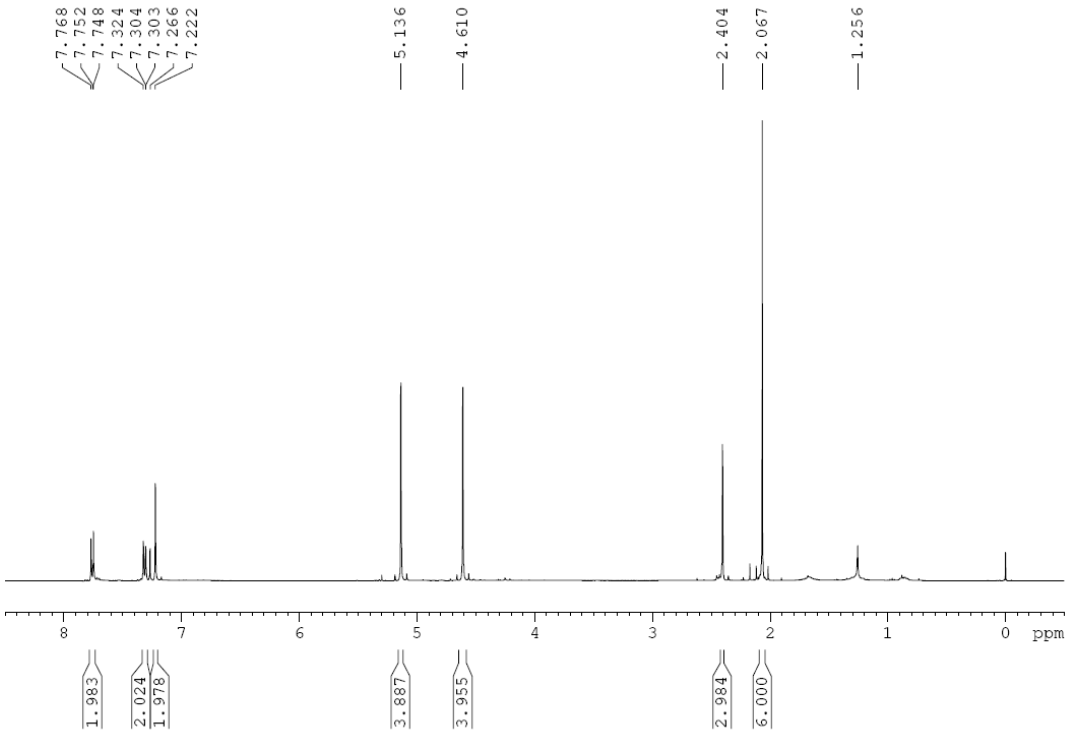

^{13}C RMN (100 MHz, $CDCl_3$)

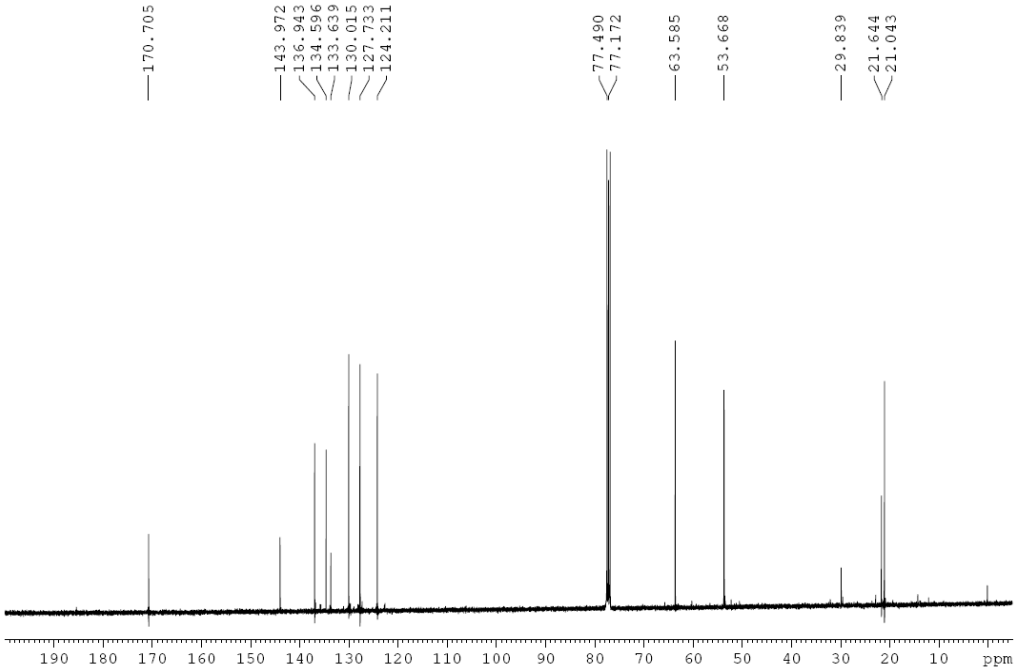

IR (ATR)

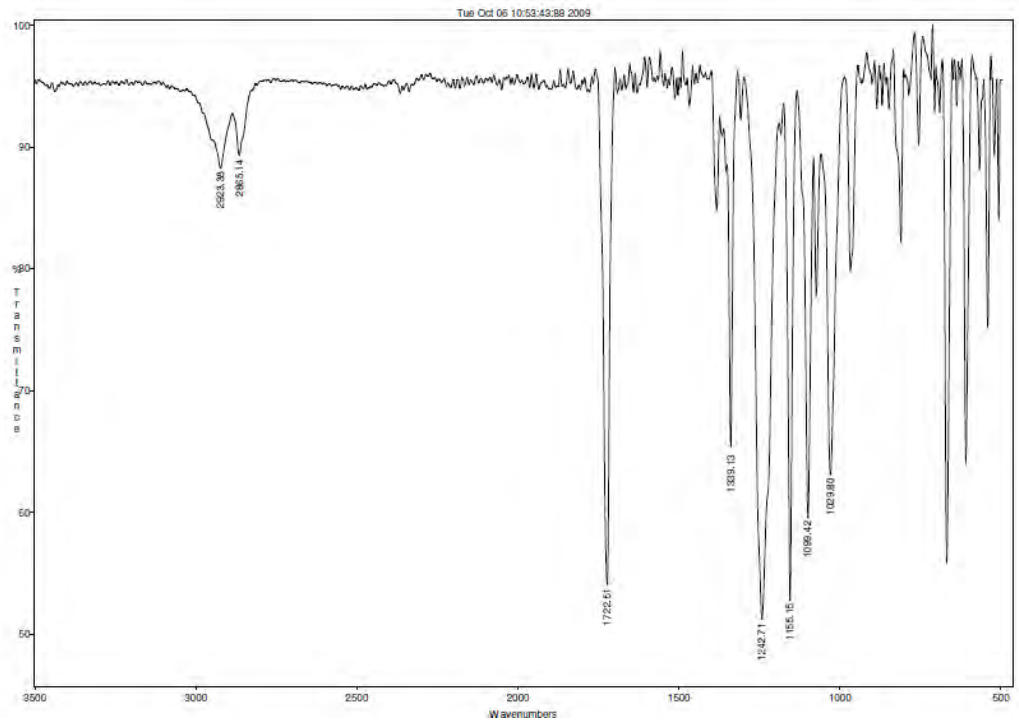

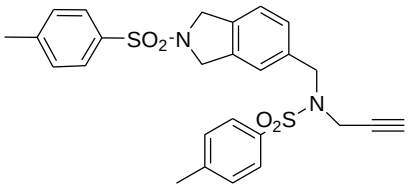

^{1}H RMN (400 MHz, $CDCl_3$)

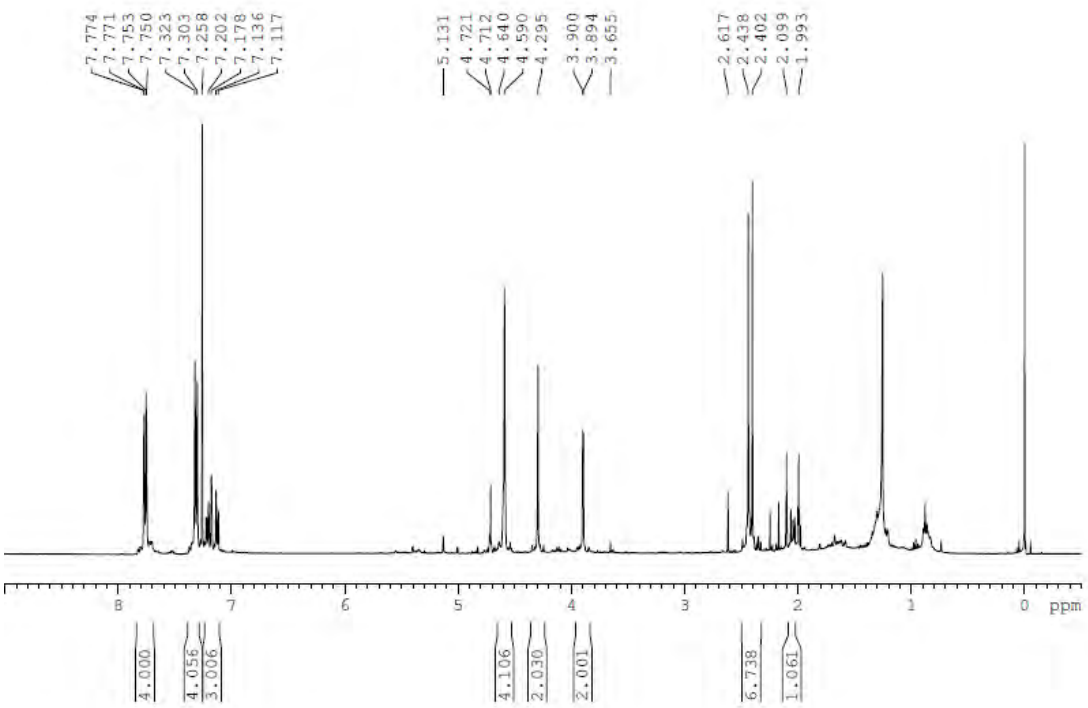

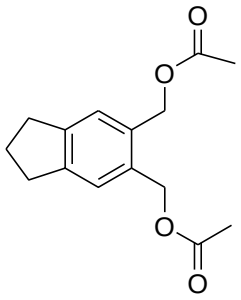

^{1}H RMN (400 MHz, $CDCl_3$)

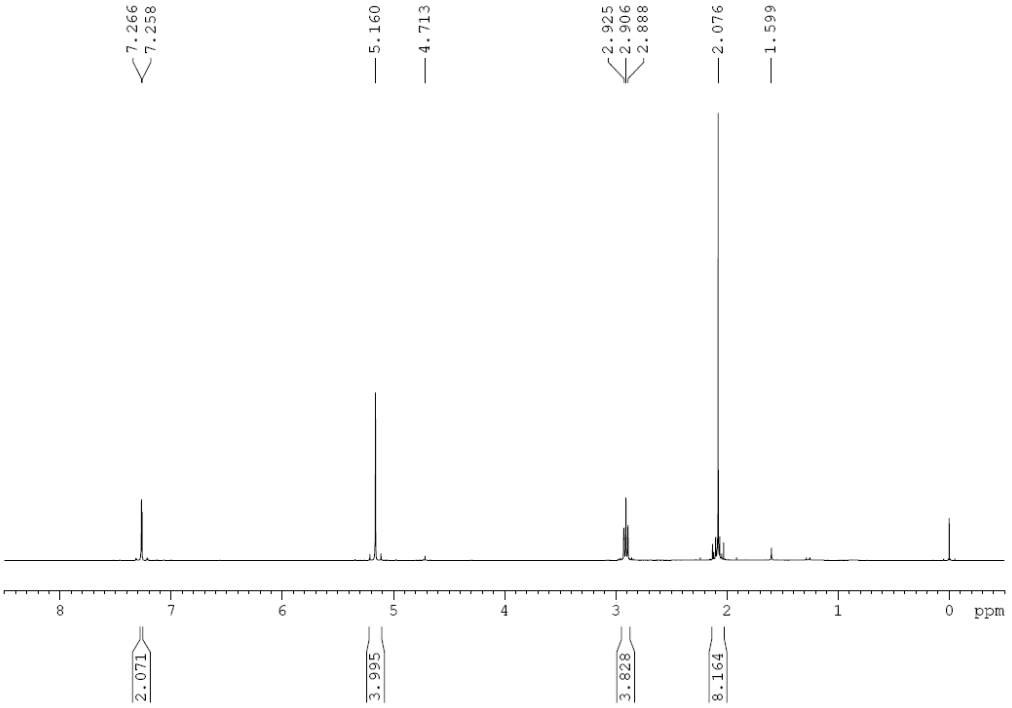

^{13}C RMN (100 MHz, $CDCl_3$)

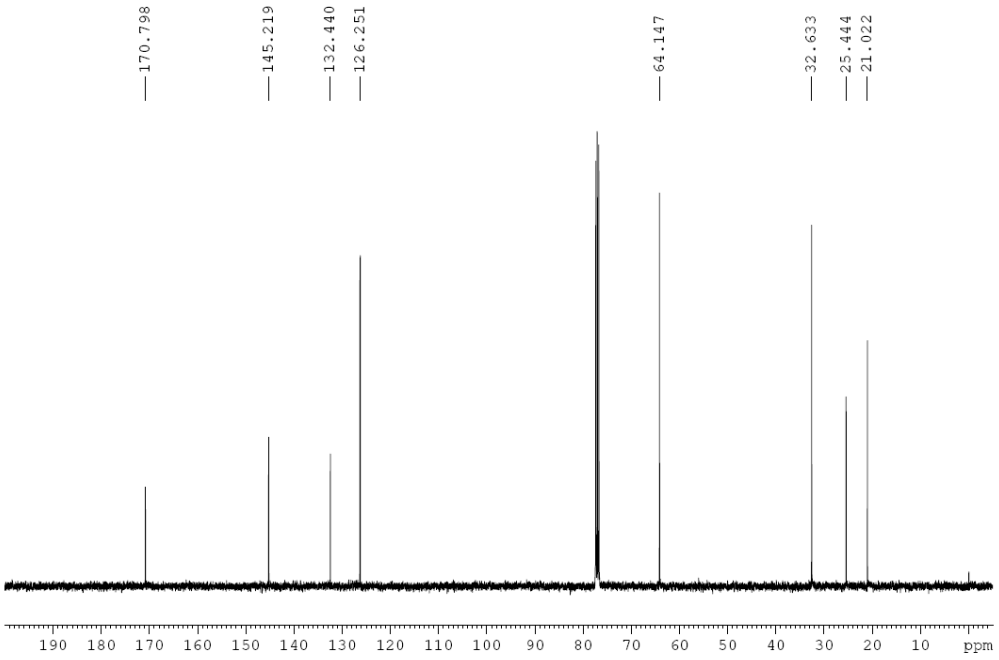

IR (ATR)

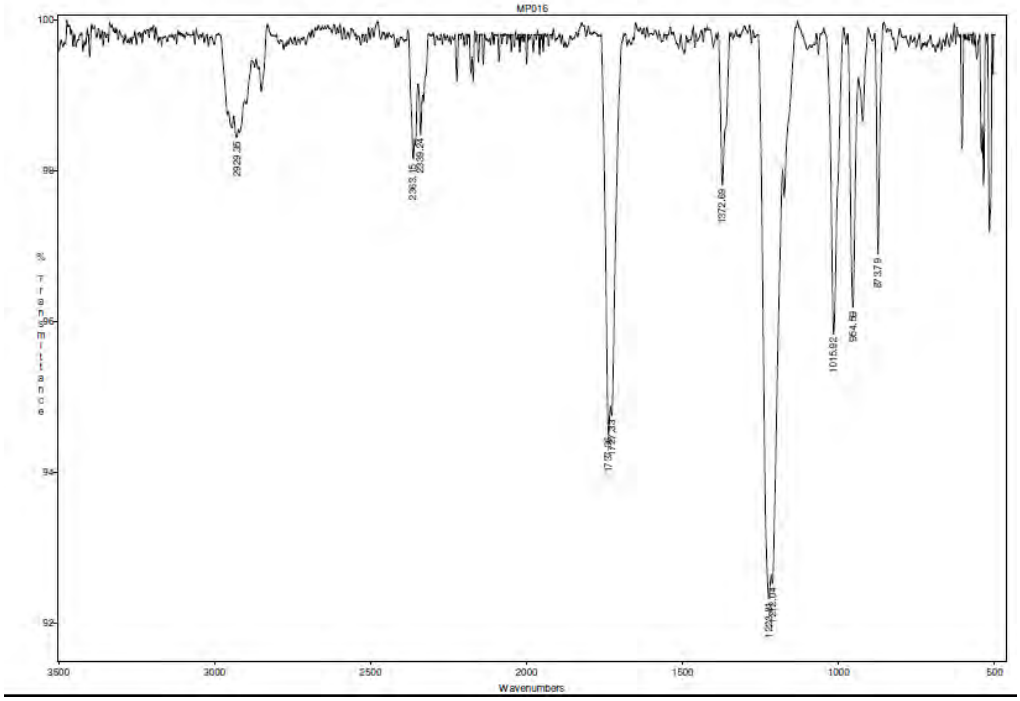

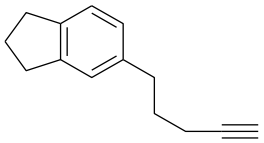

^{1}H RMN (400 MHz, $CDCl_3$)

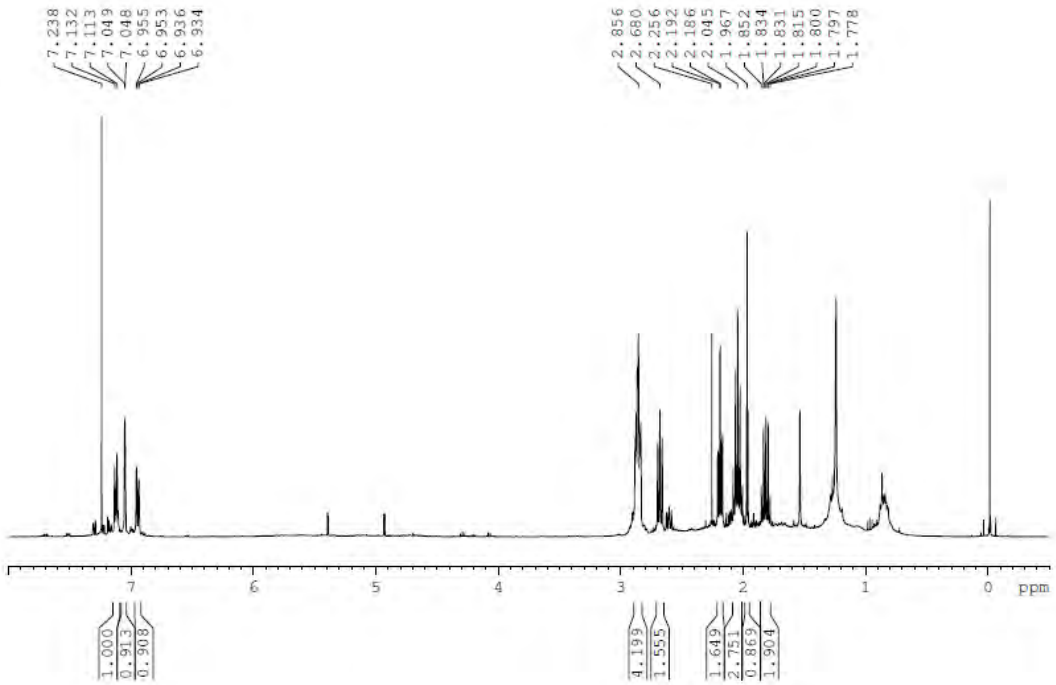

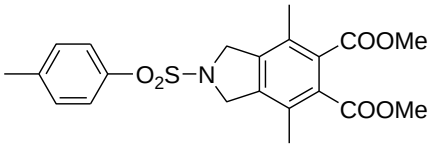

^{1}H RMN (400 MHz, $CDCl_3$)

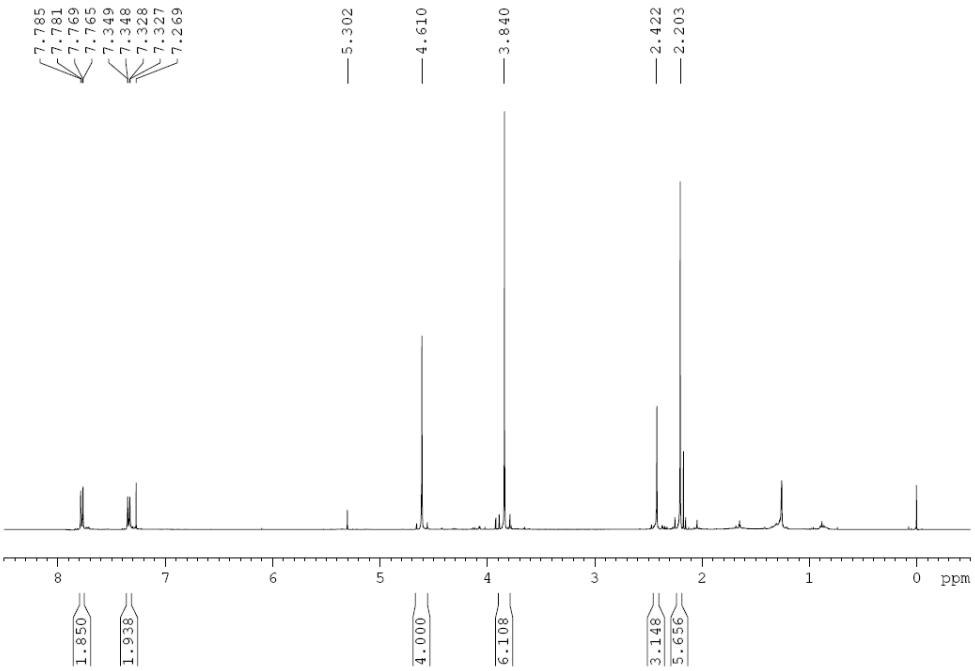

^{13}C RMN (100 MHz, $CDCl_3$)

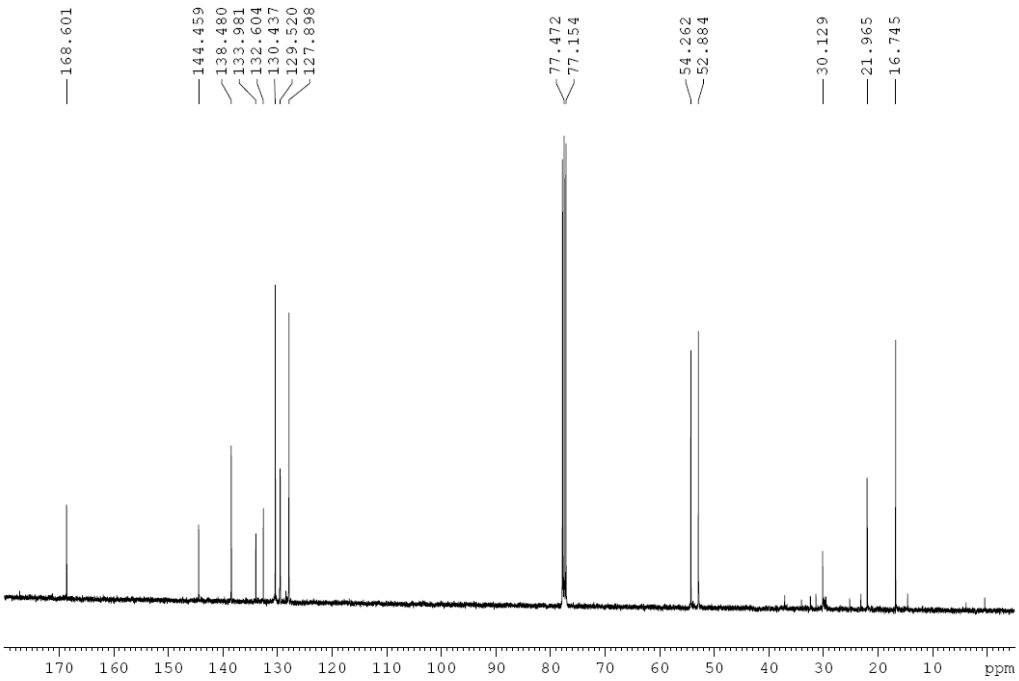

IR (ATR)

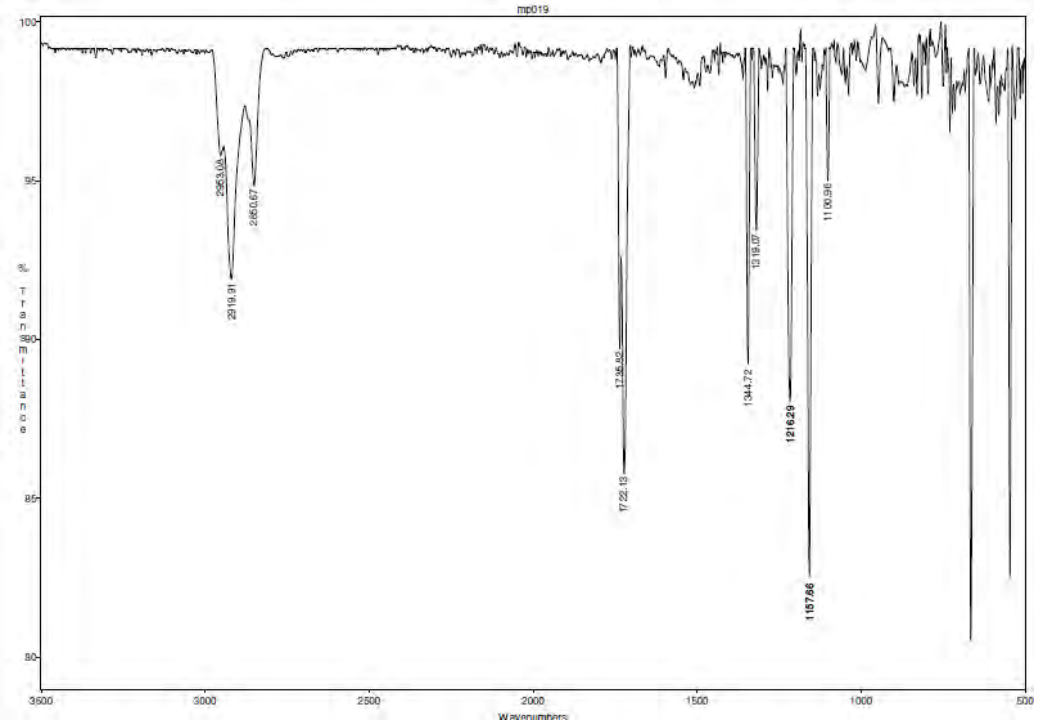
mp019
100
95
90
85
80
% Transmittance
2953.04
2919.91
2850.67
1736.85
1722.13
1344.72
1318.07
1216.29
1157.66
1100.96
3500
3000
2500
2000
1500
1000
500
Wavenumbers

ESI-MS(+)

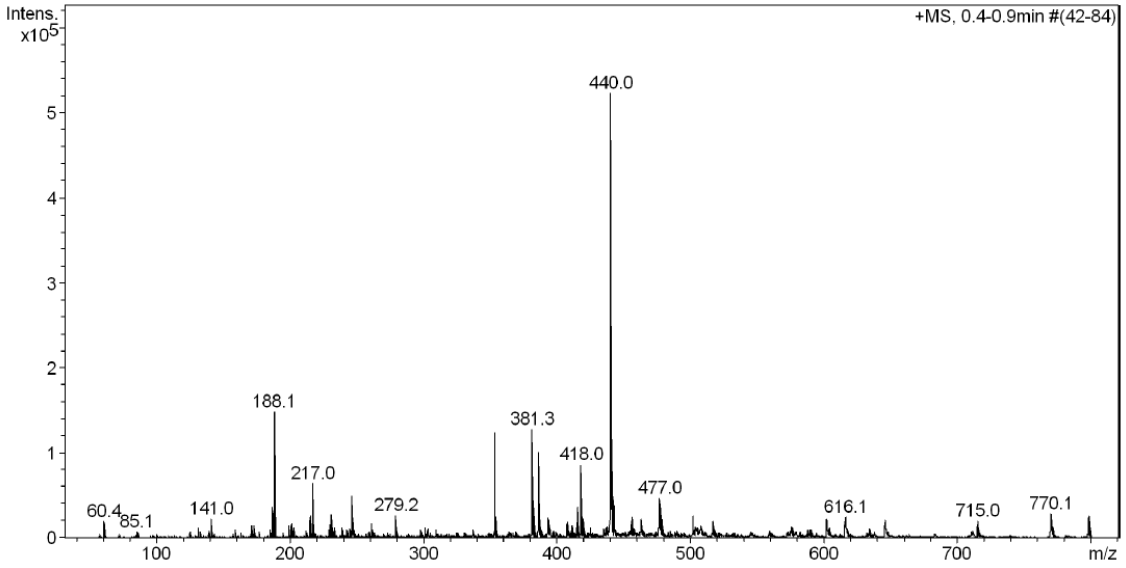
Intens.
x10^5
+MS, 0.4-0.9min #(42-84)
440.0
188.1
381.3
418.0
217.0
477.0
60.4
85.1
141.0
279.2
616.1
715.0
770.1
m/z

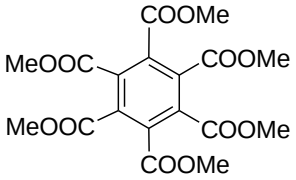

^{1}H RMN (400 MHz, $CDCl_3$)

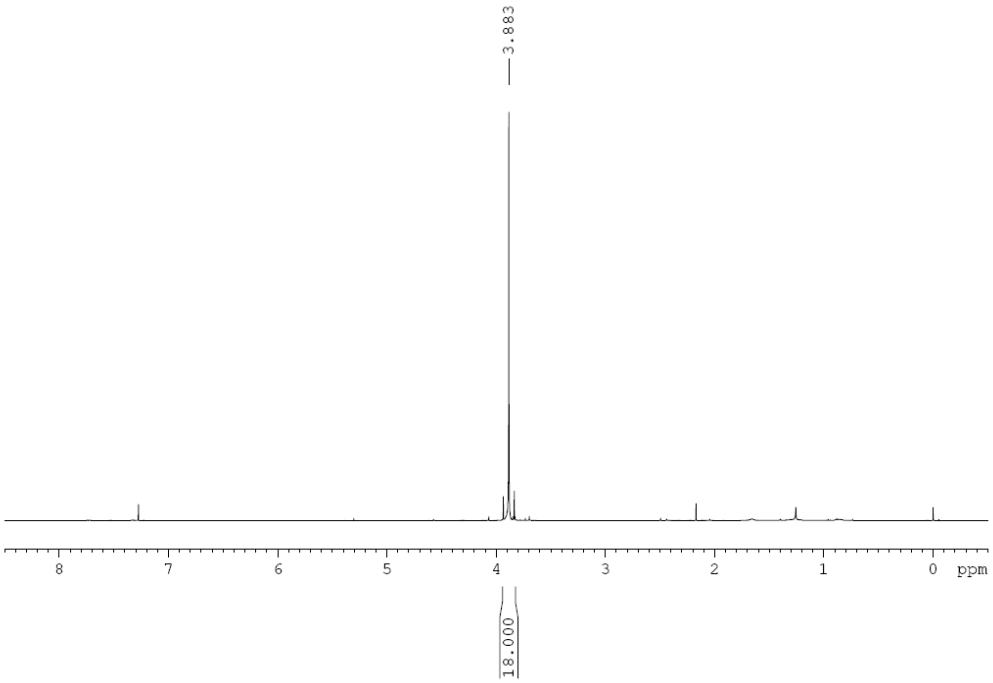

^{13}C RMN (100 MHz, $CDCl_3$)

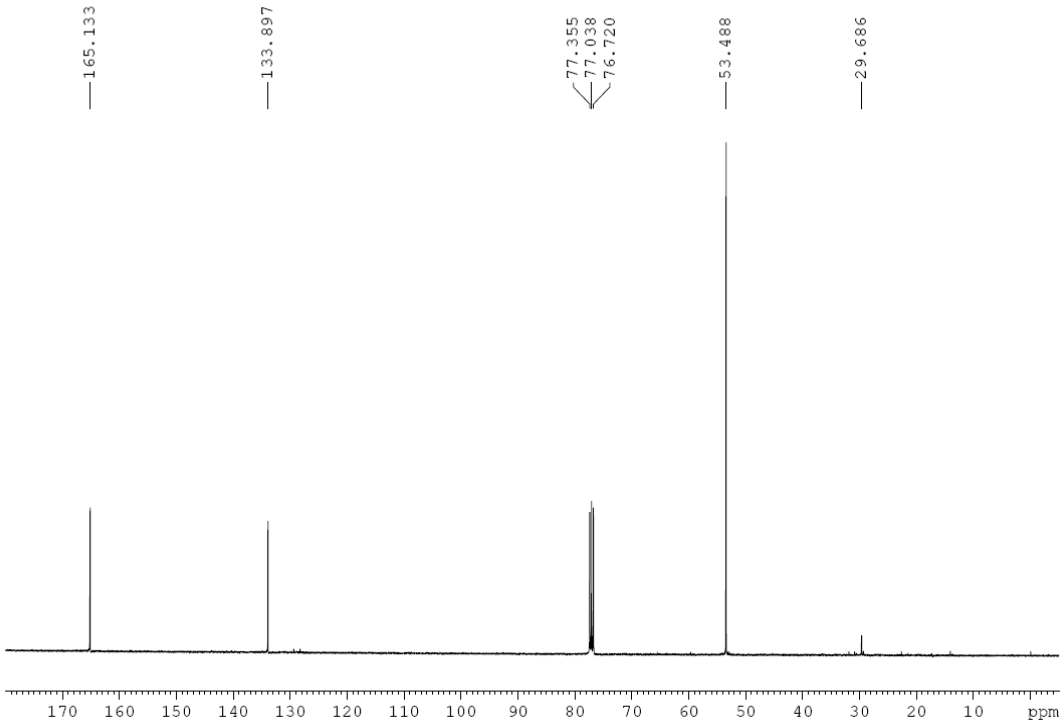

IR (ATR)

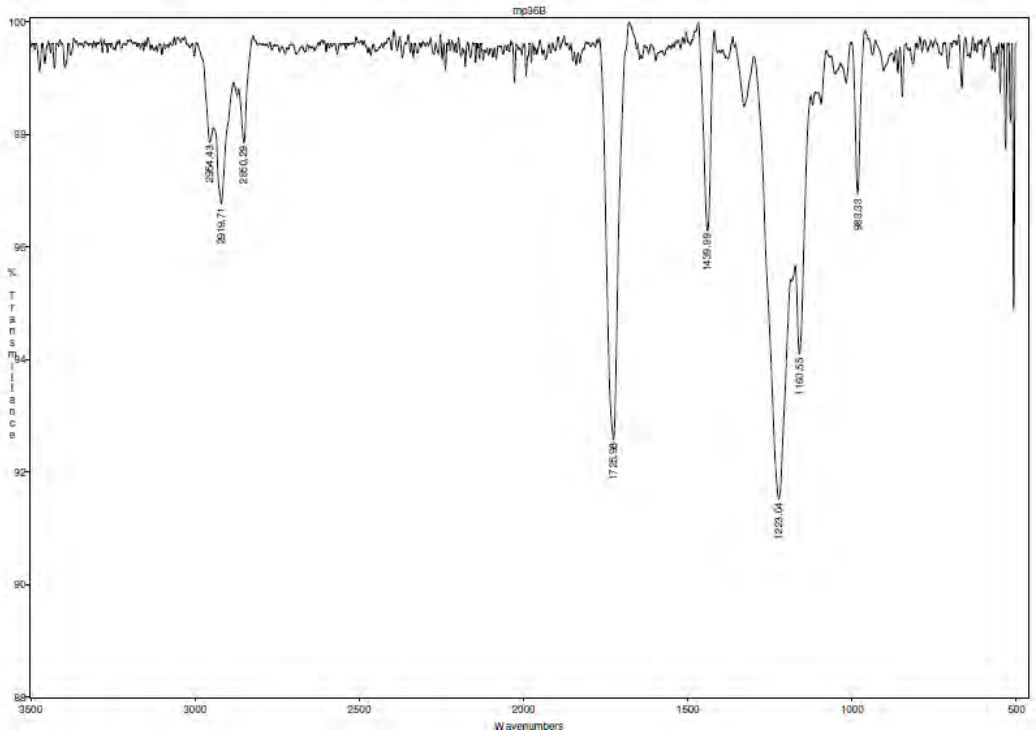

^{1}H RMN (400 MHz, $CDCl_3$)

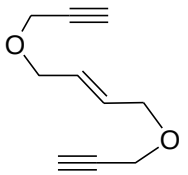

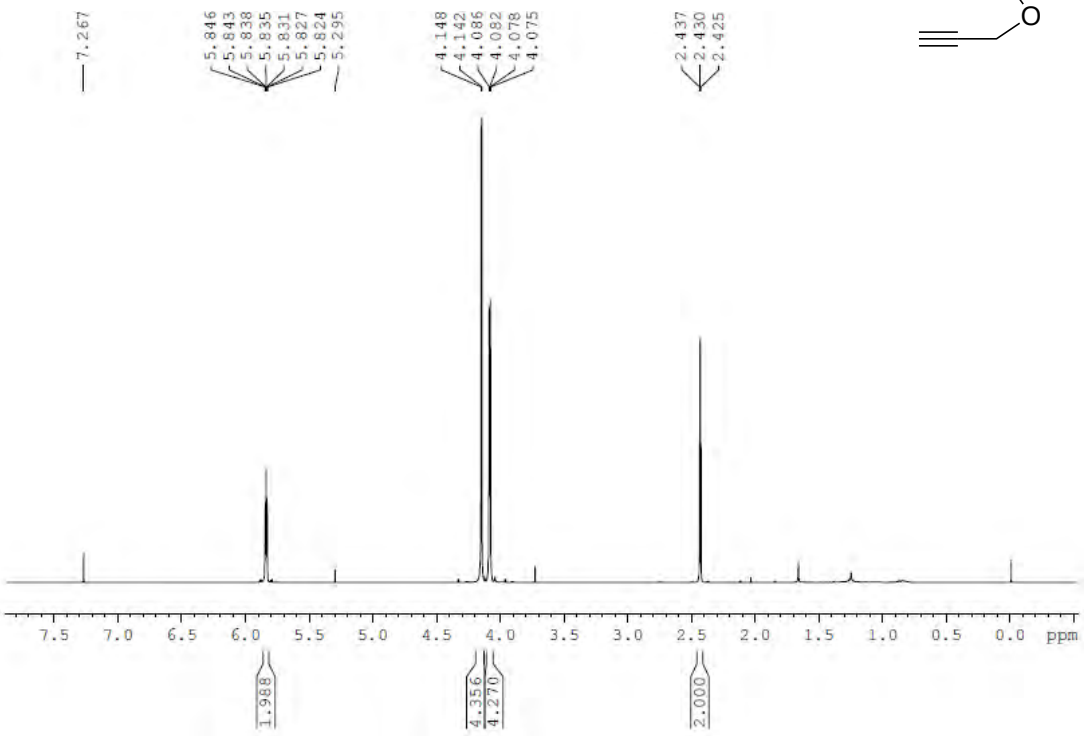

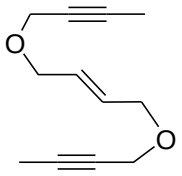

^{1}H RMN (300 MHz, $CDCl_3$)

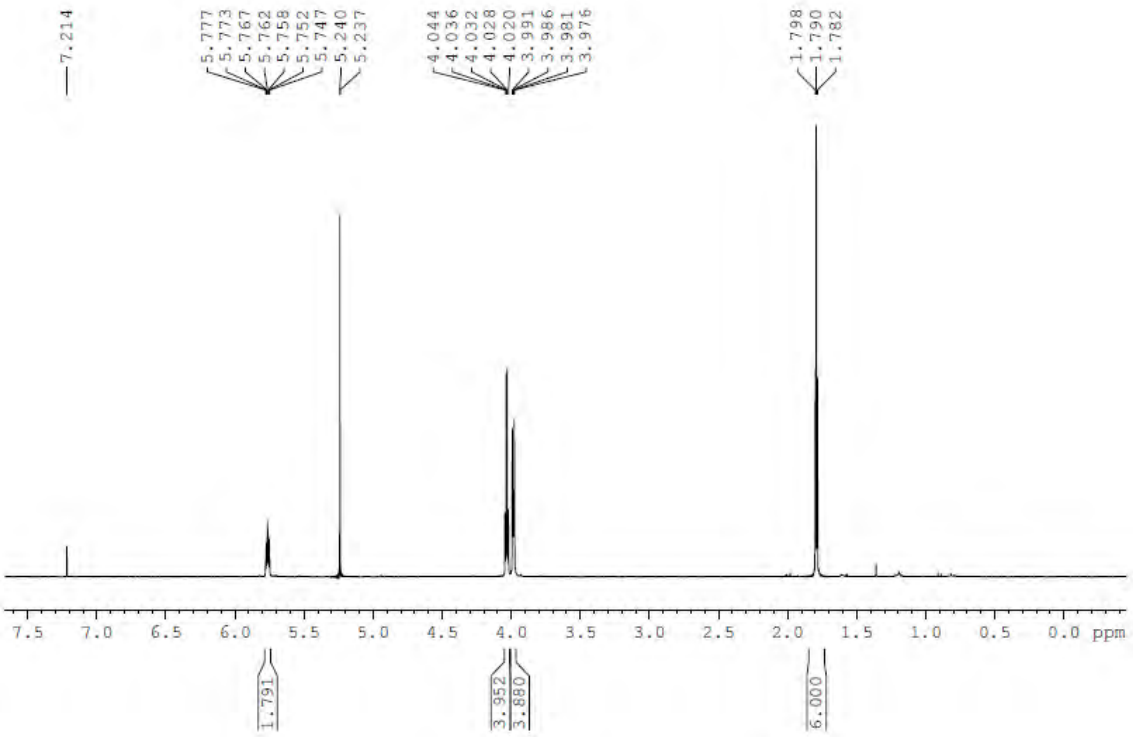

^{13}C RMN (75 MHz, $CDCl_3$)

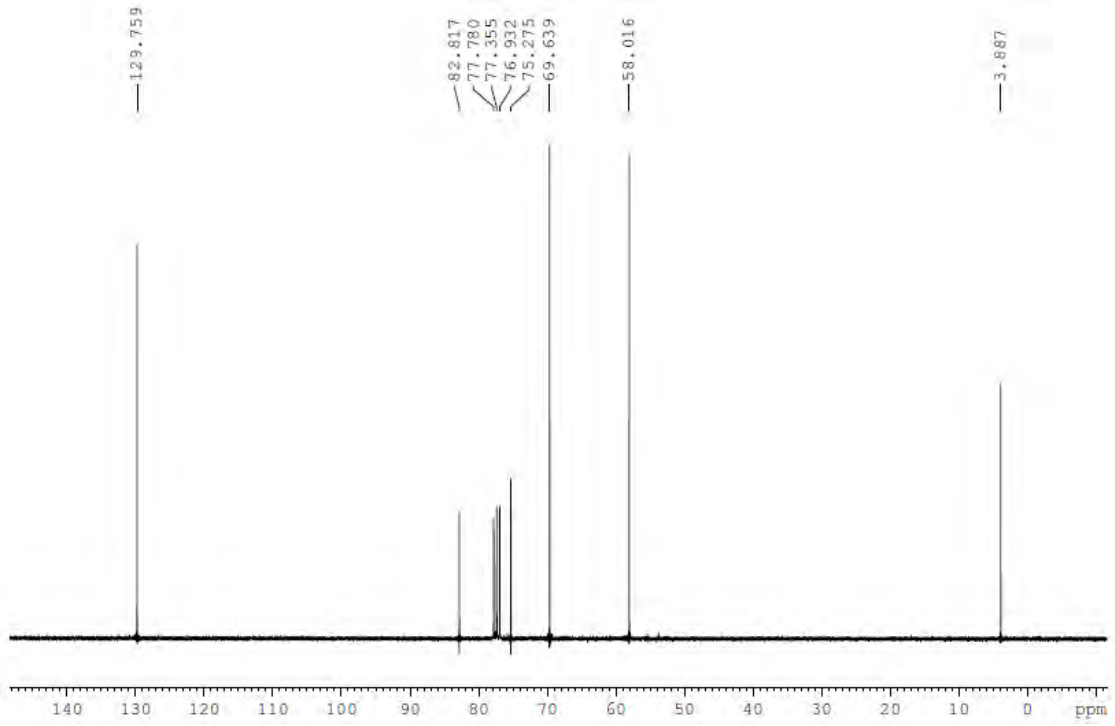

IR(ATR)

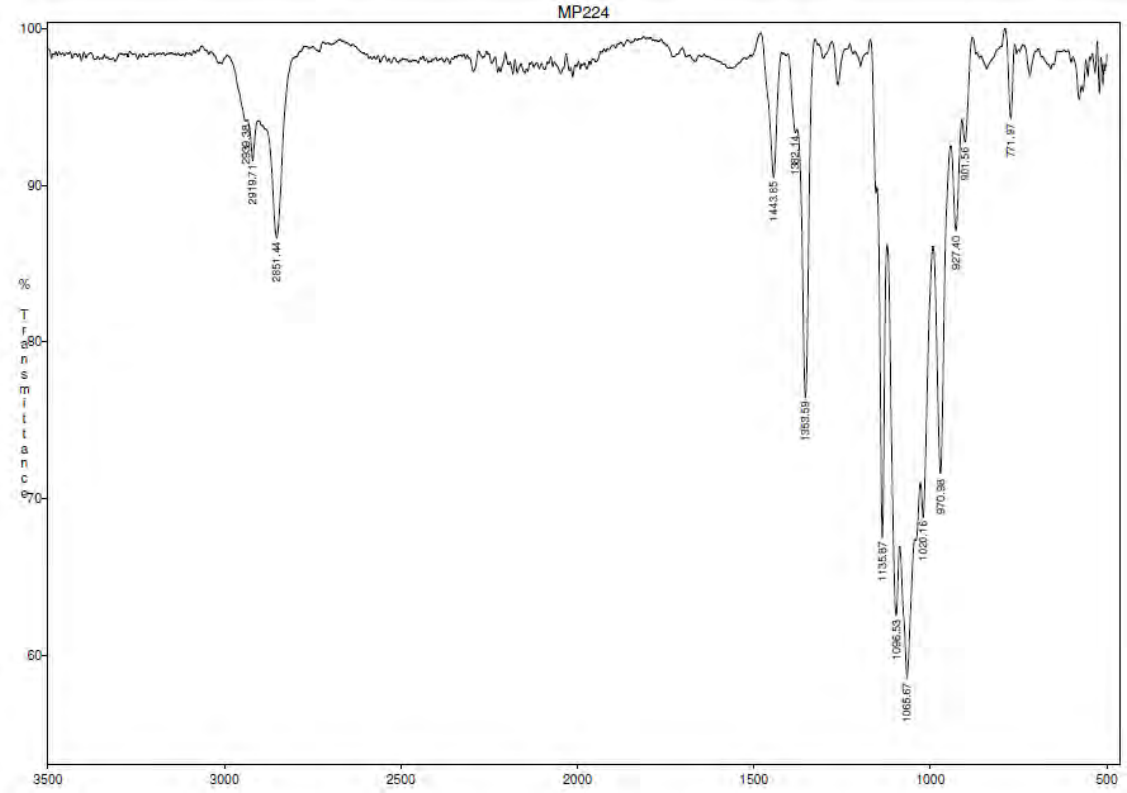

^{1}H RMN (400 MHz, $CDCl_3$)

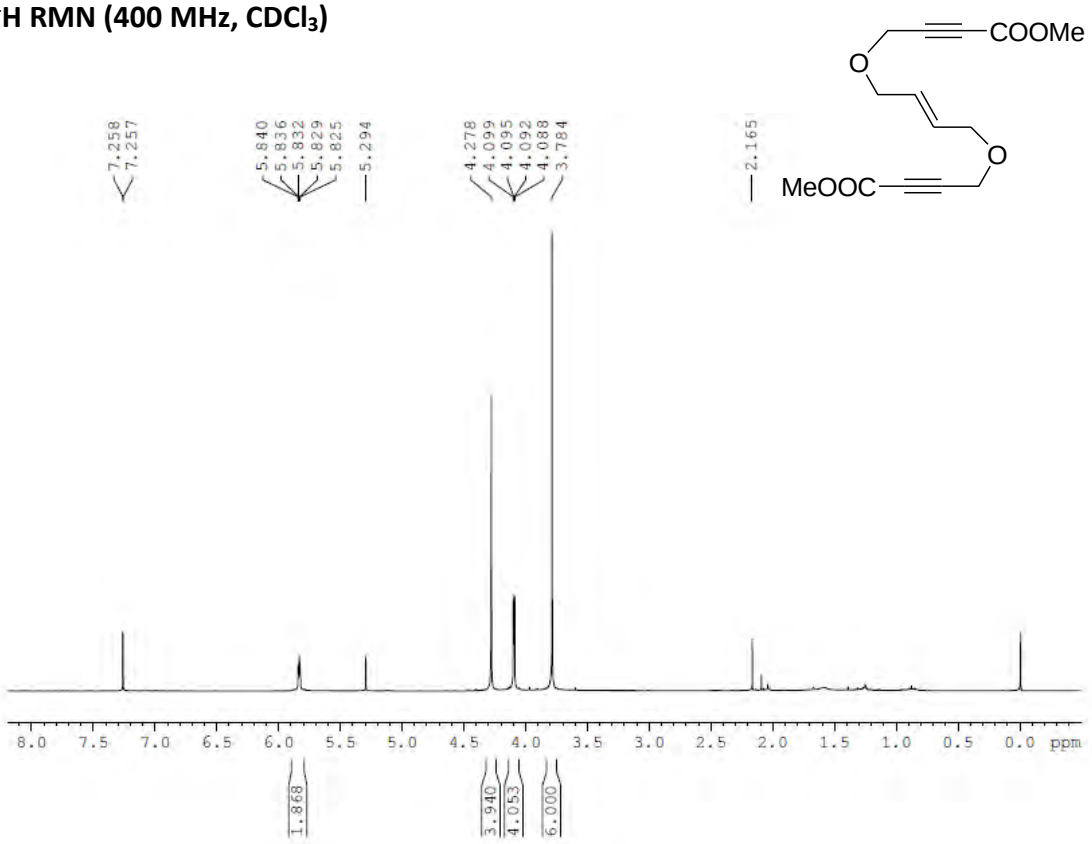

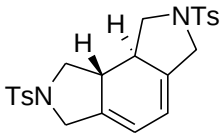

^{1}H RMN (400 MHz, $CDCl_3$)

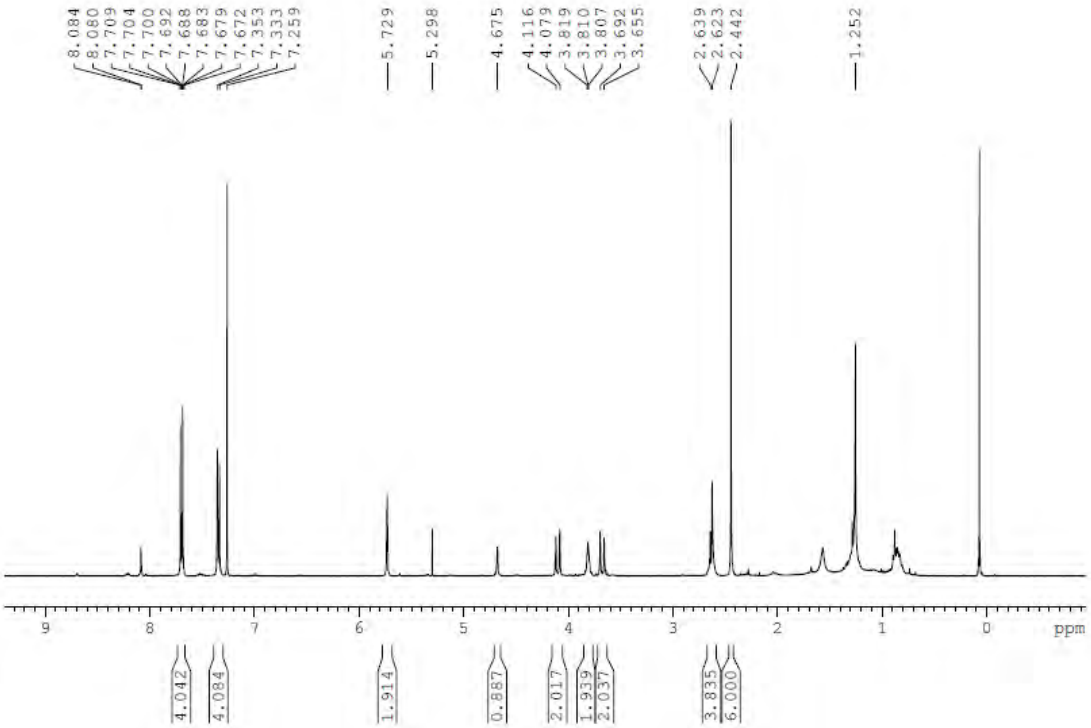

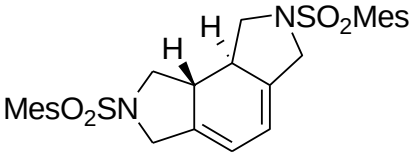

^{1}H RMN (400 MHz, $CDCl_3$)

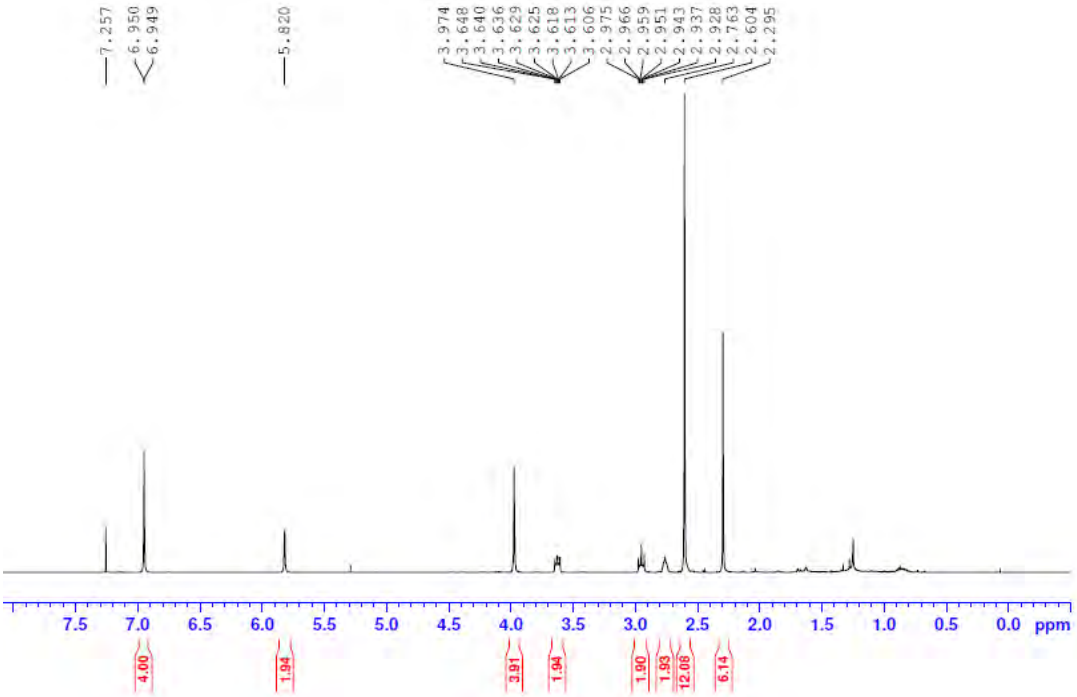

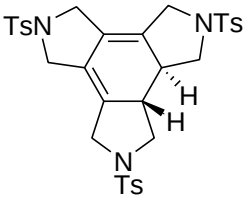

^{1}H RMN (400 MHz, $CDCl_3$)

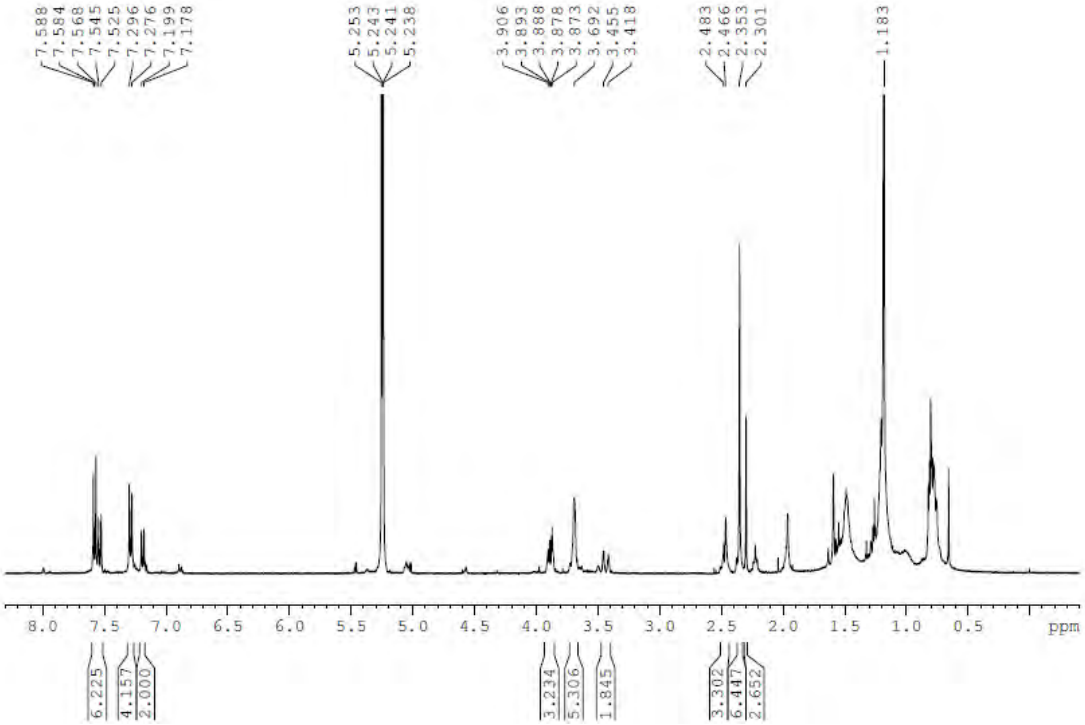

^{1}H NMR ($CDCl_3$, 250 MHz)

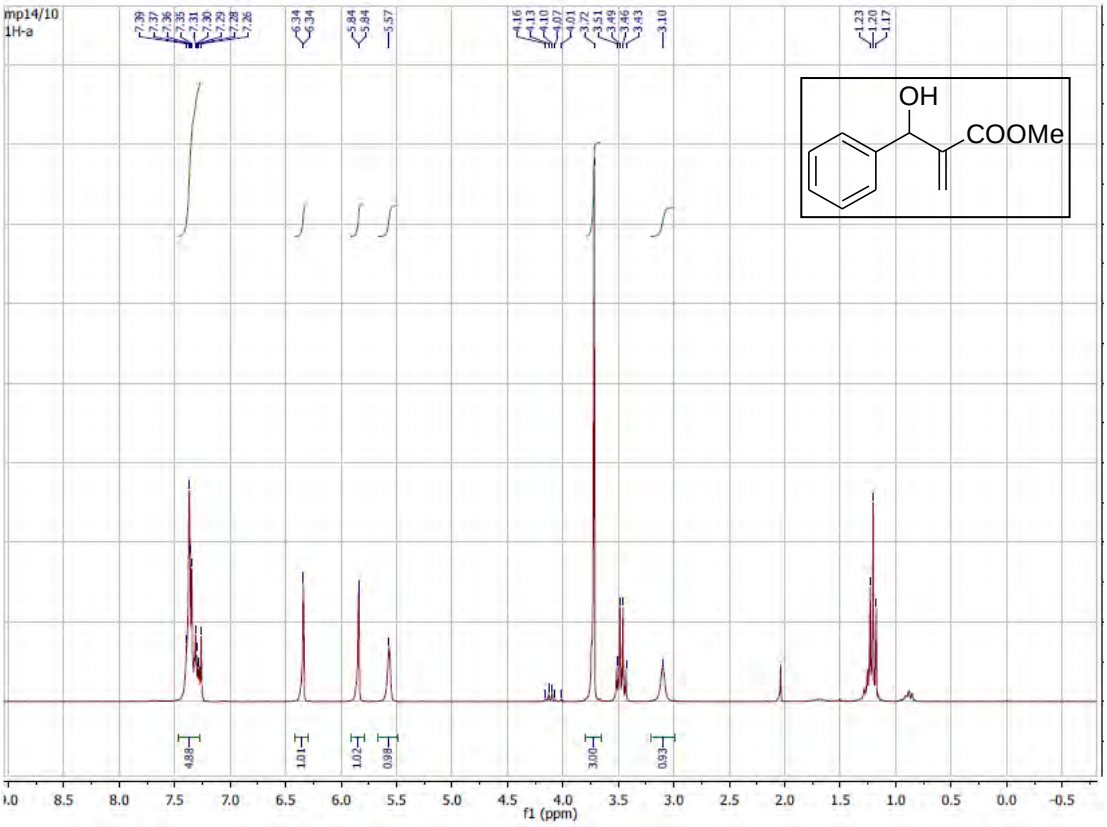

^{13}C NMR ($CDCl_3$, 62.5 MHz)

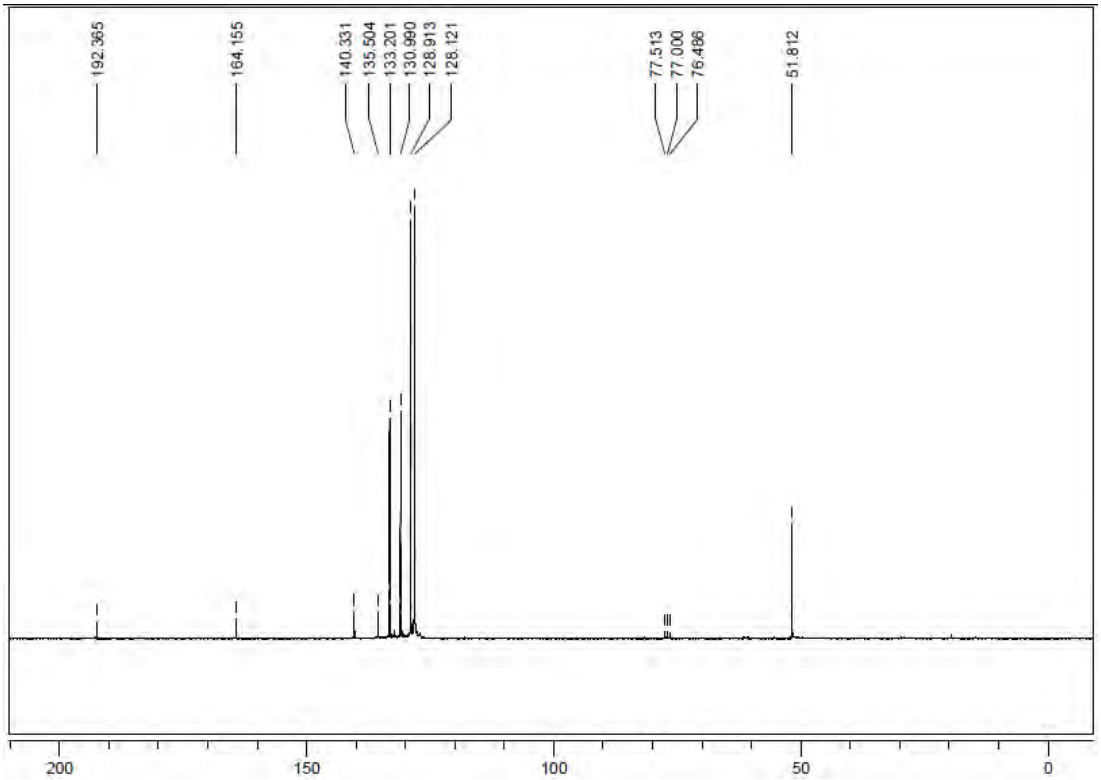

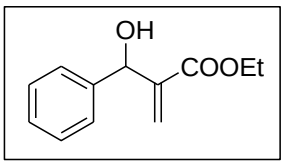

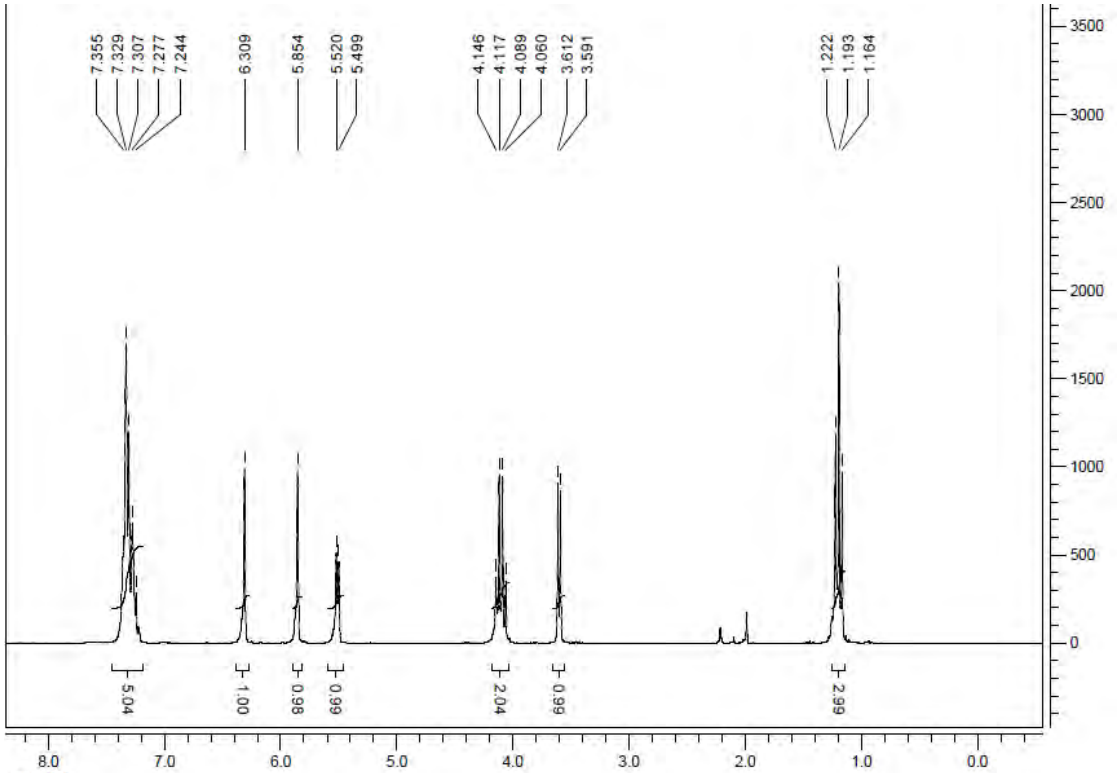

^{13}C NMR ($CDCl_3$, 62.5 MHz)

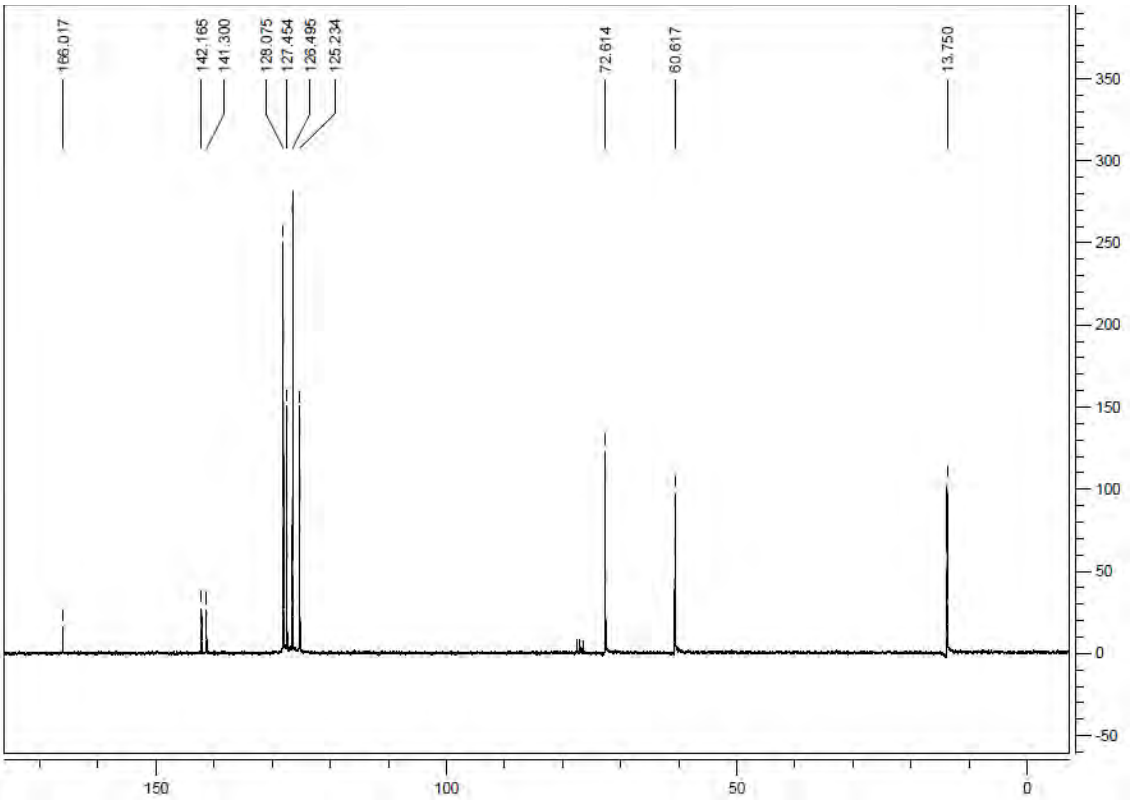

^{1}H NMR ($CDCl_3$, 250 MHz)

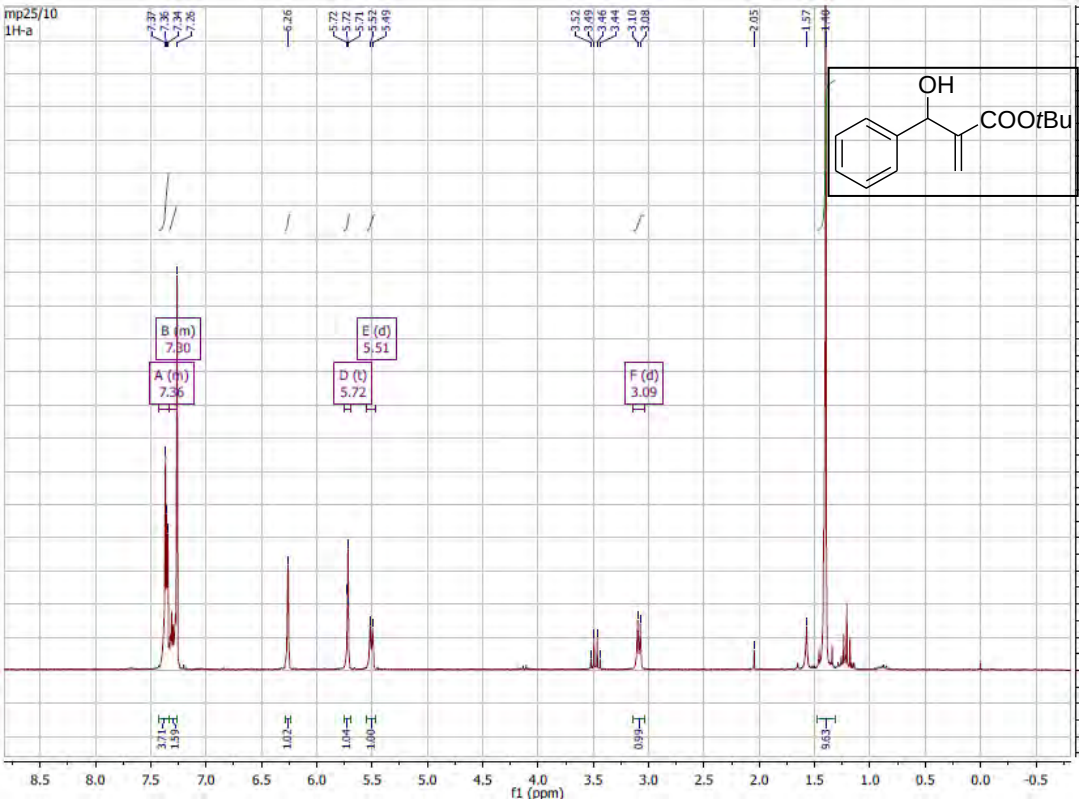

^{1}H NMR ($CDCl_3$, 250 MHz)

^{1}H NMR ($CDCl_3$, 250 MHz)

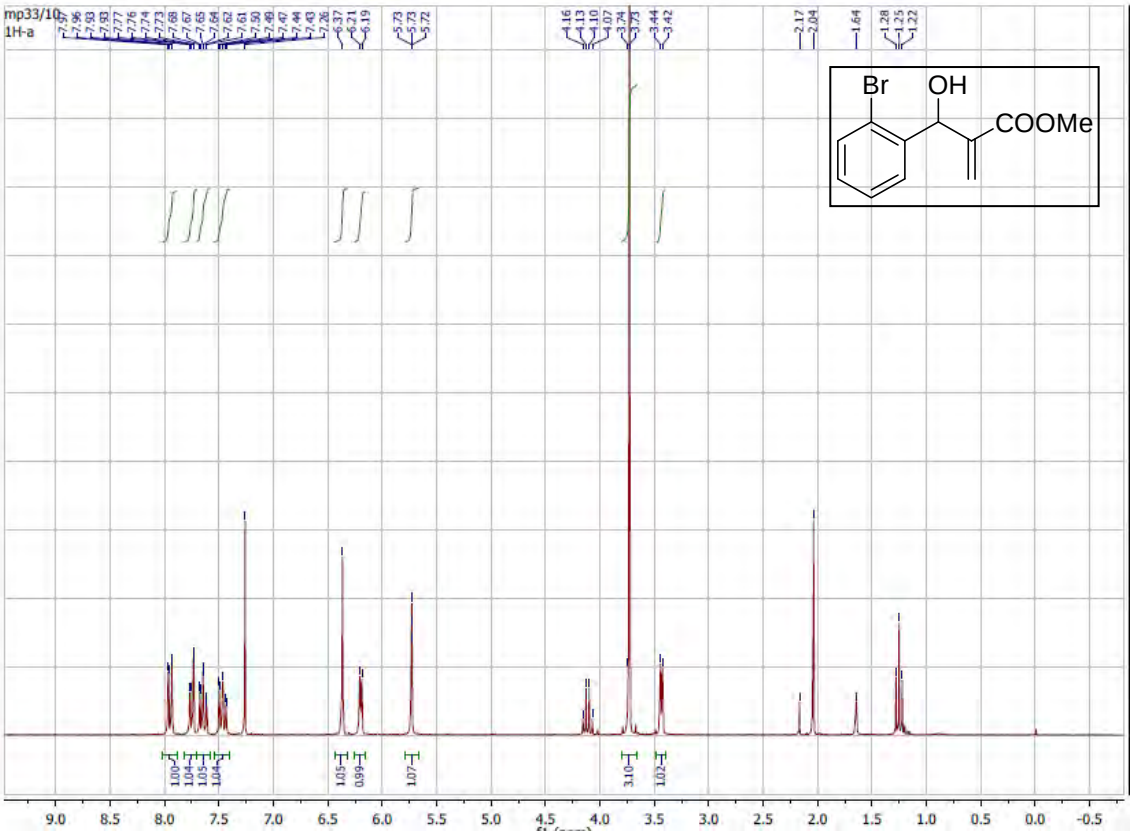

^{1}H NMR ($CDCl_3$, 250 MHz)

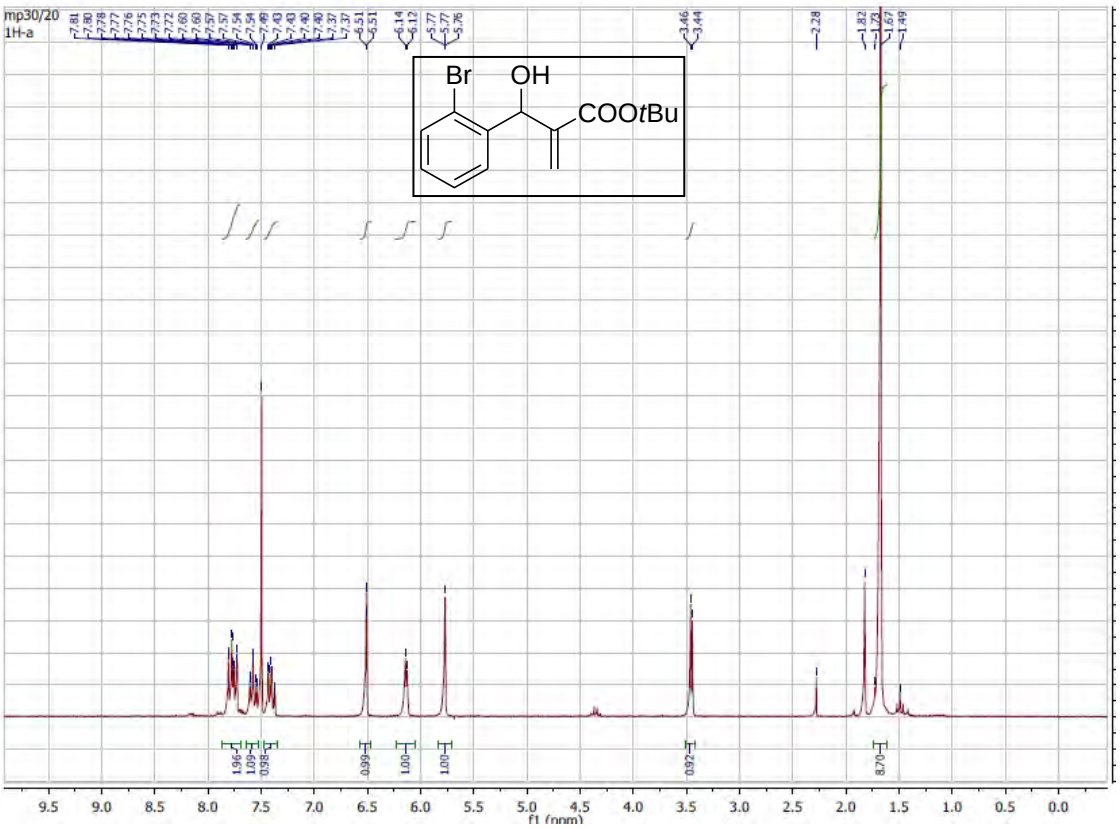

^{1}H NMR ($CDCl_3$, 250 MHz)

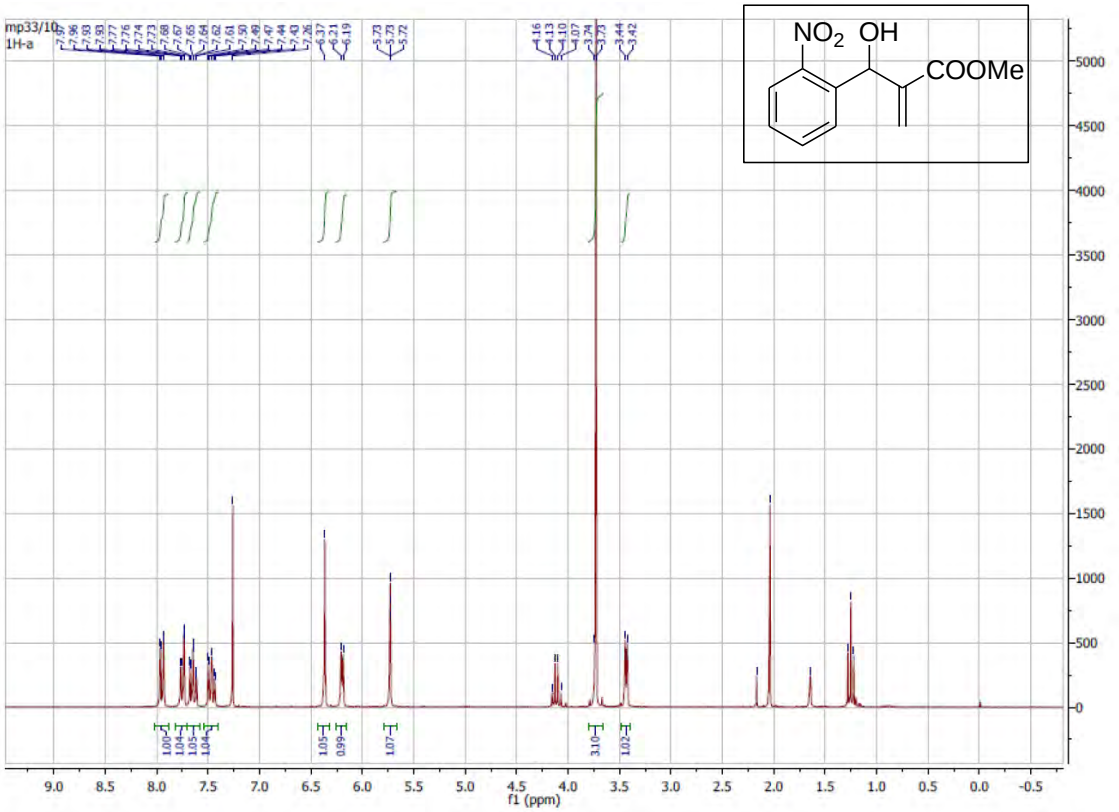

^{1}H NMR ($CDCl_3$, 250 MHz)

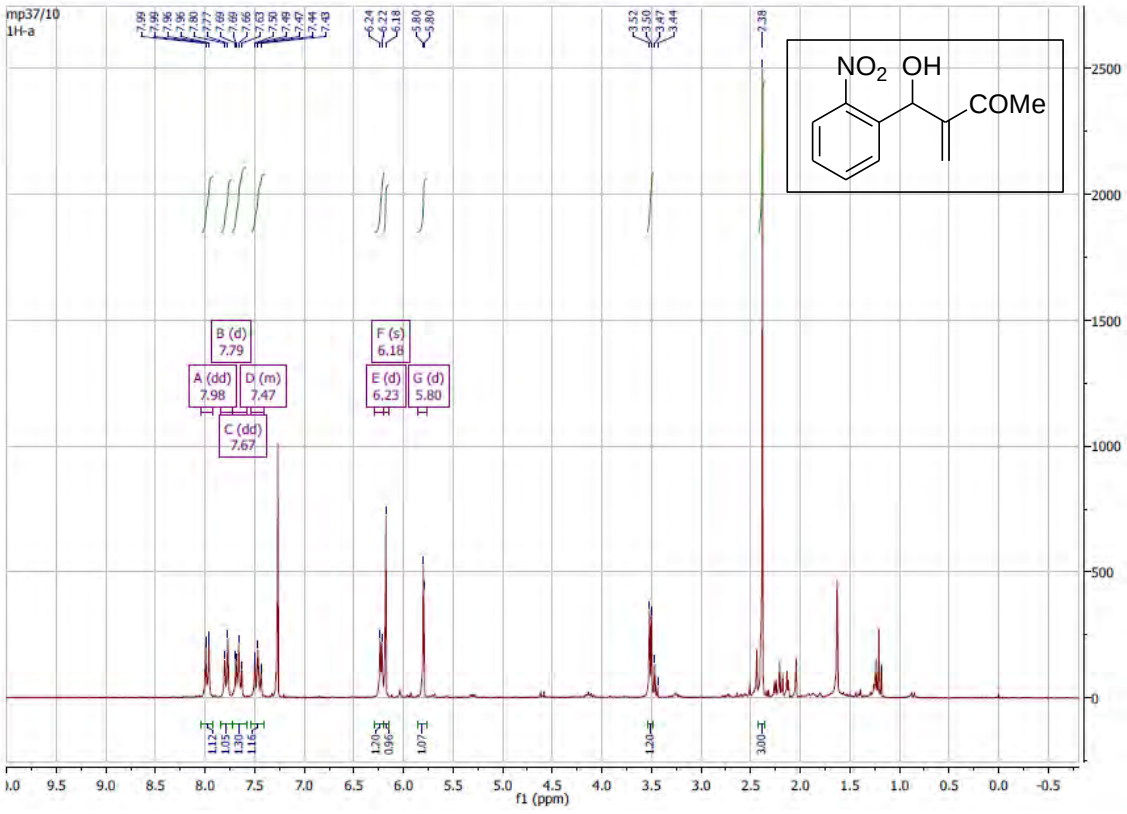

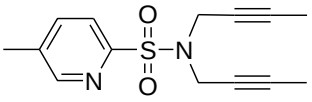

^{1}H NMR ($CDCl_3$, 400 MHz)

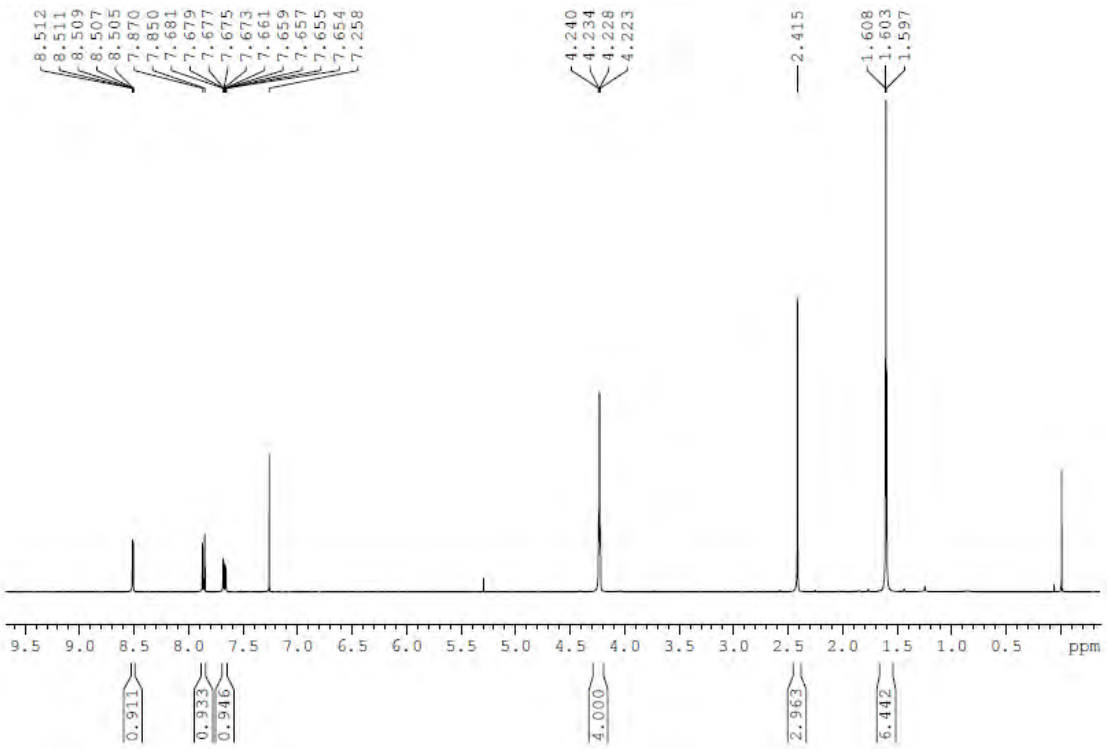

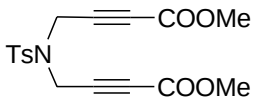

^{1}H NMR ($CDCl_3$, 300 MHz)

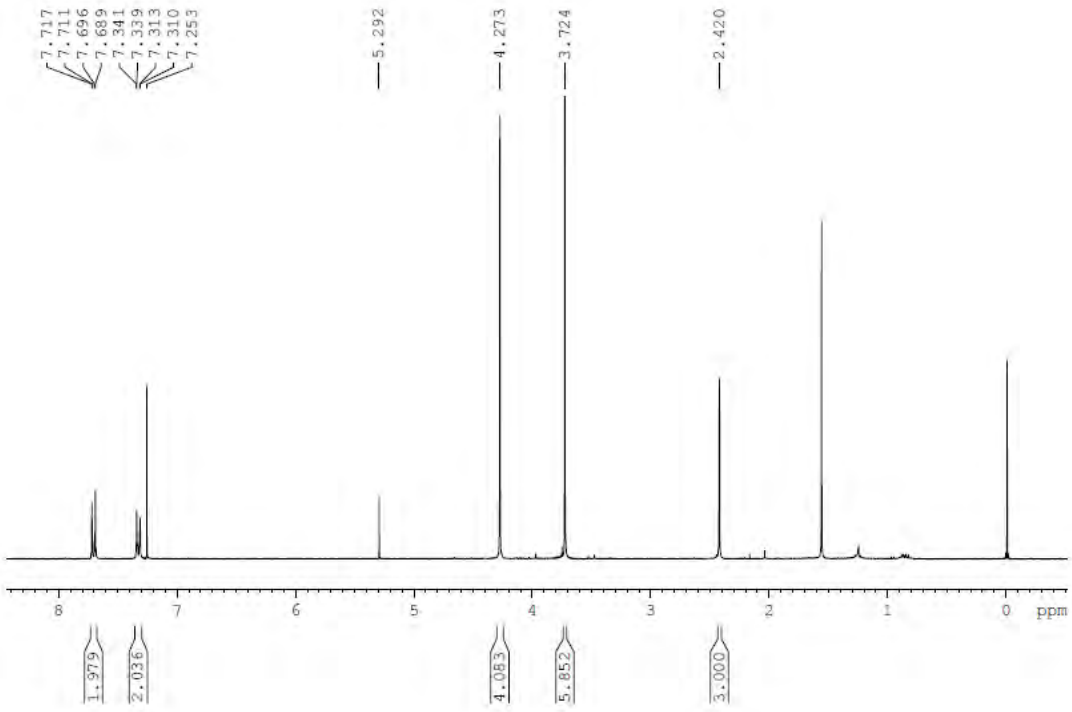

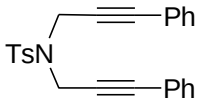

^{1}H NMR ($CDCl_3$, 300 MHz)

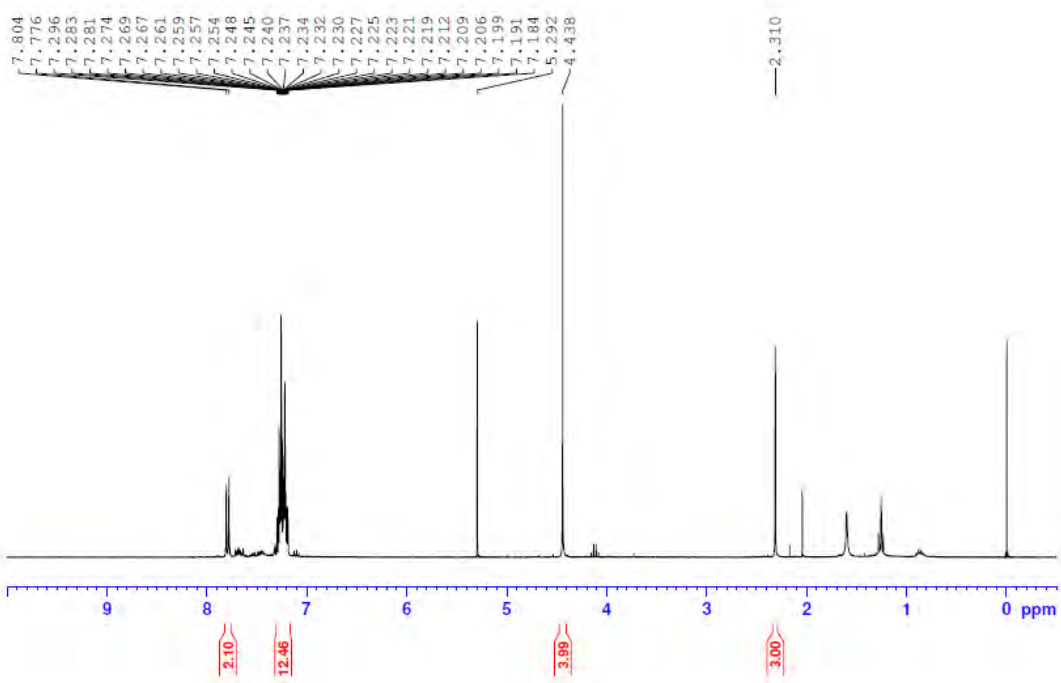

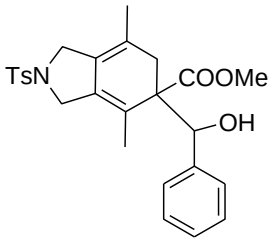

^{1}H NMR ($CDCl_3$, 300 MHz)

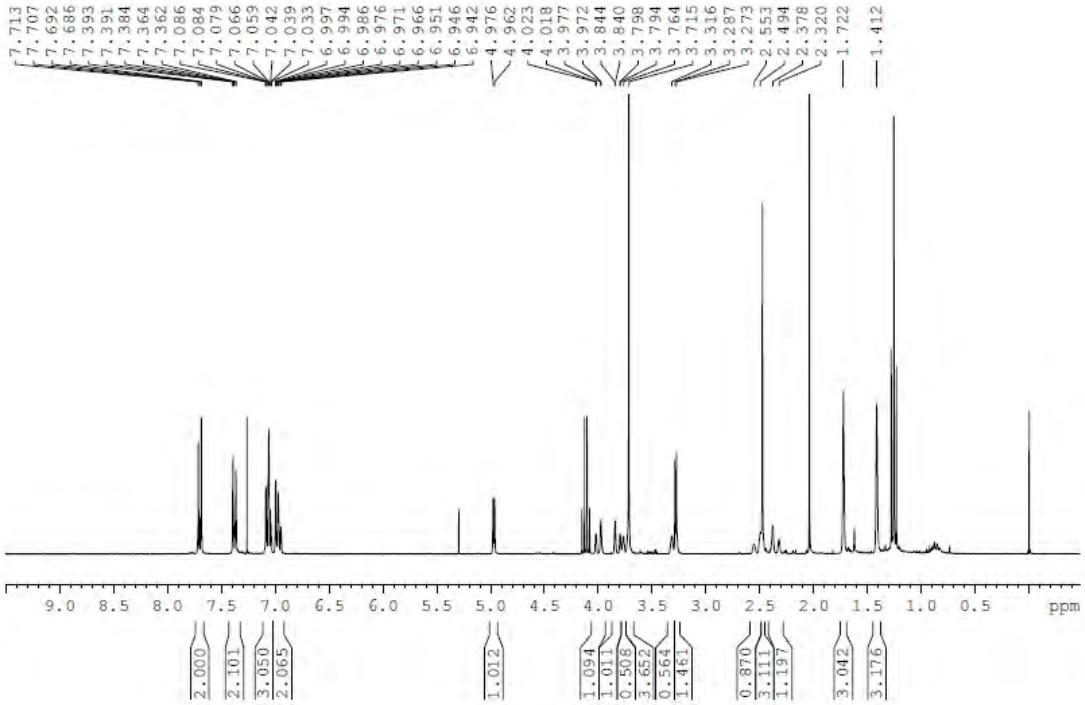

^{13}C NMR ($CDCl_3$, 100 MHz)

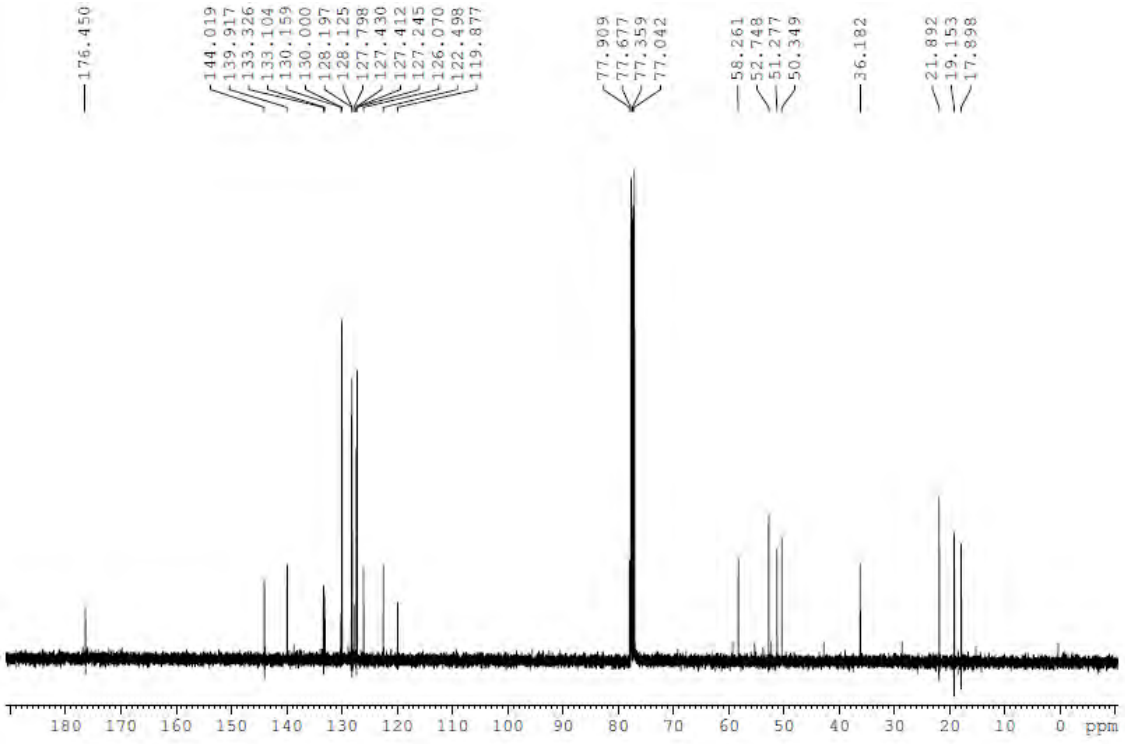

IR (ATR)

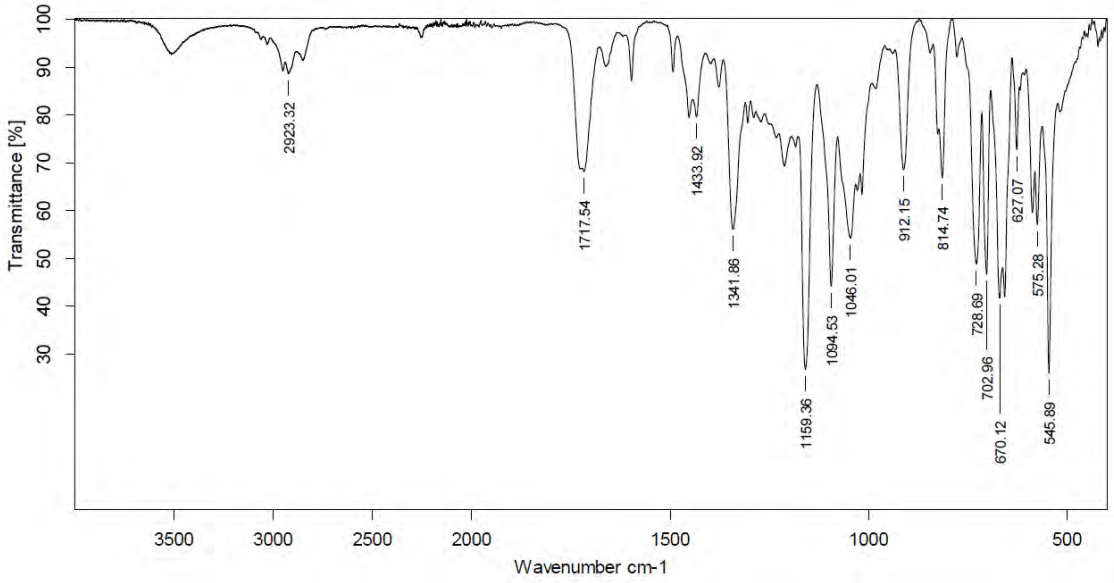
Transmittance [%]
100
90
80
70
60
50
40
30
2923.32
1717.54
1433.92
1341.86
1159.36
1094.53
1046.01
912.15
814.74
728.69
702.96
670.12
627.07
575.28
545.89
3500
3000
2500
2000
1500
1000
500
Wavenumber cm-1

ESI-MS (+)

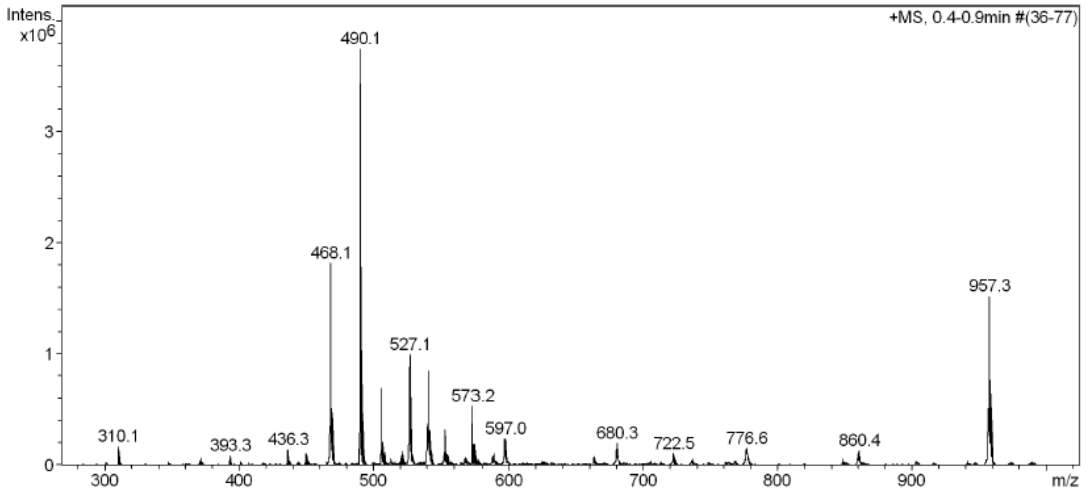
Intens.
x10^6
+MS, 0.4-0.9min #(36-77)
3
2
1
0
490.1
468.1
957.3
527.1
573.2
597.0
310.1
393.3
436.3
680.3
722.5
776.6
860.4
300
400
500
600
700
800
900
m/z

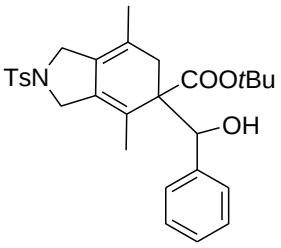

^{1}H NMR ($CDCl_3$, 400 MHz)

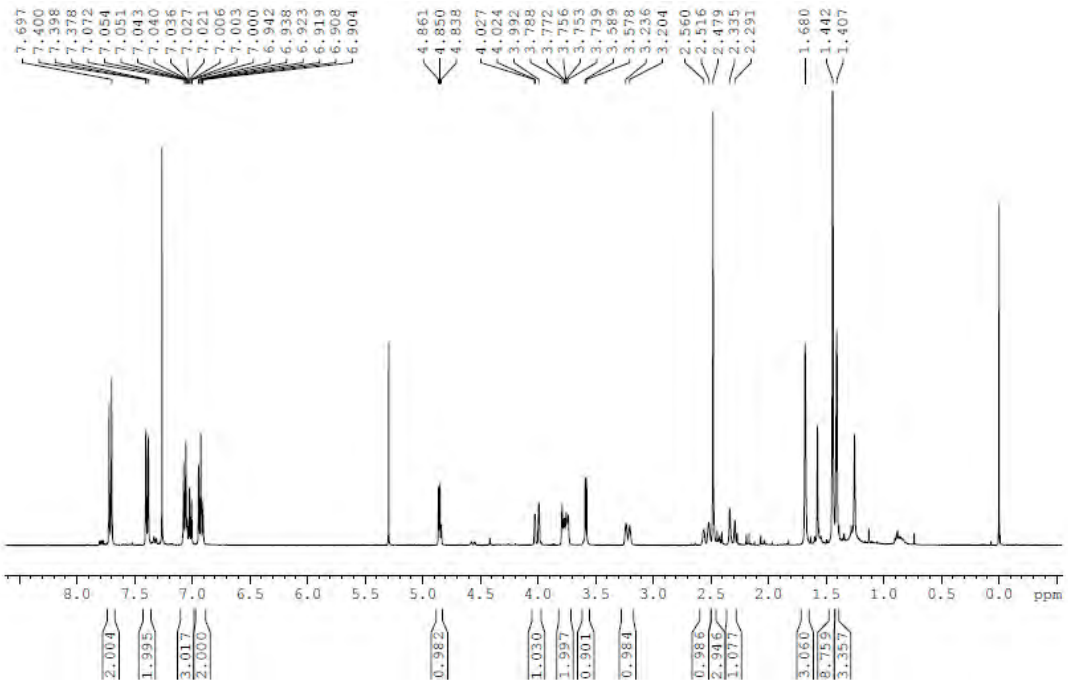

^{13}C NMR ($CDCl_3$, 75 MHz)

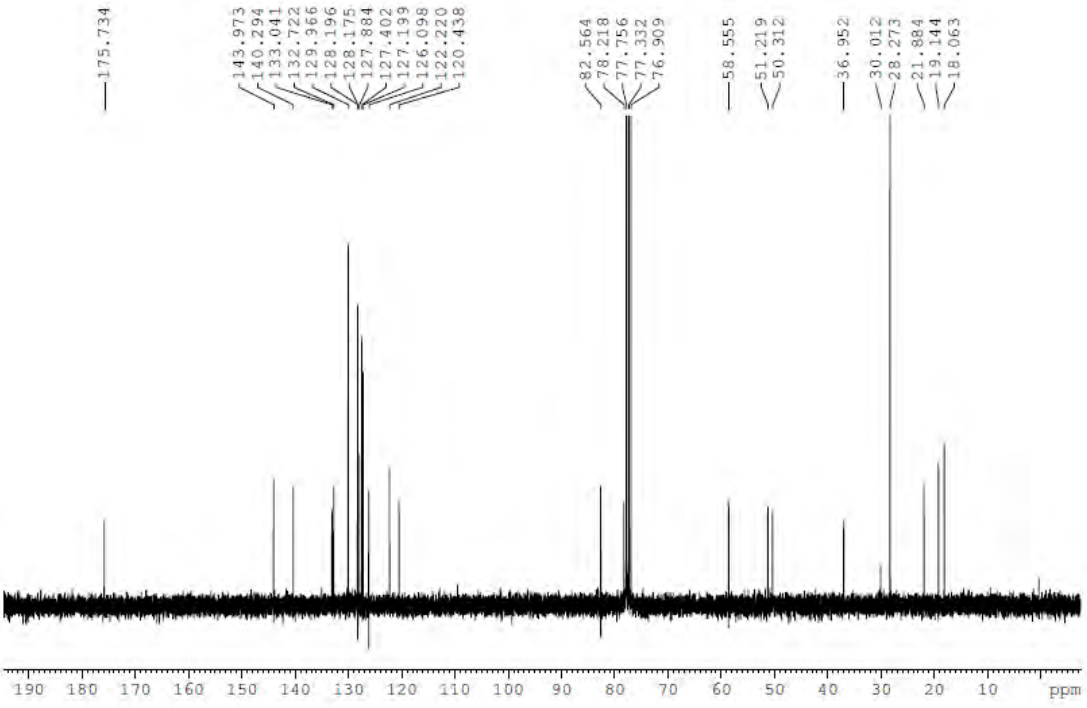

ESI-MS (+)

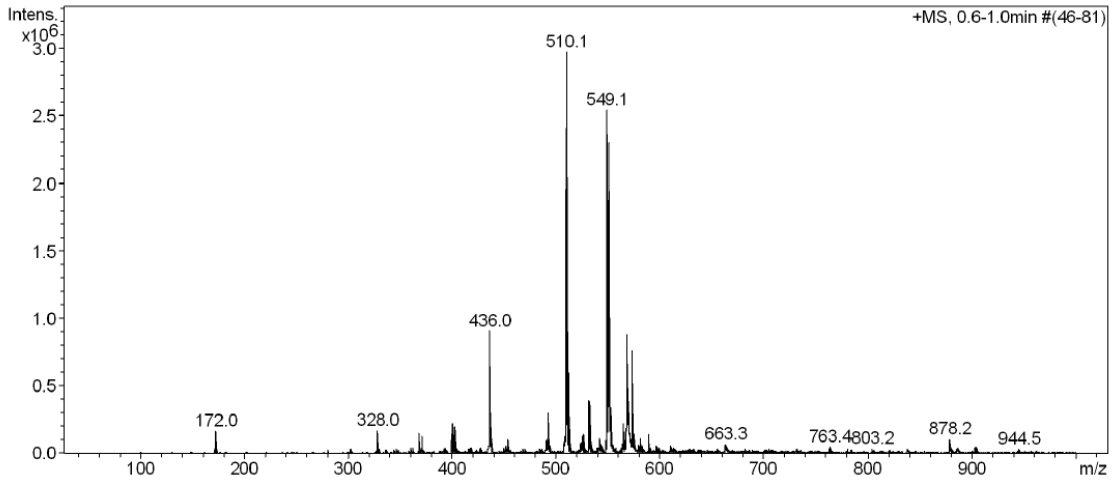

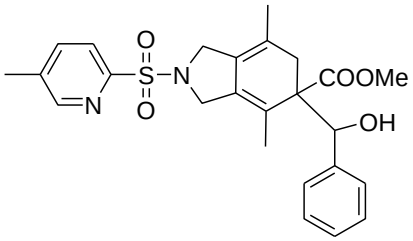

^{1}H NMR ($CDCl_3$, 300 MHz)

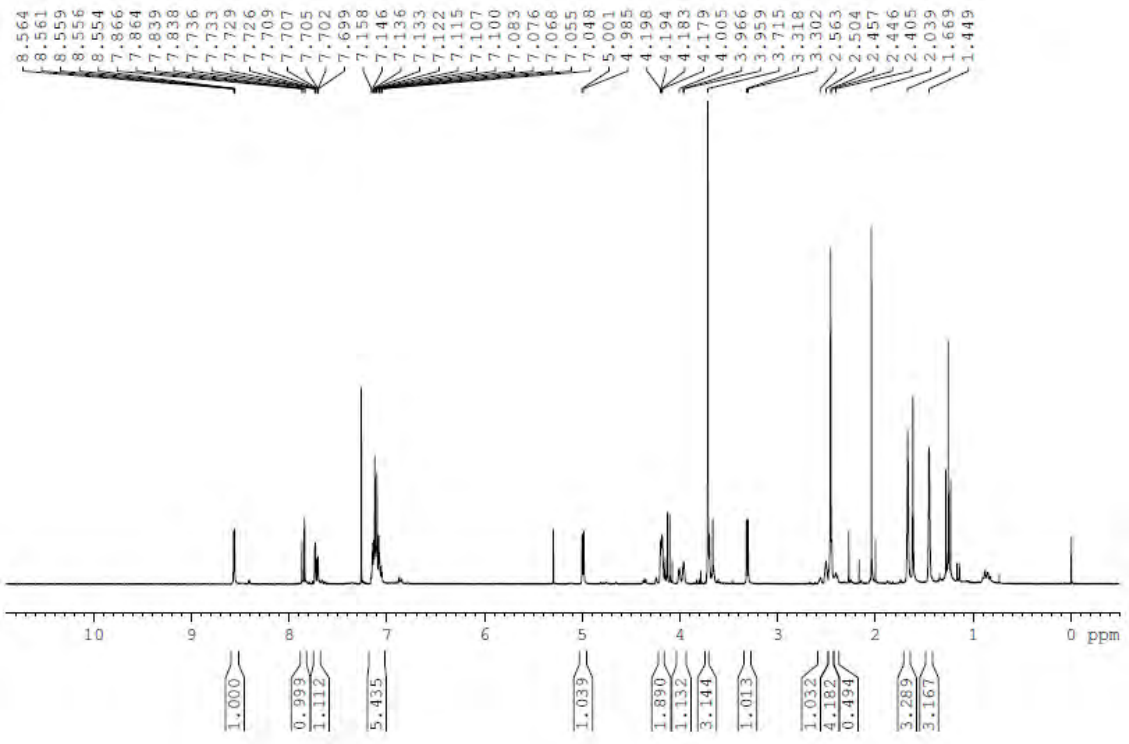

^{13}C NMR ($CDCl_3$, 75 MHz)

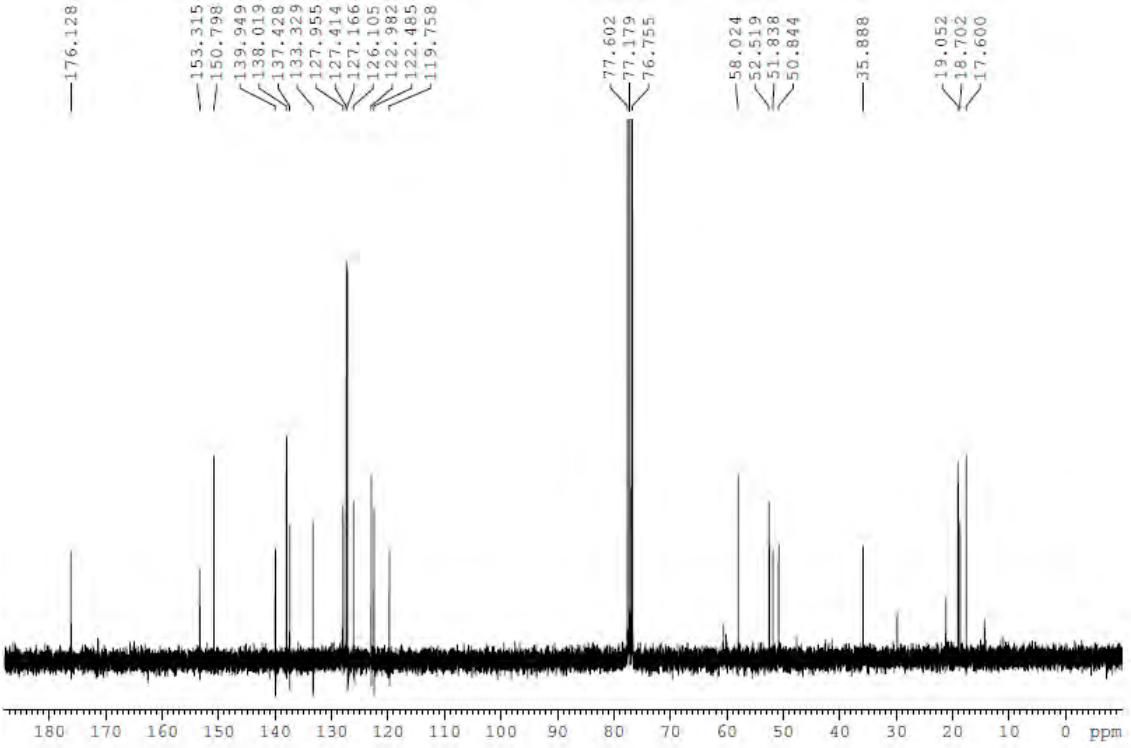

IR (ATR)

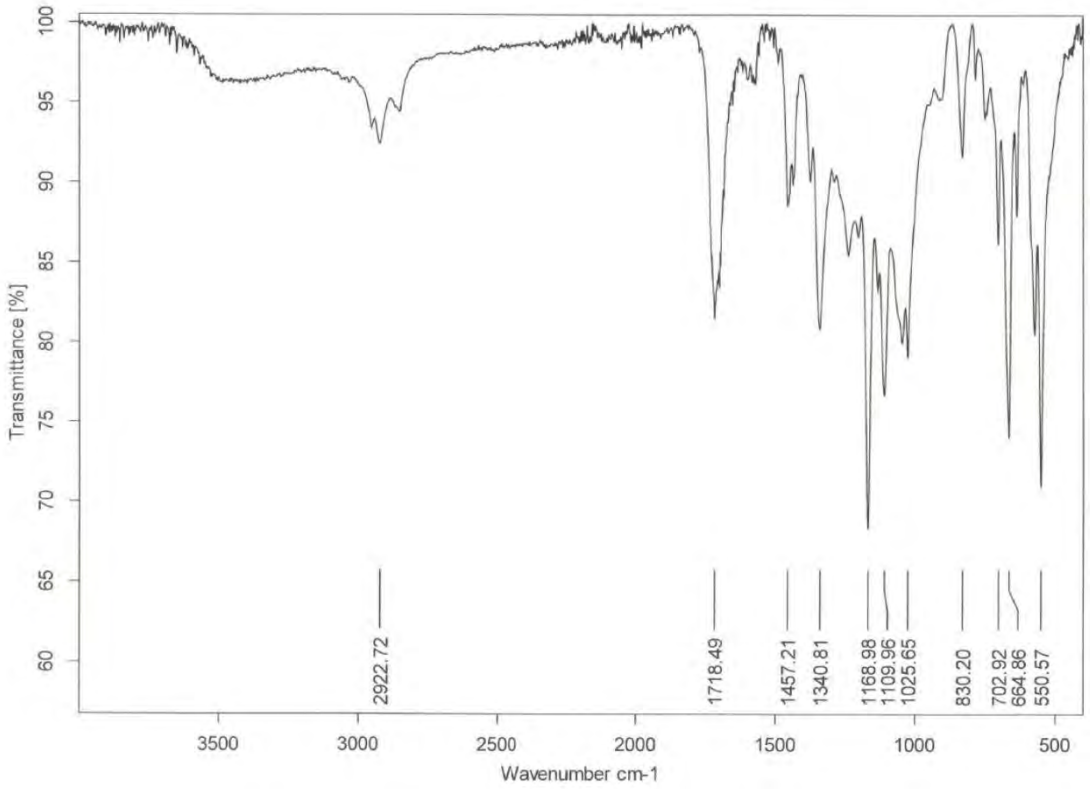

ESI-MS (+)

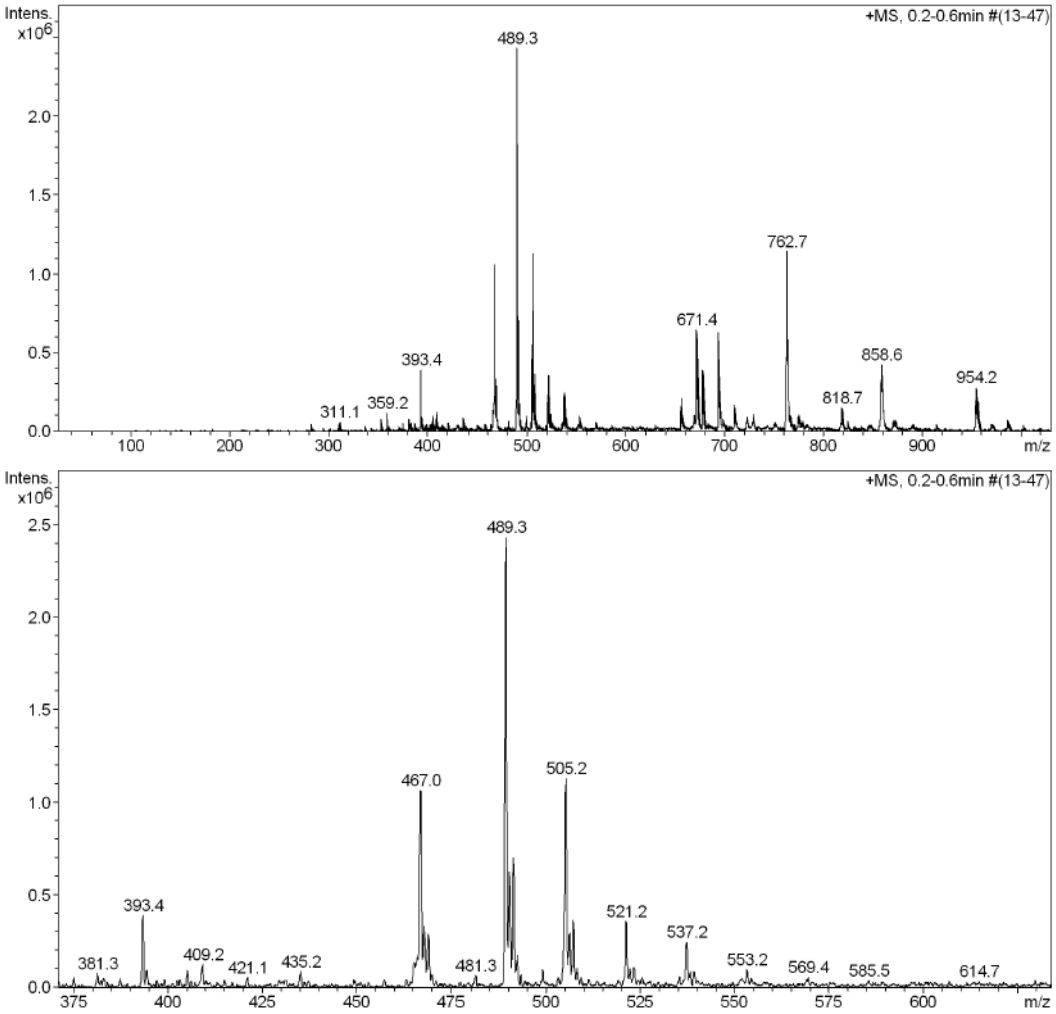
Intens.
x10^6
+MS, 0.2-0.6min #(13-47)
489.3
762.7
671.4
393.4
858.6
954.2
818.7
359.2
311.1
m/z
Intens.
x10^6
+MS, 0.2-0.6min #(13-47)
489.3
467.0
505.2
393.4
521.2
537.2
381.3
409.2
421.1
435.2
481.3
553.2
569.4
585.5
614.7
m/z

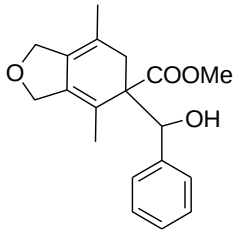

^{1}H NMR ($CDCl_3$, 400 MHz)

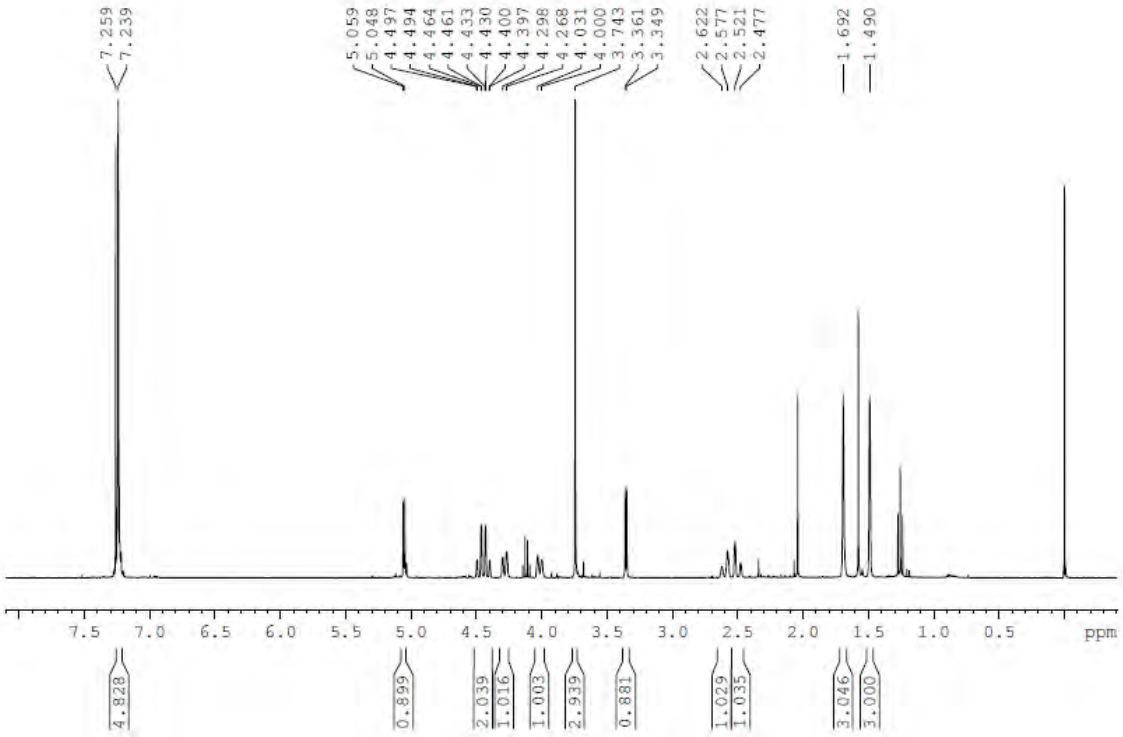

^{13}C NMR ($CDCl_3$, 75 MHz)

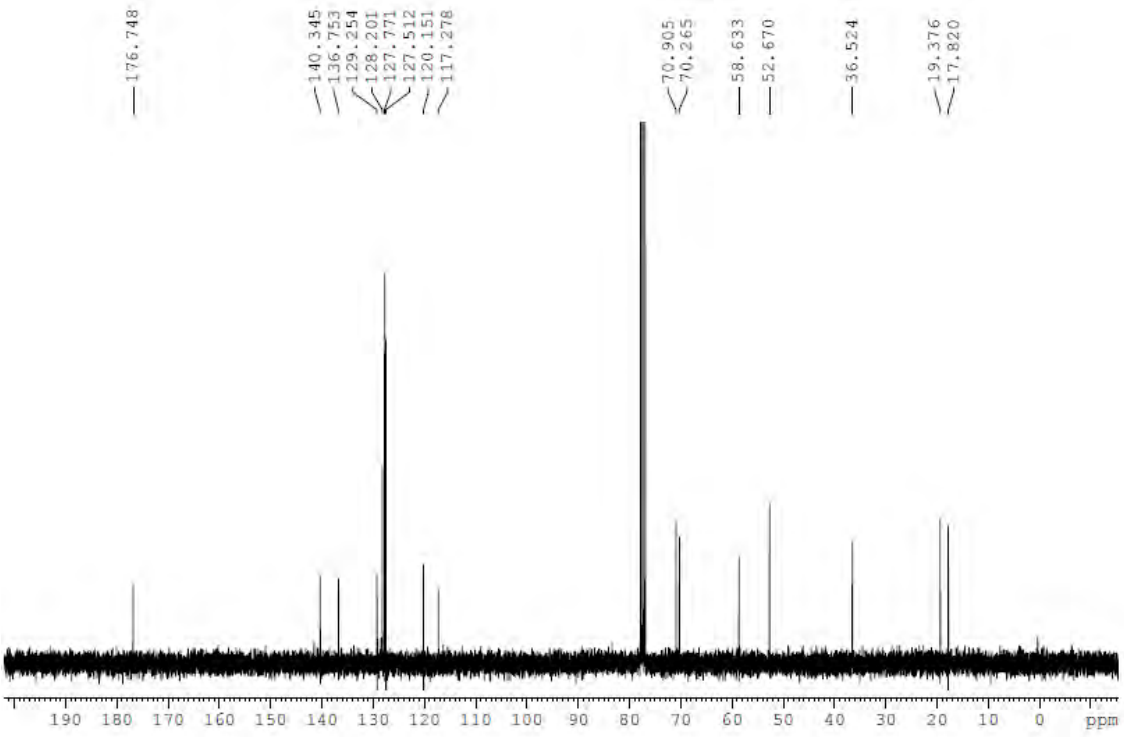

IR (ATR)

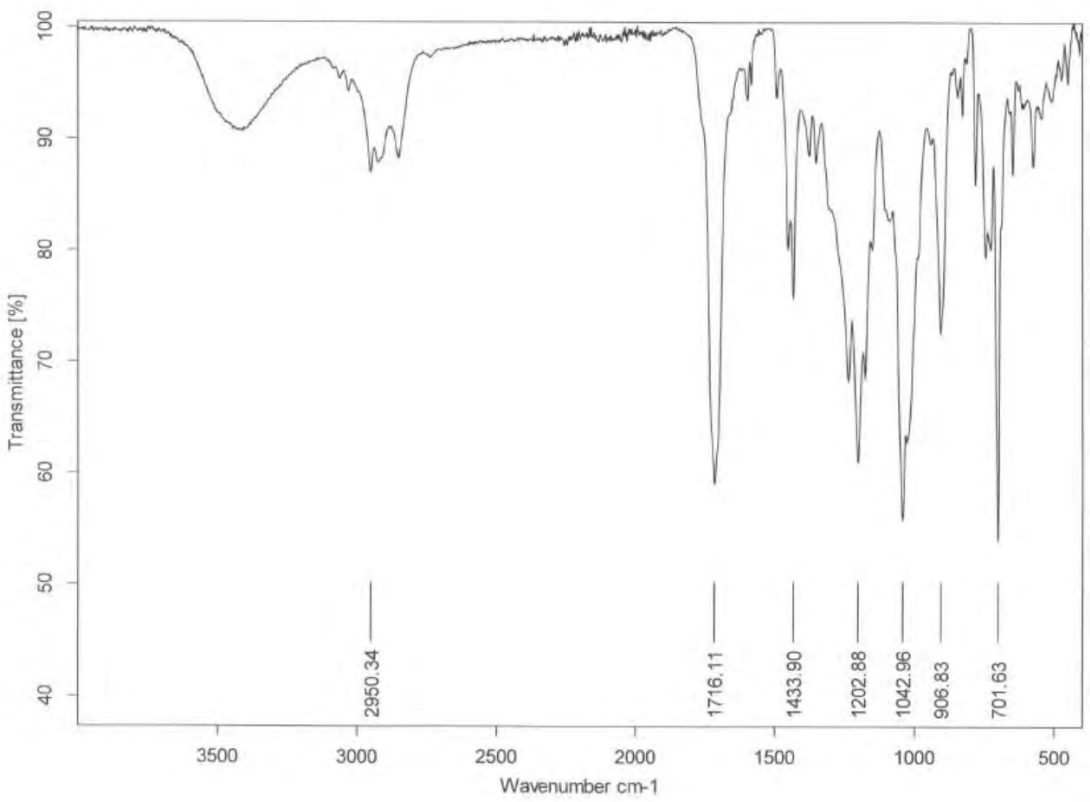
Transmittance [%]
100
90
80
70
60
50
40
2950.34
1716.11
1433.90
1202.88
1042.96
906.83
701.63
3500
3000
2500
2000
1500
1000
500
Wavenumber cm-1

ESI-MS (+)

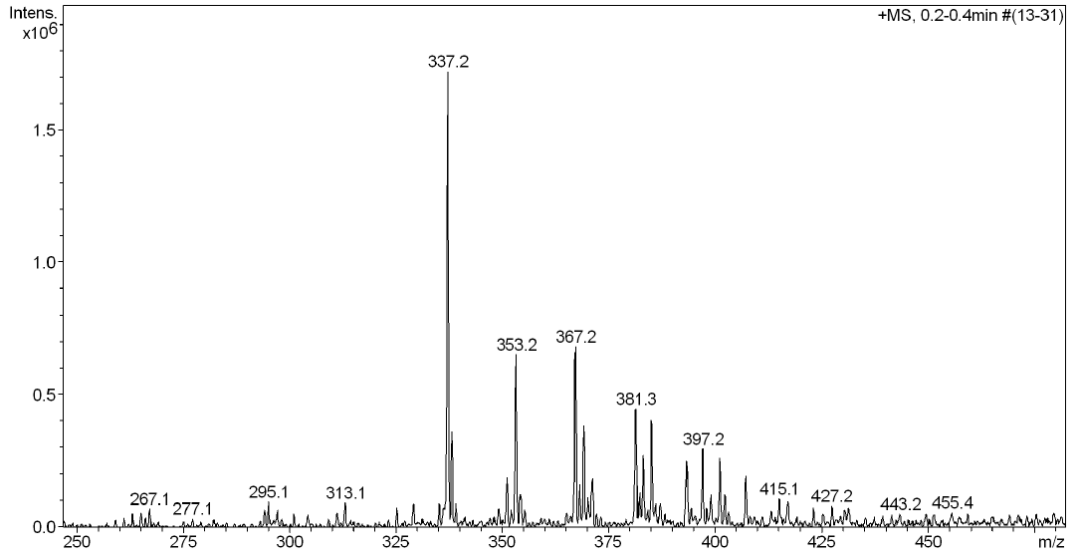
Intens.
x10^6
+MS, 0.2-0.4min #(13-31)
1.5
1.0
0.5
0.0
337.2
353.2
367.2
381.3
397.2
267.1
277.1
295.1
313.1
415.1
427.2
443.2
455.4
250
275
300
325
350
375
400
425
450
m/z

ESI-HRMS (+)

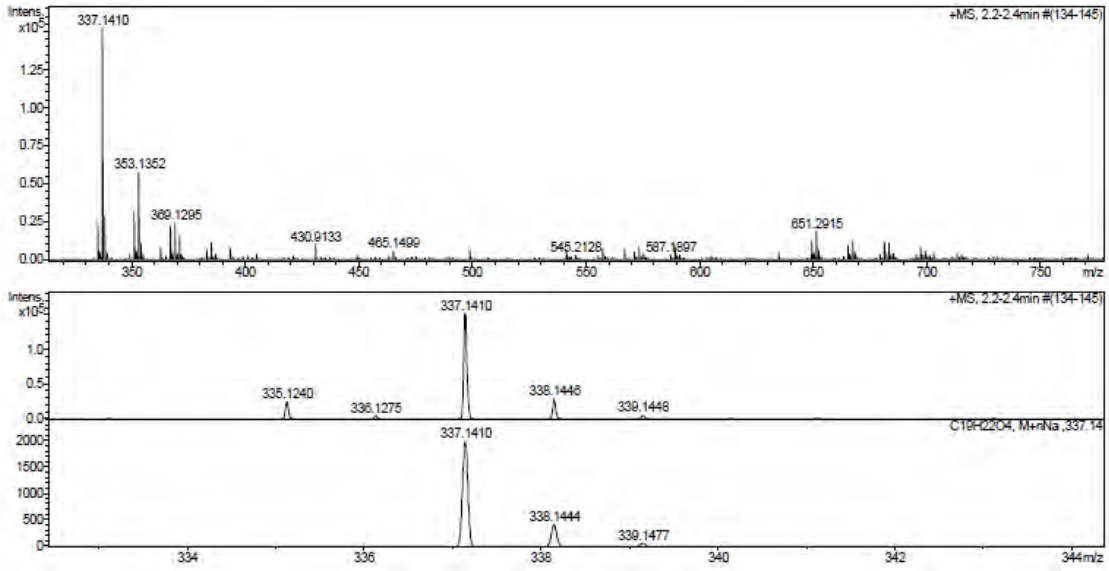

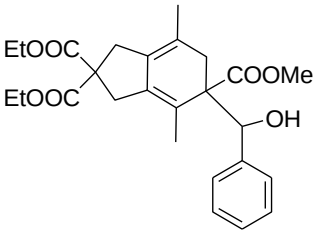

^{1}H NMR ($CDCl_3$, 400 MHz)

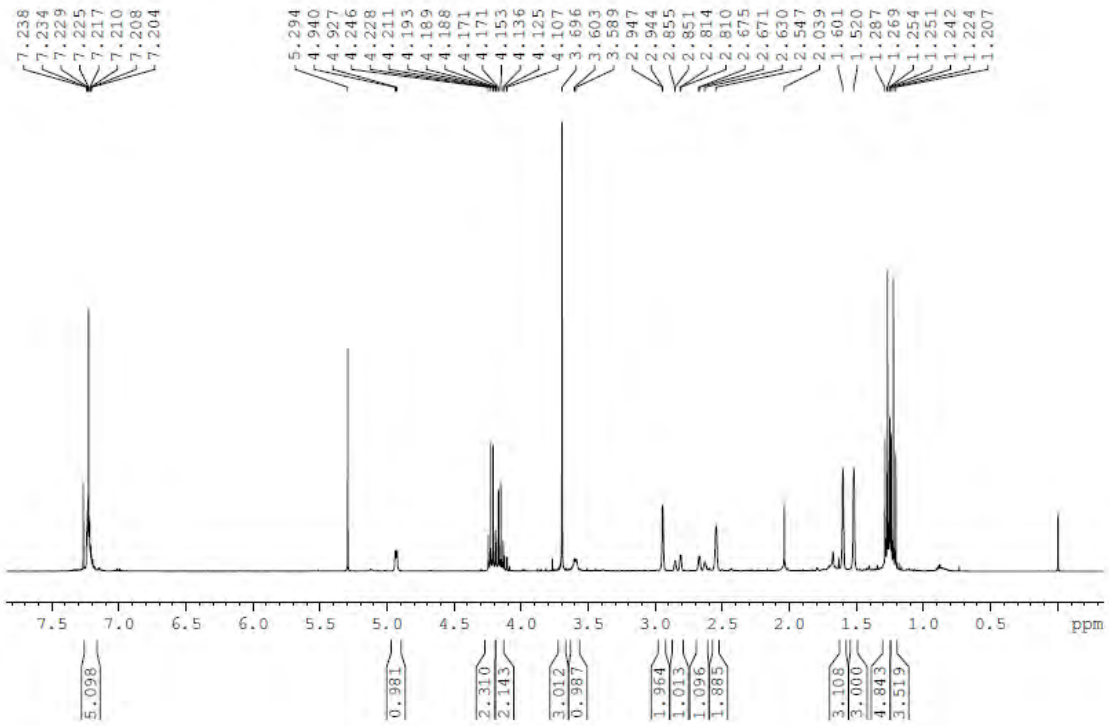

^{13}C NMR ($CDCl_3$, 75 MHz)

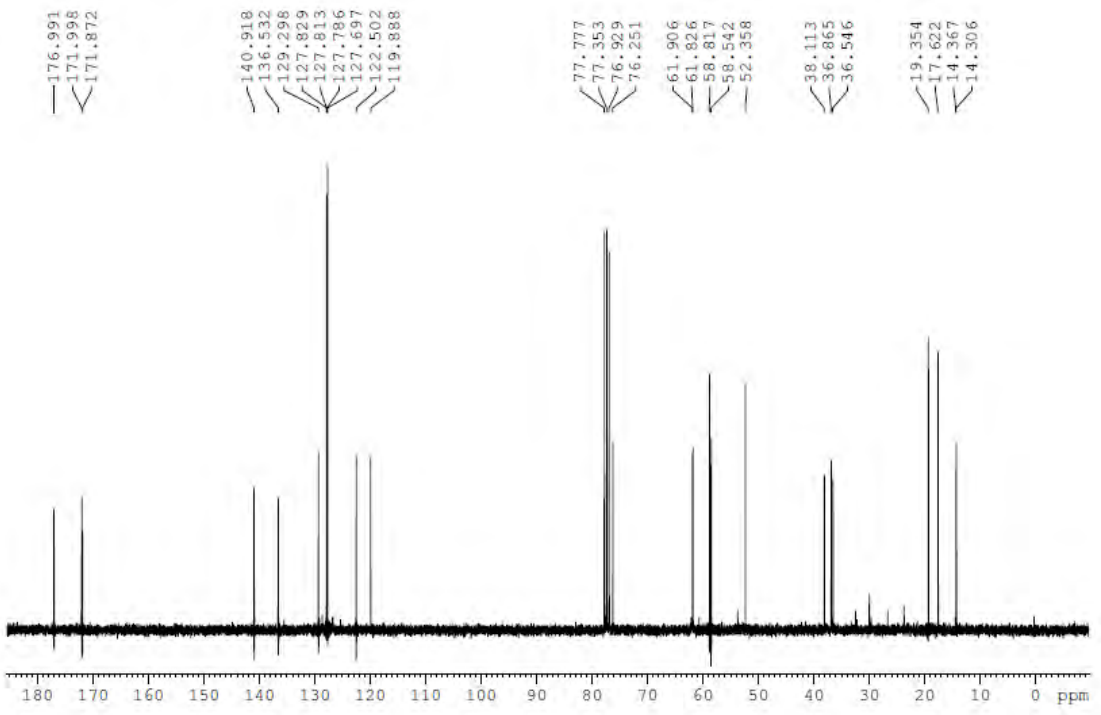

IR (ATR)

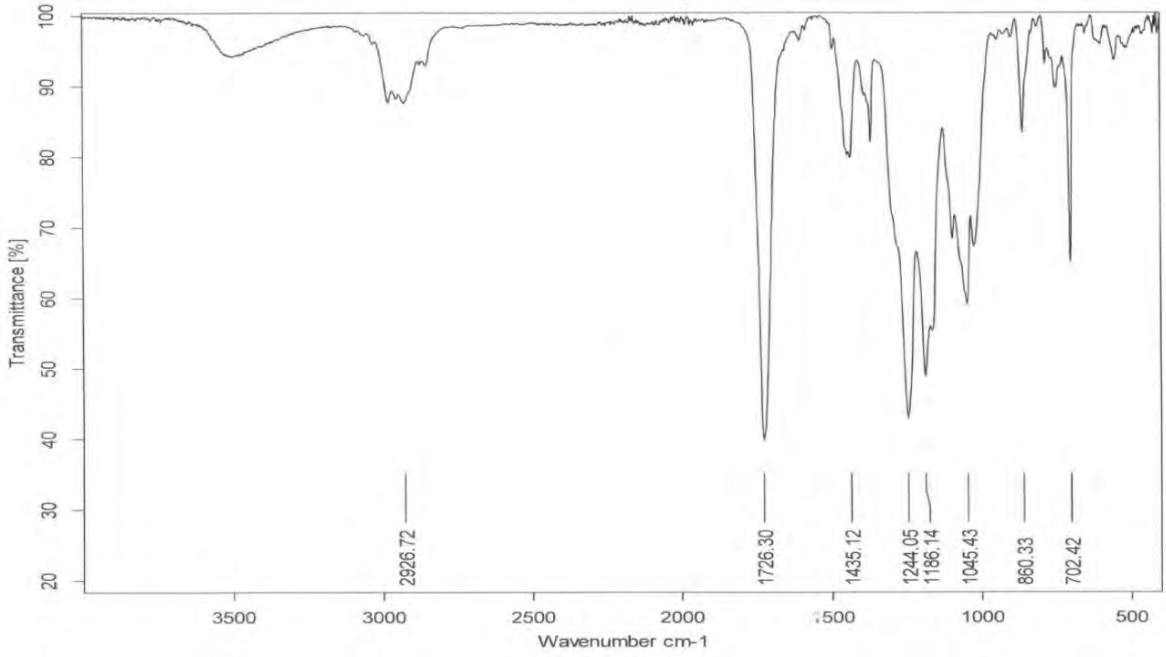

ESI-MS (+)

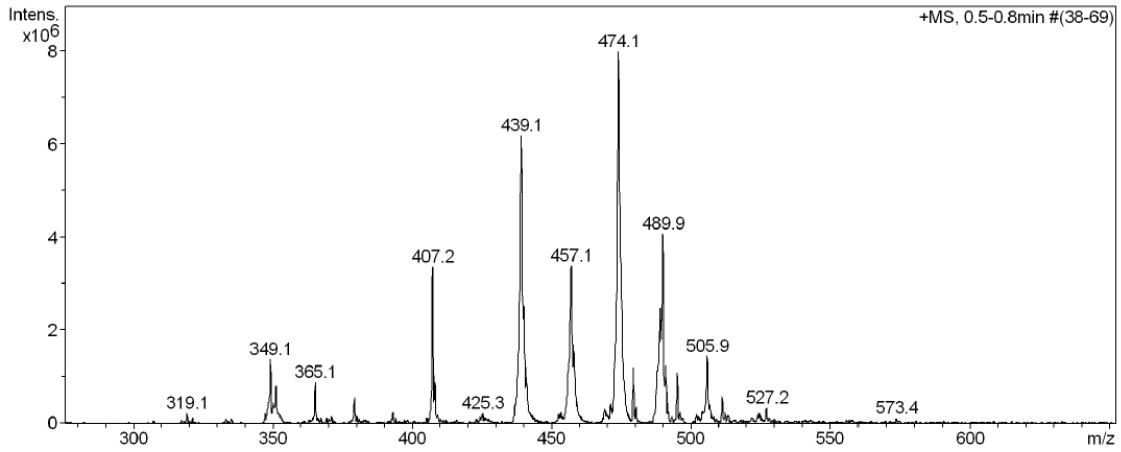

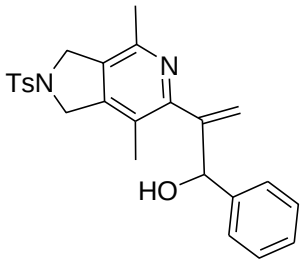

^{1}H NMR ($CDCl_3$, 300 MHz)

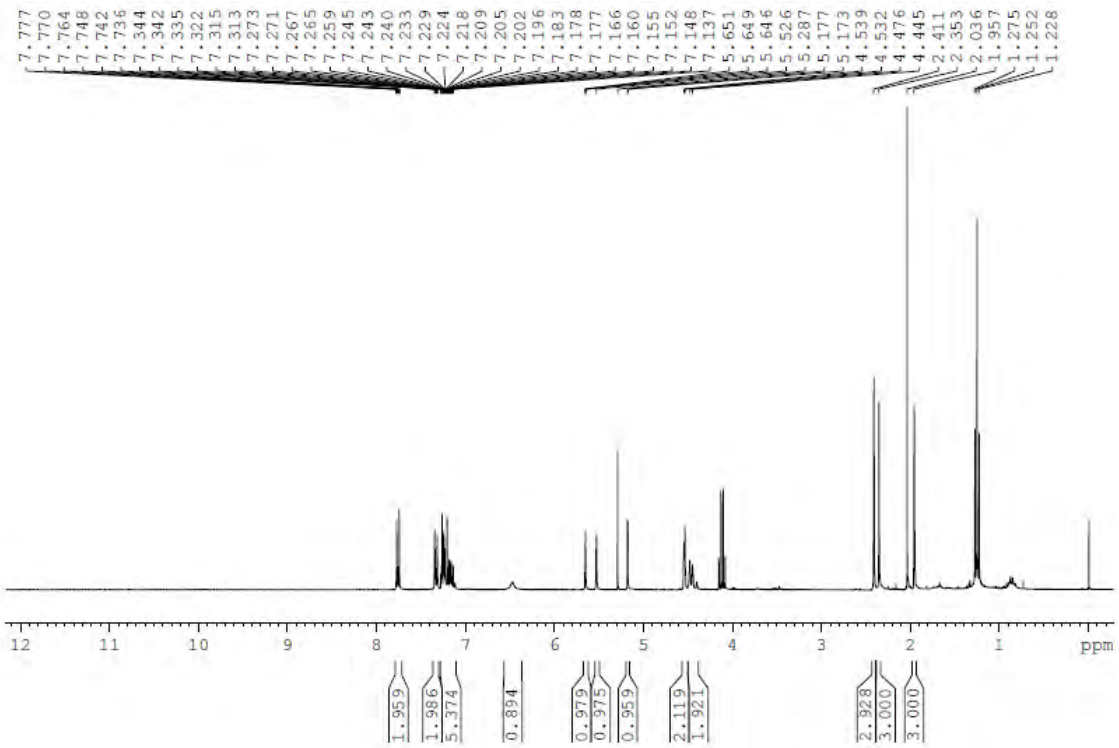

^{13}C NMR (CDCl3, 75 MHz)

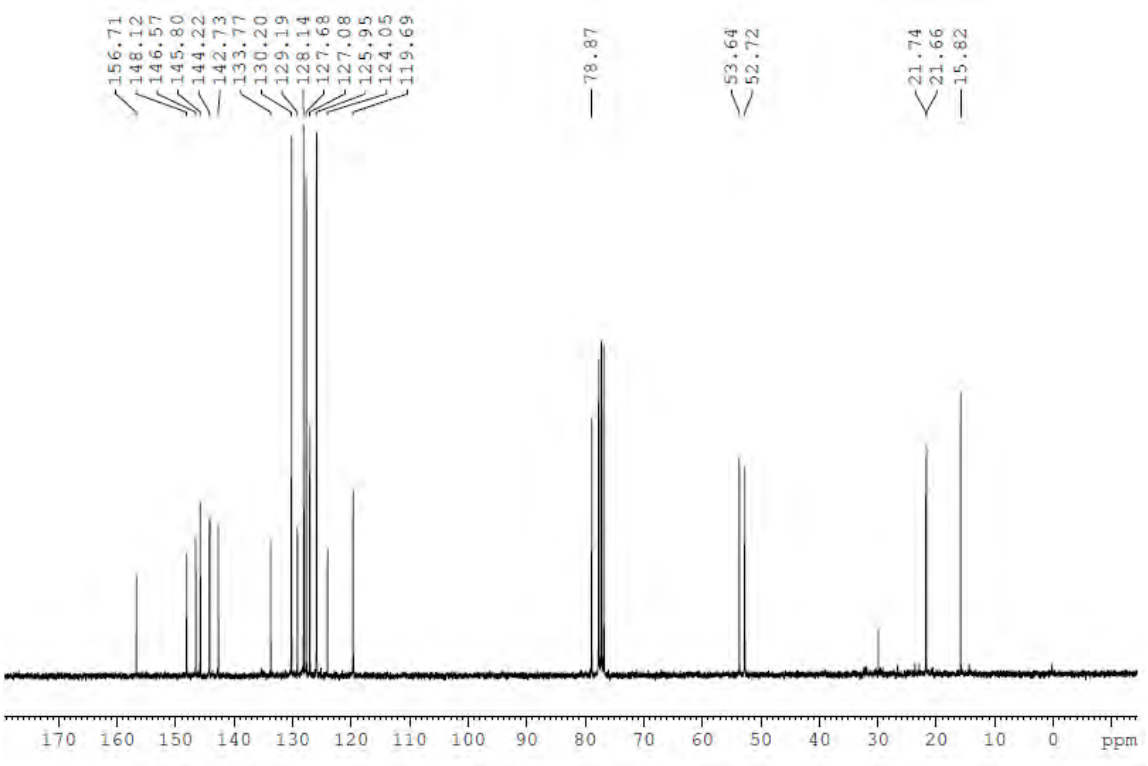

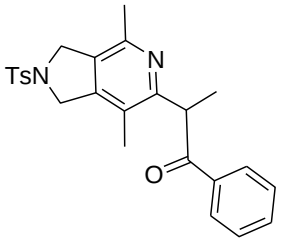

^{1}H NMR ($CDCl_3$, 300 MHz)

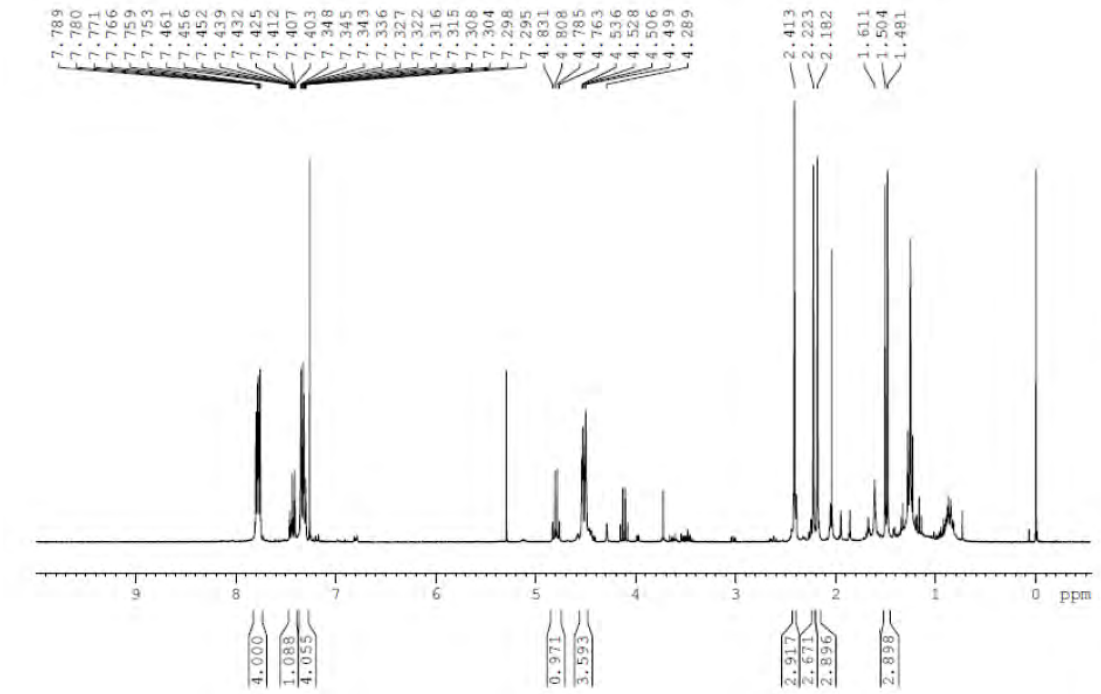

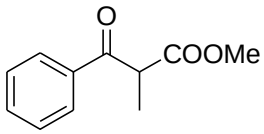

^{1}H NMR ($CDCl_3$, 300 MHz)

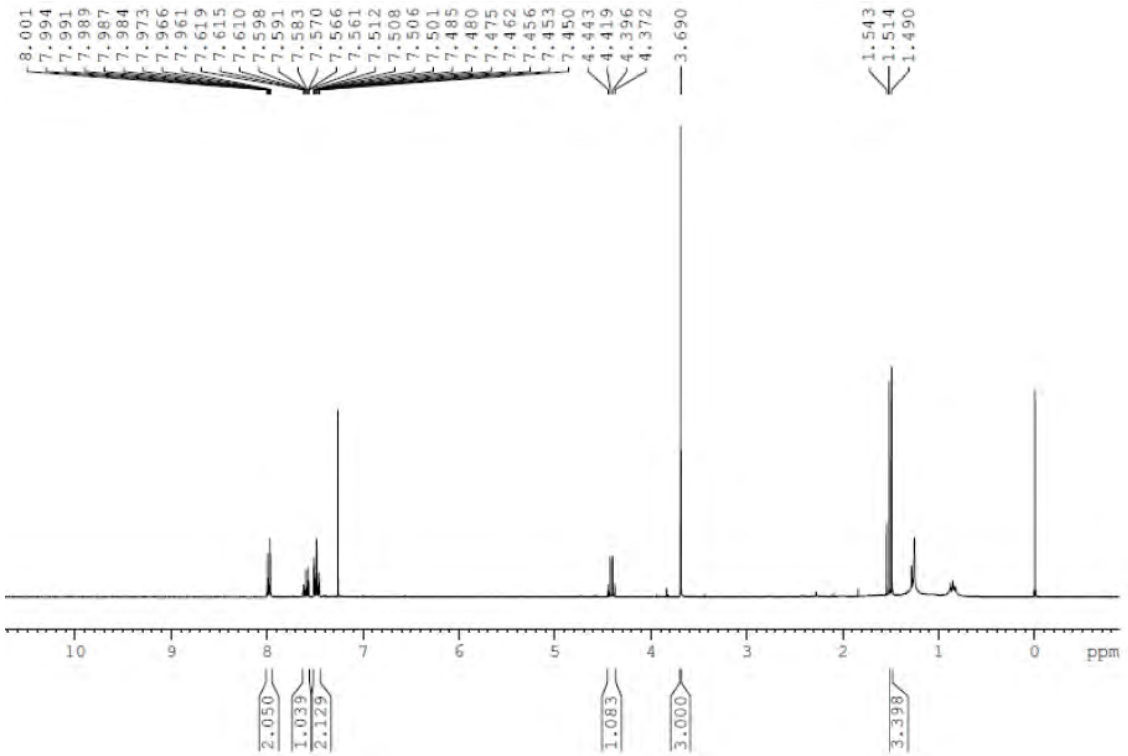

^{13}C NMR ($CDCl_3$, 75 MHz)

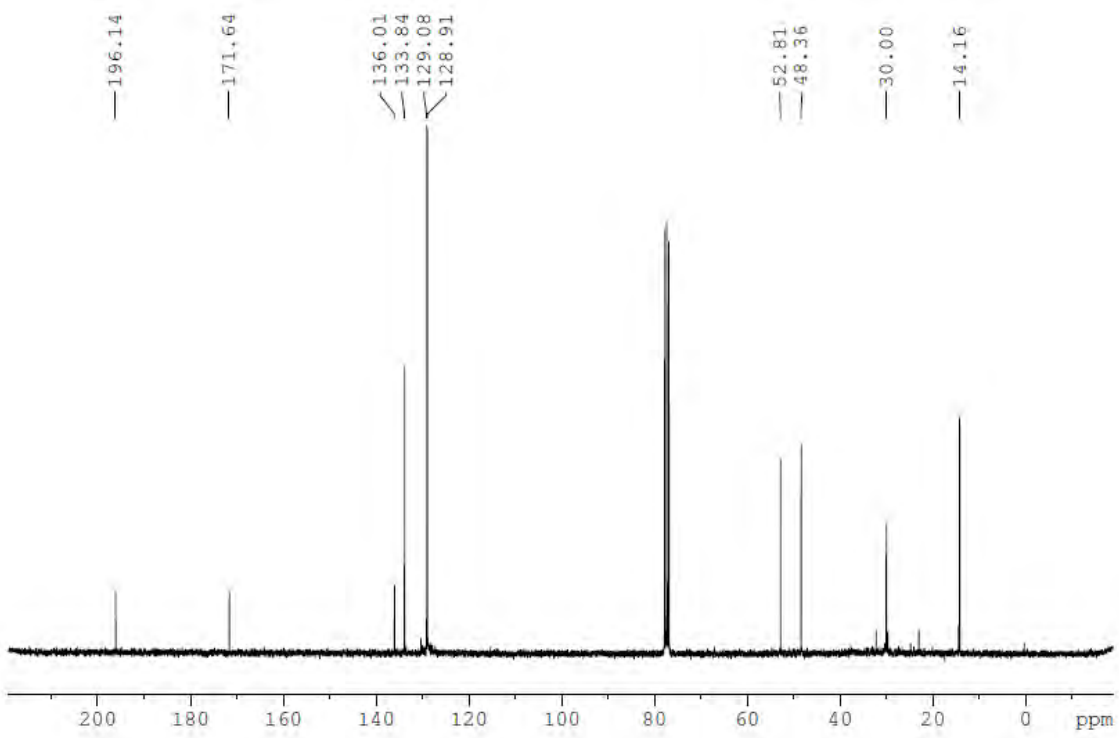

ESI-MS(+)

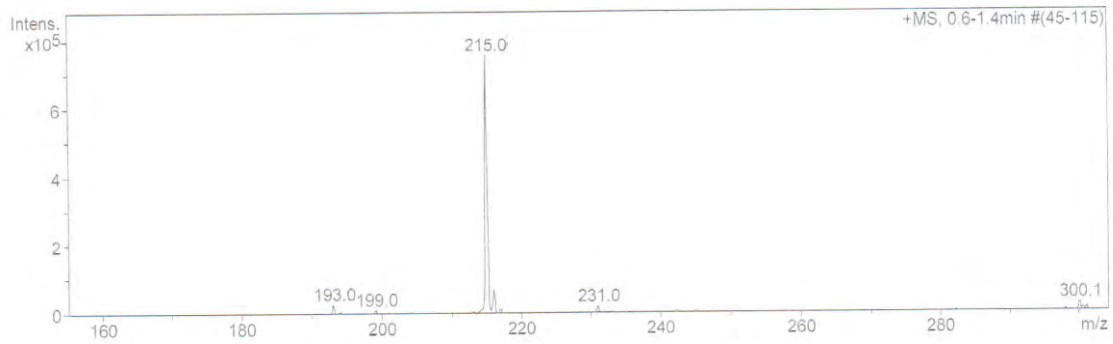

Figure 1. Chromatogram of *rac*-**38aa** (using IPA/heptanes 50:50 as eluent)

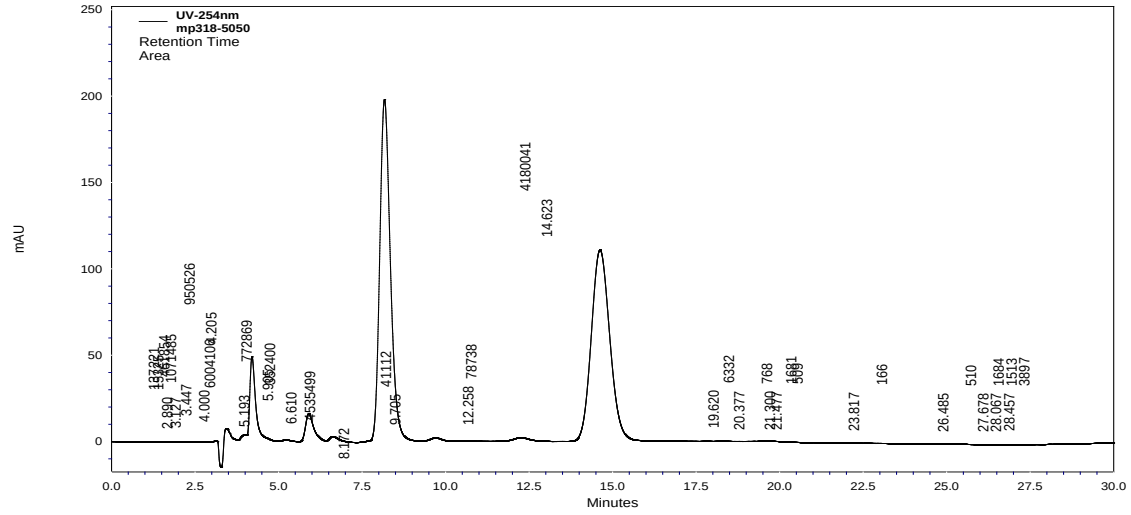

Figure 2. Chromatogram of **38aa** (using (*R*)-BINAP)

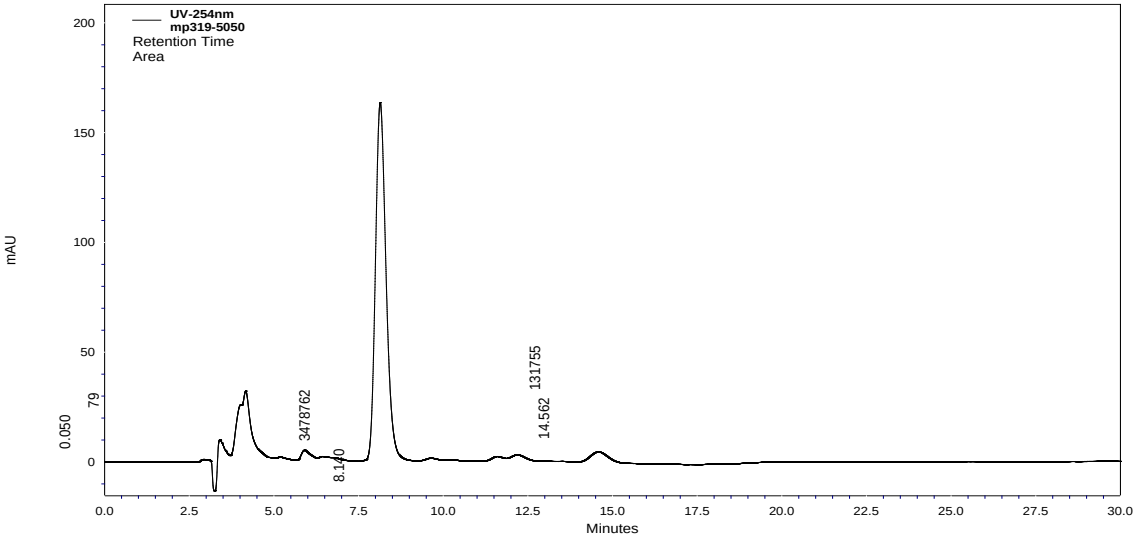

Figure 3. Chromatogram of **38aa** (using (*S*)-BINAP)

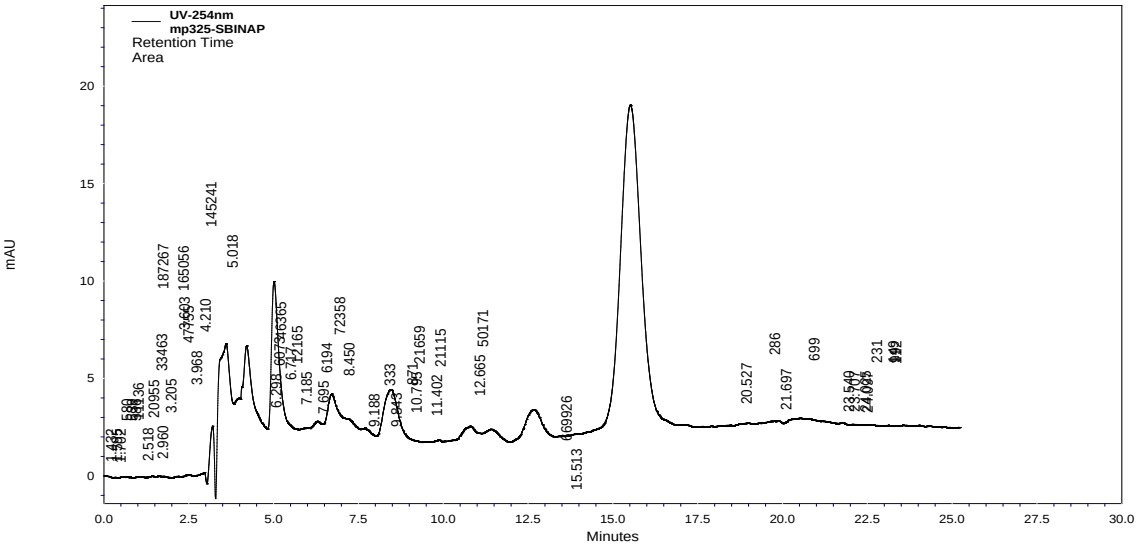

Figure 4. Chromatogram *rac*-**38ab** (using IPA/heptanes 60:40 as eluent)

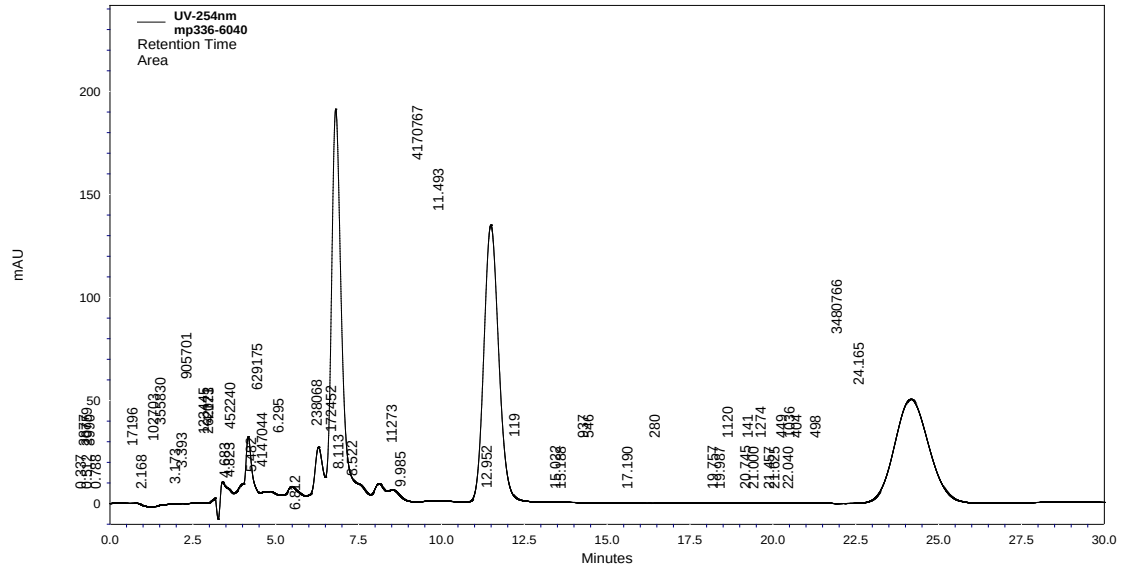

Figure 5. Chromatogram **38ab** (using (*R*)-BINAP)

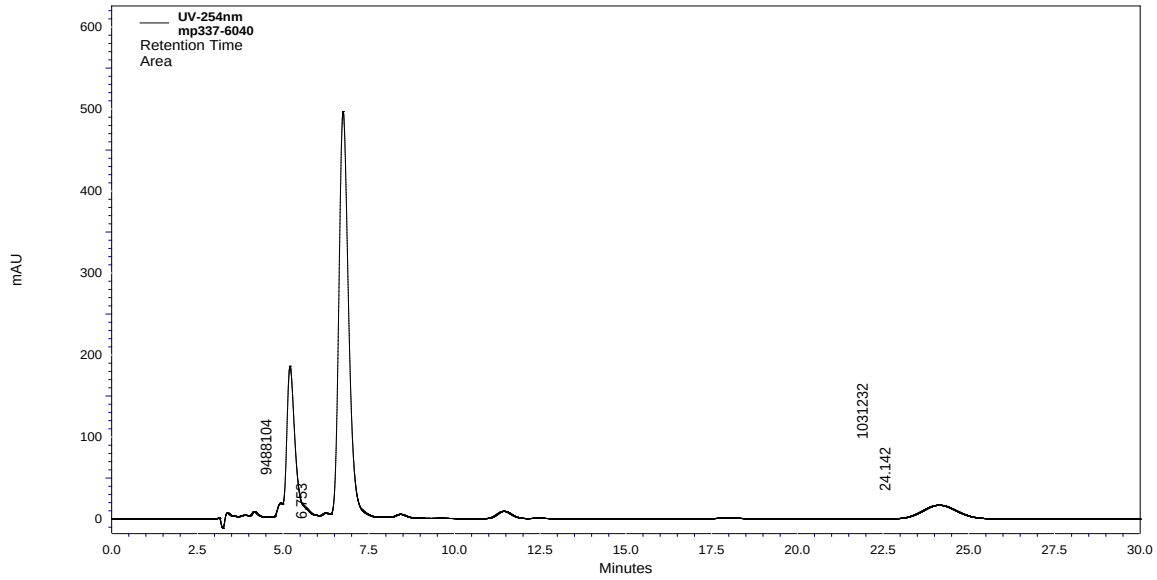

Figure 6. Chromatogram of *rac*-**38ac** + homocoupling product of diyne **16a** (using IPA/heptanes 40:60 as eluent).

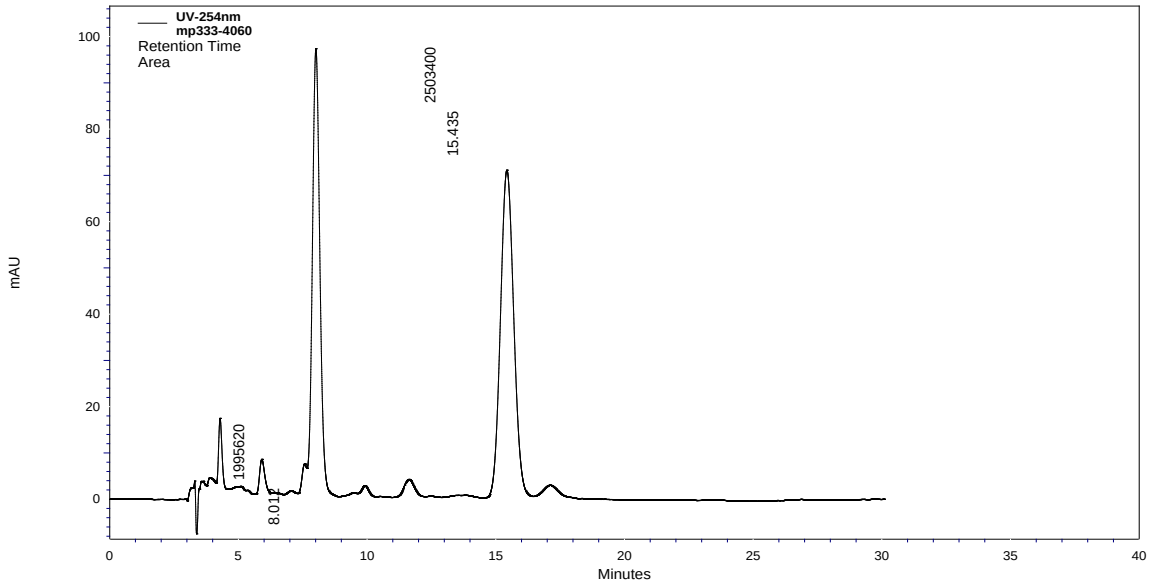

Figure 7. Chromatogram of **38ac** (using (*R*)-BINAP)

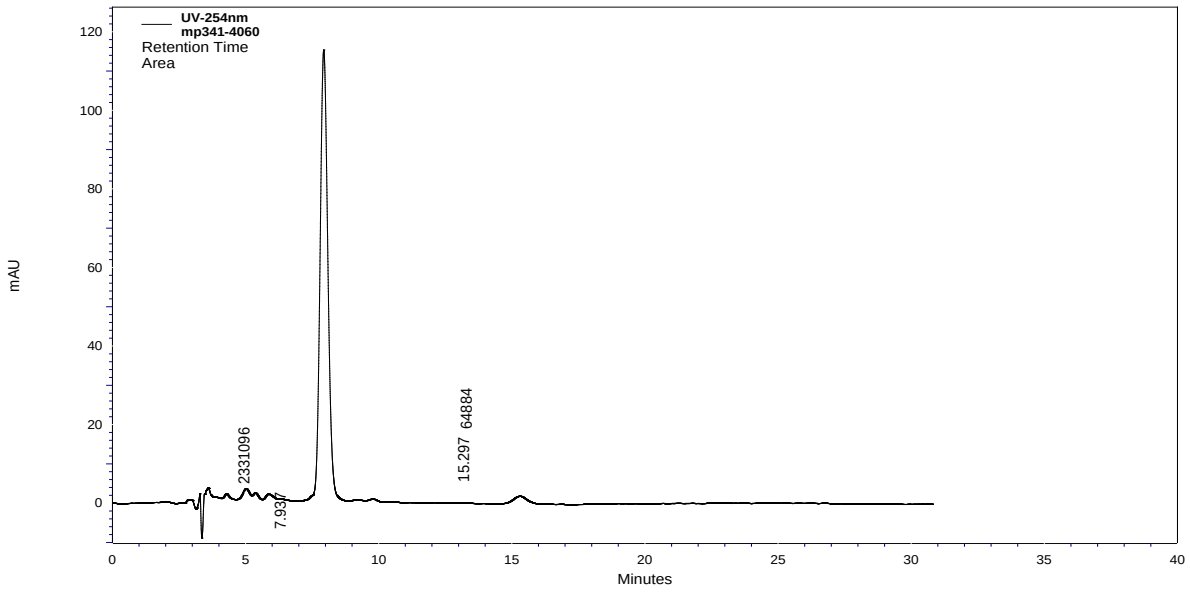

Figure 8. Chromatogram *rac*-**38ba** (using IPA/heptanes 5:95 as eluent).

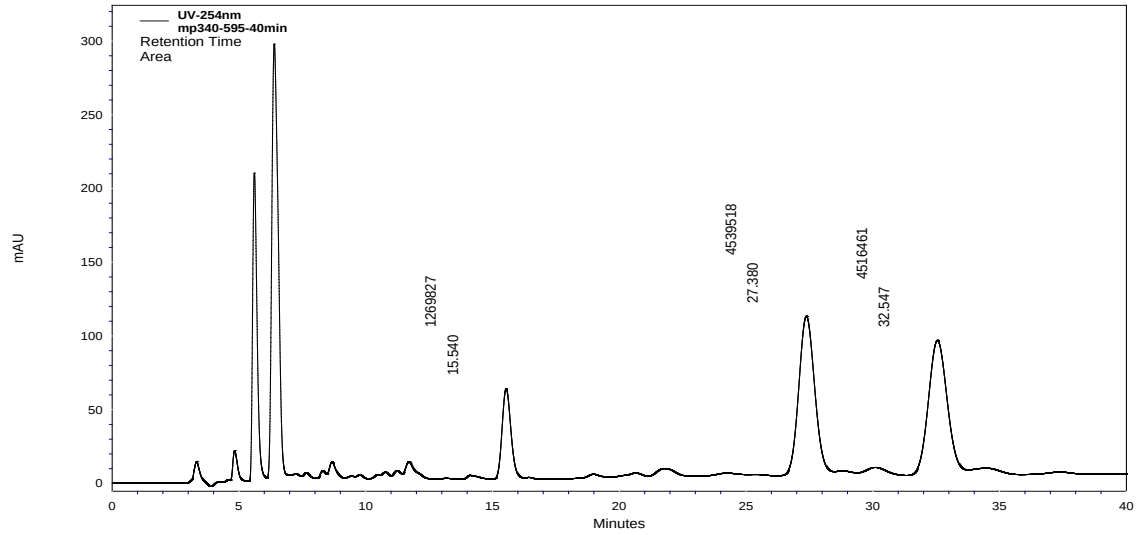

Figure 9. Chromatogram **38ba** (using (*R*)-BINAP)

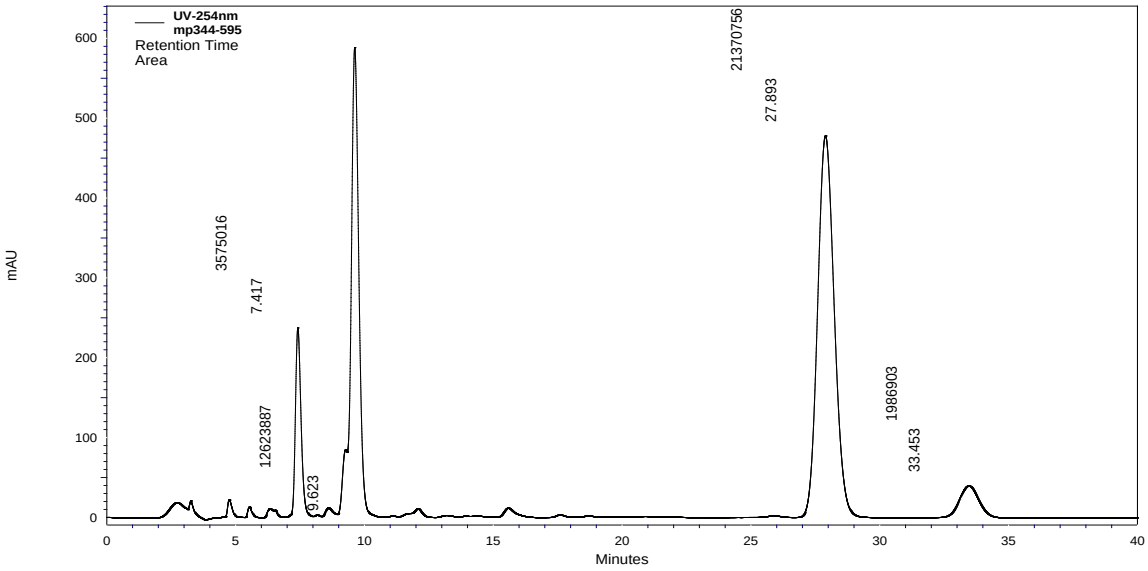

Figure 10. Chromatogram **38ca** (using (*R*)-BINAP and IPA/heptanes 5:95 as eluent).

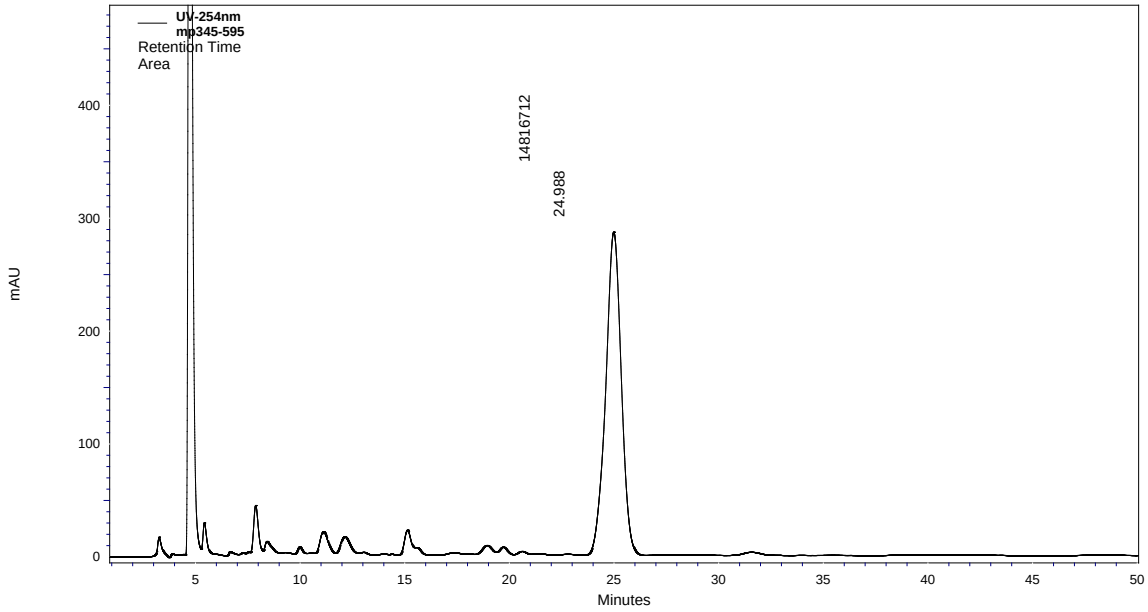

Figure 11. Chromatogram *rac*-**38da** (using IPA/heptanes 40:60 as eluent).

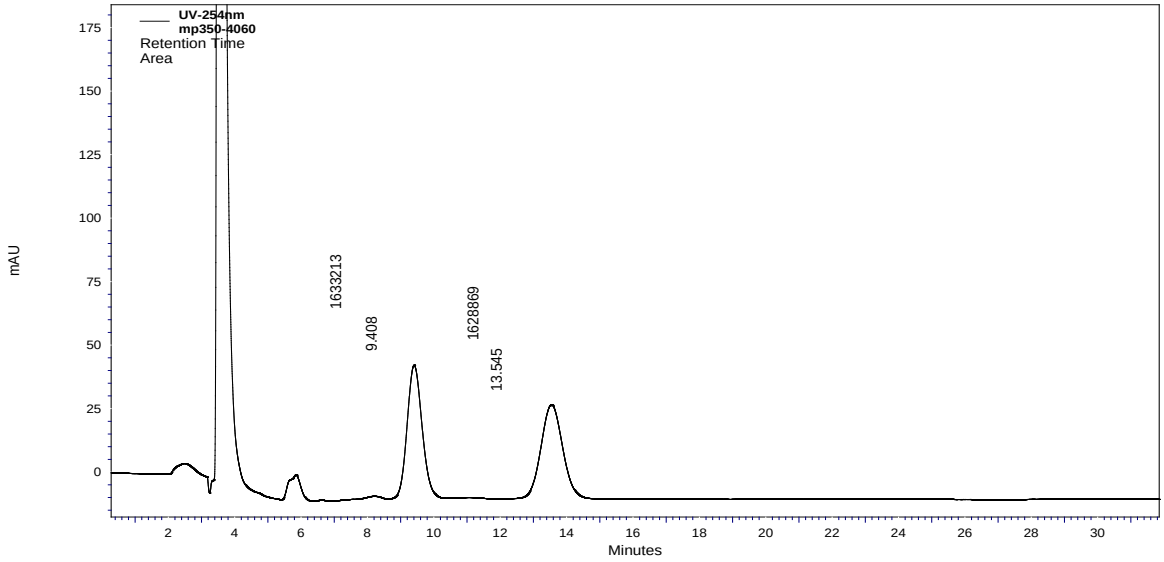

Figure 12. Chromatogram **38da** (using (*R*)-BINAP)

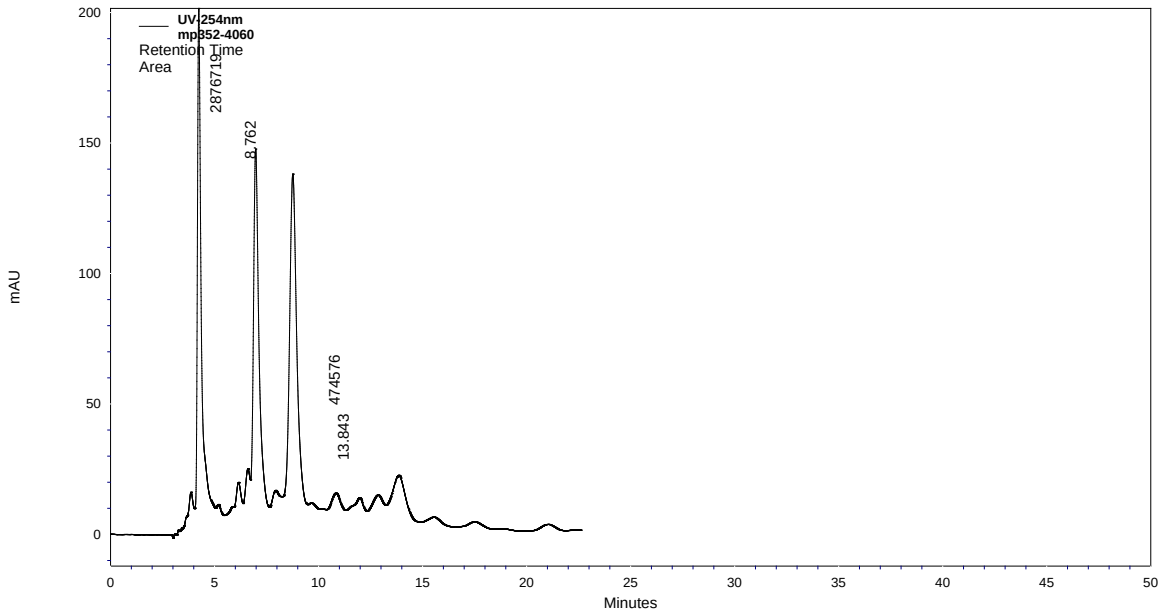

Figure 10. Chromatogram **38bb** (using (*R*)-BINAP and IPA/heptanes 5:95 as eluent).

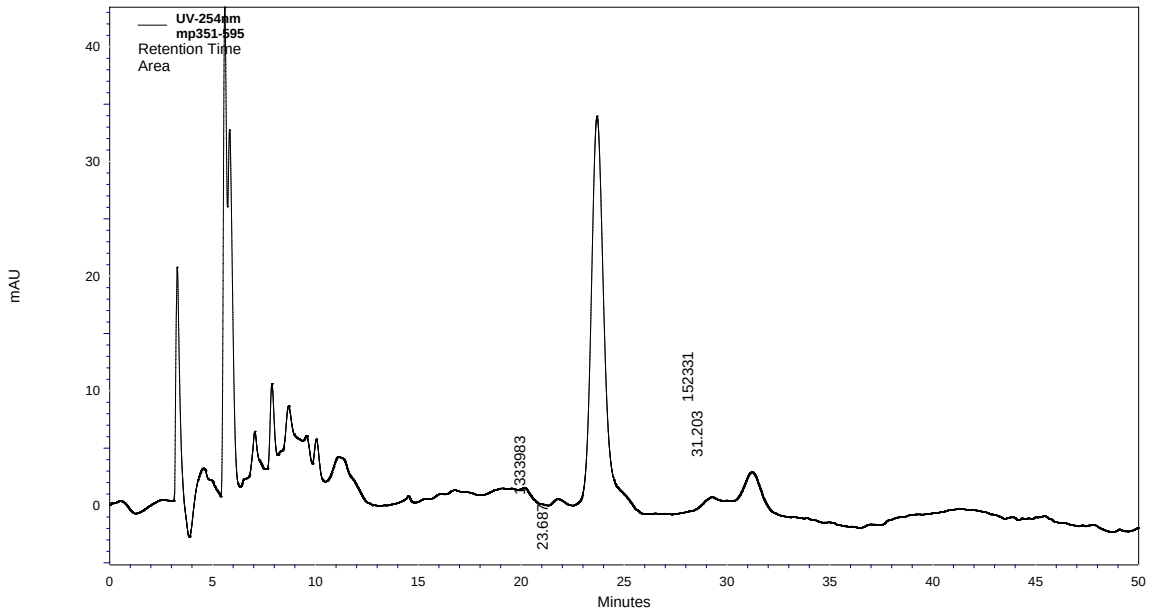

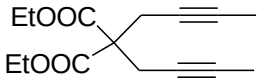

^{1}H NMR (400 MHz, $CDCl_3$)

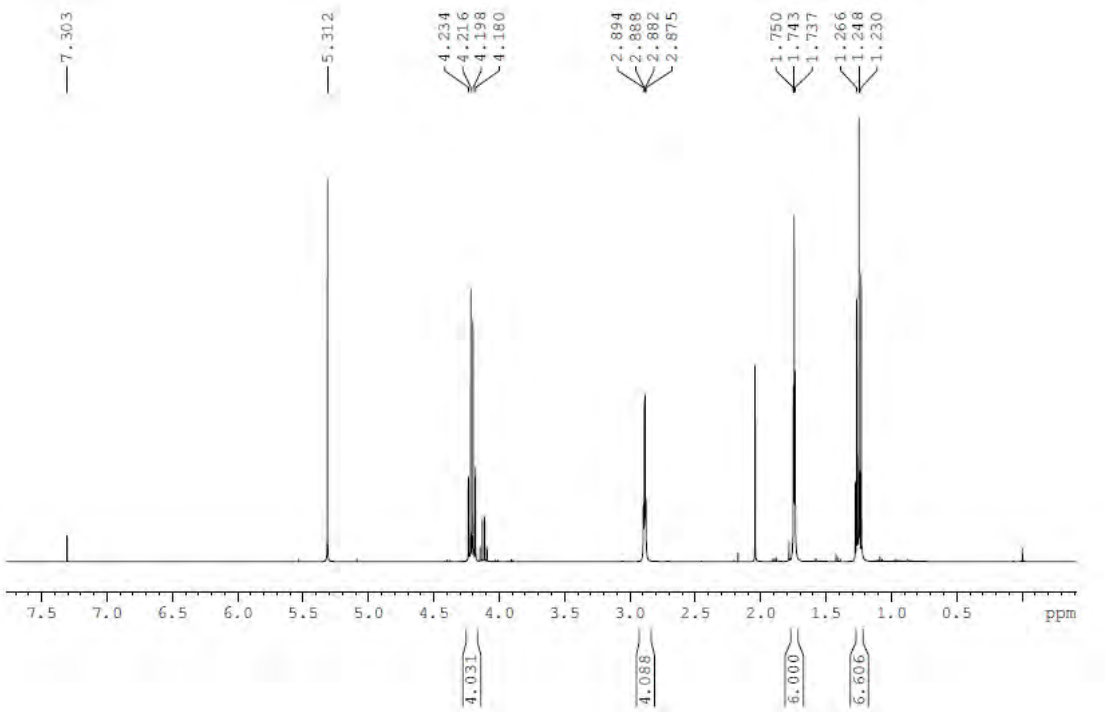

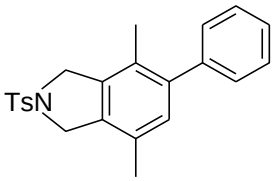

^{1}H NMR (400 MHz, $CDCl_3$)

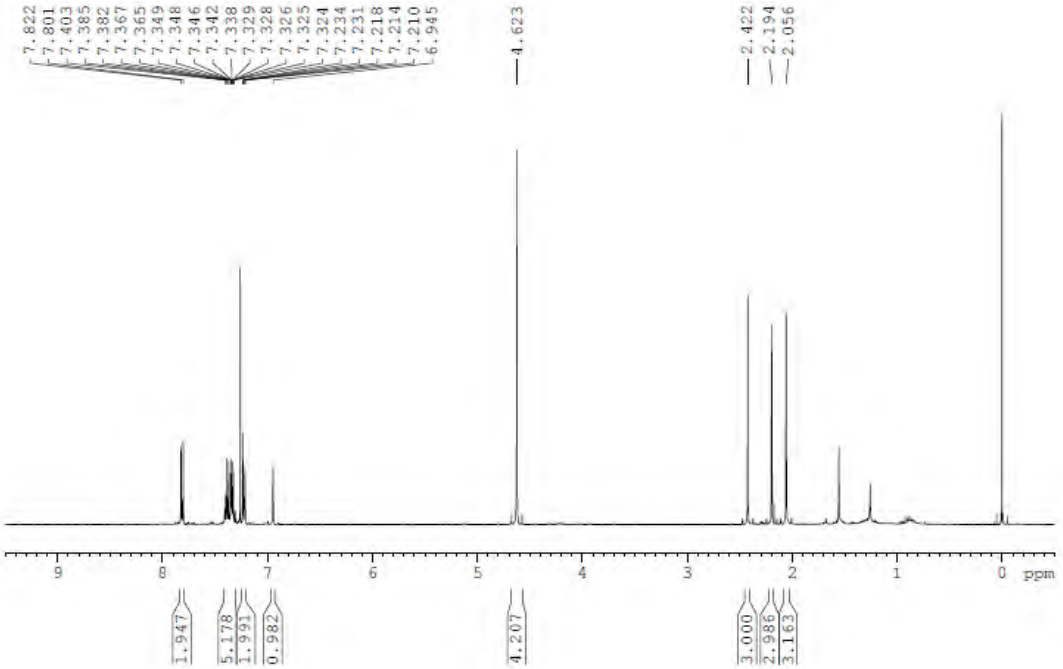

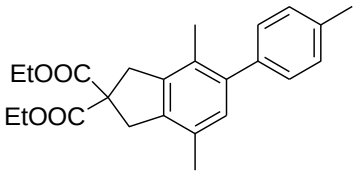

^{1}H NMR (300 MHz, $CDCl_3$)

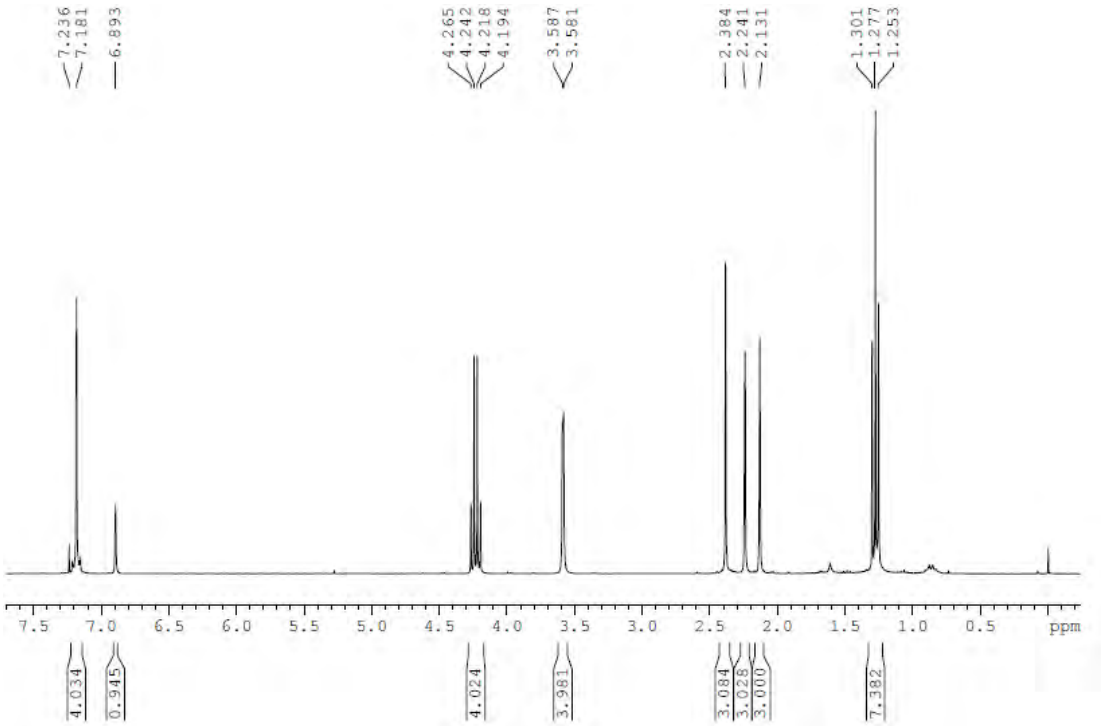

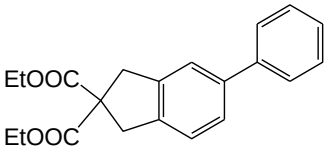

^{1}H NMR (400 MHz, $CDCl_3$)

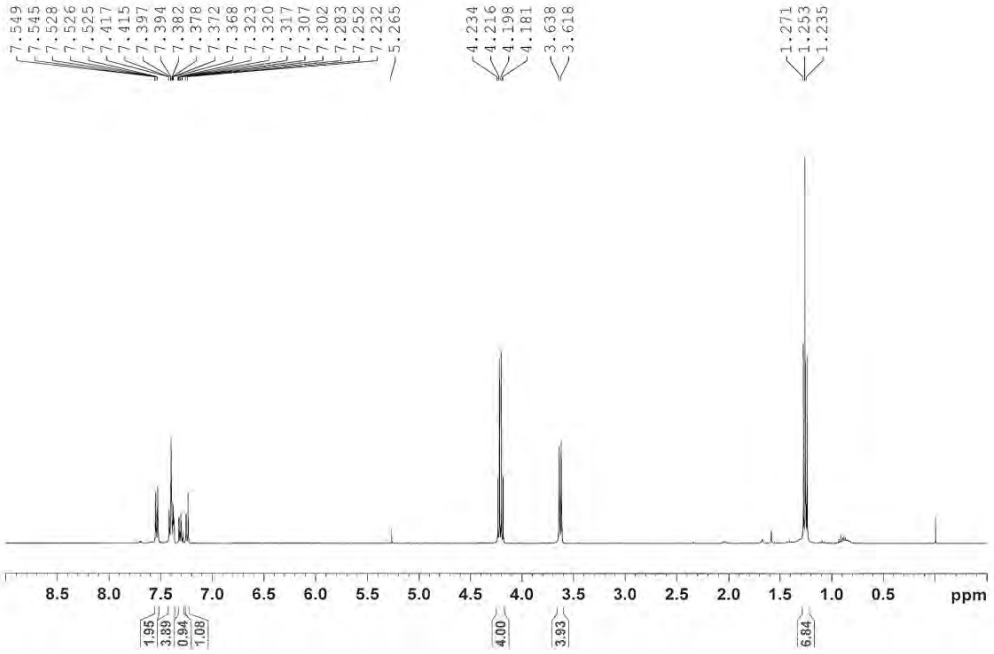

ESI-MS(+)

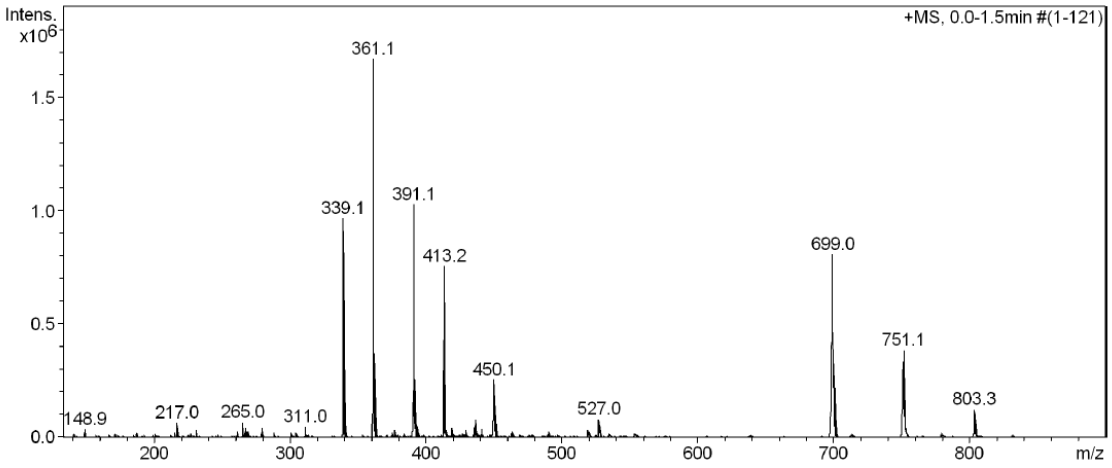

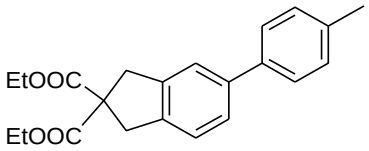

^{1}H NMR (300 MHz, $CDCl_3$)

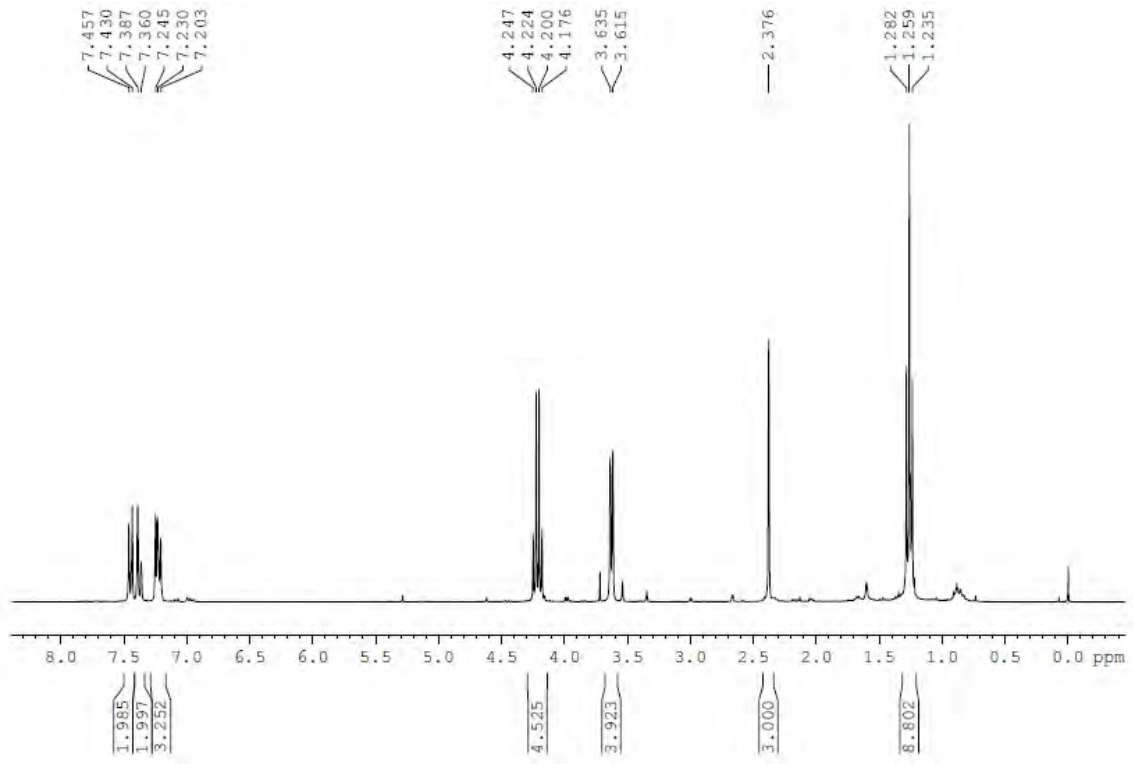

IR(ATR)

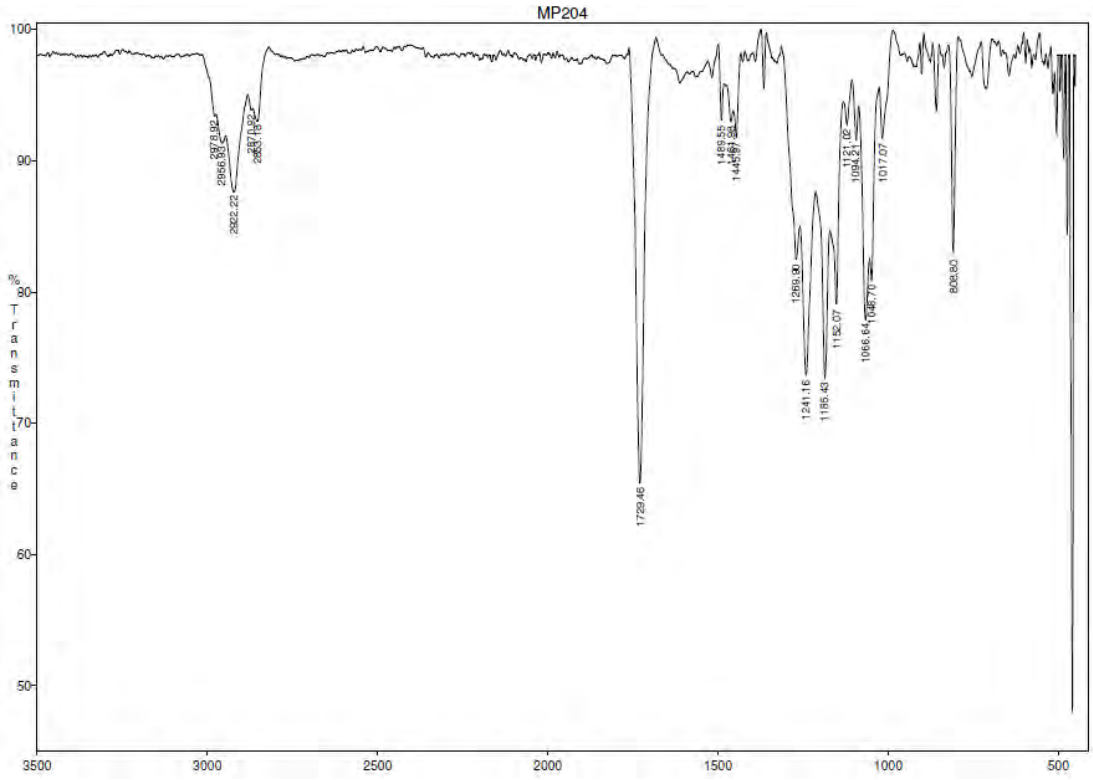

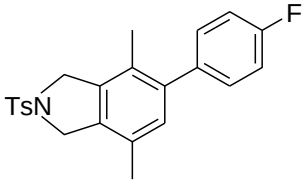

^{1}H NMR (400 MHz, $CDCl_3$)

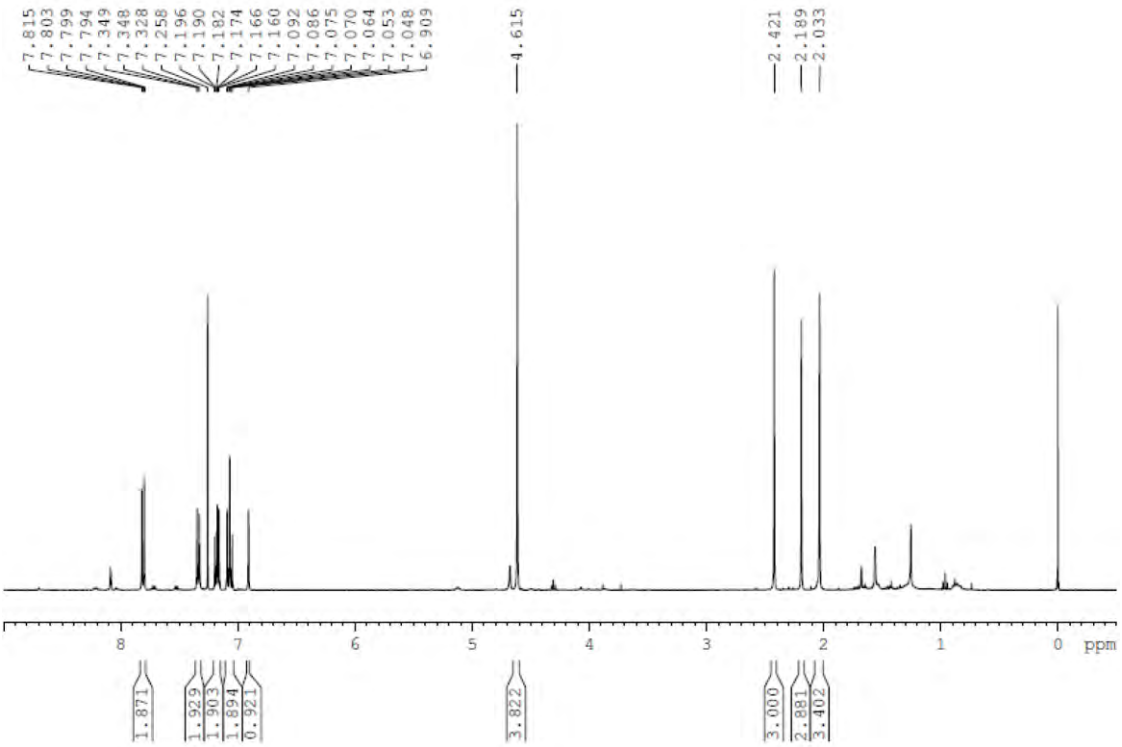

^{13}C NMR (75 MHz, $CDCl_3$)

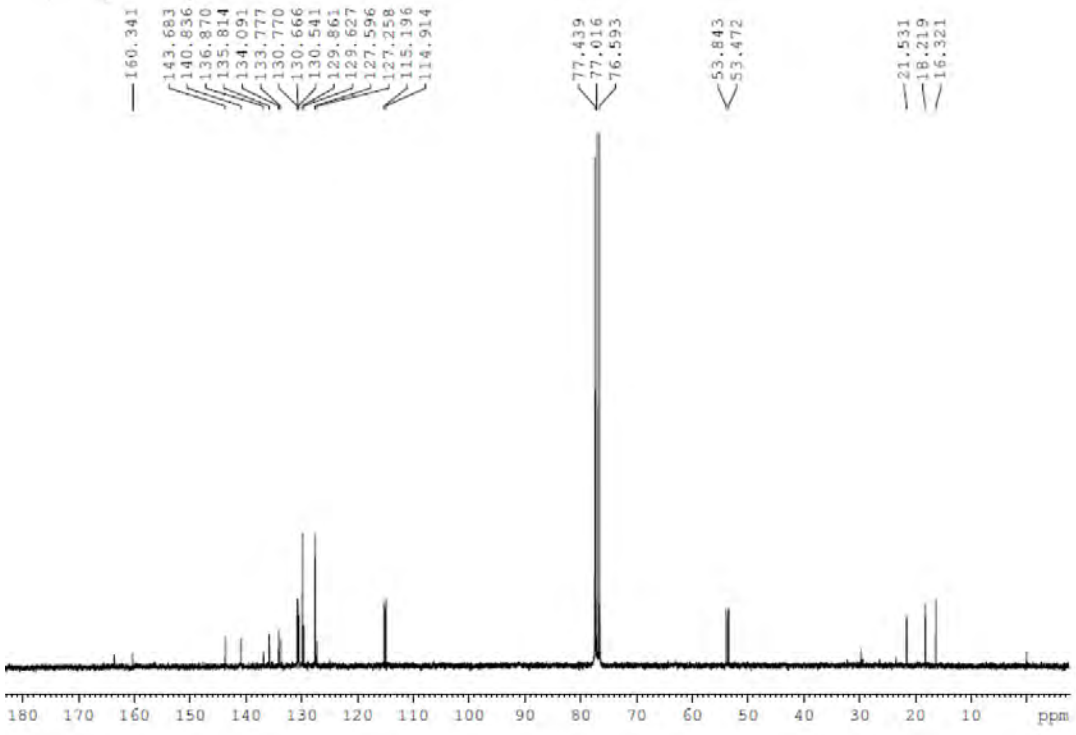

IR (ATR)

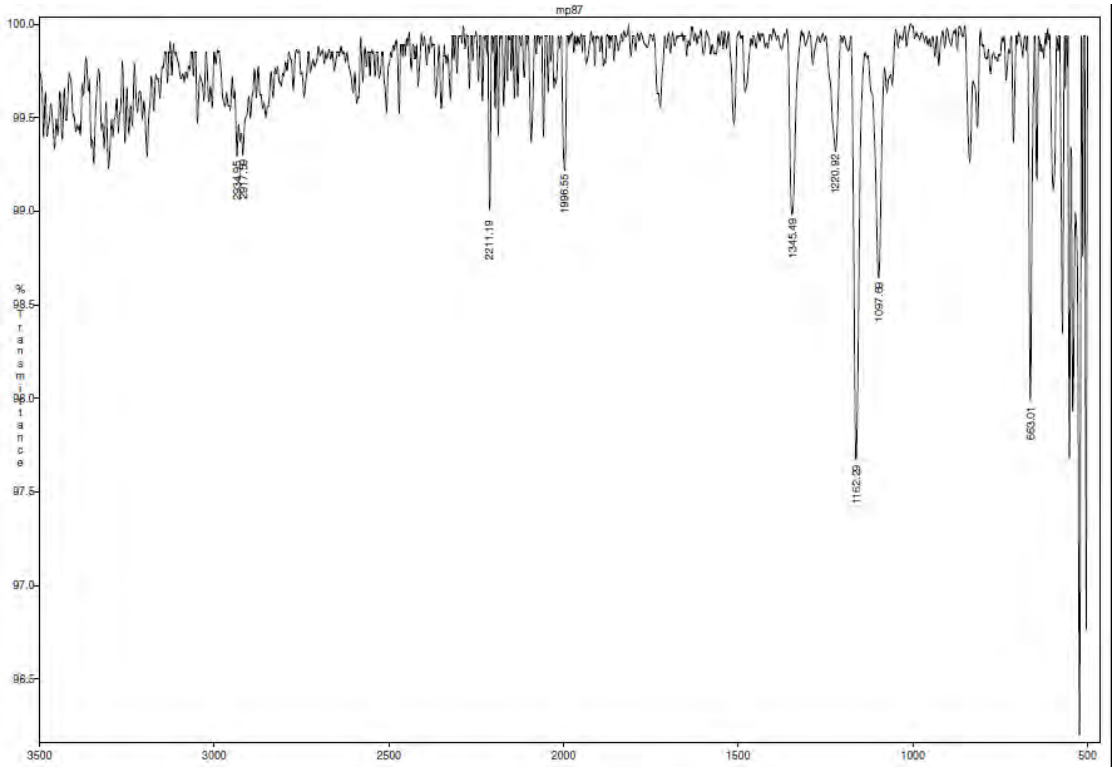

ESI-MS (+)

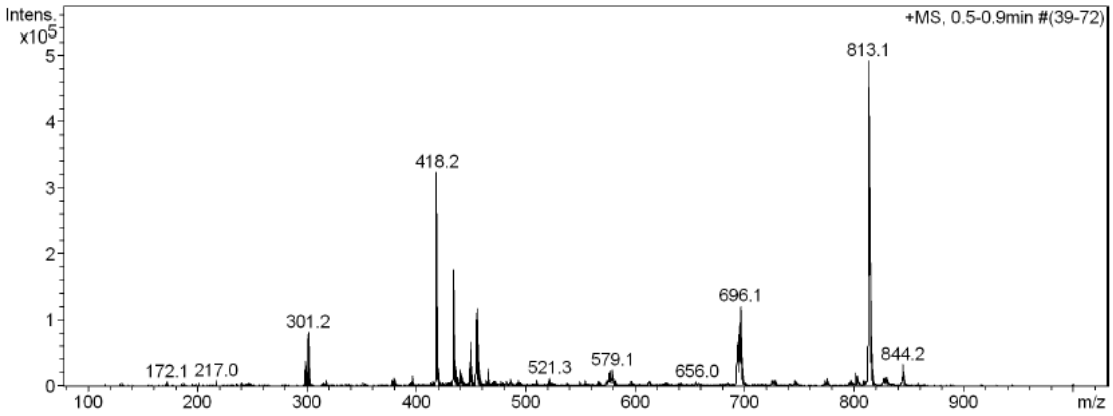

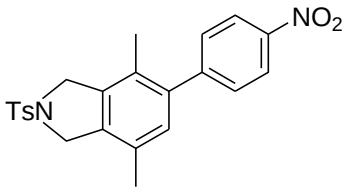

^{1}H NMR (300 MHz, $CDCl_3$)

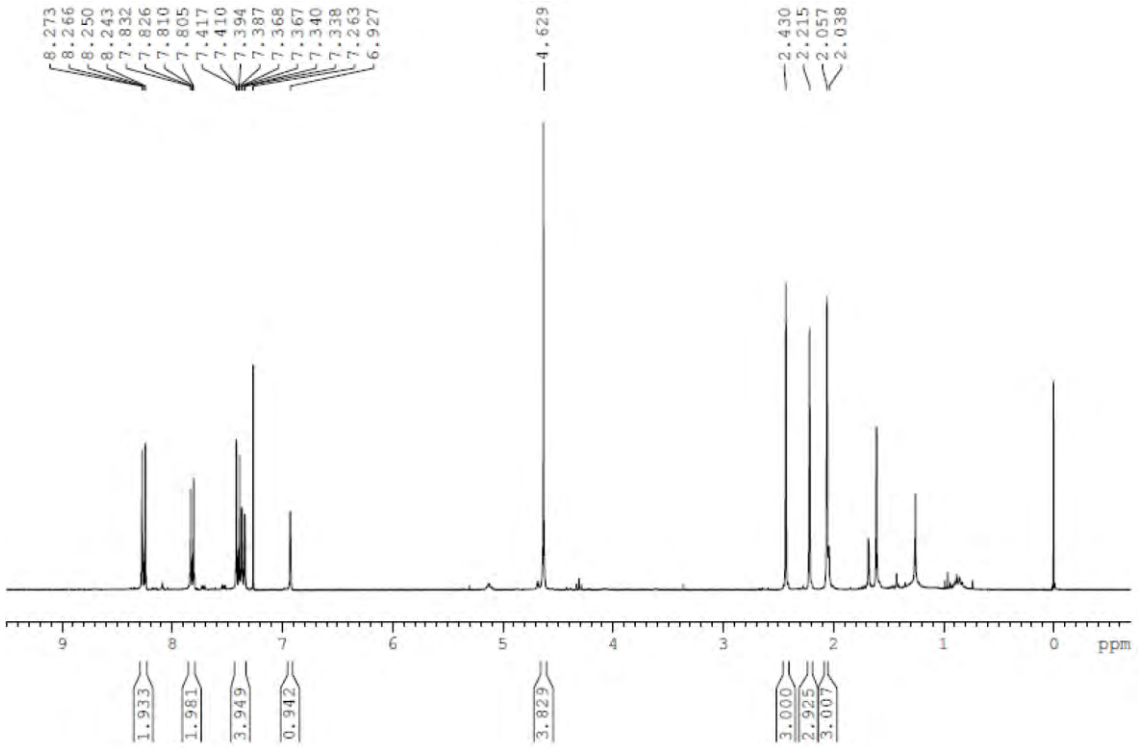

^{13}C NMR (75 MHz, $CDCl_3$)

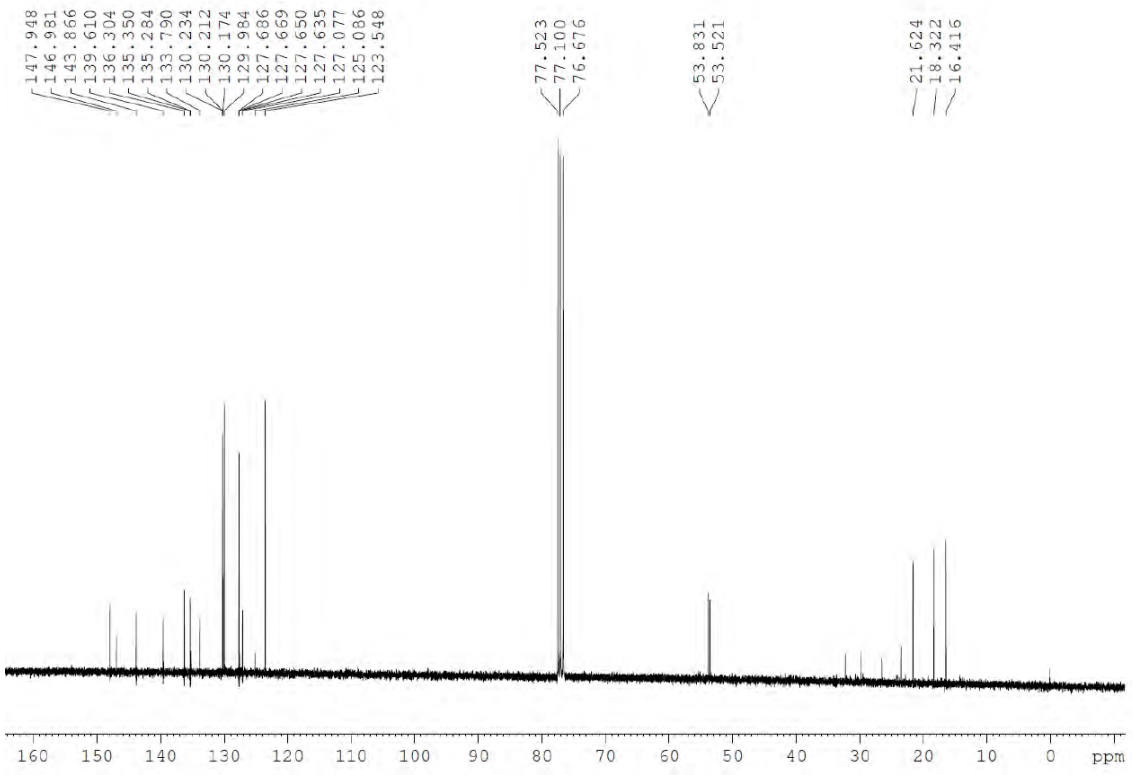

IR (ATR)

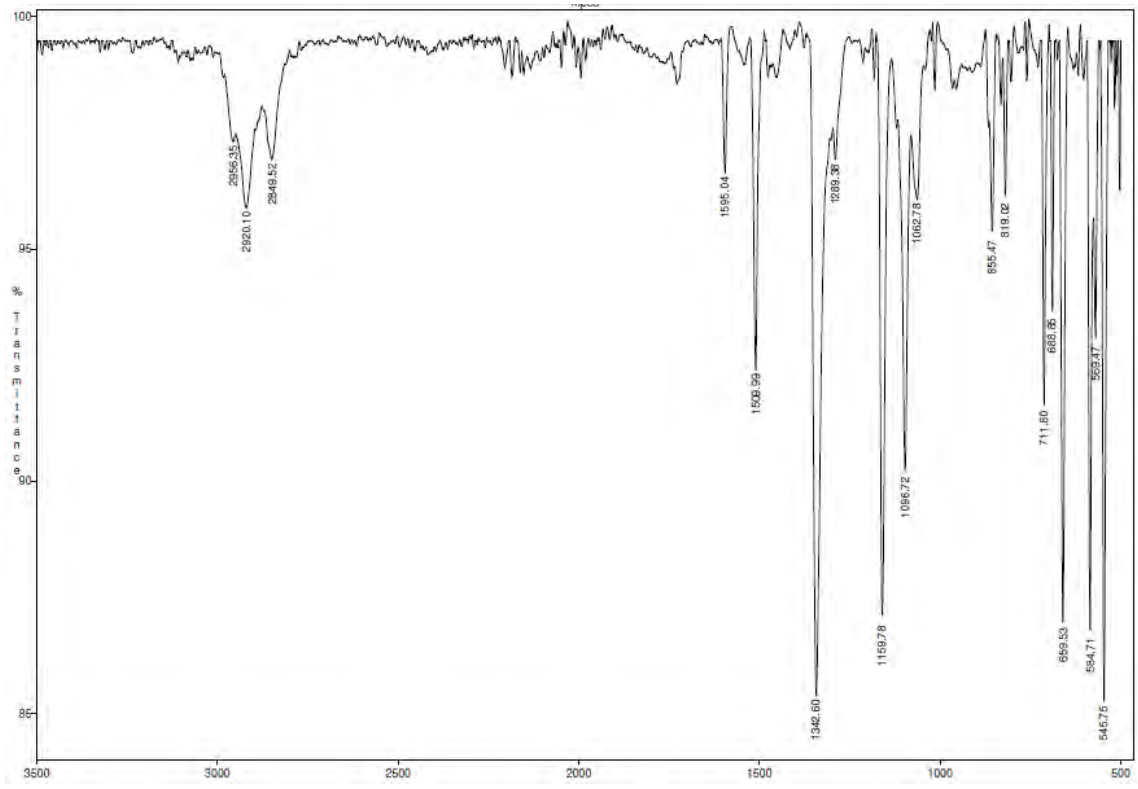

ESI-MS(+)

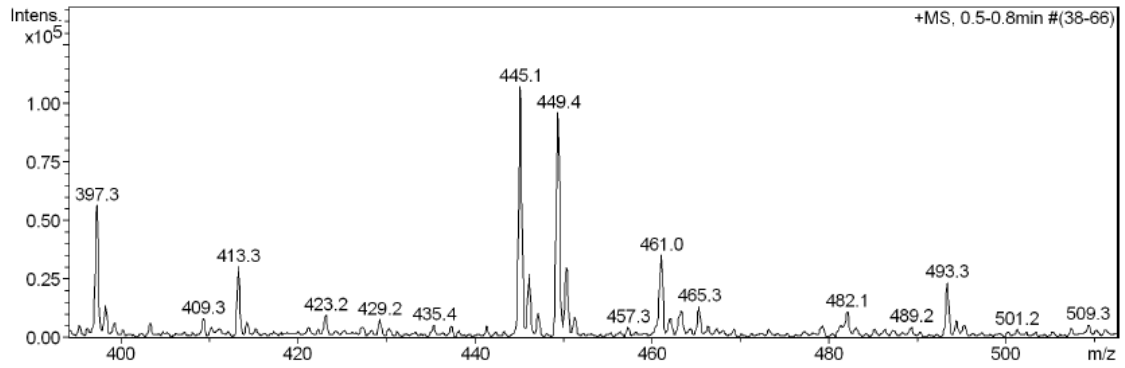

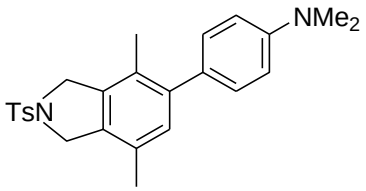

^{1}H NMR (400 MHz, $CDCl_3$)

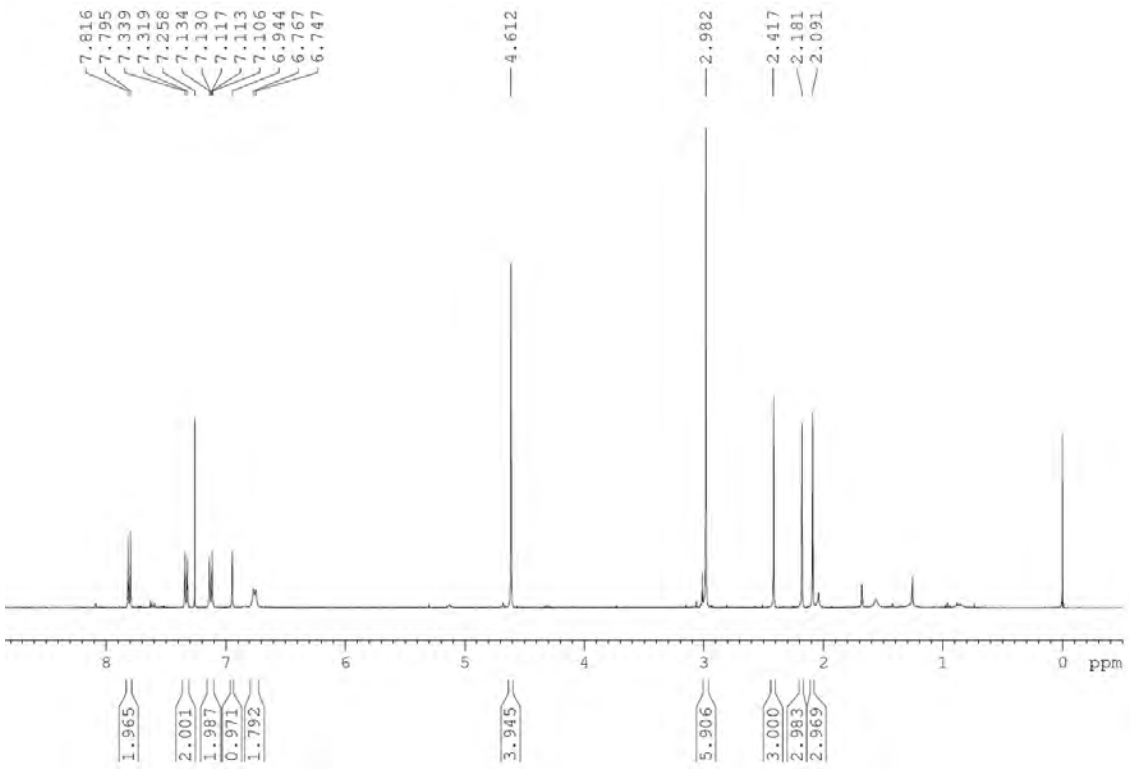

^{13}C NMR (75 MHz, $CDCl_3$)

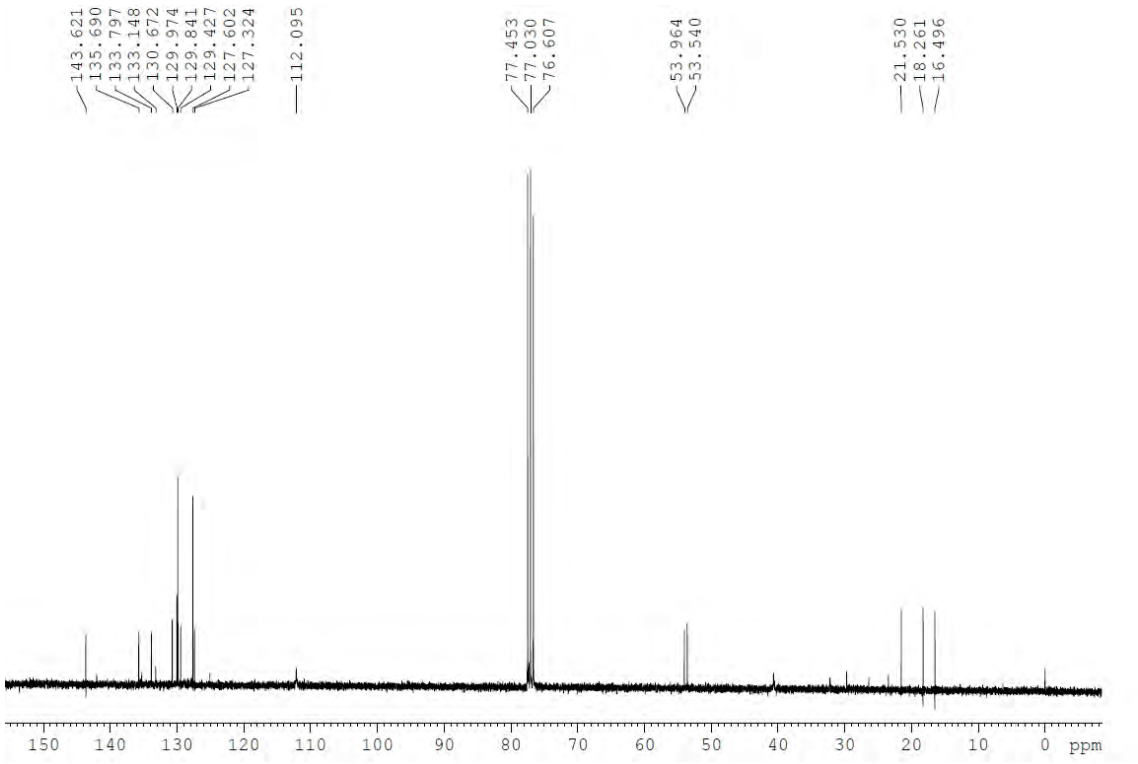

IR(ATR)

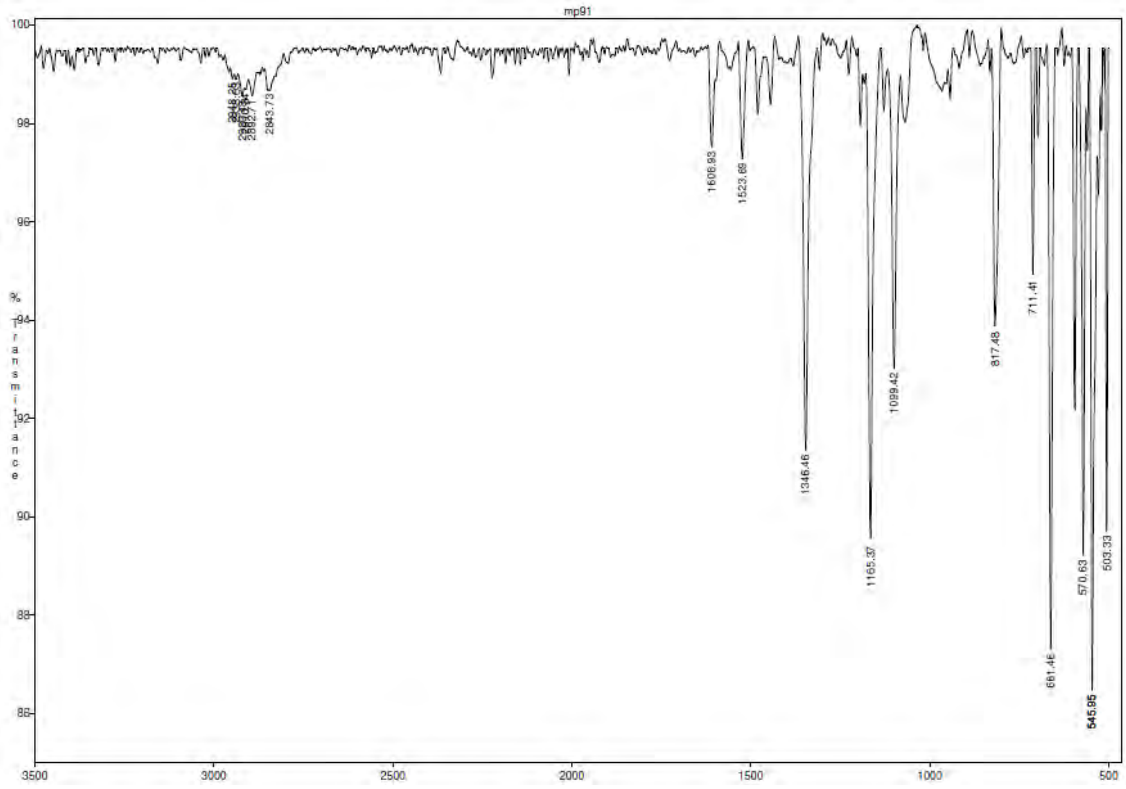

ESI-MS(+)

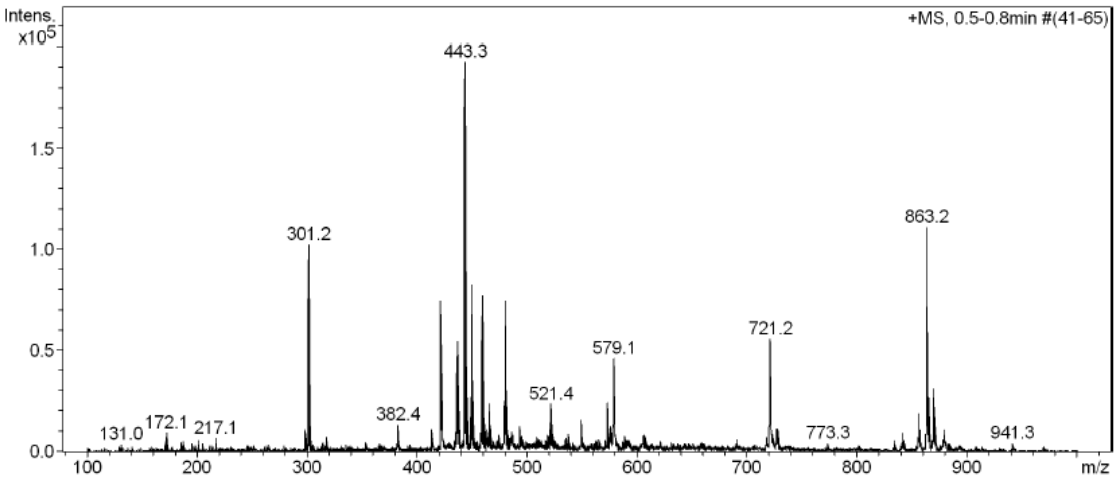

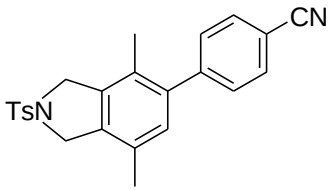

^{1}H NMR (400 MHz, $CDCl_3$)

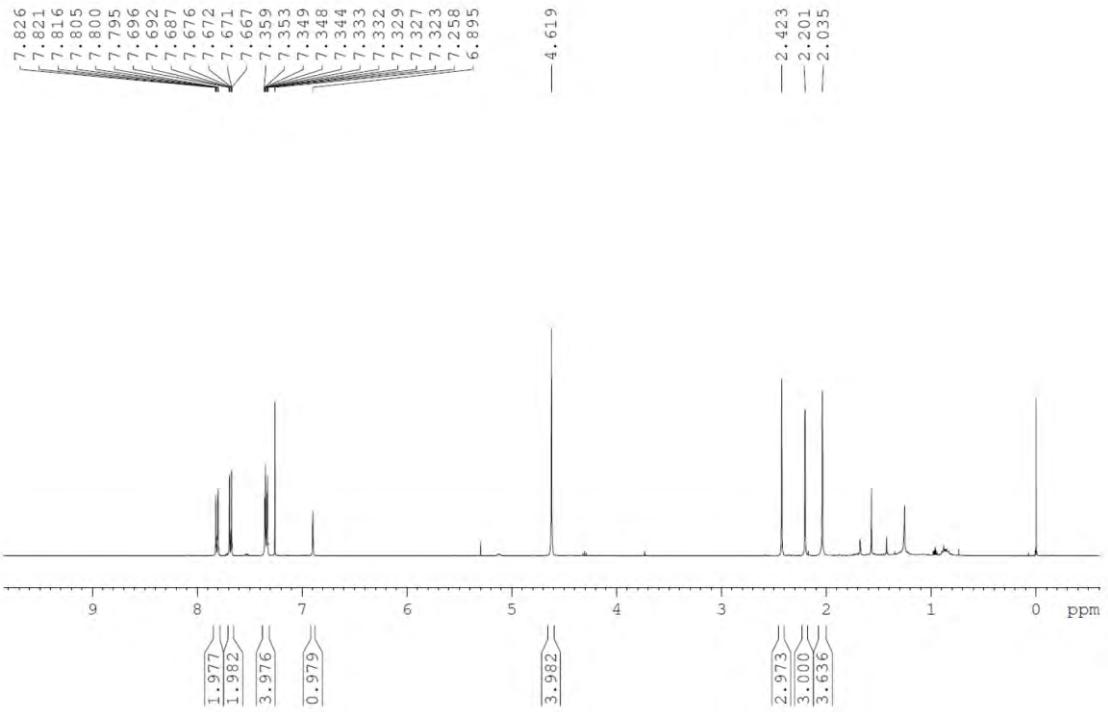

^{13}C NMR (75 MHz, $CDCl_3$)

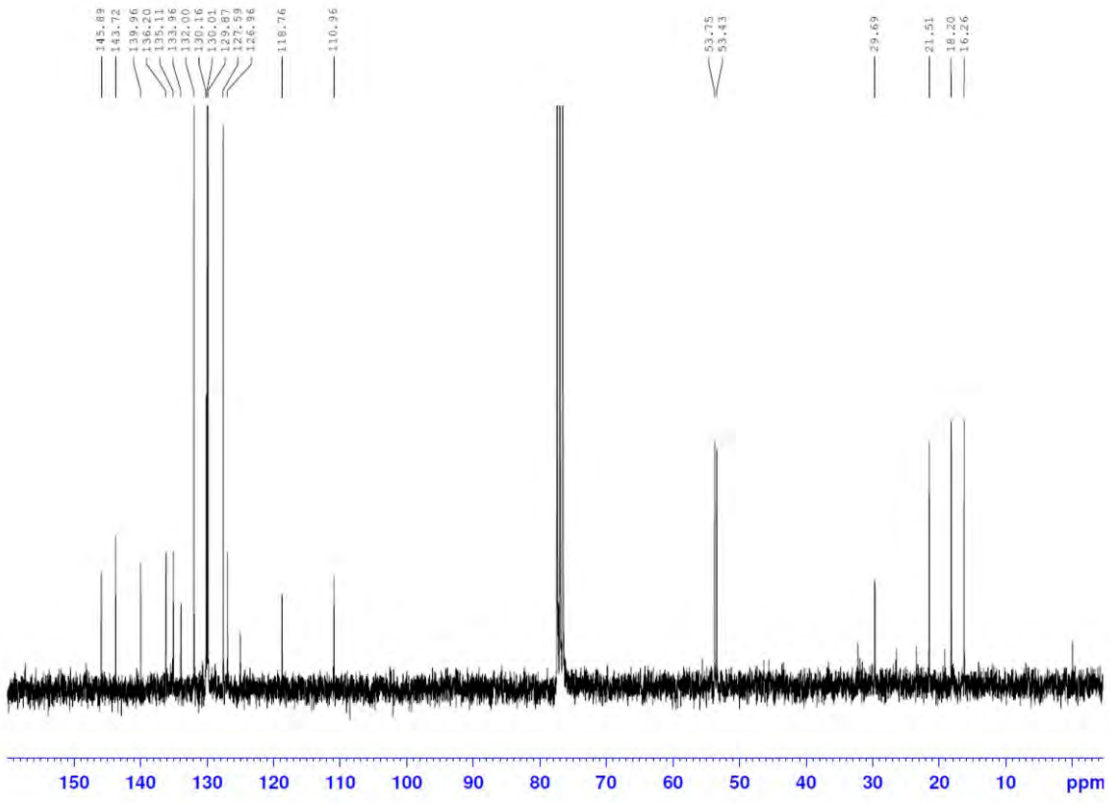

IR (ATR)

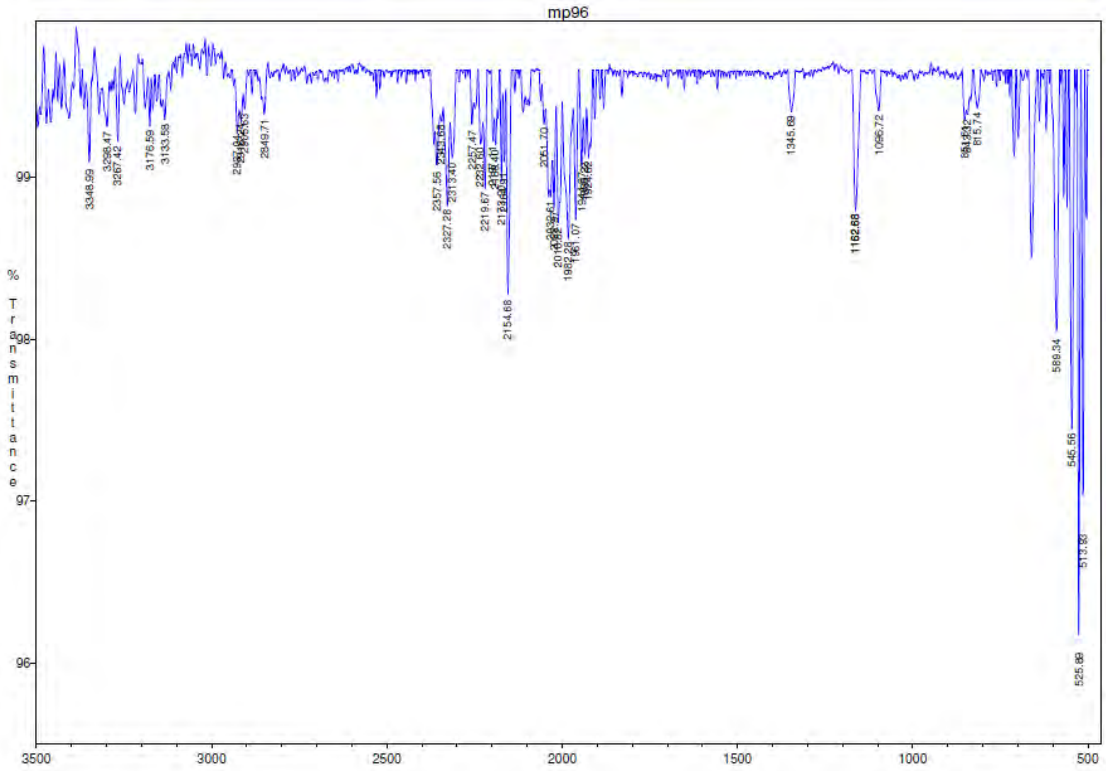

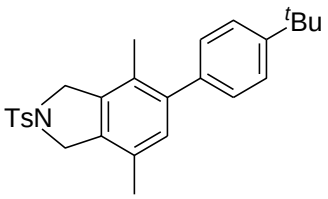

^{1}H NMR (400 MHz, $CDCl_3$)

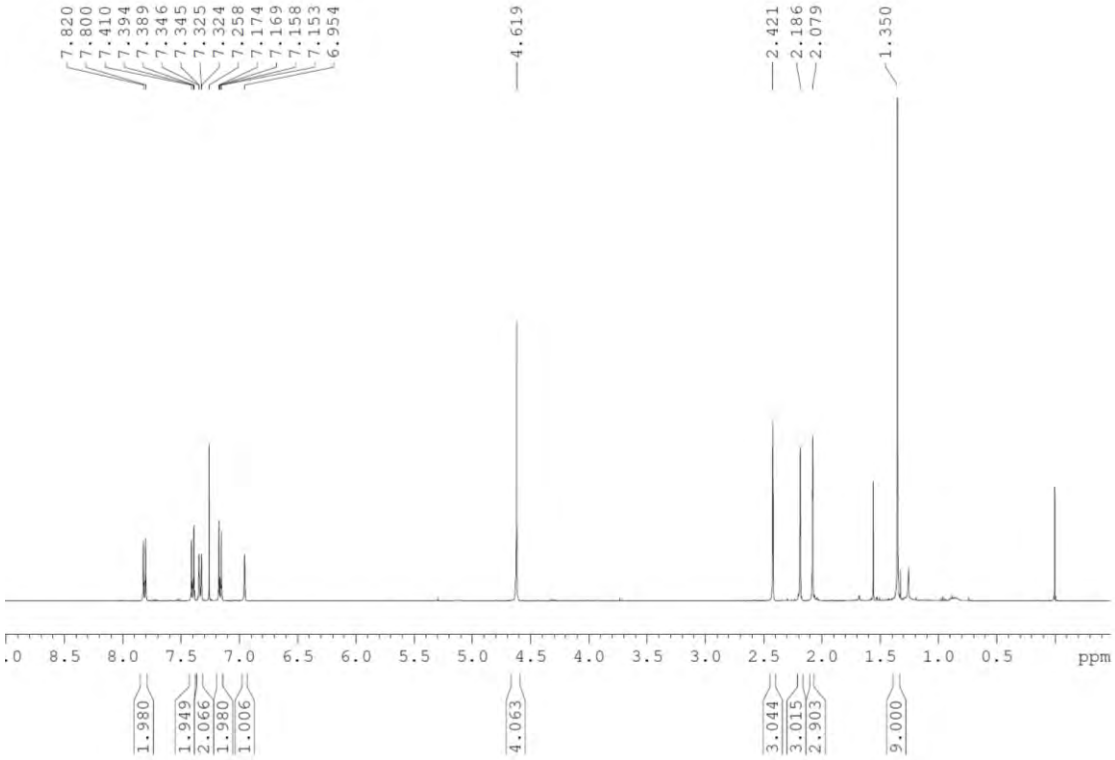

^{13}C NMR (75 MHz, $CDCl_3$)

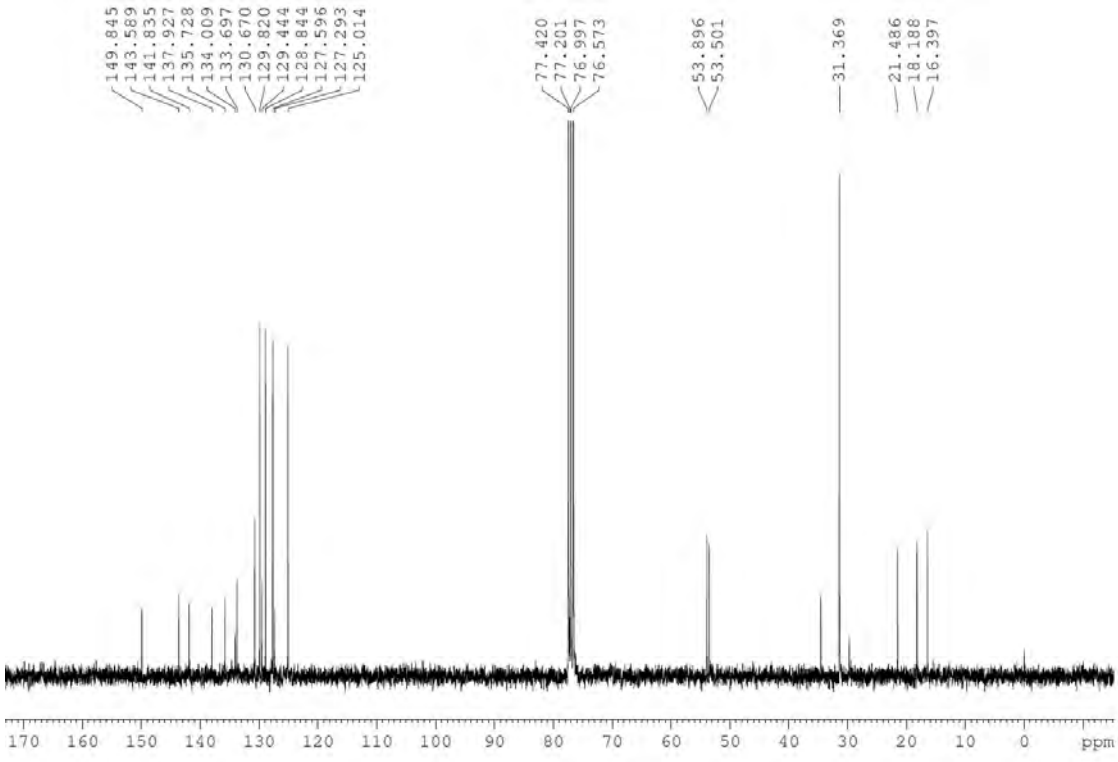

IR(ATR)

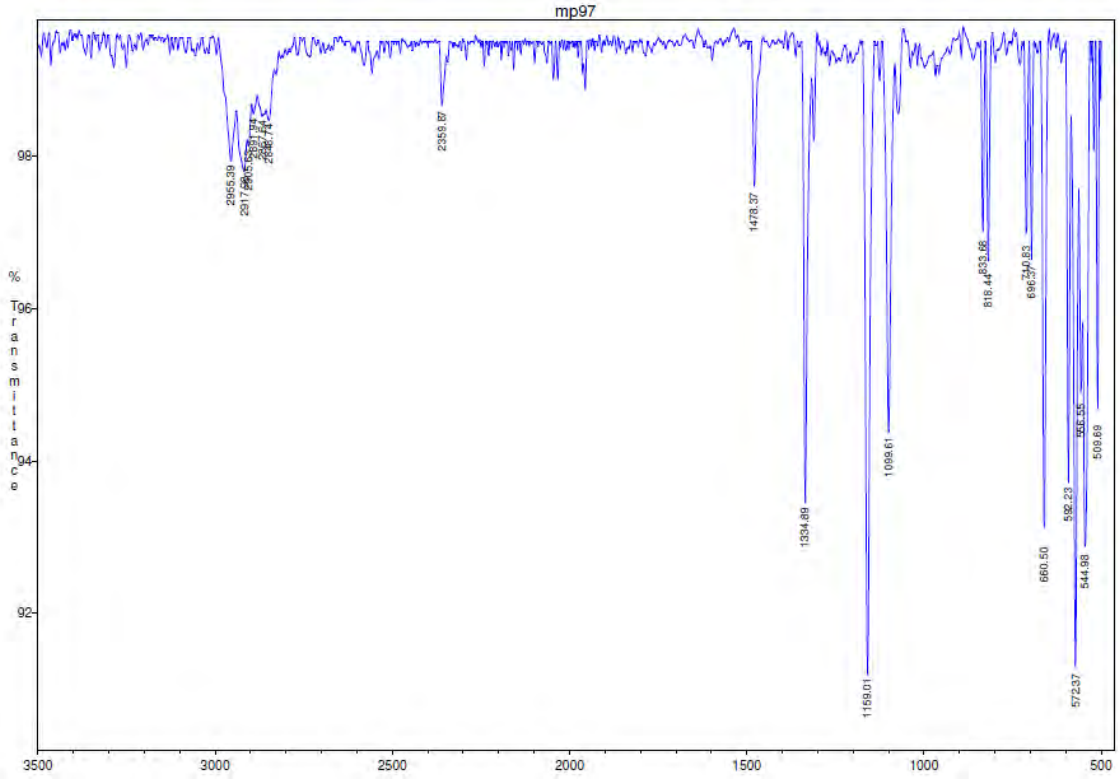

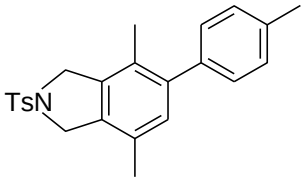

^{1}H NMR (300 MHz, $CDCl_3$)

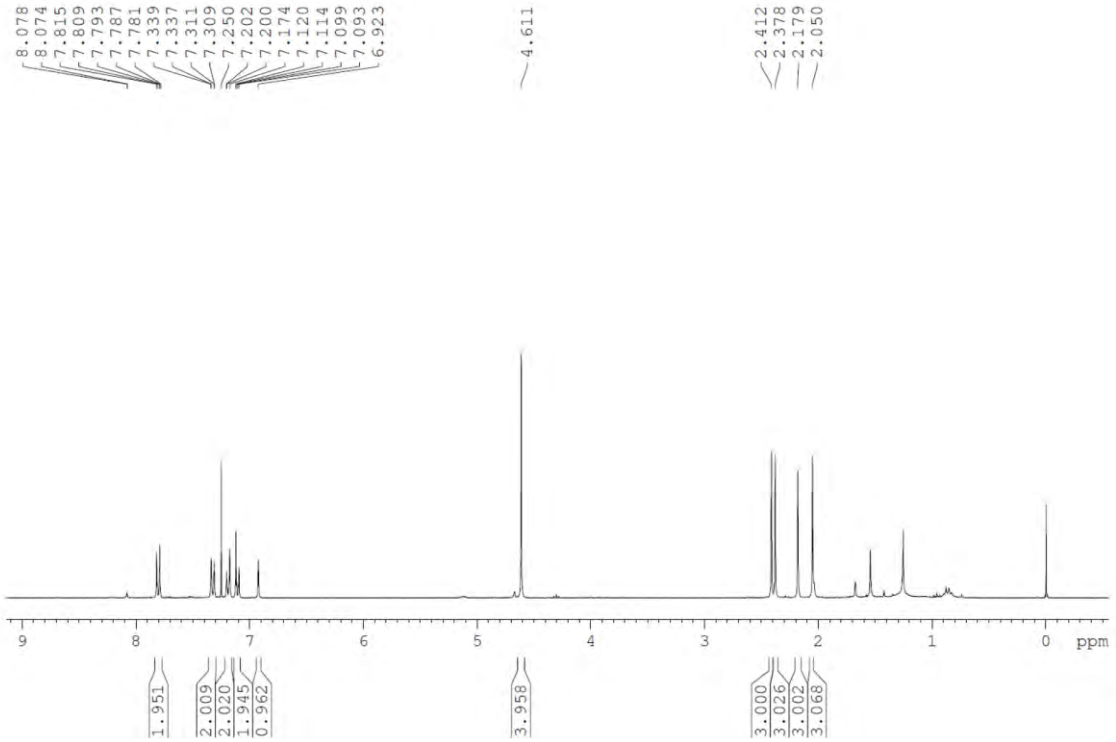

^{13}C NMR (75 MHz, $CDCl_3$)

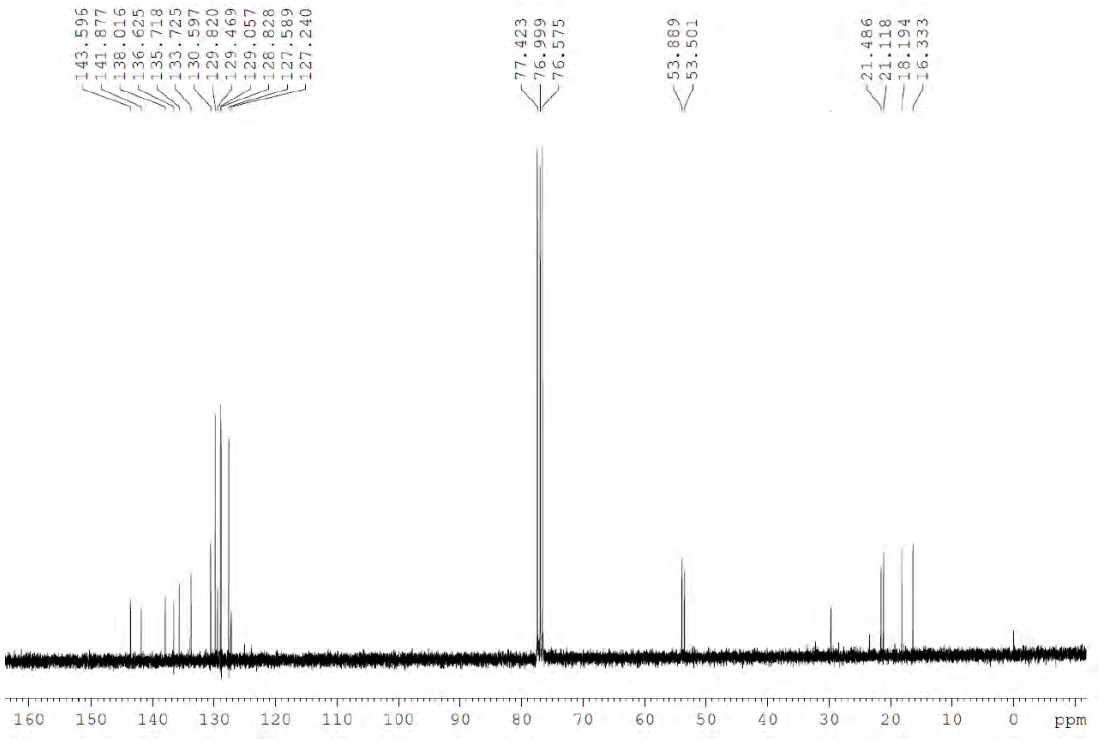

IR(ATR)

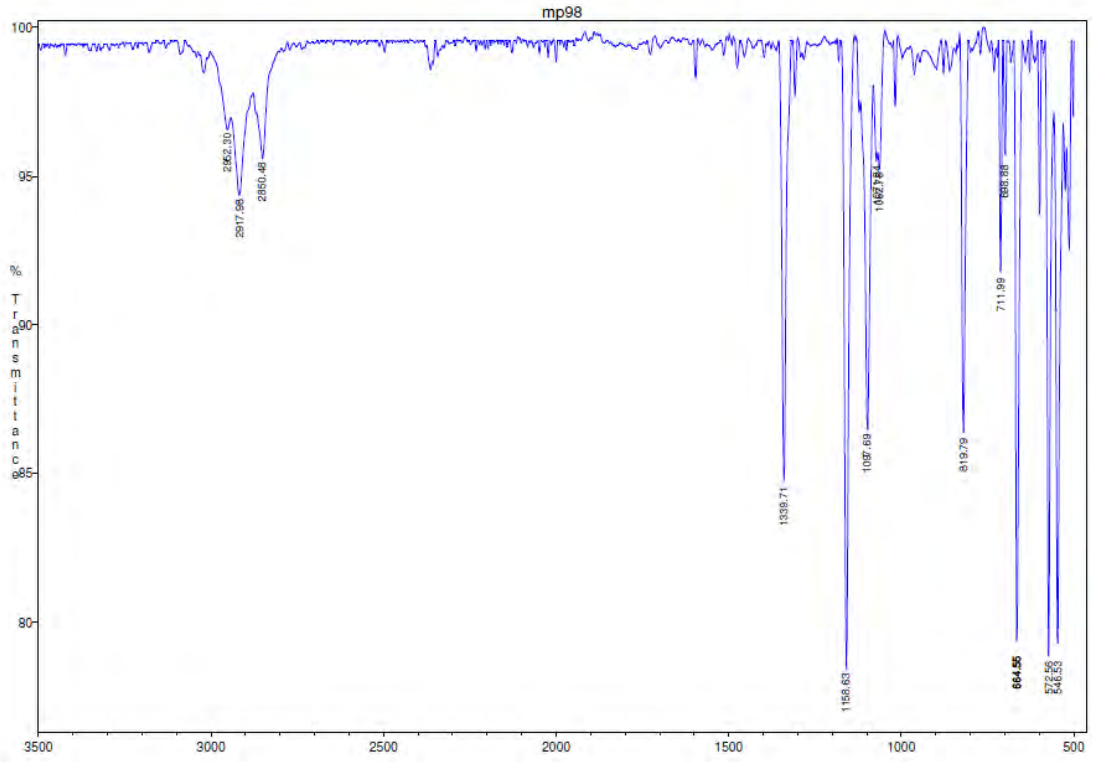

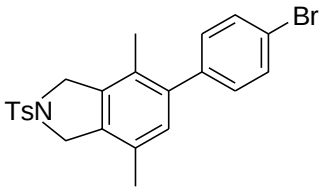

^{1}H NMR (300 MHz, $CDCl_3$)

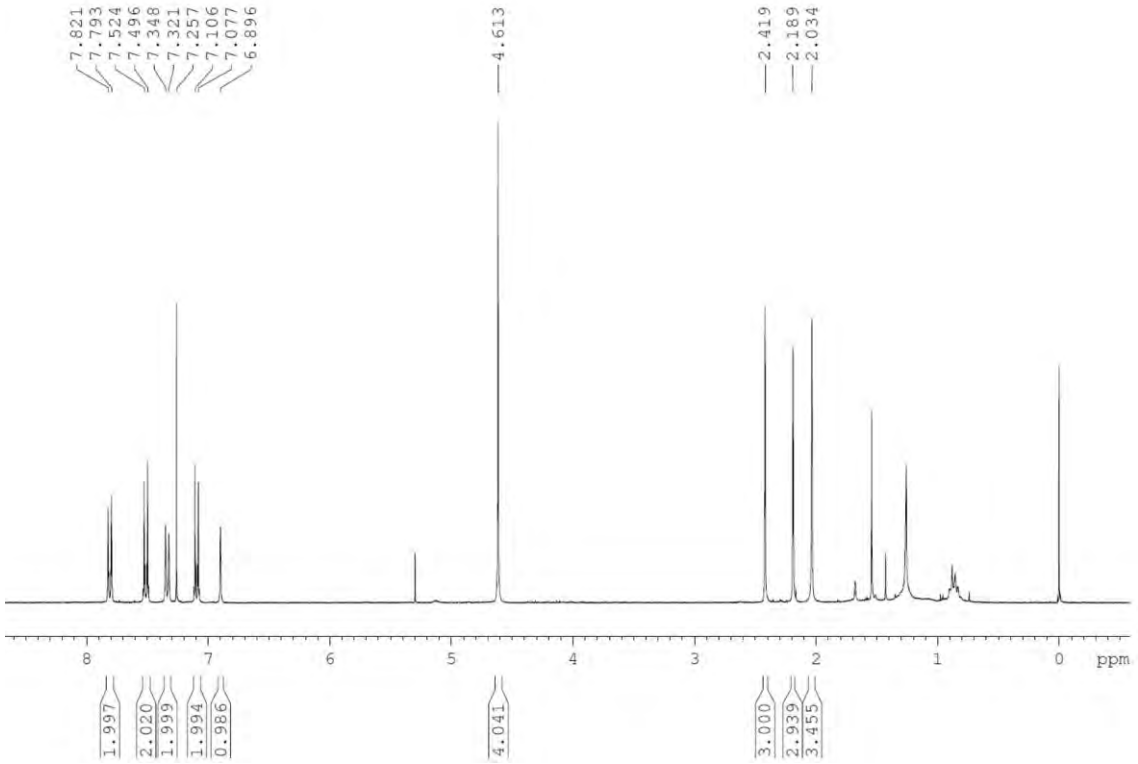

^{13}C NMR (75 MHz, $CDCl_3$)

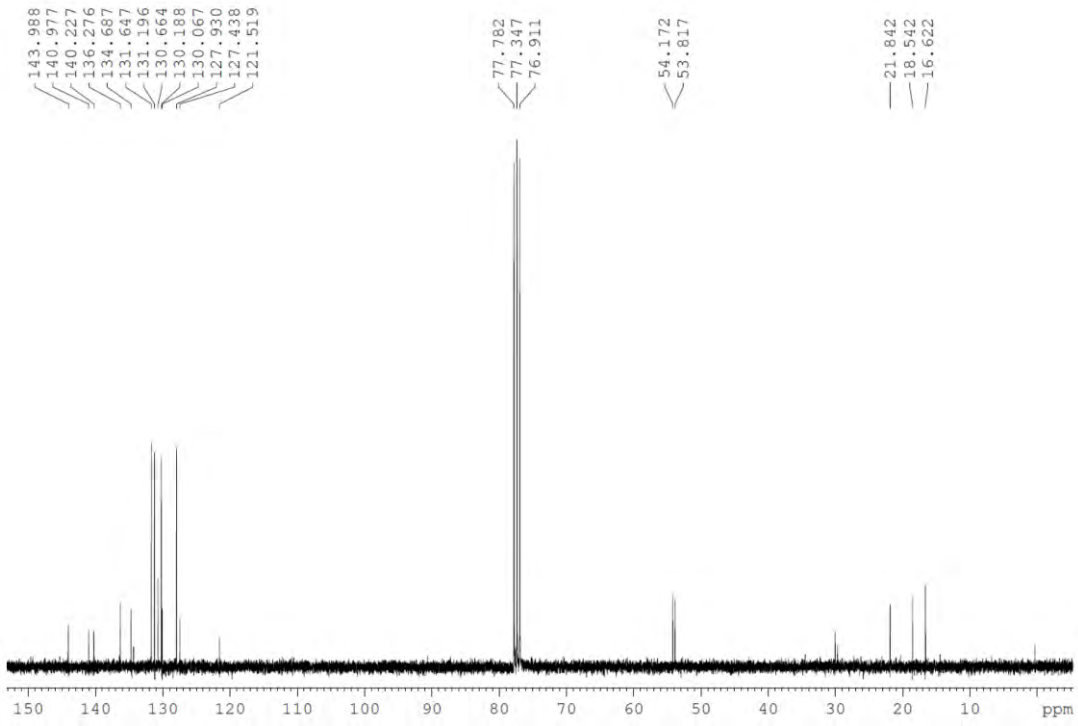

IR(ATR)

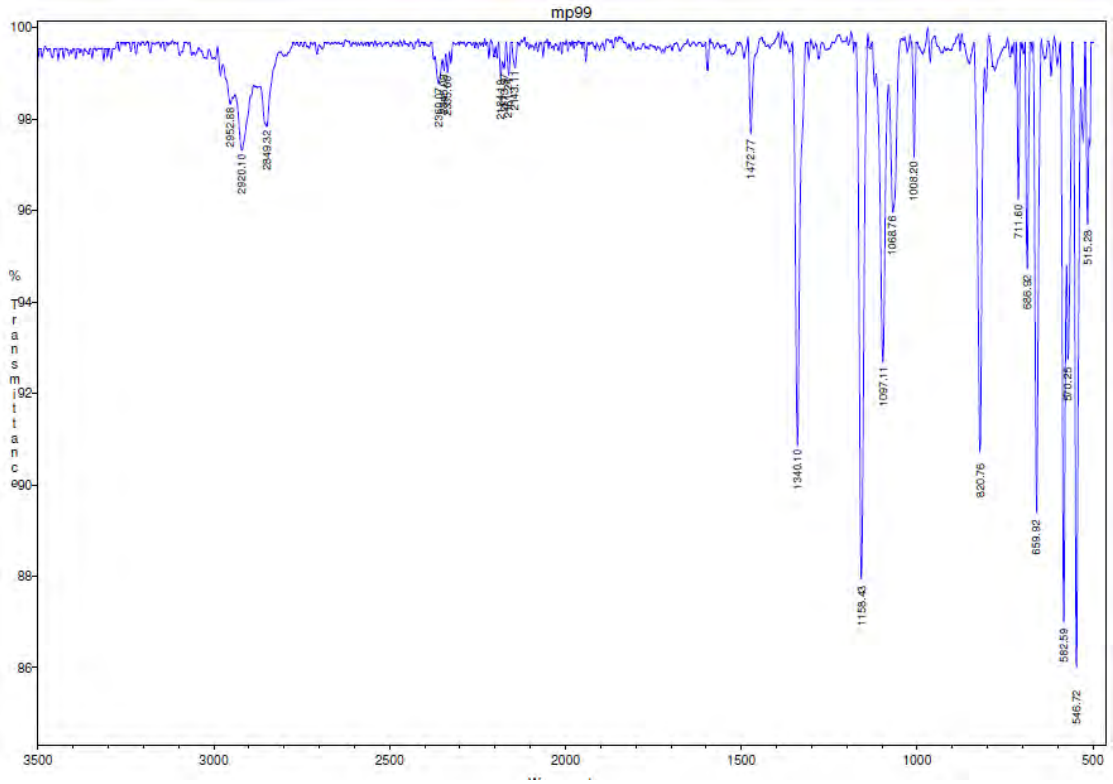

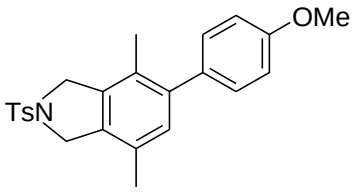

^{1}H NMR (400 MHz, $CDCl_3$)

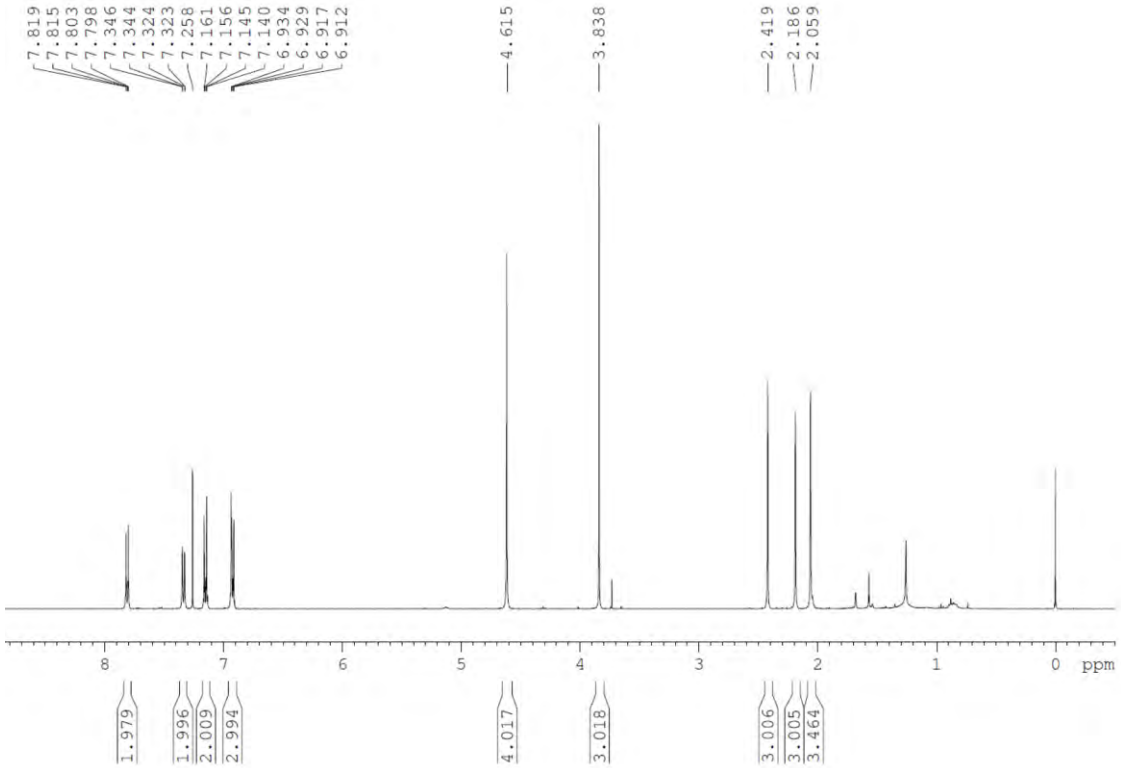

^{13}C NMR (75 MHz, $CDCl_3$)

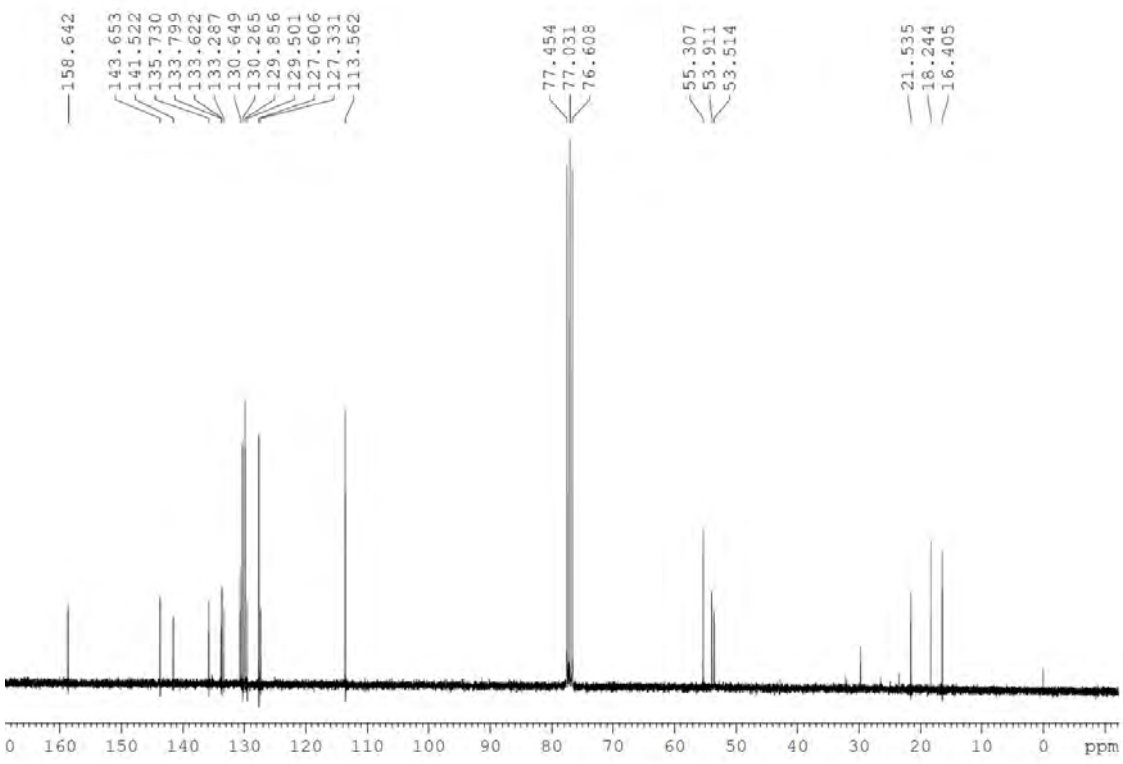

IR(ATR)

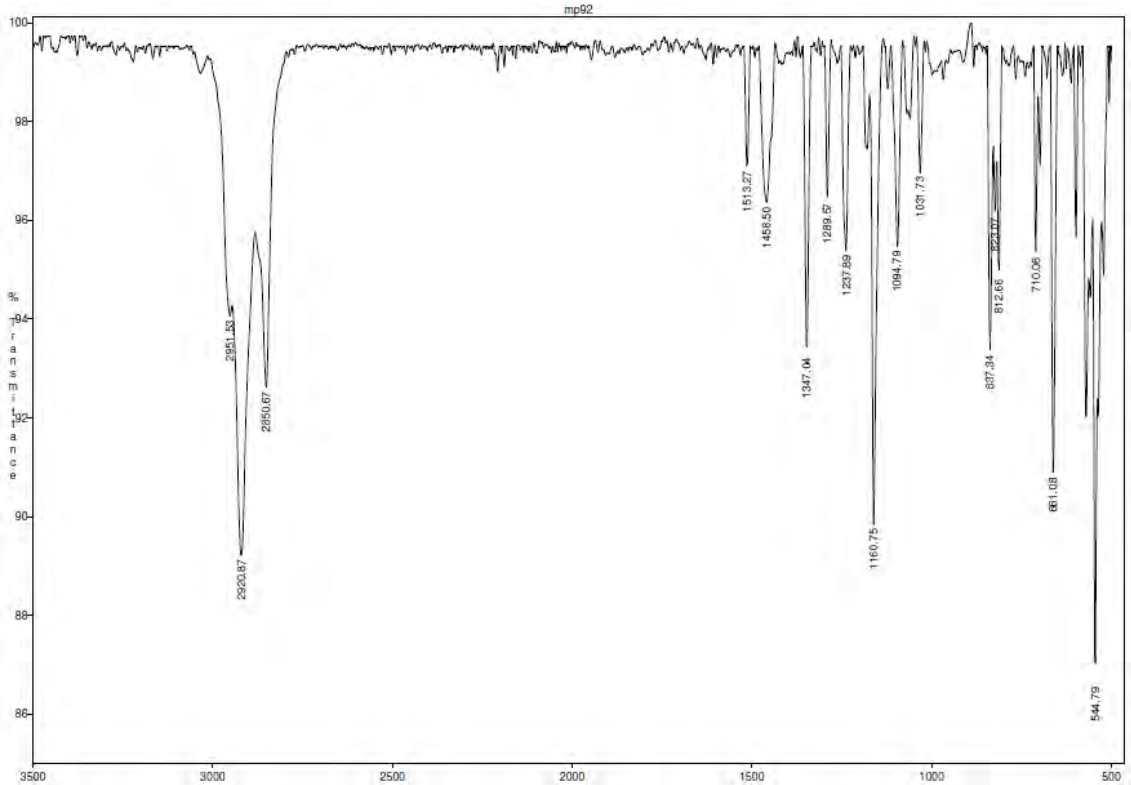

ESI-MS(+)

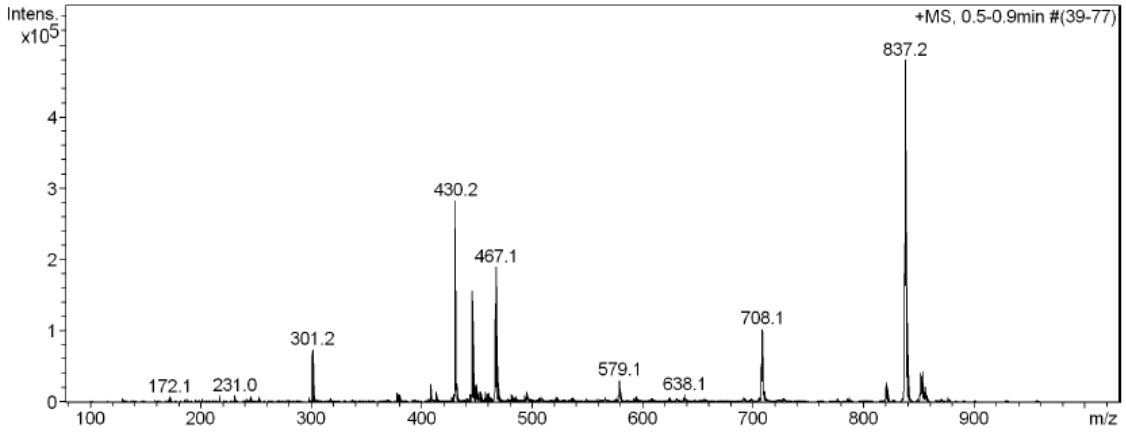
Intens.
x10^5
+MS, 0.5-0.9min #(39-77)
837.2
430.2
467.1
708.1
301.2
579.1
638.1
172.1
231.0
m/z

Direct Detection of Key Intermediates in Rhodium(I)-Catalyzed [2+2+2] Cycloadditions of Alkynes by ESI-MS

Magda Parera, Anna Dachs, Miquel Solà, Anna Pla-Quintana,* and Anna Roglans*

Figure S1. ESI(+) mass spectrum of a solution of $[Rh(COD)_2]BF_4$ diluted in methanol.

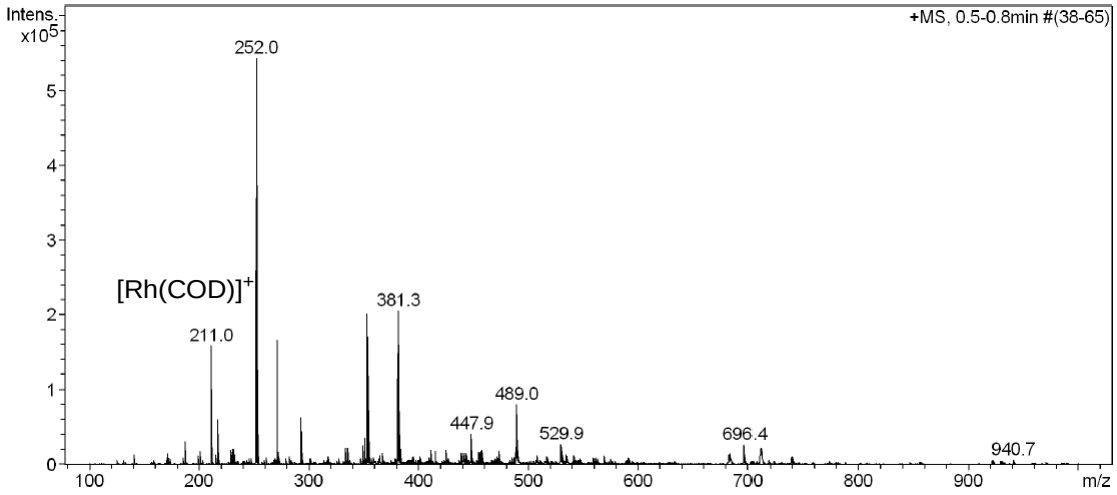

Figure S2. ESI(+) mass spectrum of a solution of BINAP ((*R*)-(+)-2,2′-Bis(diphenylphosphino)-1,1′-binaphthyl) diluted in methanol.

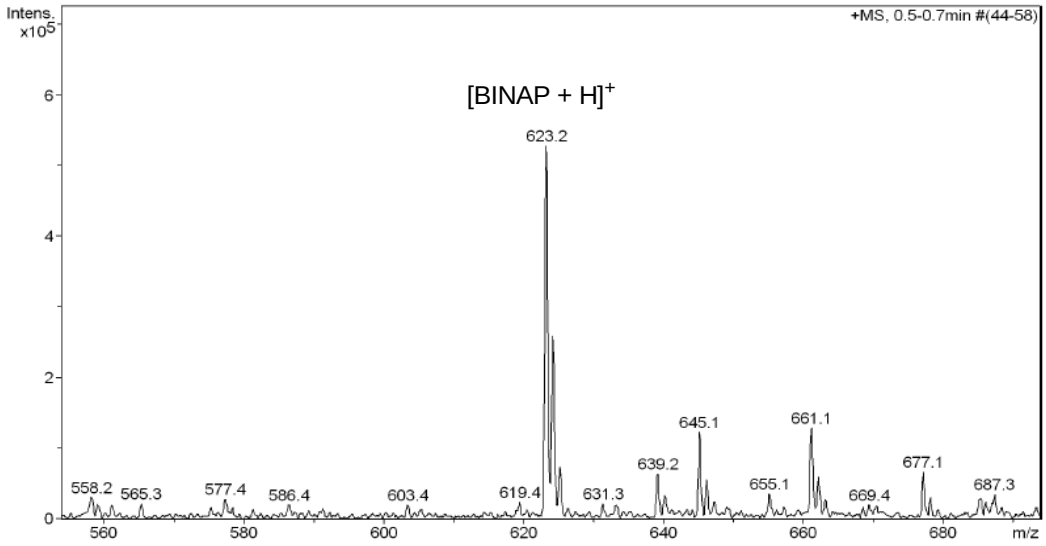

Figure S3. ESI(+) mass spectrum of a solution of $[Rh(COD)_2]BF_4$/BINAP (1:1) diluted in methanol (*m/z* range of 770 to 910).

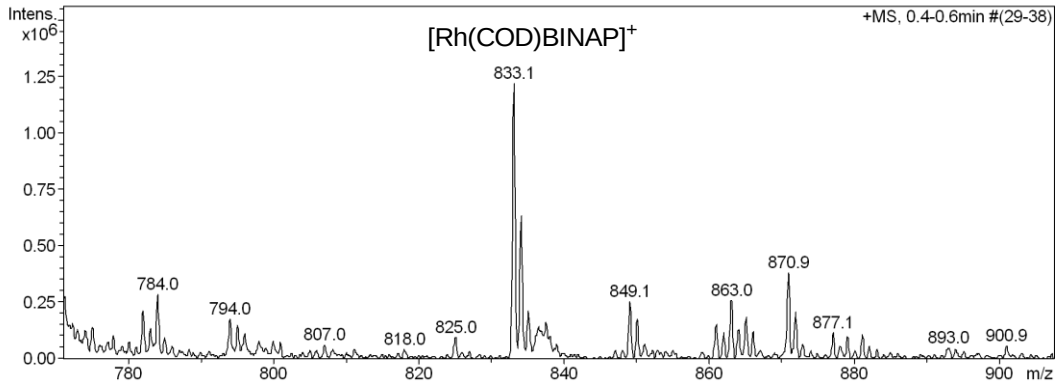

Figure S3. ESI(+) mass spectrum of a solution of $[Rh(COD)_2]BF_4$/BINAP (1:1) diluted in methanol (*m/z* range of 1270 to 1470).

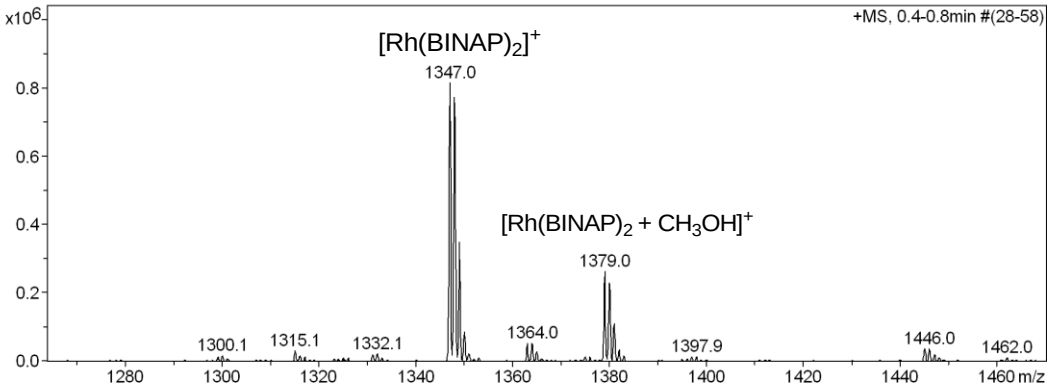

Figure S4. ESI(+)-MS/MS spectrum of the ion $[Rh(COD)(BINAP)]^+$ at *m/z* = 833 (collision energy of 1 V, width = 4 *m/z*).

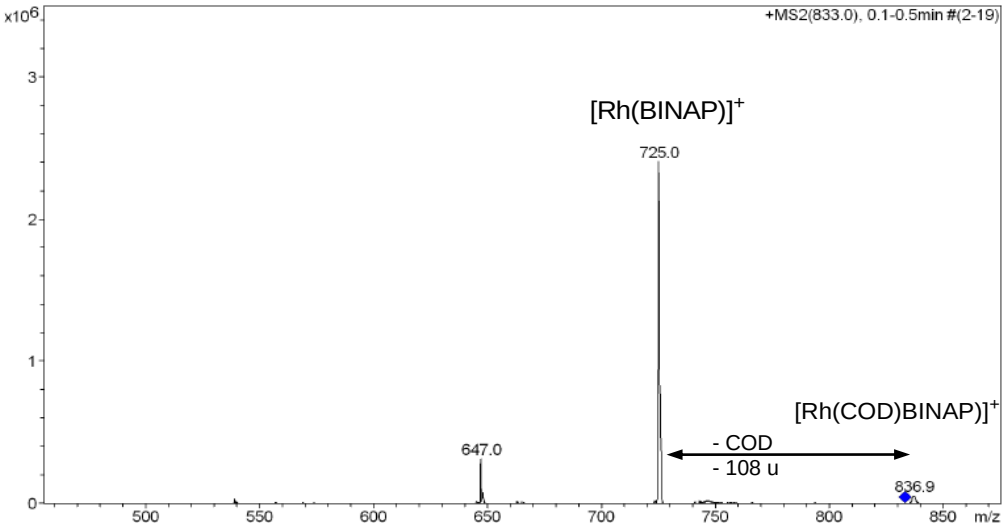

Scheme S2. [2+2+2] cycloaddition reaction between diyne **1** and *p*-methylphenylacetylene **2a**.

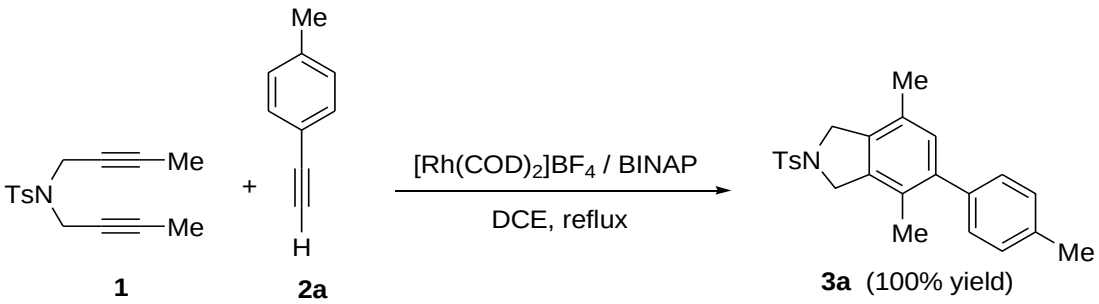

1 **2a** **3a** (100% yield)

Figure S5. ESI(+) mass spectrum of a solution of diyne **1** in methanol.

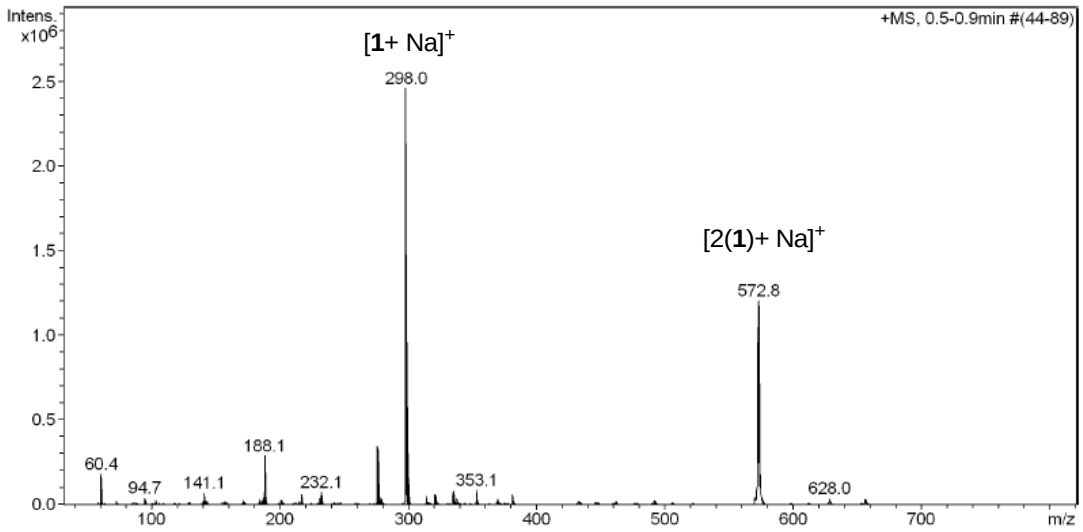

Figure S6. ESI(+) mass spectrum of a solution of cycloadduct **3a** in methanol.

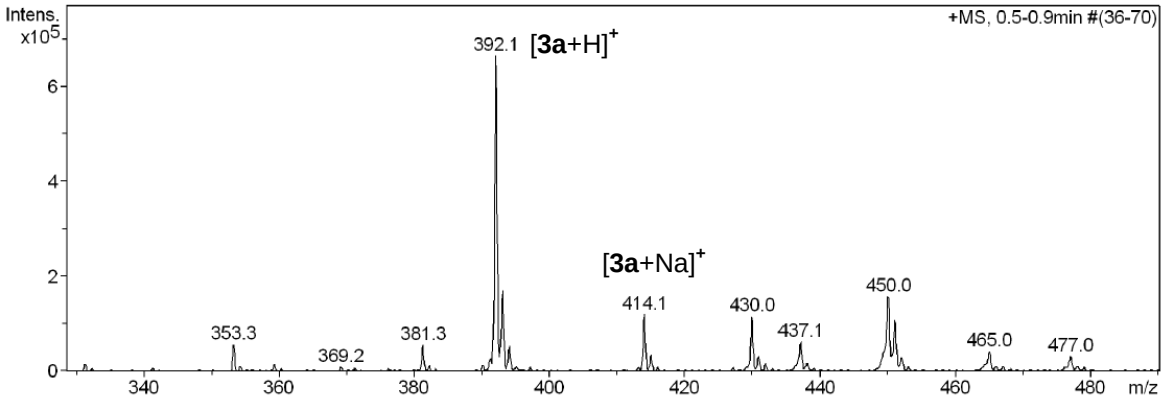

Figure S7. ESI(+) mass spectrum of a solution of the mixture of $[Rh(COD)_2]BF_4$/BINAP (5% molar) + **3a** in methanol.

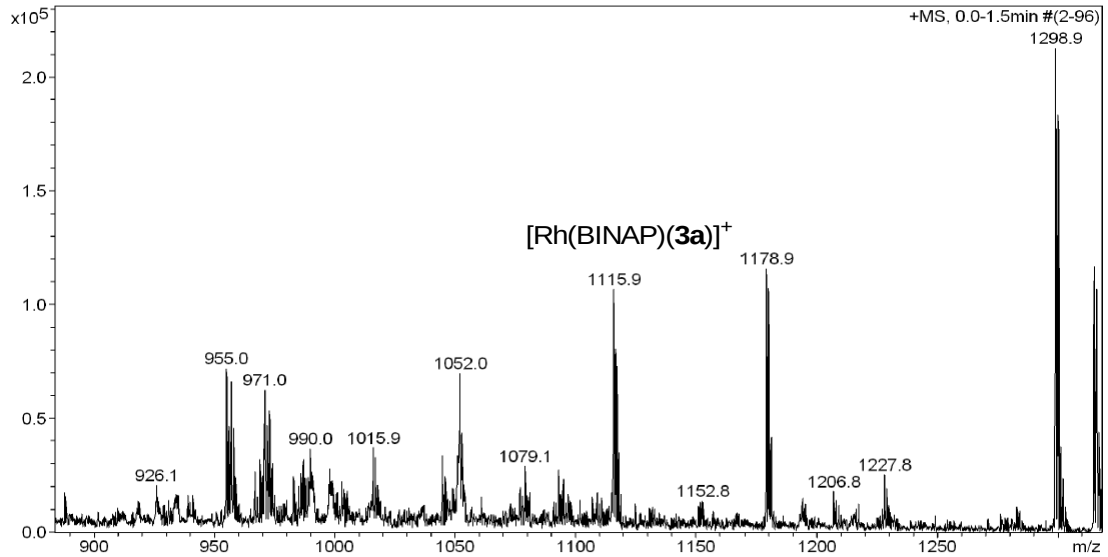

Scheme S3. [2+2+2] cycloaddition reaction between diyne **1** and *p*-methylphenylacetylene **2b**.

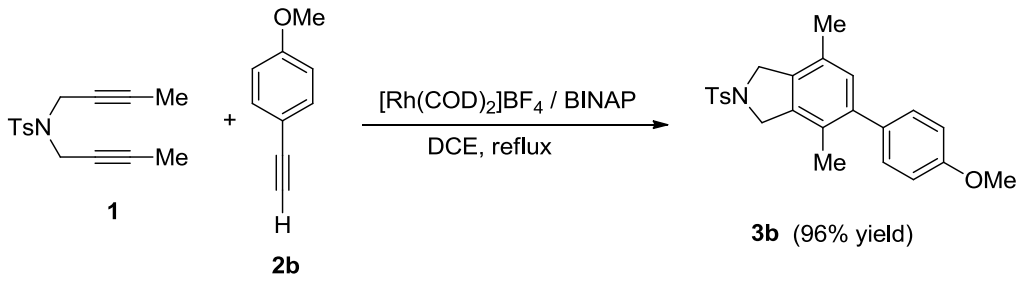

Figure S8. ESI(+) mass spectrum of a solution of the mixture of $[Rh(COD)_2]BF_4$/BINAP (5% molar) + diyne **1** + phenylacetylene **2b** diluted in methanol.

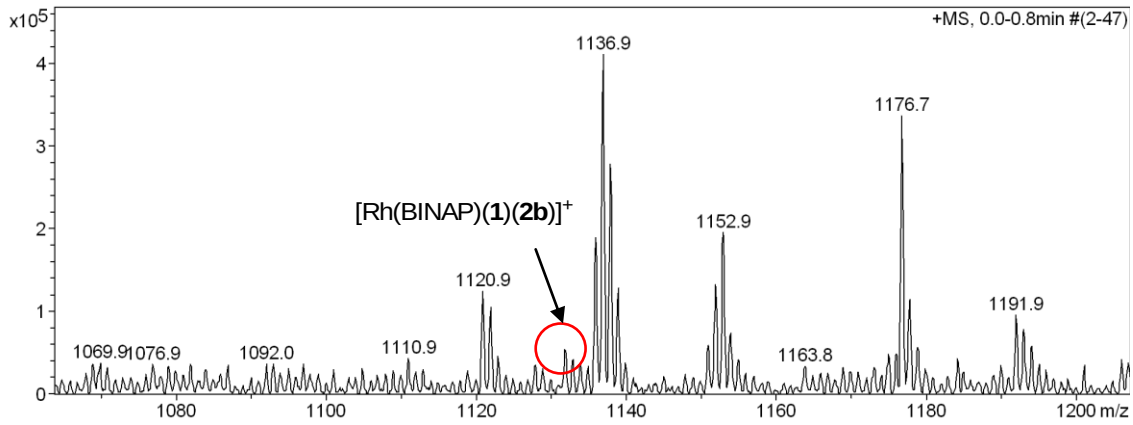

Figure S8. ESI(+)MS/MS spectrum of the ion $[Rh(BINAP)(\mathbf{1})(\mathbf{2b})]^+$ at *m/z* = 1132 (collision energy of 0,95 V, width = 4 *m/z*).

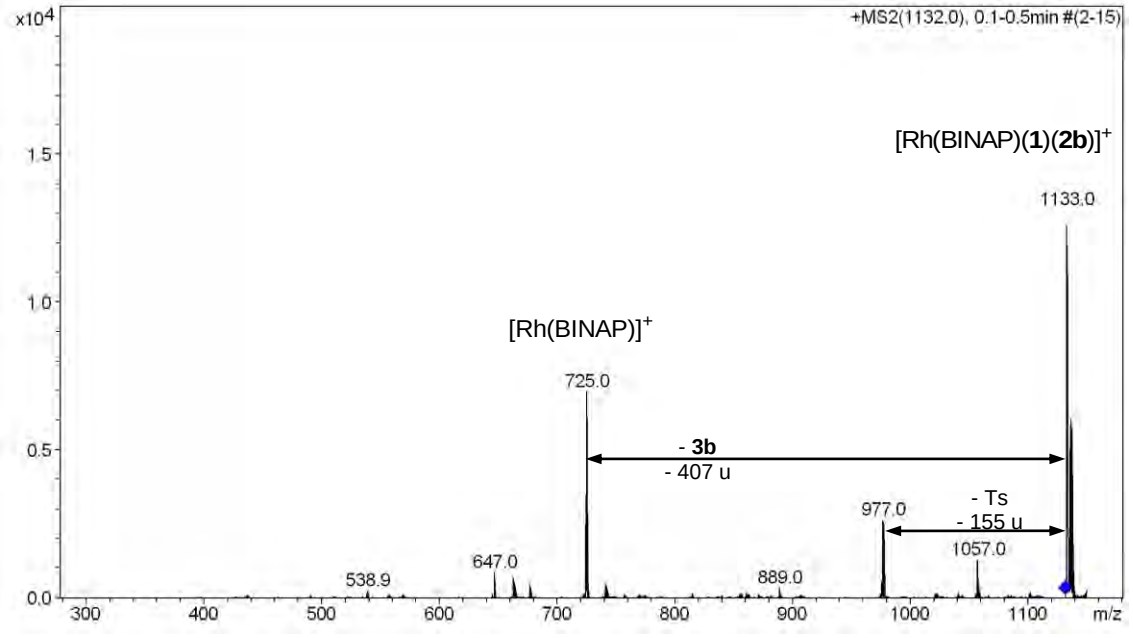

Figure S9. ESI(+)-MS/MS of the ion [Rh(BINAP)(**3b**)]$^+$ at 1132 (collision energy of 0,95 V, width = 4 *m*/*z*).

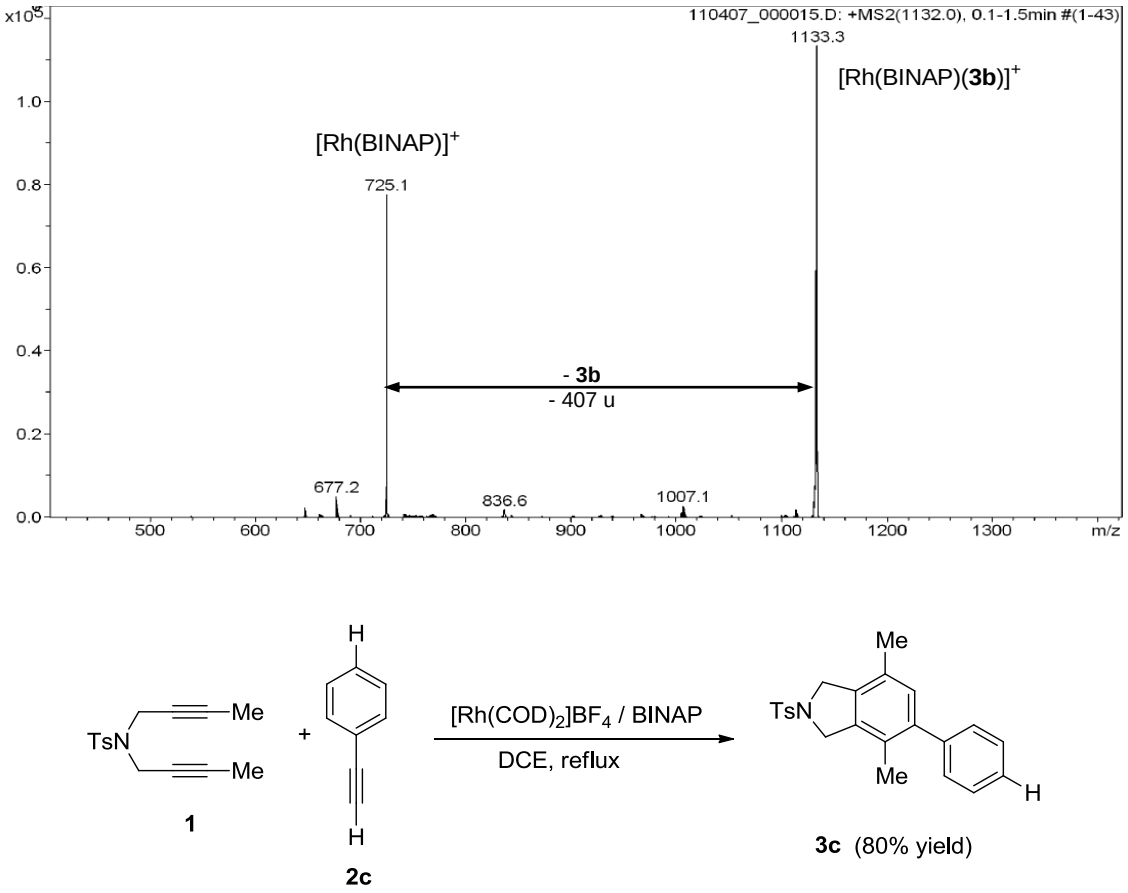

Figure S10. ESI(+) mass spectrum of a solution of the mixture of [Rh(COD)$_2$]BF$_4$/BINAP (5% molar) + **1** + **2c** at the reaction time of 15 min diluted in methanol.

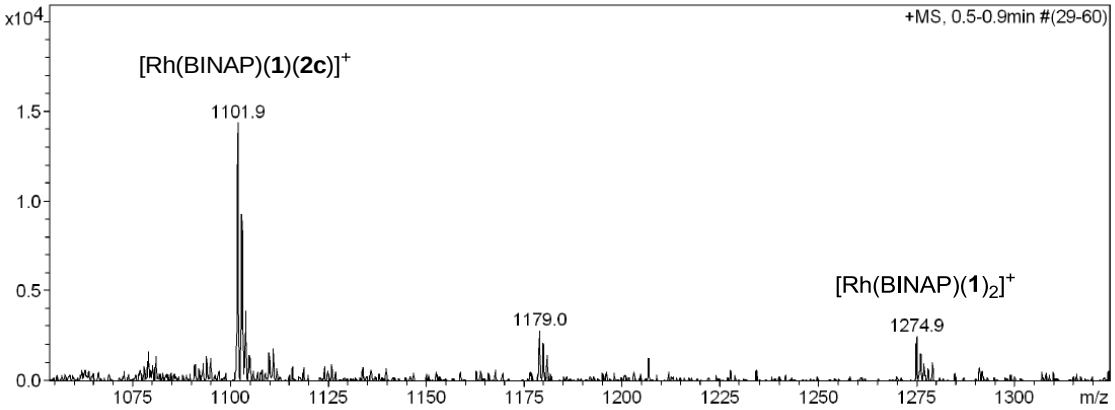

Figure S11. ESI(+)MS/MS spectrum of the ion [Rh(BINAP)(**1**)(**2c**)]$^+$ at *m/z* = 1102 (collision energy of 0,95 V, width = 4 *m/z*).

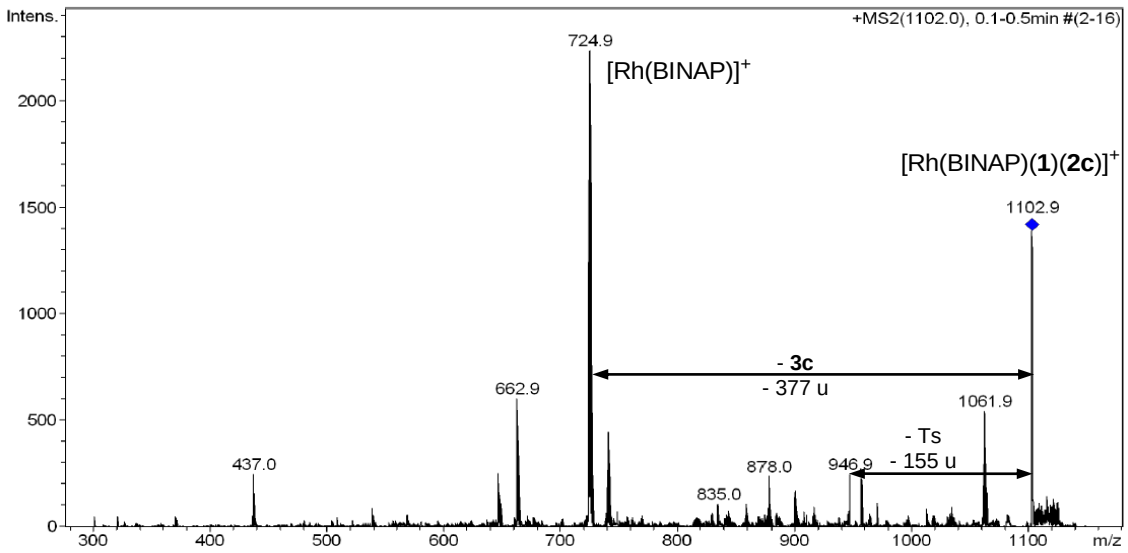

Figure S12. ESI(+)MS/MS spectrum of the ion [Rh(BINAP)(**3c**)]$^+$ at *m/z* = 1102 (collision energy of 0,95 V, width = 4 *m/z*).

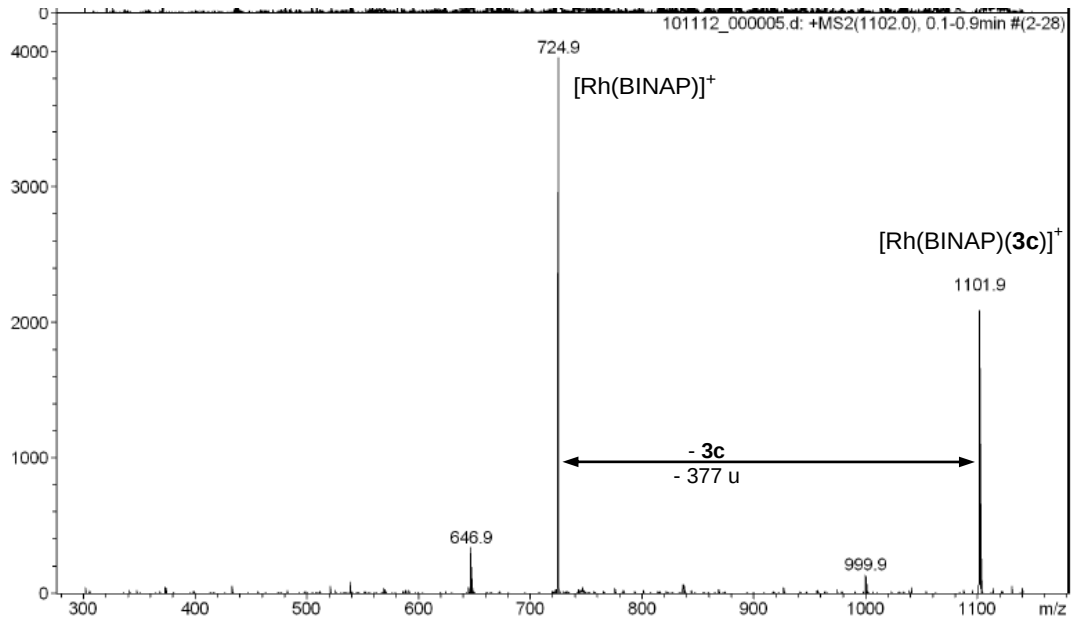

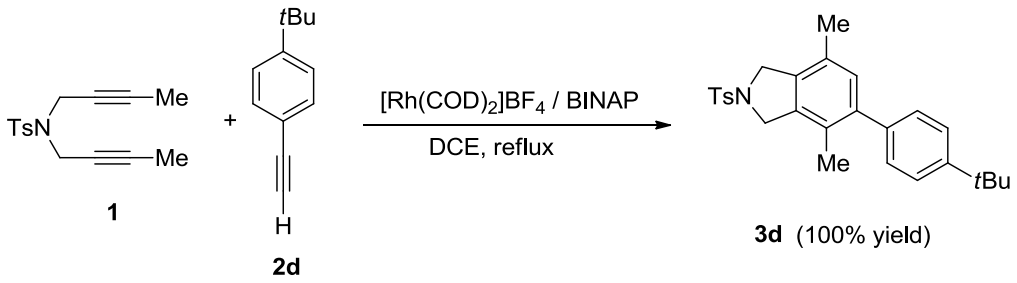

Figure S13. ESI(+) mass spectrum of a solution of the mixture of $[Rh(COD)_2]BF_4$/BINAP (5% molar) + **1** + **2d** diluted in methanol.

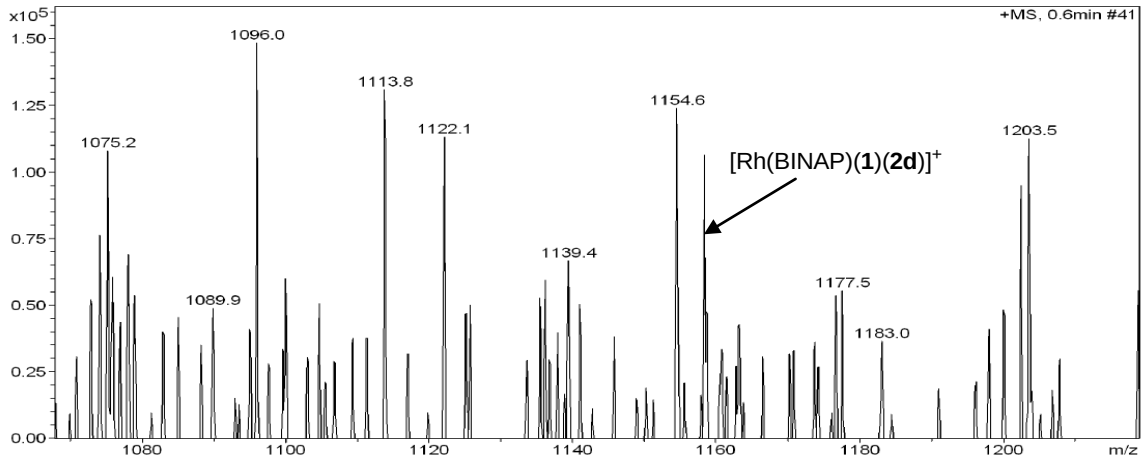

Figure S14: ESI(+)MS/MS spectrum of the ion $[Rh(BINAP)(\mathbf{1})(\mathbf{2d})]^+$ at *m/z* = 1158.0 (collision energy of 1,40 V, width = 4 *m/z*).

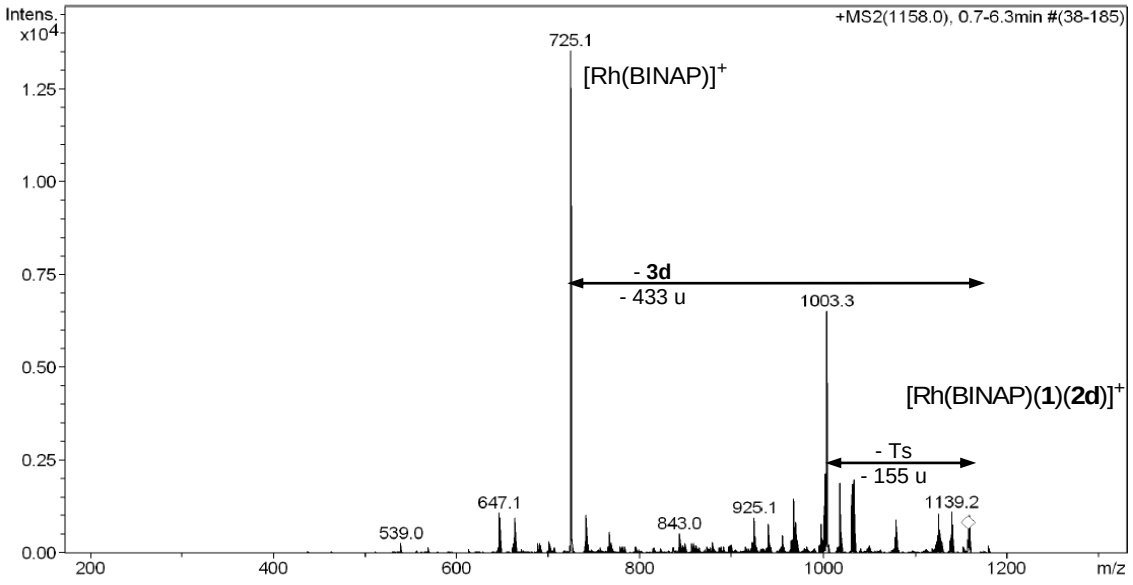

Figure S15. ESI(+)MS/MS spectrum of the ion [Rh(BINAP)(**3d**)]$^+$ at *m/z* = 1158 (collision energy of 0,95 V, width = 4 *m/z*).

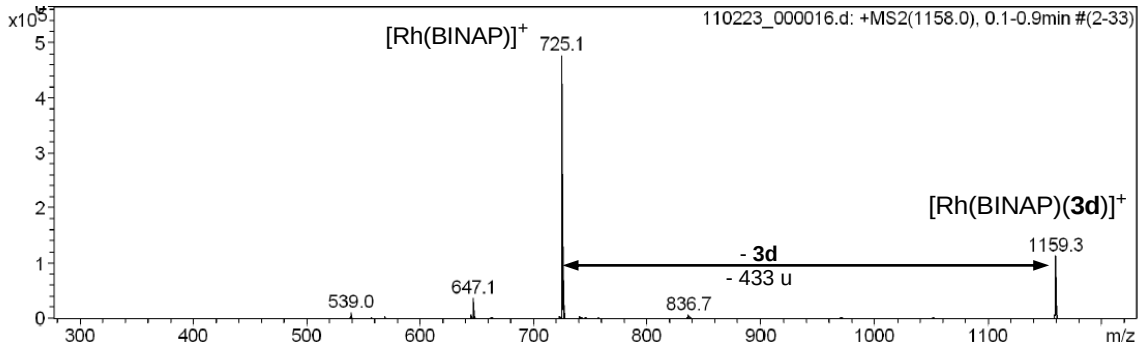

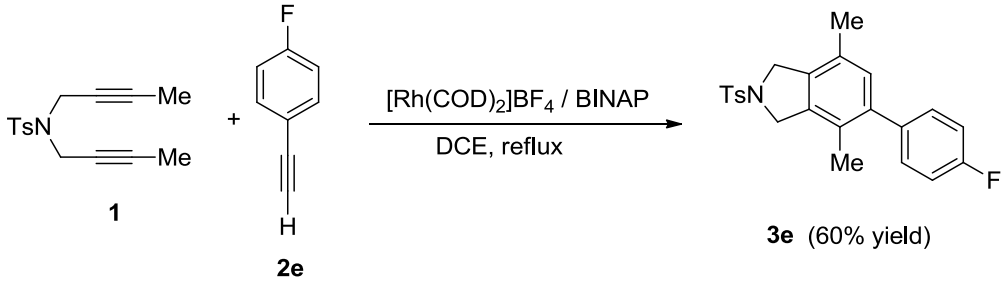

Figure S16. ESI(+) mass spectrum of a solution of the mixture of [Rh(COD)$_2$]BF$_4$/BINAP (5% molar) + **1** + **2e** diluted in methanol.

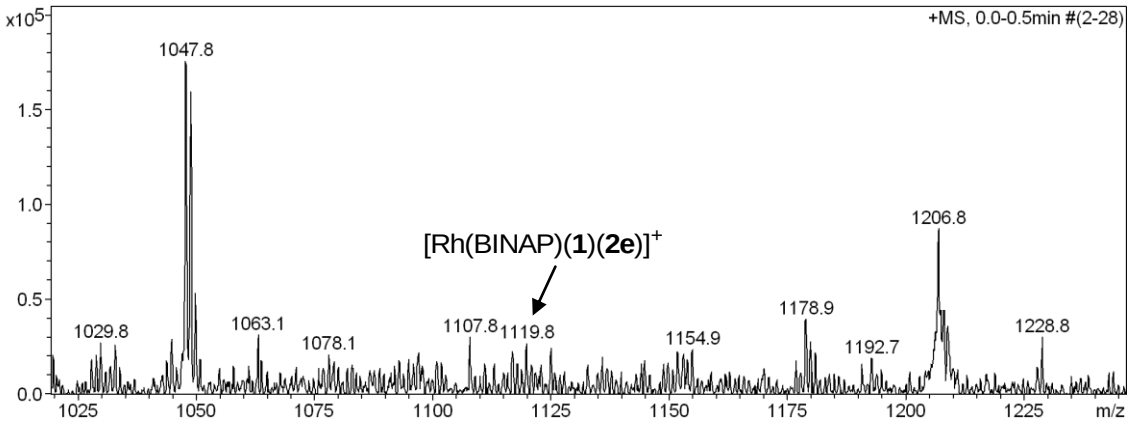

Figure S17. ESI(+)MS/MS spectrum of the ion [Rh(BINAP)(**1**)(**2e**)]$^+$ at *m/z* = 1120 (collision energy of 0,95 V, width = 4 *m/z*).

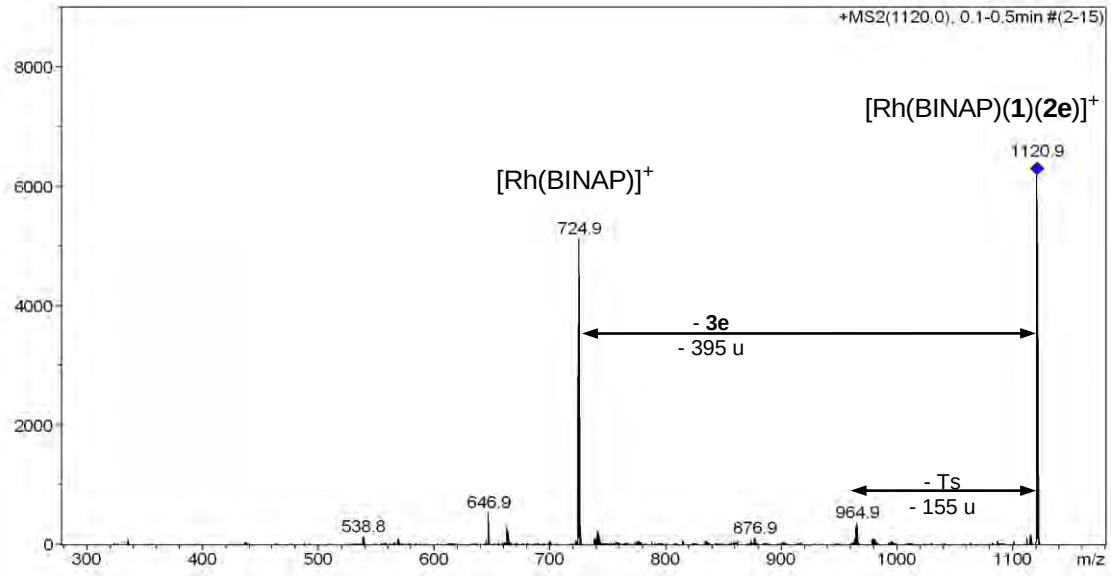

Figure S18. ESI(+)MS/MS spectrum of the ion [Rh(BINAP)(**3e**)]$^+$ at *m/z* = 1120 (collision energy of 0,95 V, width = 4 *m/z*).

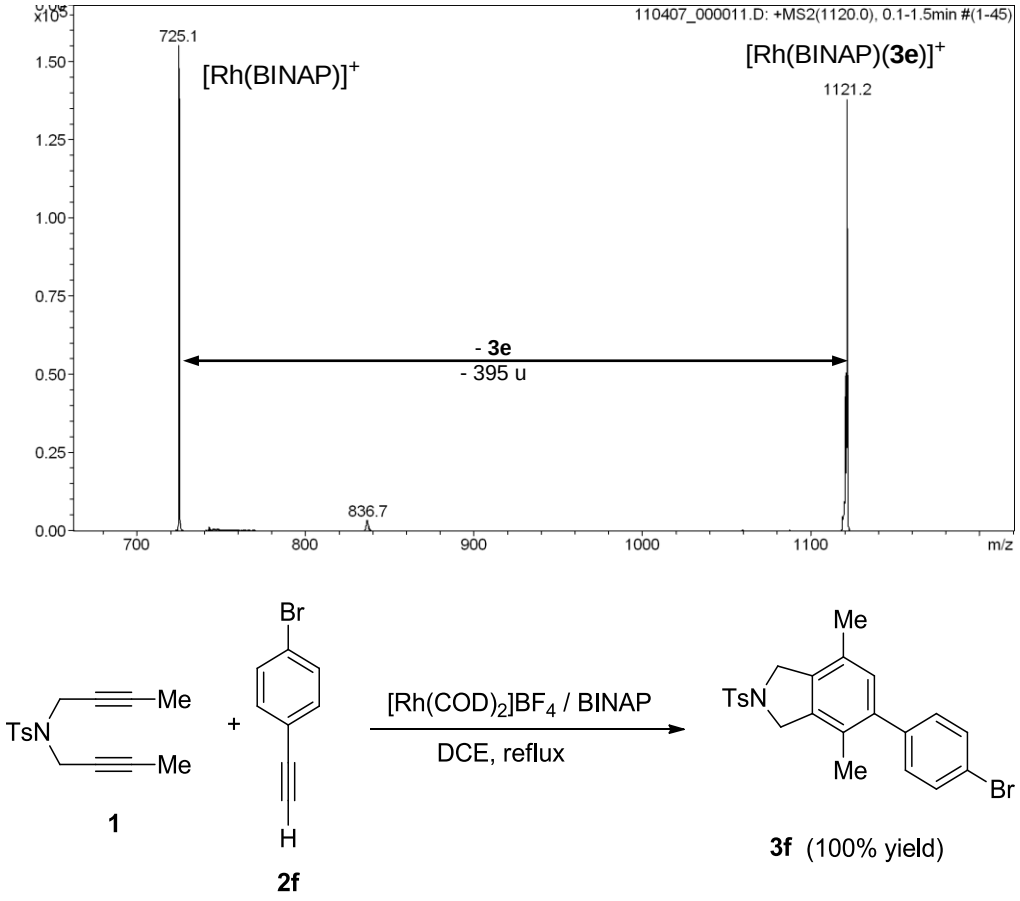

Figure S19. ESI(+) mass spectrum of a solution of the mixture of $[Rh(COD)_2]BF_4$/BINAP (5% molar) + **1** + **2f** diluted in methanol.

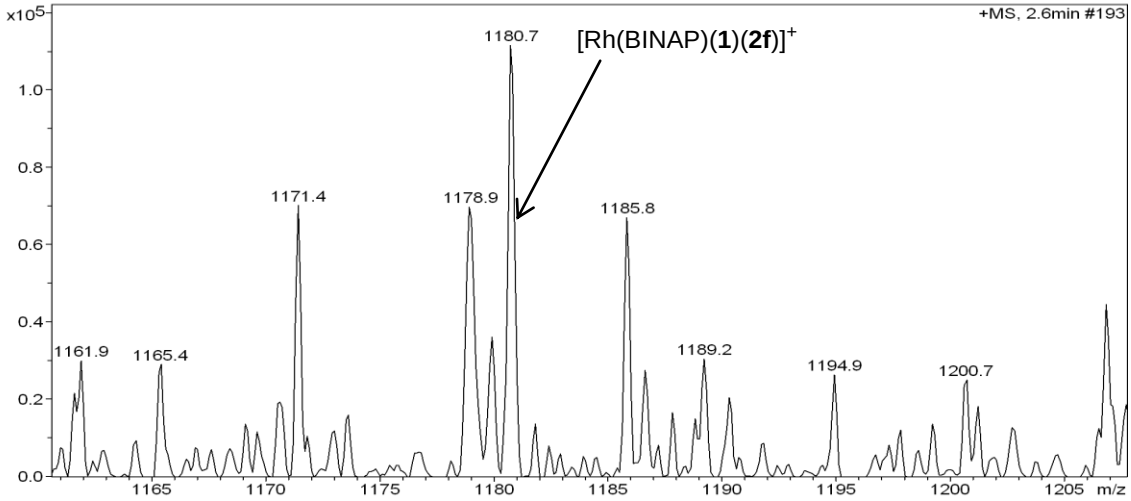

Figure S20. ESI(+)MS/MS spectrum of the ion $[Rh(BINAP)(\mathbf{1})(\mathbf{2f})]^+$ at *m/z* = 1182 (collision energy of 1,5 V, width = 4 *m/z*).

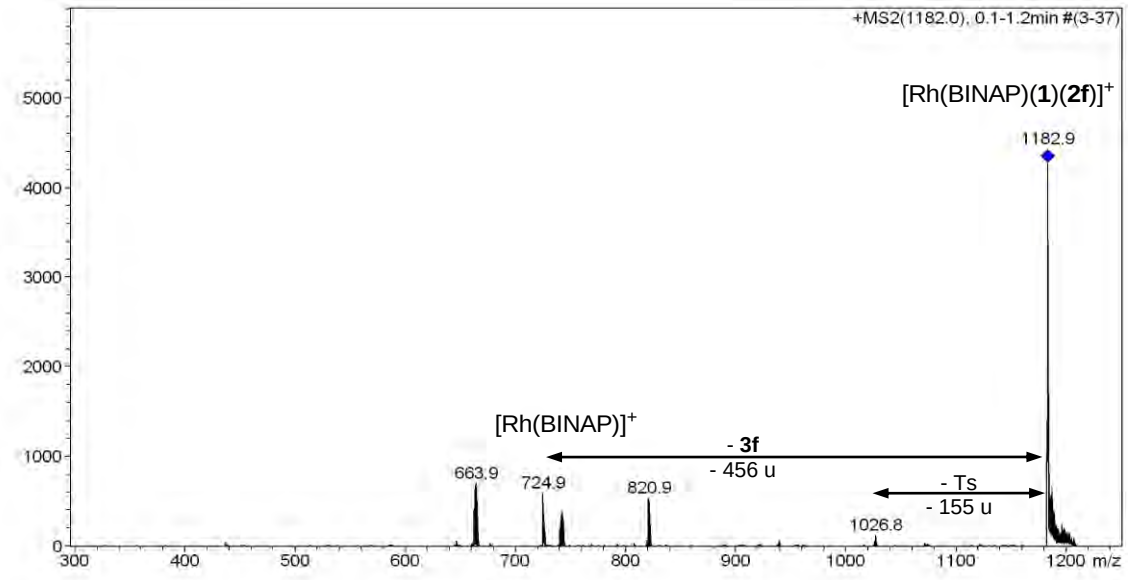

Figure S21. ESI(+)MS/MS spectrum of the ion [Rh(BINAP)(**3f**)]$^+$ at *m/z* = 1182 (collision energy of 0,95 V, width = 4 *m/z*).

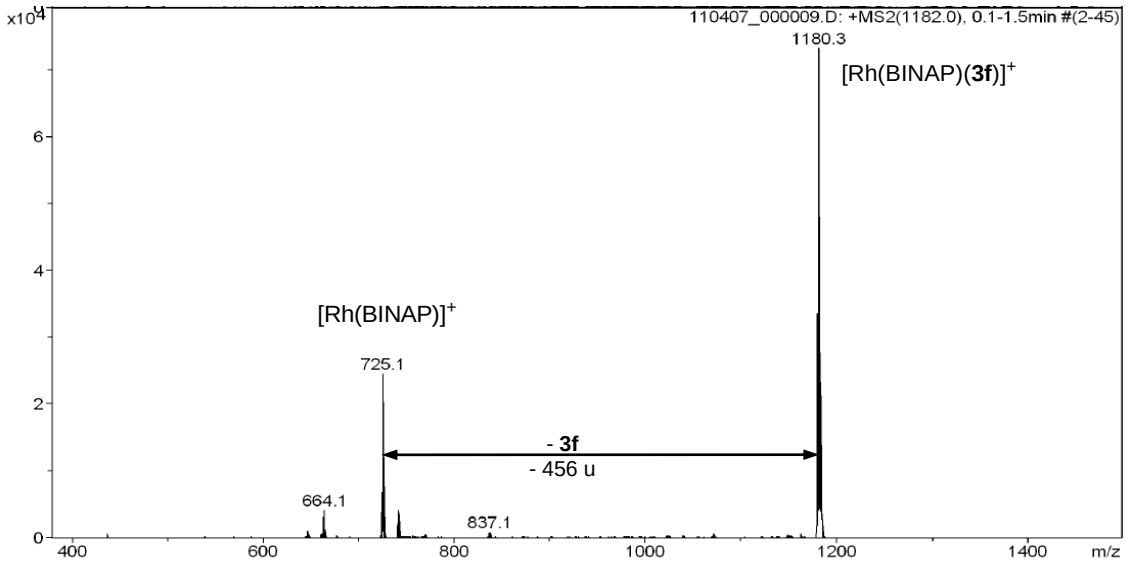

Scheme 4. [2+2+2] Cycloaddition reactions between diyne **4** and phenylacetylene **2c** studied by ESI-MS.

Figure S22. ESI(+) mass spectrum of a solution of diyne **4** in methanol.

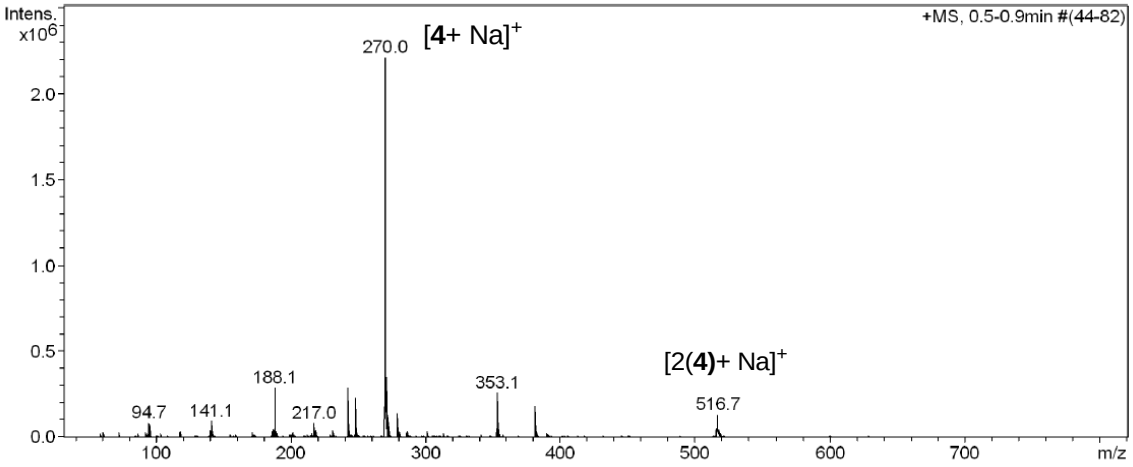

Figure S23. ESI(+) mass spectrum of a solution of cycloadduct **5** in methanol.

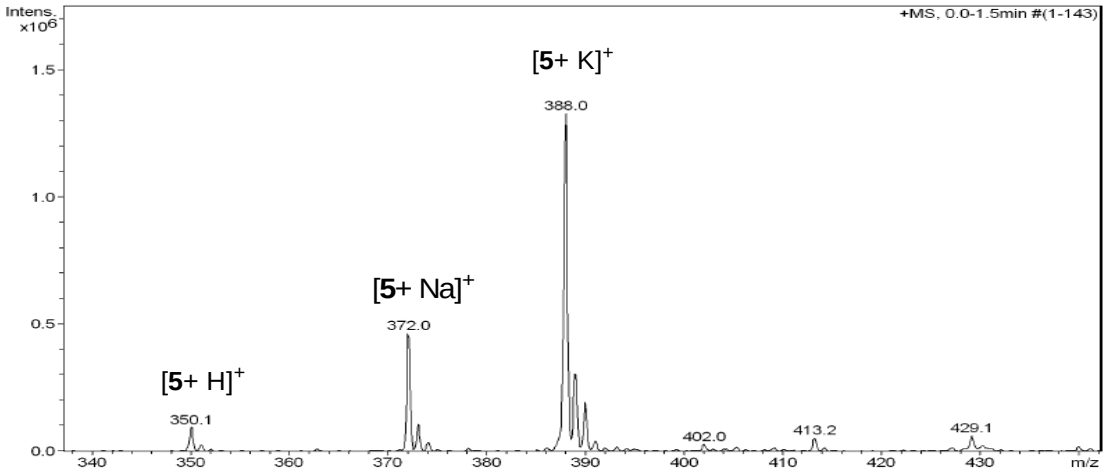

Figure S24. ESI(+)-MS/MS spectrum of the ion [**5**+H]$^+$ at *m/z* = 350 (collision energy of 1 V, width = 4 *m/z*) in methanol.

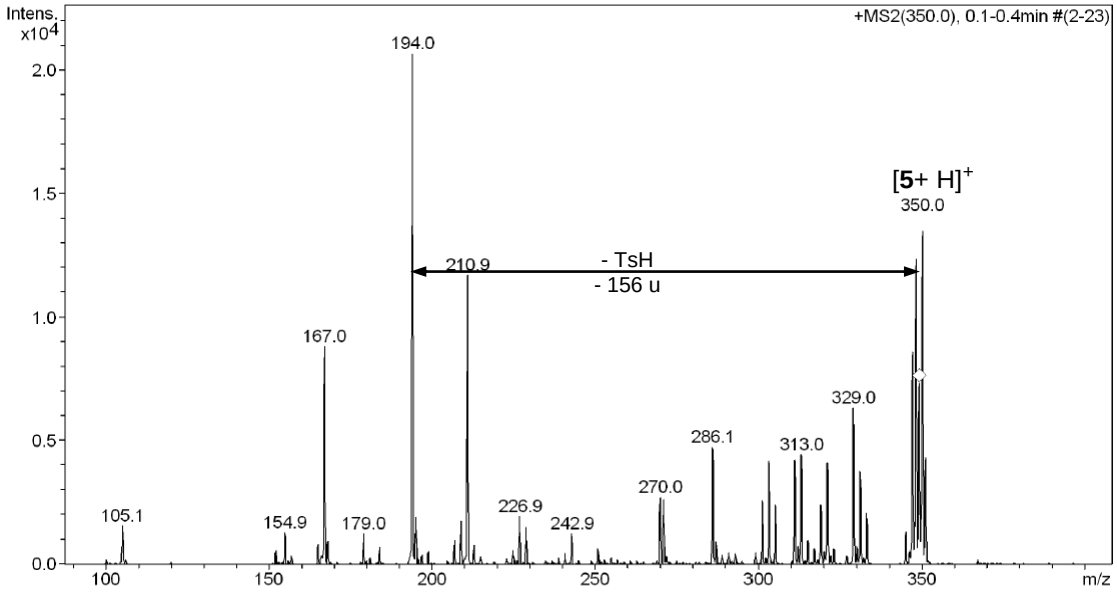

Figure S25. ESI(+) mass spectra(a and b) of a solution of the mixture of $[Rh(COD)_2]BF_4$/BINAP (5% molar) + **4** + **2c** diluted in methanol.

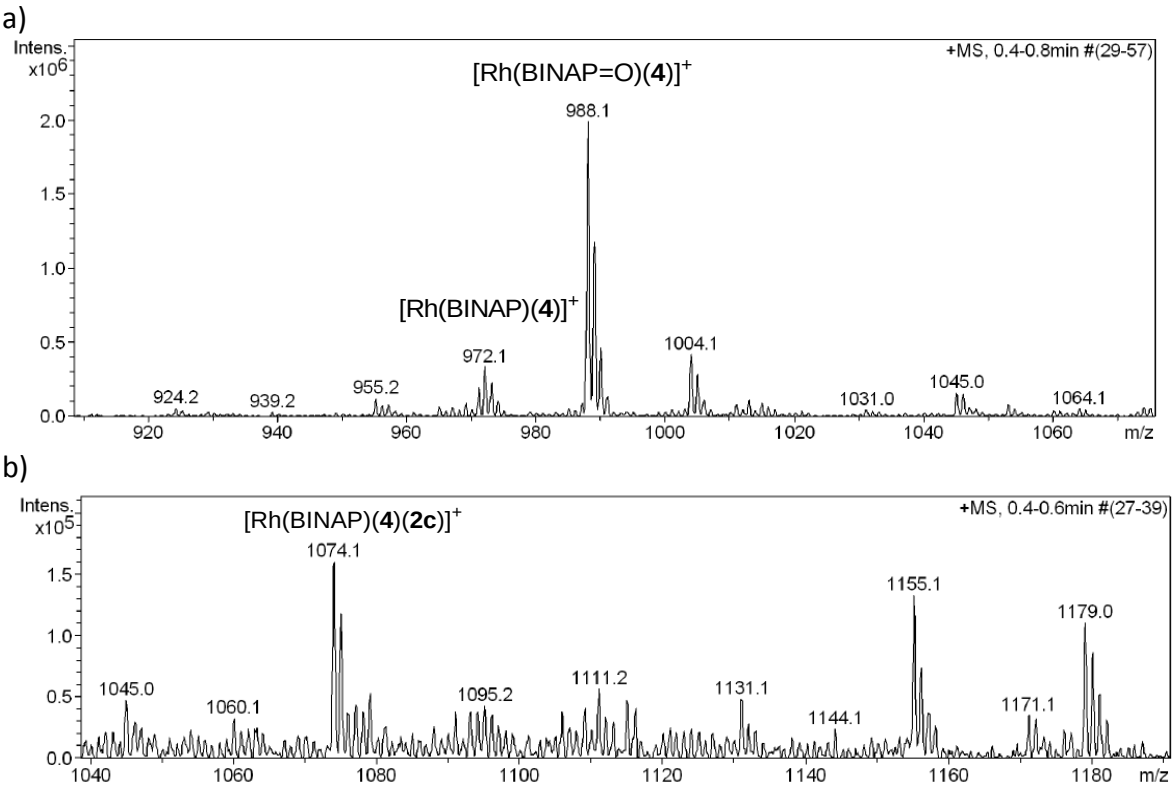

Figure S26. ESI(+)MS/MS spectrum of the ions at: a) *m/z* = 972 ([Rh(BINAP)(**4**)]$^+$), b) *m/z* = 988 ([Rh(BINAP=O)(**4**)]$^+$) and c) *m/z* = 1074 ([Rh(BINAP)(**4**)(**2c**)]$^+$) (collision energy of 1 V, width = 4 *m/z*).

a) and b):

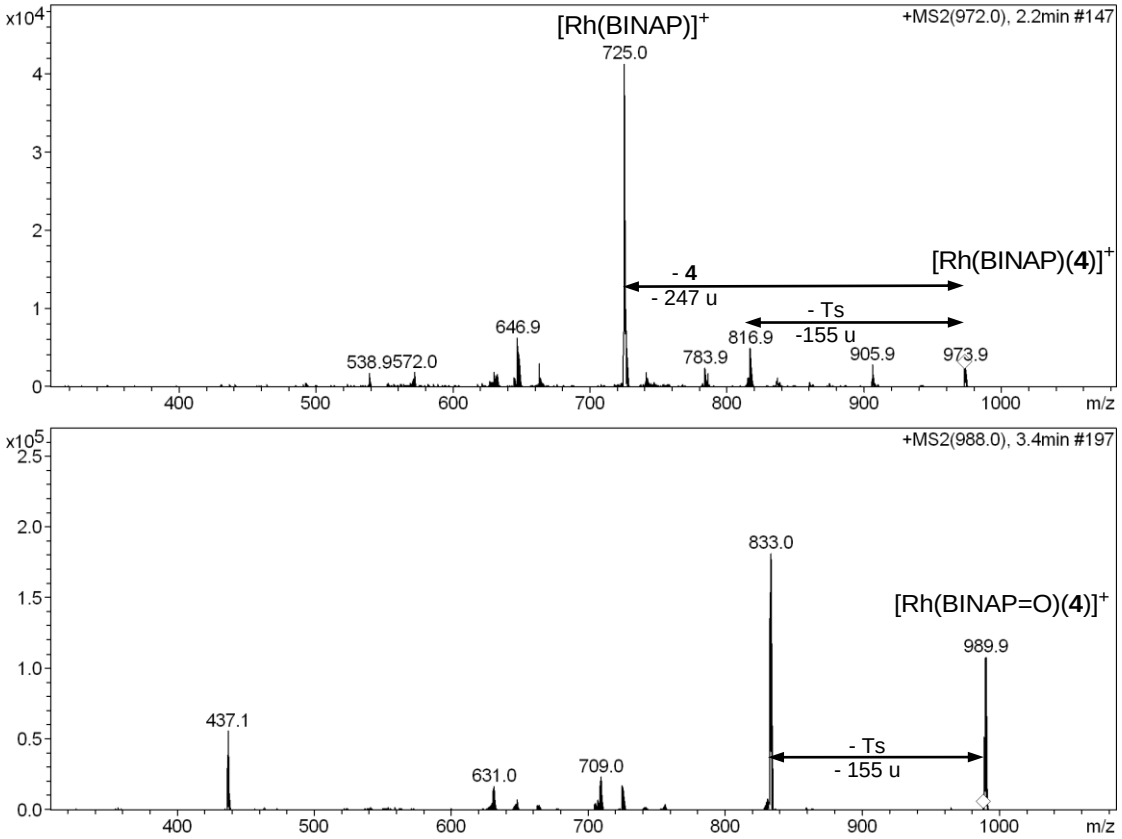

c)

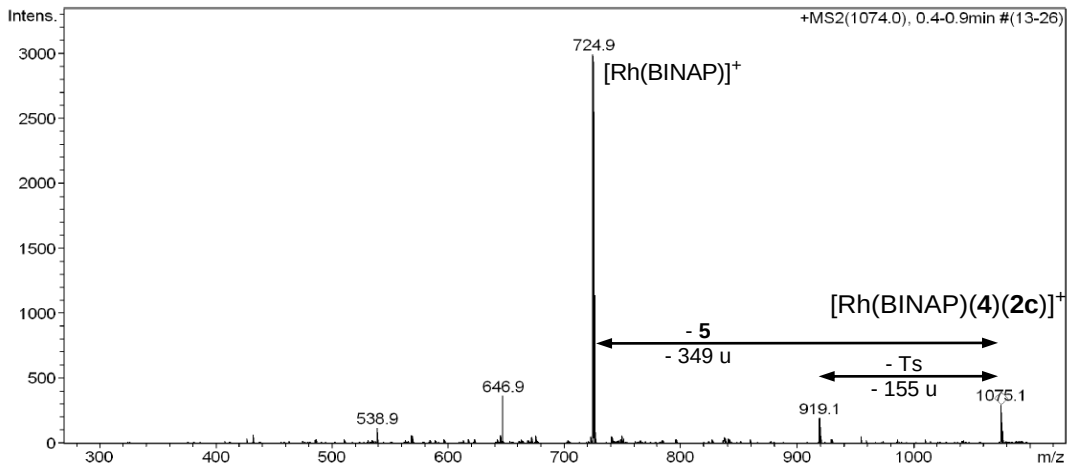

Figure S27. a) ESI(+) mass spectra of a solution of the mixture of $[Rh(COD)_2]BF_4$/BINAP (5% molar) + **4** + **2c** at the reaction time of 60 min diluted in methanol.

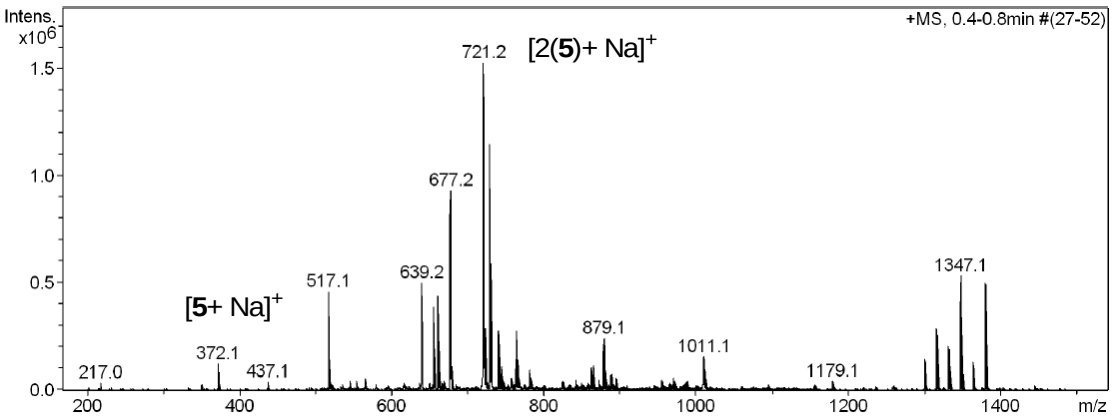

Figure S28. ESI(+) mass spectrum of a solution of the mixture of $[Rh(COD)_2]BF_4$/BINAP (5% molar) + **5** in methanol.

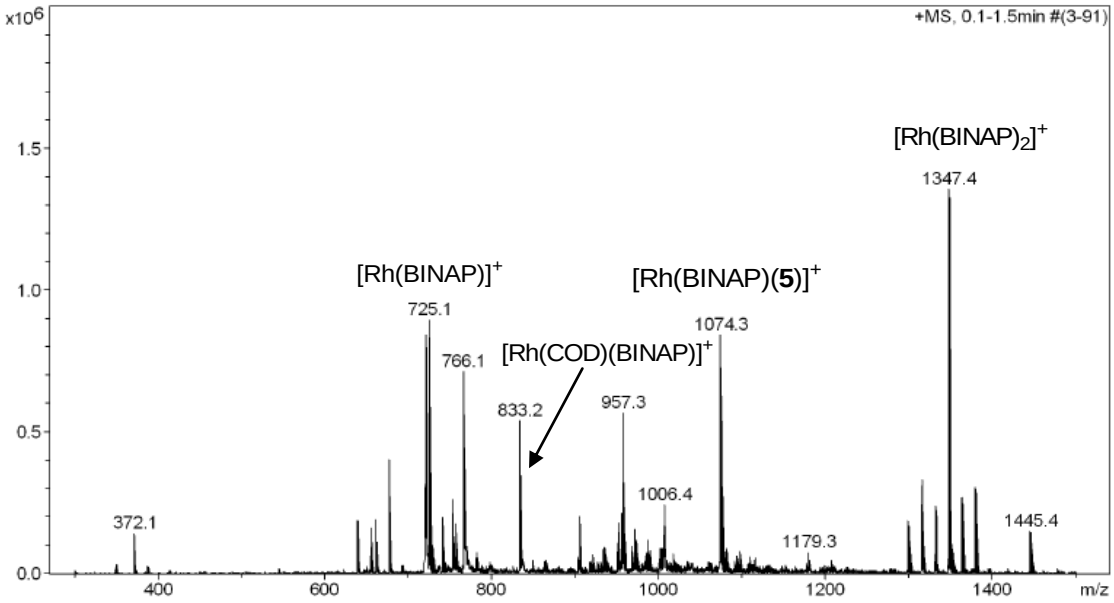

Figure S29. ESI(+)MS/MS spectrum of the ion [Rh(BINAP)(**5**)]$^+$ at *m/z* = 1074 (collision energy of 0,20 V, width = 4 *m/z*).

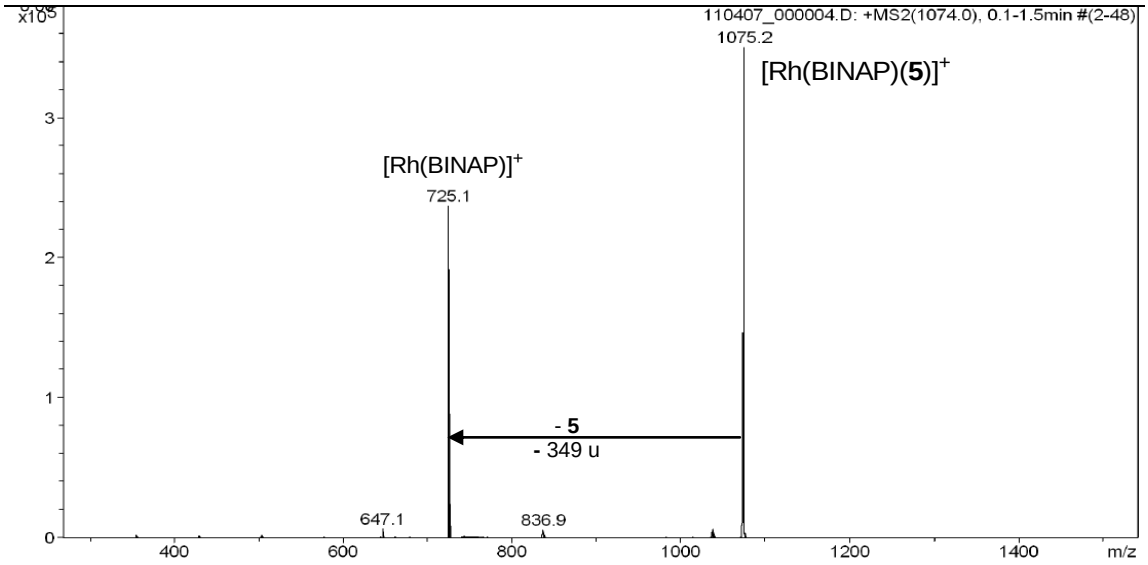

Scheme 6. [2+2+2] Cycloaddition reactions between malonate tethered diyne **6** and p-methylphenylacetylene **2a** studied by ESI-MS.

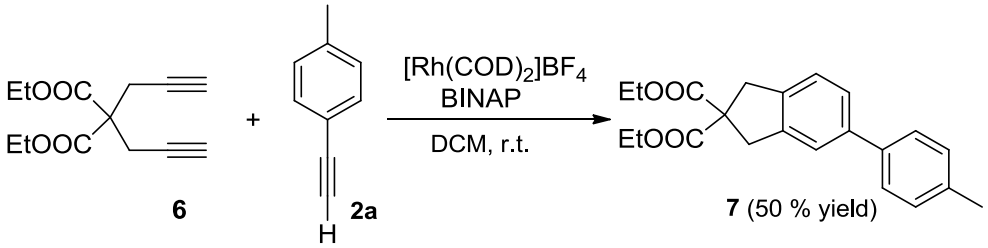

Figure S30. a) ESI(+) mass spectra of a solution of the mixture of $[Rh(COD)_2]BF_4$/BINAP (5% molar) + **6** + **2a** at the reaction time of 1 min diluted in methanol. b) Expansion of the range of the second intermediate.

a)

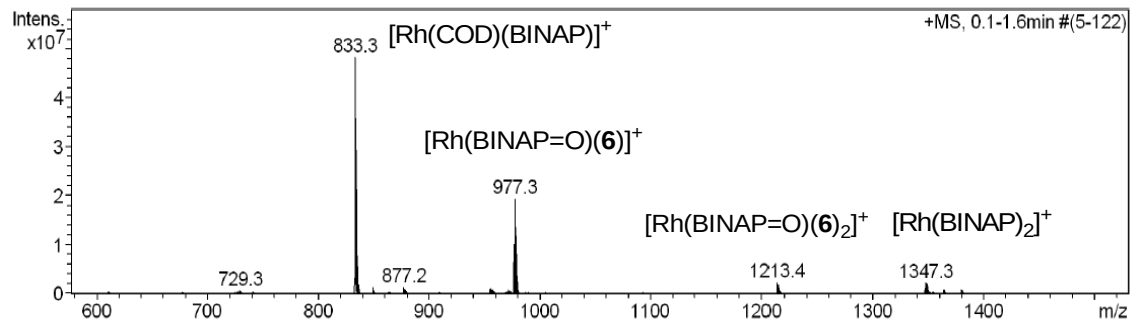

b)

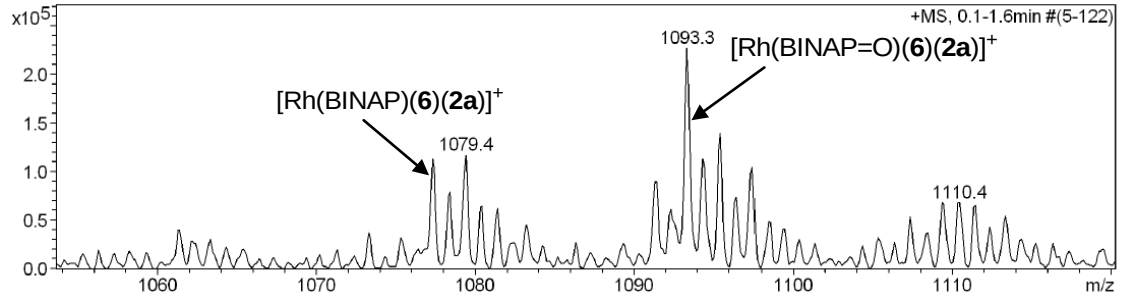

Figure S31. a) ESI(+)MS/MS and b) ESI(+)MS/MS^3 spectra of the ion [Rh(BINAP=O)(**6**)]$^+$ at *m/z* = 977.3 (collision energy of 0,30 V, width = 4 *m/z*).

a)

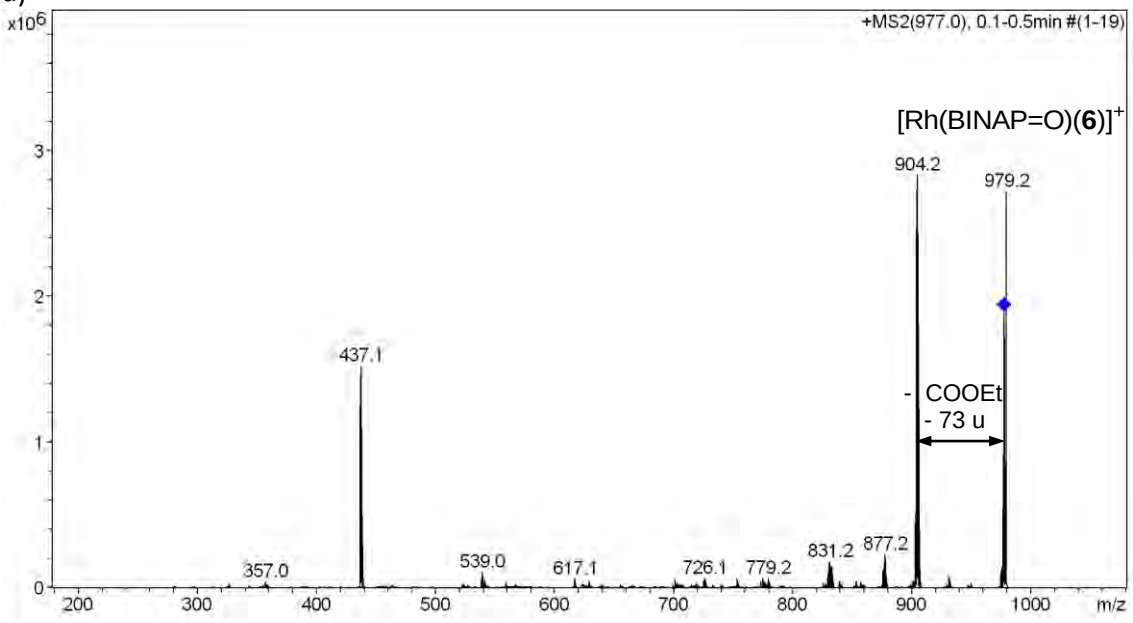

b)

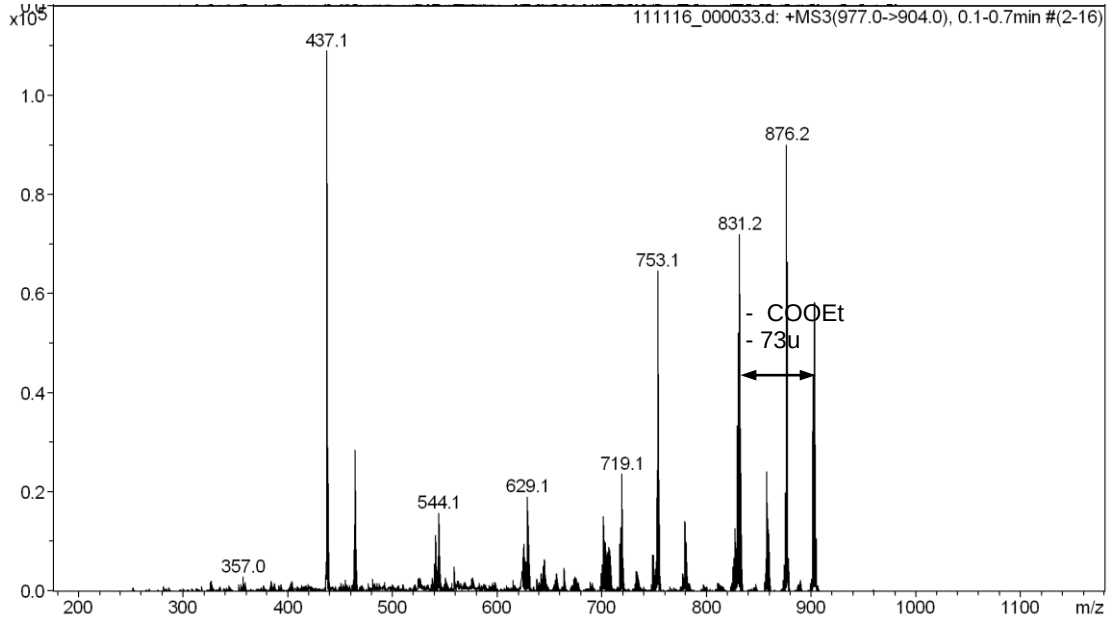

Figure S32. ESI(+)MS/MS spectrum of the ion [Rh(BINAP)(**7**)]$^+$ at *m/z* = 1077.3 (collision energy of 0,30 V, width = 4 *m/z*).

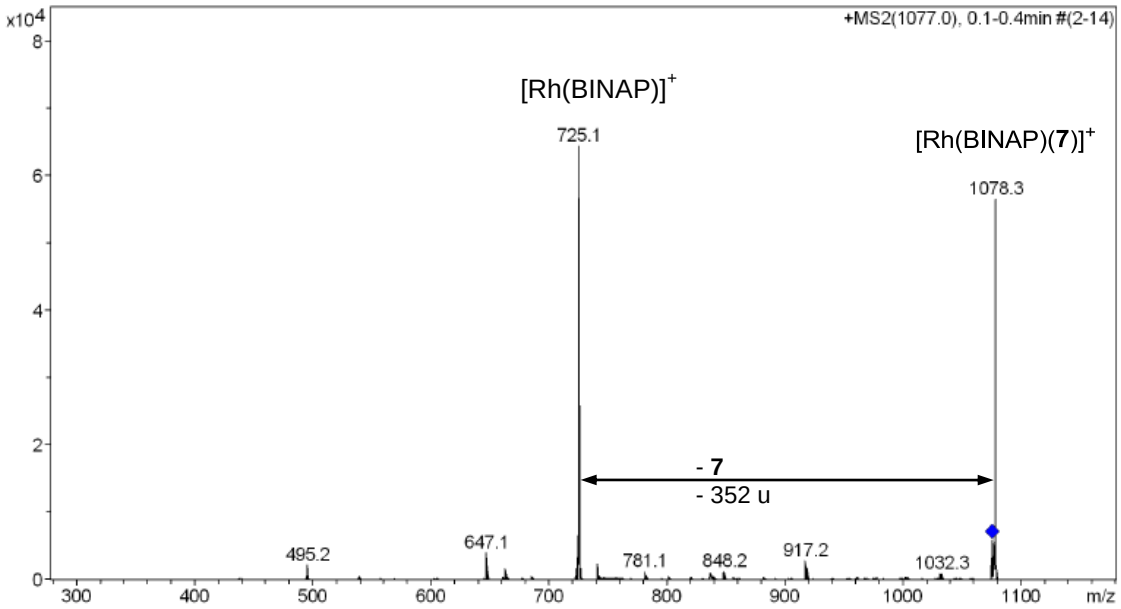

Figure S33. a) ESI(+)MS/MS and b) ESI(+)MS/MS^3 spectra of the ion [Rh(BINAP=O)(**6**)(**2a**)]$^+$ at *m/z* = 1093.3 (collision energy of 0,30 V, width = 4 *m/z*).

a)

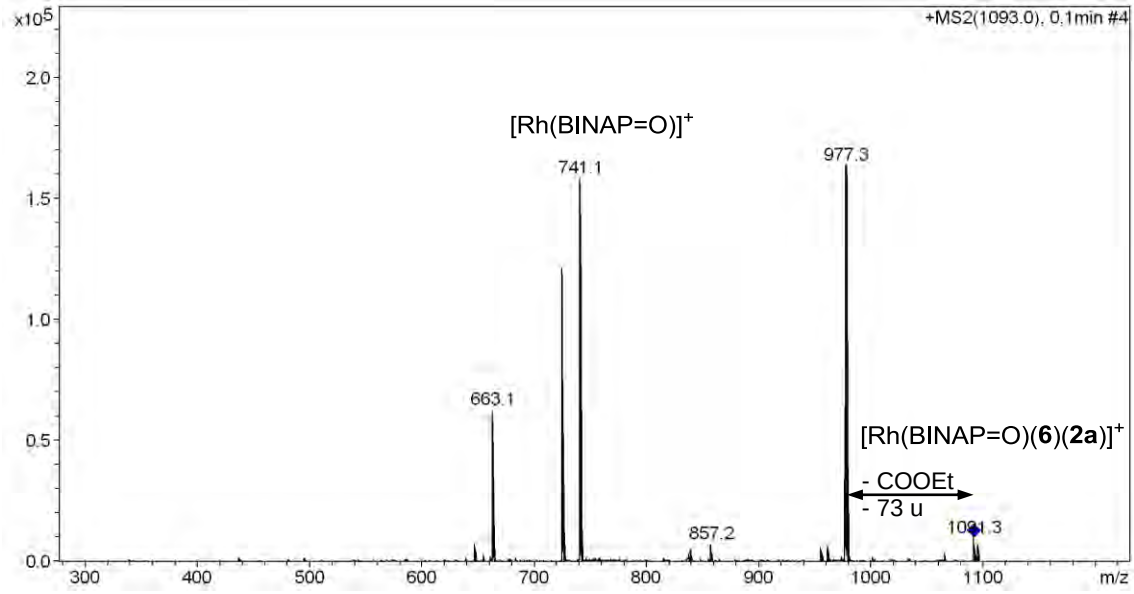

b)

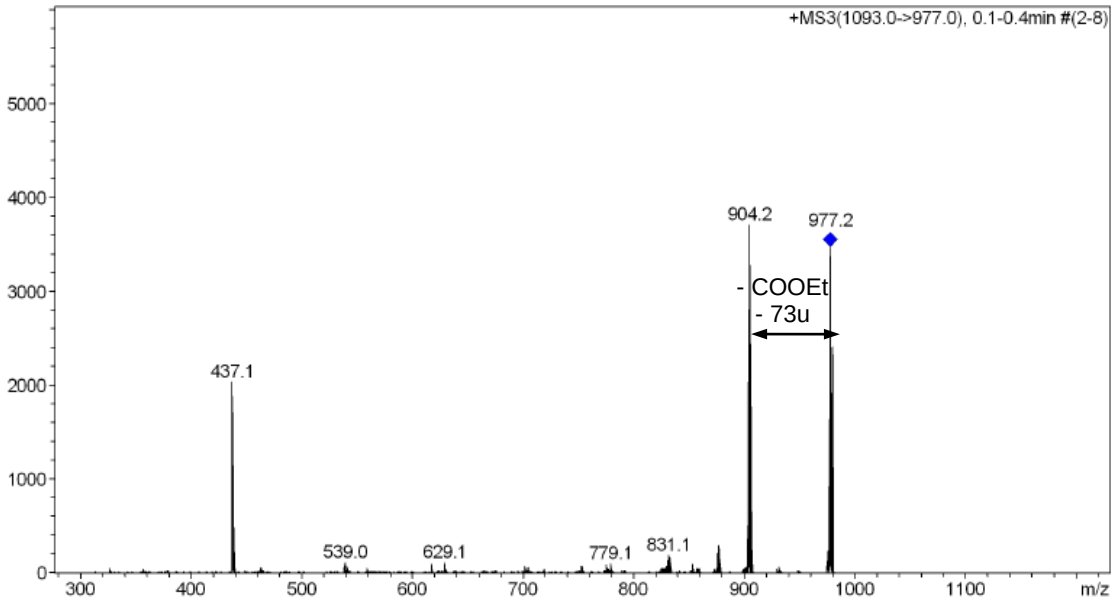

Figure S34. ESI(+)MS/MS spectrum of the ion $[Rh(BINAP)(\mathbf{6})_2]^+$ at *m/z* = 1197.0 (collision energy of 0,30 V, width = 4 *m/z*).

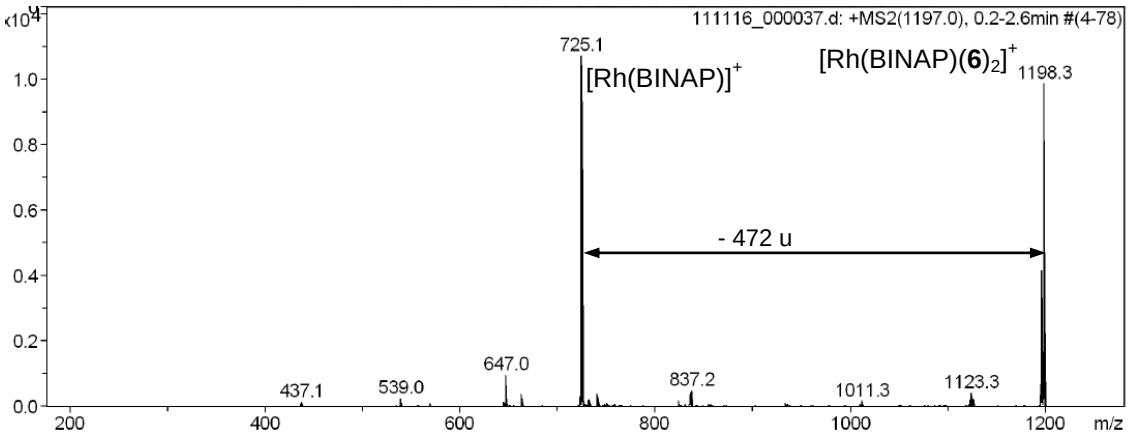

Figure S35. ESI(+)MS/MS spectrum of the ion $[Rh(BINAP{=}O)(\mathbf{6})_2]^+$ at *m/z* = 1213.4 (collision energy of 0,30 V, width = 4 *m/z*).

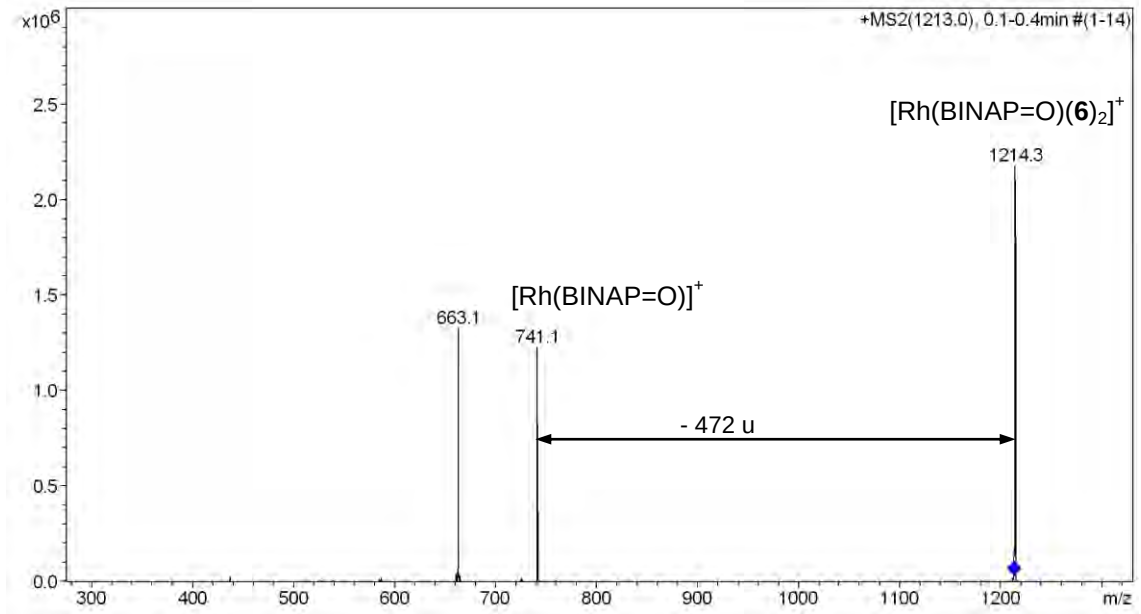

Figure S36. a) ESI(+)MS/MS spectrum of the ion [**7** + H]$^+$ at *m/z* = 353.0 (collision energy of 0,30 V, width = 4 *m/z*).

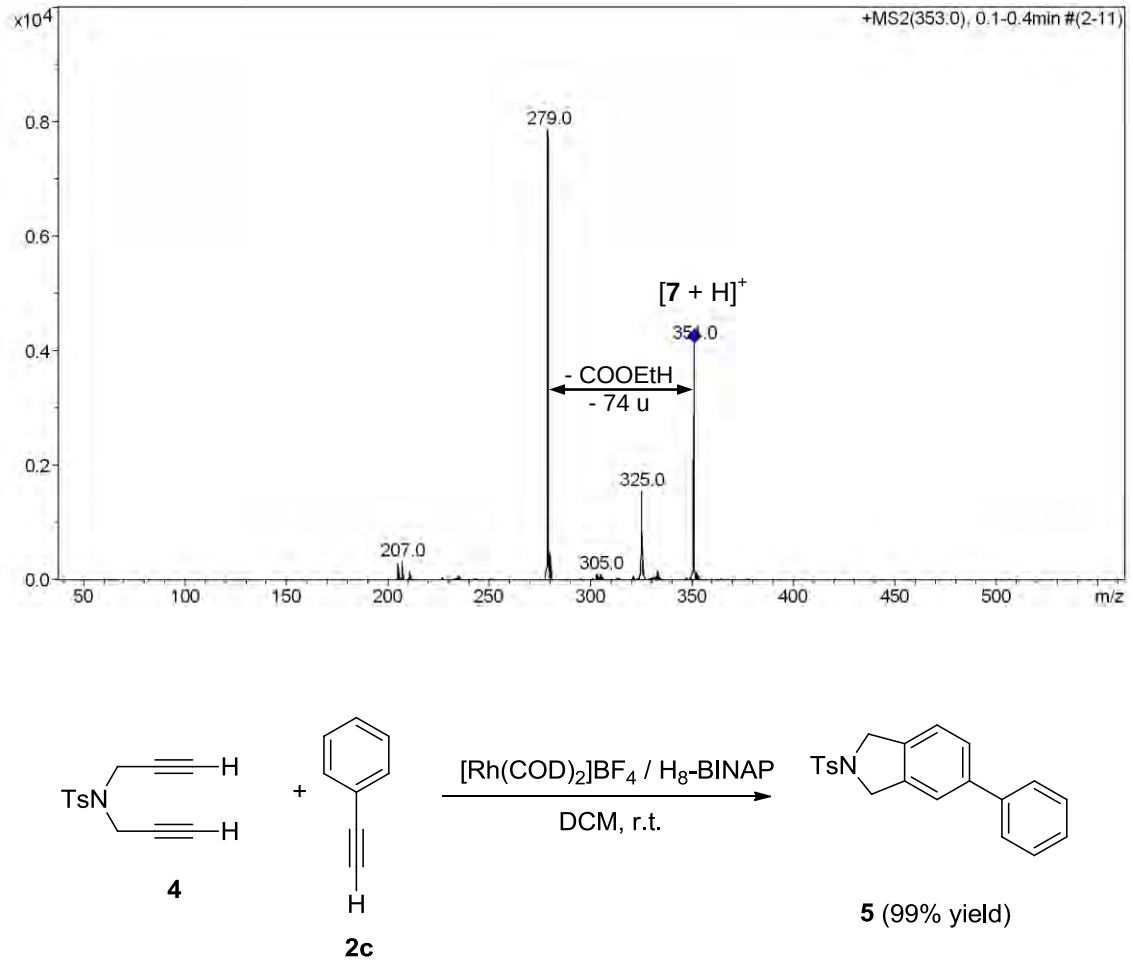

Figure S37. ESI(+) mass spectrum of a solution of $[Rh(COD)_2]BF_4$/H_8-BINAP (5% molar) + **4** + **2c** diluted in methanol.

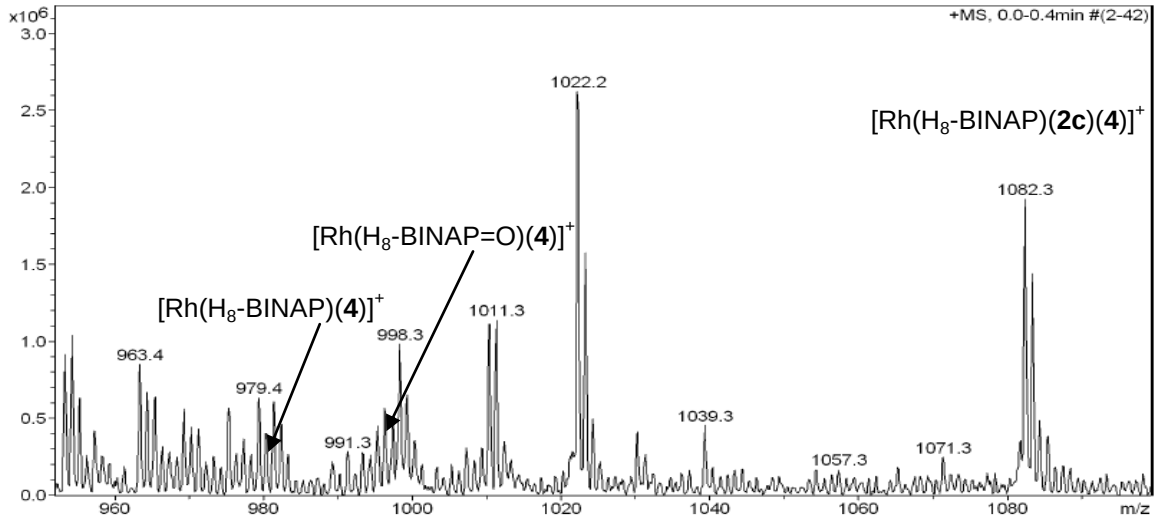

Figure S38. ESI(+)-MS/MS spectrum of the ion [Rh(H_8-BINAP)(**4**)]$^+$ at *m/z* = 980.3 (collision energy of 1 V, width = 4 *m/z*).

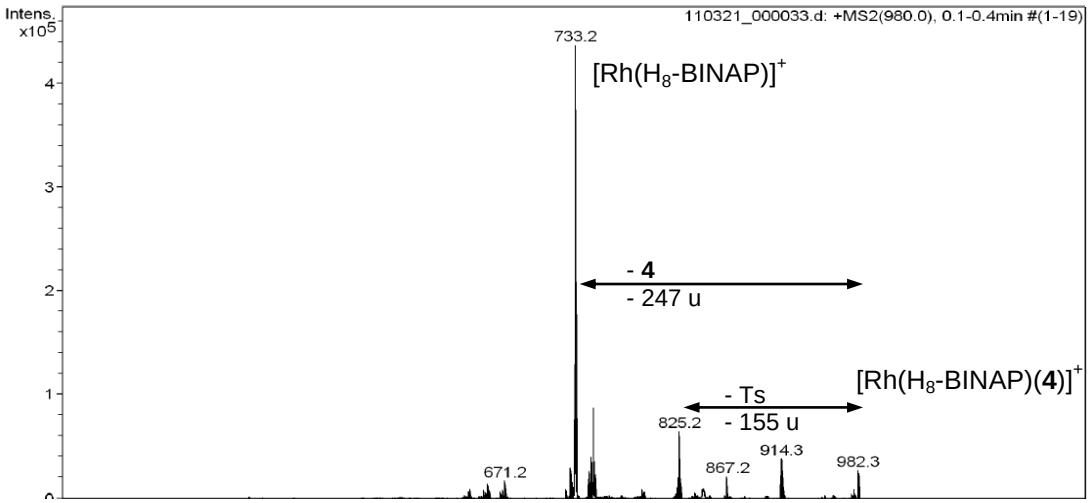

Figure S39. ESI(+)-MS/MS spectrum of the ion [Rh(H_8-BINAP=O)(**4**)]$^+$ at *m/z* = 996.3 (collision energy of 1 V, width = 4 *m/z*).

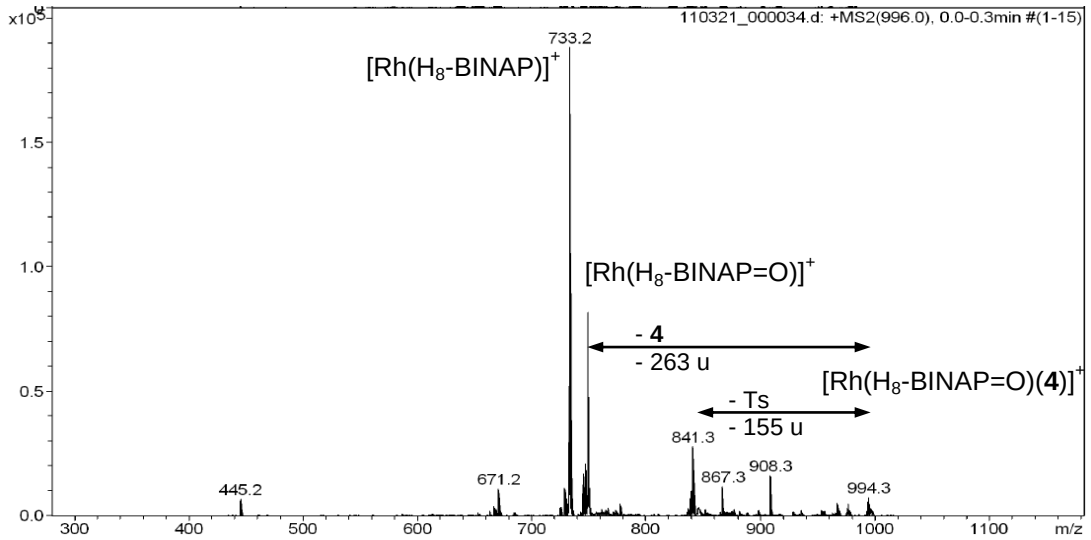

Figure S40. ESI(+)-MS/MS spectrum of the ion $[Rh(H_8\text{-BINAP})(\mathbf{4})(\mathbf{2a})]^+$ at *m/z* = 1082 (collision energy of 1 V, width = 4 *m/z*).

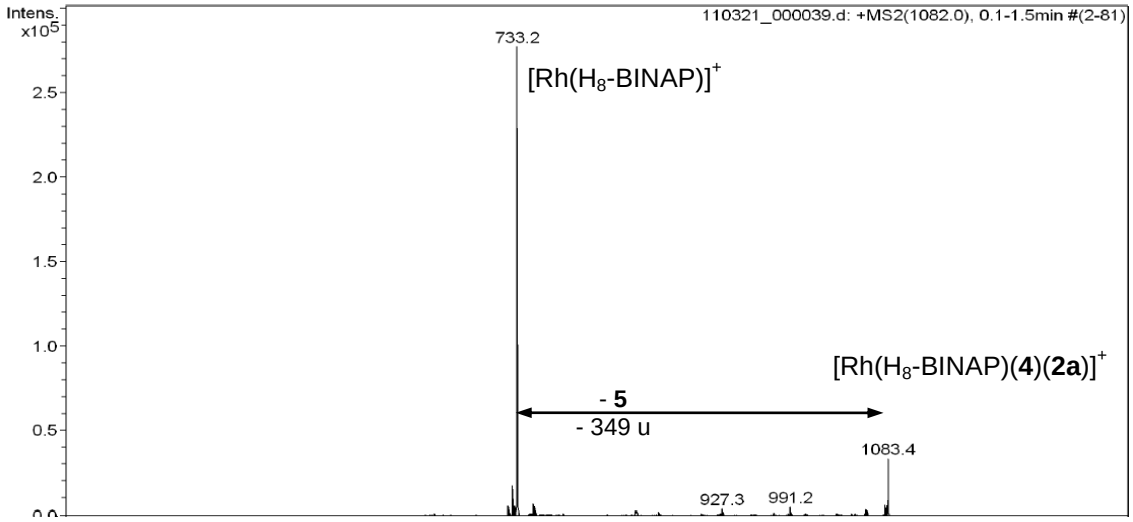

Figure S33. ESI(+)-MS/MS spectrum of the ion $[Rh(H_8\text{-BINAP})(\mathbf{4})_2]^+$ at *m/z* = 1227 (collision energy of 1 V, width = 4 *m/z*).

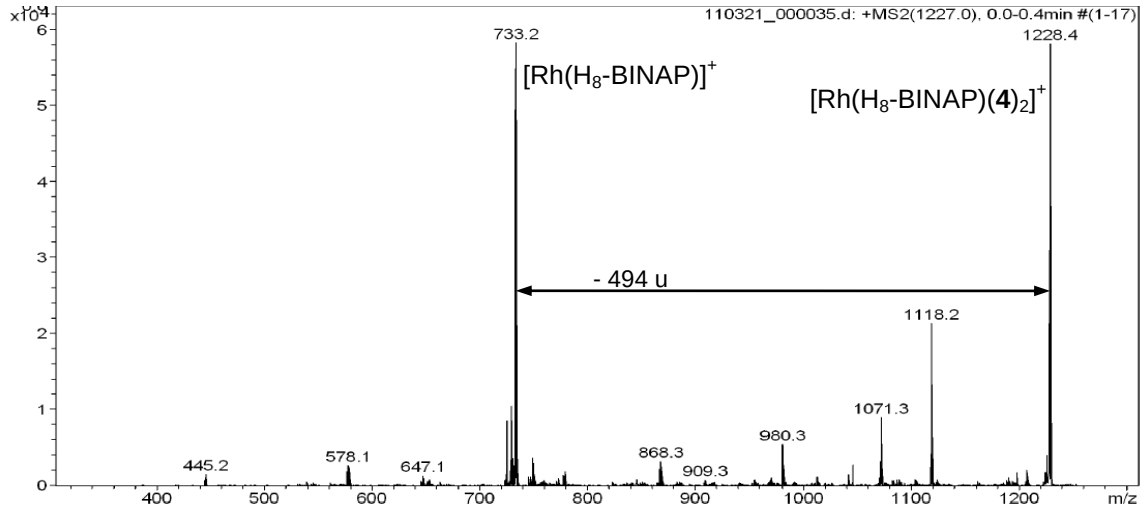

Figure S34. ESI(+) mass spectrum of a solution of the mixture of $[Rh(COD)_2]BF_4$/BIPHEP (5% molar) + **4** + **2c** diluted in methanol.

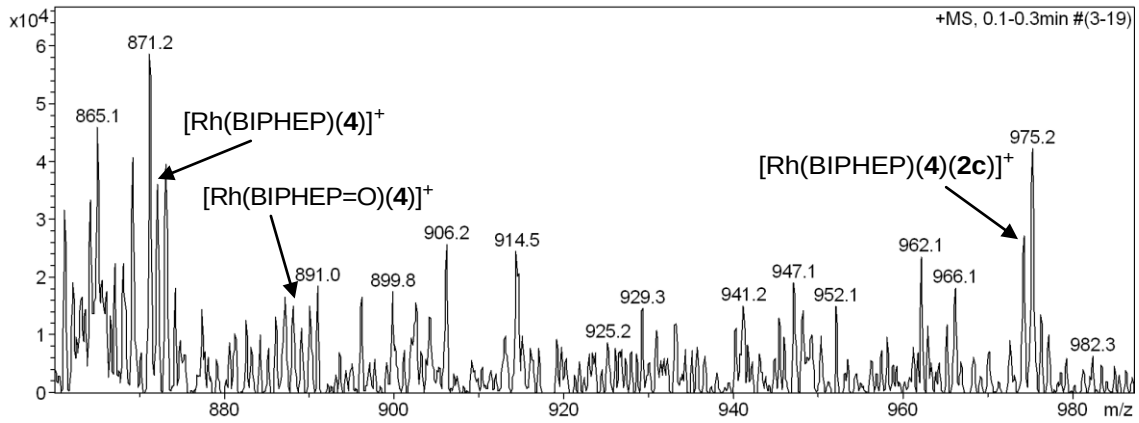

Figure S35. ESI(+)MS/MS spectra of the ions at a) *m/z* = 872 $[Rh(BIPHEP)(\mathbf{4})]^+$ and b) 888 $[Rh(BIPHEP{=}O)(\mathbf{4})]^+$ (collision energy of 0,35 V, width = 4 *m/z*).

a)

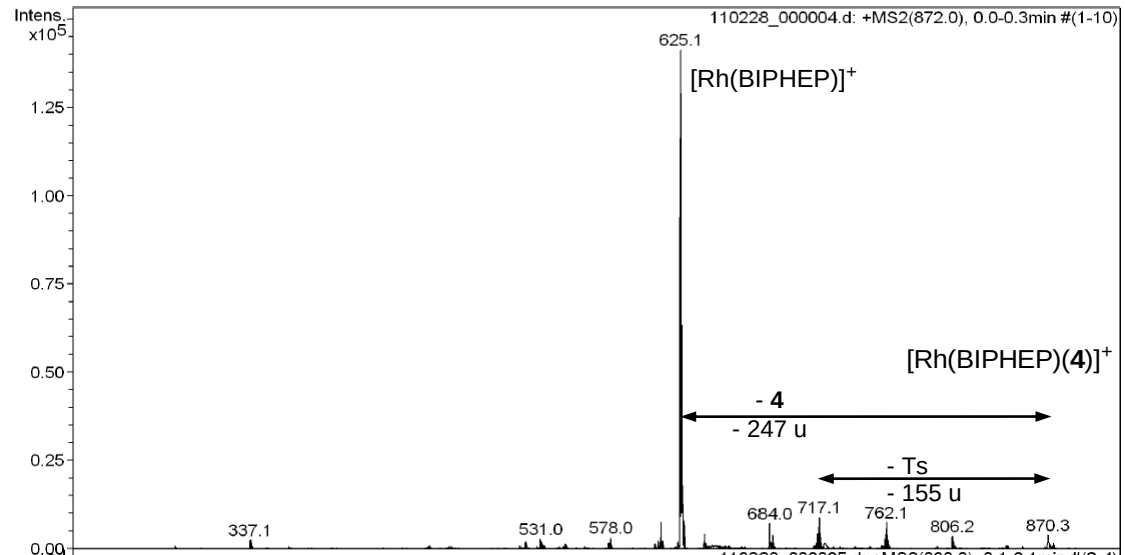

b)

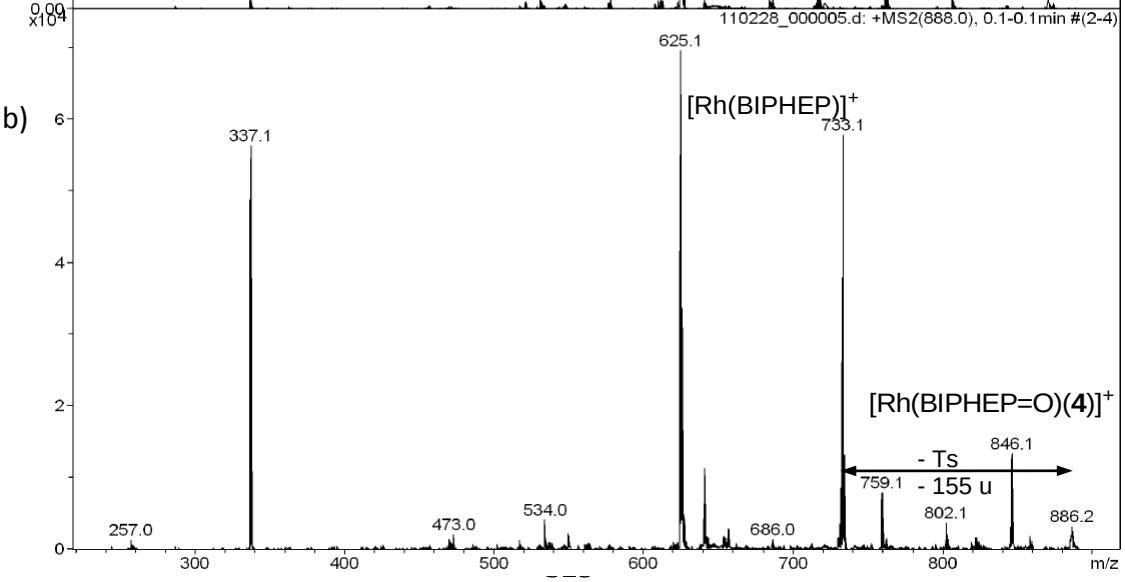

Figure S36. a) ESI(+)MS/MS and b) MS^3 spectra of the ion [Rh(BIPHEP)(**4**)(**2c**)]$^+$ at *m/z* = 974 (collision energy of 0,23 V, width = 4 *m/z*).

a)

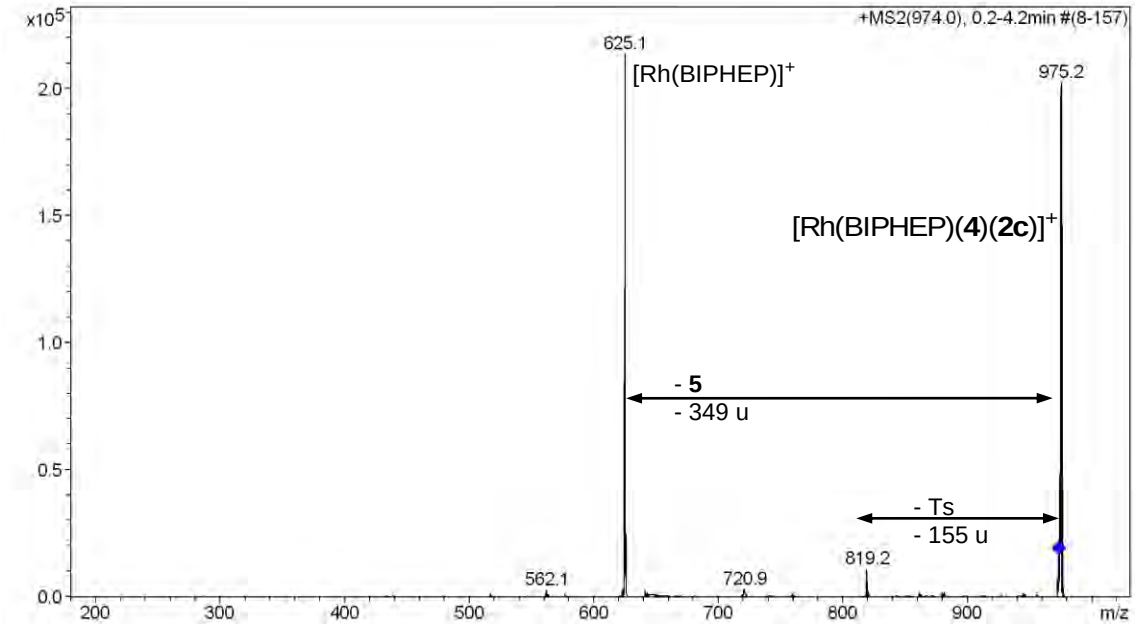

Figure S37. a) ESI(+)MS/MS and b)MS^3 spectra of the ion [Rh(BIPHEP)(**4**)$_2$]$^+$ at *m/z* = 1119 (collision energy of 0,25 V, width = 4 *m/z*).

a)

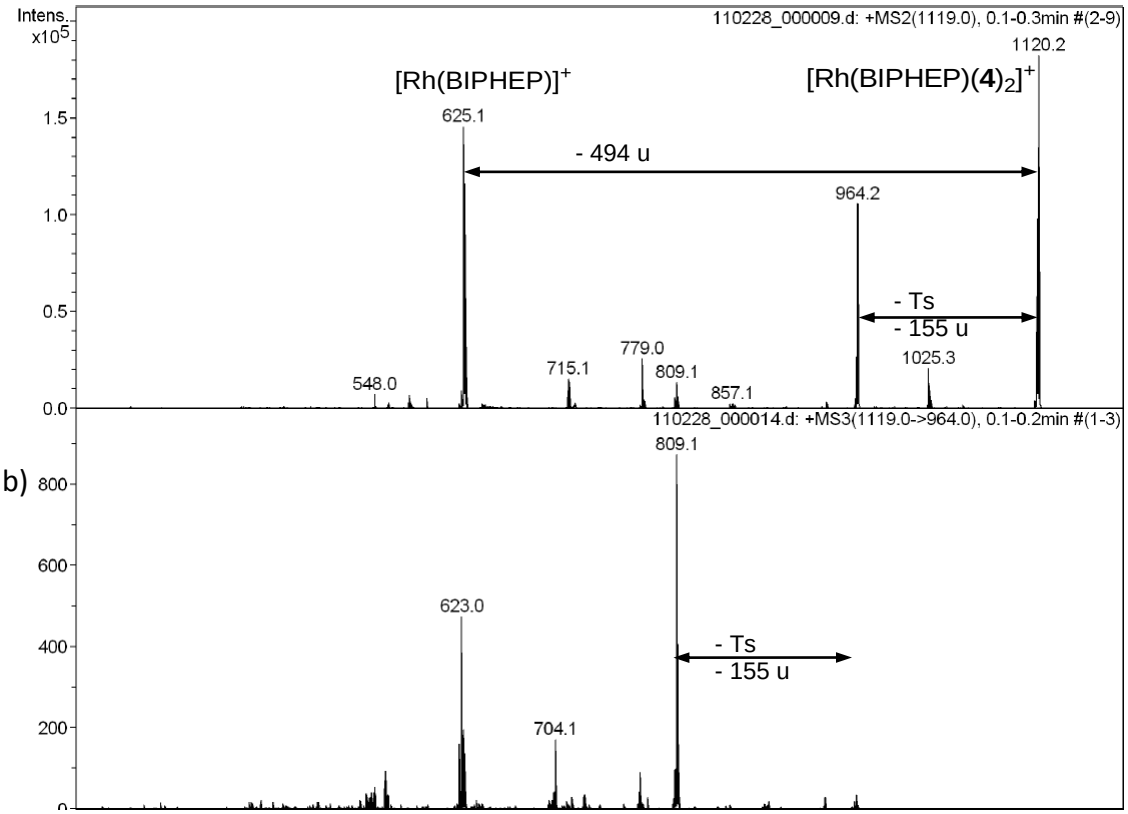

Figure S38. ESI(+) mass spectrum of a solution of the mixture of $[Rh(COD)_2]BF_4$/BIPHEP (5% molar) + **5** diluted in methanol.

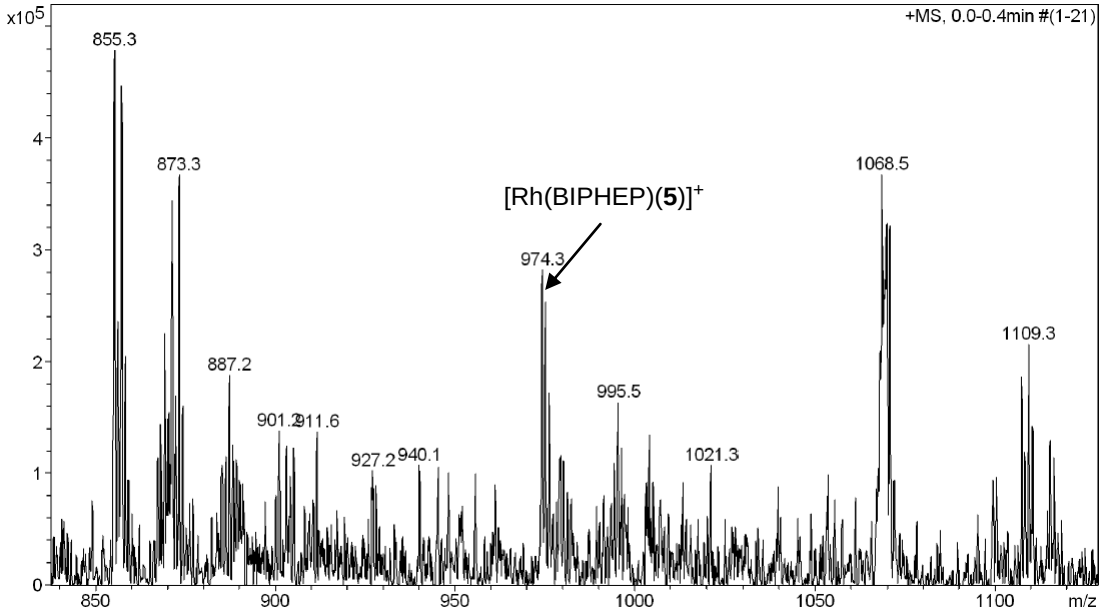

Figure S39. ESI(+)-MS/MS spectrum of the ion $[Rh(BIPHEP)(\mathbf{5})]^+$ at *m/z* = 974 (collision energy of 0,20 V, width = 4 *m/z*).

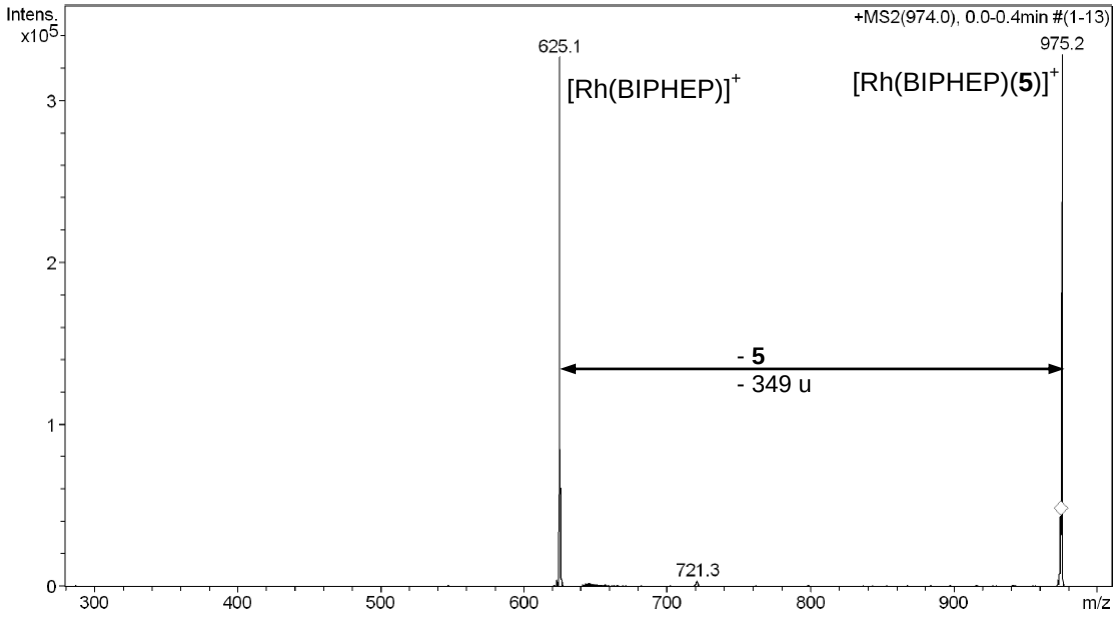

Brun, S.; Parera, M.; Pla-Quintana, A.; Roglans, A.; León, T.; Achard, T.; Solà, J.; Verdaguer, X.; Riera, A. "Chiral N-phosphino sulfinamide ligands in rhodium(I)-catalyzed [2+2+2] cycloaddition reactions". *Tetrahedron*. Vol. 66, issue 46 (2010) : 9032-9040

http://dx.doi.org/10.1016/j.tet.2010.09.009

http://www.sciencedirect.com/science/article/pii/S0040402010013347#

Received 9 July 2010

Received in revised form 30 August 2010

Accepted 3 September 2010

Available online 15 September 2010

Abstract

The combination of cationic rhodium(I) complexes with N-phosphino tert-butylsulfinamides (PNSO) ligands is efficient for catalytic intra- and intermolecular [2+2+2] cycloaddition reactions. PNSO ligands are a new class of chiral bidentate ligands, which have the characteristic of combining the easily accessible sulfur chirality with the coordinating capacity of phosphorous. Cycloaddition of open-chained and macrocyclic E-enediynes with these chiral complexes have proved to be highly efficient in terms of yields, giving moderate enantiomeric excesses of the corresponding cyclohexadiene derivatives. In addition Rh(I)/PNSO complexes catalyzed the intermolecular cycloaddition of diynes with monoalkynes in mild reaction conditions and short reaction times.

Keywords

[2+2+2] Cycloaddition; Rhodium; Sulfinamide ligands; Alkynes; Enediynes

León, T.; Parera, M.; Roglans, A.; Riera, A. Verdaguer, X. Angew. "P-Stereogenic Secondary Iminophosphorane Ligands and Their Rhodium(I) Complexes: Taking Advantage of NH/PH Tautomerism". *Angewandte Chemie International Edition*. Vol. 51, Issue 28 (July 9, 2012) :6951-6955

http://dx.doi.org/10.1002/anie.201201031

http://onlinelibrary.wiley.com/doi/10.1002/anie.201201031/abstract

Issue published online: 4 JUL 2012

Article first published online: 13 JUN 2012

Manuscript Revised: 12 APR 2012

Manuscript Received: 7 FEB 2012

Abstract

Have a good SIP: P-stereogenic secondary iminophosphorane (SIP) ligands with a sulfonyl group attached to nitrogen have been prepared. In the presence of rhodium, the tautomeric equilibrium is shifted from the favored PH tautomer towards the PIII tautomer, thereby allowing coordination of the SIP ligand through the P and O atoms. The resulting Rh complexes are effective in the [2+2+2] cycloaddition of enediynes with terminal alkynes.

Keywords

asymmetric catalysis; cycloaddition reactions; ligand design; phosphorus; rhodium

Parera, M.; Dachs, A.; Solà, M.; Pla-Quintana, A.; Roglans, A. “Direct Detection of Key Intermediates in Rhodium(I)-Catalyzed [2+2+2] Cycloadditions of Alkynes by ESI-MS”. *Chemistry A European Journal*. Vol. 18, Issue 4 (October 8, 2012) : 13097–13107

http://dx.doi.org/10.1002/chem.201200880

http://onlinelibrary.wiley.com/doi/10.1002/chem.201200880/abstract

Issue published online: 27 SEP 2012

Article first published online: 30 AUG 2012

Manuscript Revised: 3 JUL 2012

Manuscript Received: 15 MAR 2012

Abstract

The mechanism of the Rh-catalysed [2+2+2] cycloaddition reaction of diynes with monoynes has been examined using ESI-MS and ESI-CID-MS analysis. The catalytic system used consisted of the combination of a cationic rhodium(I) complex with bisphosphine ligands, which generates highly active complexes that can be detected by ESI(+) experiments. ESI-MS on-line monitoring has allowed the detection for the first time of all of the intermediates in the catalytic cycle, supporting the mechanistic proposal based mainly on theoretical calculations. For all ESI-MS experiments, the structural assignments of ions are supported by tandem mass spectrometry analyses. Computer model studies based on density functional theory (DFT) support the structural proposal made for the monoyne insertion intermediate. The collective studies provide new insight into the reactivity of cationic rhodacyclopentadienes, which should facilitate the design of related rhodium-catalysed C[BOND]C couplings.

Keywords

cycloaddition; density functional calculations; electrospray ionization; mass spectrometry; rhodium